UNIVERSITY
OF TRENTO

DIPARTIMENTO DI INGEGNERIA E SCIENZA DELL'INFORMAZIONE

38123 Povo – Trento (Italy), Via Sommarive 14
http://www.disi.unitn.it

IMAGING OF DIELECTRIC OBJECTS BY BCS-TE

L. Poli, G. Oliveri, P. Rocca, and A. Massa

June 2013

Technical Report # DISI-13-010

Contents

Part I
Problem Statement

1 Mathematical Formulation

1.1 2D TE Inverse Scattering Formulation

Si consideri un cilindro dielettrico di sezione arbitraria infinitamente esteso lungo l'asse z parallelo all'asse del cilidro stesso, sul quale incide un onda di tipo trasverso elettrico TE, ossia un'onda elettromagnetica caratterizzata da un vettore di campo elettrico perpendicolare all'asse del cilindro. Dato il tipo di illuminazione, il campo incidente elettrico $\overline{E}_{inc}$ sarà privo della componente lungo l'asse z:

$$\overline{E}_{inc}(x,y) = E^x_{inc}(x,y)\,\widehat{x} + E^y_{inc}(x,y)\,\widehat{y} \tag{1}$$

dove $\widehat{x}$ e $\widehat{y}$ rappresentano i versori paralleli rispettivamente all' asse x e all' asse y del sistema di riferimento.

Si assume che il cilindro dielettrico abbia la stessa permeabilita' magnetica del vuoto ($\mu = \mu_0$); si assume che il materiale dielettrico sia lineare e isotropo, ma che potrebbe essere non omogeneo lungo le coordinate trasverse:

$$\tilde{\varepsilon} = \tilde{\varepsilon}(x,y) \tag{2}$$

dove ε rappresenta la permettivita' dielettrica complessa del materiale.

Sia $\overline{E}_{tot}$ il campo elettrico totale, ovvero il campo il campo generato da una sorgente in presenza del cilindro dielettrico; il campo scatterato $\overline{E}_{scatt}$ e' definito come la differenza tra il campo totale $\overline{E}_{tot}$ e il campo incidente $\overline{E}_{inc}$:

$$\overline{E}_{tot}(x,y) = \overline{E}_{inc}(x,y) + \overline{E}_{scatt}(x,y) \tag{3}$$

Dato il tipo di illuminazione abbiamo che:

$$\overline{E}_{tot}(x,y) = E^x_{tot}(x,y)\,\widehat{x} + E^y_{tot}(x,y)\,\hat{y} \tag{4}$$

$$\overline{E}_{scatt}(x,y) = E^x_{scatt}(x,y)\,\widehat{x} + E^y_{scatt}(x,y)\,\hat{y} \tag{5}$$

Dal principio di equivalenza possiamo considerare il campo scatterato come generato da una corrente equivalente che irradia in spazio libero, dove la densita' di corrente e' definita come:

$$\overline{J}_{eq}(x,y) = \tau(x,y)\,\overline{E}_{tot}(x,y) \tag{6}$$

che in questo caso puo' essere definita anche come:

$$\overline{J}_{eq}(x,y) = J^x_{eq}(x,y)\,\widehat{x} + J^y_{eq}(x,y)\,\hat{y} \tag{7}$$

Si puo' dimostrare che:

$$\overline{E}_{scatt}(x,y) = \int_s \overline{\overline{G}}(x,y/x',y')\,\tau(x',y')\,\overline{E}_{tot}(x',y')\,dx'dy' \tag{8}$$

Sostituendo la (8) nella (3) si ottiene

$$\int_s \tau(x',y')\,\overline{E}_{tot}(x',y')\,\overline{\overline{G}}(x,y/x',y')\,dx'dy' = \overline{E}_{tot}(x,y) - \overline{E}_{inc}(x,y) \tag{9}$$

La (9) e' un' equazione vettoriale che, dalla (6) puo' essere riscritta come

$$\int_s \overline{J}_{eq}(x,y)\,\overline{\overline{G}}(x,y/x',y')\,dx'dy' = \overline{E}_{tot}(x,y) - \overline{E}_{inc}(x,y) \tag{10}$$

Le componenti scalari dell'equazione (10) sono ricavabili osservando che

$$\overline{\overline{G}}(x,y/x',y') = \overline{G}^x\widehat{x} + \overline{G}^y\widehat{y} \qquad \overline{J} = J^x_{eq}\widehat{x} + J^y_{eq}\widehat{y} \tag{11}$$

e

$$\overline{J}_{eq} = J^x_{eq}\widehat{x} + J^y_{eq}\widehat{y} \tag{12}$$

$$\overline{J}_{eq} \cdot \overline{\overline{G}} = \left(J_{eq}^{x}\widehat{x} + J_{eq}^{y}\widehat{y}\right)\left(\overline{G}^{x}\widehat{x} + \overline{G}^{y}\widehat{y}\right) \tag{13}$$

che per simmetria della diadica di Green $\overline{\overline{G}}$ si puo' scrivere anche

$$\overline{\overline{G}} \cdot \overline{J}_{eq} = \left(\overline{G}^{x}\widehat{x} + \overline{G}^{y}\widehat{y}\right)\left(J_{eq}^{x}\widehat{x} + J_{eq}^{y}\widehat{y}\right) \tag{14}$$

Quindi si ricava

$$\overline{J}_{eq} \cdot \overline{\overline{G}} = \left(J_{eq}^{x}G^{xx} + J_{eq}^{y}G^{xy}\right)\widehat{x} + \left(J_{eq}^{x}G^{yx} + J_{eq}^{y}G^{yy}\right)\widehat{y} \tag{15}$$

Noto questo e' possibile riscrivere la (10) nelle sue componenti scalari come segue

$$\int_{s}\left(J_{eq}^{x}G^{xx} + J_{eq}^{y}G^{xy}\right)dx'dy' = E_{tot}^{x}(x,y) - E_{inc}^{x}(x,y) \tag{16}$$

$$\int_{s}\left(J_{eq}^{x}G^{yx} + J_{eq}^{y}G^{yy}\right)dx'dy' = E_{tot}^{y}(x,y) - E_{inc}^{y}(x,y) \tag{17}$$

La (16) e la (20) rappresentano le equazioni fondamentali dello scattering inverso, le quali costituiscono un sistema di due equazioni in due incognite, rappresentate da J_{eq}^{x} e J_{eq}^{y}. Per poter risolvere con tecniche numeriche vengono discretizzate secondo la procedura di Richmond [4]. Il dominio di indagine e' suddiviso in N celle rettangolari ($D_{ind}^{(n)}$) su cui sono definite altrettante funzioni base ad impulso rettangolare; si assume che le celle siano sufficientemente piccole affinche' sia la costante dielettrica (e quindi la funzione oggetto $\tau(x_n, y_n)$) che l' intensita' del campo elettrico $E_{tot}^{x,v}(x_n, y_n)$e $E_{tot}^{y,v}(x_n, y_n)$ siano uniformi all' interno delle stesse. In forma discretizzata:

$$E_{tot}^{x,v}(x,y) \simeq \sum_{n=1}^{N} E_{tot}^{x,v}(x_n, y_n)\,\psi_n(x,y) \tag{18}$$

$$E_{tot}^{y,v}(x,y) \simeq \sum_{n=1}^{N} E_{tot}^{y,v}(x_n, y_n)\,\psi_n(x,y) \tag{19}$$

$$\tau(x,y) \simeq \sum_{n=1}^{N} \tau(x_n, y_n)\,\psi_n(x,y) \tag{20}$$

dove

$$\psi_n(x,y) = \left\{ \begin{array}{l} 1 \;\; (x,y) \in D_{ind}^{(n)} \\ 0 \;\; (x,y) \notin D_{ind}^{(n)} \end{array} \right\} \tag{21}$$

Approssimando le celle rettangolari $D_{ind}^{(n)}$ con equivalenti celle circolari si ottiene una notevole semplificazione delle espressioni. Il raggio della cella n-esima e' dato da:

$$a_n = \sqrt{\frac{dx_n dy_n}{\pi}} \tag{22}$$

Elaborando questa procedura, utilizzando delle funzioni di test impulsive ed introducendo inoltre M punti di misura, si giunge al seguente sistema algebrico

$$\begin{aligned} E_{scatt}^{x,v}(x_m^v, y_m^v) \;\; = \;\; & \sum_{n=1}^{N} \left\{ \tau(x_n, y_n)\, E_{tot}^{x,v}(x_n, y_n)\, G_{2d}^{xx,ext}(\rho_{nm}) + \right. \\ & \left. \tau(x_n, y_n)\, E_{tot}^{y,v}(x_n, y_n)\, G_{2d}^{xy,ext}(\rho_{nm}) \right\} \quad m = 1, ..., M \end{aligned} \tag{23}$$

$$E_{scatt}^{y,v}\left(x_m^v, y_m^v\right) = \sum_{n=1}^{N} \left\{ \tau\left(x_n, y_n\right) E_{tot}^{x,v}\left(x_n, y_n\right) G_{2d}^{yx,ext}\left(\rho_{nm}\right) + \right.$$

$$\left. \tau\left(x_n, y_n\right) E_{tot}^{y,v}\left(x_n, y_n\right) G_{2d}^{yy,ext}\left(\rho_{nm}\right) \right\} \quad m = 1, ..., M \tag{24}$$

dove

$$G_{2d}^{xx,ext}\left(\rho_{nm}\right) = \begin{cases} 1 - \frac{j\pi k_0 a_n H_1^{(2)}(k_0 a_n)}{4} & se\ \rho_{nm} \leq a_n \\ \left(-\frac{j\pi a_n J_1(k_0 a_n)}{2\rho_{nm}^3}\right) \left[k_0 \rho_{nm} \left(y_m - y_n\right)^2 H_0^{(2)}(k_0 \rho_{nm}) + \right. & \\ \left. \left[\left(x_m - x_n\right)^2 - \left(y_m - y_n\right)^2\right] \cdot H_1^{(2)}\left(k\rho_{nm}\right)\right] & se\ \rho_{nm} > a_n \end{cases} \tag{25}$$

$$G_{2d}^{xy,ext}\left(\rho_{nm}\right) = G_{2d}^{yx,ext}\left(\rho_{nm}\right) = \begin{cases} 0 & se\ \rho_{nm} \leq a_n \\ \left(-\frac{j\pi a_n J_1(k_0 a_n)}{2\rho_{nm}^3}\right) \left(x_m - x_n\right)\left(y_m - y_n\right) \left[2H_1^{(2)}(k_0\rho_{nm}) - \right. & \\ \left. k_0 \rho_{nm} H_0^{(2)}(k_0 \rho_{nm})\right] & se\ \rho_{nm} > a_n \end{cases} \tag{26}$$

$$G_{2d}^{yy,ext}\left(\rho_{nm}\right) = \begin{cases} \left[1 - \frac{j\pi k_0 a_n H_1^{(2)}(k_0 a_n)}{4}\right] & se\ \rho_{nm} \leq a_n \\ \left(-\frac{j\pi a_n J_1(k a_n)}{2\rho_{nm}^3}\right) \left[k_0 \rho_{nm} \left(x_m - x_n\right)^2 H_0^{(2)}(k_0 \rho_{nm}) + \right. & \\ \left. \left[\left(y_m - y_n\right)^2 - \left(x_m - x_n\right)^2\right] \cdot H_1^{(2)}\left(k_0 \rho_{nm}\right)\right. & se\ \rho_{nm} > a_n \end{cases} \tag{27}$$

dove J_1 e' la funzione di Bessel di ordine 1, $H_0^{(2)}$ e' la funzione di Hankel di seconda specie e di ordine 0, $H_1^{(2)}$ e' la funzione di Hankel di seconda specie di ordine 1, (x_m, y_m) sono le coordinate del generico m-esimo punto di misura, (x_n, y_n) sono le coordinate del centro della generica n-esima cella del dominio di indagine discretizzato, dove

$$\rho_{mn} = \sqrt{\left[\left(x_m - x_n\right)^2 + \left(y_m - y_n\right)^2\right]} \tag{28}$$

$$k_0 = \omega\sqrt{\varepsilon_0 \mu_0} \tag{29}$$

1.2 Inverse CS Problem - Scattering TE Planewave

1.2.1 Single-Task BCS

La tecnica del Bayesian Compressive Sampling permette di risolvere un problema lineare del tipo: dato $\overline{y} = \overline{A} \cdot \overline{x}$ trovare $\underline{x} \in C^M$ tale che $\underline{x} \in C^M$ e $\underline{x}$ è sparso. Considerando la tecnica single-task BCS, possiamo definire

$$\overline{y} = \begin{bmatrix} E_{scatt}^{x,v}\left(x_1, y_1\right) \\ ... \\ E_{scatt}^{x,v}\left(x_M, y_M\right) \\ E_{scatt}^{y,v}\left(x_1, y_1\right) \\ ... \\ E_{scatt}^{y,v}\left(x_M, y_M\right) \end{bmatrix} \tag{30}$$

di dimensione $2M \times 1$;

$$\overline{A} = \begin{bmatrix} G_{2d}^{xx,ext}(\rho_{11}) & ... & G_{2d}^{xx,ext}(\rho_{1N}) & G_{2d}^{xy,ext}(\rho_{11}) & ... & G_{2d}^{xy,ext}(\rho_{1N}) \\ ... & ... & ... & ... & ... & ... \\ G_{2d}^{xx,ext}(\rho_{M1}) & ... & G_{2d}^{xx,ext}(\rho_{MN}) & G_{2d}^{xy,ext}(\rho_{M1}) & ... & G_{2d}^{xy,ext}(\rho_{MN}) \\ G_{2d}^{yx,ext}(\rho_{11}) & ... & G_{2d}^{yx,ext}(\rho_{1N}) & G_{2d}^{yy,ext}(\rho_{11}) & ... & G_{2d}^{yy,ext}(\rho_{1N}) \\ ... & ... & ... & ... & ... & ... \\ G_{2d}^{yx,ext}(\rho_{M1}) & ... & G_{2d}^{yx,ext}(\rho_{MN}) & G_{2d}^{yy,ext}(\rho_{M1}) & ... & G_{2d}^{yy,ext}(\rho_{MN}) \end{bmatrix} \tag{31}$$

di dimensione $2M \times 2N$;

$$\overline{x} = \begin{bmatrix} J_{eq}^{x,v}(x_1, y_1) \\ ... \\ J_{eq}^{x,v}(x_N, y_N) \\ J_{eq}^{y,v}(x_N, y_N) \\ ... \\ J_{eq}^{y,v}(x_N, y_N) \end{bmatrix} \tag{32}$$

di dimensione $2N \times 1$.
Analogamente a quanto visto per le eq. (23) e (24), possiamo scrivere le equazioni di "stato"

$$\tau(x_n, y_n) E_{inc}^{x,v}(x_n, y_n) = J_{eq}^{x,v}(x_n, y_n) - \sum_{q=1}^{N} \Big\{ \tau(x_q, y_q) E_{tot}^{x,v} G_{2d}^{xx,int}(\rho_{nq}) \\ \tau(x_q, y_q) E_{tot}^{y,v} G_{2d}^{xy,int}(\rho_{nq}) \Big\} \quad n = 1, ..., N \tag{33}$$

$$\tau(x_n, y_n) E_{inc}^{y,v}(x_n, y_n) = J_{eq}^{y,v}(x_n, y_n) - \sum_{q=1}^{N} \Big\{ \tau(x_q, y_q) E_{tot}^{x,v} G_{2d}^{yx,int}(\rho_{nq}) \\ \tau(x_q, y_q) E_{tot}^{y,v} G_{2d}^{yy,int}(\rho_{nq}) \Big\} \quad n = 1, ..., N \tag{34}$$

dove

$$G_{2d}^{xx,int}(\rho_{qn}) = \begin{cases} \left(-\frac{j\pi a_q J_1(ka_q)}{2\rho_{qn}^3}\right) \Big[k_0 \rho_{qn} (y_n - y_q)^2 H_0^{(2)}(k_0\rho_{qn}) + \\ \Big[(x_n - x_q)^2 - (y_n - y_q)^2 \Big] \cdot H_1^{(2)}(k_0\rho_{qn}) \quad se \quad q \neq n \\ 1 - \frac{j\pi k_0 a_q H_1^{(2)}(k_0 a_q)}{4} \quad se\, q = n \end{cases} \tag{35}$$

$$G_{2d}^{xy,int}(\rho_{qn}) = G_{2d}^{yx,int}(\rho_{qn}) = \begin{cases} \left(-\frac{j\pi a_q J_1(k_0 a_q)}{2\rho_{qn}^3}\right) \Big[(x_n - x_q)(y_n - y_q) \Big[2H_1^{(2)}(k_0\rho_{qn}) - \\ k_0 \rho_{qn} H_0^{(2)}(k_0\rho_{qn}) \Big] \Big] \quad se\, q \neq n \\ 0 \qquad\qquad se\, q = n \end{cases} \tag{36}$$

$$G_{2d}^{yy,int}(\rho_{qn}) = \begin{cases} \left(-\frac{j\pi a_q J_1(ka_q)}{2\rho_{qn}^3}\right) \Big[k_0 \rho_{qn} (x_n - x_q)^2 H_0^{(2)}(k_0\rho_{qn}) + \\ \Big[(y_n - y_q)^2 - (x_n - x_q)^2 \Big] \cdot H_1^{(2)}(k_0\rho_{qn}) \quad se \quad q \neq n \\ 1 - \frac{j\pi k_0 a_q H_1^{(2)}(k_0 a_q)}{4} \quad se\, q = n \end{cases} \tag{37}$$

Per calcolare $\tau(x_n, y_n)$, prima troviamo il campo scatterato interno

$$E_{scatt}^{x,v}(x_n,y_n) = \sum_{n=1}^{N}\left\{J_{eq}^{x,v}(x_q,y_q)\,G_{2d}^{xx,ext}(\rho_{nm}) + J_{eq}^{y,v}(x_q,y_q)\,G_{2d}^{xy,ext}(\rho_{nm})\right\} \quad n=1,...,N \tag{38}$$

$$E_{scatt}^{y,v}(x_n,y_n) = \sum_{n=1}^{N}\left\{J_{eq}^{x,v}(x_q,y_q)\,G_{2d}^{yx,ext}(\rho_{nm}) + J_{eq}^{y,v}(x_q,y_q)\,G_{2d}^{yy,ext}(\rho_{nm})\right\} \quad n=1,...,N \tag{39}$$

Quindi, calcoliamo il campo totale interno:

$$E_{tot}^{x,v}(x_n,y_n) = E_{scatt}^{x,v}(x_n,y_n) + E_{int}^{x,v}(x_n,y_n) \quad n=1,...,N \tag{40}$$

$$E_{tot}^{y,v}(x_n,y_n) = E_{scatt}^{y,v}(x_n,y_n) + E_{int}^{y,v}(x_n,y_n) \quad n=1,...,N \tag{41}$$

e per finire:

$$\tau(x_n,y_n) = \frac{1}{2V}\sum_{v=1}^{V}\left\{\frac{\left[J_{eq}^{x,v}(x_n,y_n)\right]}{E_{tot}^{x,v}(x_n,y_n)} + \frac{\left[J_{eq}^{y,v}(x_n,y_n)\right]}{E_{tot}^{y,v}(x_n,y_n)}\right\} \tag{42}$$

1.2.2 Multi-Task BCS

Considerando invece la tecnica multi-task BCS, possiamo scomporre il problema in due problemi lineari, sfruttando la correlazione tra le componenti x-y di campo elettrico

$$\begin{cases} \overline{y}' = \overline{A}' \cdot \overline{x}' \\ \overline{y}'' = \overline{A}'' \cdot \overline{x}'' \end{cases} \tag{43}$$

$$\overline{y}' = \begin{bmatrix} E_{scatt}^{x,v}(x_1,y_1) \\ ... \\ E_{scatt}^{x,v}(x_M,y_M) \end{bmatrix}, \overline{y}'' = \begin{bmatrix} E_{scatt}^{y,v}(x_1,y_1) \\ ... \\ E_{scatt}^{y,v}(x_M,y_M) \end{bmatrix} \tag{44}$$

di dimensione $M \times 1$;

$$\overline{A}' = \begin{bmatrix} G_{2d}^{xx,ext}(\rho_{11}) & ... & G_{2d}^{xx,ext}(\rho_{1N}) & G_{2d}^{xy,ext}(\rho_{11}) & ... & G_{2d}^{xy,ext}(\rho_{1N}) \\ ... & ... & ... & ... & ... & ... \\ G_{2d}^{xx,ext}(\rho_{M1}) & ... & G_{2d}^{xx,ext}(\rho_{MN}) & G_{2d}^{xy,ext}(\rho_{M1}) & ... & G_{2d}^{xy,ext}(\rho_{MN}) \end{bmatrix} \tag{45}$$

$$\overline{A}'' = \begin{bmatrix} G_{2d}^{yx,ext}(\rho_{11}) & ... & G_{2d}^{yx,ext}(\rho_{1N}) & G_{2d}^{yy,ext}(\rho_{11}) & ... & G_{2d}^{yy,ext}(\rho_{1N}) \\ ... & ... & ... & ... & ... & ... \\ G_{2d}^{yx,ext}(\rho_{M1}) & ... & G_{2d}^{yx,ext}(\rho_{MN}) & G_{2d}^{yy,ext}(\rho_{M1}) & ... & G_{2d}^{yy,ext}(\rho_{MN}) \end{bmatrix} \tag{46}$$

di dimensione $M \times 2N$, e infine

$$\overline{x}' = \begin{bmatrix} J_{eq}^{xx,v}(x_1,y_1) \\ ... \\ J_{eq}^{xx,v}(x_N,y_N) \\ J_{eq}^{xy,v}(x_1,y_1) \\ ... \\ J_{eq}^{xy,v}(x_N,y_N) \end{bmatrix}, \overline{x}'' = \begin{bmatrix} J_{eq}^{yx,v}(x_1,y_1) \\ ... \\ J_{eq}^{yx,v}(x_N,y_N) \\ J_{eq}^{yy,v}(x_1,y_1) \\ ... \\ J_{eq}^{yy,v}(x_N,y_N) \end{bmatrix} \tag{47}$$

di dimensione $N \times 1$.
Per calcolare $\tau(x_n,y_n)$, prima troviamo il campo scatterato interno

$$E_{scatt}^{x,v}(x_n,y_n) = \sum_{n=1}^{N}\left\{J_{eq}^{xx,v}(x_q,y_q)\,G_{2d}^{xx,ext}(\rho_{nm}) + J_{eq}^{xy,v}(x_q,y_q)\,G_{2d}^{xy,ext}(\rho_{nm})\right\} \quad n=1,...,N \tag{48}$$

$$E_{scatt}^{y,v}(x_n, y_n) = \sum_{n=1}^{N} \left\{ J_{eq}^{yx,v}(x_q, y_q) G_{2d}^{yx,ext}(\rho_{nm}) + J_{eq}^{yy,v}(x_q, y_q) G_{2d}^{yy,ext}(\rho_{nm}) \right\} \quad n = 1, ..., N \quad (49)$$

Quindi, calcoliamo il campo totale interno:

$$E_{tot}^{x,v}(x_n, y_n) = E_{scatt}^{x,v}(x_n, y_n) + E_{int}^{x,v}(x_n, y_n) \quad n = 1, ..., N \quad (50)$$

$$E_{tot}^{y,v}(x_n, y_n) = E_{scatt}^{y,v}(x_n, y_n) + E_{int}^{y,v}(x_n, y_n) \quad n = 1, ..., N \quad (51)$$

e per finire:

$$\tau(x_n, y_n) = \frac{1}{4V} \sum_{v=1}^{V} \left\{ \frac{\left[J_{eq}^{xx,v}(x_n, y_n) \right]}{E_{tot}^{x,v}(x_n, y_n)} + \frac{\left[J_{eq}^{xy,v}(x_n, y_n) \right]}{E_{tot}^{y,v}(x_n, y_n)} + \frac{\left[J_{eq}^{yx,v}(x_n, y_n) \right]}{E_{tot}^{x,v}(x_n, y_n)} + \frac{\left[J_{eq}^{yy,v}(x_n, y_n) \right]}{E_{tot}^{y,v}(x_n, y_n)} \right\} \quad (52)$$

1.3 Legenda

- ST-BCS: versione Single-Task BCS che considera entrambe le componenti x-y di campo elettrico, secondo l'implementazione esposta nella sotto-sezione 1.2.1;
- X-ST-BCS: versione Single-Task BCS che considera esclusivamente la componente x di campo elettrico;
- Y-ST-BCS: versione Single-Task BCS che considera esclusivamente la componente y di campo elettrico;
- XY-MT-BCS: versione Multi-Task BCS che considera entrambe le componenti x-y di campo elettrico, secondo l'implementazione esposta nella sotto-sezione 1.2.2, e ne sfrutta la correlazione;
- MV-MT-BCS: versione Multi-Task BCS che considera entrambe le componenti x-y di campo elettrico, secondo l'implementazione esposta nella sotto-sezione 1.2.1, sfruttando però la correlazione tra le viste e non tra le 2 componenti di campo;
- MV-X-MT-BCS: versione Multi-Task BCS che considera esclusivamente la componente x di campo elettrico, sfruttando la correlazione tra le viste;
- MV-Y-MT-BCS: versione Multi-Task BCS che considera esclusivamente la componente y di campo elettrico, sfruttando la correlazione tra le viste;
- MV-XY-MT-BCS: versione Multi-Task BCS che considera entrambe le componenti x-y di campo elettrico, secondo l'implementazione esposta nella sotto-sezione 1.2.2 sfruttando sia la correlazione tra le 2 componenti di campo che la correlazione tra le viste;

Part II
Numerical Validation

2 ST-BCS

2.1 ST-BCS - Calibration

TEST CASE: Square Cylinder $L = 0.16\lambda$

Goal: show the performances of BCS when dealing with a sparse scatterer

- Number of Views: V
- Number of Measurements: M
- Number of Cells for the Inversion: N
- Number of Cells for the Direct solver: D
- Side of the investigation domain: L

Test Case Description

Direct solver:

- Square domain divided in $\sqrt{D} \times \sqrt{D}$ cells
- Domain side: $L = 3\lambda$
- $D = 1296$ (discretization for the direct solver: $< \lambda/10$)

Investigation domain:

- Square domain divided in $\sqrt{N} \times \sqrt{N}$ cells
- $L = 3\lambda$
- $2ka = 2 \times \frac{2\pi}{\lambda} \times \frac{L\sqrt{2}}{2} = 6\pi\sqrt{2} = 26.65$
- $\#DOF = \frac{(2ka)^2}{2} = \frac{(2 \times \frac{2\pi}{\lambda} \times \frac{L\sqrt{2}}{2})^2}{2} = 4\pi^2 \left(\frac{L}{\lambda}\right)^2 = 4\pi^2 \times 9 \approx 355.3$
- N scelto in modo da essere vicino a $\#DOF$: $N = 324$ (18×18)

Measurement domain:

- Measurement points taken on a circle of radius $\rho = 3\lambda$
- Full-aspect measurements
- $M \approx 2ka \rightarrow M = 27$

Sources:

- Plane waves
- $V \approx 2ka \rightarrow V = 27$
- Amplitude: $A = 1$
- Frequency: 300 MHz ($\lambda = 1$)

Object:

- Square cylinder of side $\frac{\lambda}{6} = 0.1667$
- $\varepsilon_r = 2.0$

- $\sigma = 0$ [S/m]

BCS parameters:

- Initial estimate of the noise: $n_0 = \in \{1.0 \times 10^{-6}, 2.0 \times 10^{-6}, 5.0 \times 10^{-6}, 1.0 \times 10^{-5}, 2.0 \times 10^{-5}, 5.0 \times 10^{-5}, 1.0 \times 10^{-4}, 2.0 \times 10^{-4}, 5.0 \times 10^{-4}, 1.0 \times 10^{-3}, 2.0 \times 10^{-3}, 5.0 \times 10^{-3}, 1.0 \times 10^{-2}\}$
- Convergenze parameter: $\tau = 1.0 \times 10^{-8}$

RESULTS: Calibration

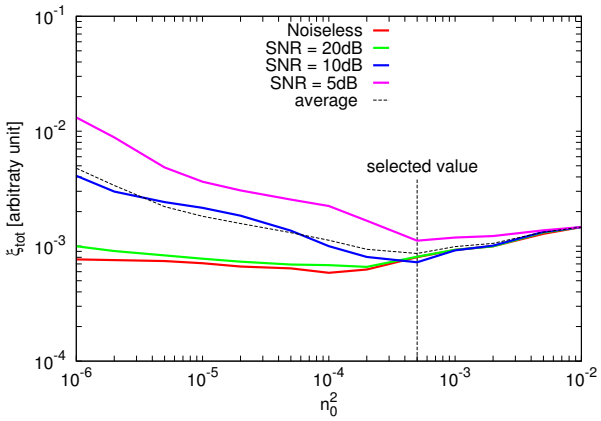

(a)

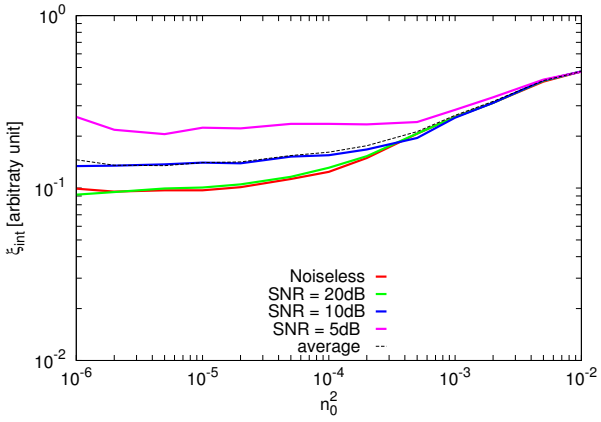

(b)

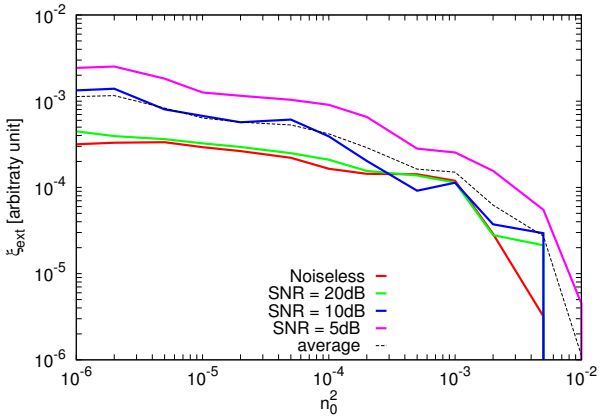

(c)

Figure 1. Behaviour of error figures as a function of the initial estimate of the noise n_0, for different SNR values: (a) total error ξ_{tot}, (b) internal error ξ_{int}, (c) external error ξ_{ext}.

2.2 ST-BCS - Basic Tests

TEST CASE: Square Cylinder $L = 0.16\lambda$

Goal: show the performances of BCS when dealing with a sparse scatterer

- Number of Views: V
- Number of Measurements: M
- Number of Cells for the Inversion: N
- Number of Cells for the Direct solver: D
- Side of the investigation domain: L

Test Case Description

Direct solver:

- Square domain divided in $\sqrt{D} \times \sqrt{D}$ cells
- Domain side: $L = 3\lambda$
- $D = 1296$ (discretization for the direct solver: $< \lambda/10$)

Investigation domain:

- Square domain divided in $\sqrt{N} \times \sqrt{N}$ cells
- $L = 3\lambda$
- $2ka = 2 \times \frac{2\pi}{\lambda} \times \frac{L\sqrt{2}}{2} = 6\pi\sqrt{2} = 26.65$
- $\#DOF = \frac{(2ka)^2}{2} = \frac{(2 \times \frac{2\pi}{\lambda} \times \frac{L\sqrt{2}}{2})^2}{2} = 4\pi^2 \left(\frac{L}{\lambda}\right)^2 = 4\pi^2 \times 9 \approx 355.3$
- N scelto in modo da essere vicino a $\#DOF$: $N = 324$ (18×18)

Measurement domain:

- Measurement points taken on a circle of radius $\rho = 3\lambda$
- Full-aspect measurements
- $M \approx 2ka \rightarrow M = 27$

Sources:

- Plane waves
- $V \approx 2ka \rightarrow V = 27$
- Amplitude: $A = 1$
- Frequency: 300 MHz ($\lambda = 1$)

Object:

- Square cylinder of side $\frac{\lambda}{6} = 0.1667$
- $\varepsilon_r \in \{1.5, 2.0, 2.5, 3.0, 3.5, 4.0, 4.5, 5.0\}$

- $\sigma = 0$ [S/m]

BCS parameters:

- Initial estimate of the noise: $n_0 = 5.0 \times 10^{-4}$
- Convergenze parameter: $\tau = 1.0 \times 10^{-8}$

RESULTS: $\varepsilon_r = 1.5$

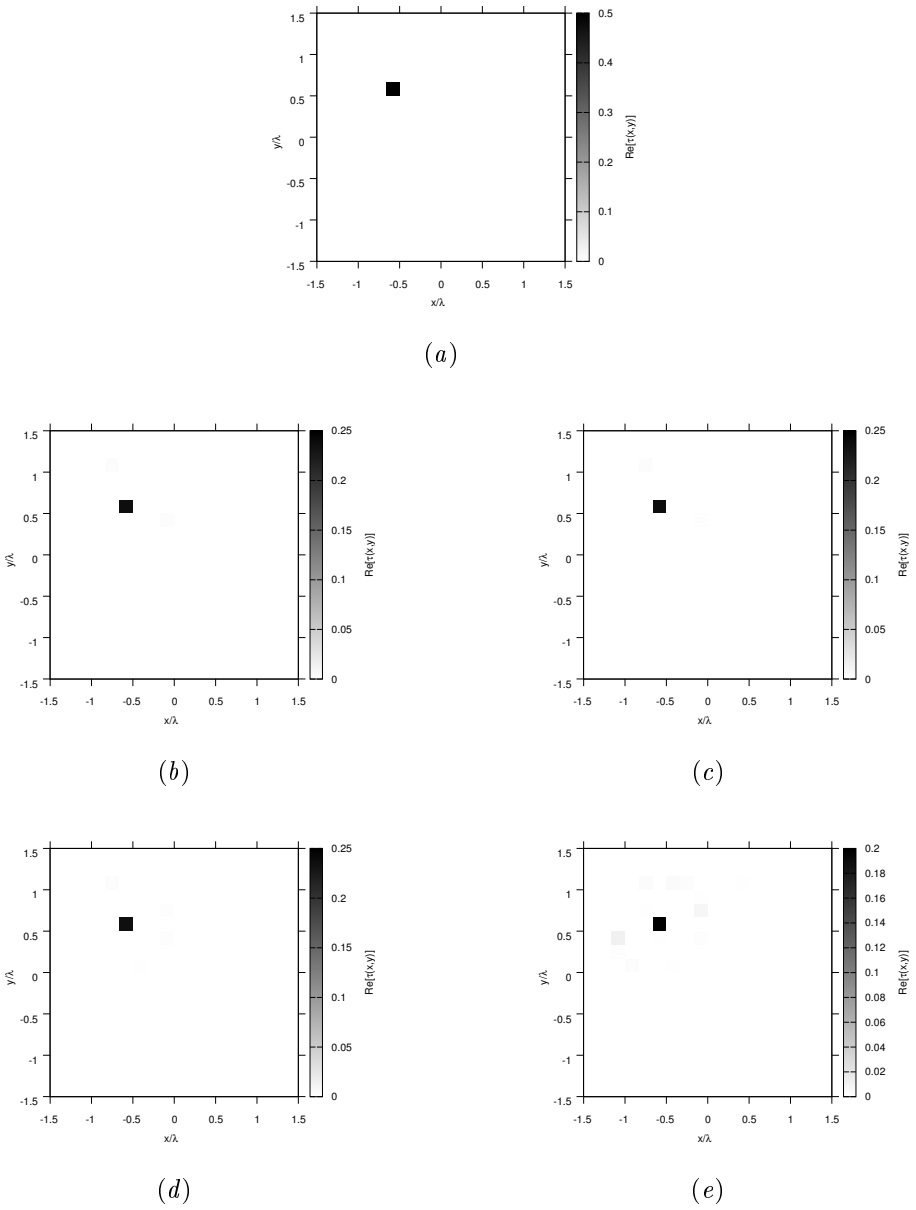

(a)

(b)

(c)

(d)

(e)

Figure 2. Actual object (a) and BCS reconstructed object for (b) Noiseless case, (c) $SNR = 20$ [dB] , (d) $SNR = 10$ [dB] , (e) $SNR = 5$ [dB].

RESULTS: $\varepsilon_r = 2.0$

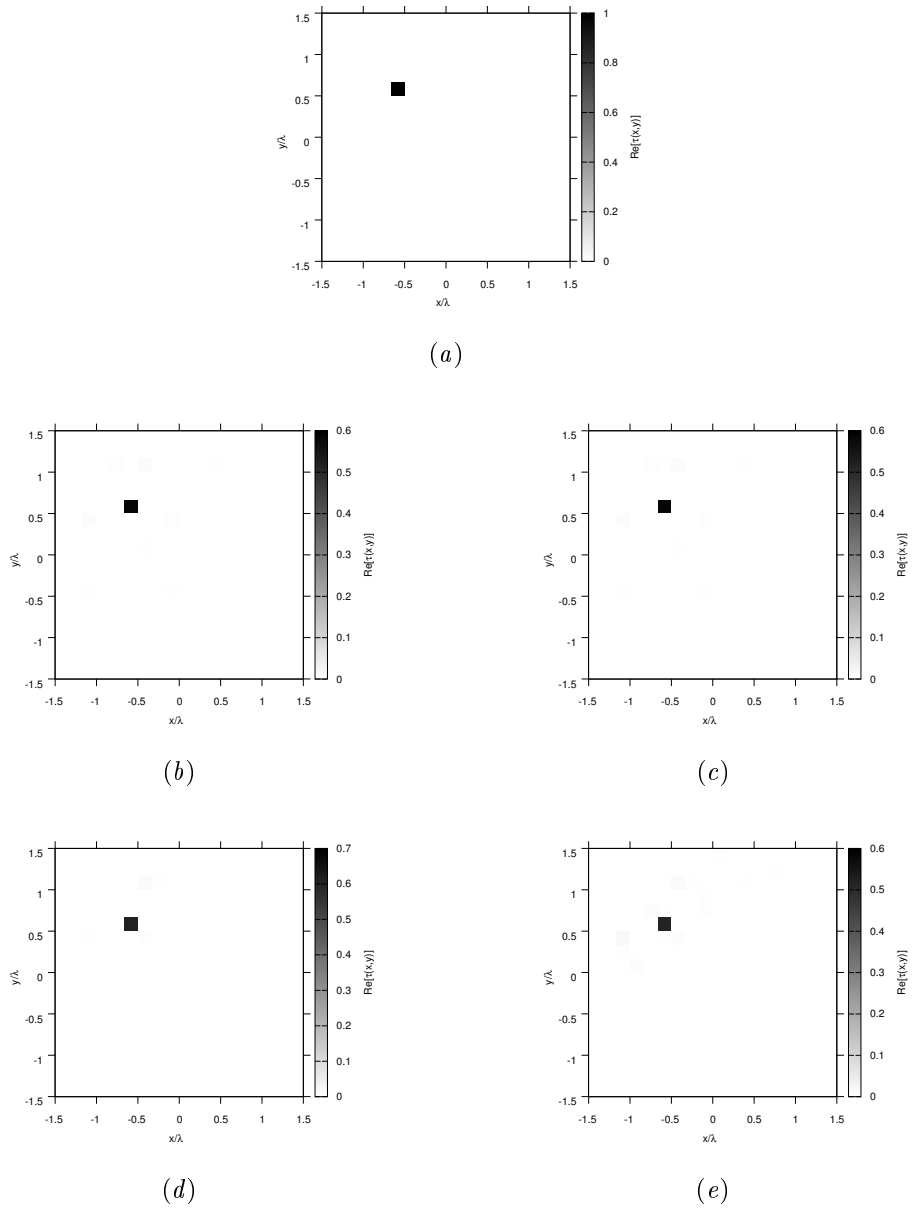

(a)

(b)

(c)

(d)

(e)

Figure 3. Actual object (a) and BCS reconstructed object for (b) Noiseless case, (c) $SNR = 20$ [dB] , (d) $SNR = 10$ [dB] , (e) $SNR = 5$ [dB].

RESULTS: $\varepsilon_r = 5.0$

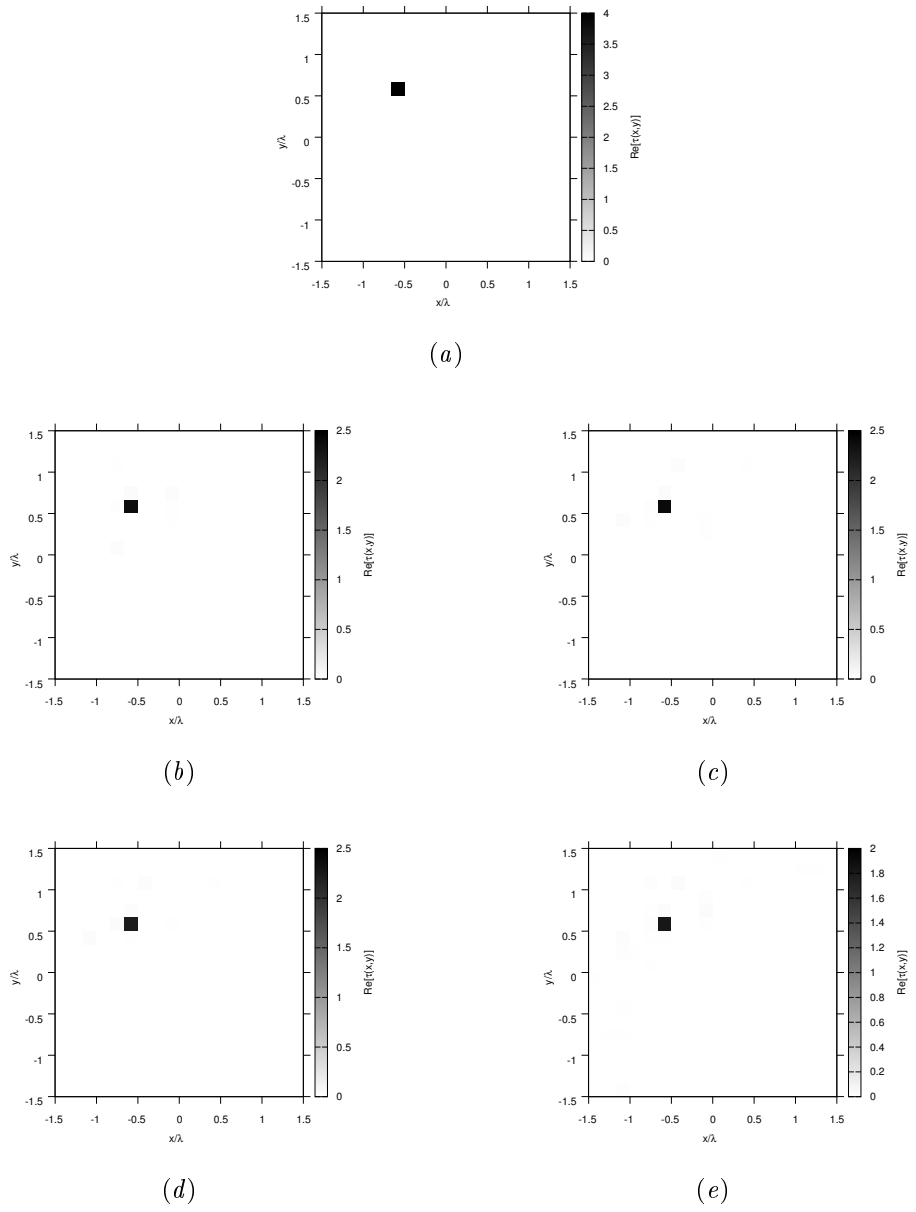

(a)

(b)

(c)

(d)

(e)

Figure 4. Actual object (a) and BCS reconstructed object for (b) Noiseless case, (c) $SNR = 20$ [dB] , (d) $SNR = 10$ [dB] , (e) $SNR = 5$ [dB].

RESULTS: Error Figures

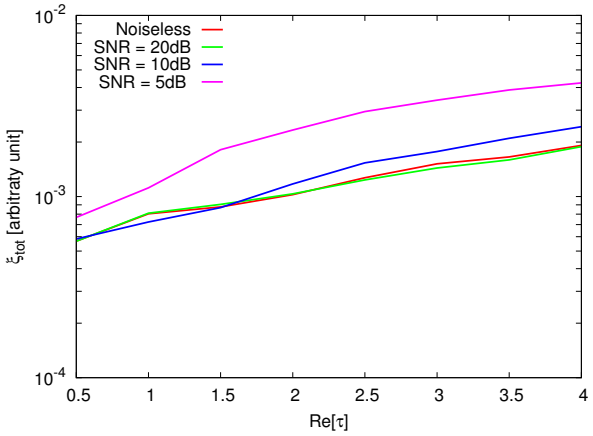

(a)

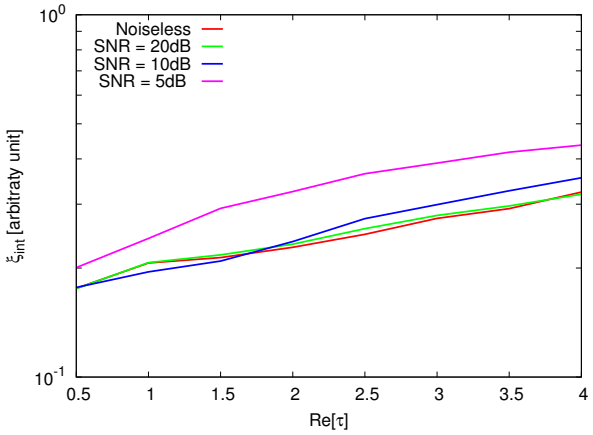

(b)

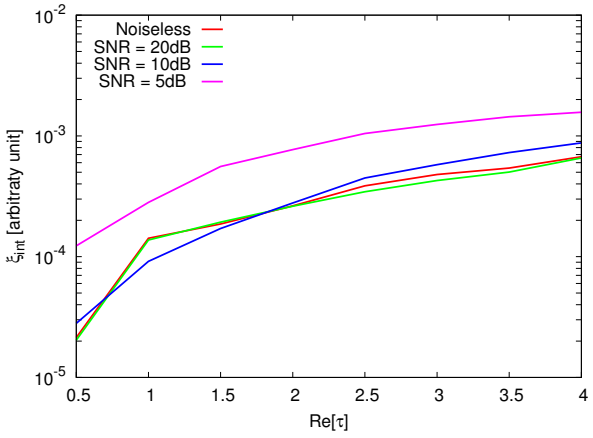

(c)

Figure 5. Behaviour of error figures as a function of ε_r, for different SNR values: (a) total error ξ_{tot}, (b) internal error ξ_{int}, (c) external error ξ_{ext}.

TEST CASE: Two Square Cylinders $L = 0.16\lambda$

Goal: show the performances of BCS when dealing with a sparse scatterer

- Number of Views: V
- Number of Measurements: M
- Number of Cells for the Inversion: N
- Number of Cells for the Direct solver: D
- Side of the investigation domain: L

Test Case Description

Direct solver:

- Square domain divided in $\sqrt{D} \times \sqrt{D}$ cells
- Domain side: $L = 3\lambda$
- $D = 1296$ (discretization for the direct solver: $< \lambda/10$)

Investigation domain:

- Square domain divided in $\sqrt{N} \times \sqrt{N}$ cells
- $L = 3\lambda$
- $2ka = 2 \times \frac{2\pi}{\lambda} \times \frac{L\sqrt{2}}{2} = 6\pi\sqrt{2} = 26.65$
- $\#DOF = \frac{(2ka)^2}{2} = \frac{(2 \times \frac{2\pi}{\lambda} \times \frac{L\sqrt{2}}{2})^2}{2} = 4\pi^2 \left(\frac{L}{\lambda}\right)^2 = 4\pi^2 \times 9 \approx 355.3$
- N scelto in modo da essere vicino a $\#DOF$: $N = 324$ (18×18)

Measurement domain:

- Measurement points taken on a circle of radius $\rho = 3\lambda$
- Full-aspect measurements
- $M \approx 2ka \rightarrow M = 27$

Sources:

- Plane waves
- $V \approx 2ka \rightarrow V = 27$
- Amplitude: $A = 1$
- Frequency: 300 MHz $(\lambda = 1)$

Object:

- Two square cylinders of side $\frac{\lambda}{6} = 0.1667$
- $\varepsilon_r \in \{1.5, 2.0, 2.5, 3.0, 3.5, 4.0, 4.5, 5.0\}$ (one square), $\varepsilon_r = 1.5$ (one square)
- $\sigma = 0$ [S/m]

BCS parameters:

- Initial estimate of the noise: $n_0 = 5.0 \times 10^{-4}$
- Convergenze parameter: $\tau = 1.0 \times 10^{-8}$

RESULTS: $\varepsilon_r = 1.5$

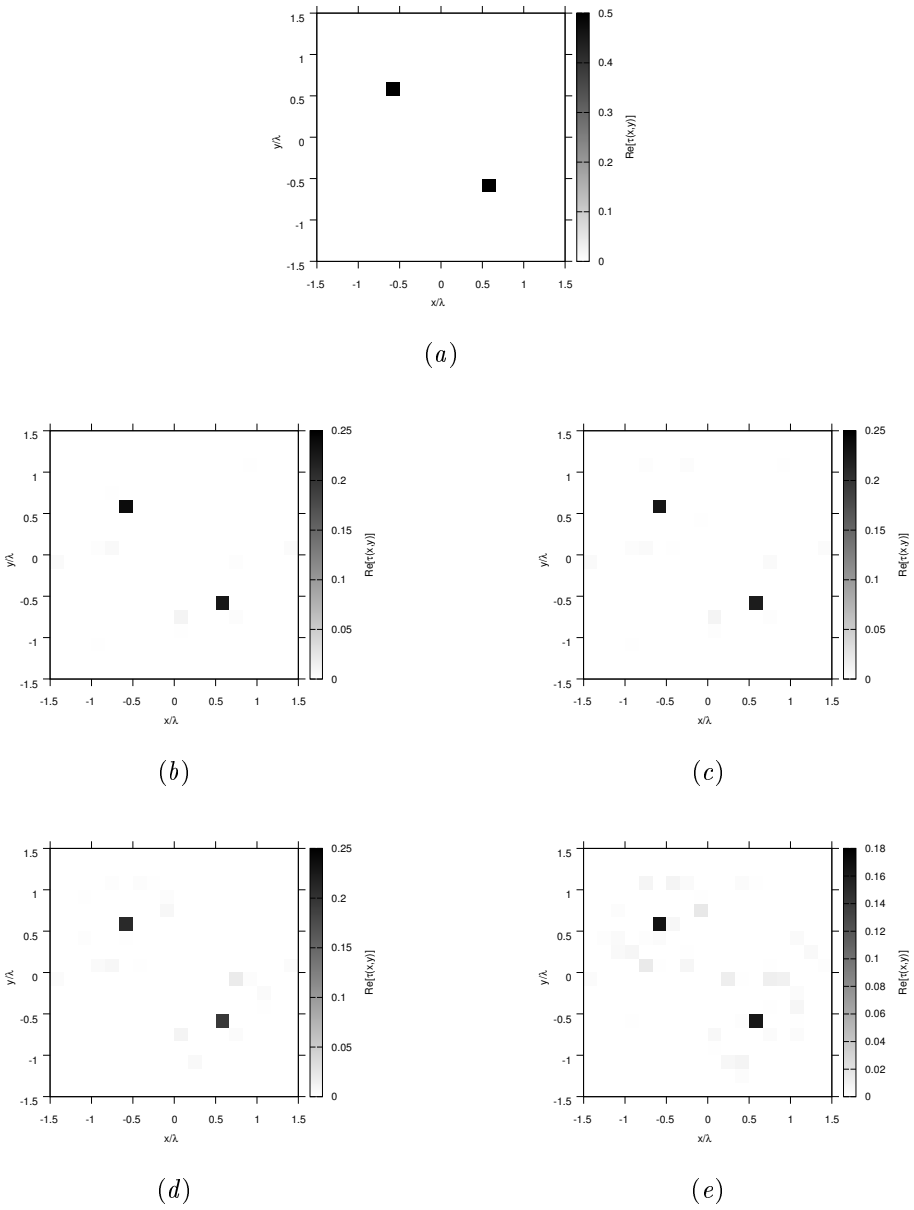

(a)

(b)

(c)

(d)

(e)

Figure 6. Actual object (a) and BCS reconstructed object for (b) Noiseless case, (c) $SNR = 20$ [dB] , (d) $SNR = 10$ [dB] , (e) $SNR = 5$ [dB].

RESULTS: $\varepsilon_r = 2.0$

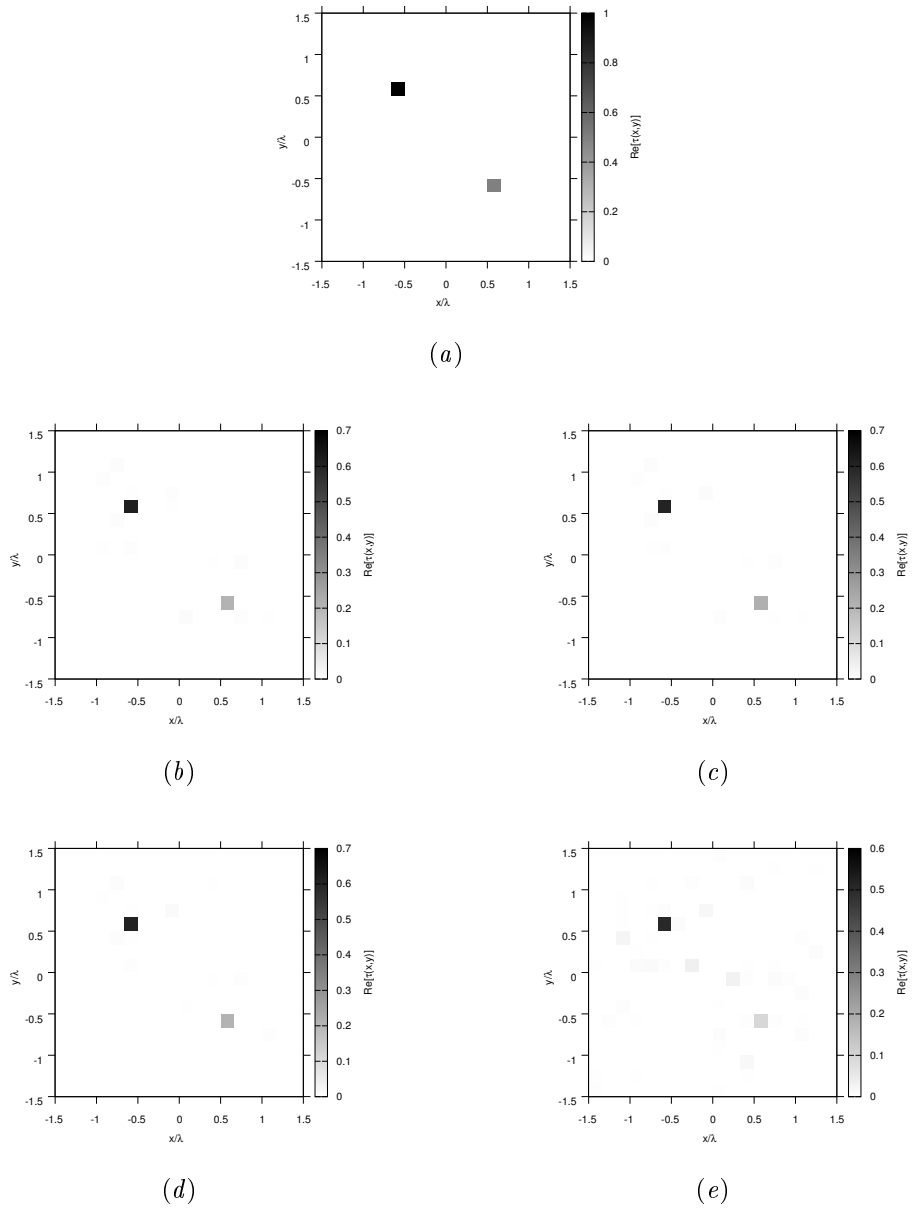

(a) (b) (c) (d) (e)

Figure 7. Actual object (a) and BCS reconstructed object for (b) Noiseless case, (c) $SNR = 20$ [dB] , (d) $SNR = 10$ [dB] , (e) $SNR = 5$ [dB].

RESULTS: $\varepsilon_r = 5.0$

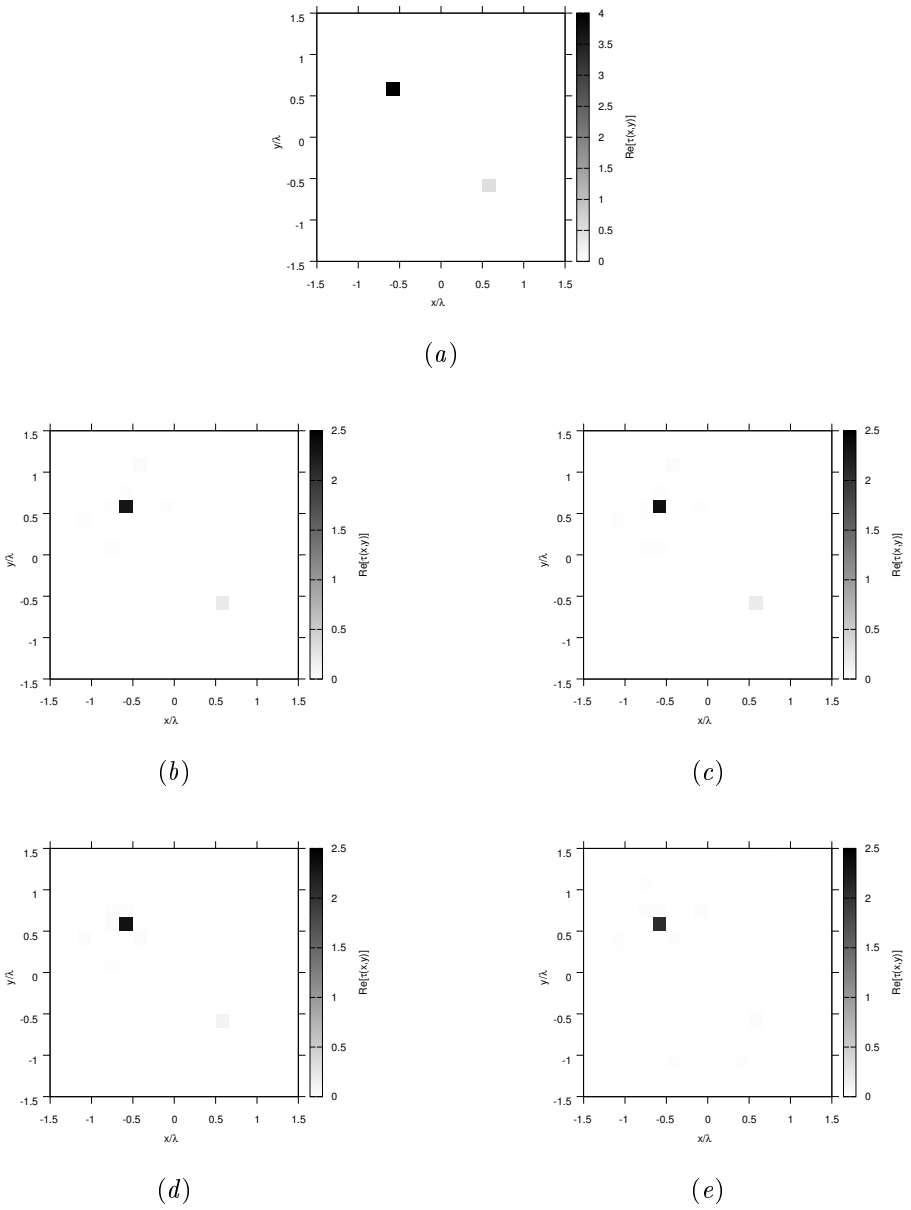

(a) (b) (c) (d) (e)

Figure 8. Actual object (a) and BCS reconstructed object for (b) Noiseless case, (c) $SNR = 20$ [dB] , (d) $SNR = 10$ [dB] , (e) $SNR = 5$ [dB].

RESULTS: Error Figures

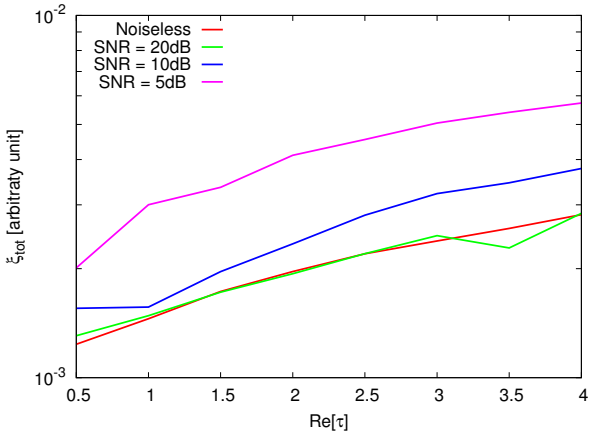

(a)

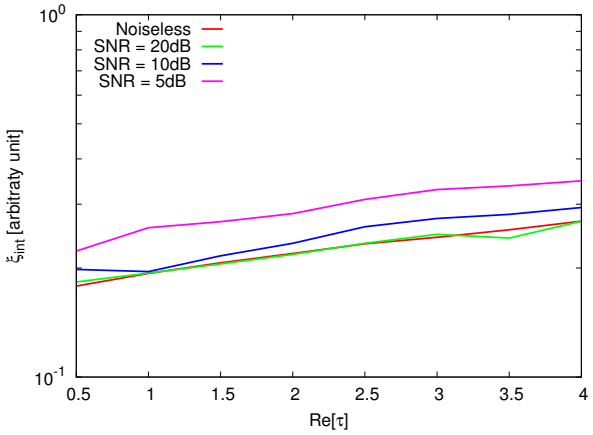

(b)

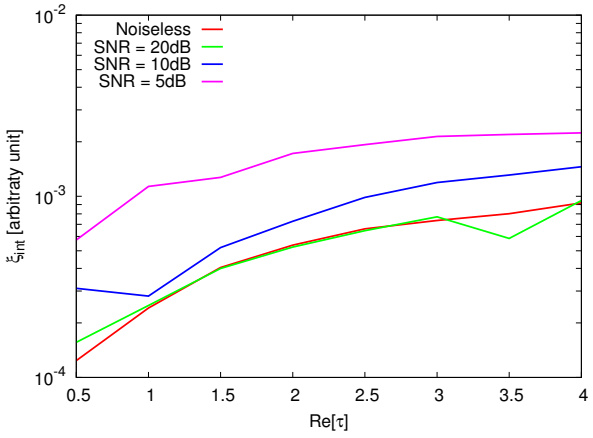

(c)

Figure 9. Behaviour of error figures as a function of ε_r, for different SNR values: (a) total error ξ_{tot}, (b) internal error ξ_{int}, (c) external error ξ_{ext}.

TEST CASE: Square Cylinder $L = 0.33\lambda$

Goal: show the performances of BCS when dealing with a sparse scatterer

- Number of Views: V
- Number of Measurements: M
- Number of Cells for the Inversion: N
- Number of Cells for the Direct solver: D
- Side of the investigation domain: L

Test Case Description

Direct solver:

- Square domain divided in $\sqrt{D} \times \sqrt{D}$ cells
- Domain side: $L = 3\lambda$
- $D = 1296$ (discretization for the direct solver: $< \lambda/10$)

Investigation domain:

- Square domain divided in $\sqrt{N} \times \sqrt{N}$ cells
- $L = 3\lambda$
- $2ka = 2 \times \frac{2\pi}{\lambda} \times \frac{L\sqrt{2}}{2} = 6\pi\sqrt{2} = 26.65$
- $\#DOF = \frac{(2ka)^2}{2} = \frac{(2 \times \frac{2\pi}{\lambda} \times \frac{L\sqrt{2}}{2})^2}{2} = 4\pi^2 \left(\frac{L}{\lambda}\right)^2 = 4\pi^2 \times 9 \approx 355.3$
- N scelto in modo da essere vicino a $\#DOF$: $N = 324$ (18×18)

Measurement domain:

- Measurement points taken on a circle of radius $\rho = 3\lambda$
- Full-aspect measurements
- $M \approx 2ka \rightarrow M = 27$

Sources:

- Plane waves
- $V \approx 2ka \rightarrow V = 27$
- Amplitude: $A = 1$
- Frequency: 300 MHz $(\lambda = 1)$

Object:

- Square cylinder of side $\frac{\lambda}{3} = 0.33$
- $\varepsilon_r \in \{1.5, 2.0, 2.5, 3.0, 3.5, 4.0, 4.5, 5.0\}$
- $\sigma = 0$ [S/m]

BCS parameters:

- Initial estimate of the noise: $n_0 = 5.0 \times 10^{-4}$
- Convergenze parameter: $\tau = 1.0 \times 10^{-8}$

RESULTS: $\varepsilon_r = 1.5$

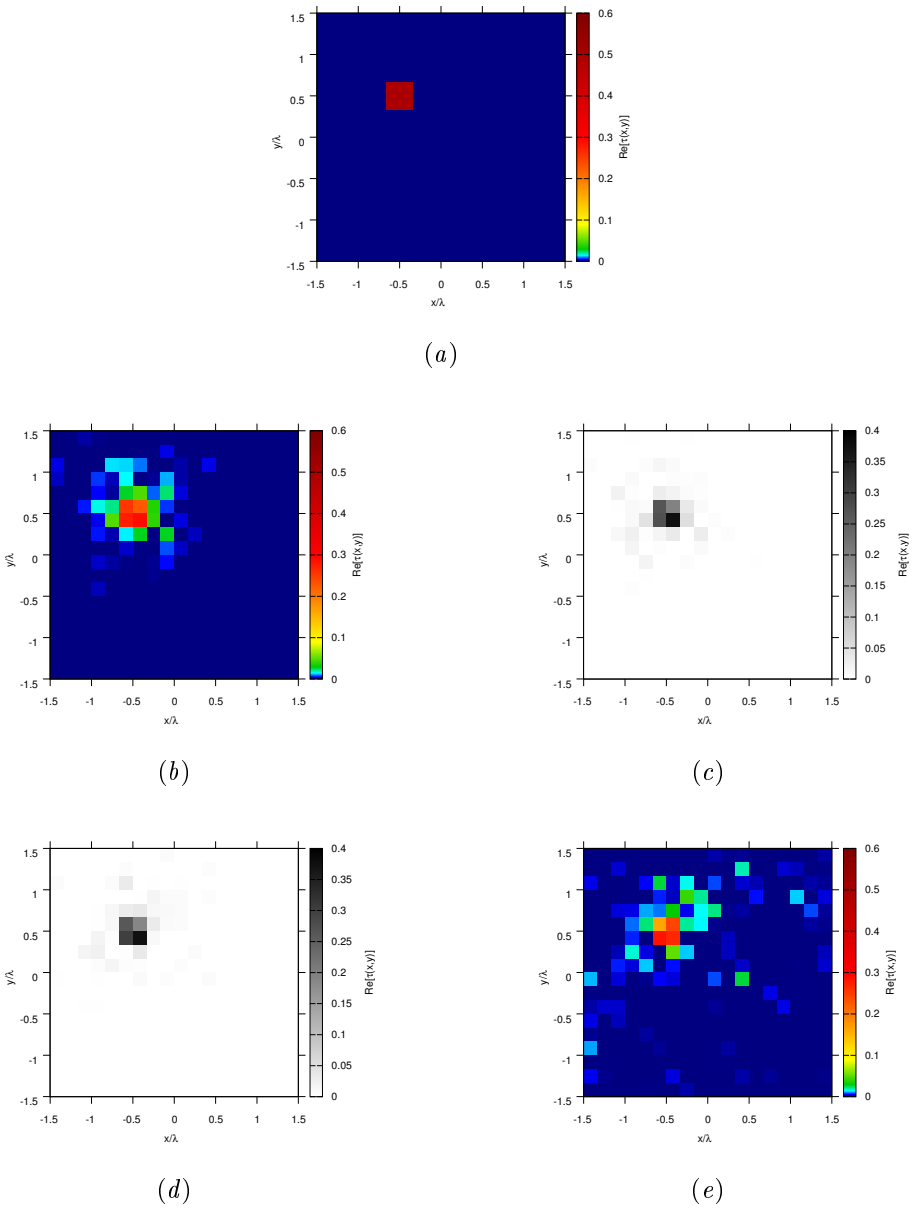

(a)

(b) (c)

(d) (e)

Figure 10. Actual object (a) and BCS reconstructed object for (b) Noiseless case, (c) $SNR = 20$ [dB] , (d) $SNR = 10$ [dB] , (e) $SNR = 5$ [dB].

RESULTS: $\varepsilon_r = 2.0$

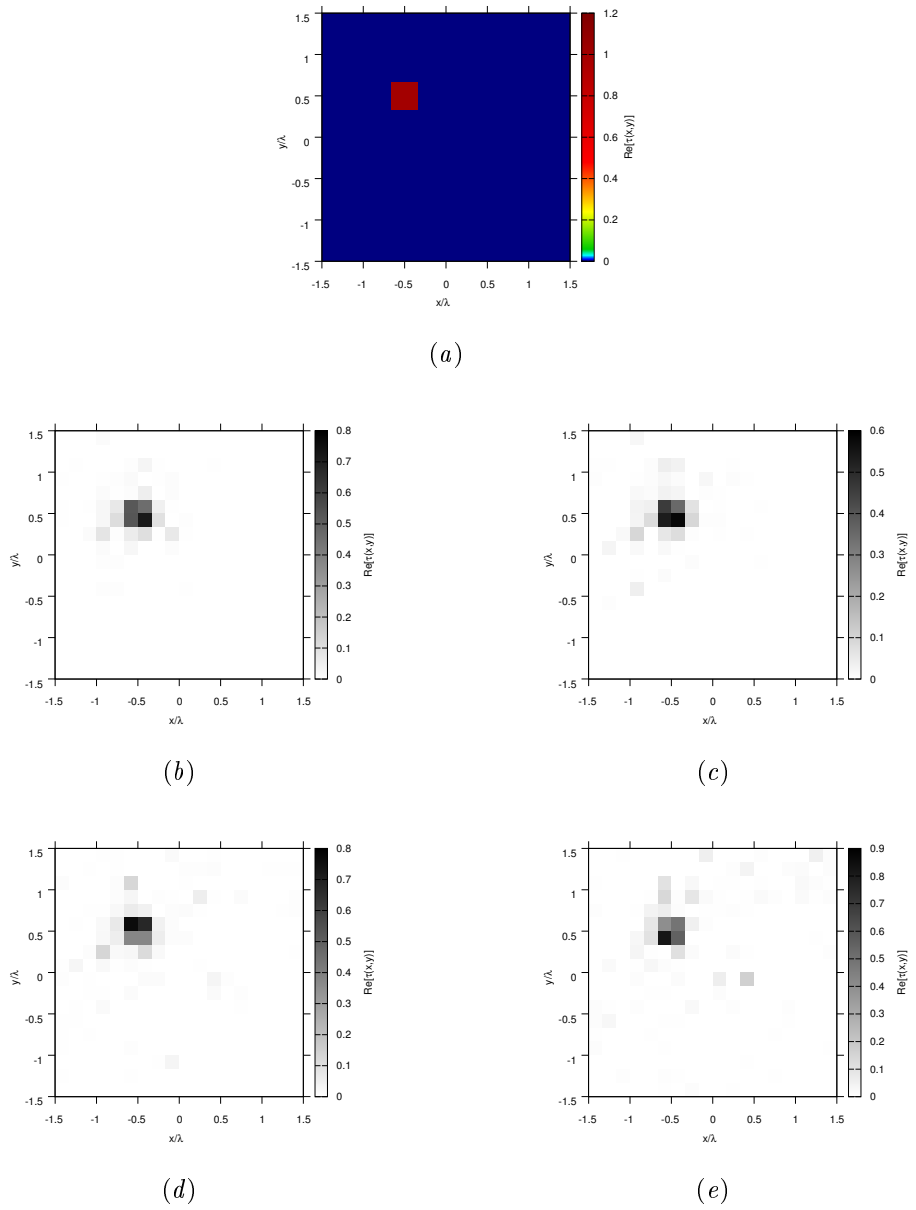

Figure 11. Actual object (a) and BCS reconstructed object for (b) Noiseless case, (c) $SNR = 20$ [dB] , (d) $SNR = 10$ [dB] , (e) $SNR = 5$ [dB].

RESULTS: $\varepsilon_r = 3.0$

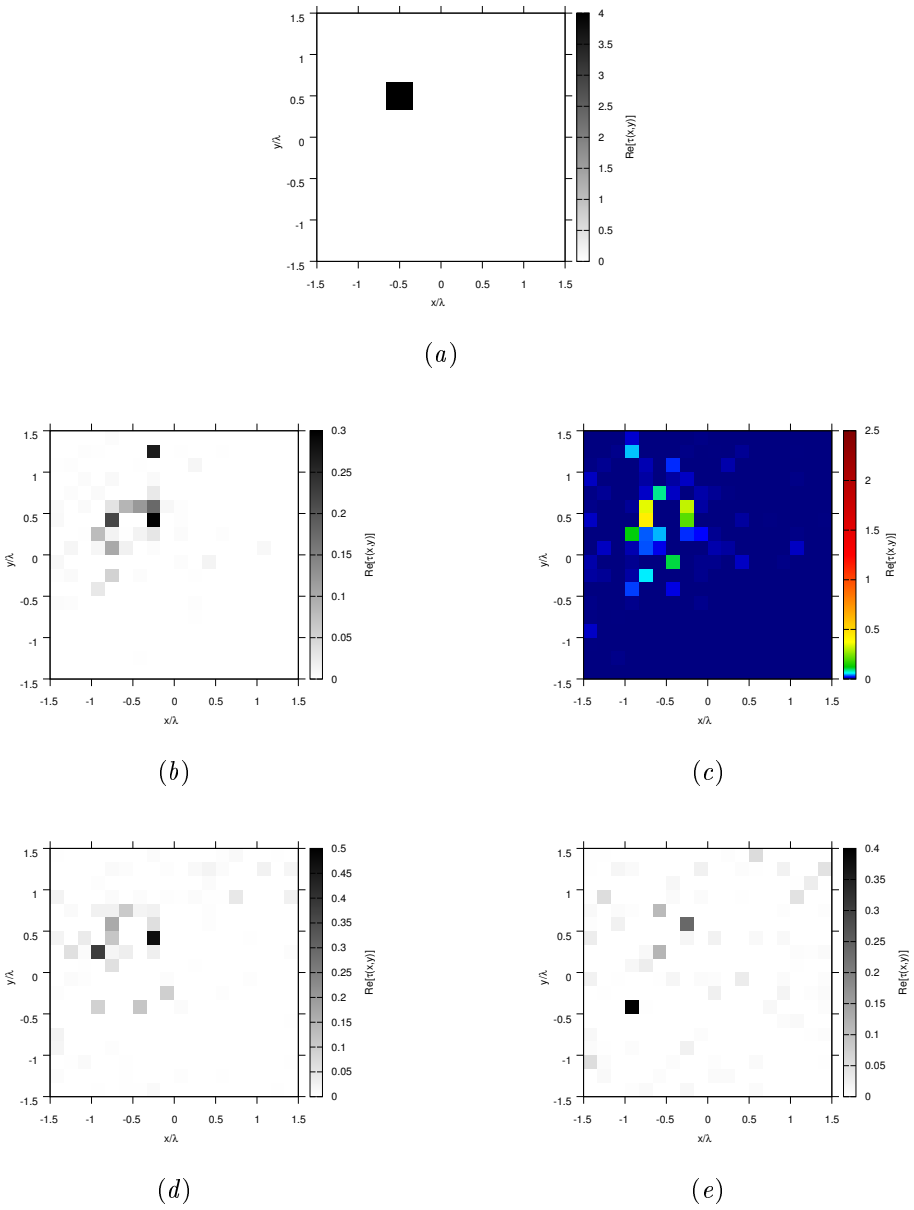

(a) (b) (c) (d) (e)

Figure 12. Actual object (a) and BCS reconstructed object for (b) Noiseless case, (c) $SNR = 20$ [dB] , (d) $SNR = 10$ [dB] , (e) $SNR = 5$ [dB].

RESULTS: Error Figures

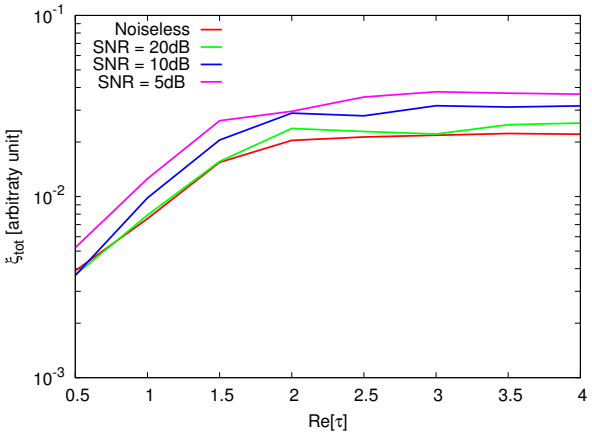

(a)

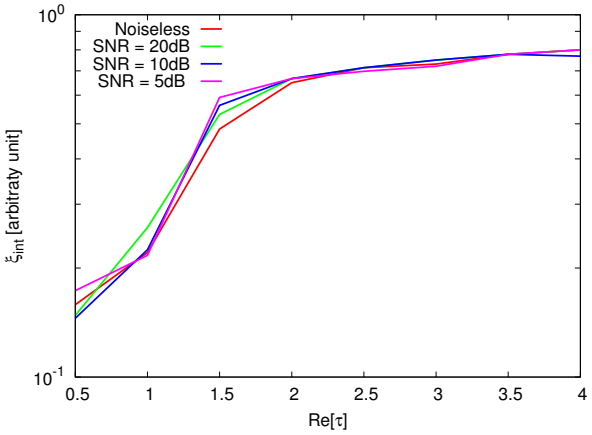

(b)

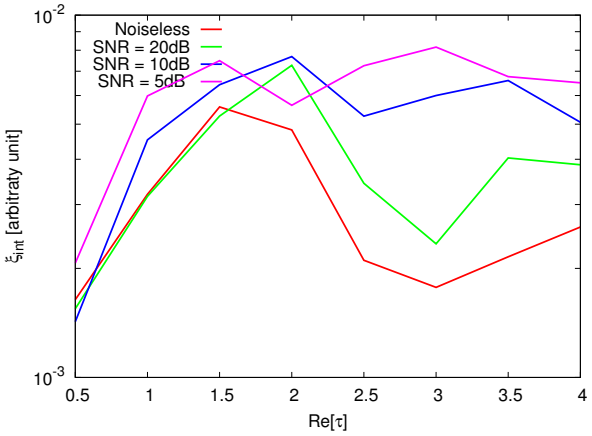

(c)

Figure 13. Behaviour of error figures as a function of ε_r, for different SNR values: (a) total error ξ_{tot}, (b) internal error ξ_{int}, (c) external error ξ_{ext}.

TEST CASE: Cross-Shaped Cylinder

Goal: show the performances of BCS when dealing with a sparse scatterer

- Number of Views: V
- Number of Measurements: M
- Number of Cells for the Inversion: N
- Number of Cells for the Direct solver: D
- Side of the investigation domain: L

Test Case Description

Direct solver:

- Square domain divided in $\sqrt{D} \times \sqrt{D}$ cells
- Domain side: $L = 3\lambda$
- $D = 1296$ (discretization for the direct solver: $< \lambda/10$)

Investigation domain:

- Square domain divided in $\sqrt{N} \times \sqrt{N}$ cells
- $L = 3\lambda$
- $2ka = 2 \times \frac{2\pi}{\lambda} \times \frac{L\sqrt{2}}{2} = 6\pi\sqrt{2} = 26.65$
- $\#DOF = \frac{(2ka)^2}{2} = \frac{(2 \times \frac{2\pi}{\lambda} \times \frac{L\sqrt{2}}{2})^2}{2} = 4\pi^2 \left(\frac{L}{\lambda}\right)^2 = 4\pi^2 \times 9 \approx 355.3$
- N scelto in modo da essere vicino a $\#DOF$: $N = 324$ (18×18)

Measurement domain:

- Measurement points taken on a circle of radius $\rho = 3\lambda$
- Full-aspect measurements
- $M \approx 2ka \rightarrow M = 27$

Sources:

- Plane waves
- $V \approx 2ka \rightarrow V = 27$
- Amplitude: $A = 1$
- Frequency: 300 MHz $(\lambda = 1)$

Object:

- Cross-shaped cylinder
- $\varepsilon_r \in \{1.5, 2.0, 2.5, 3.0, 3.5, 4.0, 4.5, 5.0\}$
- $\sigma = 0$ [S/m]

BCS parameters:

- Initial estimate of the noise: $n_0 = 5.0 \times 10^{-4}$
- Convergenze parameter: $\tau = 1.0 \times 10^{-8}$

RESULTS: $\varepsilon_r = 1.5$

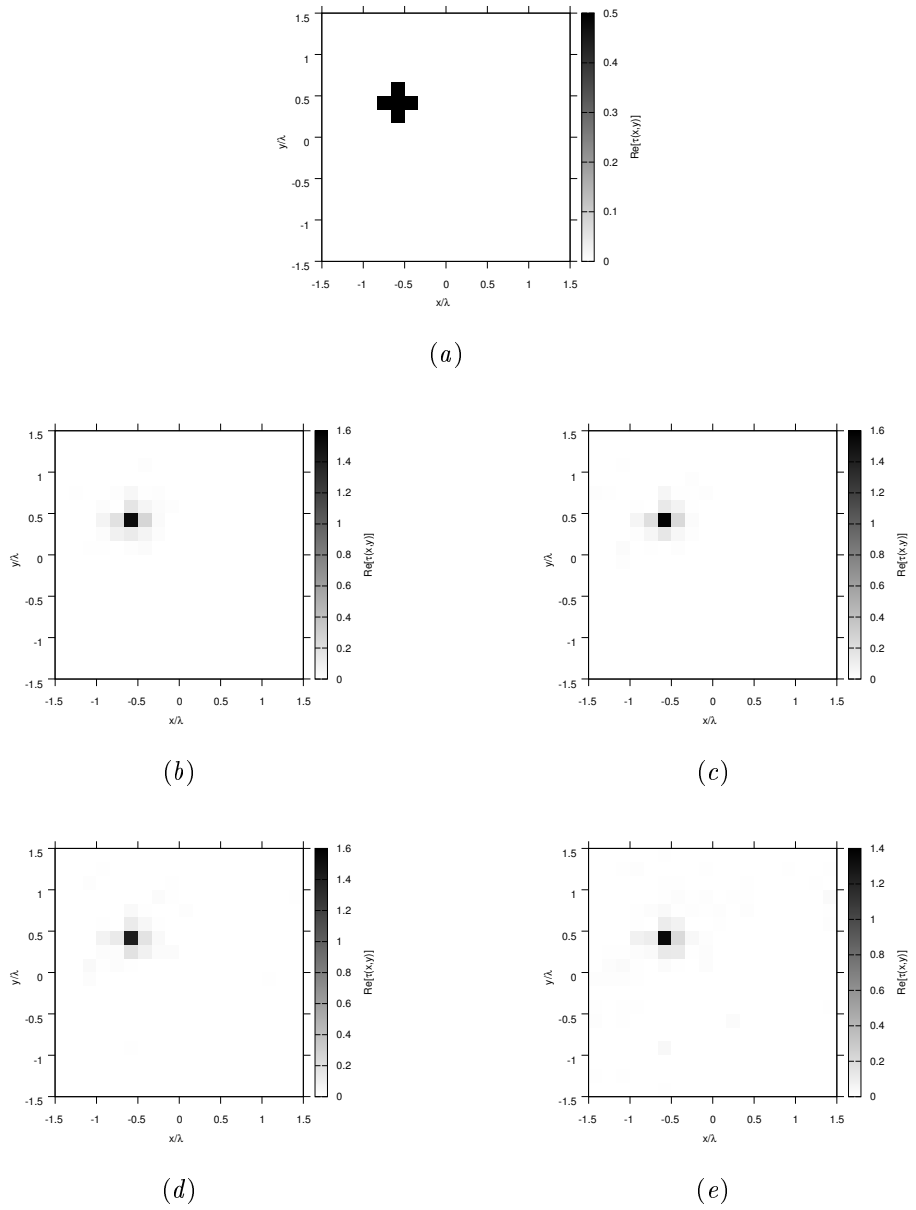

(a) (b) (c) (d) (e)

Figure 14. Actual object (a) and BCS reconstructed object for (b) Noiseless case, (c) $SNR = 20$ [dB] , (d) $SNR = 10$ [dB] , (e) $SNR = 5$ [dB].

RESULTS: $\varepsilon_r = 2.0$

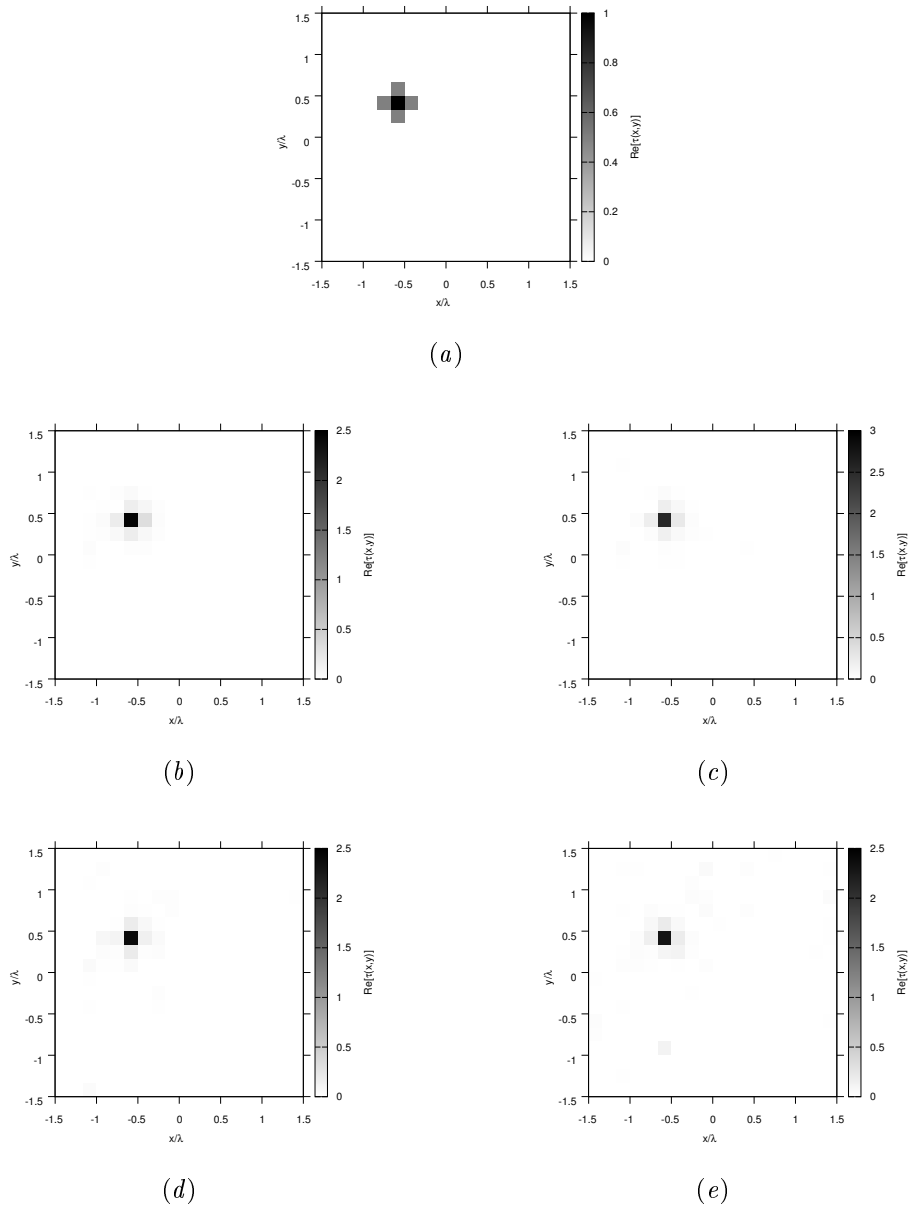

(a)

(b)

(c)

(d)

(e)

Figure 15. Actual object (a) and BCS reconstructed object for (b) Noiseless case, (c) $SNR = 20$ [dB] , (d) $SNR = 10$ [dB] , (e) $SNR = 5$ [dB].

RESULTS: $\varepsilon_r = 3.0$

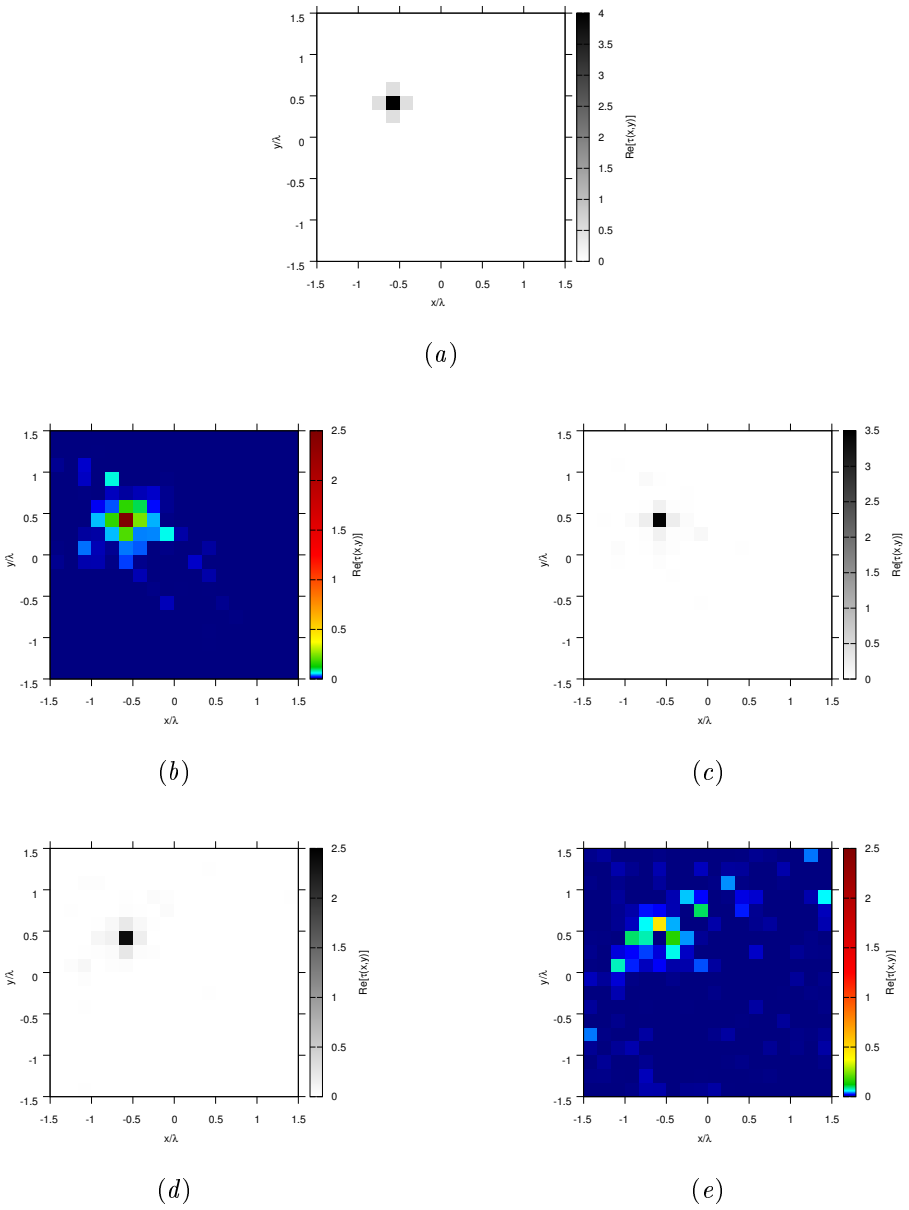

(a)

(b)

(c)

(d)

(e)

Figure 16. Actual object (a) and BCS reconstructed object for (b) Noiseless case, (c) $SNR = 20$ [dB] , (d) $SNR = 10$ [dB] , (e) $SNR = 5$ [dB].

RESULTS: Error Figures

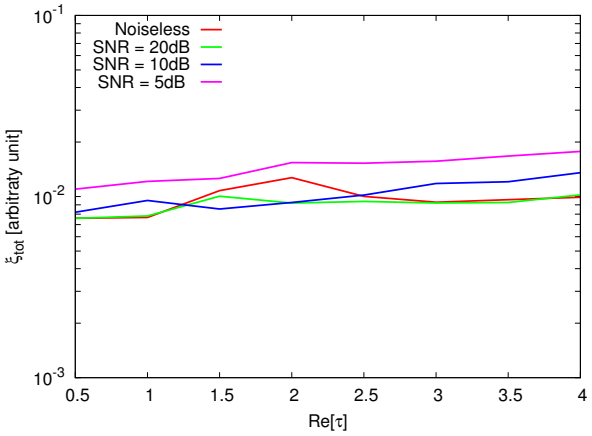

(a)

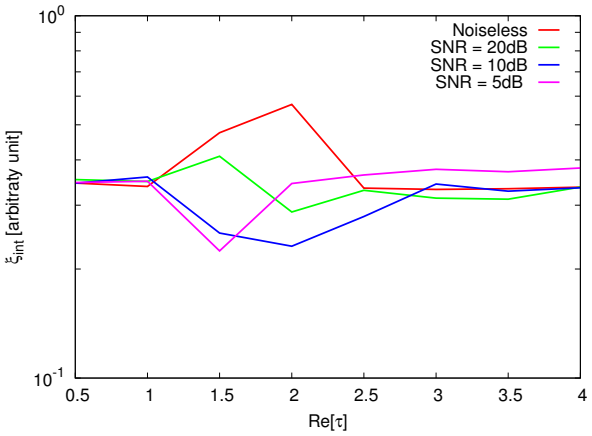

(b)

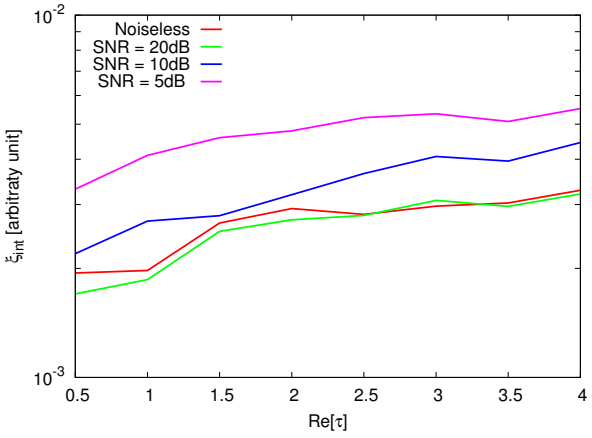

(c)

Figure 17. Behaviour of error figures as a function of ε_r, for different SNR values: (a) total error ξ_{tot}, (b) internal error ξ_{int}, (c) external error ξ_{ext}.

TEST CASE: L-Shaped Cylinder

Goal: show the performances of BCS when dealing with a sparse scatterer

- Number of Views: V
- Number of Measurements: M
- Number of Cells for the Inversion: N
- Number of Cells for the Direct solver: D
- Side of the investigation domain: L

Test Case Description

Direct solver:

- Square domain divided in $\sqrt{D} \times \sqrt{D}$ cells
- Domain side: $L = 3\lambda$
- $D = 1296$ (discretization for the direct solver: $< \lambda/10$)

Investigation domain:

- Square domain divided in $\sqrt{N} \times \sqrt{N}$ cells
- $L = 3\lambda$
- $2ka = 2 \times \frac{2\pi}{\lambda} \times \frac{L\sqrt{2}}{2} = 6\pi\sqrt{2} = 26.65$
- $\#DOF = \frac{(2ka)^2}{2} = \frac{(2 \times \frac{2\pi}{\lambda} \times \frac{L\sqrt{2}}{2})^2}{2} = 4\pi^2 \left(\frac{L}{\lambda}\right)^2 = 4\pi^2 \times 9 \approx 355.3$
- N scelto in modo da essere vicino a $\#DOF$: $N = 324$ (18×18)

Measurement domain:

- Measurement points taken on a circle of radius $\rho = 3\lambda$
- Full-aspect measurements
- $M \approx 2ka \rightarrow M = 27$

Sources:

- Plane waves
- $V \approx 2ka \rightarrow V = 27$
- Amplitude $A = 1$
- Frequency: 300 MHz $(\lambda = 1)$

Object:

- L-shaped cylinder
- $\varepsilon_r \in \{1.5, 2.0, 2.5, 3.0, 3.5, 4.0, 4.5, 5.0\}$
- $\sigma = 0$ [S/m]

BCS parameters:

- Initial estimate of the noise: $n_0 = 5.0 \times 10^{-4}$
- Convergenze parameter: $\tau = 1.0 \times 10^{-8}$

RESULTS: $\varepsilon_r = 1.5$

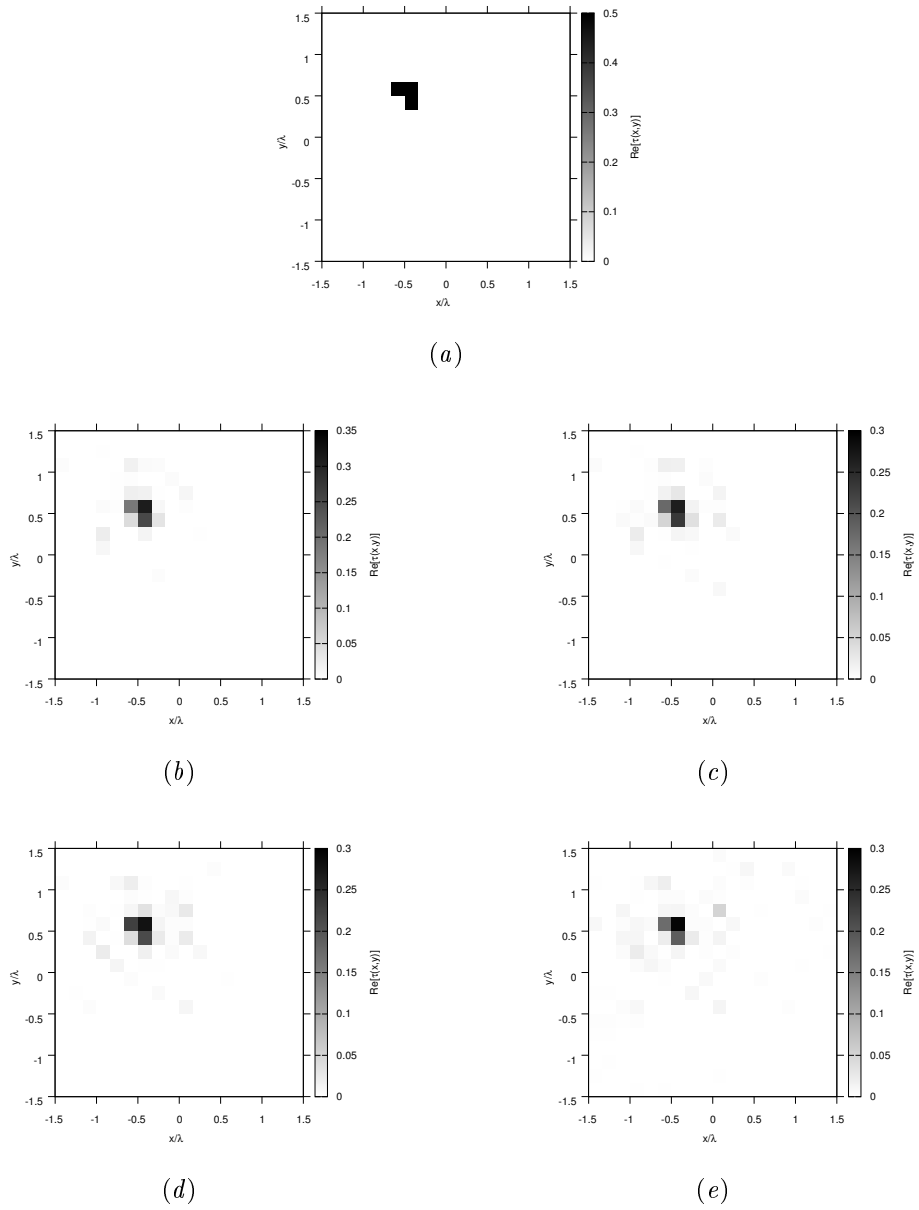

(a)

(b) (c)

(d) (e)

Figure 18. Actual object (a) and BCS reconstructed object for (b) Noiseless case, (c) $SNR = 20$ [dB] , (d) $SNR = 10$ [dB] , (e) $SNR = 5$ [dB].

RESULTS: $\varepsilon_r = 2.0$

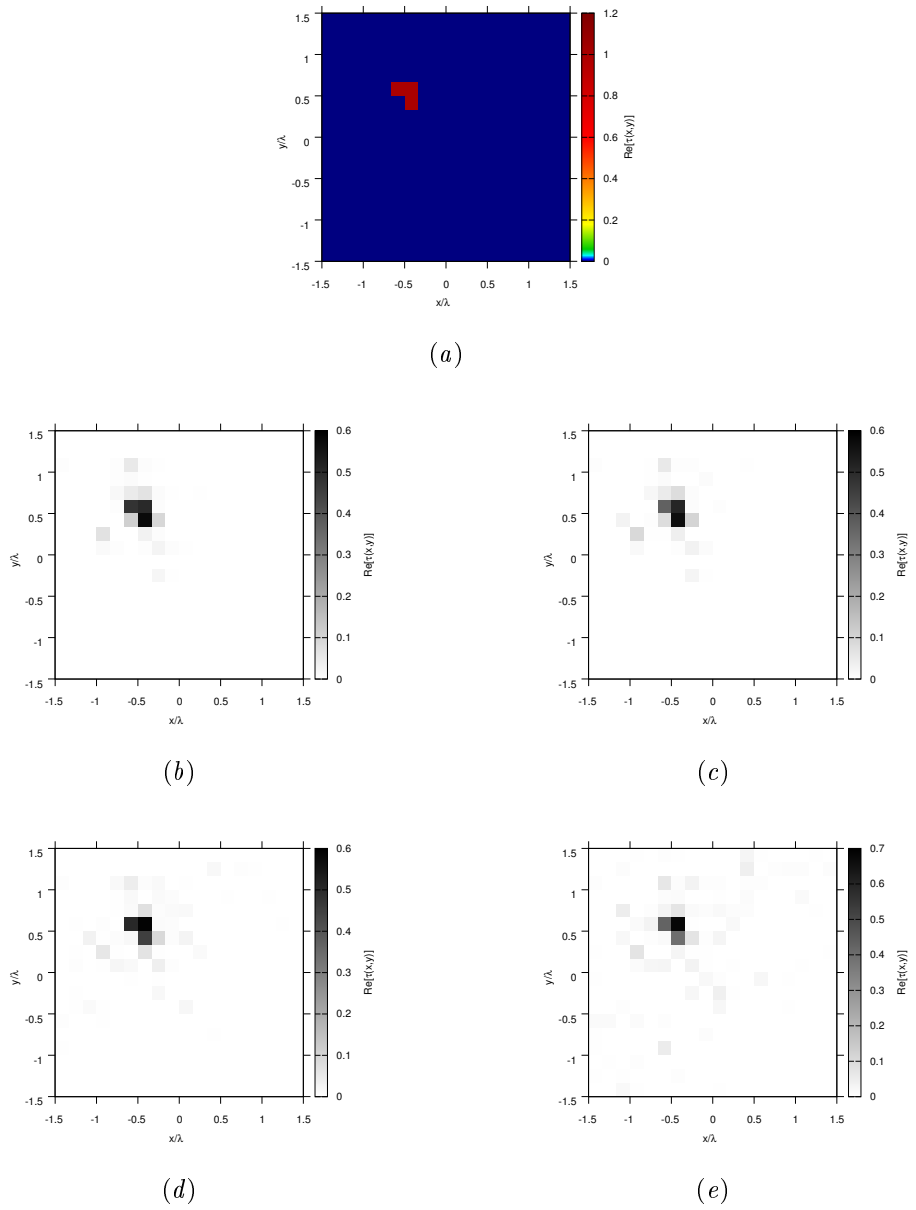

Figure 19. Actual object (a) and BCS reconstructed object for (b) Noiseless case, (c) $SNR = 20$ [dB] , (d) $SNR = 10$ [dB] , (e) $SNR = 5$ [dB].

RESULTS: $\varepsilon_r = 3.0$

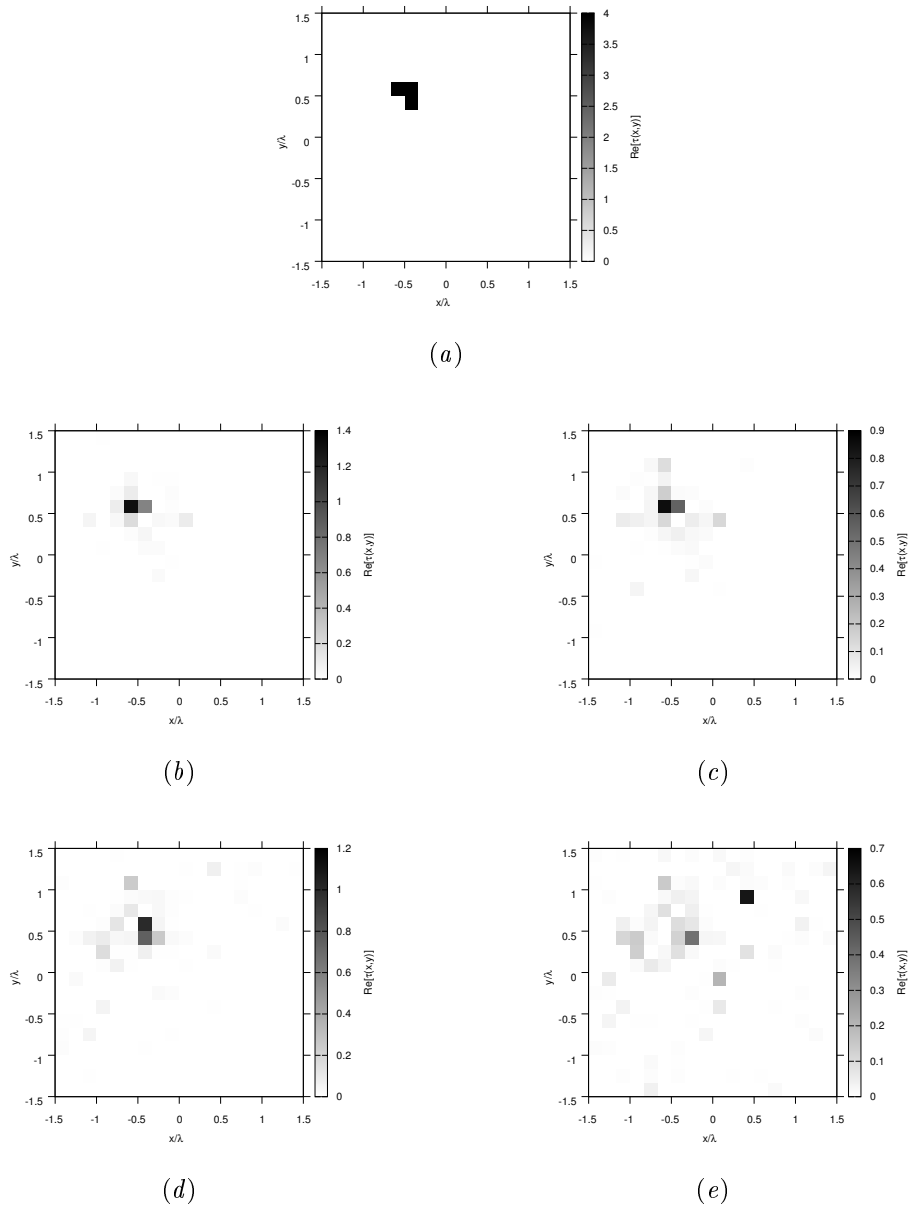

(a) (b) (c) (d) (e)

Figure 20. Actual object (a) and BCS reconstructed object for (b) Noiseless case, (c) $SNR = 20$ [dB] , (d) $SNR = 10$ [dB] , (e) $SNR = 5$ [dB].

RESULTS: Error Figures

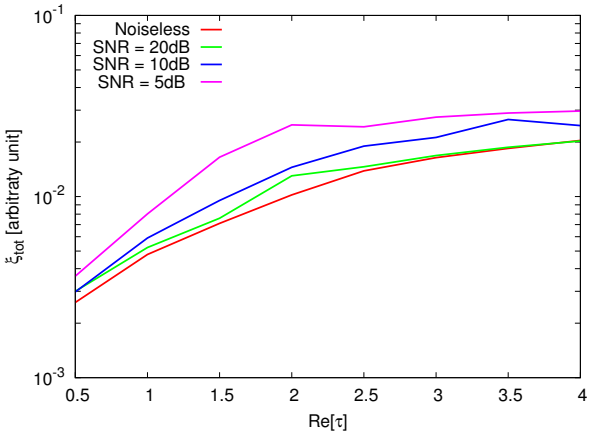

(a)

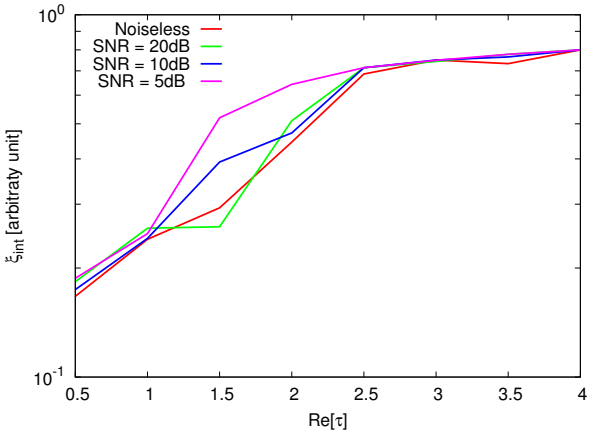

(b)

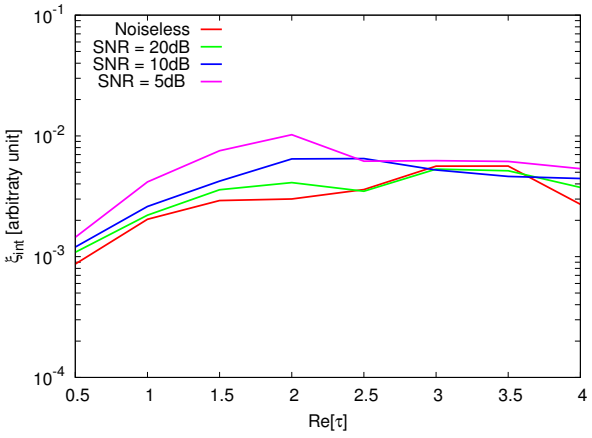

(c)

Figure 21. Behaviour of error figures as a function of ε_r, for different SNR values: (a) total error ξ_{tot}, (b) internal error ξ_{int}, (c) external error ξ_{ext}.

TEST CASE: Inhomogeneous L-Shaped Cylinder

Goal: show the performances of BCS when dealing with a sparse scatterer

- Number of Views: V
- Number of Measurements: M
- Number of Cells for the Inversion: N
- Number of Cells for the Direct solver: D
- Side of the investigation domain: L

Test Case Description

Direct solver:

- Square domain divided in $\sqrt{D} \times \sqrt{D}$ cells
- Domain side: $L = 3\lambda$
- $D = 1296$ (discretization for the direct solver: $< \lambda/10$)

Investigation domain:

- Square domain divided in $\sqrt{N} \times \sqrt{N}$ cells
- $L = 3\lambda$
- $2ka = 2 \times \frac{2\pi}{\lambda} \times \frac{L\sqrt{2}}{2} = 6\pi\sqrt{2} = 26.65$
- $\#DOF = \frac{(2ka)^2}{2} = \frac{(2 \times \frac{2\pi}{\lambda} \times \frac{L\sqrt{2}}{2})^2}{2} = 4\pi^2 \left(\frac{L}{\lambda}\right)^2 = 4\pi^2 \times 9 \approx 355.3$
- N scelto in modo da essere vicino a $\#DOF$: $N = 324$ (18×18)

Measurement domain:

- Measurement points taken on a circle of radius $\rho = 3\lambda$
- Full-aspect measurements
- $M \approx 2ka \rightarrow M = 27$

Sources:

- Plane waves
- $V \approx 2ka \rightarrow V = 27$
- Amplitude $A = 1$
- Frequency: 300 MHz $(\lambda = 1)$

Object:

- Inhomogeneous L-shaped cylinder
- $\varepsilon_r \in \{1.5, 2.0, 2.5, 3.0, 3.5, 4.0, 4.5, 5.0\}$
- $\sigma = 0$ [S/m]

BCS parameters:

- Initial estimate of the noise: $n_0 = 5.0 \times 10^{-4}$
- Convergenze parameter: $\tau = 1.0 \times 10^{-8}$

RESULTS: $\varepsilon_r = 1.5$

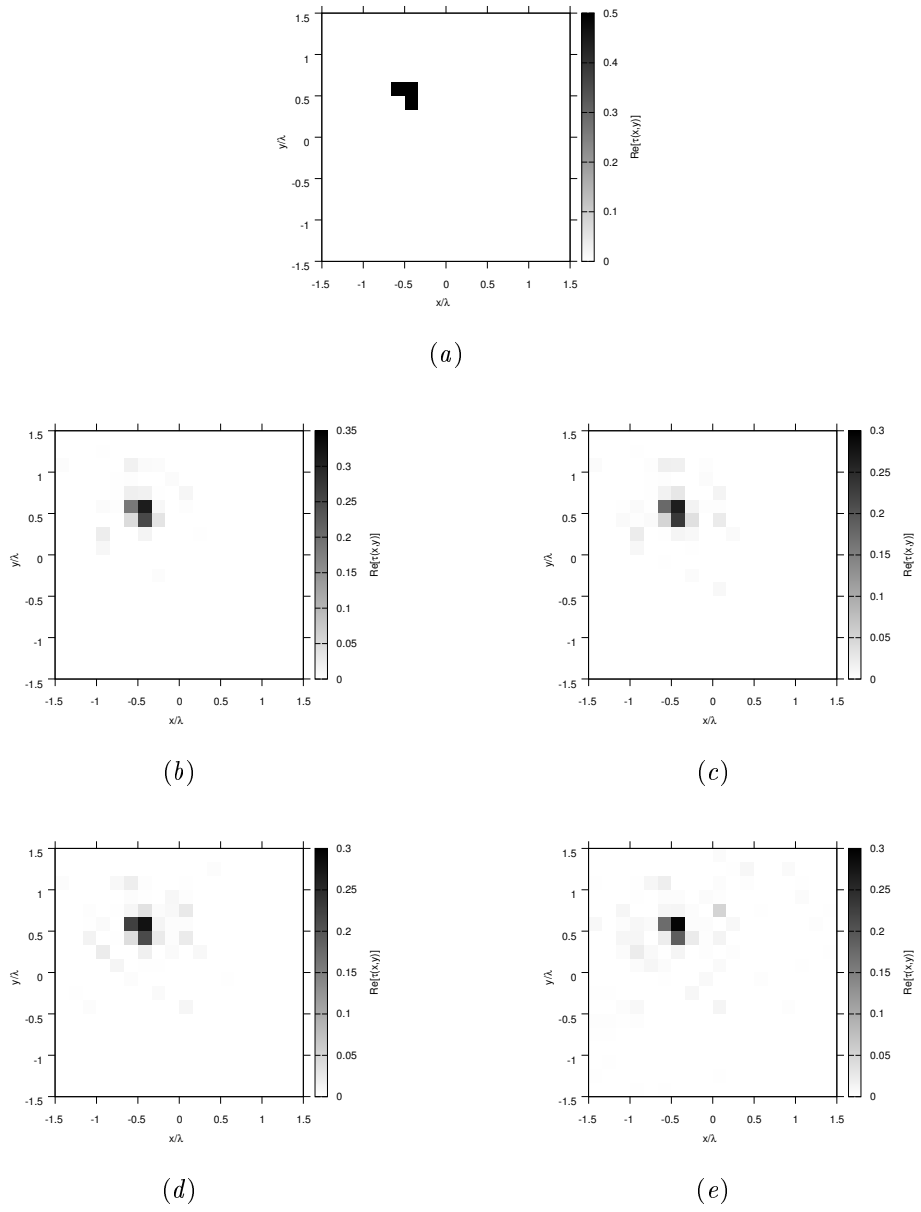

(a)

(b)

(c)

(d)

(e)

Figure 22. Actual object (a) and BCS reconstructed object for (b) Noiseless case, (c) $SNR = 20$ [dB] , (d) $SNR = 10$ [dB] , (e) $SNR = 5$ [dB].

RESULTS: $\varepsilon_r = 2.0$

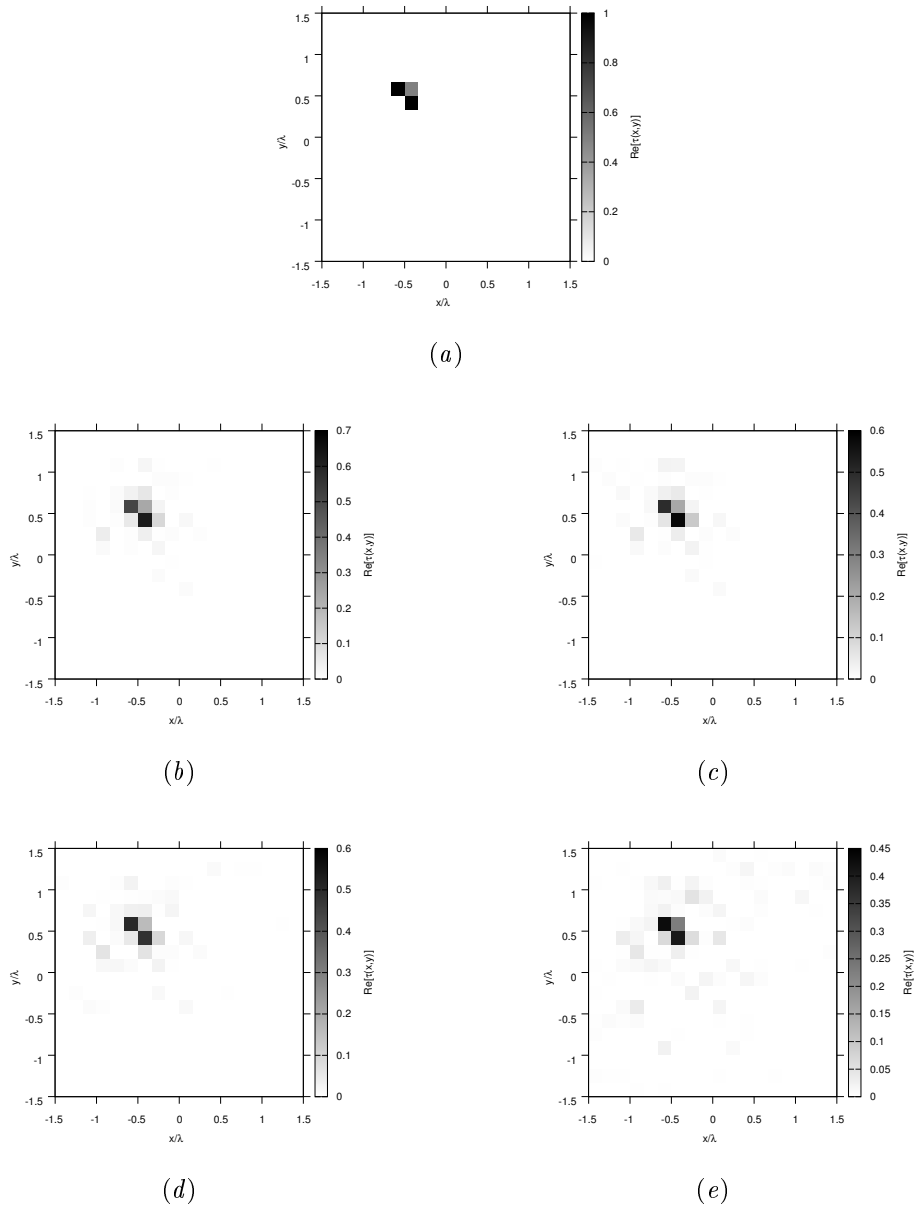

(a)

(b)

(c)

(d)

(e)

Figure 23. Actual object (a) and BCS reconstructed object for (b) Noiseless case, (c) $SNR = 20$ [dB] , (d) $SNR = 10$ [dB] , (e) $SNR = 5$ [dB].

RESULTS: $\varepsilon_r = 3.0$

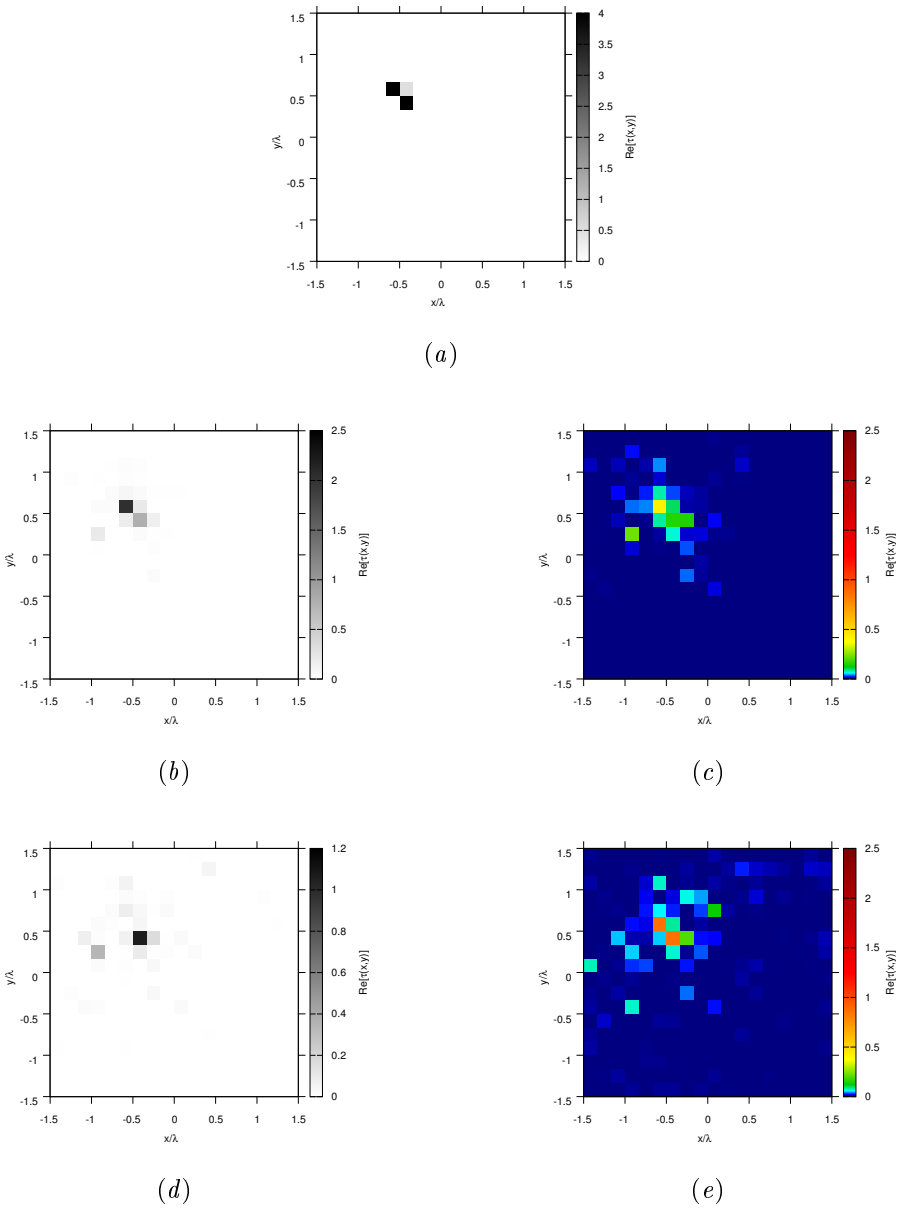

(a)

(b)

(c)

(d)

(e)

Figure 24. Actual object (a) and BCS reconstructed object for (b) Noiseless case, (c) $SNR = 20$ [dB] , (d) $SNR = 10$ [dB] , (e) $SNR = 5$ [dB].

RESULTS: Error Figures

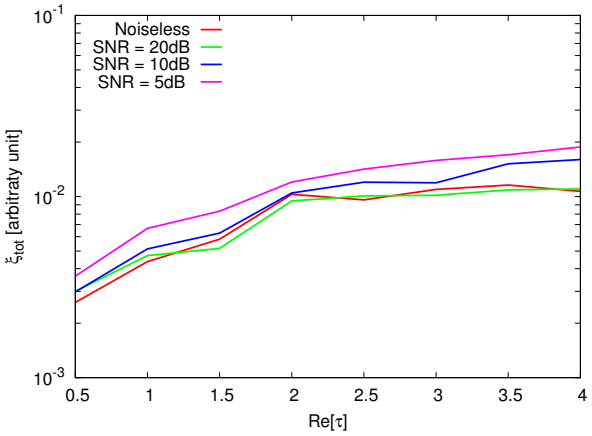

(a)

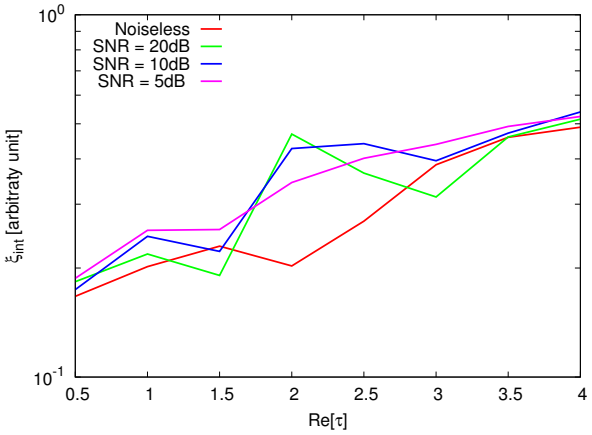

(b)

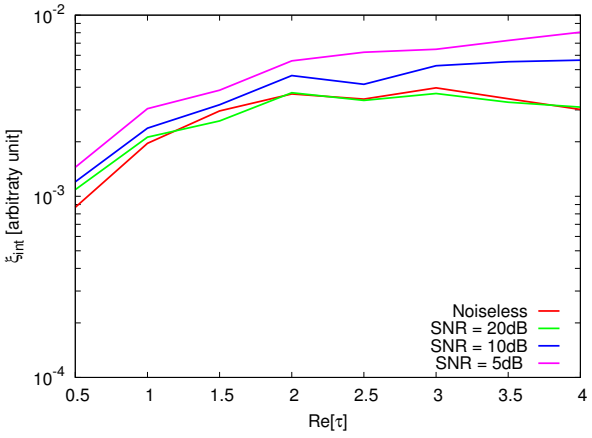

(c)

Figure 25. Behaviour of error figures as a function of ε_r, for different SNR values: (a) total error ξ_{tot}, (b) internal error ξ_{int}, (c) external error ξ_{ext}.

TEST CASE: Line-Shaped Cylinder $L = 0.5\lambda$

Goal: show the performances of BCS when dealing with a sparse scatterer

- Number of Views: V
- Number of Measurements: M
- Number of Cells for the Inversion: N
- Number of Cells for the Direct solver: D
- Side of the investigation domain: L

Test Case Description

Direct solver:

- Square domain divided in $\sqrt{D} \times \sqrt{D}$ cells
- Domain side: $L = 3\lambda$
- $D = 1296$ (discretization for the direct solver: $< \lambda/10$)

Investigation domain:

- Square domain divided in $\sqrt{N} \times \sqrt{N}$ cells
- $L = 3\lambda$
- $2ka = 2 \times \frac{2\pi}{\lambda} \times \frac{L\sqrt{2}}{2} = 6\pi\sqrt{2} = 26.65$
- $\#DOF = \frac{(2ka)^2}{2} = \frac{(2 \times \frac{2\pi}{\lambda} \times \frac{L\sqrt{2}}{2})^2}{2} = 4\pi^2 \left(\frac{L}{\lambda}\right)^2 = 4\pi^2 \times 9 \approx 355.3$
- N scelto in modo da essere vicino a $\#DOF$: $N = 324$ (18×18)

Measurement domain:

- Measurement points taken on a circle of radius $\rho = 3\lambda$
- Full-aspect measurements
- $M \approx 2ka \rightarrow M = 27$

Sources:

- Plane waves
- $V \approx 2ka \rightarrow V = 27$
- Amplitude $A = 1$
- Frequency: 300 MHz $(\lambda = 1)$

Object:

- Inhomogeneous L-shaped cylinder
- $\varepsilon_r \in \{1.5, 2.0, 2.5, 3.0, 3.5, 4.0, 4.5, 5.0\}$
- $\sigma = 0$ [S/m]

BCS parameters:

- Initial estimate of the noise: $n_0 = 5.0 \times 10^{-4}$
- Convergenze parameter: $\tau = 1.0 \times 10^{-8}$

RESULTS: $\varepsilon_r = 1.5$

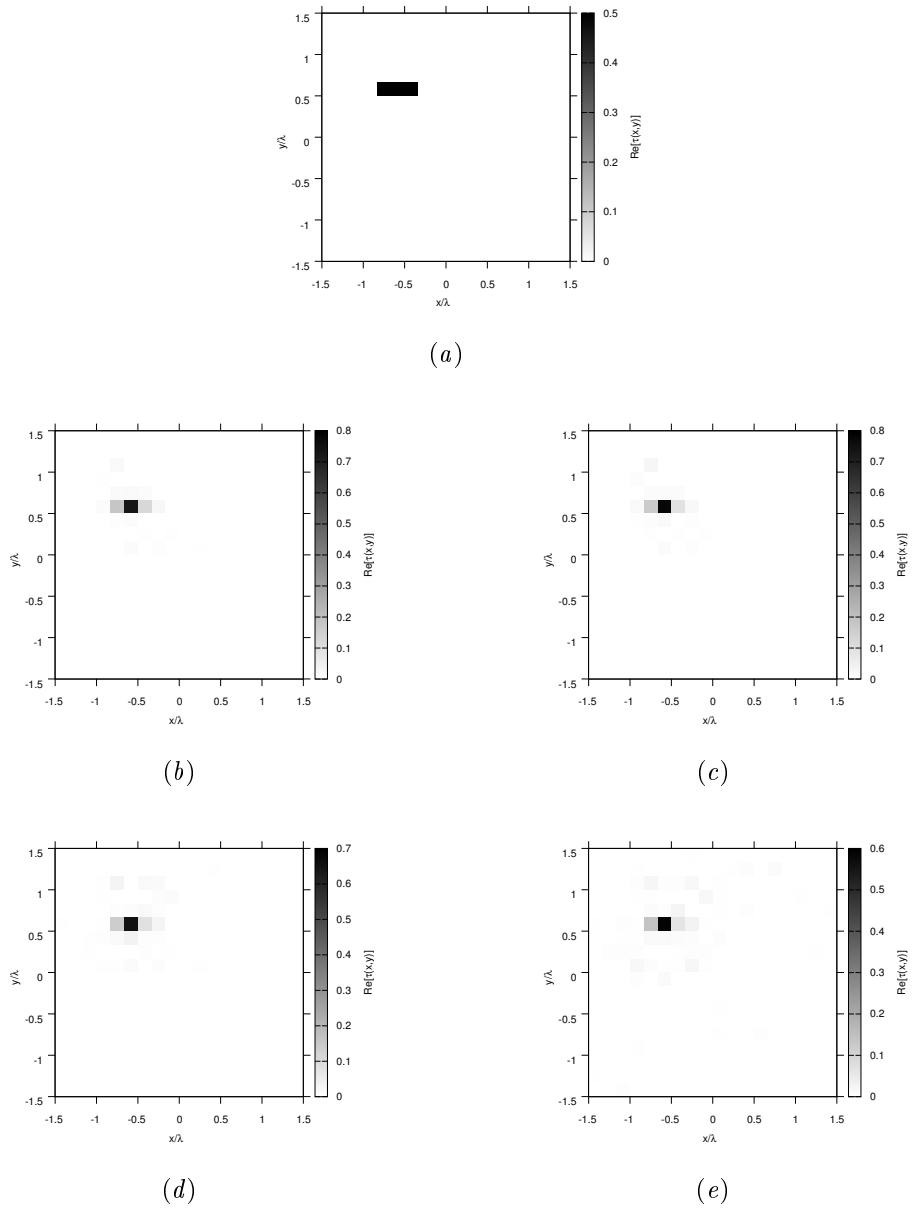

Figure 26. Actual object (a) and BCS reconstructed object for (b) Noiseless case, (c) $SNR = 20$ [dB] , (d) $SNR = 10$ [dB] , (e) $SNR = 5$ [dB].

RESULTS: $\varepsilon_r = 2.0$

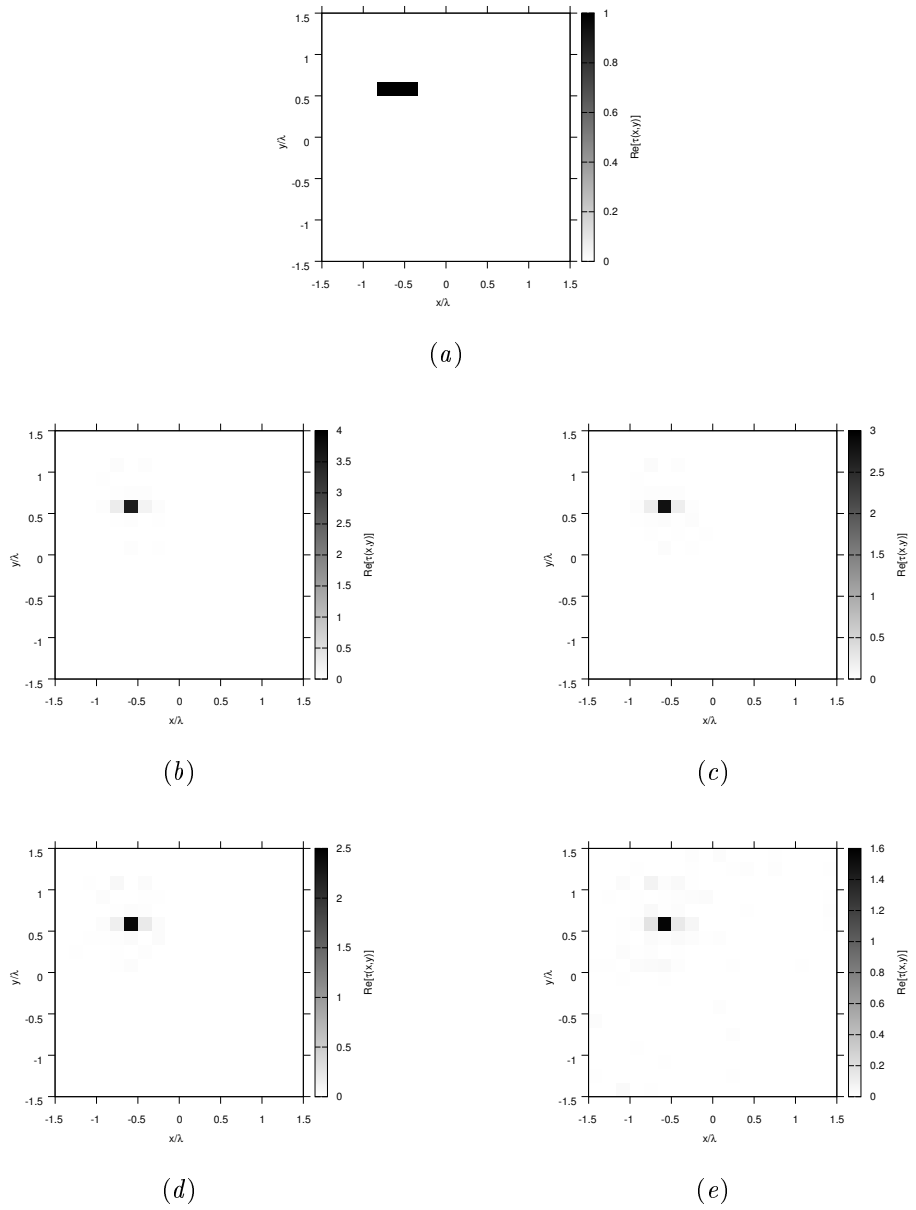

(a) (b) (c) (d) (e)

Figure 27. Actual object (a) and BCS reconstructed object for (b) Noiseless case, (c) $SNR = 20$ [dB] , (d) $SNR = 10$ [dB] , (e) $SNR = 5$ [dB].

RESULTS: $\varepsilon_r = 3.0$

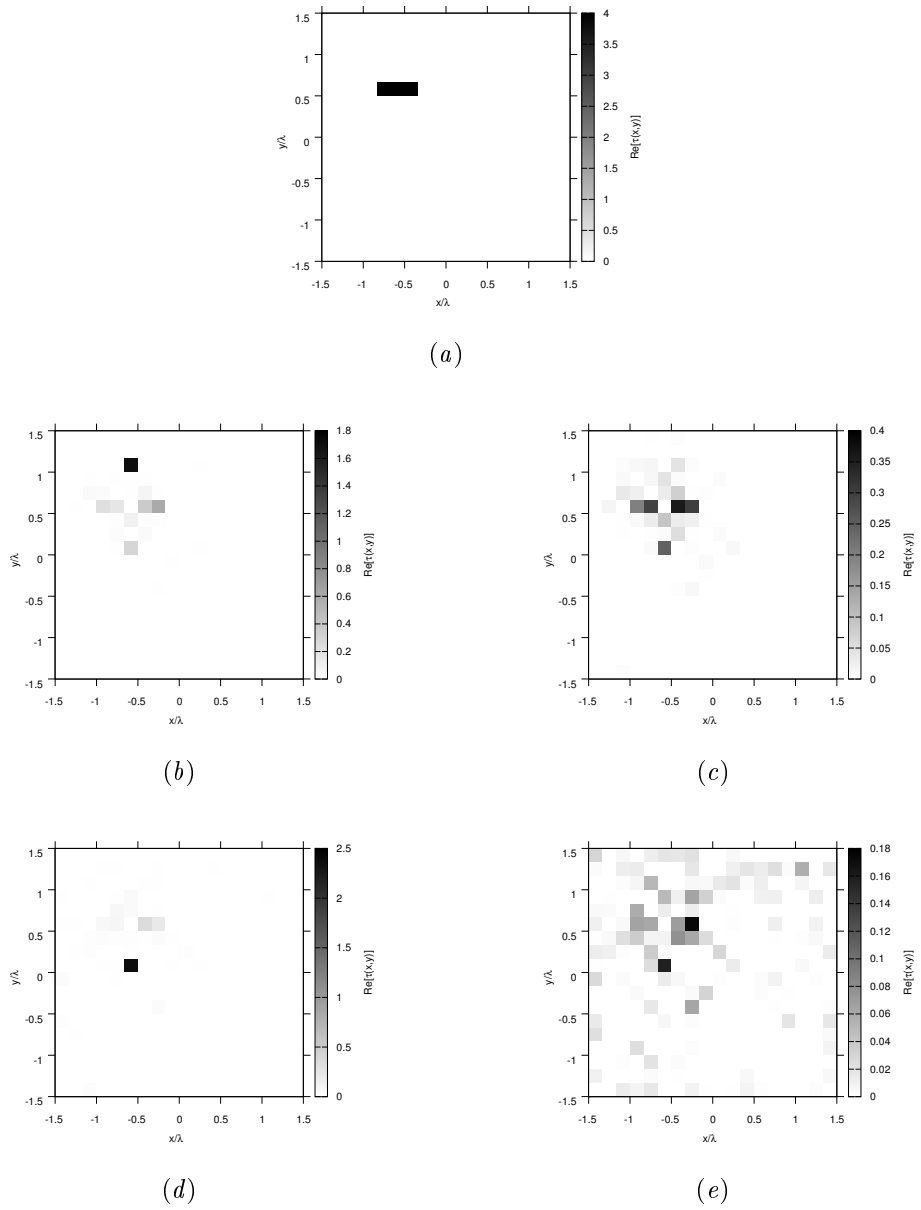

(a)

(b)

(c)

(d)

(e)

Figure 28. Actual object (a) and BCS reconstructed object for (b) Noiseless case, (c) $SNR = 20$ [dB] , (d) $SNR = 10$ [dB] , (e) $SNR = 5$ [dB].

RESULTS: Error Figures

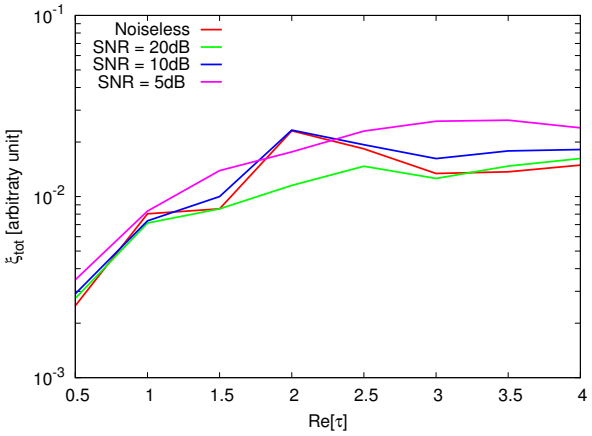

(a)

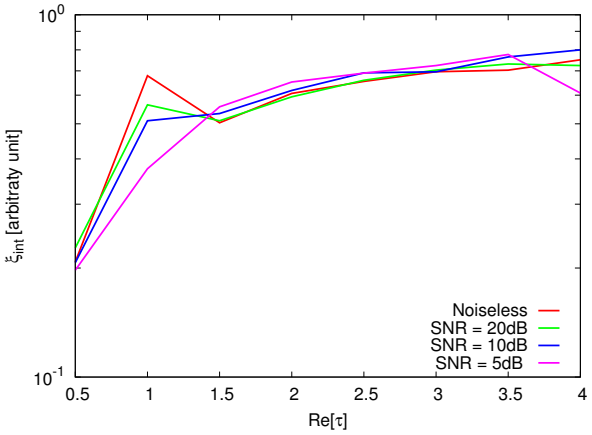

(b)

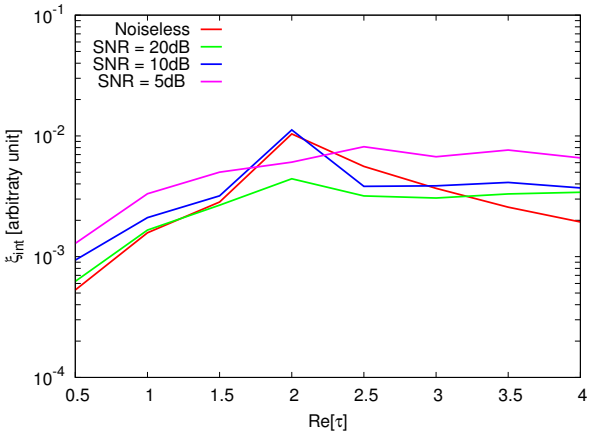

(c)

Figure 29. Behaviour of error figures as a function of ε_r, for different SNR values: (a) total error ξ_{tot}, (b) internal error ξ_{int}, (c) external error ξ_{ext}.

3 XY-MT-BCS (Exploiting Correlation between x-y Field Components)

3.1 XY-MT-BCS - Calibration

TEST CASE: Square Cylinder

Goal: show the performances of BCS when dealing with a sparse scatterer

- Number of Views: V
- Number of Measurements: M
- Number of Cells for the Inversion: N
- Number of Cells for the Direct solver: D
- Side of the investigation domain: L

Test Case Description

Direct solver:

- Square domain divided in $\sqrt{D} \times \sqrt{D}$ cells
- Domain side: $L = 3\lambda$
- $D = 1296$ (discretization for the direct solver: $< \lambda/10$)

Investigation domain:

- Square domain divided in $\sqrt{N} \times \sqrt{N}$ cells
- $L = 3\lambda$
- $2ka = 2 \times \frac{2\pi}{\lambda} \times \frac{L\sqrt{2}}{2} = 6\pi\sqrt{2} = 26.65$
- $\#DOF = \frac{(2ka)^2}{2} = \frac{(2 \times \frac{2\pi}{\lambda} \times \frac{L\sqrt{2}}{2})^2}{2} = 4\pi^2 \left(\frac{L}{\lambda}\right)^2 = 4\pi^2 \times 9 \approx 355.3$
- N scelto in modo da essere vicino a $\#DOF$: $N = 324$ (18×18)

Measurement domain:

- Measurement points taken on a circle of radius $\rho = 3\lambda$
- Full-aspect measurements
- $M \approx 2ka \rightarrow M = 27$

Sources:

- Plane waves
- $V \approx 2ka \rightarrow V = 27$
- Amplitude: $A = 1$
- Frequency: 300 MHz ($\lambda = 1$)

Object:

- Square cylinder of side $\frac{\lambda}{6} = 0.1667$
- $\varepsilon_r = 2.0$

- $\sigma = 0$ [S/m]

BCS parameters:

- Gamma prior on noise variance parameter: $a \in \{1 \times 10^{-1}, 2 \times 10^{-1}, 5 \times 10^{-1}\ 1 \times 10^{0}, 2 \times 10^{0}, 5 \times 10^{0}, 1 \times 10^{+1}, 2 \times 10^{+1}, 5 \times 10^{+1}, 1 \times 10^{+2}, 2 \times 10^{+2}, 5 \times 10^{+2}, 1 \times 10^{+3}, 2 \times 10^{+3}, 5 \times 10^{+3}, 1 \times 10^{+4}\}$
- Gamma prior on noise variance parameter: $b \in \{1 \times 10^{+0}, 5 \times 10^{-1}, 2 \times 10^{-1}, 1 \times 10^{-1}, 5 \times 10^{-2}, 2 \times 10^{-2}\ 1 \times 10^{-2}, 5 \times 10^{-3}, 2 \times 10^{-3}, 1 \times 10^{-3}, 5 \times 10^{-4}, 2 \times 10^{-4}, 1 \times 10^{-4}\}$
- Convergenze parameter: $\tau = 1.0 \times 10^{-8}$

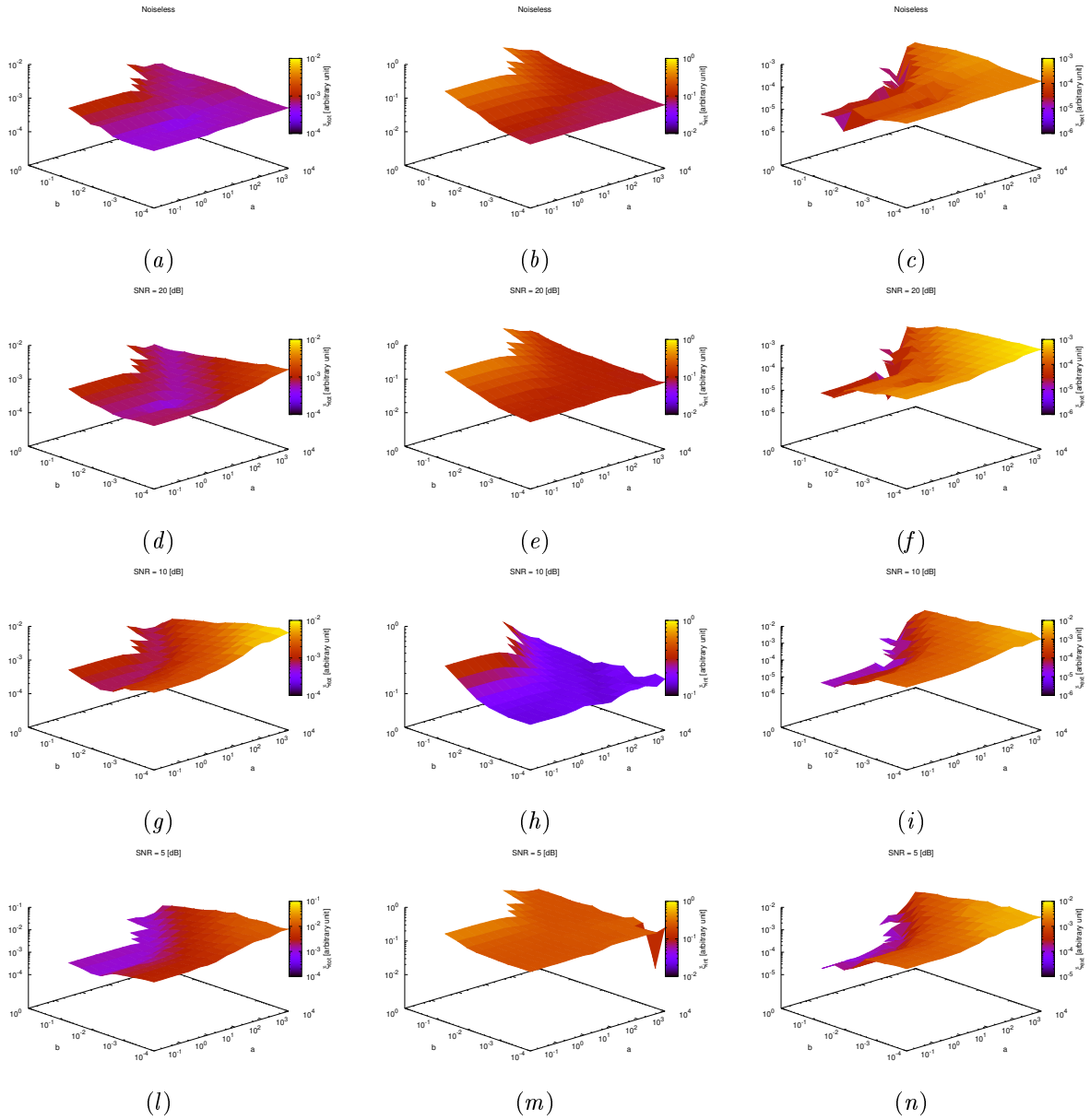

Figure 30. Behaviour of error figures as a function of the initial estimate of the Gamma prior on the noise variance parameters a and b, for different SNR values: (a), (d), (g) and (l) total error ξ_{tot}, (b), (e), (h) and (m) internal error ξ_{int}, (c), (f), (i) and (n) external error ξ_{ext}, for (a), (b) and (c) Noiseless case, (d), (e) and (f) $SNR = 20dB$, (g), (h) and (i) $SNR = 10dB$ and (l), (m) and (n) $SNR = 5dB$.

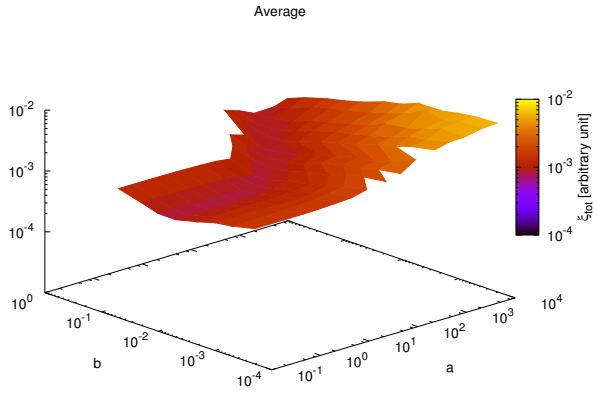

(a)

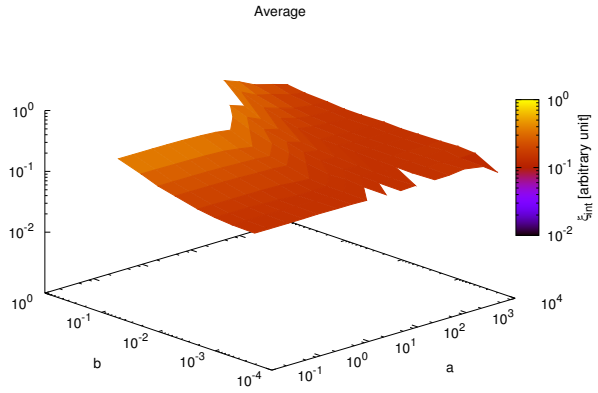

(b)

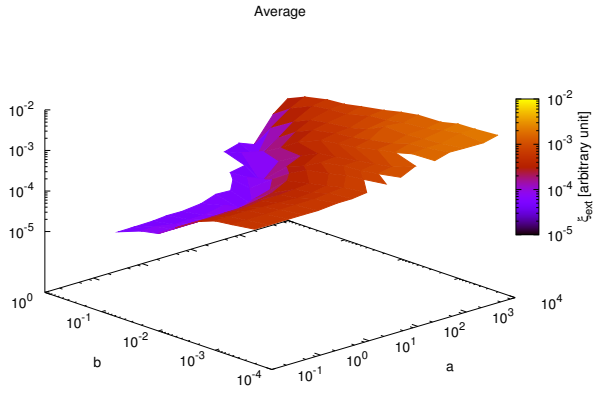

(c)

Figure 31. Averaged behaviour of error figures as a function of the initial estimate of the Gamma prior on the noise variance parameters a and b: (a) total error ξ_{tot}, (b) internal error ξ_{int}, (c) external error ξ_{ext}.

3.2 XY-MT-BCS - Basic Tests

TEST CASE: Square Cylinder $L = 0.16\lambda$

Goal: show the performances of BCS when dealing with a sparse scatterer

- Number of Views: V
- Number of Measurements: M
- Number of Cells for the Inversion: N
- Number of Cells for the Direct solver: D
- Side of the investigation domain: L

Test Case Description

Direct solver:

- Square domain divided in $\sqrt{D} \times \sqrt{D}$ cells
- Domain side: $L = 3\lambda$
- $D = 1296$ (discretization for the direct solver: $< \lambda/10$)

Investigation domain:

- Square domain divided in $\sqrt{N} \times \sqrt{N}$ cells
- $L = 3\lambda$
- $2ka = 2 \times \frac{2\pi}{\lambda} \times \frac{L\sqrt{2}}{2} = 6\pi\sqrt{2} = 26.65$
- $\#DOF = \frac{(2ka)^2}{2} = \frac{(2 \times \frac{2\pi}{\lambda} \times \frac{L\sqrt{2}}{2})^2}{2} = 4\pi^2 \left(\frac{L}{\lambda}\right)^2 = 4\pi^2 \times 9 \approx 355.3$
- N scelto in modo da essere vicino a $\#DOF$: $N = 324$ (18×18)

Measurement domain:

- Measurement points taken on a circle of radius $\rho = 3\lambda$
- Full-aspect measurements
- $M \approx 2ka \rightarrow M = 27$

Sources:

- Plane waves
- $V \approx 2ka \rightarrow V = 27$
- Amplitude: $A = 1$
- Frequency: 300 MHz ($\lambda = 1$)

Object:

- Square cylinder of side $\frac{\lambda}{6} = 0.1667$
- $\varepsilon_r \in \{1.5, 2.0, 2.5, 3.0, 3.5, 4.0, 4.5, 5.0\}$

- $\sigma = 0$ [S/m]

BCS parameters:

- Gamma prior on noise variance parameters: $a = 2 \times 10^{+2}$, $b = 1 \times 10^{-1}$
- Convergenze parameter: $\tau = 1.0 \times 10^{-8}$

RESULTS: $\varepsilon_r = 1.5$

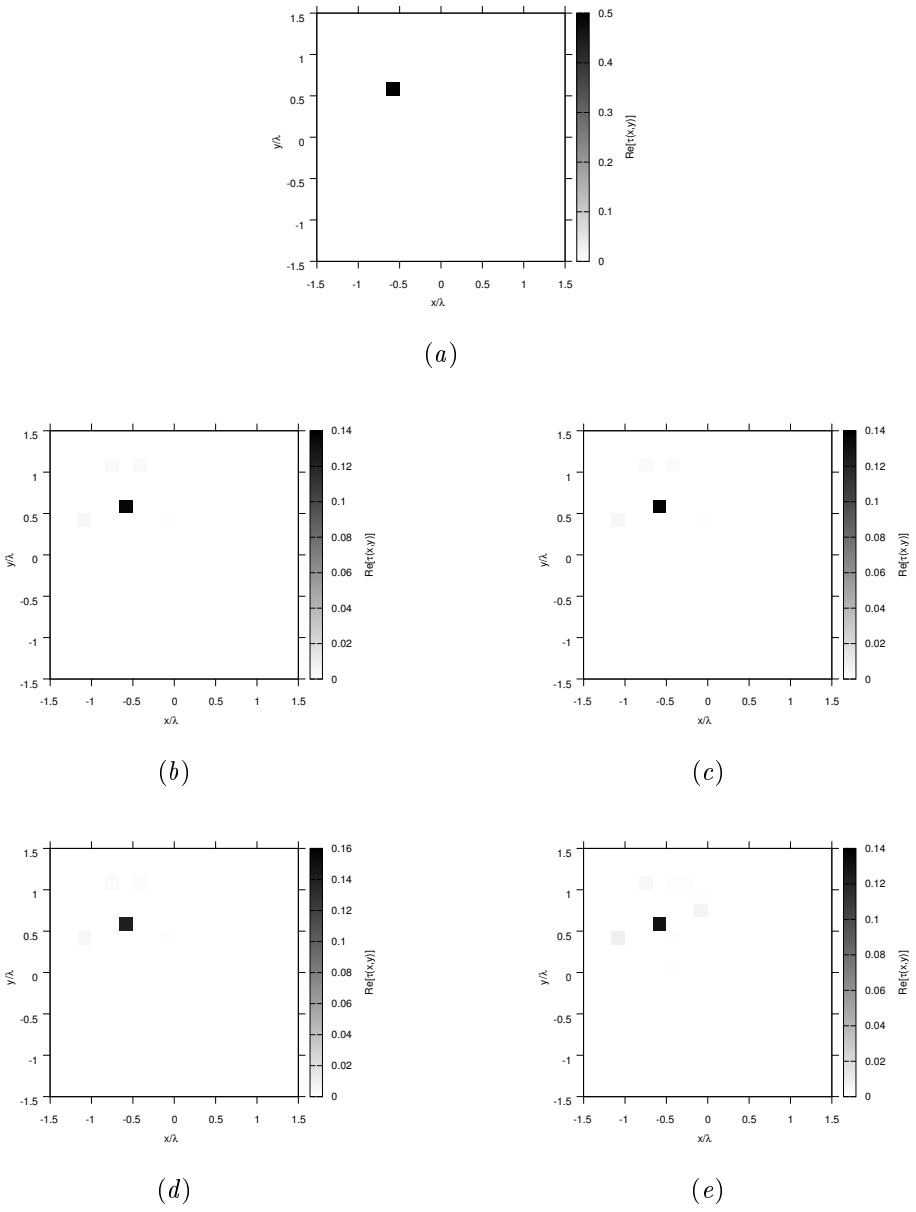

(a) (b) (c) (d) (e)

Figure 32. Actual object (a) and BCS reconstructed object for (b) Noiseless case, (c) $SNR = 20$ [dB] , (d) $SNR = 10$ [dB] , (e) $SNR = 5$ [dB].

RESULTS: $\varepsilon_r = 2.0$

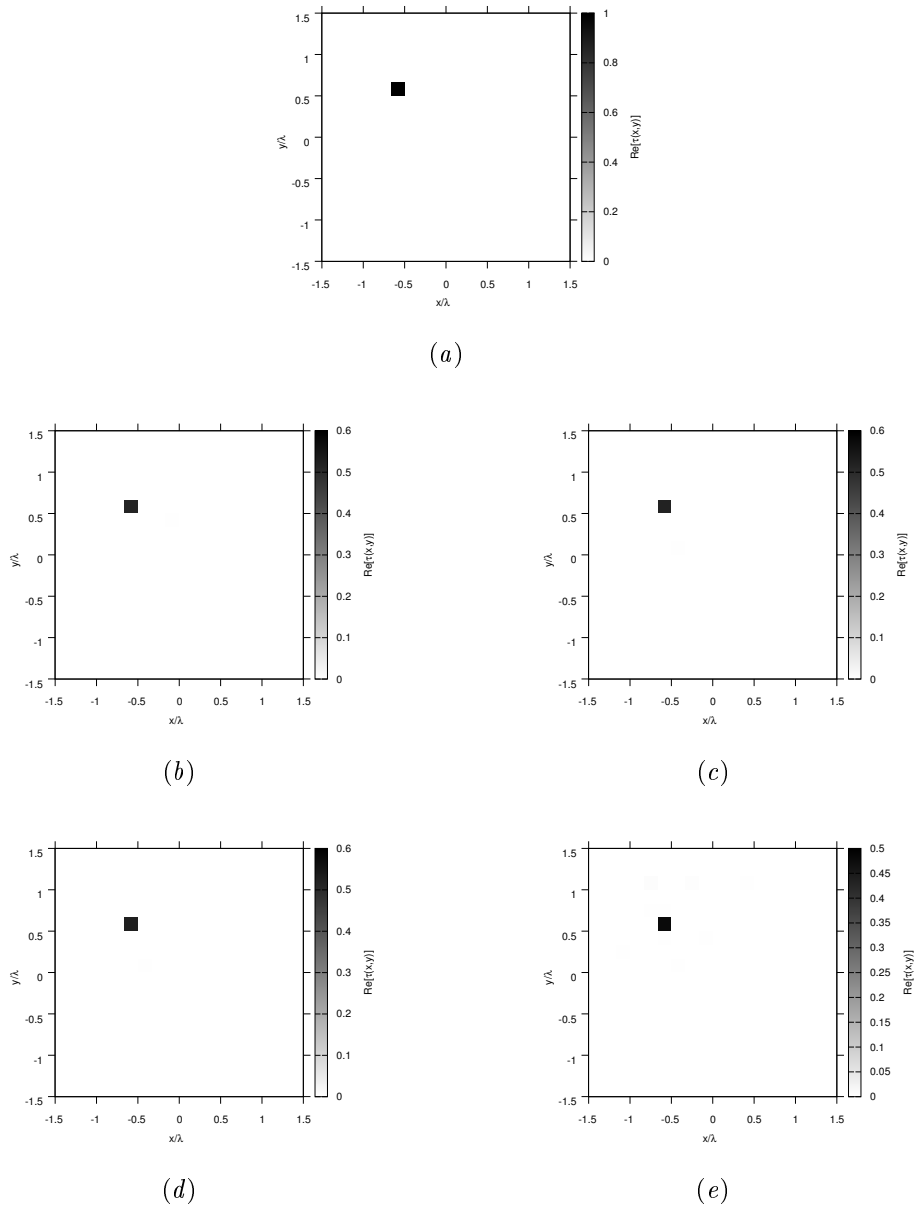

(a)

(b)

(c)

(d)

(e)

Figure 33. Actual object (a) and BCS reconstructed object for (b) Noiseless case, (c) $SNR = 20$ [dB] , (d) $SNR = 10$ [dB] , (e) $SNR = 5$ [dB].

RESULTS: $\varepsilon_r = 5.0$

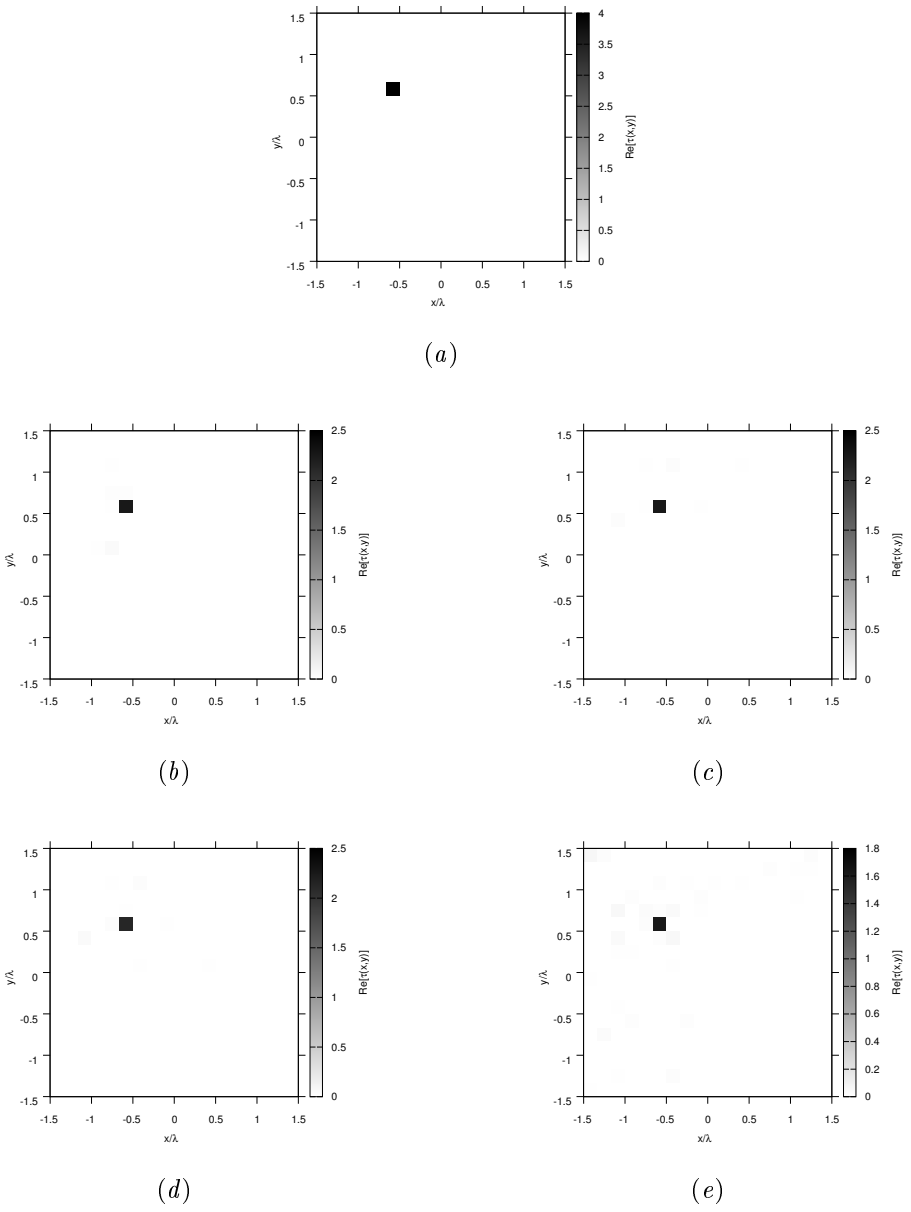

(a) (b) (c) (d) (e)

Figure 34. Actual object (a) and BCS reconstructed object for (b) Noiseless case, (c) $SNR = 20$ [dB] , (d) $SNR = 10$ [dB] , (e) $SNR = 5$ [dB].

RESULTS: Error Figures

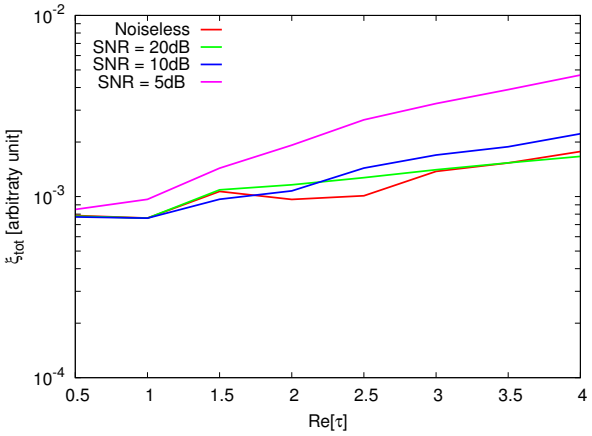

(a)

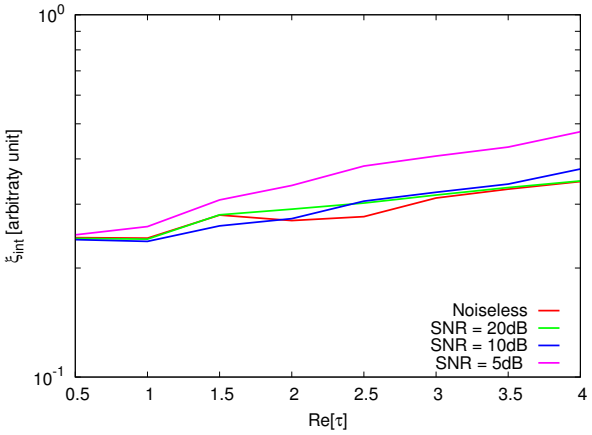

(b)

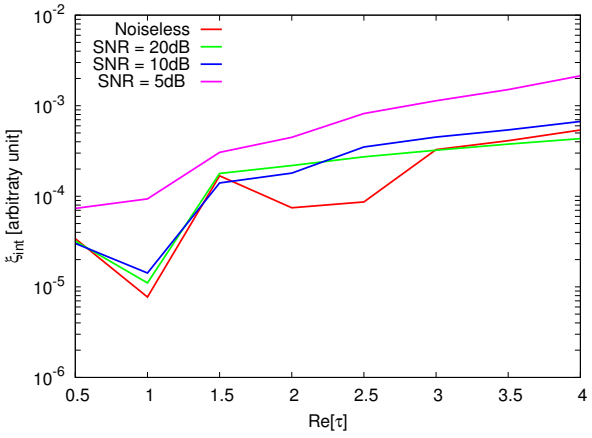

(c)

Figure 35. Behaviour of error figures as a function of ε_r, for different SNR values: (a) total error ξ_{tot}, (b) internal error ξ_{int}, (c) external error ξ_{ext}.

TEST CASE: Two Square Cylinders $L = 0.16\lambda$

Goal: show the performances of BCS when dealing with a sparse scatterer

- Number of Views: V
- Number of Measurements: M
- Number of Cells for the Inversion: N
- Number of Cells for the Direct solver: D
- Side of the investigation domain: L

Test Case Description

Direct solver:

- Square domain divided in $\sqrt{D} \times \sqrt{D}$ cells
- Domain side: $L = 3\lambda$
- $D = 1296$ (discretization for the direct solver: $< \lambda/10$)

Investigation domain:

- Square domain divided in $\sqrt{N} \times \sqrt{N}$ cells
- $L = 3\lambda$
- $2ka = 2 \times \frac{2\pi}{\lambda} \times \frac{L\sqrt{2}}{2} = 6\pi\sqrt{2} = 26.65$
- $\#DOF = \frac{(2ka)^2}{2} = \frac{(2 \times \frac{2\pi}{\lambda} \times \frac{L\sqrt{2}}{2})^2}{2} = 4\pi^2 \left(\frac{L}{\lambda}\right)^2 = 4\pi^2 \times 9 \approx 355.3$
- N scelto in modo da essere vicino a $\#DOF$: $N = 324$ (18×18)

Measurement domain:

- Measurement points taken on a circle of radius $\rho = 3\lambda$
- Full-aspect measurements
- $M \approx 2ka \rightarrow M = 27$

Sources:

- Plane waves
- $V \approx 2ka \rightarrow V = 27$
- Amplitude: $A = 1$
- Frequency: 300 MHz $(\lambda = 1)$

Object:

- Two square cylinders of side $\frac{\lambda}{6} = 0.1667$
- $\varepsilon_r \in \{1.5, 2.0, 2.5, 3.0, 3.5, 4.0, 4.5, 5.0\}$ (one square), $\varepsilon_r = 1.5$ (one square)
- $\sigma = 0$ [S/m]

BCS parameters:

- Gamma prior on noise variance parameters: $a = 2 \times 10^{+2}$, $b = 1 \times 10^{-1}$
- Convergenze parameter: $\tau = 1.0 \times 10^{-8}$

RESULTS: $\varepsilon_r = 1.5$

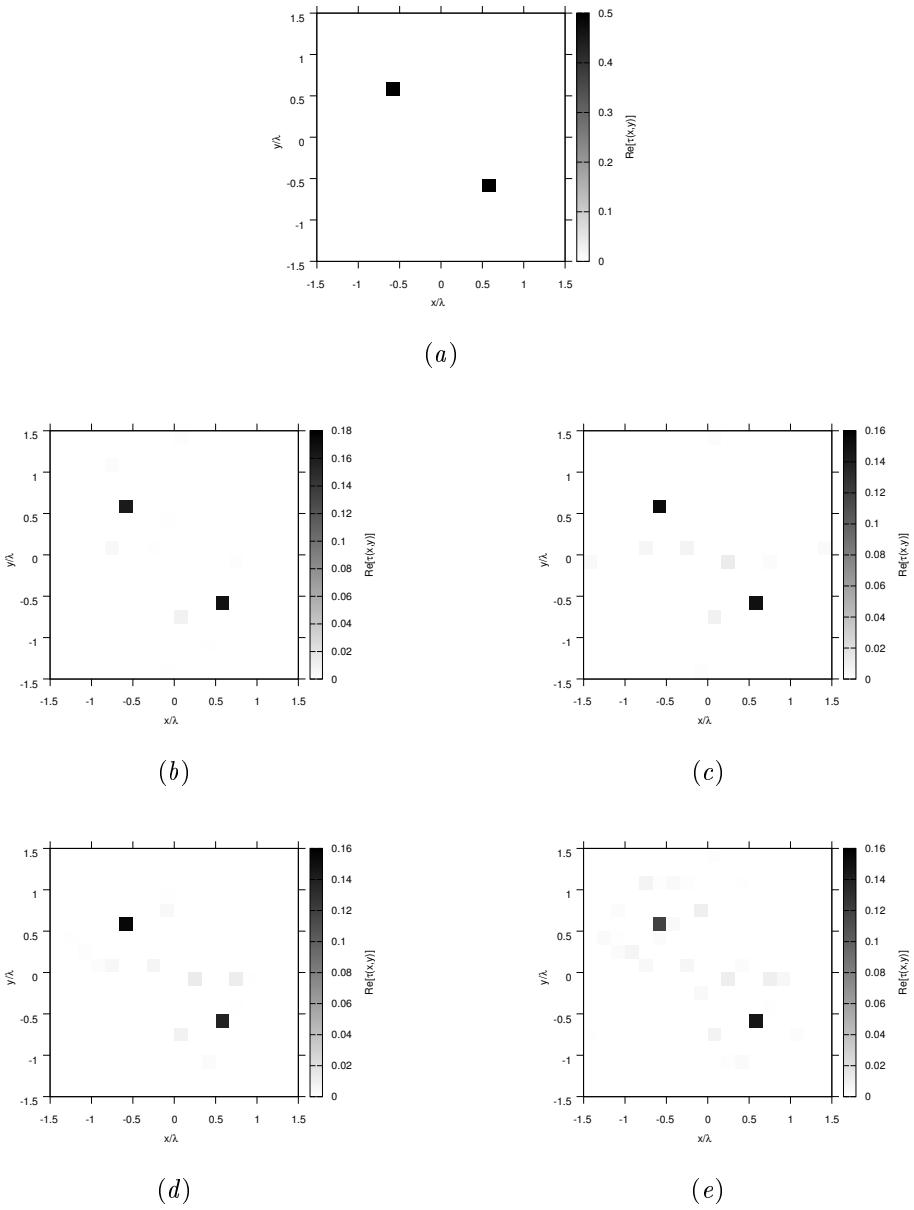

(a)

(b)

(c)

(d)

(e)

Figure 36. Actual object (a) and BCS reconstructed object for (b) Noiseless case, (c) $SNR = 20$ [dB] , (d) $SNR = 10$ [dB] , (e) $SNR = 5$ [dB].

RESULTS: $\varepsilon_r = 2.0$

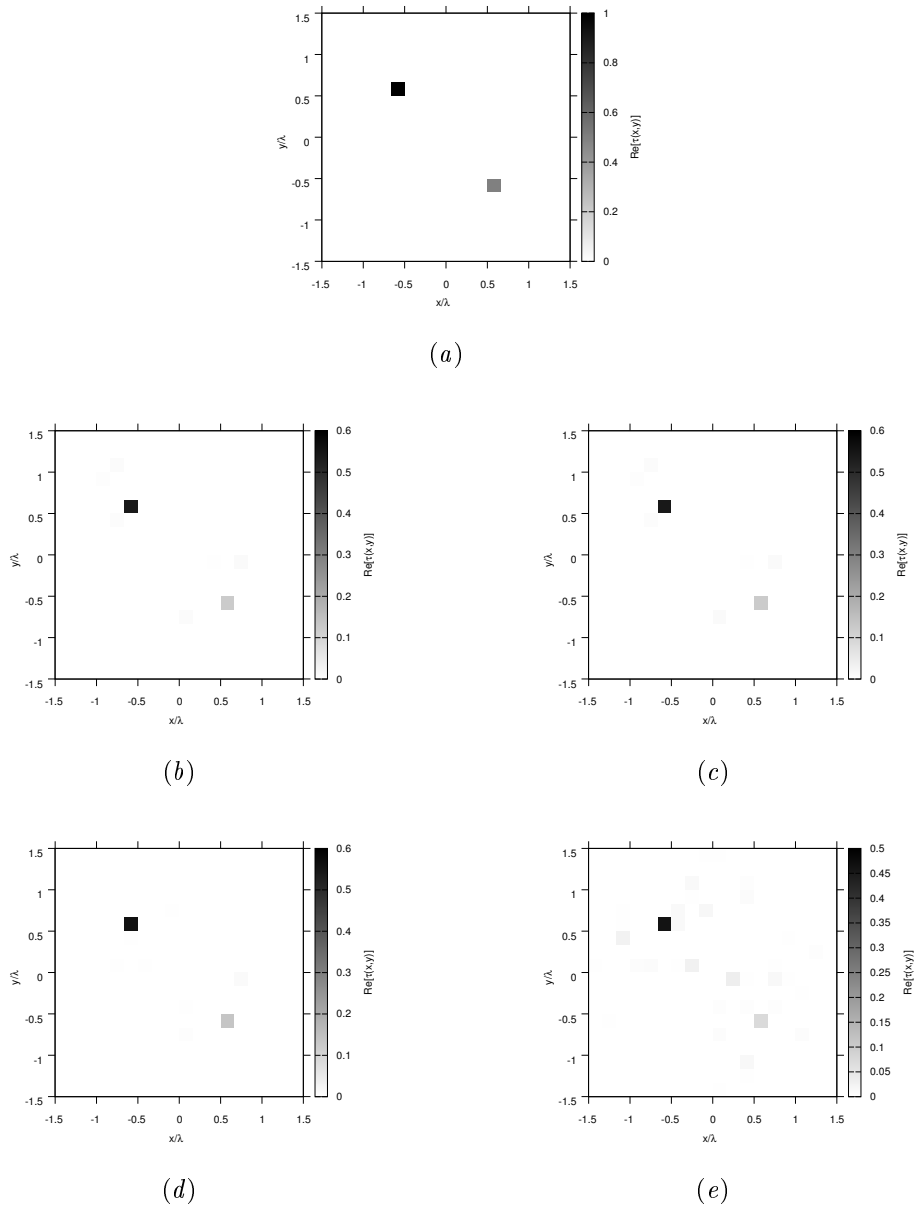

(a)

(b)

(c)

(d)

(e)

Figure 37. Actual object (a) and BCS reconstructed object for (b) Noiseless case, (c) $SNR = 20$ [dB] , (d) $SNR = 10$ [dB] , (e) $SNR = 5$ [dB].

RESULTS: $\varepsilon_r = 5.0$

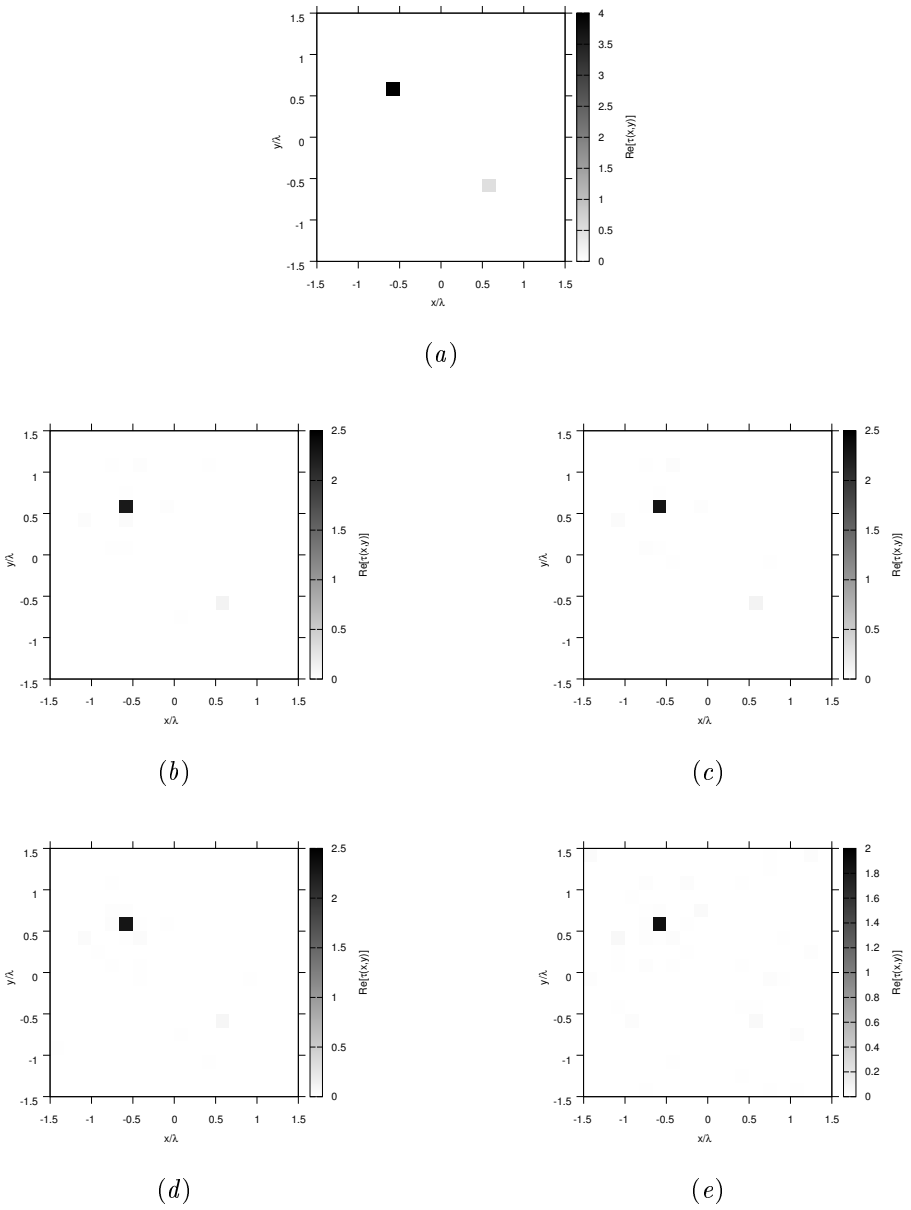

(a)

(b)

(c)

(d)

(e)

Figure 38. Actual object (a) and BCS reconstructed object for (b) Noiseless case, (c) $SNR = 20$ [dB] , (d) $SNR = 10$ [dB] , (e) $SNR = 5$ [dB].

RESULTS: Error Figures

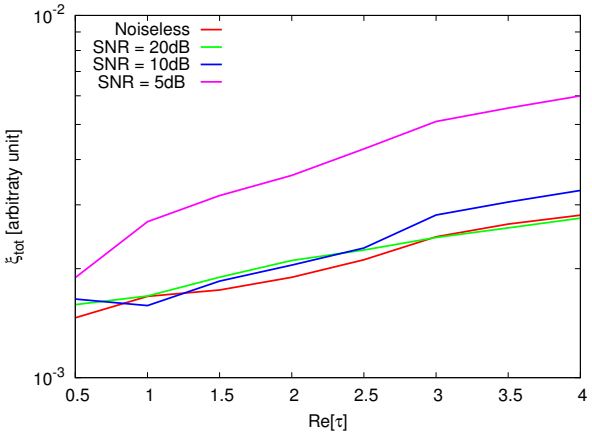

(a)

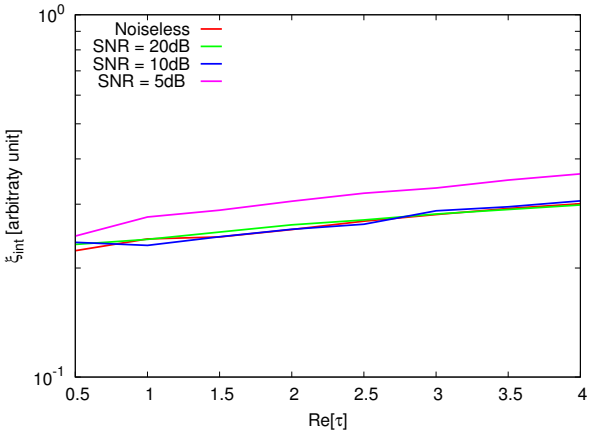

(b)

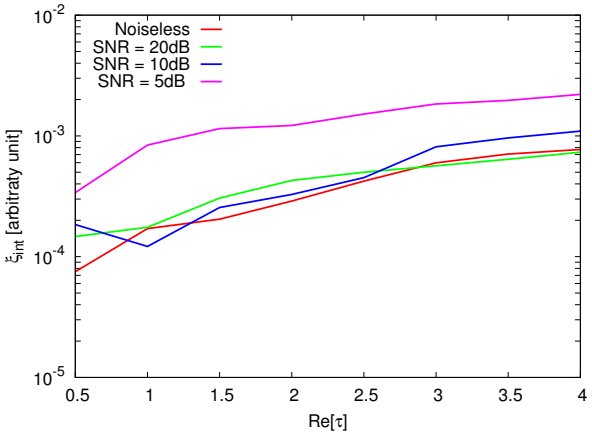

(c)

Figure 39. Behaviour of error figures as a function of ε_r, for different SNR values: (a) total error ξ_{tot}, (b) internal error ξ_{int}, (c) external error ξ_{ext}.

TEST CASE: Square Cylinder $L = 0.33\lambda$

Goal: show the performances of BCS when dealing with a sparse scatterer

- Number of Views: V
- Number of Measurements: M
- Number of Cells for the Inversion: N
- Number of Cells for the Direct solver: D
- Side of the investigation domain: L

Test Case Description

Direct solver:

- Square domain divided in $\sqrt{D} \times \sqrt{D}$ cells
- Domain side: $L = 3\lambda$
- $D = 1296$ (discretization for the direct solver: $< \lambda/10$)

Investigation domain:

- Square domain divided in $\sqrt{N} \times \sqrt{N}$ cells
- $L = 3\lambda$
- $2ka = 2 \times \frac{2\pi}{\lambda} \times \frac{L\sqrt{2}}{2} = 6\pi\sqrt{2} = 26.65$
- $\#DOF = \frac{(2ka)^2}{2} = \frac{(2 \times \frac{2\pi}{\lambda} \times \frac{L\sqrt{2}}{2})^2}{2} = 4\pi^2 \left(\frac{L}{\lambda}\right)^2 = 4\pi^2 \times 9 \approx 355.3$
- N scelto in modo da essere vicino a $\#DOF$: $N = 324$ (18×18)

Measurement domain:

- Measurement points taken on a circle of radius $\rho = 3\lambda$
- Full-aspect measurements
- $M \approx 2ka \rightarrow M = 27$

Sources:

- Plane waves
- $V \approx 2ka \rightarrow V = 27$
- Amplitude: $A = 1$
- Frequency: 300 MHz $(\lambda = 1)$

Object:

- Square cylinder of side $\frac{\lambda}{3} = 0.33$
- $\varepsilon_r \in \{1.5, 2.0, 2.5, 3.0, 3.5, 4.0, 4.5, 5.0\}$
- $\sigma = 0$ [S/m]

BCS parameters:

- Gamma prior on noise variance parameters: $a = 2 \times 10^{+2}$, $b = 1 \times 10^{-1}$
- Convergenze parameter: $\tau = 1.0 \times 10^{-8}$

RESULTS: $\varepsilon_r = 1.5$

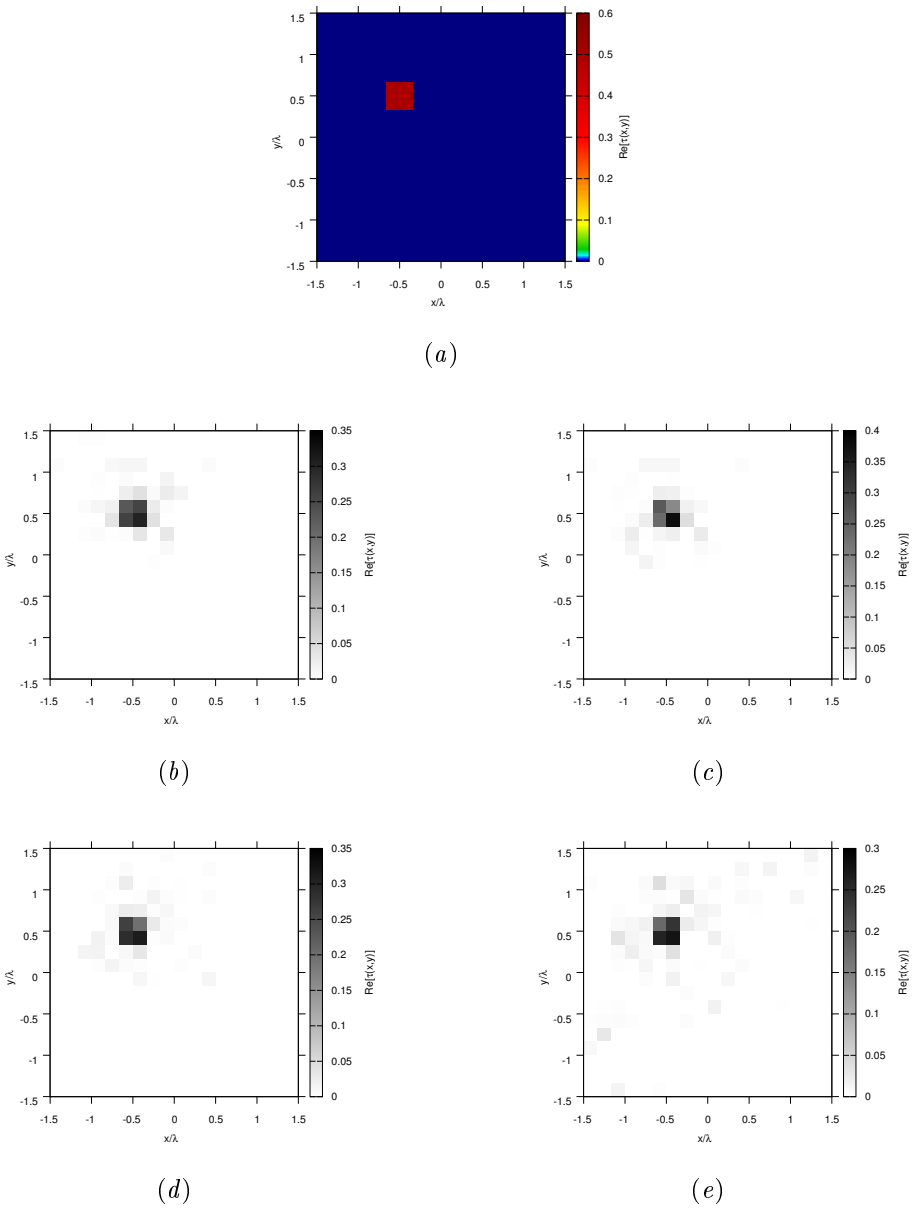

Figure 40. Actual object (a) and BCS reconstructed object for (b) Noiseless case, (c) $SNR = 20$ [dB] , (d) $SNR = 10$ [dB] , (e) $SNR = 5$ [dB].

RESULTS: $\varepsilon_r = 2.0$

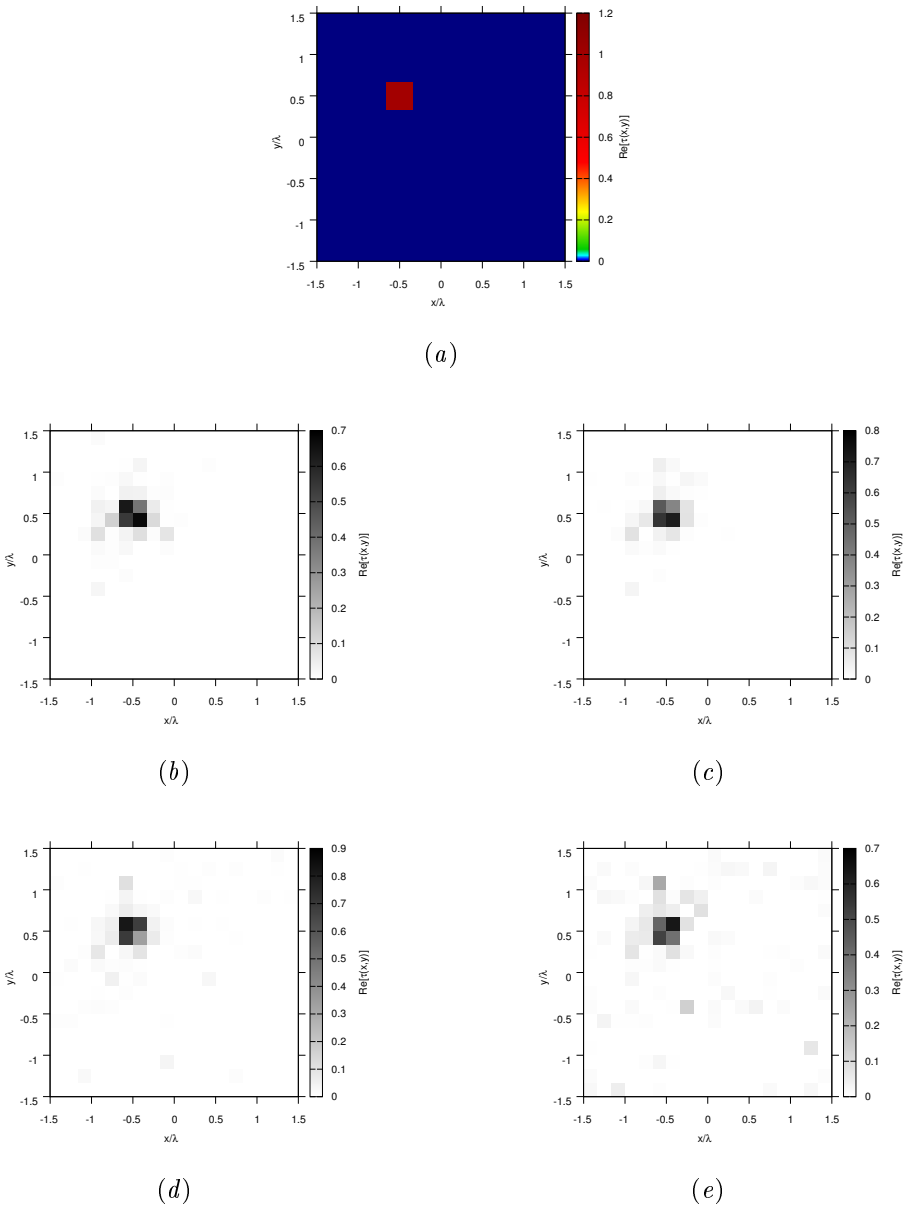

(a) (b) (c) (d) (e)

Figure 41. Actual object (a) and BCS reconstructed object for (b) Noiseless case, (c) $SNR = 20$ [dB] , (d) $SNR = 10$ [dB] , (e) $SNR = 5$ [dB].

RESULTS: $\varepsilon_r = 3.0$

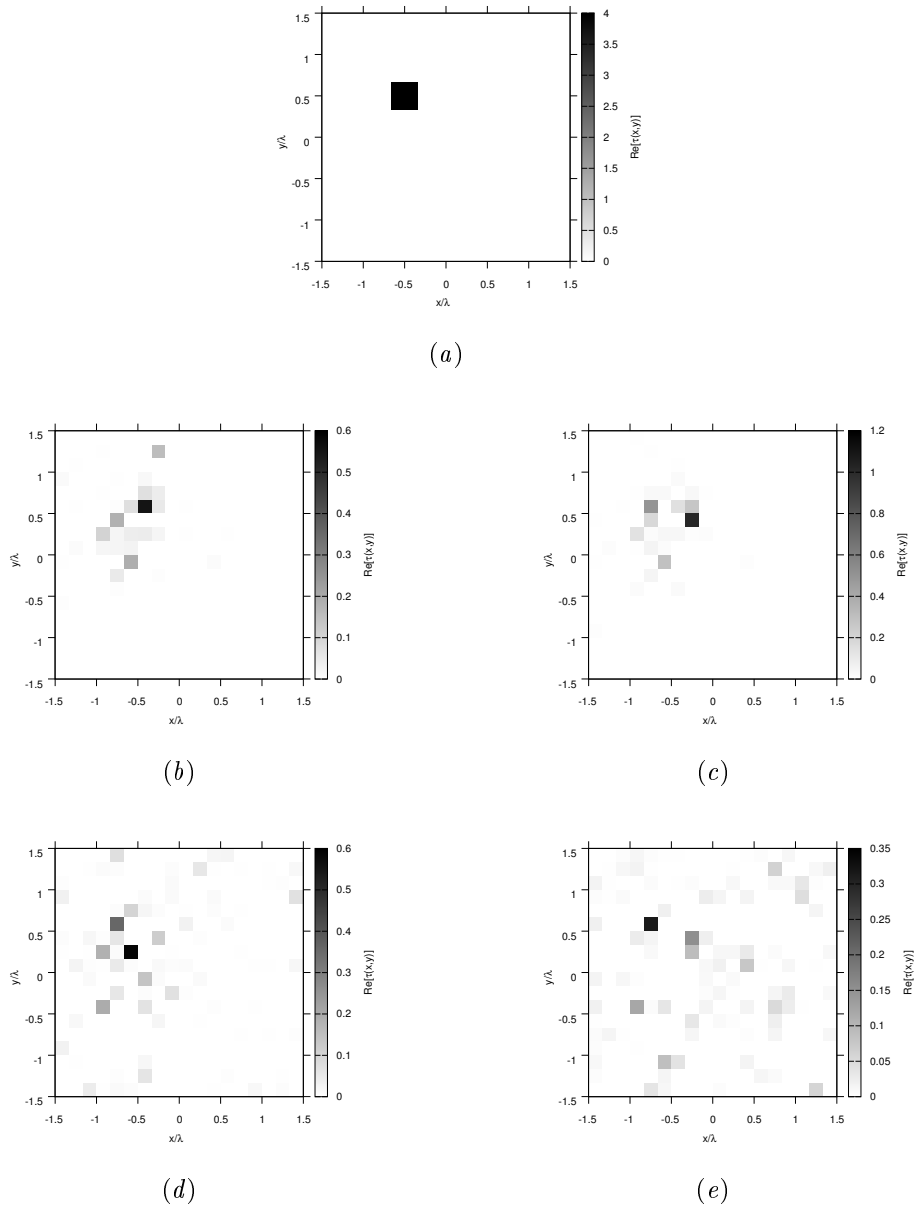

Figure 42. Actual object (a) and BCS reconstructed object for (b) Noiseless case, (c) $SNR = 20$ [dB] , (d) $SNR = 10$ [dB] , (e) $SNR = 5$ [dB].

RESULTS: Error Figures

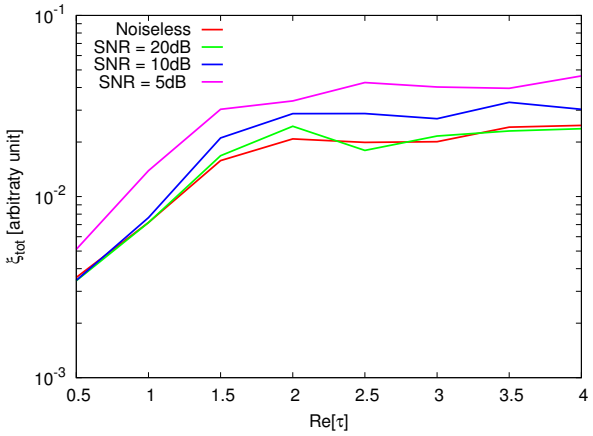

(a)

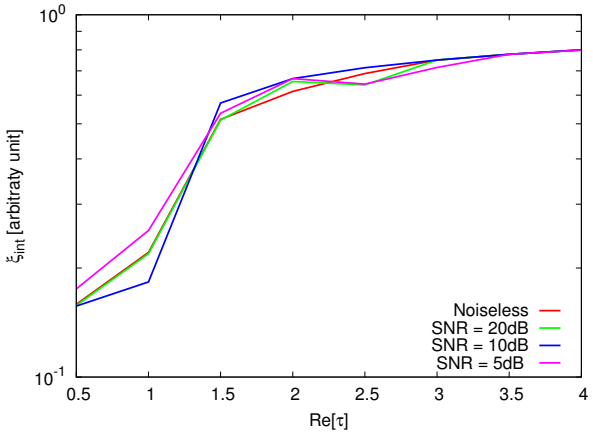

(b)

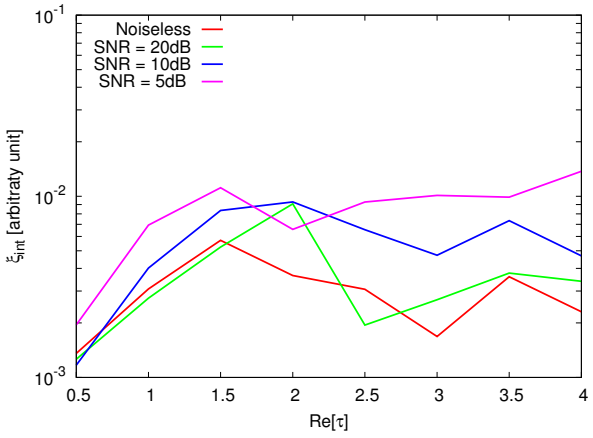

(c)

Figure 43. Behaviour of error figures as a function of ε_r, for different SNR values: (a) total error ξ_{tot}, (b) internal error ξ_{int}, (c) external error ξ_{ext}.

TEST CASE: Cross-Shaped Cylinder

Goal: show the performances of BCS when dealing with a sparse scatterer

- Number of Views: V
- Number of Measurements: M
- Number of Cells for the Inversion: N
- Number of Cells for the Direct solver: D
- Side of the investigation domain: L

Test Case Description

Direct solver:

- Square domain divided in $\sqrt{D} \times \sqrt{D}$ cells
- Domain side: $L = 3\lambda$
- $D = 1296$ (discretization for the direct solver: $< \lambda/10$)

Investigation domain:

- Square domain divided in $\sqrt{N} \times \sqrt{N}$ cells
- $L = 3\lambda$
- $2ka = 2 \times \frac{2\pi}{\lambda} \times \frac{L\sqrt{2}}{2} = 6\pi\sqrt{2} = 26.65$
- $\#DOF = \frac{(2ka)^2}{2} = \frac{(2 \times \frac{2\pi}{\lambda} \times \frac{L\sqrt{2}}{2})^2}{2} = 4\pi^2 \left(\frac{L}{\lambda}\right)^2 = 4\pi^2 \times 9 \approx 355.3$
- N scelto in modo da essere vicino a $\#DOF$: $N = 324$ (18×18)

Measurement domain:

- Measurement points taken on a circle of radius $\rho = 3\lambda$
- Full-aspect measurements
- $M \approx 2ka \rightarrow M = 27$

Sources:

- Plane waves
- $V \approx 2ka \rightarrow V = 27$
- Amplitude: $A = 1$
- Frequency: 300 MHz $(\lambda = 1)$

Object:

- Cross-shaped cylinder
- $\varepsilon_r \in \{1.5, 2.0, 2.5, 3.0, 3.5, 4.0, 4.5, 5.0\}$
- $\sigma = 0$ [S/m]

BCS parameters:

- Gamma prior on noise variance parameters: $a = 2 \times 10^{+2}$, $b = 1 \times 10^{-1}$
- Convergenze parameter: $\tau = 1.0 \times 10^{-8}$

RESULTS: $\varepsilon_r = 1.5$

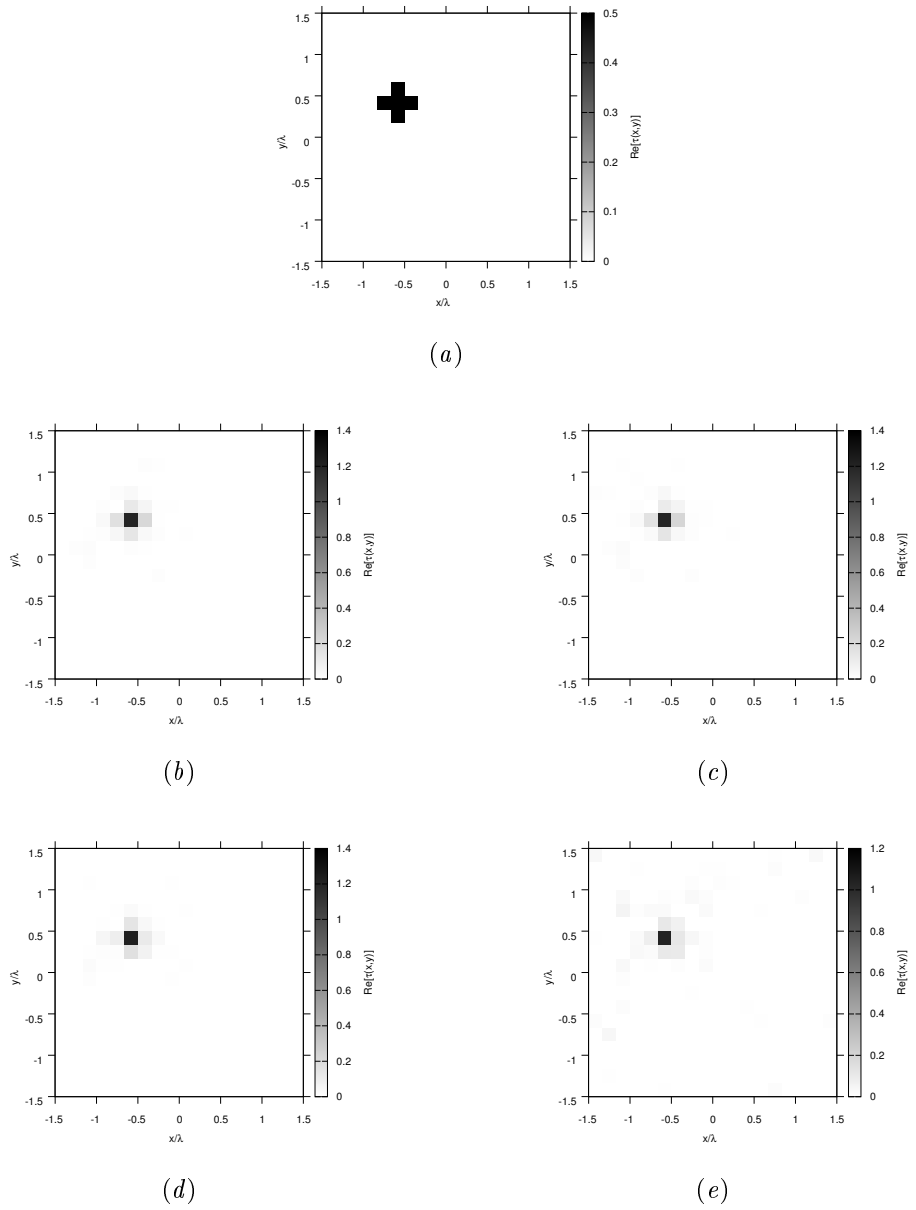

(a)

(b)

(c)

(d)

(e)

Figure 44. Actual object (a) and BCS reconstructed object for (b) Noiseless case, (c) $SNR = 20$ [dB] , (d) $SNR = 10$ [dB] , (e) $SNR = 5$ [dB].

RESULTS: $\varepsilon_r = 2.0$

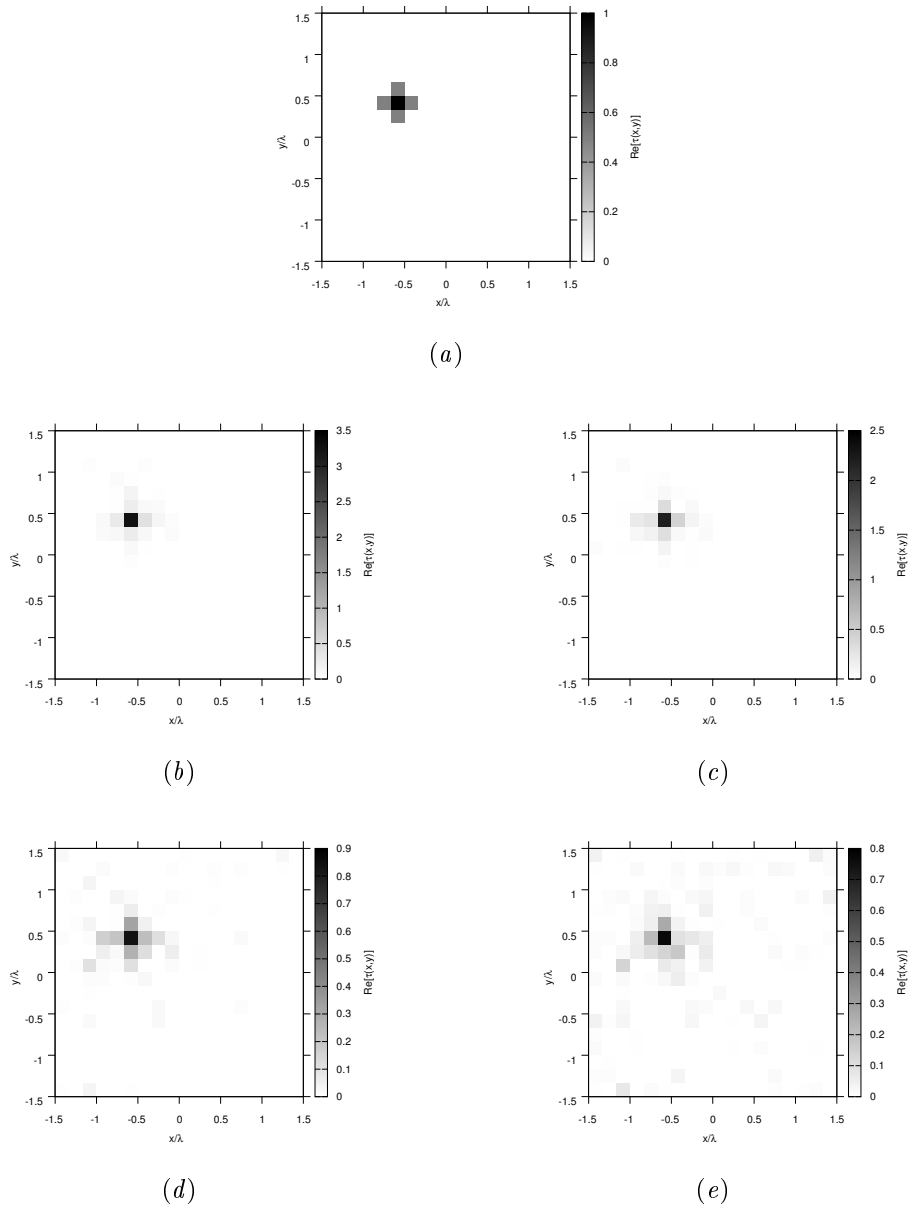

(a) (b) (c) (d) (e)

Figure 45. Actual object (a) and BCS reconstructed object for (b) Noiseless case, (c) $SNR = 20$ [dB] , (d) $SNR = 10$ [dB] , (e) $SNR = 5$ [dB].

RESULTS: $\varepsilon_r = 3.0$

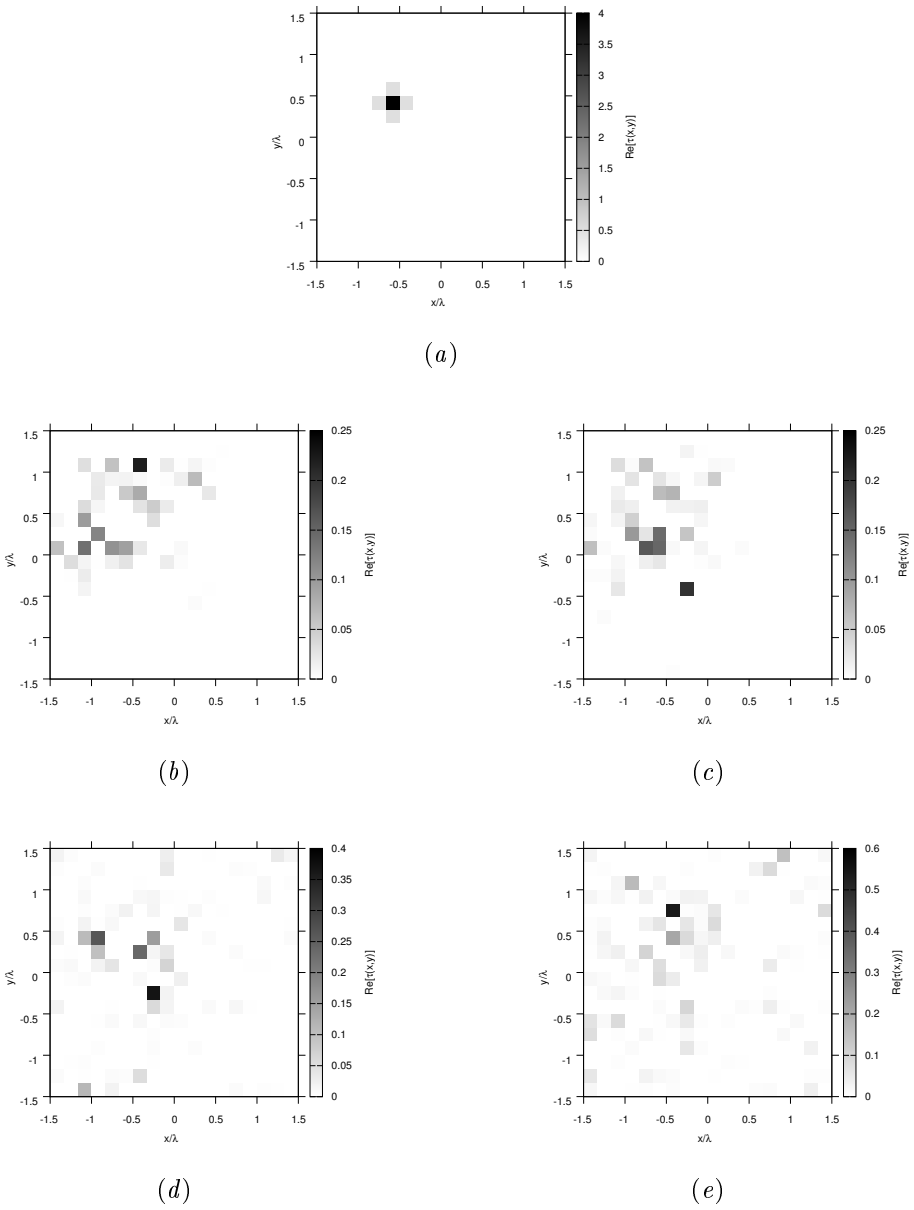

Figure 46. Actual object (a) and BCS reconstructed object for (b) Noiseless case, (c) $SNR = 20$ [dB] , (d) $SNR = 10$ [dB] , (e) $SNR = 5$ [dB].

RESULTS: Error Figures

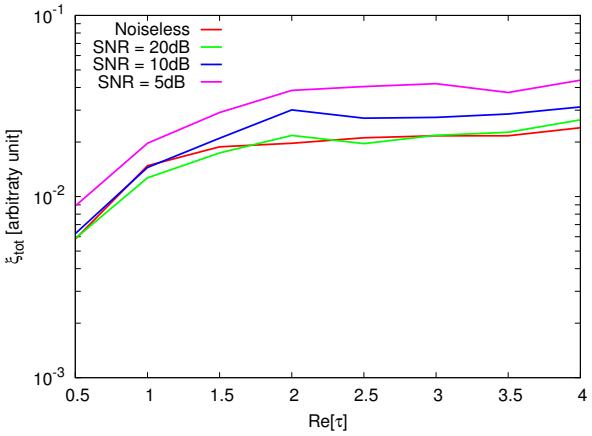

(a)

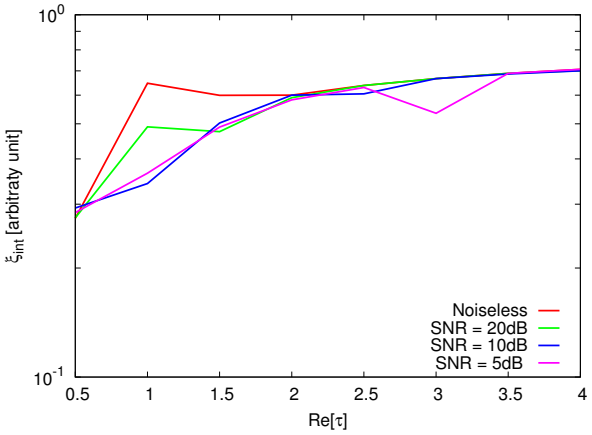

(b)

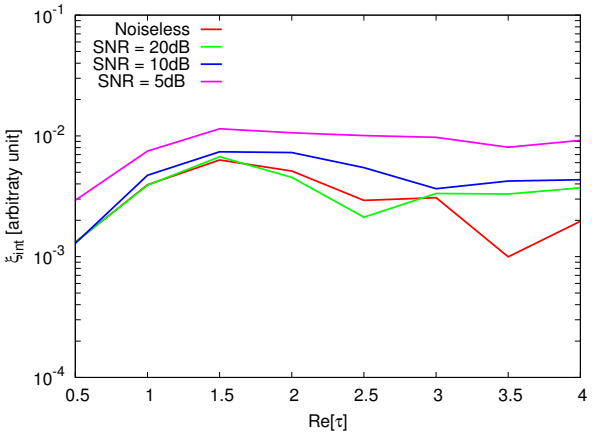

(c)

Figure 47. Behaviour of error figures as a function of ε_r, for different SNR values: (a) total error ξ_{tot}, (b) internal error ξ_{int}, (c) external error ξ_{ext}.

TEST CASE: L-Shaped Cylinder

Goal: show the performances of BCS when dealing with a sparse scatterer

- Number of Views: V
- Number of Measurements: M
- Number of Cells for the Inversion: N
- Number of Cells for the Direct solver: D
- Side of the investigation domain: L

Test Case Description

Direct solver:

- Square domain divided in $\sqrt{D} \times \sqrt{D}$ cells
- Domain side: $L = 3\lambda$
- $D = 1296$ (discretization for the direct solver: $< \lambda/10$)

Investigation domain:

- Square domain divided in $\sqrt{N} \times \sqrt{N}$ cells
- $L = 3\lambda$
- $2ka = 2 \times \frac{2\pi}{\lambda} \times \frac{L\sqrt{2}}{2} = 6\pi\sqrt{2} = 26.65$
- $\#DOF = \frac{(2ka)^2}{2} = \frac{(2 \times \frac{2\pi}{\lambda} \times \frac{L\sqrt{2}}{2})^2}{2} = 4\pi^2 \left(\frac{L}{\lambda}\right)^2 = 4\pi^2 \times 9 \approx 355.3$
- N scelto in modo da essere vicino a $\#DOF$: $N = 324$ (18×18)

Measurement domain:

- Measurement points taken on a circle of radius $\rho = 3\lambda$
- Full-aspect measurements
- $M \approx 2ka \rightarrow M = 27$

Sources:

- Plane waves
- $V \approx 2ka \rightarrow V = 27$
- Amplitude $A = 1$
- Frequency: 300 MHz $(\lambda = 1)$

Object:

- L-shaped cylinder
- $\varepsilon_r \in \{1.5, 2.0, 2.5, 3.0, 3.5, 4.0, 4.5, 5.0\}$
- $\sigma = 0$ [S/m]

BCS parameters:

- Gamma prior on noise variance parameters: $a = 2 \times 10^{+2}$, $b = 1 \times 10^{-1}$
- Convergenze parameter: $\tau = 1.0 \times 10^{-8}$

RESULTS: $\varepsilon_r = 1.5$

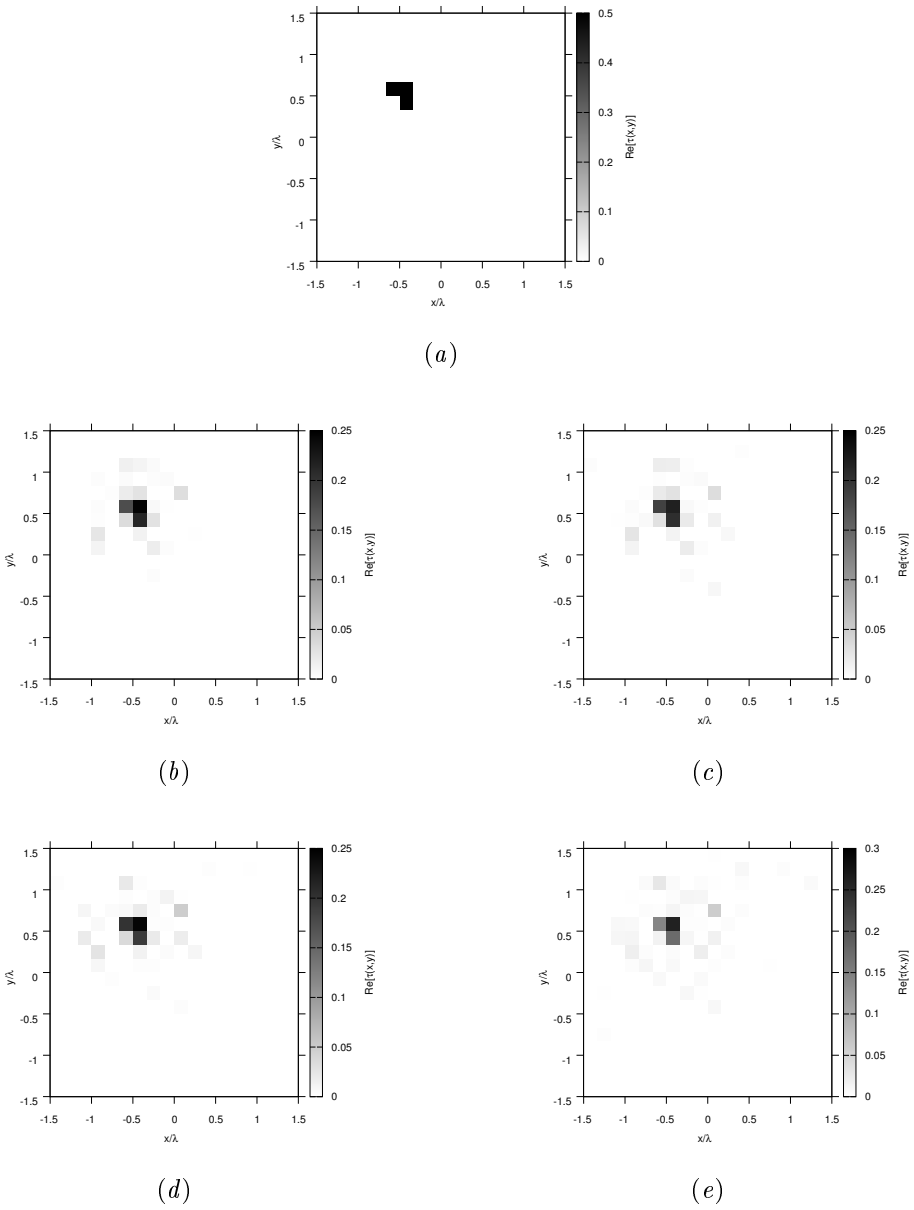

(a)

(b)

(c)

(d)

(e)

Figure 48. Actual object (a) and BCS reconstructed object for (b) Noiseless case, (c) $SNR = 20$ [dB] , (d) $SNR = 10$ [dB] , (e) $SNR = 5$ [dB].

RESULTS: $\varepsilon_r = 2.0$

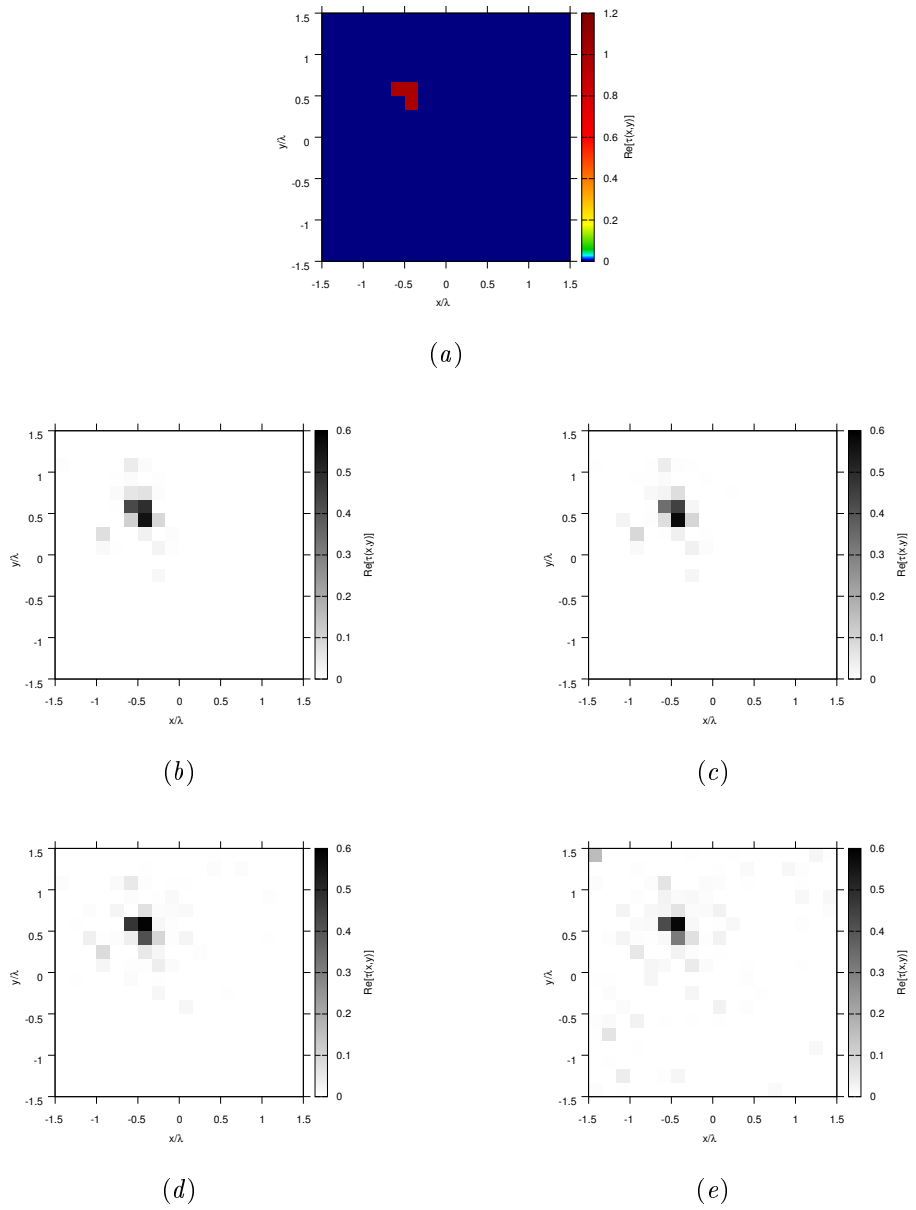

(a)

(b)

(c)

(d)

(e)

Figure 49. Actual object (a) and BCS reconstructed object for (b) Noiseless case, (c) $SNR = 20$ [dB] , (d) $SNR = 10$ [dB] , (e) $SNR = 5$ [dB].

RESULTS: $\varepsilon_r = 3.0$

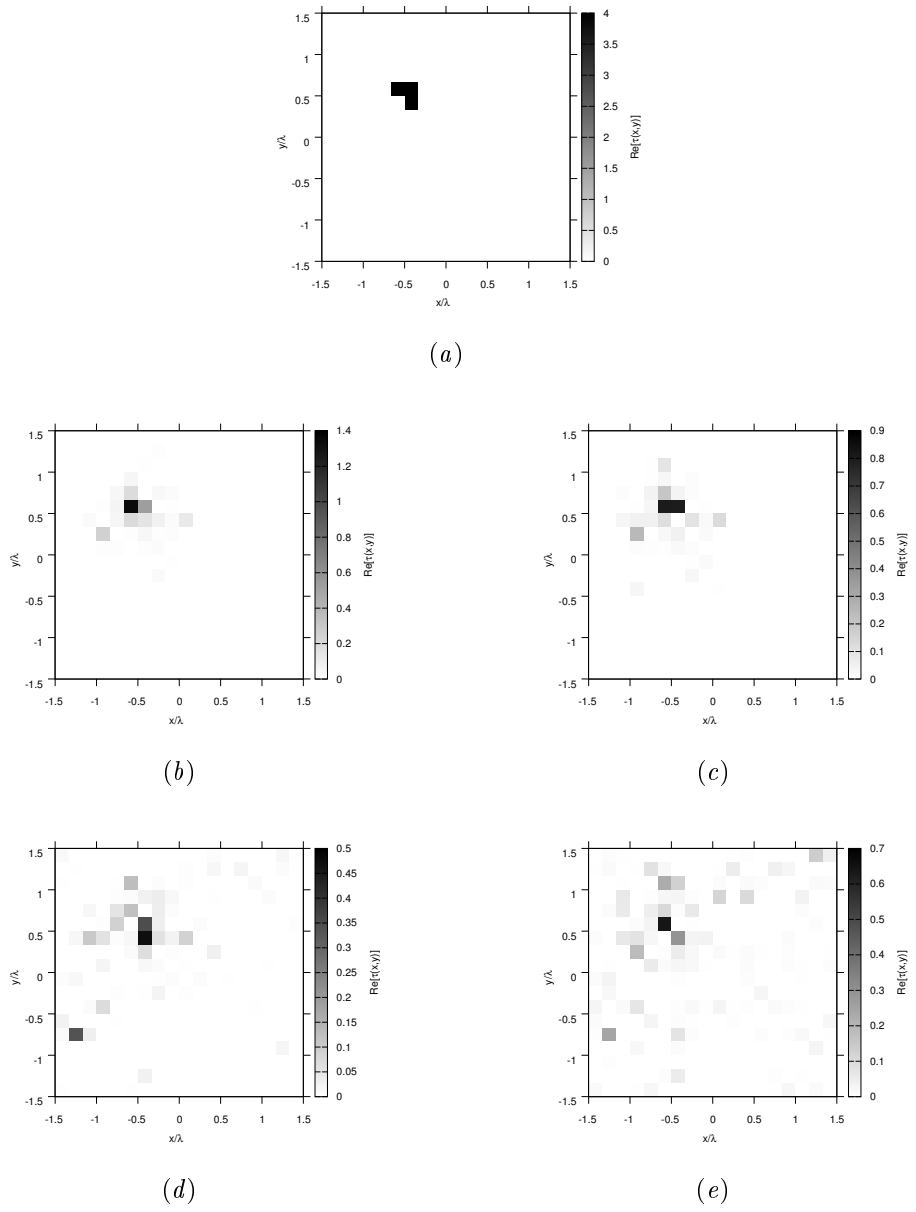

(a)

(b)

(c)

(d)

(e)

Figure 50. Actual object (a) and BCS reconstructed object for (b) Noiseless case, (c) $SNR = 20$ [dB] , (d) $SNR = 10$ [dB] , (e) $SNR = 5$ [dB].

RESULTS: Error Figures

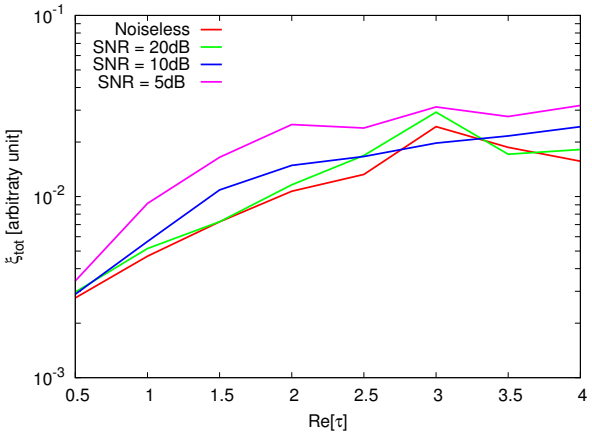

(a)

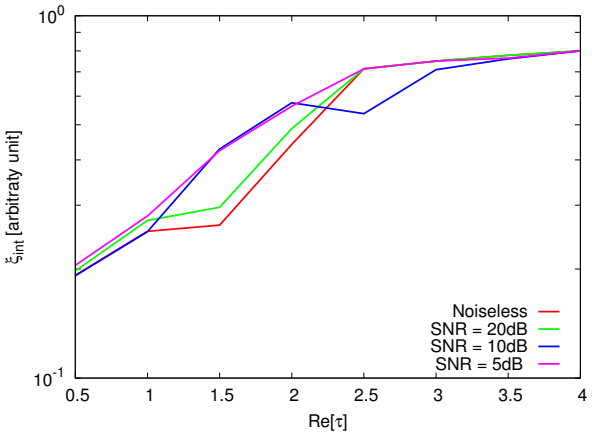

(b)

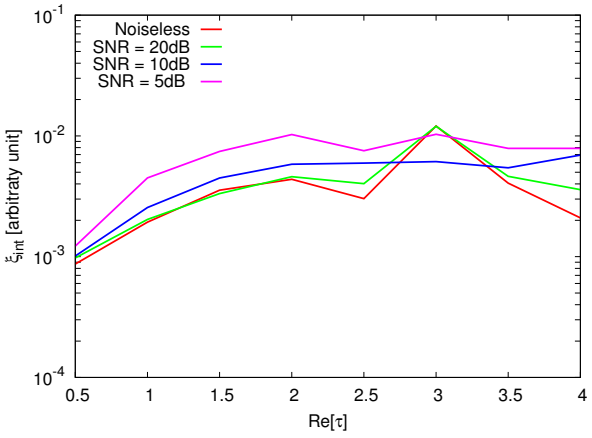

(c)

Figure 51. Behaviour of error figures as a function of ε_r, for different SNR values: (a) total error ξ_{tot}, (b) internal error ξ_{int}, (c) external error ξ_{ext}.

TEST CASE: Inhomogeneous L-Shaped Cylinder

Goal: show the performances of BCS when dealing with a sparse scatterer

- Number of Views: V
- Number of Measurements: M
- Number of Cells for the Inversion: N
- Number of Cells for the Direct solver: D
- Side of the investigation domain: L

Test Case Description

Direct solver:

- Square domain divided in $\sqrt{D} \times \sqrt{D}$ cells
- Domain side: $L = 3\lambda$
- $D = 1296$ (discretization for the direct solver: $< \lambda/10$)

Investigation domain:

- Square domain divided in $\sqrt{N} \times \sqrt{N}$ cells
- $L = 3\lambda$
- $2ka = 2 \times \frac{2\pi}{\lambda} \times \frac{L\sqrt{2}}{2} = 6\pi\sqrt{2} = 26.65$
- $\#DOF = \frac{(2ka)^2}{2} = \frac{(2 \times \frac{2\pi}{\lambda} \times \frac{L\sqrt{2}}{2})^2}{2} = 4\pi^2 \left(\frac{L}{\lambda}\right)^2 = 4\pi^2 \times 9 \approx 355.3$
- N scelto in modo da essere vicino a $\#DOF$: $N = 324$ (18×18)

Measurement domain:

- Measurement points taken on a circle of radius $\rho = 3\lambda$
- Full-aspect measurements
- $M \approx 2ka \rightarrow M = 27$

Sources:

- Plane waves
- $V \approx 2ka \rightarrow V = 27$
- Amplitude $A = 1$
- Frequency: 300 MHz $(\lambda = 1)$

Object:

- Inhomogeneous L-shaped cylinder
- $\varepsilon_r \in \{1.5, 2.0, 2.5, 3.0, 3.5, 4.0, 4.5, 5.0\}$
- $\sigma = 0$ [S/m]

BCS parameters:

- Gamma prior on noise variance parameters: $a = 2 \times 10^{+2}$, $b = 1 \times 10^{-1}$
- Convergenze parameter: $\tau = 1.0 \times 10^{-8}$

RESULTS: $\varepsilon_r = 1.5$

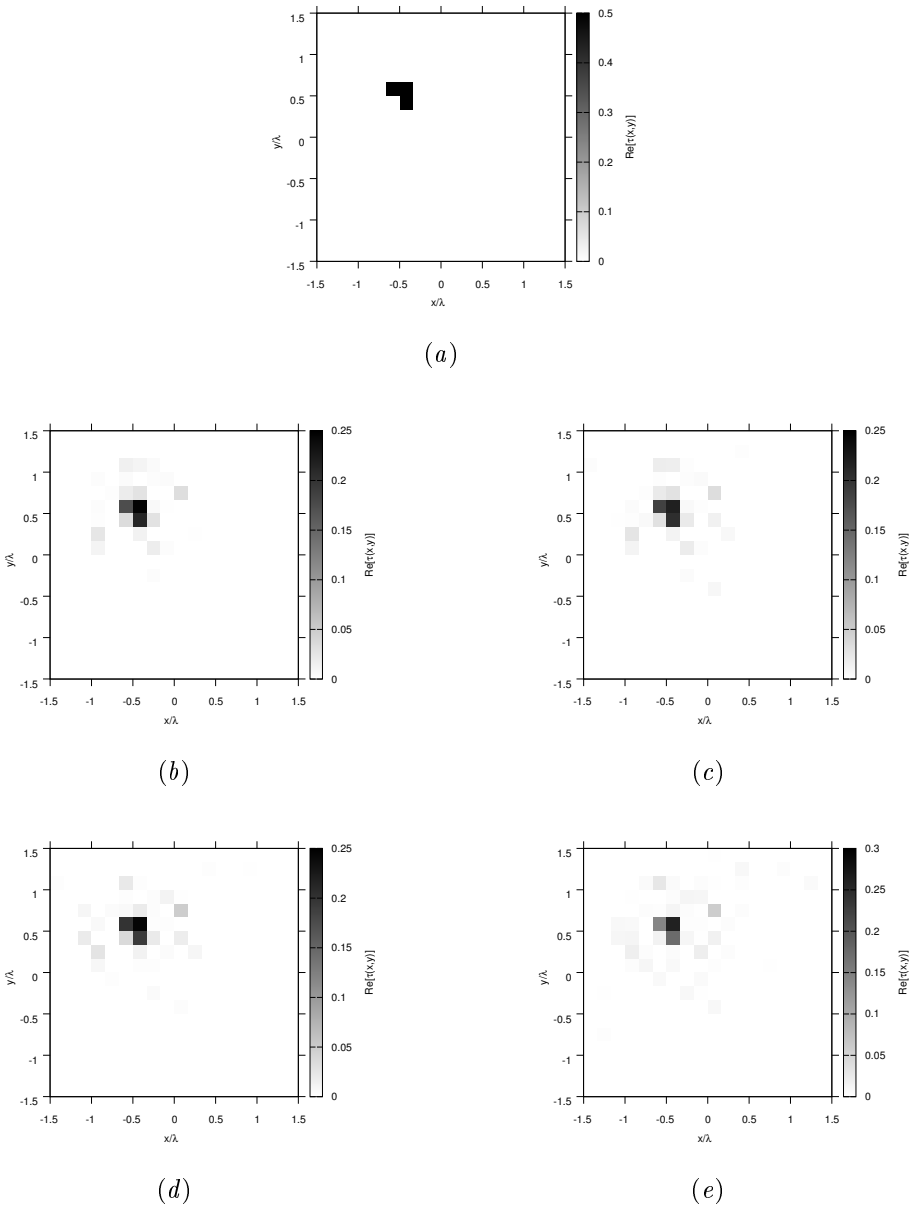

(a)

(b) (c)

(d) (e)

Figure 52. Actual object (a) and BCS reconstructed object for (b) Noiseless case, (c) $SNR = 20$ [dB] , (d) $SNR = 10$ [dB] , (e) $SNR = 5$ [dB].

RESULTS: $\varepsilon_r = 2.0$

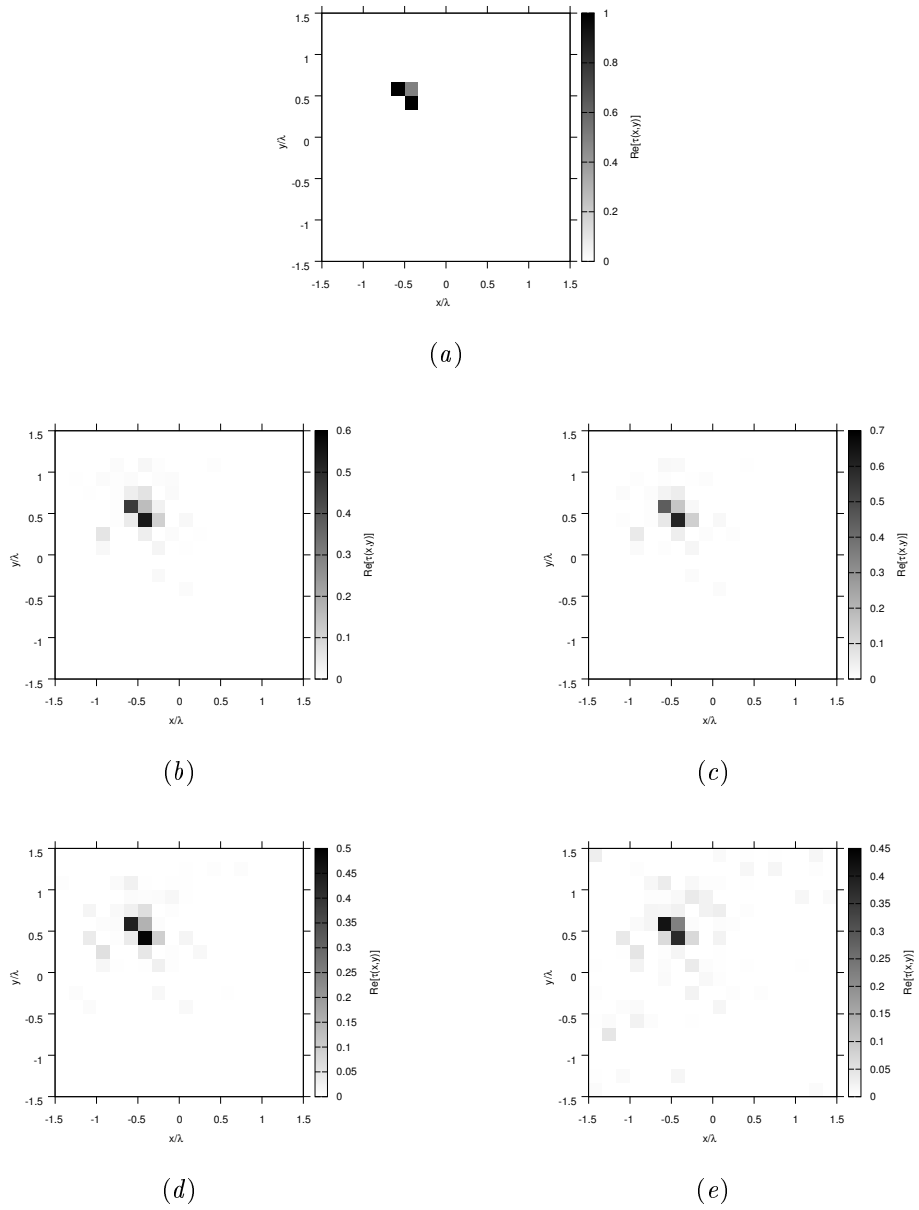

(a) (b) (c) (d) (e)

Figure 53. Actual object (a) and BCS reconstructed object for (b) Noiseless case, (c) $SNR = 20$ [dB] , (d) $SNR = 10$ [dB] , (e) $SNR = 5$ [dB].

RESULTS: $\varepsilon_r = 3.0$

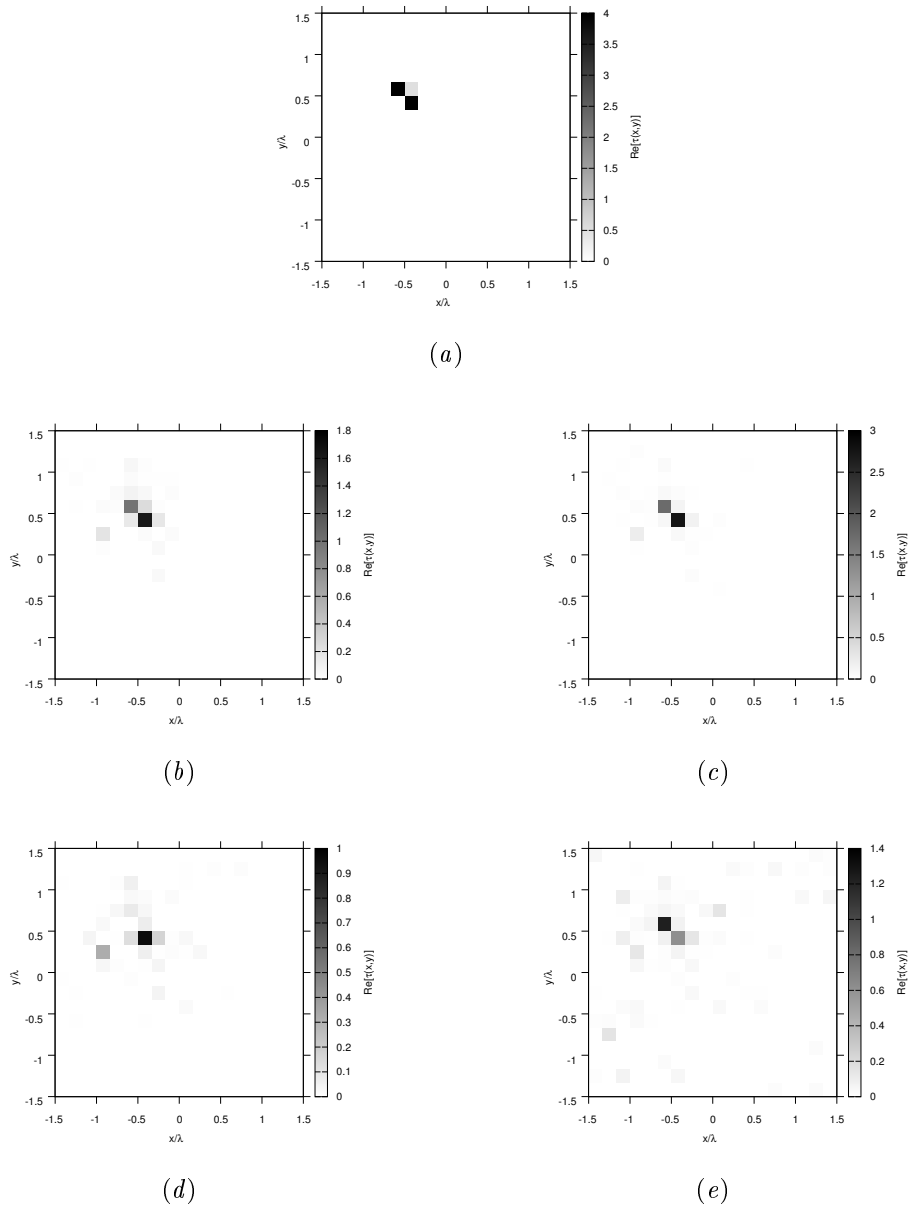

Figure 54. Actual object (a) and BCS reconstructed object for (b) Noiseless case, (c) $SNR = 20$ [dB] , (d) $SNR = 10$ [dB] , (e) $SNR = 5$ [dB].

RESULTS: Error Figures

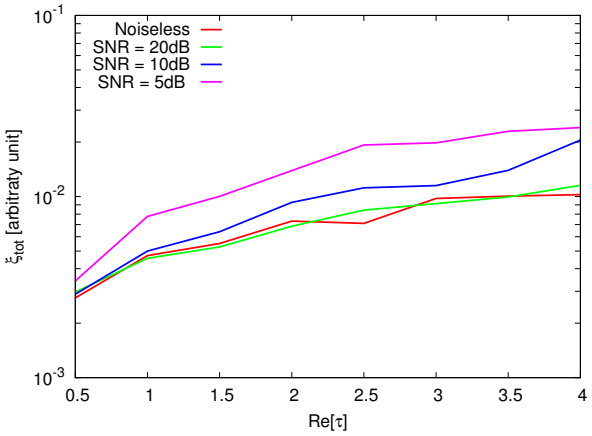

(a)

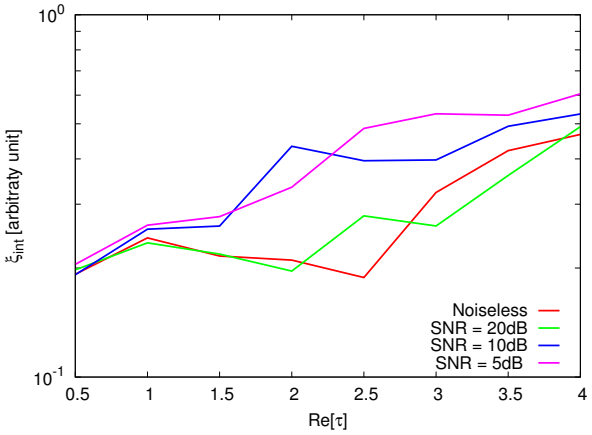

(b)

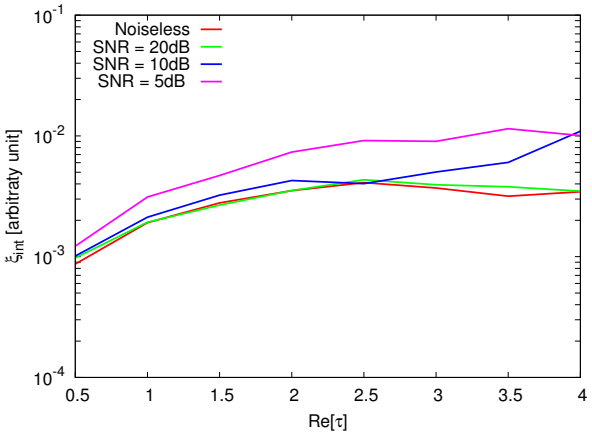

(c)

Figure 55. Behaviour of error figures as a function of ε_r, for different SNR values: (a) total error ξ_{tot}, (b) internal error ξ_{int}, (c) external error ξ_{ext}.

TEST CASE: Line-Shaped Cylinder $L = 0.5\lambda$

Goal: show the performances of BCS when dealing with a sparse scatterer

- Number of Views: V
- Number of Measurements: M
- Number of Cells for the Inversion: N
- Number of Cells for the Direct solver: D
- Side of the investigation domain: L

Test Case Description

Direct solver:

- Square domain divided in $\sqrt{D} \times \sqrt{D}$ cells
- Domain side: $L = 3\lambda$
- $D = 1296$ (discretization for the direct solver: $< \lambda/10$)

Investigation domain:

- Square domain divided in $\sqrt{N} \times \sqrt{N}$ cells
- $L = 3\lambda$
- $2ka = 2 \times \frac{2\pi}{\lambda} \times \frac{L\sqrt{2}}{2} = 6\pi\sqrt{2} = 26.65$
- $\#DOF = \frac{(2ka)^2}{2} = \frac{(2 \times \frac{2\pi}{\lambda} \times \frac{L\sqrt{2}}{2})^2}{2} = 4\pi^2 \left(\frac{L}{\lambda}\right)^2 = 4\pi^2 \times 9 \approx 355.3$
- N scelto in modo da essere vicino a $\#DOF$: $N = 324$ (18×18)

Measurement domain:

- Measurement points taken on a circle of radius $\rho = 3\lambda$
- Full-aspect measurements
- $M \approx 2ka \rightarrow M = 27$

Sources:

- Plane waves
- $V \approx 2ka \rightarrow V = 27$
- Amplitude $A = 1$
- Frequency: 300 MHz $(\lambda = 1)$

Object:

- Line-shaped cylinder $L = 0.5\lambda$
- $\varepsilon_r \in \{1.5, 2.0, 2.5, 3.0, 3.5, 4.0, 4.5, 5.0\}$
- $\sigma = 0$ [S/m]

BCS parameters:

- Gamma prior on noise variance parameters: $a = 2 \times 10^{+2}$, $b = 1 \times 10^{-1}$
- Convergenze parameter: $\tau = 1.0 \times 10^{-8}$

RESULTS: $\varepsilon_r = 1.5$

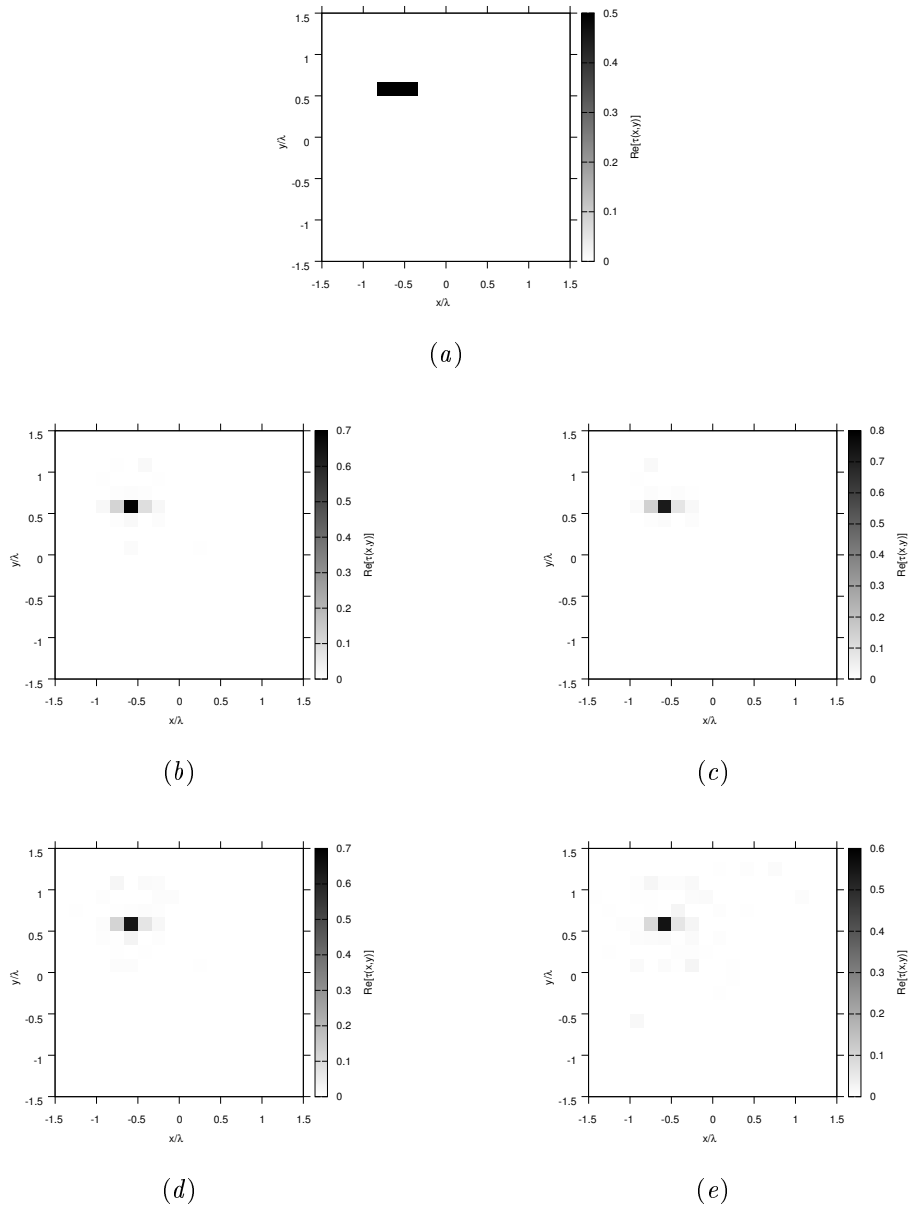

Figure 56. Actual object (a) and BCS reconstructed object for (b) Noiseless case, (c) $SNR = 20$ [dB] , (d) $SNR = 10$ [dB] , (e) $SNR = 5$ [dB].

RESULTS: $\varepsilon_r = 2.0$

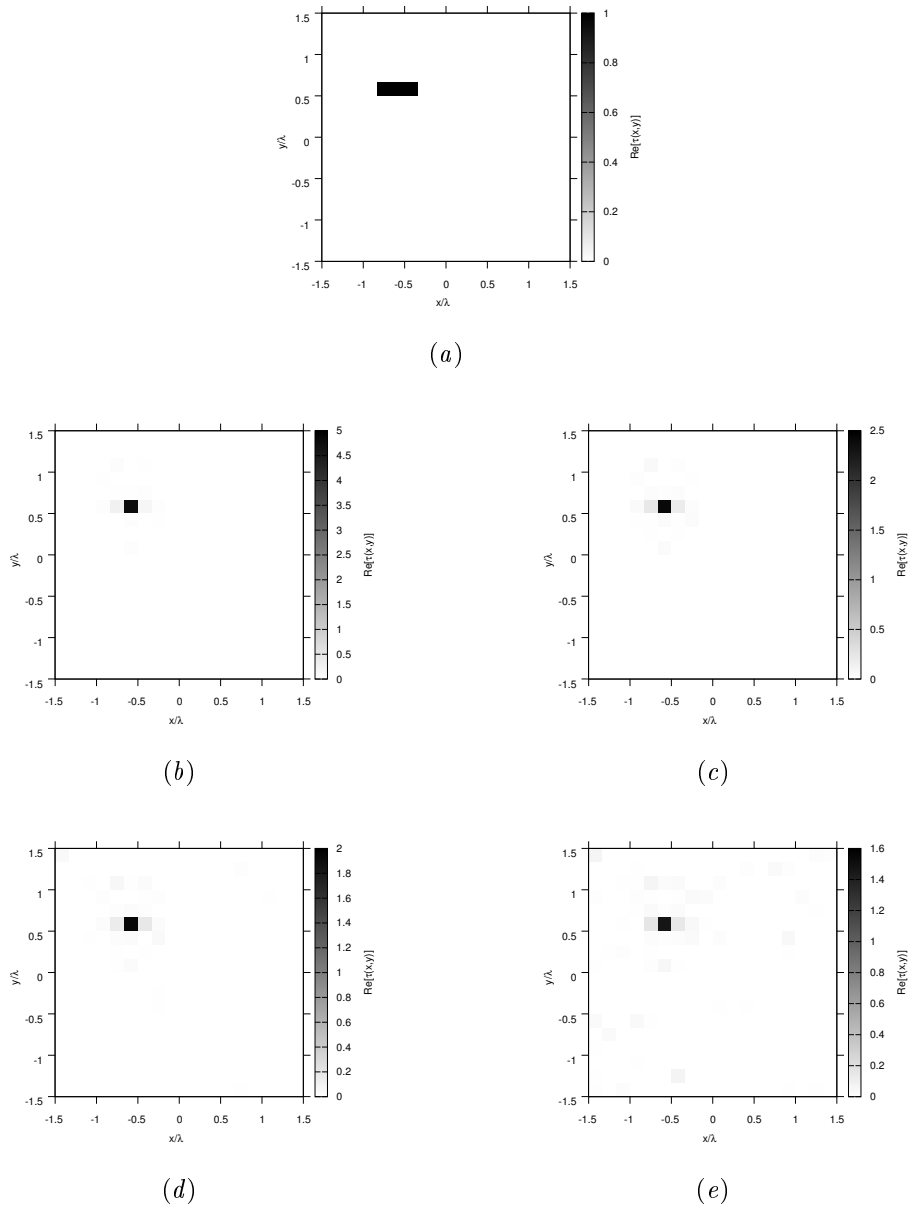

(a) (b) (c) (d) (e)

Figure 57. Actual object (a) and BCS reconstructed object for (b) Noiseless case, (c) $SNR = 20$ [dB] , (d) $SNR = 10$ [dB] , (e) $SNR = 5$ [dB].

RESULTS: $\varepsilon_r = 3.0$

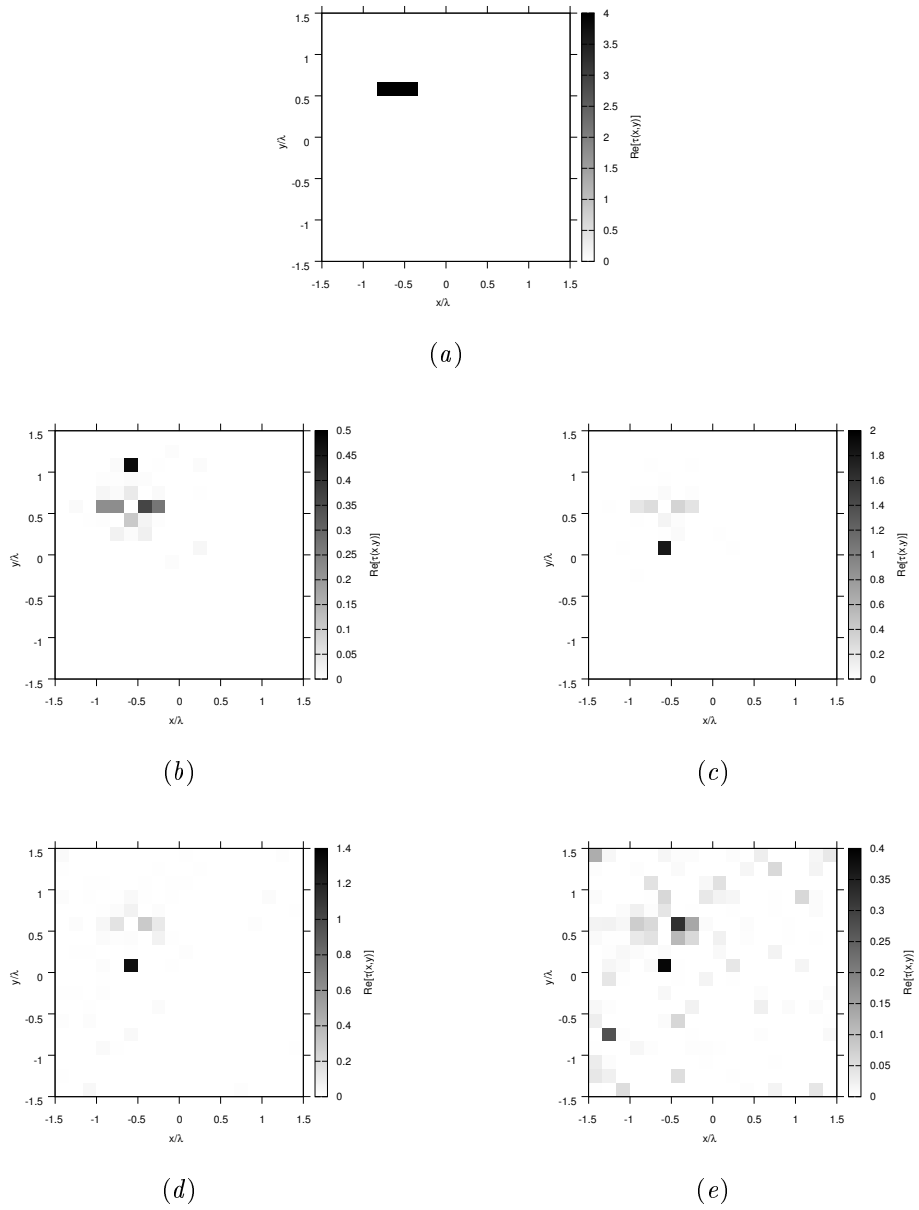

(a)

(b)

(c)

(d)

(e)

Figure 58. Actual object (a) and BCS reconstructed object for (b) Noiseless case, (c) $SNR = 20$ [dB] , (d) $SNR = 10$ [dB] , (e) $SNR = 5$ [dB].

RESULTS: Error Figures

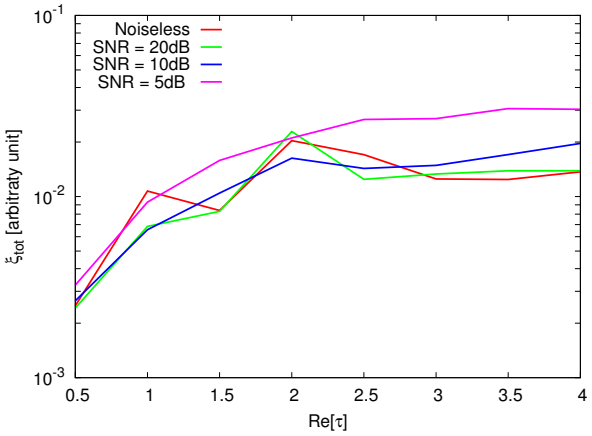

(a)

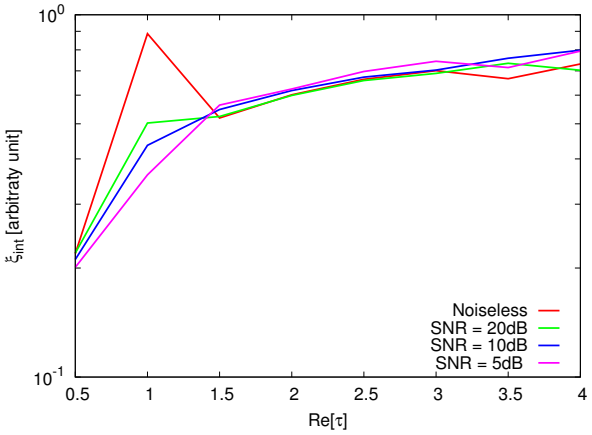

(b)

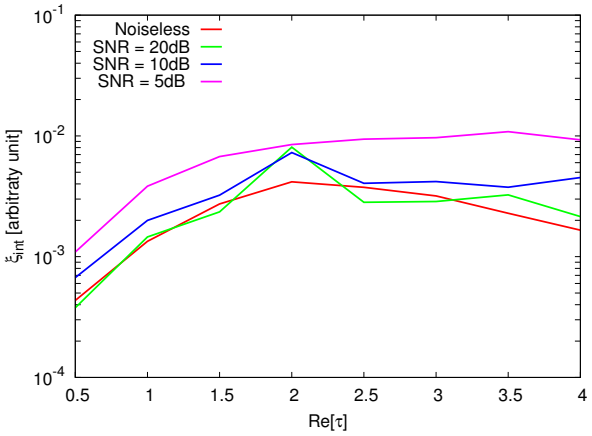

(c)

Figure 59. Behaviour of error figures as a function of ε_r, for different SNR values: (a) total error ξ_{tot}, (b) internal error ξ_{int}, (c) external error ξ_{ext}.

4 MV-MT-BCS (Exploiting Correlation between Views)

4.1 MV-MT-BCS - Calibration

TEST CASE: Square Cylinder

Goal: show the performances of BCS when dealing with a sparse scatterer

- Number of Views: V
- Number of Measurements: M
- Number of Cells for the Inversion: N
- Number of Cells for the Direct solver: D
- Side of the investigation domain: L

Test Case Description

Direct solver:

- Square domain divided in $\sqrt{D} \times \sqrt{D}$ cells
- Domain side: $L = 3\lambda$
- $D = 1296$ (discretization for the direct solver: $< \lambda/10$)

Investigation domain:

- Square domain divided in $\sqrt{N} \times \sqrt{N}$ cells
- $L = 3\lambda$
- $2ka = 2 \times \frac{2\pi}{\lambda} \times \frac{L\sqrt{2}}{2} = 6\pi\sqrt{2} = 26.65$
- $\#DOF = \frac{(2ka)^2}{2} = \frac{(2 \times \frac{2\pi}{\lambda} \times \frac{L\sqrt{2}}{2})^2}{2} = 4\pi^2 \left(\frac{L}{\lambda}\right)^2 = 4\pi^2 \times 9 \approx 355.3$
- N scelto in modo da essere vicino a $\#DOF$: $N = 324$ (18×18)

Measurement domain:

- Measurement points taken on a circle of radius $\rho = 3\lambda$
- Full-aspect measurements
- $M \approx 2ka \rightarrow M = 27$

Sources:

- Plane waves
- $V \approx 2ka \rightarrow V = 27$
- Amplitude: $A = 1$
- Frequency: 300 MHz ($\lambda = 1$)

Object:

- Square cylinder of side $\frac{\lambda}{6} = 0.1667$
- $\varepsilon_r = 2.0$

- $\sigma = 0$ [S/m]

BCS parameters:

- Gamma prior on noise variance parameter: $a \in \{1 \times 10^{-1}, 2 \times 10^{-1}, 5 \times 10^{-1}\ 1 \times 10^{0}, 2 \times 10^{0}, 5 \times 10^{0}, 1 \times 10^{+1}, 2 \times 10^{+1}, 5 \times 10^{+1}, 1 \times 10^{+2}, 2 \times 10^{+2}, 5 \times 10^{+2}, 1 \times 10^{+3}, 2 \times 10^{+3}, 5 \times 10^{+3}, 1 \times 10^{+4}\}$
- Gamma prior on noise variance parameter: $b \in \{1 \times 10^{+0}, 5 \times 10^{-1}, 2 \times 10^{-1}, 1 \times 10^{-1}, 5 \times 10^{-2}, 2 \times 10^{-2}\ 1 \times 10^{-2}, 5 \times 10^{-3}, 2 \times 10^{-3}, 1 \times 10^{-3}, 5 \times 10^{-4}, 2 \times 10^{-4}, 1 \times 10^{-4}\}$
- Convergenze parameter: $\tau = 1.0 \times 10^{-8}$

RESULTS: Calibration

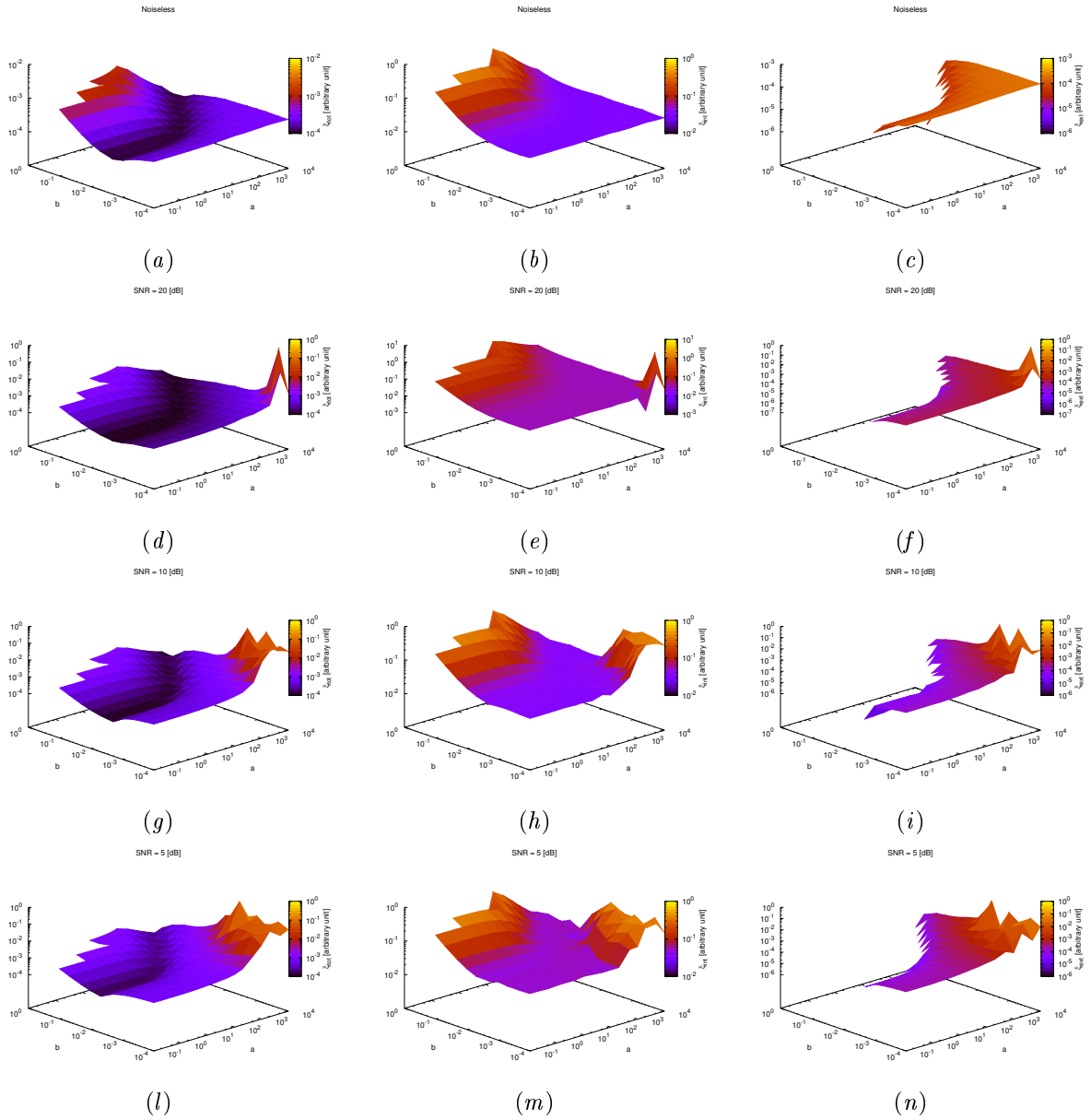

Figure 60. Behaviour of error figures as a function of the initial estimate of the Gamma prior on the noise variance parameters a and b, for different SNR values: (a), (d), (g) and (l) total error ξ_{tot}, (b), (e), (h) and (m) internal error ξ_{int}, (c), (f), (i) and (n) external error ξ_{ext}, for (a), (b) and (c) Noiseless case, (d), (e) and (f) $SNR = 20dB$, (g), (h) and (i) $SNR = 10dB$ and (l), (m) and (n) $SNR = 5dB$.

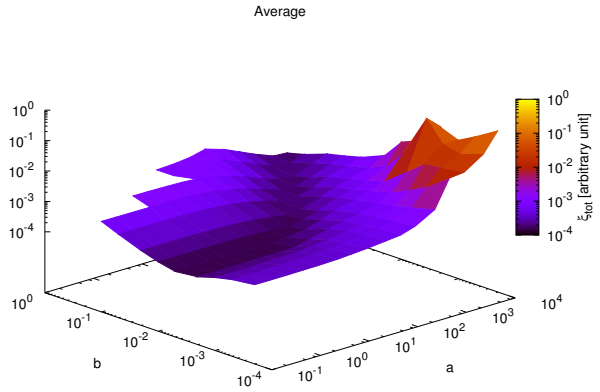

(a)

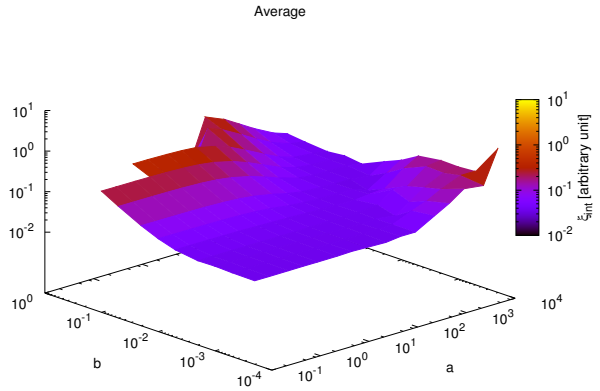

(b)

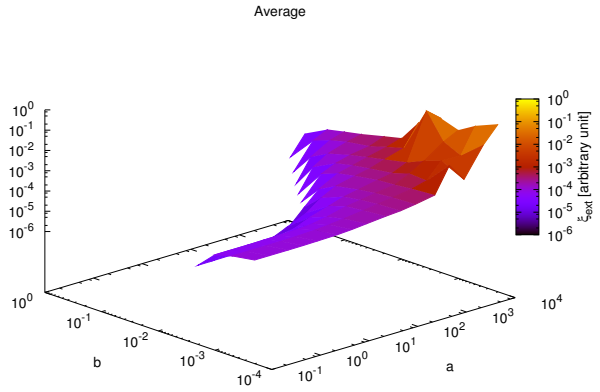

(c)

Figure 61. Averaged behaviour of error figures as a function of the initial estimate of the Gamma prior on the noise variance parameters a and b: (a) total error ξ_{tot}, (b) internal error ξ_{int}, (c) external error ξ_{ext}.

4.2 MV-MT-BCS - Basic Tests

TEST CASE: Square Cylinder $L = 0.16\lambda$

Goal: show the performances of BCS when dealing with a sparse scatterer

- Number of Views: V
- Number of Measurements: M
- Number of Cells for the Inversion: N
- Number of Cells for the Direct solver: D
- Side of the investigation domain: L

Test Case Description

Direct solver:

- Square domain divided in $\sqrt{D} \times \sqrt{D}$ cells
- Domain side: $L = 3\lambda$
- $D = 1296$ (discretization for the direct solver: $< \lambda/10$)

Investigation domain:

- Square domain divided in $\sqrt{N} \times \sqrt{N}$ cells
- $L = 3\lambda$
- $2ka = 2 \times \frac{2\pi}{\lambda} \times \frac{L\sqrt{2}}{2} = 6\pi\sqrt{2} = 26.65$
- $\#DOF = \frac{(2ka)^2}{2} = \frac{(2 \times \frac{2\pi}{\lambda} \times \frac{L\sqrt{2}}{2})^2}{2} = 4\pi^2 \left(\frac{L}{\lambda}\right)^2 = 4\pi^2 \times 9 \approx 355.3$
- N scelto in modo da essere vicino a $\#DOF$: $N = 324$ (18×18)

Measurement domain:

- Measurement points taken on a circle of radius $\rho = 3\lambda$
- Full-aspect measurements
- $M \approx 2ka \rightarrow M = 27$

Sources:

- Plane waves
- $V \approx 2ka \rightarrow V = 27$
- Amplitude: $A = 1$
- Frequency: 300 MHz ($\lambda = 1$)

Object:

- Square cylinder of side $\frac{\lambda}{6} = 0.1667$
- $\varepsilon_r \in \{1.5, 2.0, 2.5, 3.0, 3.5, 4.0, 4.5, 5.0\}$

- $\sigma = 0$ [S/m]

BCS parameters:

- Gamma prior on noise variance parameters: $a = 1 \times 10^{+1}$, $b = 5 \times 10^{-3}$
- Convergenze parameter: $\tau = 1.0 \times 10^{-8}$

RESULTS: $\varepsilon_r = 1.5$

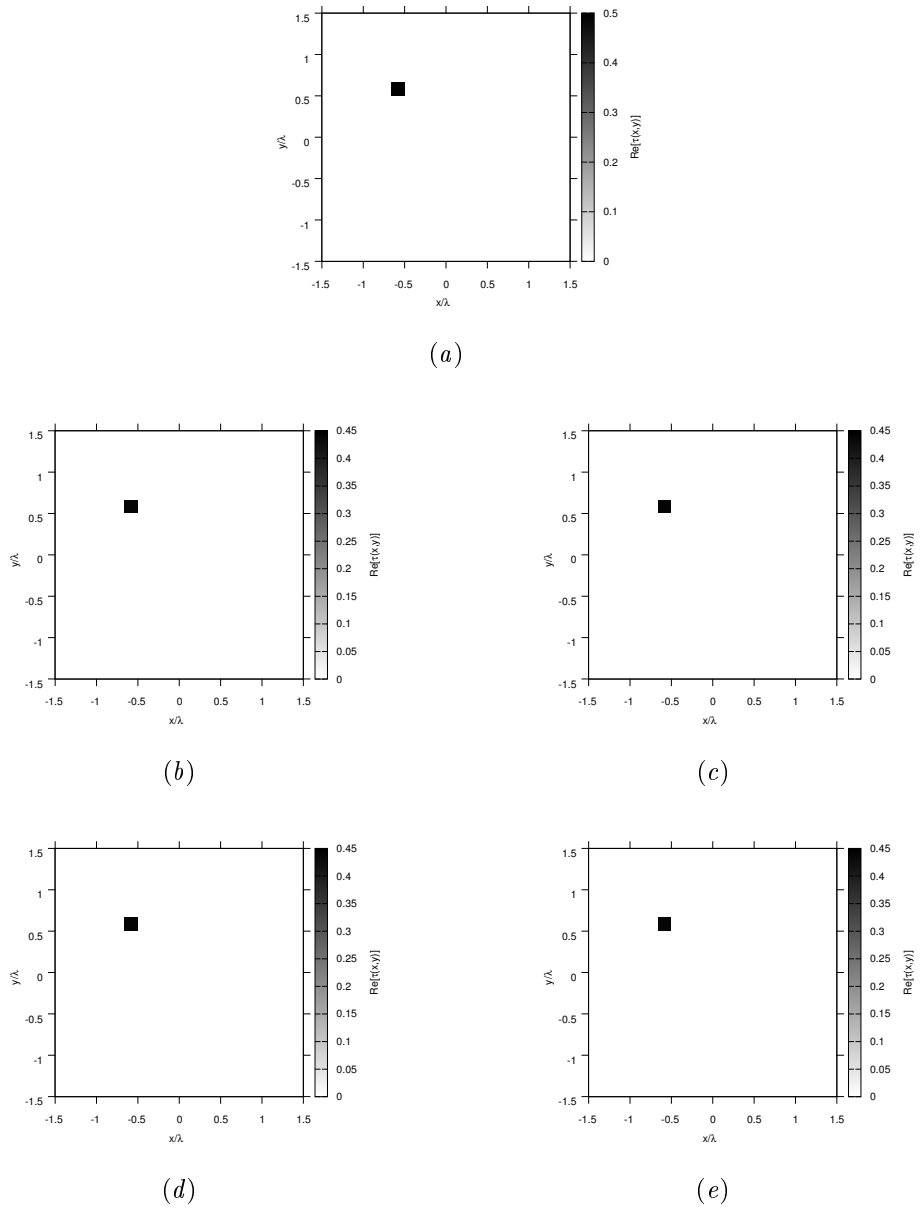

(a)

(b)

(c)

(d)

(e)

Figure 62. Actual object (a) and BCS reconstructed object for (b) Noiseless case, (c) $SNR = 20$ [dB] , (d) $SNR = 10$ [dB] , (e) $SNR = 5$ [dB].

RESULTS: $\varepsilon_r = 2.0$

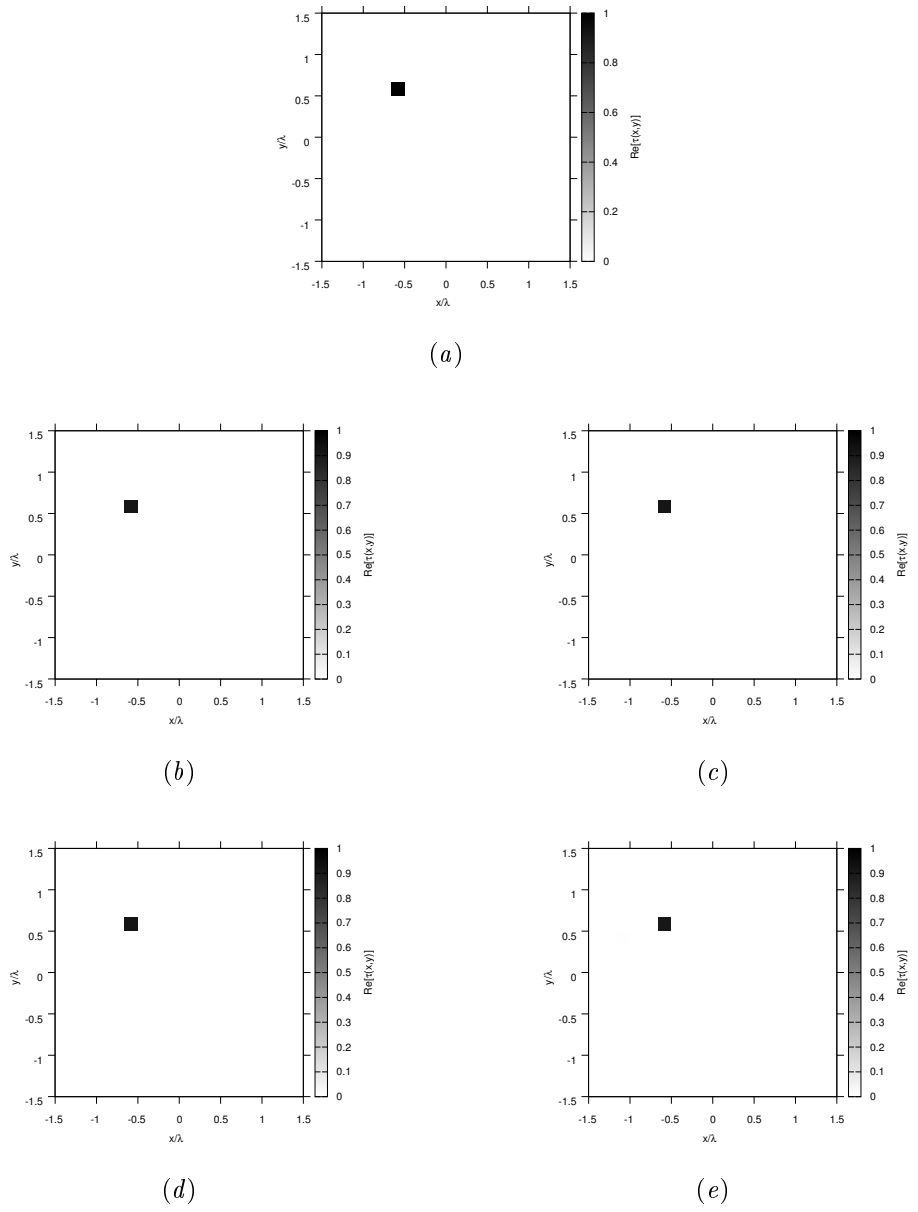

(a) (b) (c) (d) (e)

Figure 63. Actual object (a) and BCS reconstructed object for (b) Noiseless case, (c) $SNR = 20$ [dB] , (d) $SNR = 10$ [dB] , (e) $SNR = 5$ [dB].

RESULTS: $\varepsilon_r = 5.0$

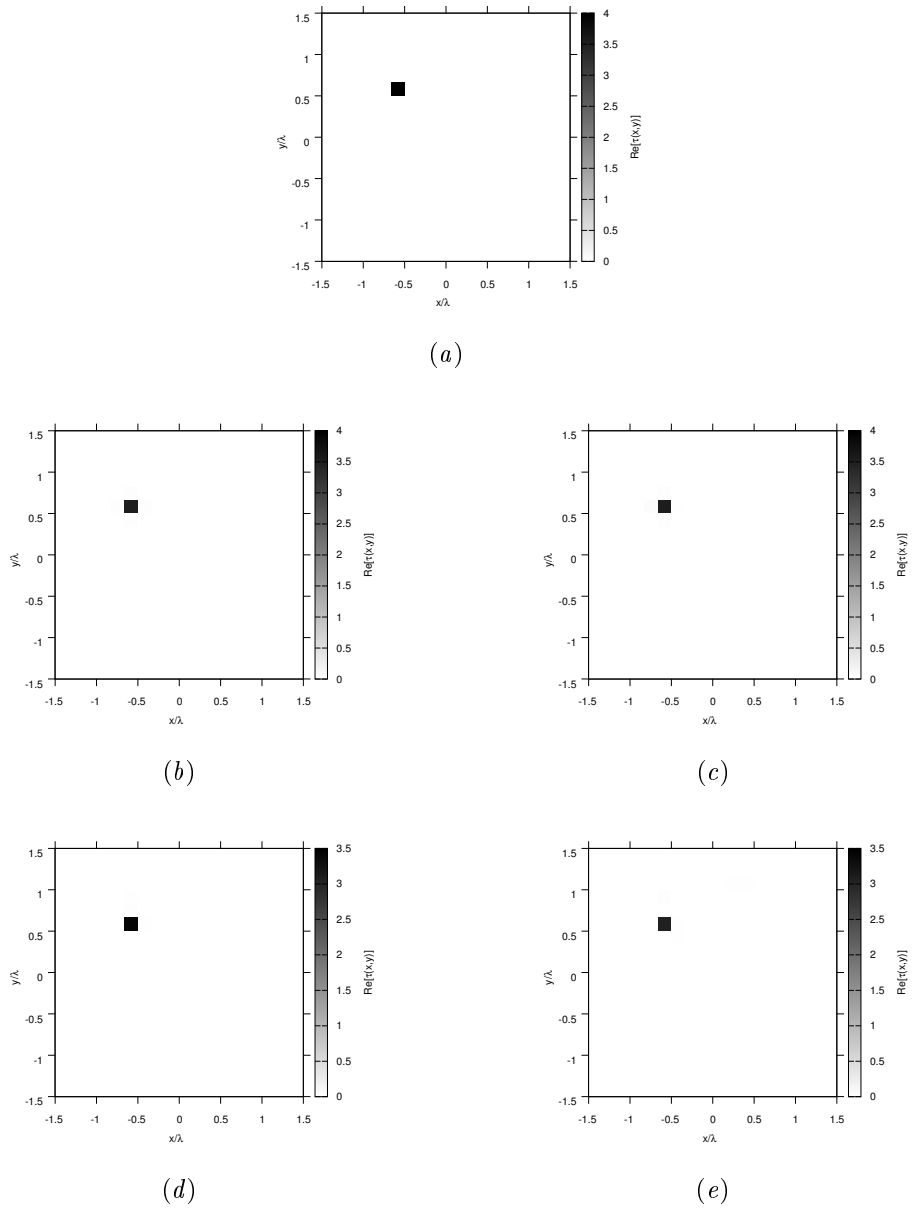

(a) (b) (c) (d) (e)

Figure 64. Actual object (a) and BCS reconstructed object for (b) Noiseless case, (c) $SNR = 20$ [dB] , (d) $SNR = 10$ [dB] , (e) $SNR = 5$ [dB].

RESULTS: Error Figures

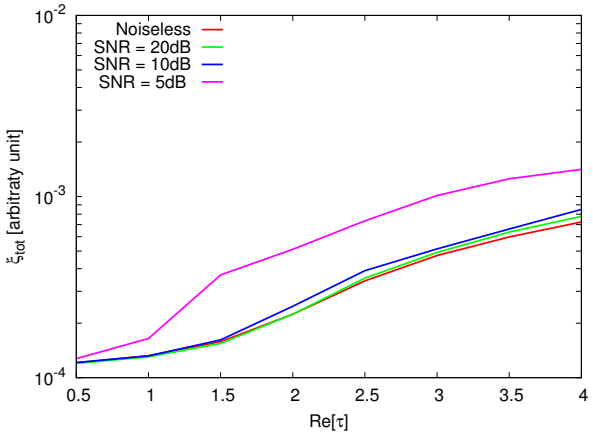

(a)

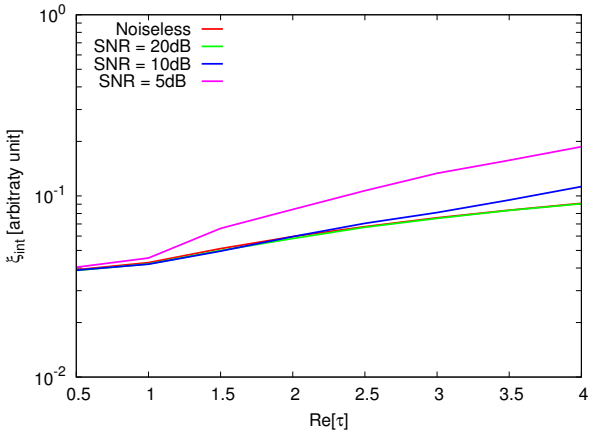

(b)

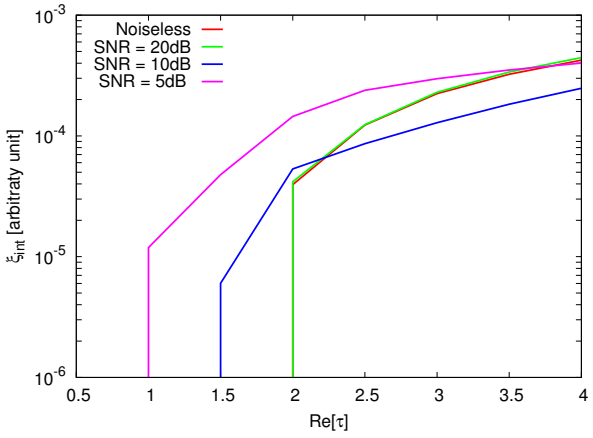

(c)

Figure 65. Behaviour of error figures as a function of ε_r, for different SNR values: (a) total error ξ_{tot}, (b) internal error ξ_{int}, (c) external error ξ_{ext}.

TEST CASE: Two Square Cylinders $L = 0.16\lambda$

Goal: show the performances of BCS when dealing with a sparse scatterer

- Number of Views: V
- Number of Measurements: M
- Number of Cells for the Inversion: N
- Number of Cells for the Direct solver: D
- Side of the investigation domain: L

Test Case Description

Direct solver:

- Square domain divided in $\sqrt{D} \times \sqrt{D}$ cells
- Domain side: $L = 3\lambda$
- $D = 1296$ (discretization for the direct solver: $< \lambda/10$)

Investigation domain:

- Square domain divided in $\sqrt{N} \times \sqrt{N}$ cells
- $L = 3\lambda$
- $2ka = 2 \times \frac{2\pi}{\lambda} \times \frac{L\sqrt{2}}{2} = 6\pi\sqrt{2} = 26.65$
- $\#DOF = \frac{(2ka)^2}{2} = \frac{(2 \times \frac{2\pi}{\lambda} \times \frac{L\sqrt{2}}{2})^2}{2} = 4\pi^2 \left(\frac{L}{\lambda}\right)^2 = 4\pi^2 \times 9 \approx 355.3$
- N scelto in modo da essere vicino a $\#DOF$: $N = 324$ (18×18)

Measurement domain:

- Measurement points taken on a circle of radius $\rho = 3\lambda$
- Full-aspect measurements
- $M \approx 2ka \rightarrow M = 27$

Sources:

- Plane waves
- $V \approx 2ka \rightarrow V = 27$
- Amplitude: $A = 1$
- Frequency: 300 MHz $(\lambda = 1)$

Object:

- Two square cylinders of side $\frac{\lambda}{6} = 0.1667$
- $\varepsilon_r \in \{1.5, 2.0, 2.5, 3.0, 3.5, 4.0, 4.5, 5.0\}$ (one square), $\varepsilon_r = 1.5$ (one square)
- $\sigma = 0$ [S/m]

BCS parameters:

- Gamma prior on noise variance parameters: $a = 1 \times 10^{+1}$, $b = 5 \times 10^{-3}$
- Convergenze parameter: $\tau = 1.0 \times 10^{-8}$

RESULTS: $\varepsilon_r = 1.5$

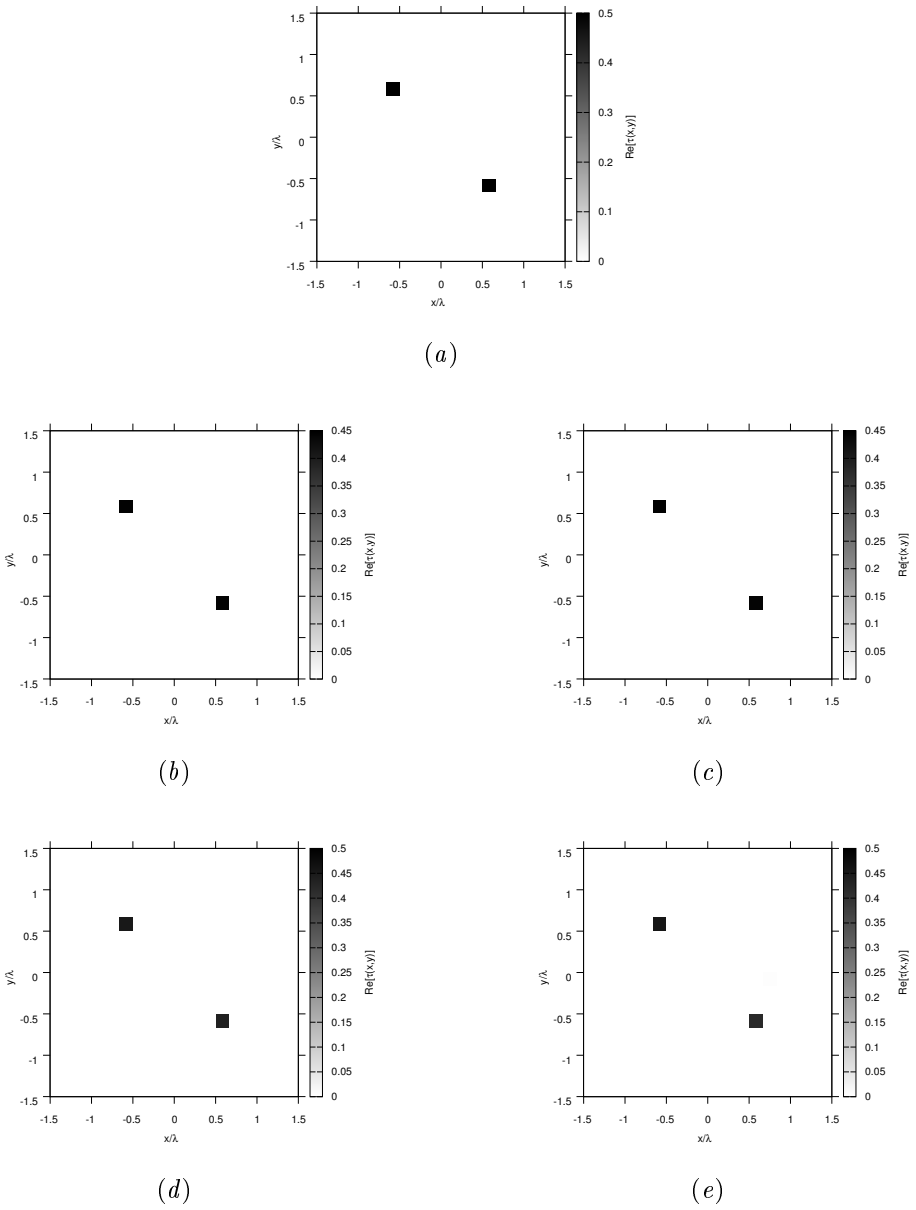

(a) (b) (c) (d) (e)

Figure 66. Actual object (a) and BCS reconstructed object for (b) Noiseless case, (c) $SNR = 20$ [dB] , (d) $SNR = 10$ [dB] , (e) $SNR = 5$ [dB].

RESULTS: $\varepsilon_r = 2.0$

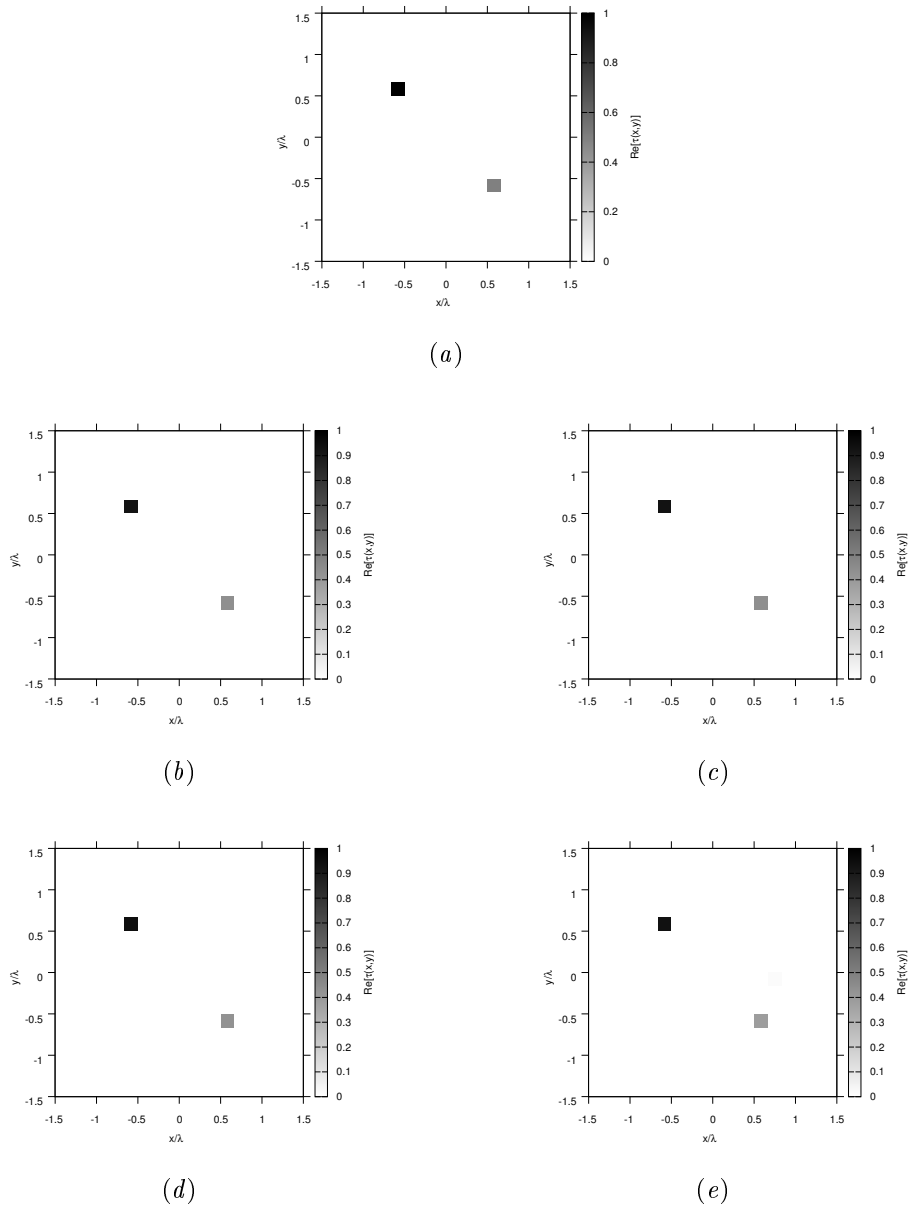

(a) (b) (c) (d) (e)

Figure 67. Actual object (a) and BCS reconstructed object for (b) Noiseless case, (c) $SNR = 20$ [dB] , (d) $SNR = 10$ [dB] , (e) $SNR = 5$ [dB].

RESULTS: $\varepsilon_r = 5.0$

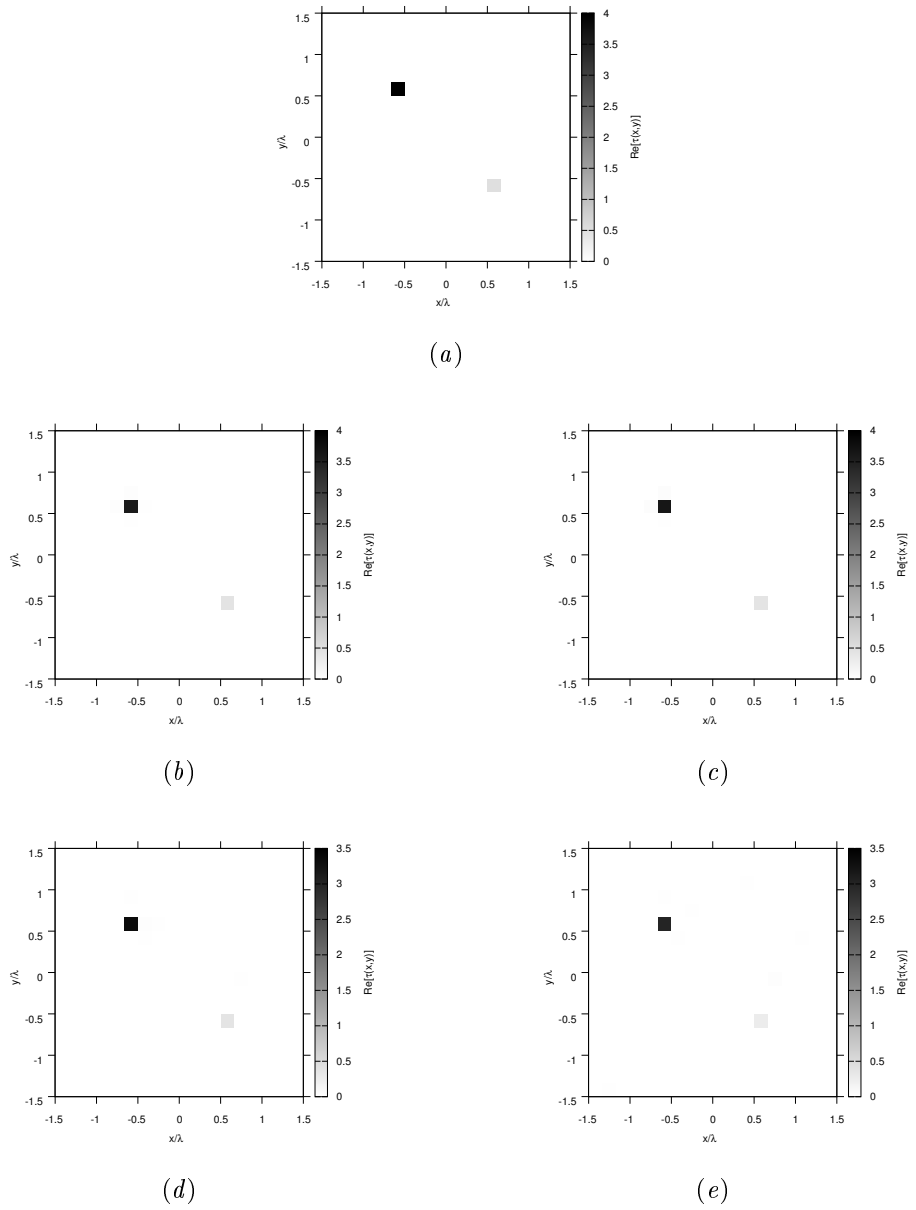

Figure 68. Actual object (a) and BCS reconstructed object for (b) Noiseless case, (c) $SNR = 20$ [dB] , (d) $SNR = 10$ [dB] , (e) $SNR = 5$ [dB].

RESULTS: Error Figures

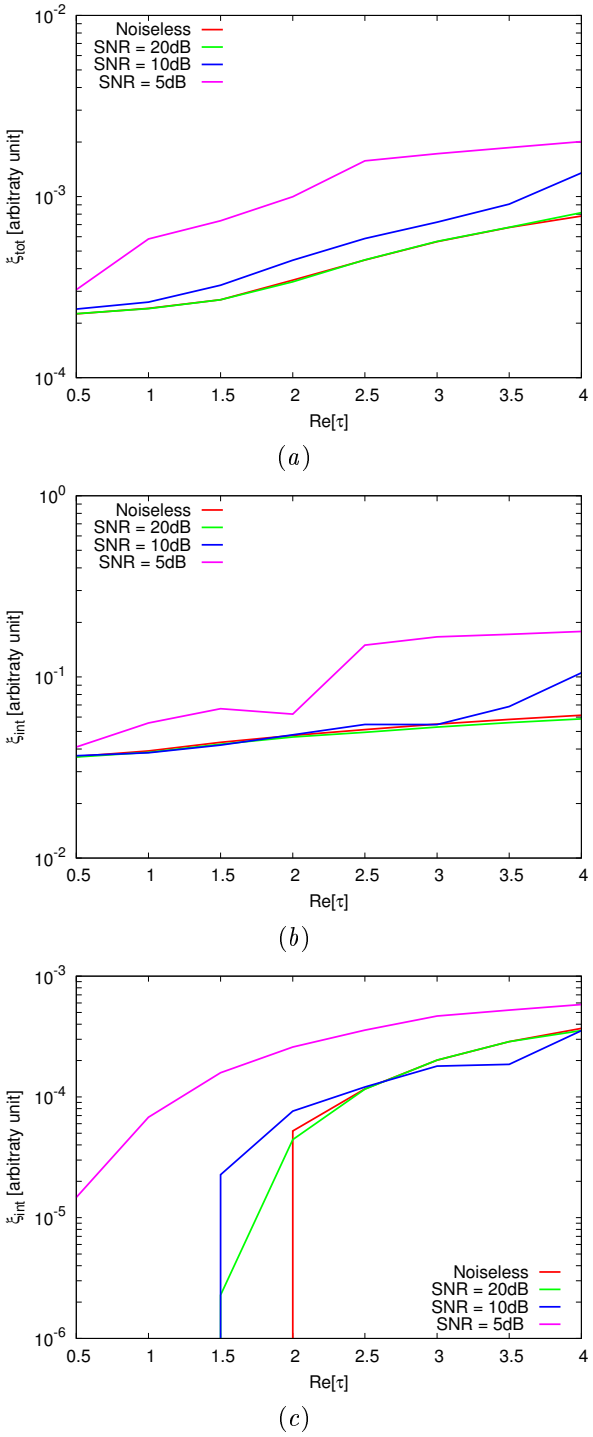

Figure 69. Behaviour of error figures as a function of ε_r, for different SNR values: (a) total error ξ_{tot}, (b) internal error ξ_{int}, (c) external error ξ_{ext}.

TEST CASE: Square Cylinder $L = 0.33\lambda$

Goal: show the performances of BCS when dealing with a sparse scatterer

- Number of Views: V
- Number of Measurements: M
- Number of Cells for the Inversion: N
- Number of Cells for the Direct solver: D
- Side of the investigation domain: L

Test Case Description

Direct solver:

- Square domain divided in $\sqrt{D} \times \sqrt{D}$ cells
- Domain side: $L = 3\lambda$
- $D = 1296$ (discretization for the direct solver: $< \lambda/10$)

Investigation domain:

- Square domain divided in $\sqrt{N} \times \sqrt{N}$ cells
- $L = 3\lambda$
- $2ka = 2 \times \frac{2\pi}{\lambda} \times \frac{L\sqrt{2}}{2} = 6\pi\sqrt{2} = 26.65$
- $\#DOF = \frac{(2ka)^2}{2} = \frac{(2 \times \frac{2\pi}{\lambda} \times \frac{L\sqrt{2}}{2})^2}{2} = 4\pi^2 \left(\frac{L}{\lambda}\right)^2 = 4\pi^2 \times 9 \approx 355.3$
- N scelto in modo da essere vicino a $\#DOF$: $N = 324$ (18×18)

Measurement domain:

- Measurement points taken on a circle of radius $\rho = 3\lambda$
- Full-aspect measurements
- $M \approx 2ka \rightarrow M = 27$

Sources:

- Plane waves
- $V \approx 2ka \rightarrow V = 27$
- Amplitude: $A = 1$
- Frequency: 300 MHz $(\lambda = 1)$

Object:

- Square cylinder of side $\frac{\lambda}{3} = 0.33$
- $\varepsilon_r \in \{1.5, 2.0, 2.5, 3.0, 3.5, 4.0, 4.5, 5.0\}$
- $\sigma = 0$ [S/m]

BCS parameters:

- Gamma prior on noise variance parameters: $a = 1 \times 10^{+1}$, $b = 5 \times 10^{-3}$
- Convergenze parameter: $\tau = 1.0 \times 10^{-8}$

RESULTS: $\varepsilon_r = 1.5$

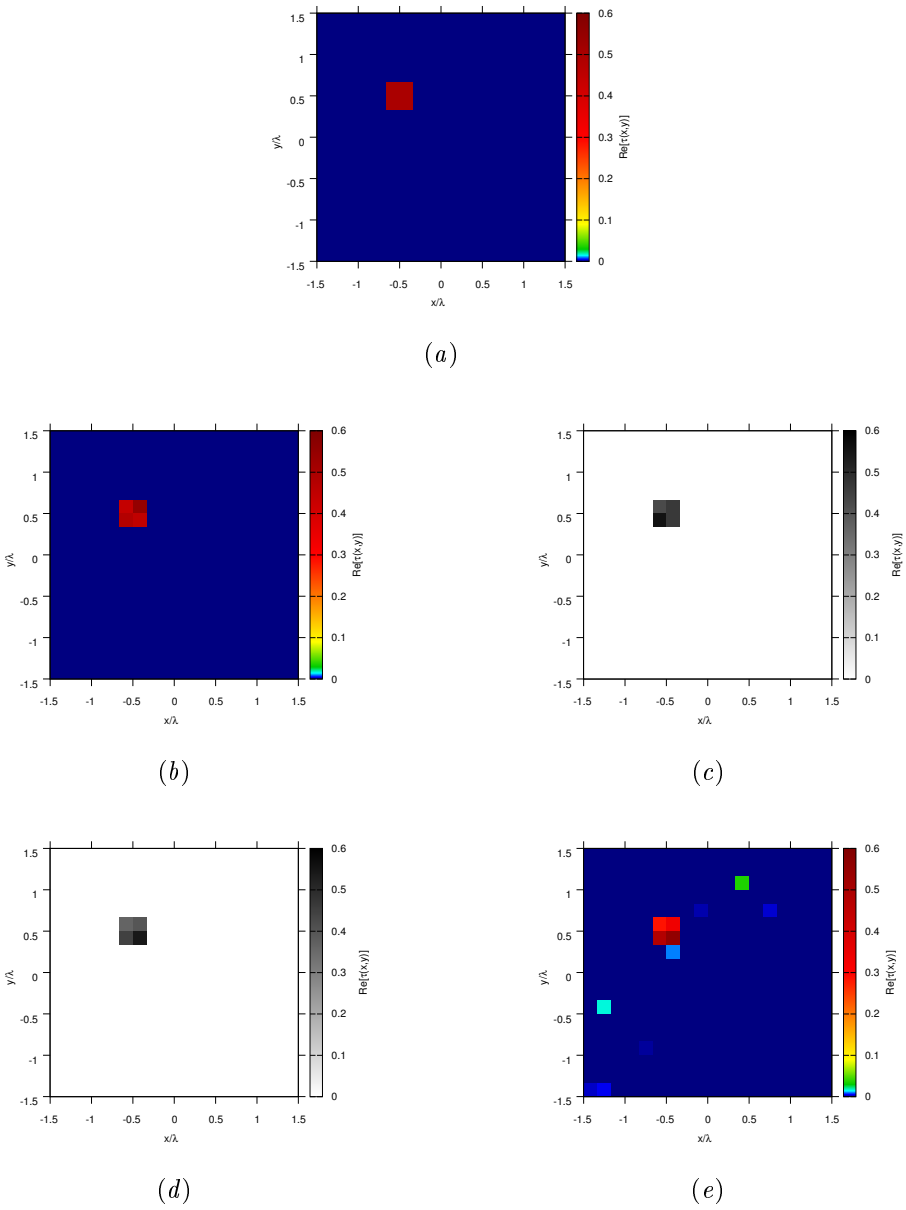

(a)

(b) (c)

(d) (e)

Figure 70. Actual object (a) and BCS reconstructed object for (b) Noiseless case, (c) $SNR = 20$ [dB] , (d) $SNR = 10$ [dB] , (e) $SNR = 5$ [dB].

RESULTS: $\varepsilon_r = 2.0$

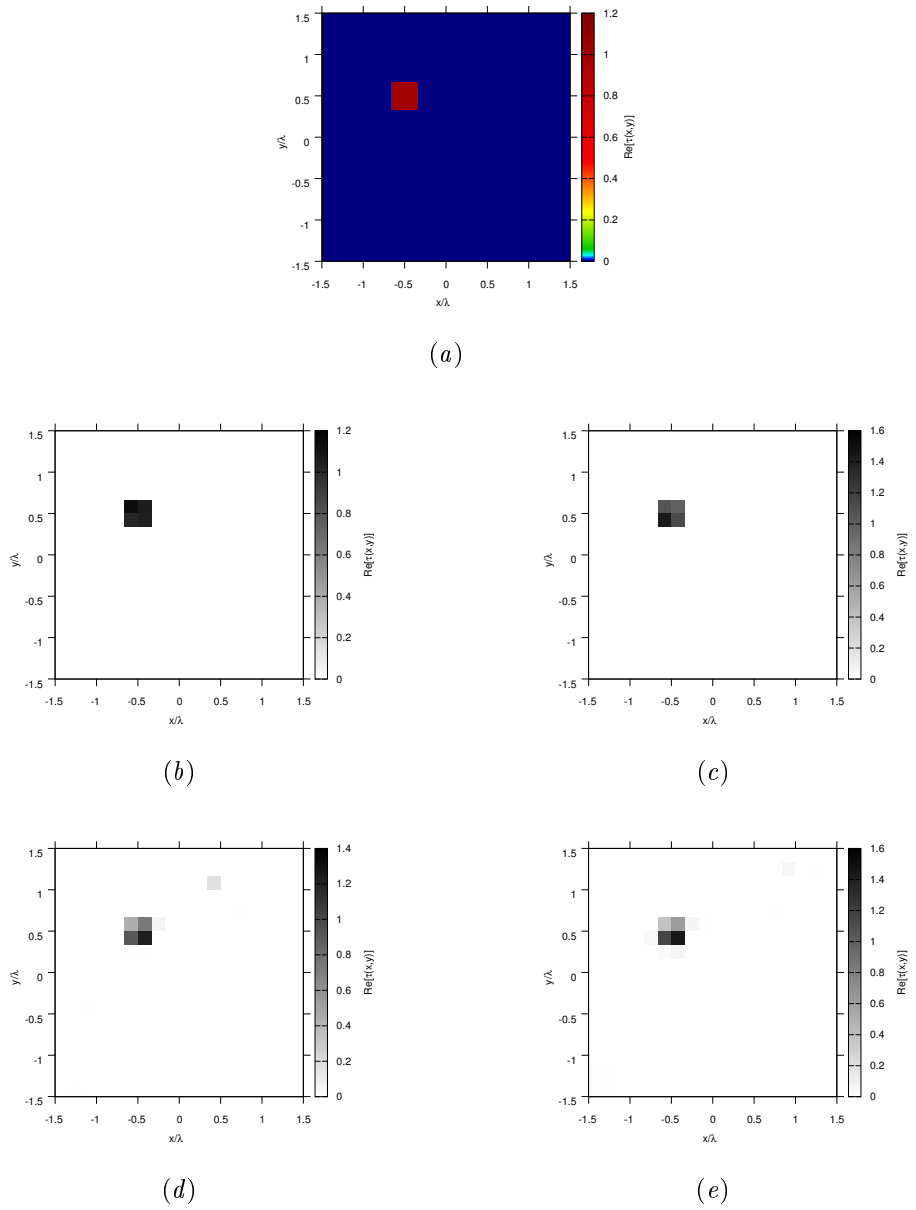

Figure 71. Actual object (a) and BCS reconstructed object for (b) Noiseless case, (c) $SNR = 20$ [dB] , (d) $SNR = 10$ [dB] , (e) $SNR = 5$ [dB].

RESULTS: $\varepsilon_r = 3.0$

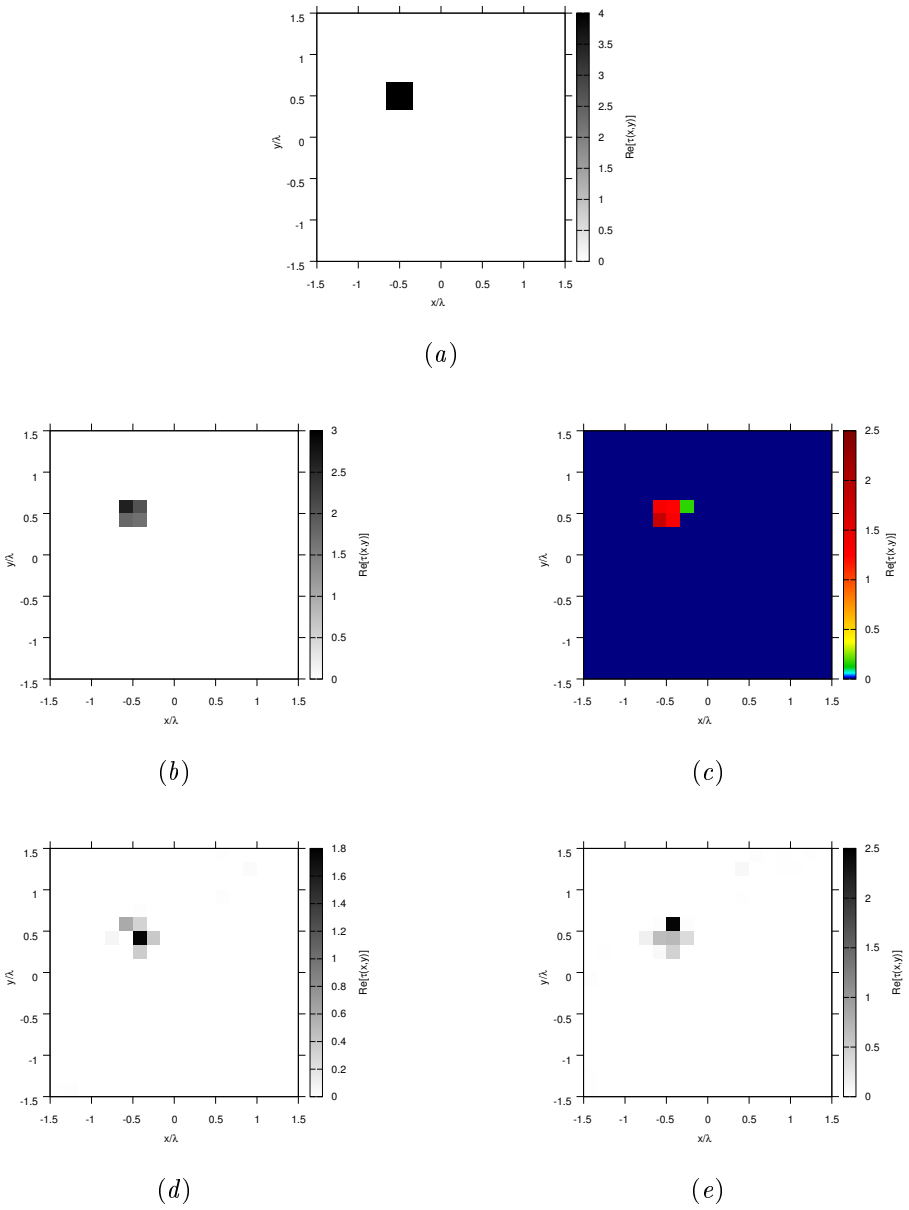

(a)

(b)

(c)

(d)

(e)

Figure 72. Actual object (a) and BCS reconstructed object for (b) Noiseless case, (c) $SNR = 20$ [dB] , (d) $SNR = 10$ [dB] , (e) $SNR = 5$ [dB].

RESULTS: Error Figures

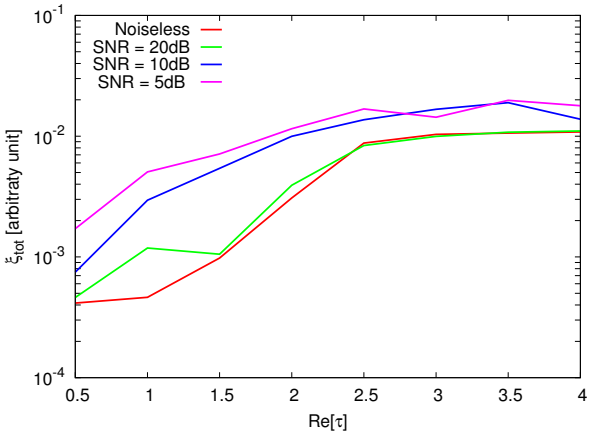

(a)

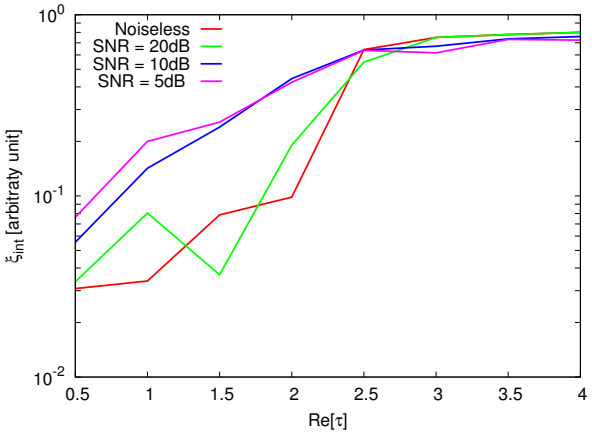

(b)

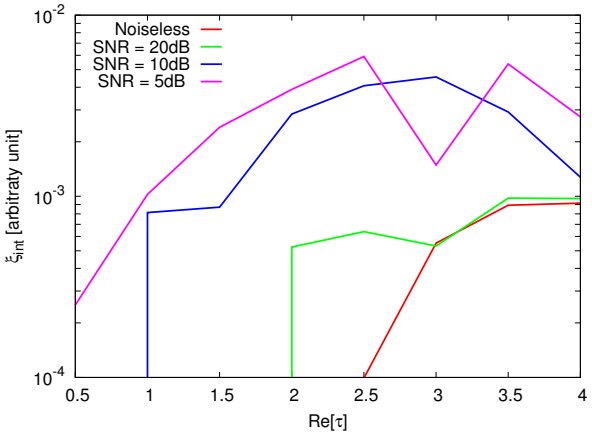

(c)

Figure 73. Behaviour of error figures as a function of ε_r, for different SNR values: (a) total error ξ_{tot}, (b) internal error ξ_{int}, (c) external error ξ_{ext}.

TEST CASE: Cross-Shaped Cylinder

Goal: show the performances of BCS when dealing with a sparse scatterer

- Number of Views: V
- Number of Measurements: M
- Number of Cells for the Inversion: N
- Number of Cells for the Direct solver: D
- Side of the investigation domain: L

Test Case Description

Direct solver:

- Square domain divided in $\sqrt{D} \times \sqrt{D}$ cells
- Domain side: $L = 3\lambda$
- $D = 1296$ (discretization for the direct solver: $< \lambda/10$)

Investigation domain:

- Square domain divided in $\sqrt{N} \times \sqrt{N}$ cells
- $L = 3\lambda$
- $2ka = 2 \times \frac{2\pi}{\lambda} \times \frac{L\sqrt{2}}{2} = 6\pi\sqrt{2} = 26.65$
- $\#DOF = \frac{(2ka)^2}{2} = \frac{(2 \times \frac{2\pi}{\lambda} \times \frac{L\sqrt{2}}{2})^2}{2} = 4\pi^2 \left(\frac{L}{\lambda}\right)^2 = 4\pi^2 \times 9 \approx 355.3$
- N scelto in modo da essere vicino a $\#DOF$: $N = 324$ (18×18)

Measurement domain:

- Measurement points taken on a circle of radius $\rho = 3\lambda$
- Full-aspect measurements
- $M \approx 2ka \rightarrow M = 27$

Sources:

- Plane waves
- $V \approx 2ka \rightarrow V = 27$
- Amplitude: $A = 1$
- Frequency: 300 MHz $(\lambda = 1)$

Object:

- Cross-shaped cylinder
- $\varepsilon_r \in \{1.5, 2.0, 2.5, 3.0, 3.5, 4.0, 4.5, 5.0\}$
- $\sigma = 0$ [S/m]

BCS parameters:

- Gamma prior on noise variance parameters: $a = 1 \times 10^{+1}$, $b = 5 \times 10^{-3}$
- Convergenze parameter: $\tau = 1.0 \times 10^{-8}$

RESULTS: $\varepsilon_r = 1.5$

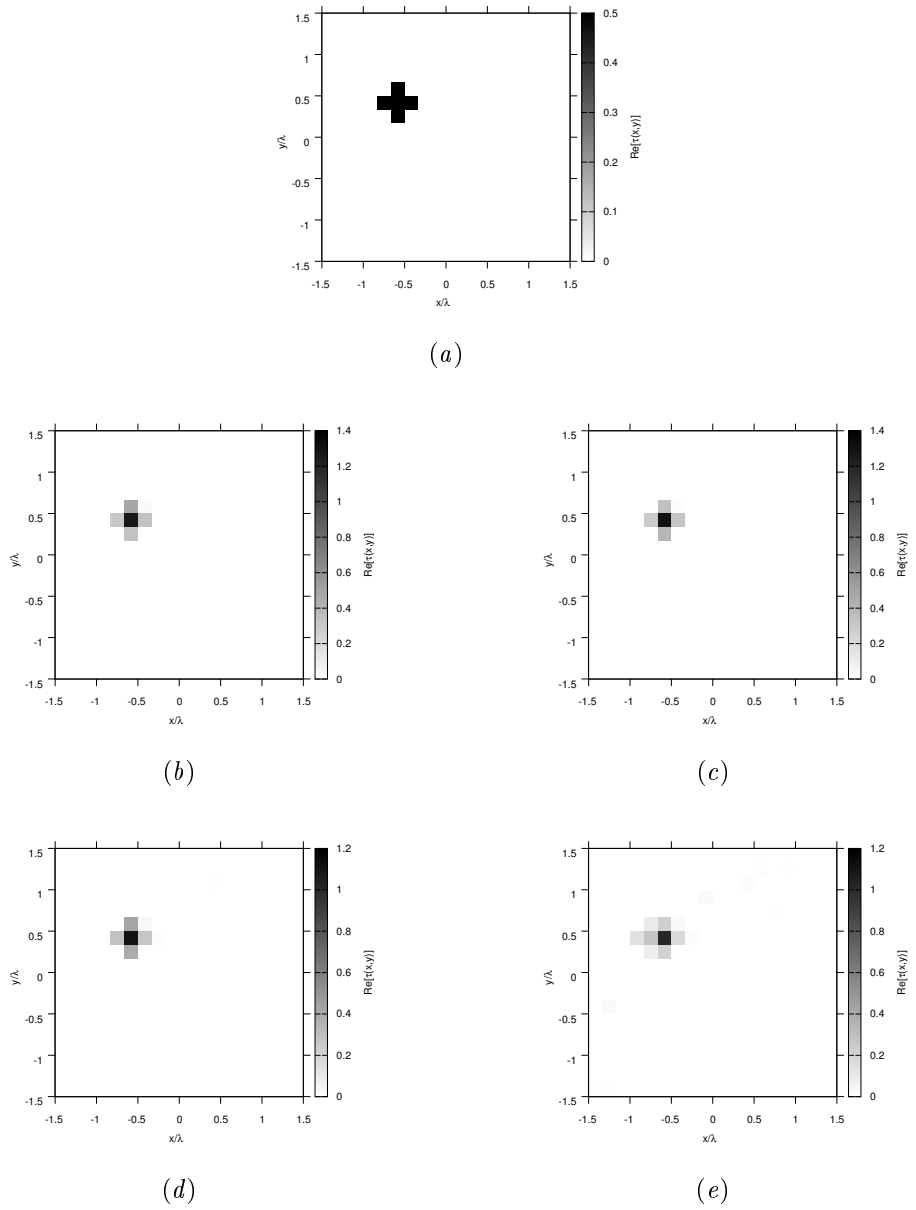

(a)

(b)

(c)

(d)

(e)

Figure 74. Actual object (a) and BCS reconstructed object for (b) Noiseless case, (c) $SNR = 20$ [dB] , (d) $SNR = 10$ [dB] , (e) $SNR = 5$ [dB].

RESULTS: $\varepsilon_r = 2.0$

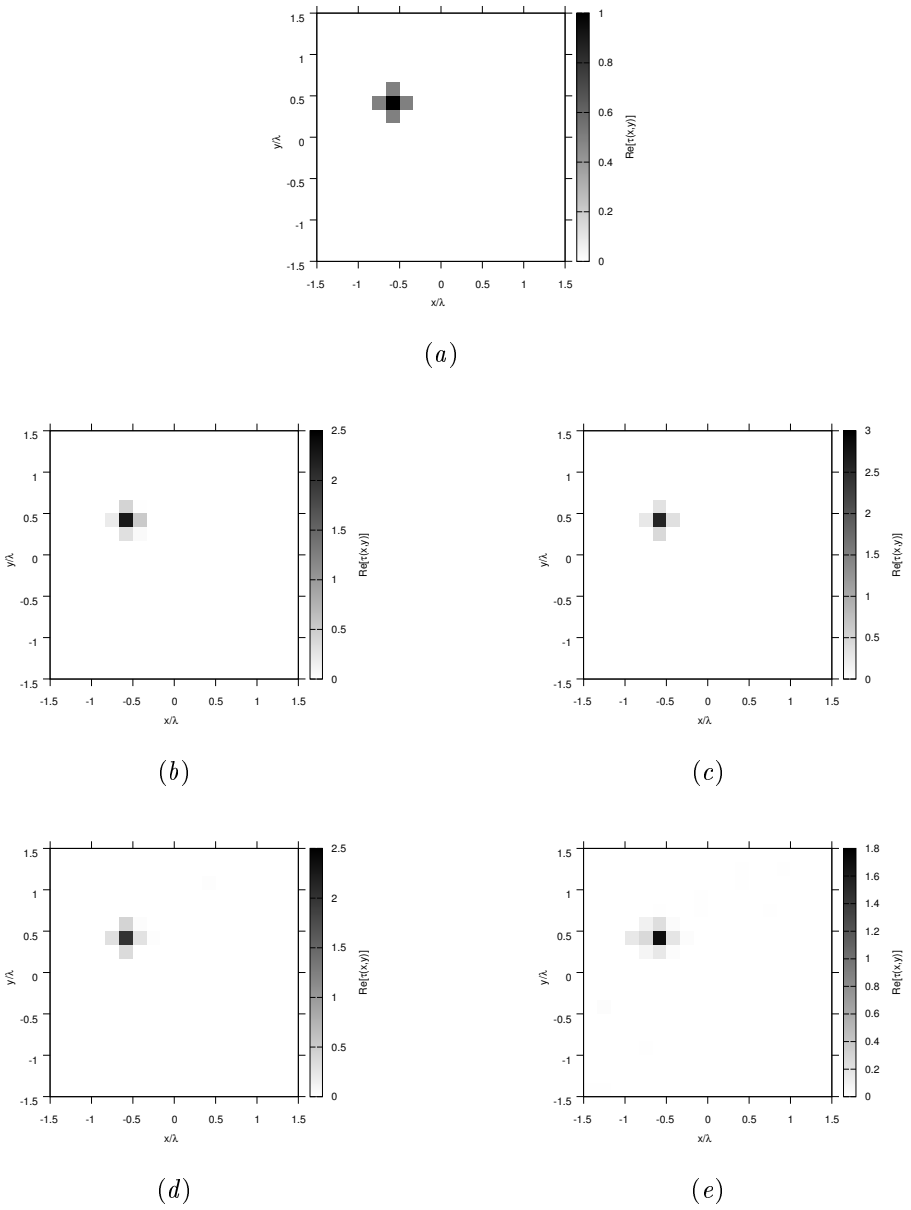

(a)

(b)

(c)

(d)

(e)

Figure 75. Actual object (a) and BCS reconstructed object for (b) Noiseless case, (c) $SNR = 20$ [dB] , (d) $SNR = 10$ [dB] , (e) $SNR = 5$ [dB].

RESULTS: $\varepsilon_r = 3.0$

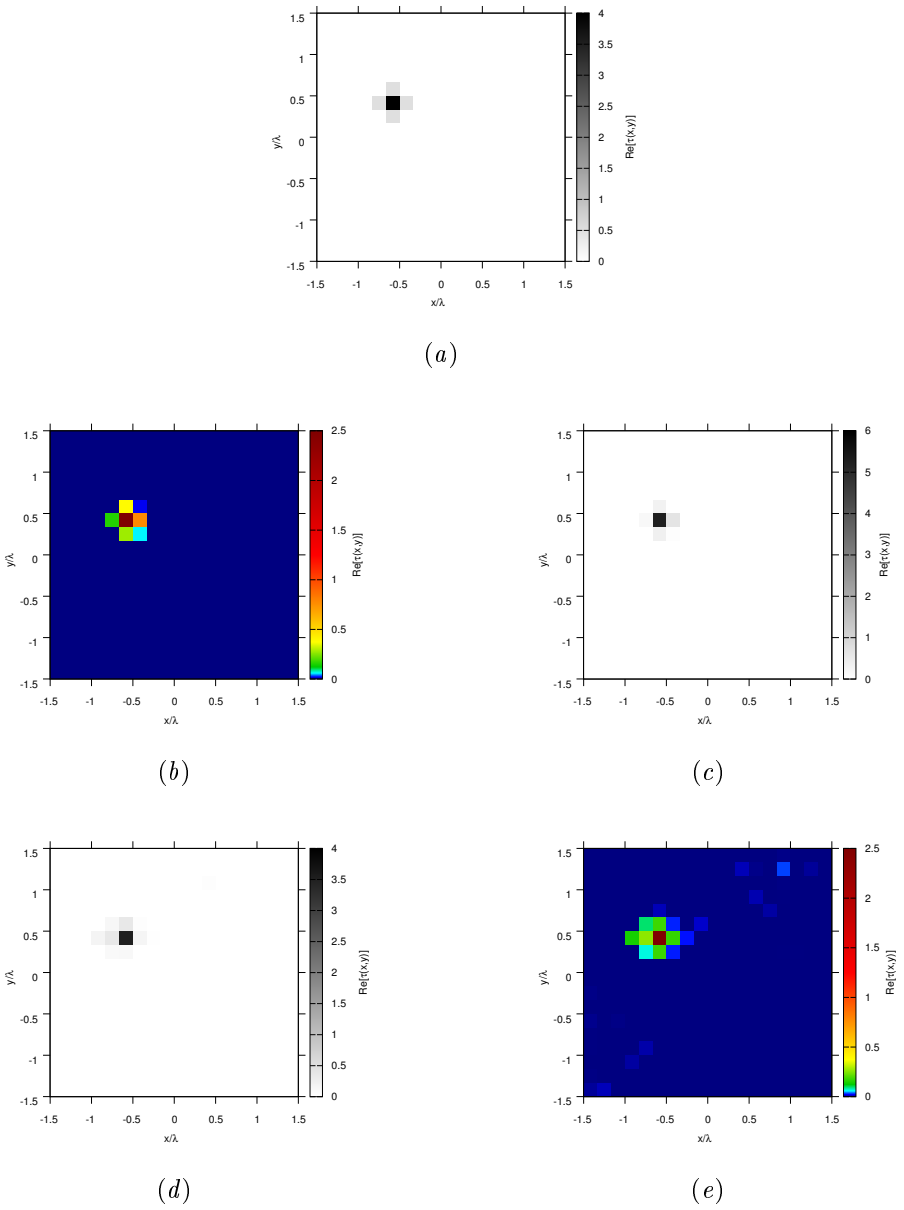

(a)

(b)

(c)

(d)

(e)

Figure 76. Actual object (a) and BCS reconstructed object for (b) Noiseless case, (c) $SNR = 20$ [dB] , (d) $SNR = 10$ [dB] , (e) $SNR = 5$ [dB].

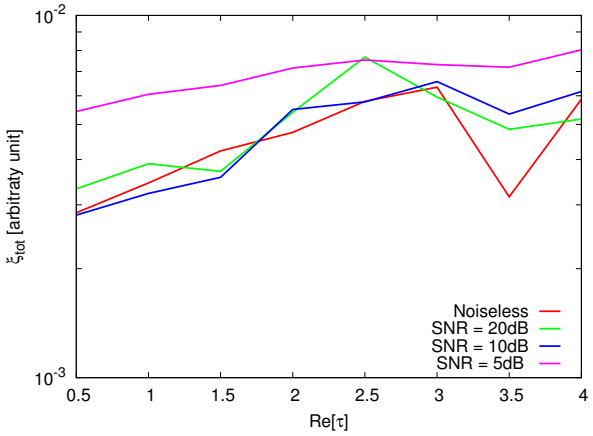

(a)

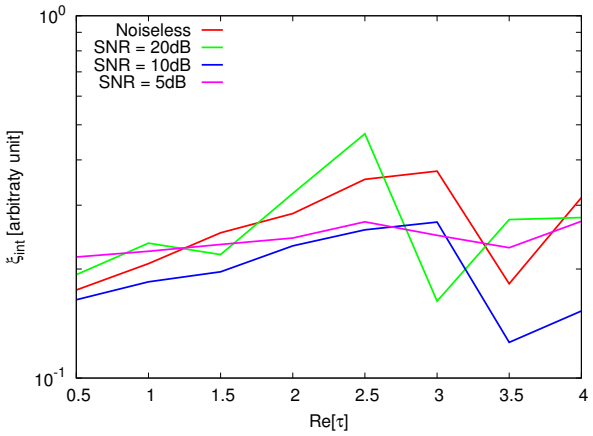

(b)

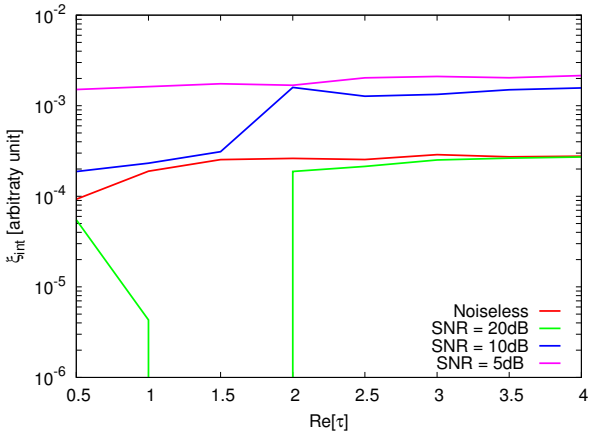

(c)

Figure 77. Behaviour of error figures as a function of ε_r, for different SNR values: (a) total error ξ_{tot}, (b) internal error ξ_{int}, (c) external error ξ_{ext}.

TEST CASE: L-Shaped Cylinder

Goal: show the performances of BCS when dealing with a sparse scatterer

- Number of Views: V
- Number of Measurements: M
- Number of Cells for the Inversion: N
- Number of Cells for the Direct solver: D
- Side of the investigation domain: L

Test Case Description

Direct solver:

- Square domain divided in $\sqrt{D} \times \sqrt{D}$ cells
- Domain side: $L = 3\lambda$
- $D = 1296$ (discretization for the direct solver: $< \lambda/10$)

Investigation domain:

- Square domain divided in $\sqrt{N} \times \sqrt{N}$ cells
- $L = 3\lambda$
- $2ka = 2 \times \frac{2\pi}{\lambda} \times \frac{L\sqrt{2}}{2} = 6\pi\sqrt{2} = 26.65$
- $\#DOF = \frac{(2ka)^2}{2} = \frac{(2 \times \frac{2\pi}{\lambda} \times \frac{L\sqrt{2}}{2})^2}{2} = 4\pi^2 \left(\frac{L}{\lambda}\right)^2 = 4\pi^2 \times 9 \approx 355.3$
- N scelto in modo da essere vicino a $\#DOF$: $N = 324$ (18×18)

Measurement domain:

- Measurement points taken on a circle of radius $\rho = 3\lambda$
- Full-aspect measurements
- $M \approx 2ka \rightarrow M = 27$

Sources:

- Plane waves
- $V \approx 2ka \rightarrow V = 27$
- Amplitude $A = 1$
- Frequency: 300 MHz $(\lambda = 1)$

Object:

- L-shaped cylinder
- $\varepsilon_r \in \{1.5, 2.0, 2.5, 3.0, 3.5, 4.0, 4.5, 5.0\}$
- $\sigma = 0$ [S/m]

BCS parameters:

- Gamma prior on noise variance parameters: $a = 1 \times 10^{+1}$, $b = 5 \times 10^{-3}$
- Convergenze parameter: $\tau = 1.0 \times 10^{-8}$

RESULTS: $\varepsilon_r = 1.5$

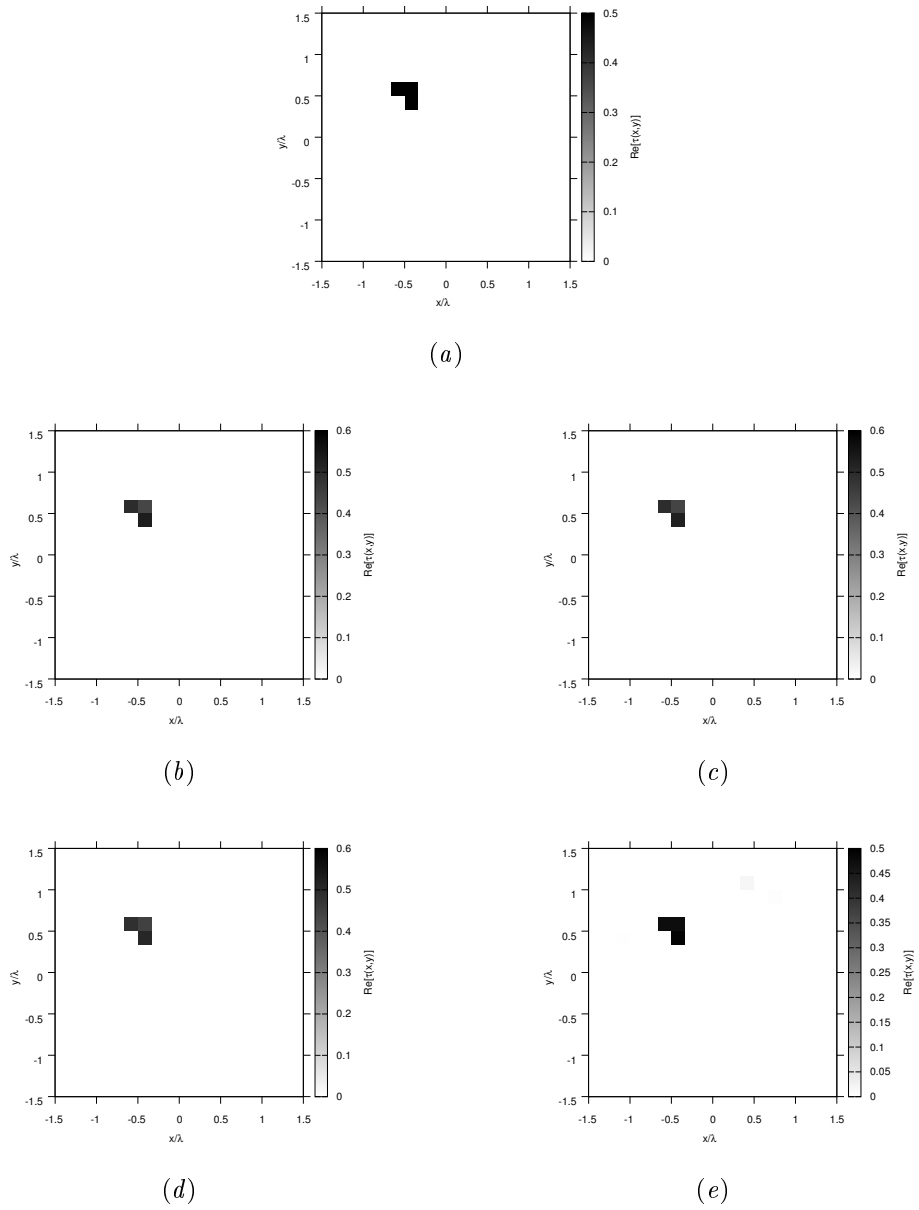

(a)

(b)

(c)

(d)

(e)

Figure 78. Actual object (a) and BCS reconstructed object for (b) Noiseless case, (c) $SNR = 20$ [dB] , (d) $SNR = 10$ [dB] , (e) $SNR = 5$ [dB].

RESULTS: $\varepsilon_r = 2.0$

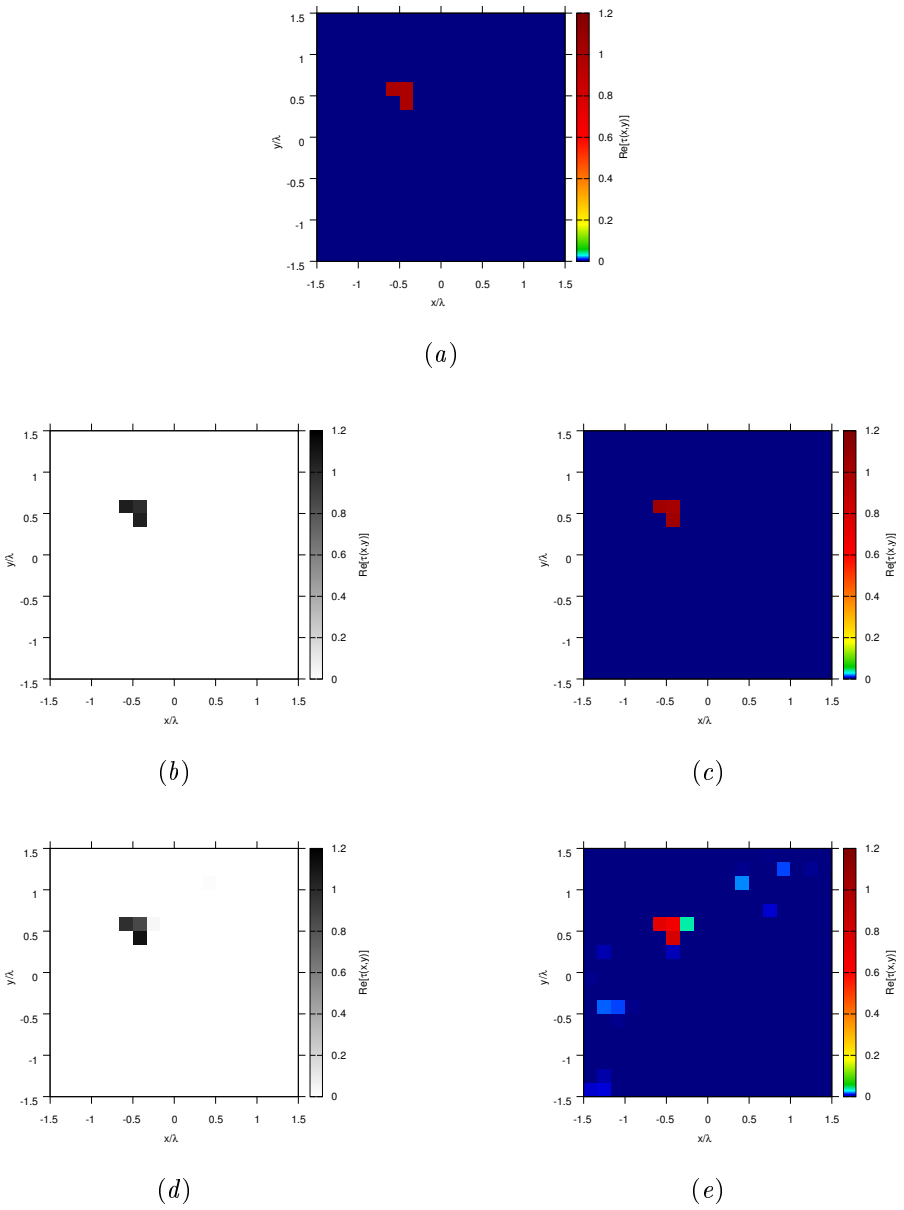

(a)

(b)

(c)

(d)

(e)

Figure 79. Actual object (a) and BCS reconstructed object for (b) Noiseless case, (c) $SNR = 20$ [dB] , (d) $SNR = 10$ [dB] , (e) $SNR = 5$ [dB].

RESULTS: $\varepsilon_r = 3.0$

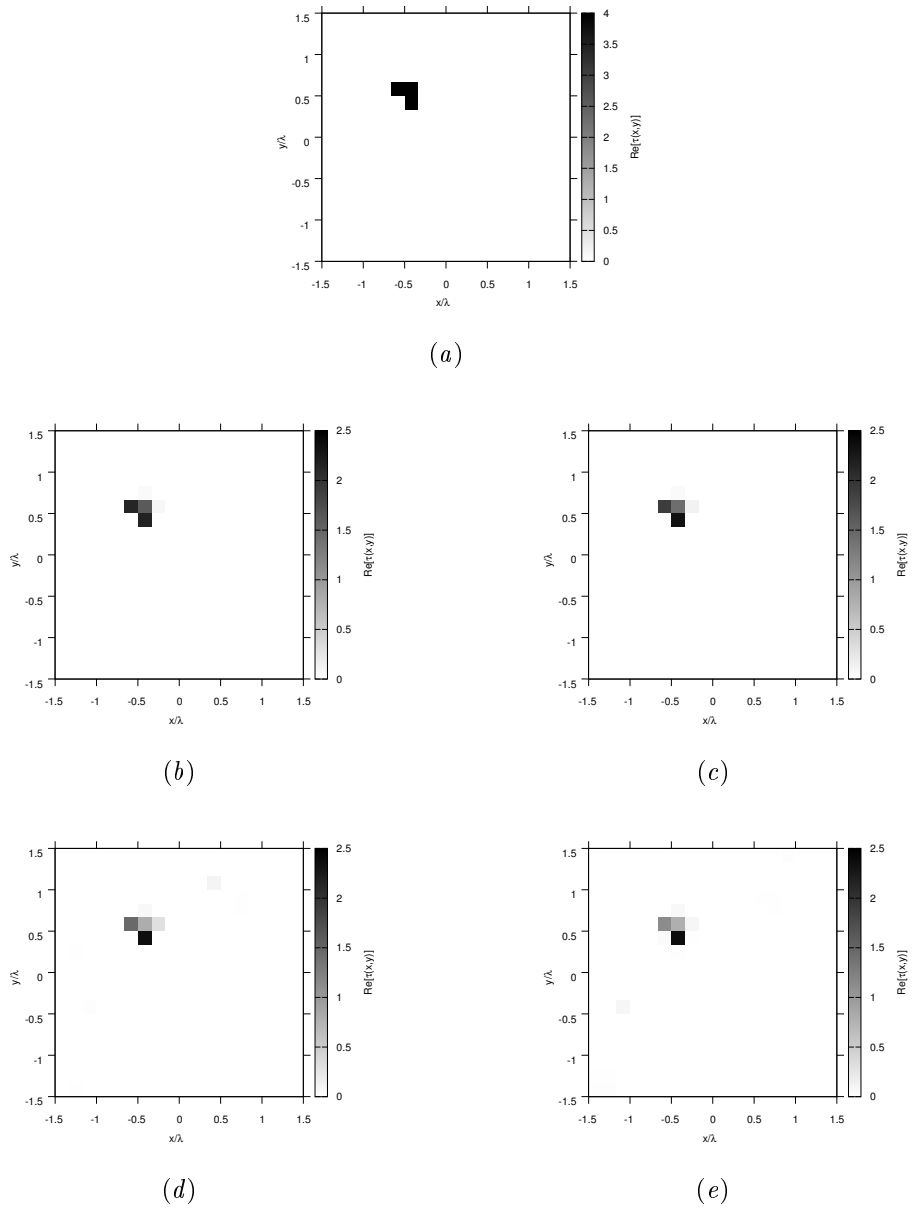

(a) (b) (c) (d) (e)

Figure 80. Actual object (a) and BCS reconstructed object for (b) Noiseless case, (c) $SNR = 20$ [dB] , (d) $SNR = 10$ [dB] , (e) $SNR = 5$ [dB].

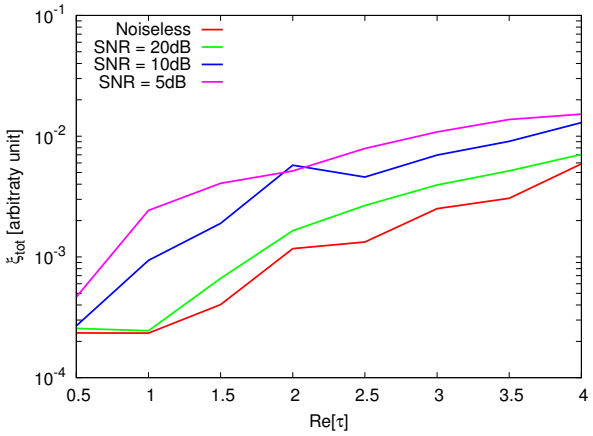

(a)

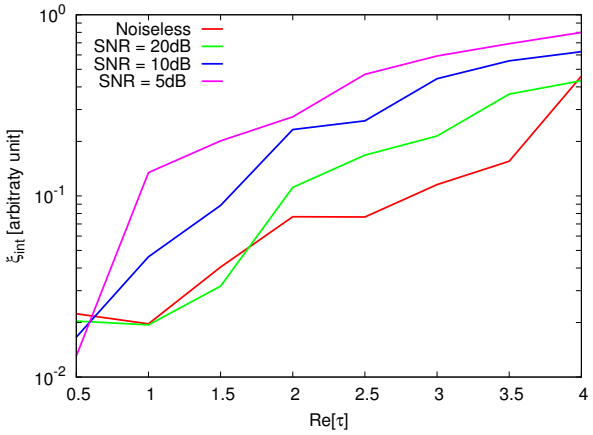

(b)

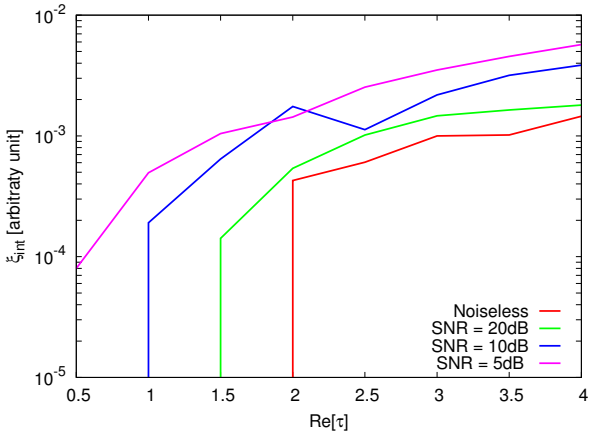

(c)

Figure 81. Behaviour of error figures as a function of ε_r, for different SNR values: (a) total error ξ_{tot}, (b) internal error ξ_{int}, (c) external error ξ_{ext}.

TEST CASE: Inhomogeneous L-Shaped Cylinder

Goal: show the performances of BCS when dealing with a sparse scatterer

- Number of Views: V
- Number of Measurements: M
- Number of Cells for the Inversion: N
- Number of Cells for the Direct solver: D
- Side of the investigation domain: L

Test Case Description

Direct solver:

- Square domain divided in $\sqrt{D} \times \sqrt{D}$ cells
- Domain side: $L = 3\lambda$
- $D = 1296$ (discretization for the direct solver: $< \lambda/10$)

Investigation domain:

- Square domain divided in $\sqrt{N} \times \sqrt{N}$ cells
- $L = 3\lambda$
- $2ka = 2 \times \frac{2\pi}{\lambda} \times \frac{L\sqrt{2}}{2} = 6\pi\sqrt{2} = 26.65$
- $\#DOF = \frac{(2ka)^2}{2} = \frac{(2 \times \frac{2\pi}{\lambda} \times \frac{L\sqrt{2}}{2})^2}{2} = 4\pi^2 \left(\frac{L}{\lambda}\right)^2 = 4\pi^2 \times 9 \approx 355.3$
- N scelto in modo da essere vicino a $\#DOF$: $N = 324$ (18×18)

Measurement domain:

- Measurement points taken on a circle of radius $\rho = 3\lambda$
- Full-aspect measurements
- $M \approx 2ka \rightarrow M = 27$

Sources:

- Plane waves
- $V \approx 2ka \rightarrow V = 27$
- Amplitude $A = 1$
- Frequency: 300 MHz $(\lambda = 1)$

Object:

- Inhomogeneous L-shaped cylinder
- $\varepsilon_r \in \{1.5, 2.0, 2.5, 3.0, 3.5, 4.0, 4.5, 5.0\}$
- $\sigma = 0$ [S/m]

BCS parameters:

- Gamma prior on noise variance parameters: $a = 1 \times 10^{+1}$, $b = 5 \times 10^{-3}$
- Convergenze parameter: $\tau = 1.0 \times 10^{-8}$

RESULTS: $\varepsilon_r = 1.5$

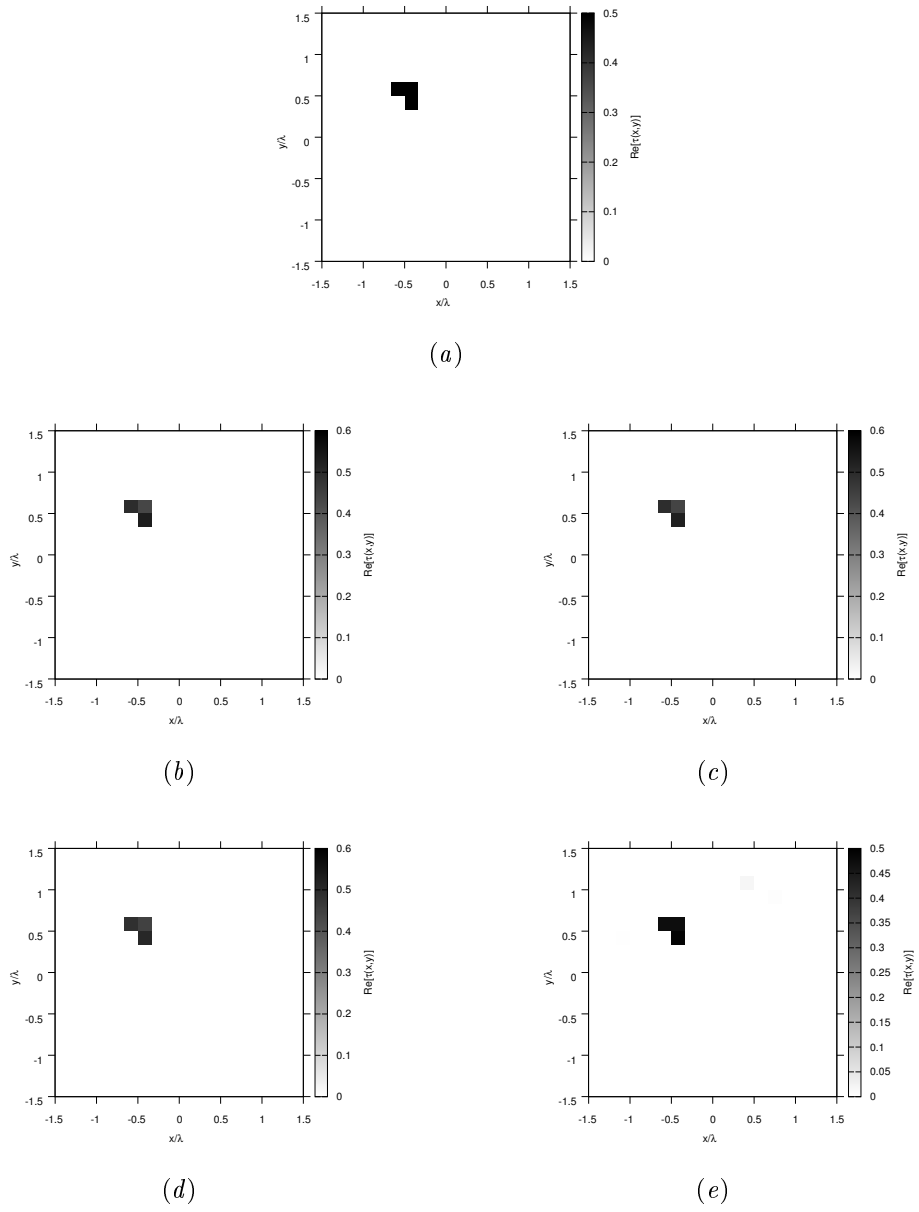

(a)

(b)

(c)

(d)

(e)

Figure 82. Actual object (a) and BCS reconstructed object for (b) Noiseless case, (c) $SNR = 20$ [dB] , (d) $SNR = 10$ [dB] , (e) $SNR = 5$ [dB].

RESULTS: $\varepsilon_r = 2.0$

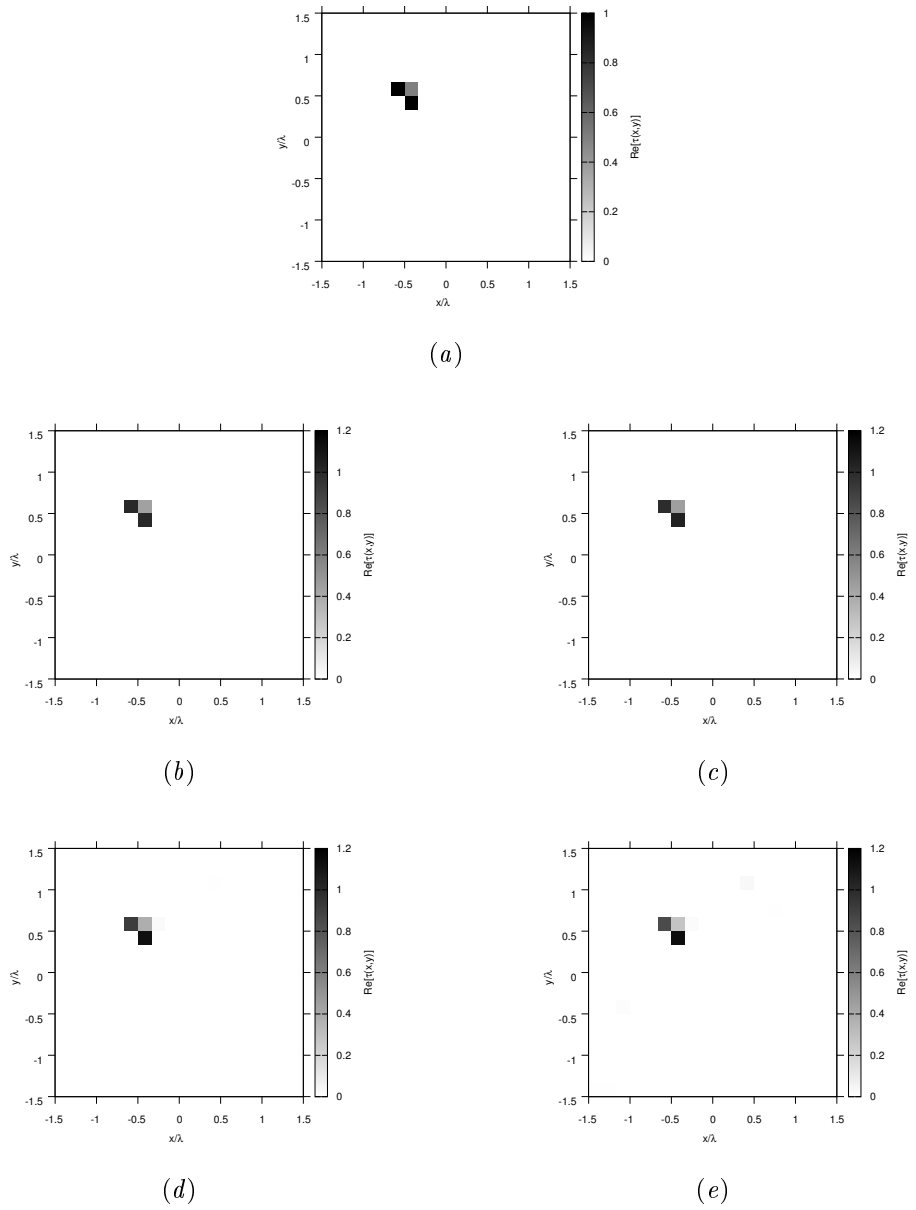

(a)

(b)

(c)

(d)

(e)

Figure 83. Actual object (a) and BCS reconstructed object for (b) Noiseless case, (c) $SNR = 20$ [dB] , (d) $SNR = 10$ [dB] , (e) $SNR = 5$ [dB].

RESULTS: $\varepsilon_r = 3.0$

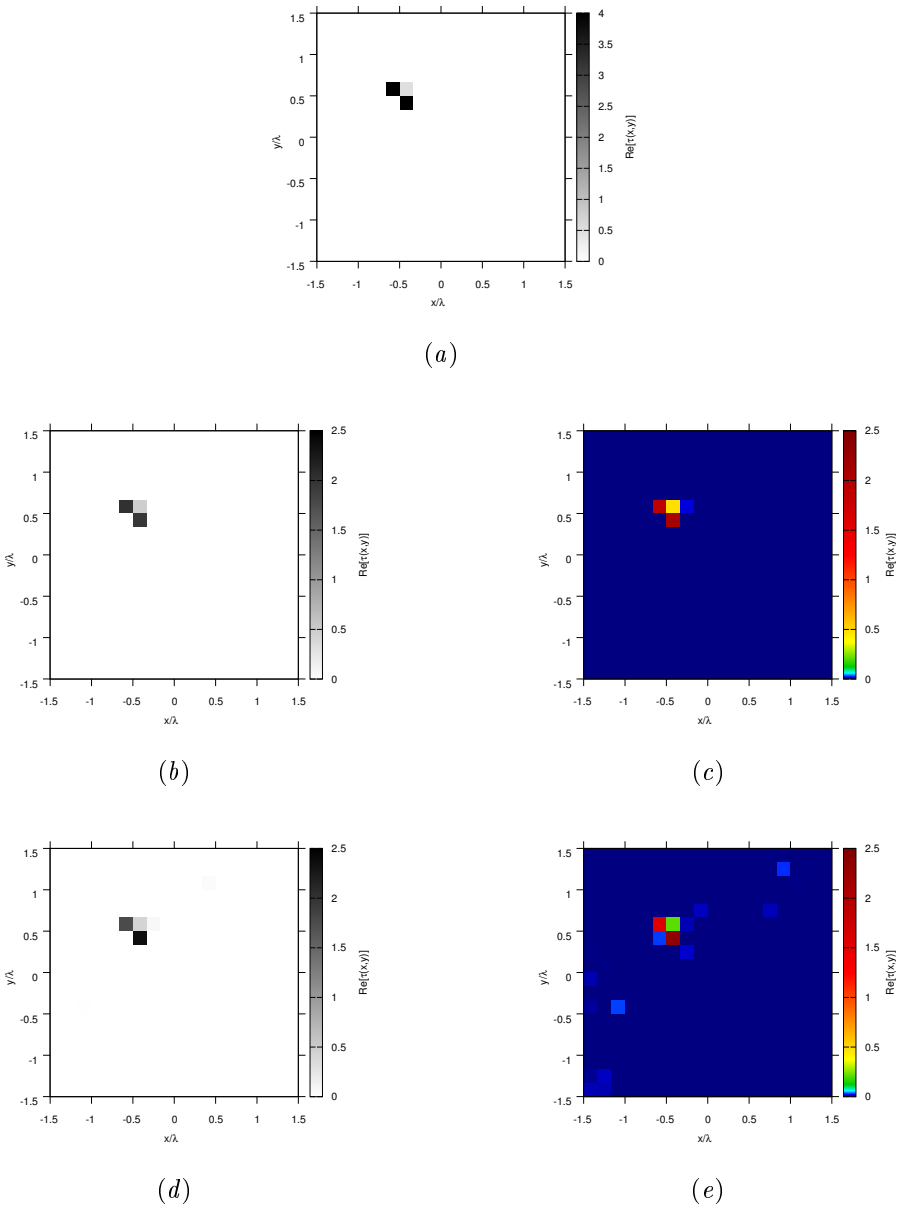

(a) (b) (c) (d) (e)

Figure 84. Actual object (a) and BCS reconstructed object for (b) Noiseless case, (c) $SNR = 20$ [dB] , (d) $SNR = 10$ [dB] , (e) $SNR = 5$ [dB].

RESULTS: $\varepsilon_r = 5.0$

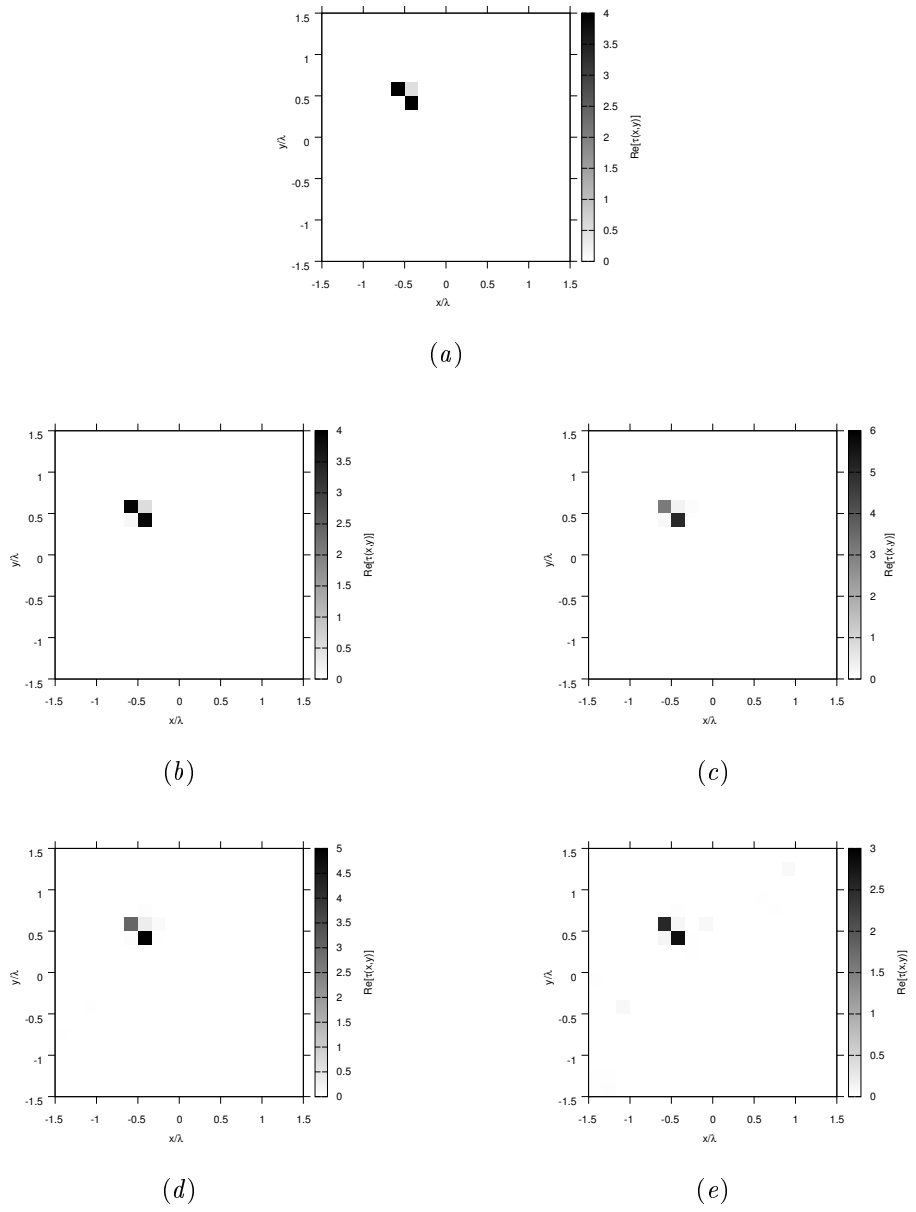

(a)

(b)

(c)

(d)

(e)

Figure 85. Actual object (a) and BCS reconstructed object for (b) Noiseless case, (c) $SNR = 20$ [dB] , (d) $SNR = 10$ [dB] , (e) $SNR = 5$ [dB].

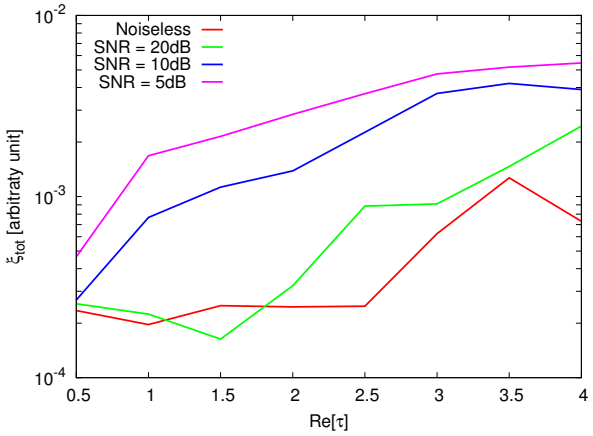

(a)

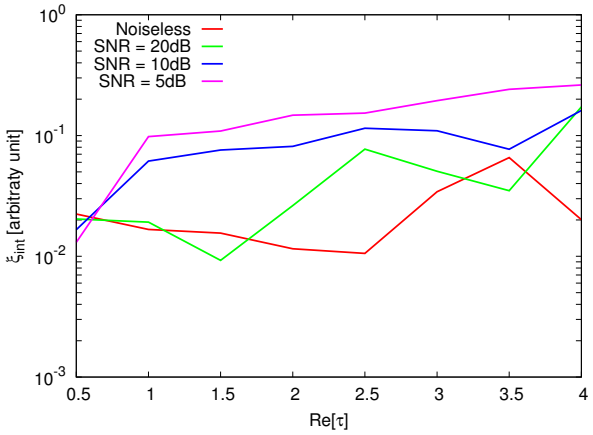

(b)

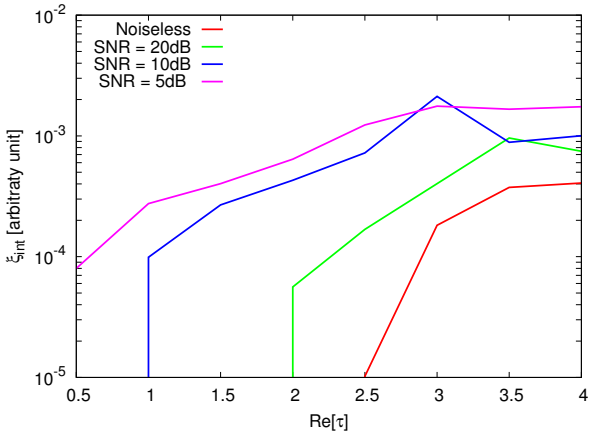

(c)

Figure 86. Behaviour of error figures as a function of ε_r, for different SNR values: (a) total error ξ_{tot}, (b) internal error ξ_{int}, (c) external error ξ_{ext}.

TEST CASE: Line-Shaped Cylinder $L = 0.5\lambda$

Goal: show the performances of BCS when dealing with a sparse scatterer

- Number of Views: V
- Number of Measurements: M
- Number of Cells for the Inversion: N
- Number of Cells for the Direct solver: D
- Side of the investigation domain: L

Test Case Description

Direct solver:

- Square domain divided in $\sqrt{D} \times \sqrt{D}$ cells
- Domain side: $L = 3\lambda$
- $D = 1296$ (discretization for the direct solver: $< \lambda/10$)

Investigation domain:

- Square domain divided in $\sqrt{N} \times \sqrt{N}$ cells
- $L = 3\lambda$
- $2ka = 2 \times \frac{2\pi}{\lambda} \times \frac{L\sqrt{2}}{2} = 6\pi\sqrt{2} = 26.65$
- $\#DOF = \frac{(2ka)^2}{2} = \frac{(2 \times \frac{2\pi}{\lambda} \times \frac{L\sqrt{2}}{2})^2}{2} = 4\pi^2 \left(\frac{L}{\lambda}\right)^2 = 4\pi^2 \times 9 \approx 355.3$
- N scelto in modo da essere vicino a $\#DOF$: $N = 324$ (18×18)

Measurement domain:

- Measurement points taken on a circle of radius $\rho = 3\lambda$
- Full-aspect measurements
- $M \approx 2ka \rightarrow M = 27$

Sources:

- Plane waves
- $V \approx 2ka \rightarrow V = 27$
- Amplitude $A = 1$
- Frequency: 300 MHz $(\lambda = 1)$

Object:

- Line-shaped cylinder $L = 0.5\lambda$
- $\varepsilon_r \in \{1.5, 2.0, 2.5, 3.0, 3.5, 4.0, 4.5, 5.0\}$
- $\sigma = 0$ [S/m]

BCS parameters:

- Gamma prior on noise variance parameters: $a = 1 \times 10^{+1}$, $b = 5 \times 10^{-3}$
- Convergenze parameter: $\tau = 1.0 \times 10^{-8}$

RESULTS: $\varepsilon_r = 1.5$

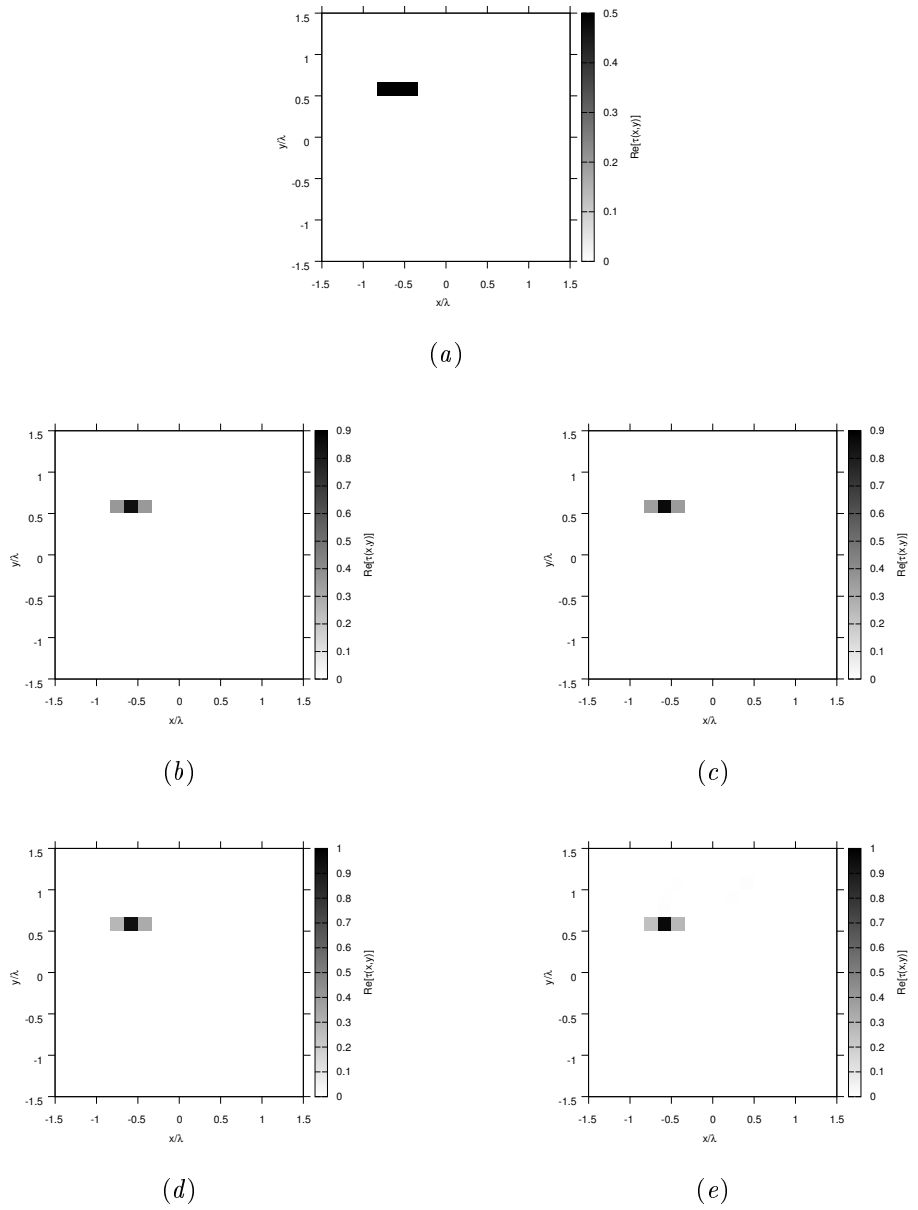

(a) (b) (c) (d) (e)

Figure 87. Actual object (a) and BCS reconstructed object for (b) Noiseless case, (c) $SNR = 20$ [dB] , (d) $SNR = 10$ [dB] , (e) $SNR = 5$ [dB].

RESULTS: $\varepsilon_r = 2.0$

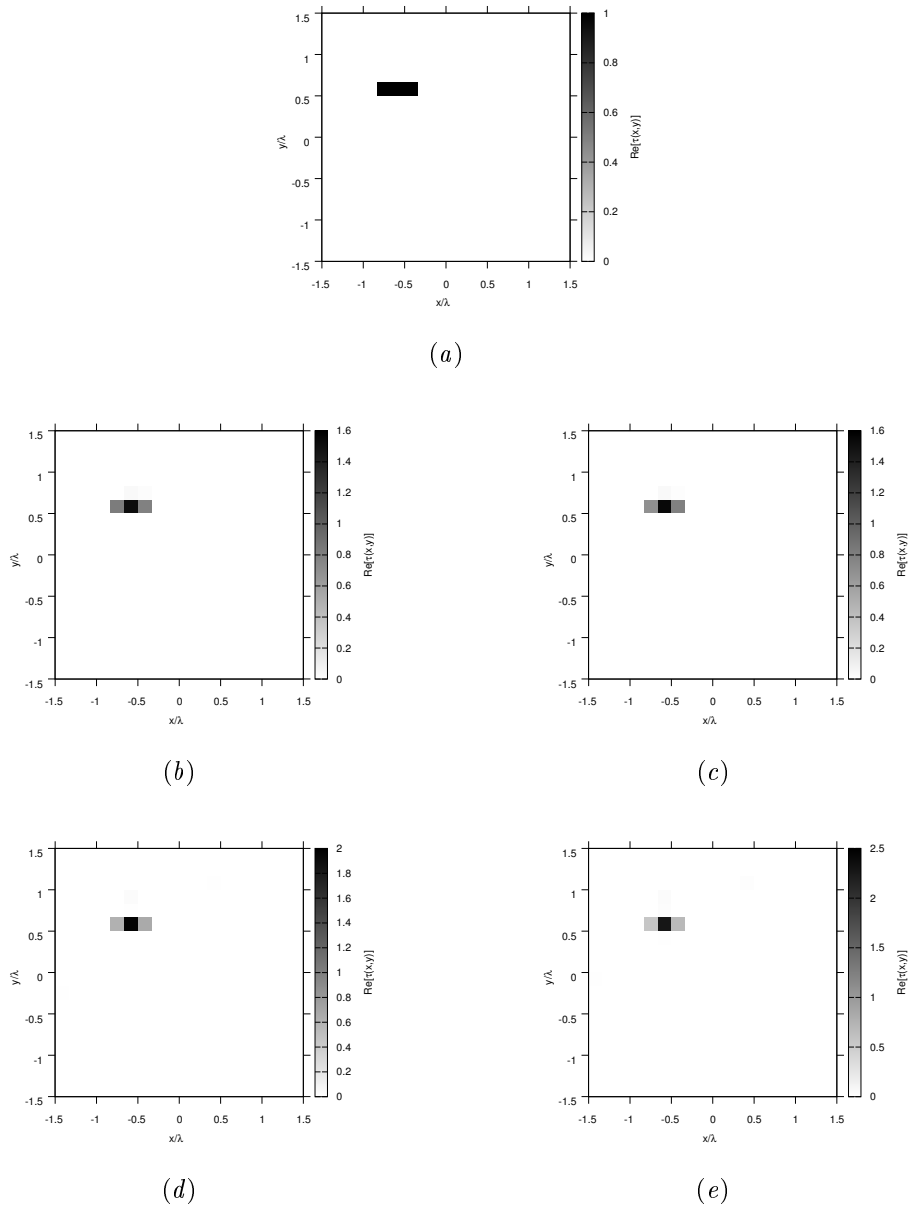

(a)

(b)

(c)

(d)

(e)

Figure 88. Actual object (a) and BCS reconstructed object for (b) Noiseless case, (c) $SNR = 20$ [dB] , (d) $SNR = 10$ [dB] , (e) $SNR = 5$ [dB].

RESULTS: $\varepsilon_r = 3.0$

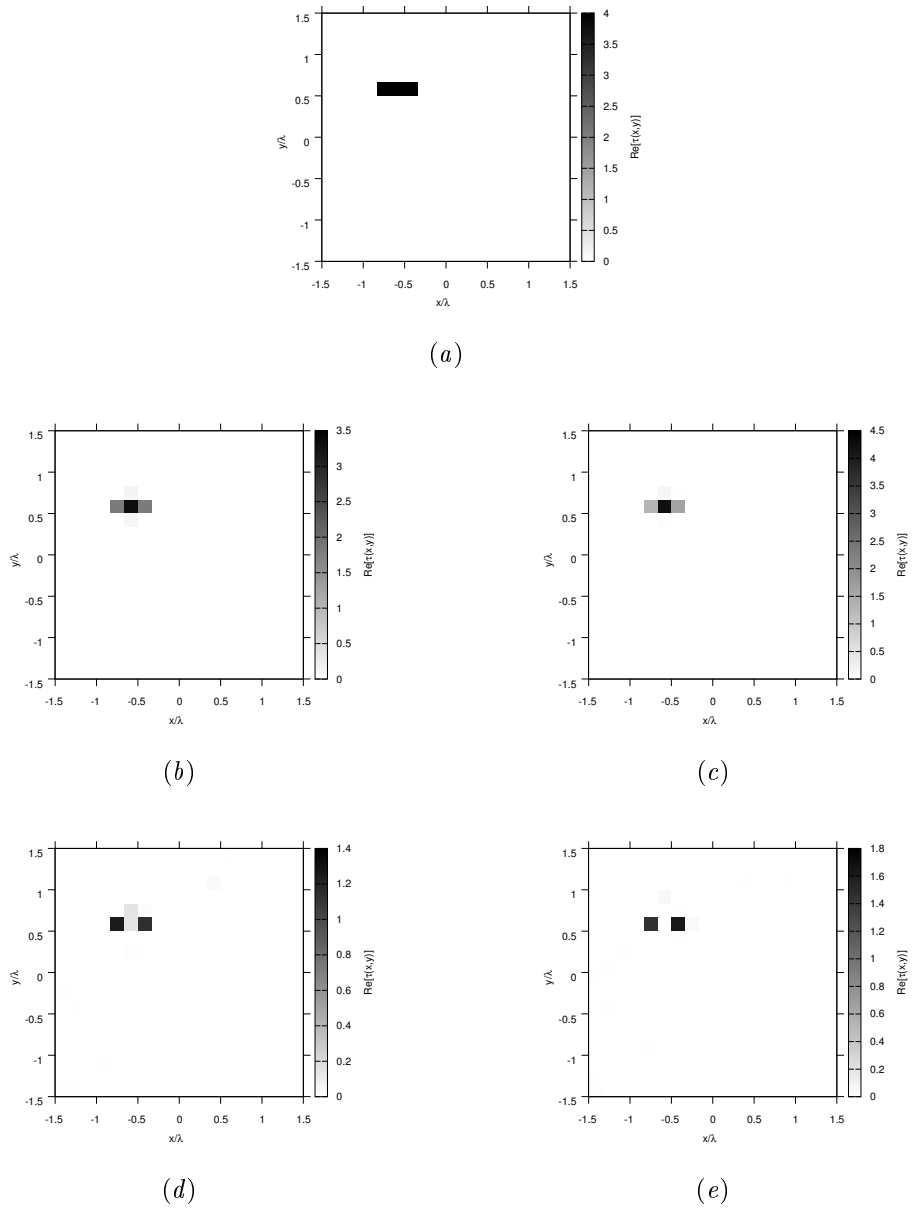

(a)

(b)

(c)

(d)

(e)

Figure 89. Actual object (a) and BCS reconstructed object for (b) Noiseless case, (c) $SNR = 20$ [dB] , (d) $SNR = 10$ [dB] , (e) $SNR = 5$ [dB].

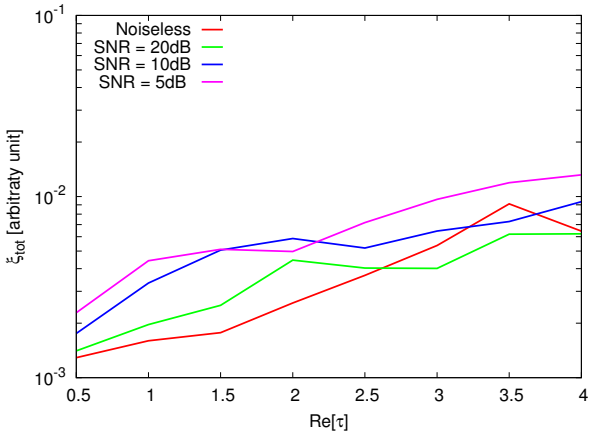

(a)

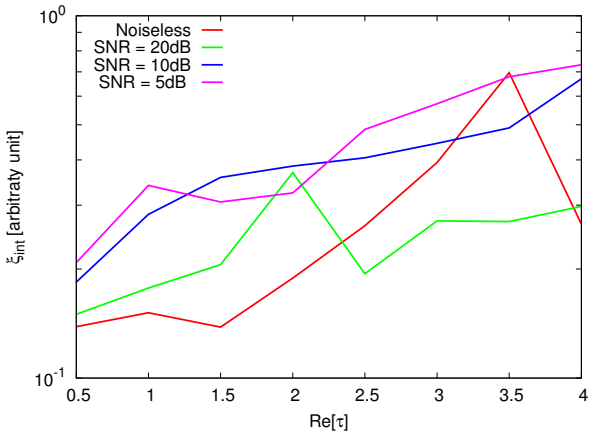

(b)

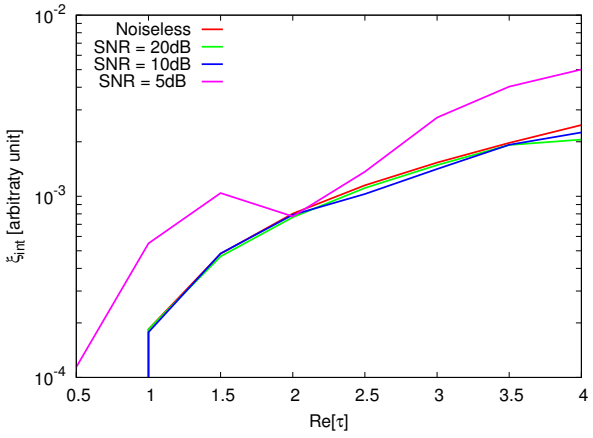

(c)

Figure 90. Behaviour of error figures as a function of ε_r, for different SNR values: (a) total error ξ_{tot}, (b) internal error ξ_{int}, (c) external error ξ_{ext}.

4.3 MV-MT-BCS - Advanced Tests

TEST CASE: Two Square Cylinders $L = 0.33\lambda$

Goal: show the performances of BCS when dealing with a sparse scatterer

- Number of Views: V
- Number of Measurements: M
- Number of Cells for the Inversion: N
- Number of Cells for the Direct solver: D
- Side of the investigation domain: L

Test Case Description

Direct solver:

- Square domain divided in $\sqrt{D} \times \sqrt{D}$ cells
- Domain side: $L = 3\lambda$
- $D = 1296$ (discretization for the direct solver: $< \lambda/10$)

Investigation domain:

- Square domain divided in $\sqrt{N} \times \sqrt{N}$ cells
- $L = 3\lambda$
- $2ka = 2 \times \frac{2\pi}{\lambda} \times \frac{L\sqrt{2}}{2} = 6\pi\sqrt{2} = 26.65$
- $\#DOF = \frac{(2ka)^2}{2} = \frac{(2 \times \frac{2\pi}{\lambda} \times \frac{L\sqrt{2}}{2})^2}{2} = 4\pi^2 \left(\frac{L}{\lambda}\right)^2 = 4\pi^2 \times 9 \approx 355.3$
- N scelto in modo da essere vicino a $\#DOF$: $N = 324$ (18×18)

Measurement domain:

- Measurement points taken on a circle of radius $\rho = 3\lambda$
- Full-aspect measurements
- $M \approx 2ka \rightarrow M = 27$

Sources:

- Plane waves
- $V \approx 2ka \rightarrow V = 27$
- Amplitude: $A = 1$
- Frequency: 300 MHz ($\lambda = 1$)

Object:

- Two square cylinders of side $\frac{\lambda}{3} = 0.33$
- $\varepsilon_r \in \{1.5, 2.0, 2.5, 3.0, 3.5, 4.0, 4.5, 5.0\}$ (two square)

- $\sigma = 0$ [S/m]

BCS parameters:

- Gamma prior on noise variance parameters: $a = 1 \times 10^{+1}$, $b = 5 \times 10^{-3}$
- Convergenze parameter: $\tau = 1.0 \times 10^{-8}$

RESULTS: $\varepsilon_r = 1.5$

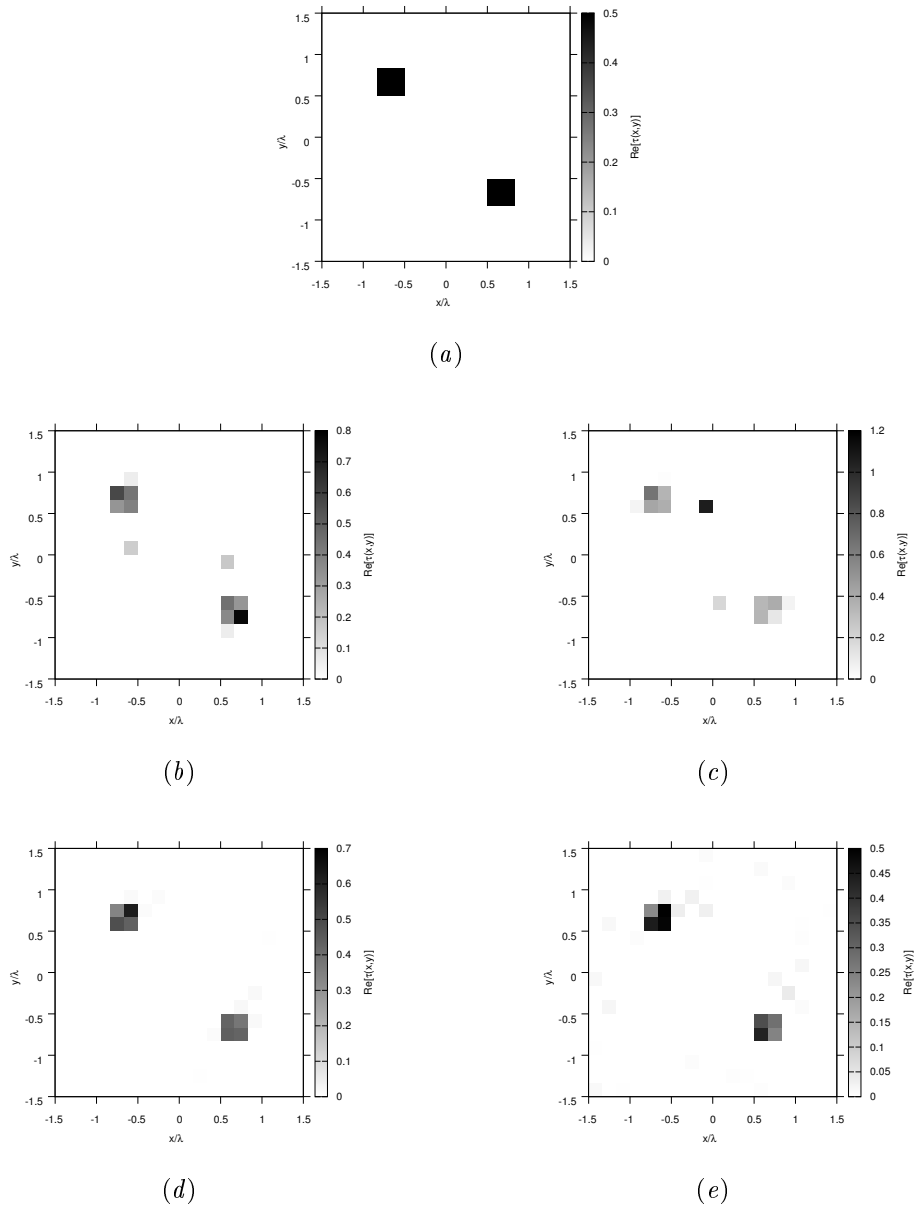

(a)

(b)

(c)

(d)

(e)

Figure 91. Actual object (a) and BCS reconstructed object for (b) Noiseless case, (c) $SNR = 20$ [dB] , (d) $SNR = 10$ [dB] , (e) $SNR = 5$ [dB].

RESULTS: $\varepsilon_r = 2.0$

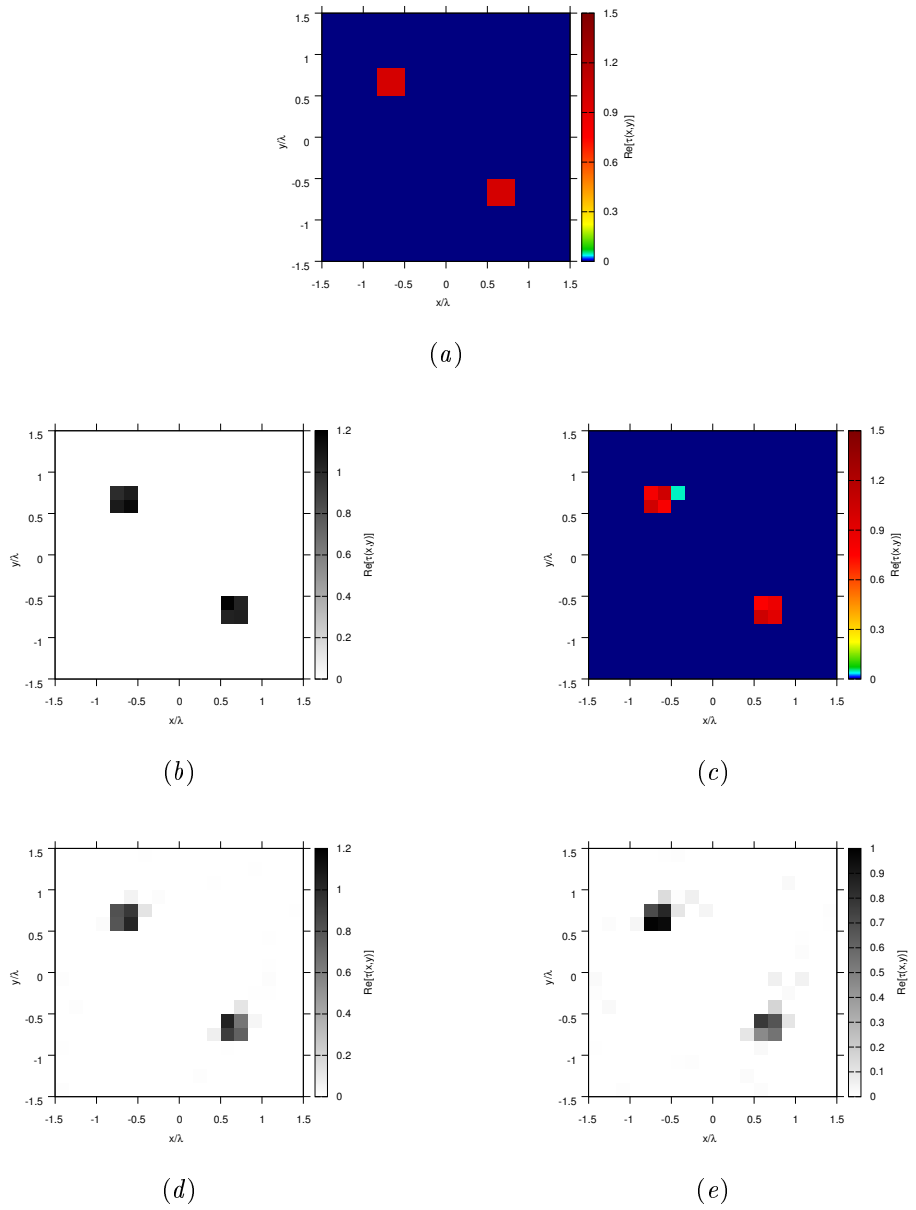

(a)

(b)

(c)

(d)

(e)

Figure 92. Actual object (a) and BCS reconstructed object for (b) Noiseless case, (c) $SNR = 20$ [dB] , (d) $SNR = 10$ [dB] , (e) $SNR = 5$ [dB].

RESULTS: $\varepsilon_r = 3.0$

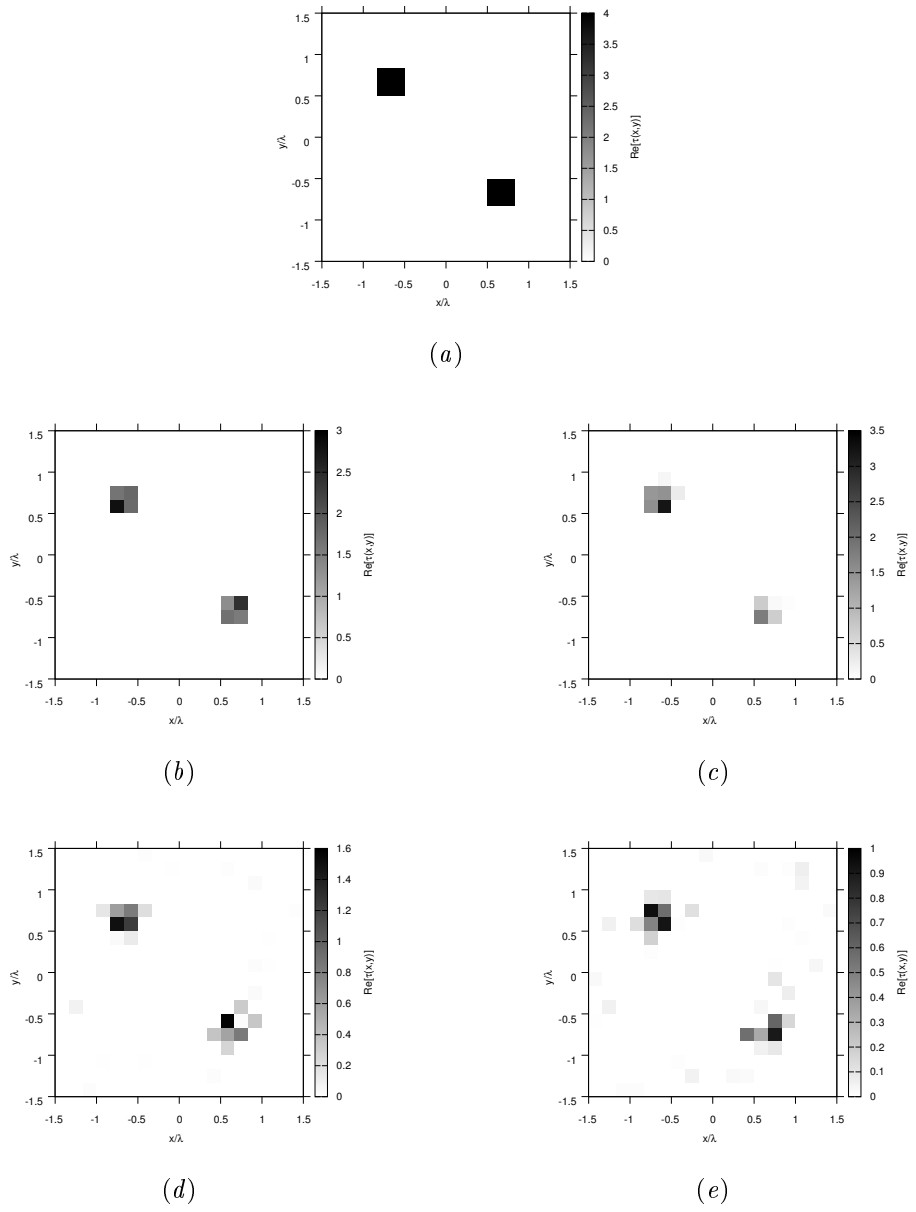

(a) (b) (c) (d) (e)

Figure 93. Actual object (a) and BCS reconstructed object for (b) Noiseless case, (c) $SNR = 20$ [dB] , (d) $SNR = 10$ [dB] , (e) $SNR = 5$ [dB].

RESULTS: Error Figures

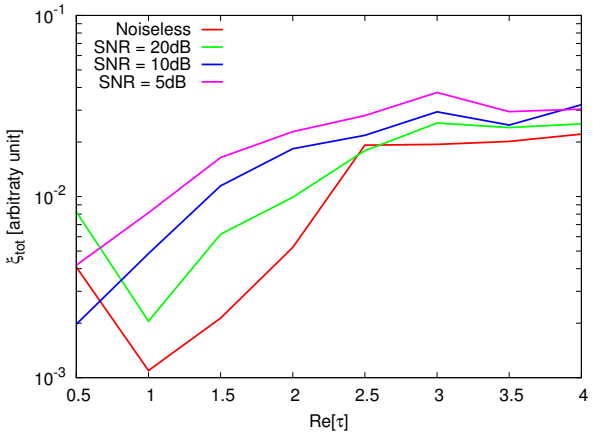

(a)

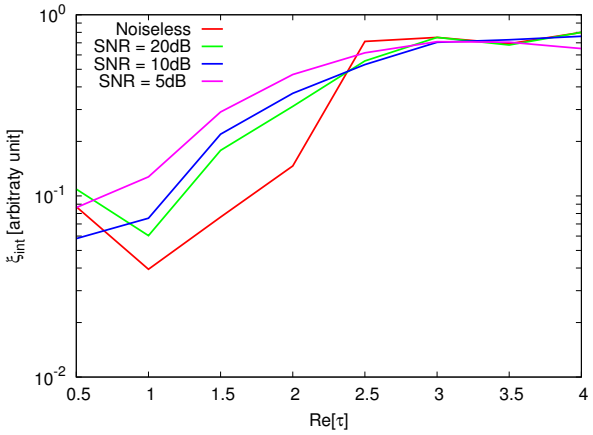

(b)

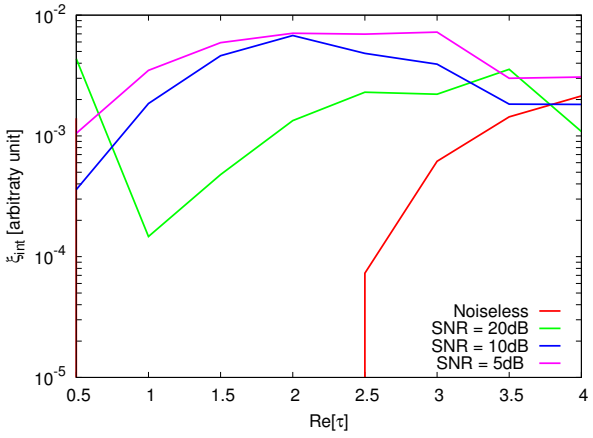

(c)

Figure 94. Behaviour of error figures as a function of ε_r, for different SNR values: (a) total error ξ_{tot}, (b) internal error ξ_{int}, (c) external error ξ_{ext}.

TEST CASE: Square Cylinder $L = 0.50\lambda$

Goal: show the performances of BCS when dealing with a sparse scatterer

- Number of Views: V
- Number of Measurements: M
- Number of Cells for the Inversion: N
- Number of Cells for the Direct solver: D
- Side of the investigation domain: L

Test Case Description

Direct solver:

- Square domain divided in $\sqrt{D} \times \sqrt{D}$ cells
- Domain side: $L = 3\lambda$
- $D = 1296$ (discretization for the direct solver: $< \lambda/10$)

Investigation domain:

- Square domain divided in $\sqrt{N} \times \sqrt{N}$ cells
- $L = 3\lambda$
- $2ka = 2 \times \frac{2\pi}{\lambda} \times \frac{L\sqrt{2}}{2} = 6\pi\sqrt{2} = 26.65$
- $\#DOF = \frac{(2ka)^2}{2} = \frac{(2 \times \frac{2\pi}{\lambda} \times \frac{L\sqrt{2}}{2})^2}{2} = 4\pi^2 \left(\frac{L}{\lambda}\right)^2 = 4\pi^2 \times 9 \approx 355.3$
- N scelto in modo da essere vicino a $\#DOF$: $N = 324$ (18×18)

Measurement domain:

- Measurement points taken on a circle of radius $\rho = 3\lambda$
- Full-aspect measurements
- $M \approx 2ka \rightarrow M = 27$

Sources:

- Plane waves
- $V \approx 2ka \rightarrow V = 27$
- Amplitude: $A = 1$
- Frequency: 300 MHz $(\lambda = 1)$

Object:

- Square cylinder of side $\frac{\lambda}{2} = 0.5$
- $\varepsilon_r \in \{1.5, 2.0, 2.5, 3.0, 3.5, 4.0, 4.5, 5.0\}$
- $\sigma = 0$ [S/m]

BCS parameters:

- Gamma prior on noise variance parameters: $a = 1 \times 10^{+1}$, $b = 5 \times 10^{-3}$
- Convergenze parameter: $\tau = 1.0 \times 10^{-8}$

RESULTS: $\varepsilon_r = 1.5$

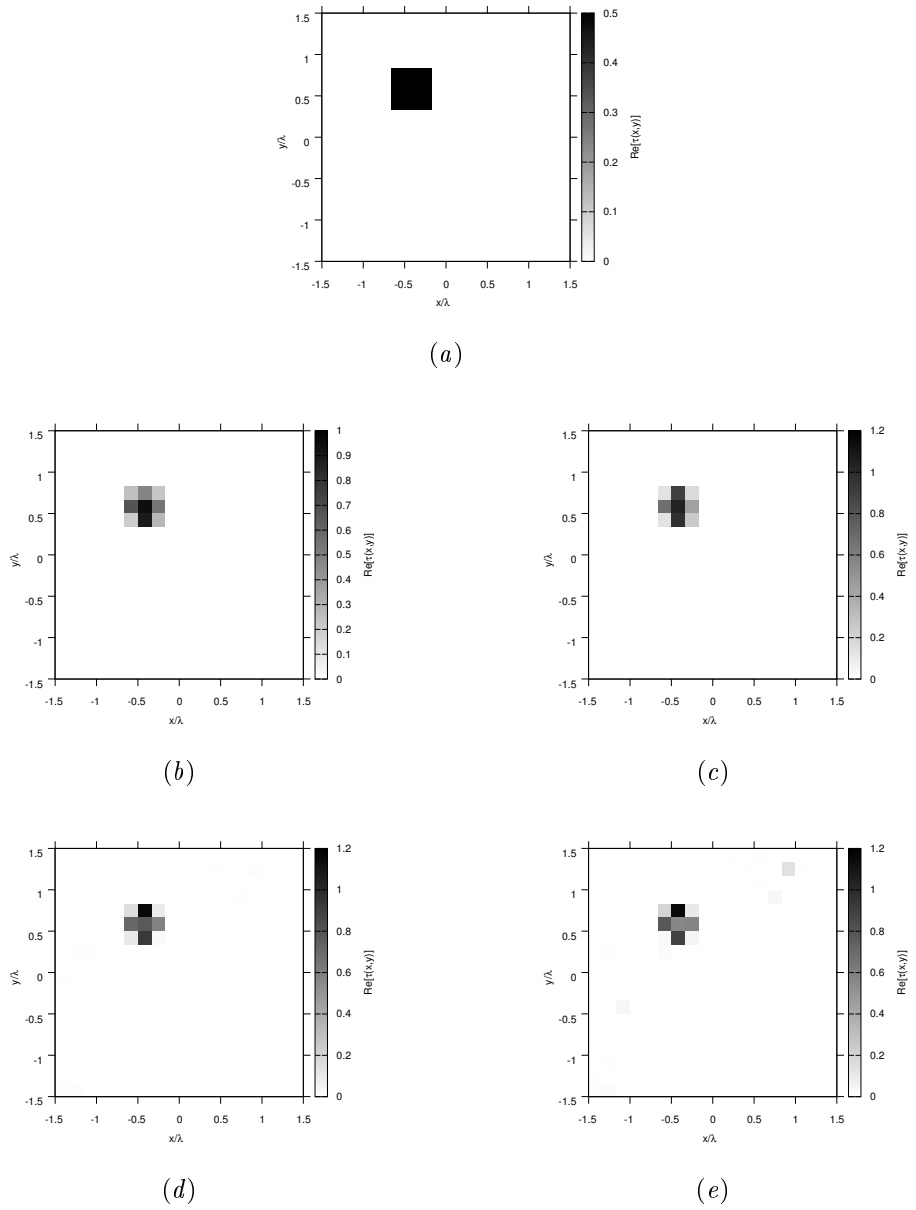

(a)

(b)

(c)

(d)

(e)

Figure 95. Actual object (a) and BCS reconstructed object for (b) Noiseless case, (c) $SNR = 20$ [dB] , (d) $SNR = 10$ [dB] , (e) $SNR = 5$ [dB].

RESULTS: Error Figures

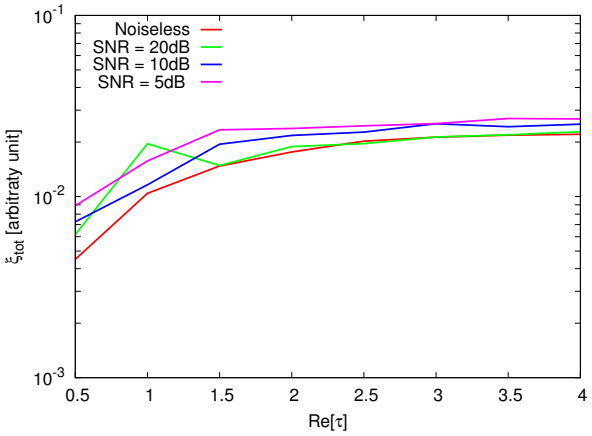

(a)

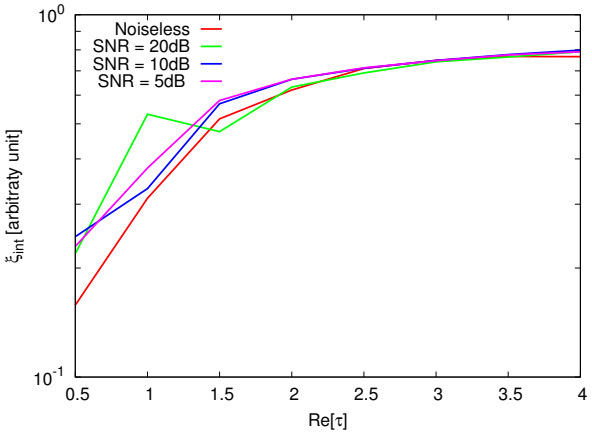

(b)

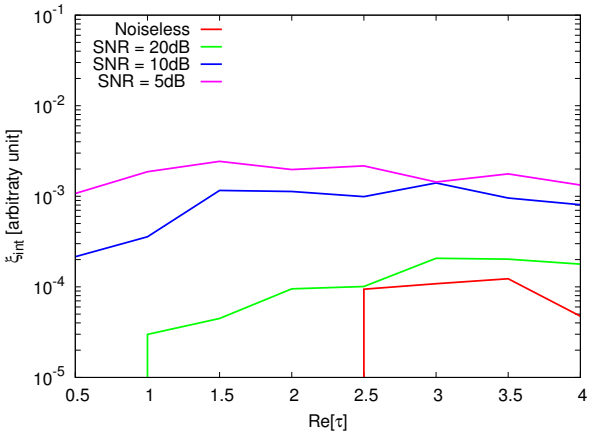

(c)

Figure 96. Behaviour of error figures as a function of ε_r, for different SNR values: (a) total error ξ_{tot}, (b) internal error ξ_{int}, (c) external error ξ_{ext}.

TEST CASE: Hollow Square Cylinder $L = 0.50\lambda$

Goal: show the performances of BCS when dealing with a sparse scatterer

- Number of Views: V
- Number of Measurements: M
- Number of Cells for the Inversion: N
- Number of Cells for the Direct solver: D
- Side of the investigation domain: L

Test Case Description

Direct solver:

- Square domain divided in $\sqrt{D} \times \sqrt{D}$ cells
- Domain side: $L = 3\lambda$
- $D = 1296$ (discretization for the direct solver: $< \lambda/10$)

Investigation domain:

- Square domain divided in $\sqrt{N} \times \sqrt{N}$ cells
- $L = 3\lambda$
- $2ka = 2 \times \frac{2\pi}{\lambda} \times \frac{L\sqrt{2}}{2} = 6\pi\sqrt{2} = 26.65$
- $\#DOF = \frac{(2ka)^2}{2} = \frac{(2 \times \frac{2\pi}{\lambda} \times \frac{L\sqrt{2}}{2})^2}{2} = 4\pi^2 \left(\frac{L}{\lambda}\right)^2 = 4\pi^2 \times 9 \approx 355.3$
- N scelto in modo da essere vicino a $\#DOF$: $N = 324$ (18×18)

Measurement domain:

- Measurement points taken on a circle of radius $\rho = 3\lambda$
- Full-aspect measurements
- $M \approx 2ka \rightarrow M = 27$

Sources:

- Plane waves
- $V \approx 2ka \rightarrow V = 27$
- Amplitude: $A = 1$
- Frequency: 300 MHz $(\lambda = 1)$

Object:

- Hollow square cylinder of side $\frac{\lambda}{2} = 0.5$
- $\varepsilon_r \in \{1.5, 2.0, 2.5, 3.0, 3.5, 4.0, 4.5, 5.0\}$
- $\sigma = 0$ [S/m]

BCS parameters:

- Gamma prior on noise variance parameters: $a = 1 \times 10^{+1}$, $b = 5 \times 10^{-3}$
- Convergenze parameter: $\tau = 1.0 \times 10^{-8}$

RESULTS: $\varepsilon_r = 1.5$

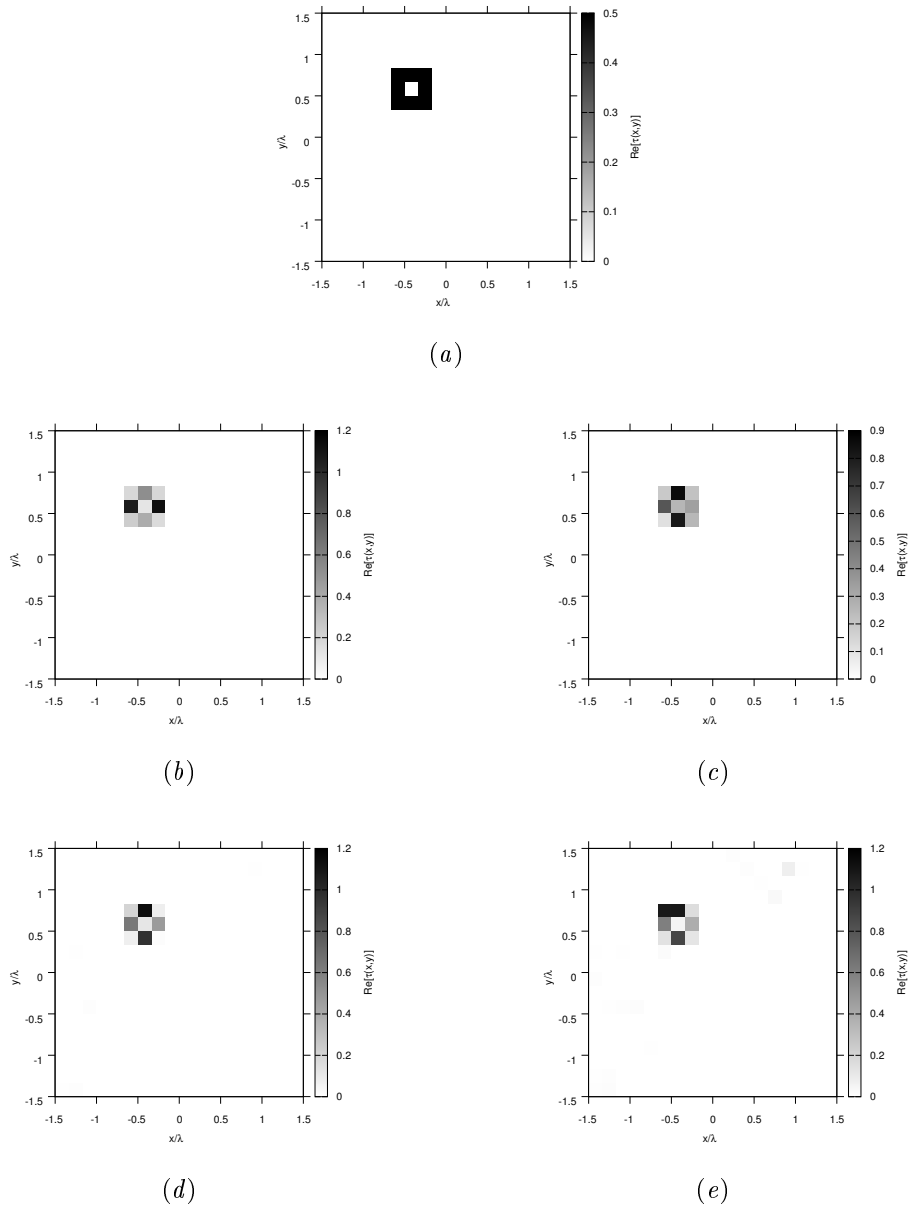

(a)

(b)

(c)

(d)

(e)

Figure 97. Actual object (a) and BCS reconstructed object for (b) Noiseless case, (c) $SNR = 20$ [dB] , (d) $SNR = 10$ [dB] , (e) $SNR = 5$ [dB].

RESULTS: $\varepsilon_r = 2.0$

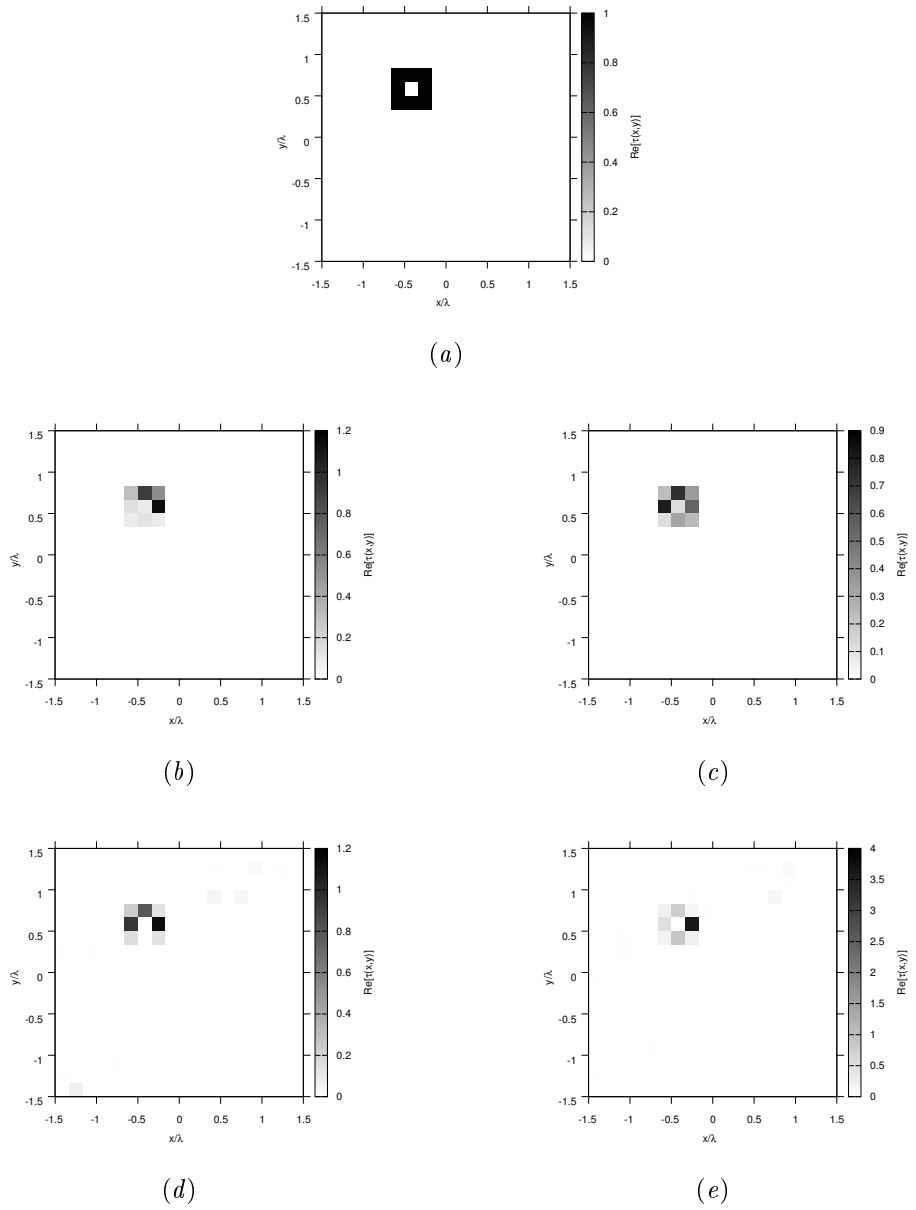

(a)

(b)

(c)

(d)

(e)

Figure 98. Actual object (a) and BCS reconstructed object for (b) Noiseless case, (c) $SNR = 20$ [dB] , (d) $SNR = 10$ [dB] , (e) $SNR = 5$ [dB].

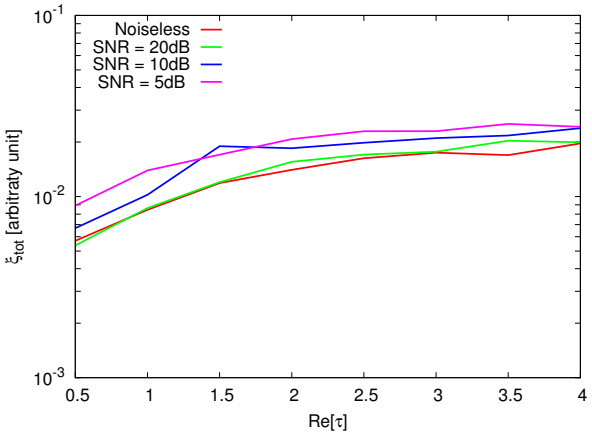

(a)

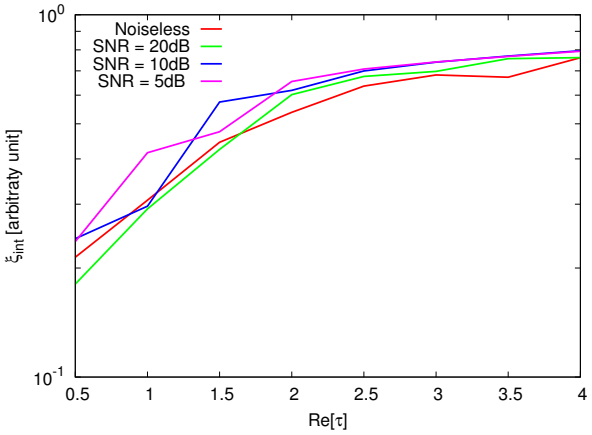

(b)

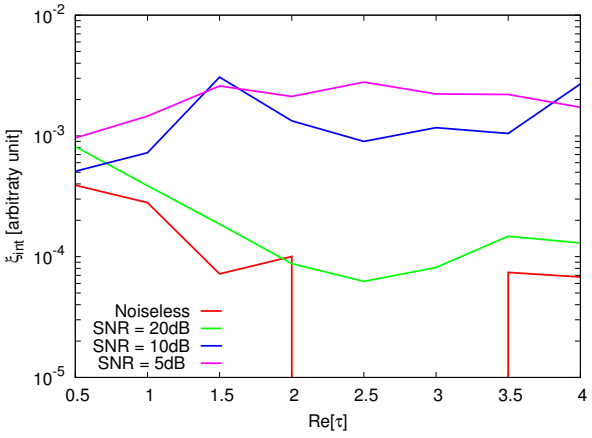

(c)

Figure 99. Behaviour of error figures as a function of ε_r, for different SNR values: (a) total error ξ_{tot}, (b) internal error ξ_{int}, (c) external error ξ_{ext}.

TEST CASE: Big L-Shaped Cylinder

Goal: show the performances of BCS when dealing with a sparse scatterer

- Number of Views: V
- Number of Measurements: M
- Number of Cells for the Inversion: N
- Number of Cells for the Direct solver: D
- Side of the investigation domain: L

Test Case Description

Direct solver:

- Square domain divided in $\sqrt{D} \times \sqrt{D}$ cells
- Domain side: $L = 3\lambda$
- $D = 1296$ (discretization for the direct solver: $< \lambda/10$)

Investigation domain:

- Square domain divided in $\sqrt{N} \times \sqrt{N}$ cells
- $L = 3\lambda$
- $2ka = 2 \times \frac{2\pi}{\lambda} \times \frac{L\sqrt{2}}{2} = 6\pi\sqrt{2} = 26.65$
- $\#DOF = \frac{(2ka)^2}{2} = \frac{(2 \times \frac{2\pi}{\lambda} \times \frac{L\sqrt{2}}{2})^2}{2} = 4\pi^2 \left(\frac{L}{\lambda}\right)^2 = 4\pi^2 \times 9 \approx 355.3$
- N scelto in modo da essere vicino a $\#DOF$: $N = 324$ (18×18)

Measurement domain:

- Measurement points taken on a circle of radius $\rho = 3\lambda$
- Full-aspect measurements
- $M \approx 2ka \rightarrow M = 27$

Sources:

- Plane waves
- $V \approx 2ka \rightarrow V = 27$
- Amplitude: $A = 1$
- Frequency: 300 MHz $(\lambda = 1)$

Object:

- Big L-shaped cylinder
- $\varepsilon_r \in \{1.5, 2.0, 2.5, 3.0, 3.5, 4.0, 4.5, 5.0\}$
- $\sigma = 0$ [S/m]

BCS parameters:

- Gamma prior on noise variance parameters: $a = 1 \times 10^{+1}$, $b = 5 \times 10^{-3}$
- Convergenze parameter: $\tau = 1.0 \times 10^{-8}$

RESULTS: $\varepsilon_r = 1.5$

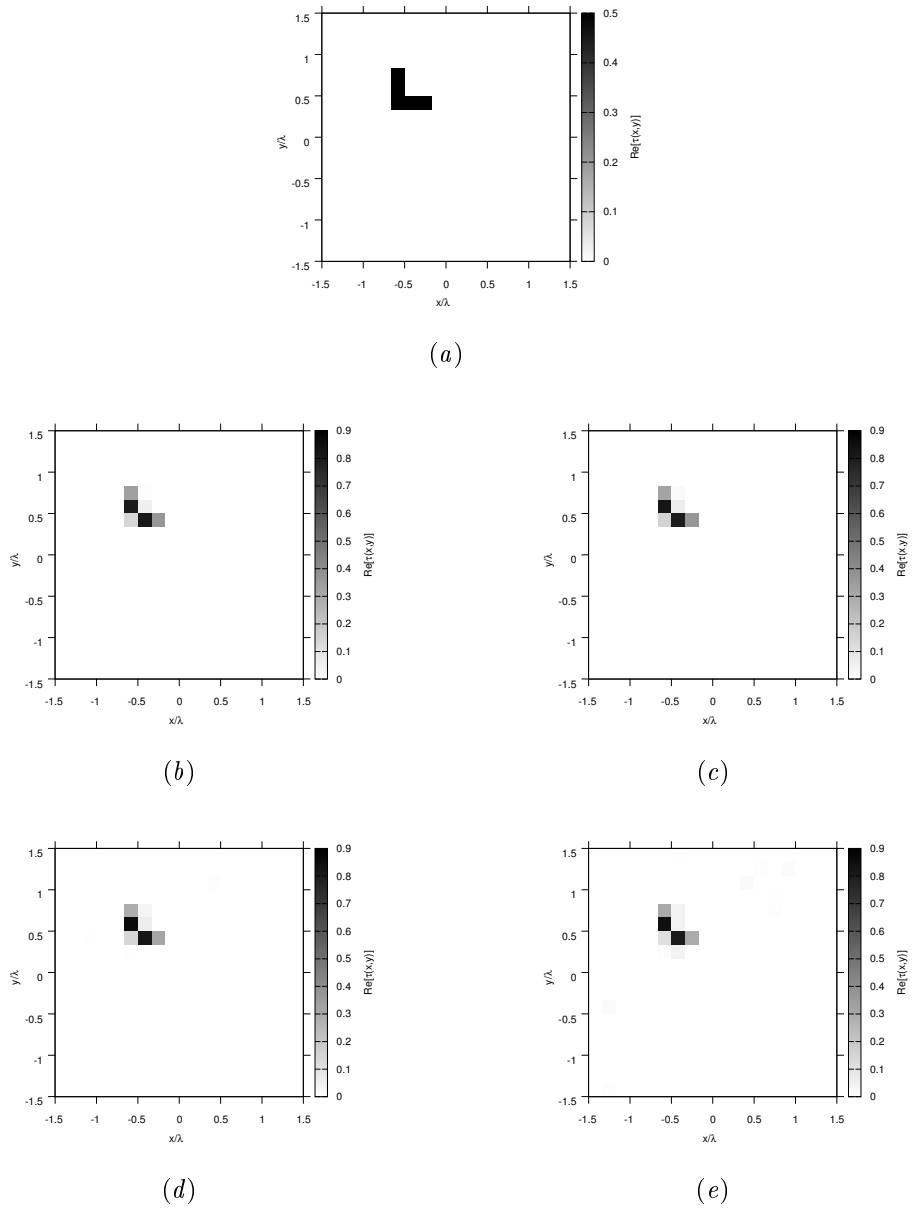

(a) (b) (c) (d) (e)

Figure 100. Actual object (a) and BCS reconstructed object for (b) Noiseless case, (c) $SNR = 20$ [dB] , (d) $SNR = 10$ [dB] , (e) $SNR = 5$ [dB].

RESULTS: $\varepsilon_r = 2.0$

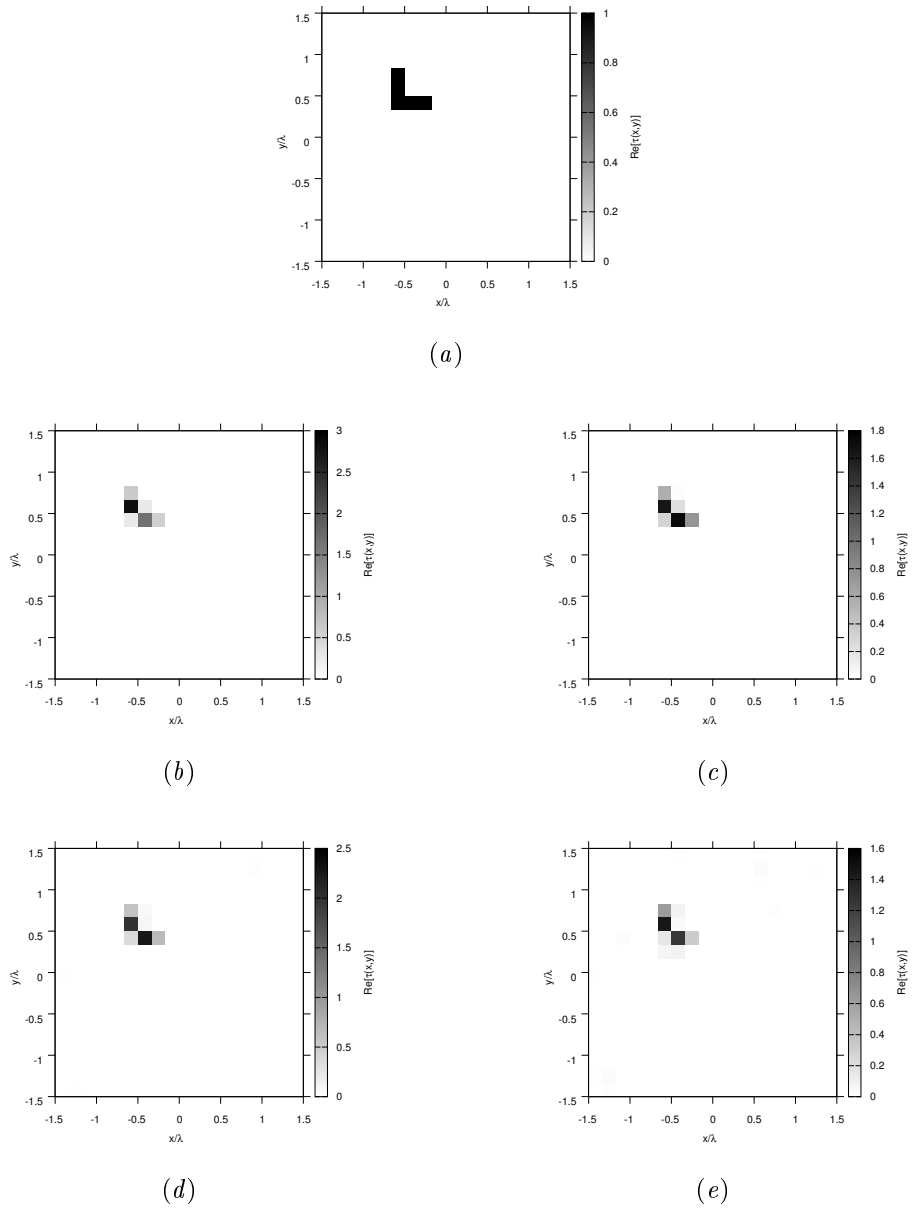

(a)

(b)

(c)

(d)

(e)

Figure 101. Actual object (a) and BCS reconstructed object for (b) Noiseless case, (c) $SNR = 20$ [dB] , (d) $SNR = 10$ [dB] , (e) $SNR = 5$ [dB].

RESULTS: $\varepsilon_r = 3.0$

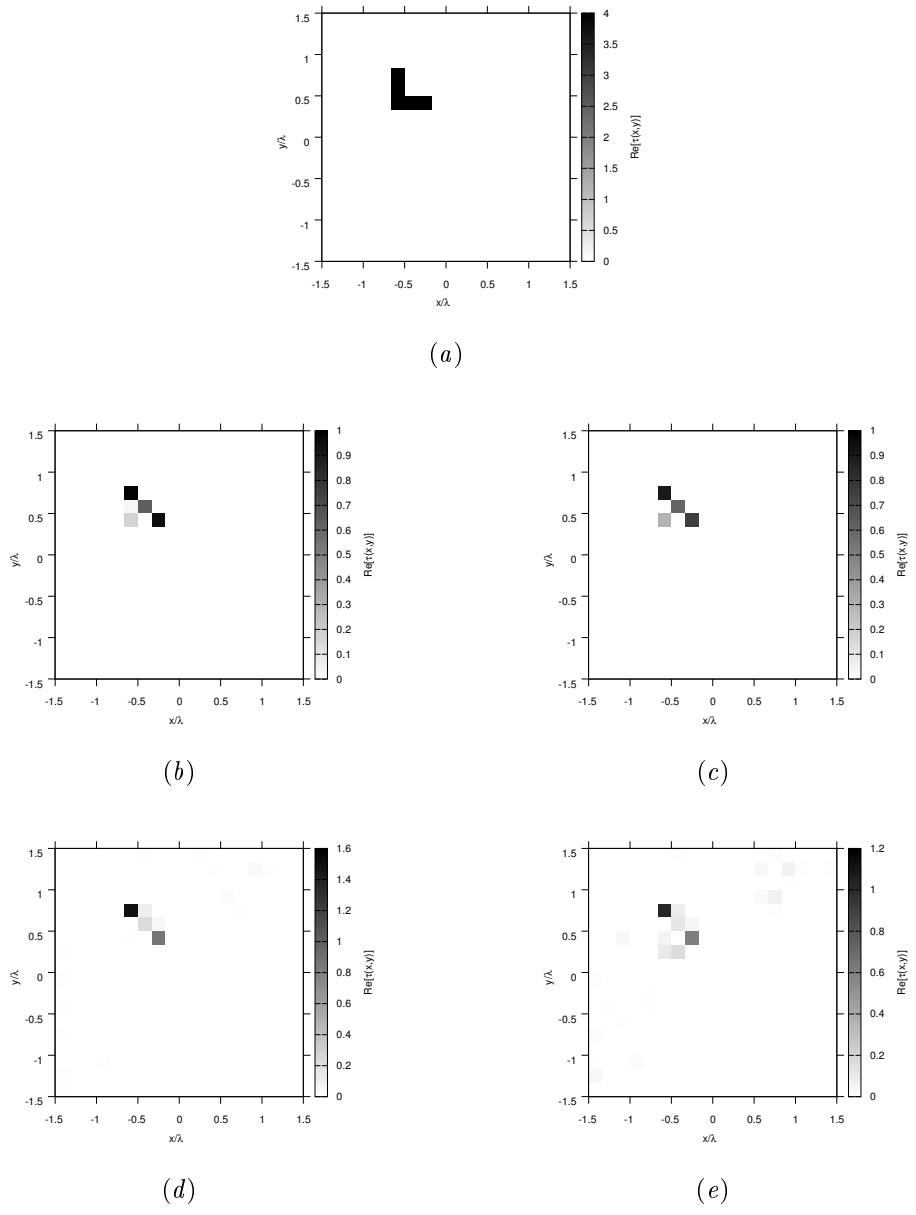

(a) (b) (c) (d) (e)

Figure 102. Actual object (a) and BCS reconstructed object for (b) Noiseless case, (c) $SNR = 20$ [dB] , (d) $SNR = 10$ [dB] , (e) $SNR = 5$ [dB].

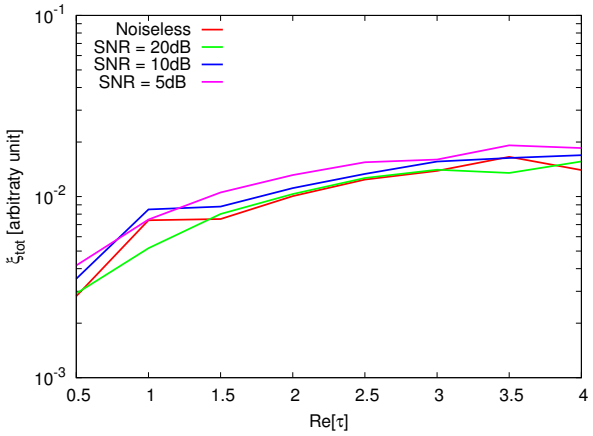

(a)

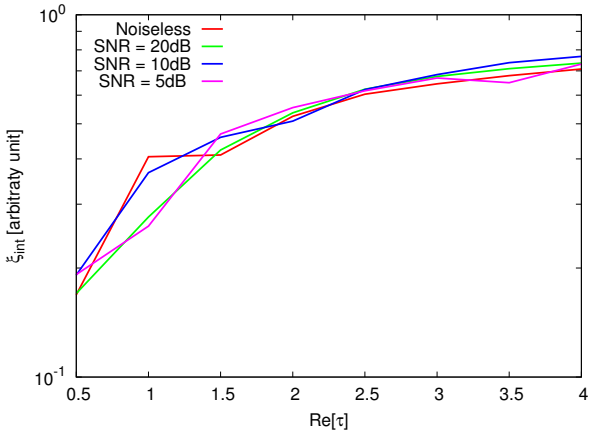

(b)

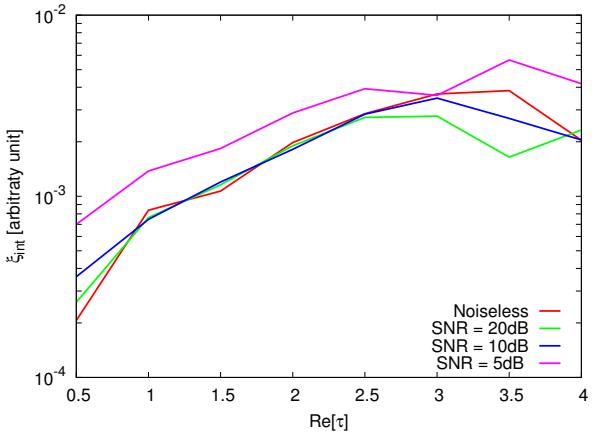

(c)

Figure 103. Behaviour of error figures as a function of ε_r, for different SNR values: (a) total error ξ_{tot}, (b) internal error ξ_{int}, (c) external error ξ_{ext}.

TEST CASE: Big T-Shaped Cylinder

Goal: show the performances of BCS when dealing with a sparse scatterer

- Number of Views: V
- Number of Measurements: M
- Number of Cells for the Inversion: N
- Number of Cells for the Direct solver: D
- Side of the investigation domain: L

Test Case Description

Direct solver:

- Square domain divided in $\sqrt{D} \times \sqrt{D}$ cells
- Domain side: $L = 3\lambda$
- $D = 1296$ (discretization for the direct solver: $< \lambda/10$)

Investigation domain:

- Square domain divided in $\sqrt{N} \times \sqrt{N}$ cells
- $L = 3\lambda$
- $2ka = 2 \times \frac{2\pi}{\lambda} \times \frac{L\sqrt{2}}{2} = 6\pi\sqrt{2} = 26.65$
- $\#DOF = \frac{(2ka)^2}{2} = \frac{(2 \times \frac{2\pi}{\lambda} \times \frac{L\sqrt{2}}{2})^2}{2} = 4\pi^2 \left(\frac{L}{\lambda}\right)^2 = 4\pi^2 \times 9 \approx 355.3$
- N scelto in modo da essere vicino a $\#DOF$: $N = 324$ (18×18)

Measurement domain:

- Measurement points taken on a circle of radius $\rho = 3\lambda$
- Full-aspect measurements
- $M \approx 2ka \rightarrow M = 27$

Sources:

- Plane waves
- $V \approx 2ka \rightarrow V = 27$
- Amplitude: $A = 1$
- Frequency: 300 MHz $(\lambda = 1)$

Object:

- Big T-shaped cylinder
- $\varepsilon_r \in \{1.5, 2.0, 2.5, 3.0, 3.5, 4.0, 4.5, 5.0\}$
- $\sigma = 0$ [S/m]

BCS parameters:

- Gamma prior on noise variance parameters: $a = 1 \times 10^{+1}$, $b = 5 \times 10^{-3}$
- Convergenze parameter: $\tau = 1.0 \times 10^{-8}$

RESULTS: $\varepsilon_r = 1.5$

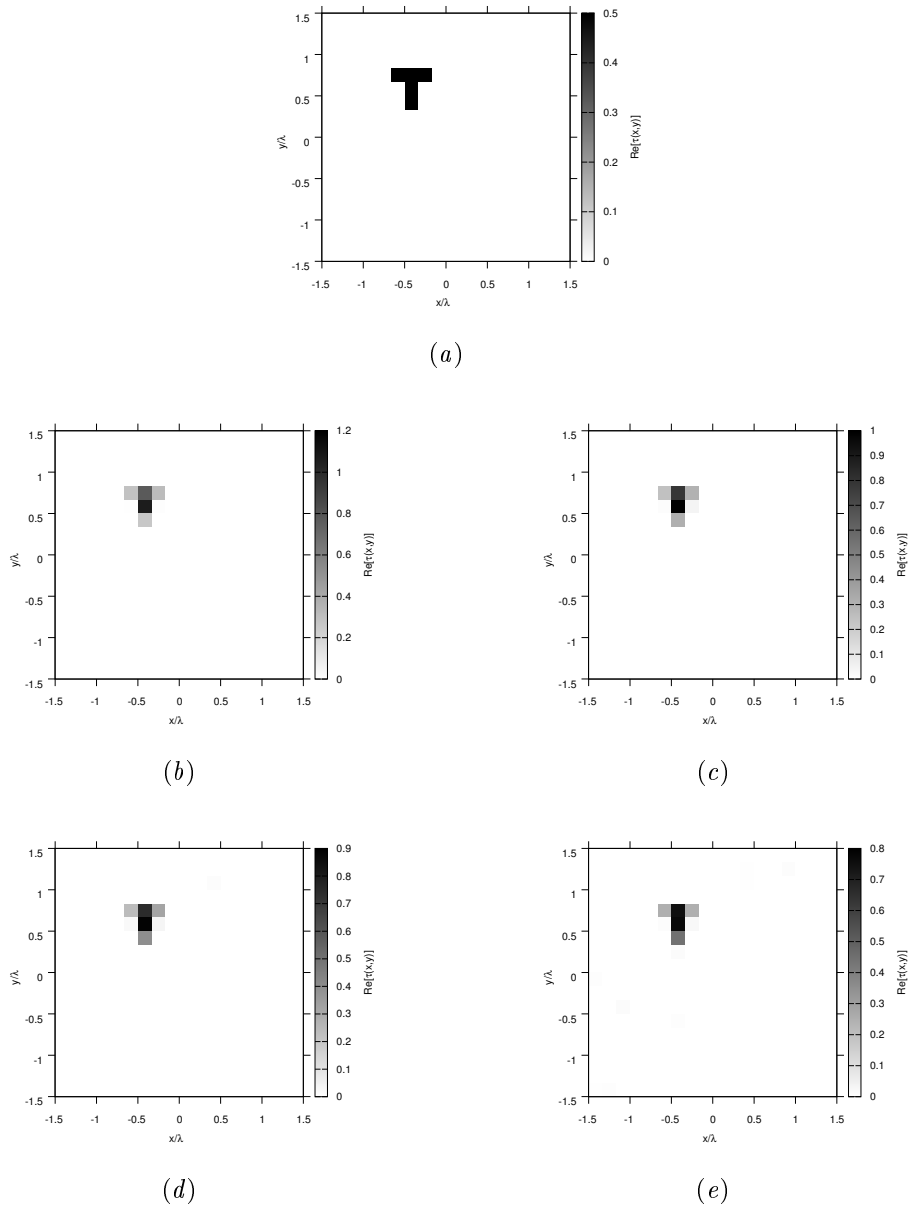

(a) (b) (c) (d) (e)

Figure 104. Actual object (a) and BCS reconstructed object for (b) Noiseless case, (c) $SNR = 20$ [dB] , (d) $SNR = 10$ [dB] , (e) $SNR = 5$ [dB].

RESULTS: $\varepsilon_r = 2.0$

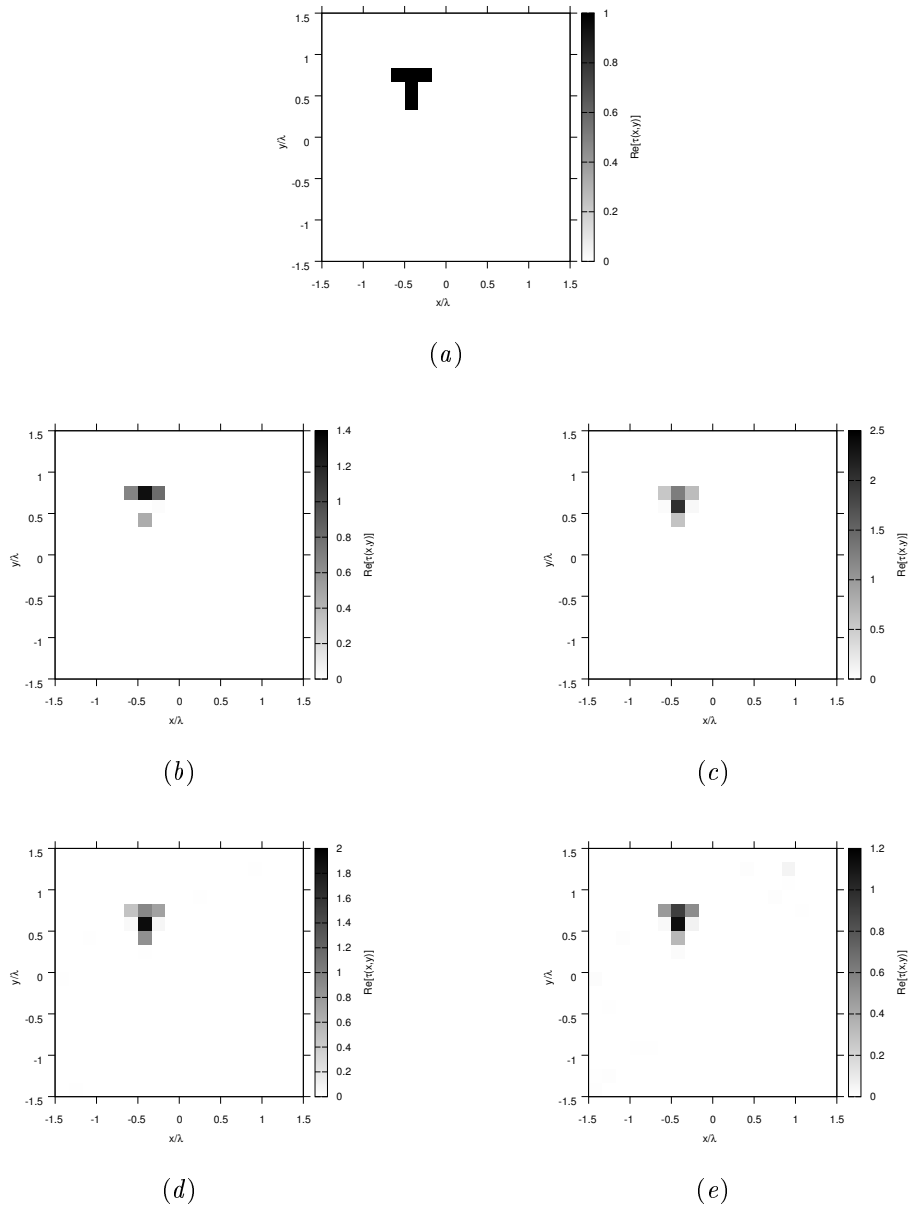

(a)

(b)

(c)

(d)

(e)

Figure 105. Actual object (a) and BCS reconstructed object for (b) Noiseless case, (c) $SNR = 20$ [dB] , (d) $SNR = 10$ [dB] , (e) $SNR = 5$ [dB].

RESULTS: $\varepsilon_r = 3.0$

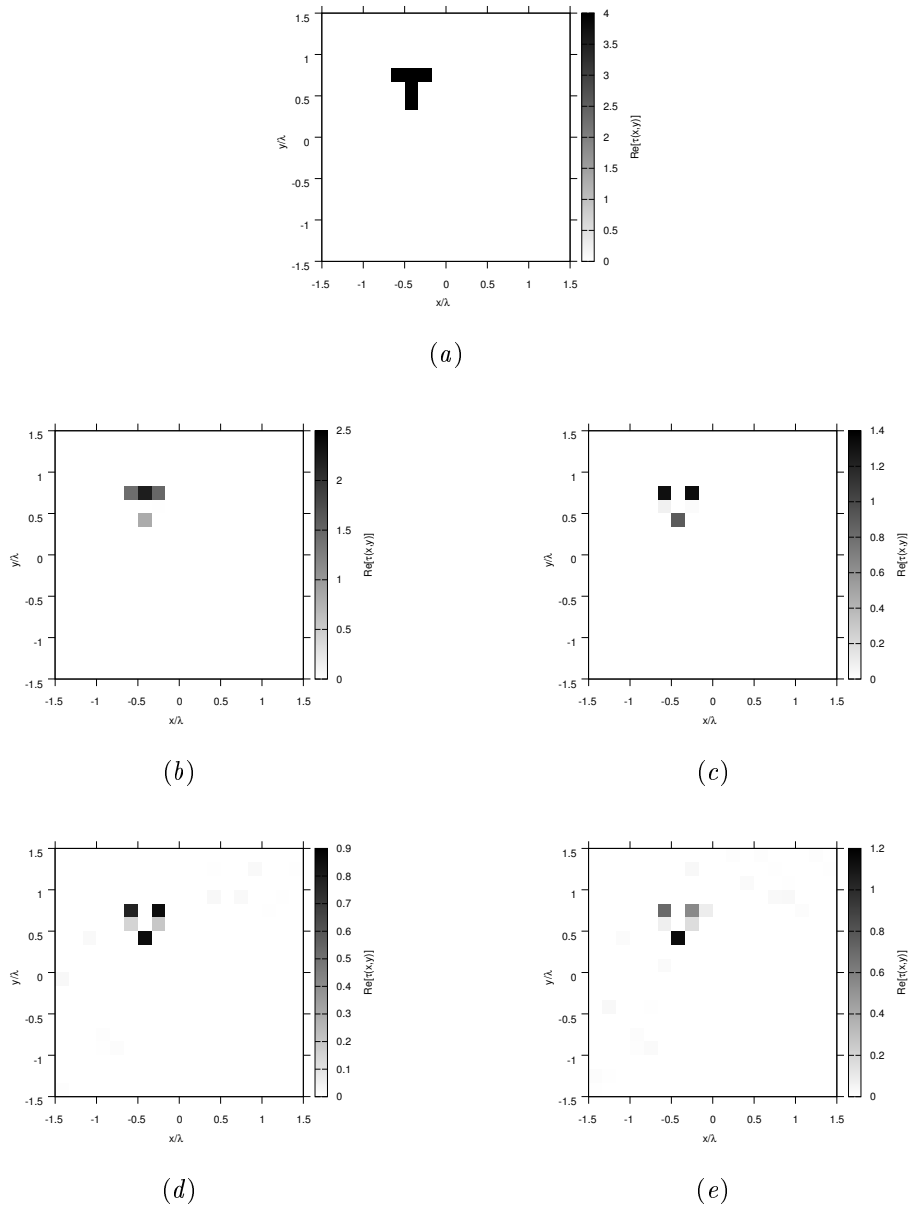

(a) (b) (c) (d) (e)

Figure 106. Actual object (a) and BCS reconstructed object for (b) Noiseless case, (c) $SNR = 20$ [dB] , (d) $SNR = 10$ [dB] , (e) $SNR = 5$ [dB].

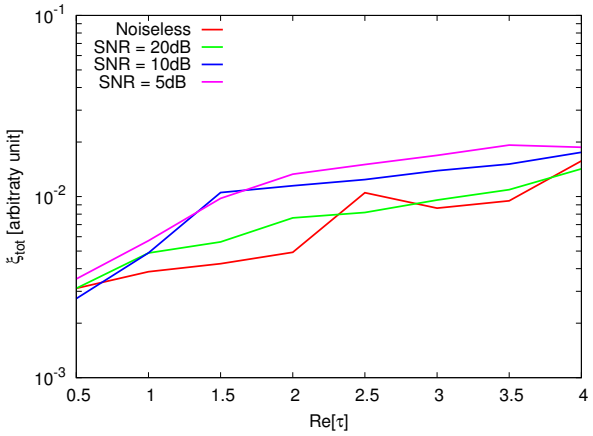

(a)

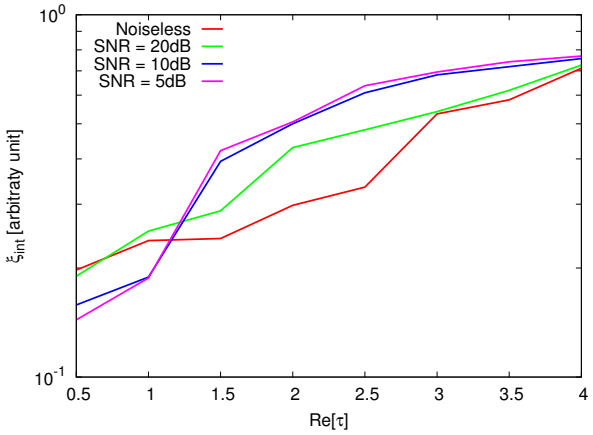

(b)

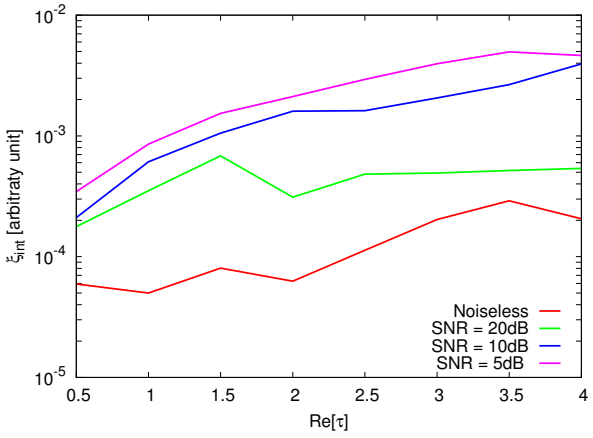

(c)

Figure 107. Behaviour of error figures as a function of ε_r, for different SNR values: (a) total error ξ_{tot}, (b) internal error ξ_{int}, (c) external error ξ_{ext}.

TEST CASE: Test Random Objects (Statistical Test)

Goal: evaluate the performances of BCS

- Number of Views: V
- Number of Measurements: M
- Number of Cells for the Inversion: N
- Number of Cells for the Direct solver: D
- Side of the investigation domain: L

Test Case Description

Direct solver:

- Square domain divided in $\sqrt{D} \times \sqrt{D}$ cells
- Domain side: $L = 3\lambda$
- $D = 1296$ (discretization for the direct solver: $< \lambda/10$)

Investigation domain:

- Square domain divided in $\sqrt{N} \times \sqrt{N}$ cells
- $L = 3\lambda$
- $N = 324$

Measurement domain:

- Measurement points taken on a circle of radius $\rho = 3\lambda$
- Full-aspect measurements
- $M \approx 2ka \rightarrow M = 27$

Sources:

- Plane waves
- $V \approx 2ka \rightarrow V = 27$
- Amplitude $A = 1$
- Frequency: 300 MHz ($\lambda = 1$)

Object:

- S square cylinders of side $\frac{\lambda}{6} = 0.16667$ ($S \in \{1, 2, 3, 4, 5, 6\}$)
- $\varepsilon_r \in \{1.5, 2.0, 3.0, 4.0, 5.0\}$
- $\sigma = 0$ [S/m]

BCS parameters:

- Gamma prior on noise variance parameters: $a = 1 \times 10^{+1}$, $b = 5 \times 10^{-3}$
- Convergenze parameter: $\tau = 1.0 \times 10^{-8}$

Statistical Analysis:

- $K = 10$ random seeds used for each case to determine the position of the objects inside the onvestigation domain

RESULTS: $\varepsilon_r = 1.5$

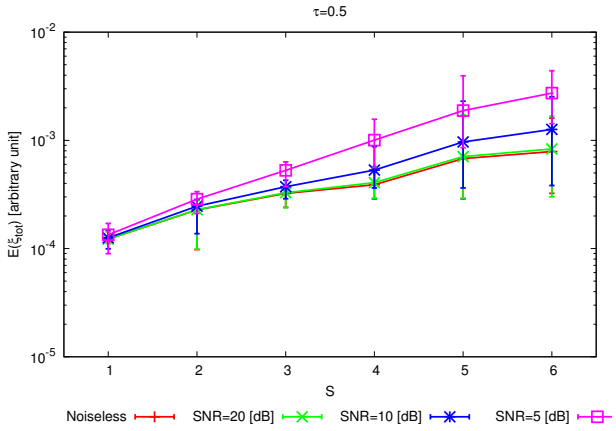

(a)

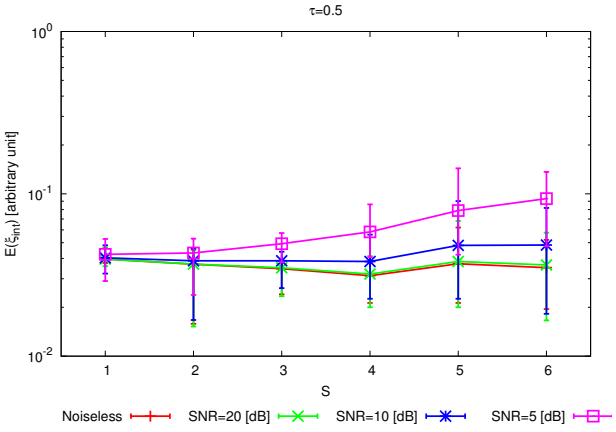

(b)

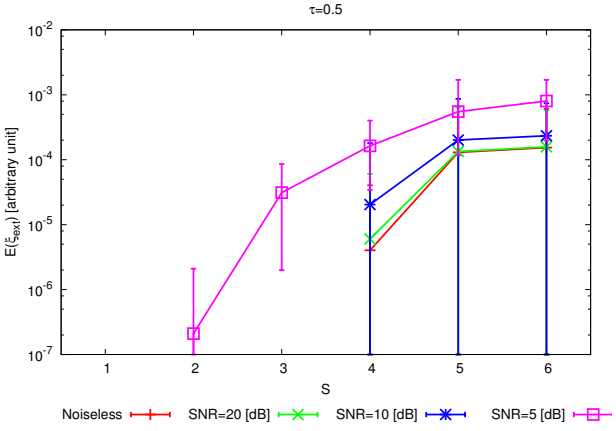

(c)

Figure 156. *Statistical analysis* $[K = 10, \varepsilon_r = 1.5]$ - Behaviour of mean, maximum and minimum of the error figures as a function of S (sparsity factor), for different SNR values: (a) total error ξ_{tot}, (b) internal error ξ_{int}, (c) external error ξ_{ext}.

RESULTS: $\varepsilon_r = 2.0$

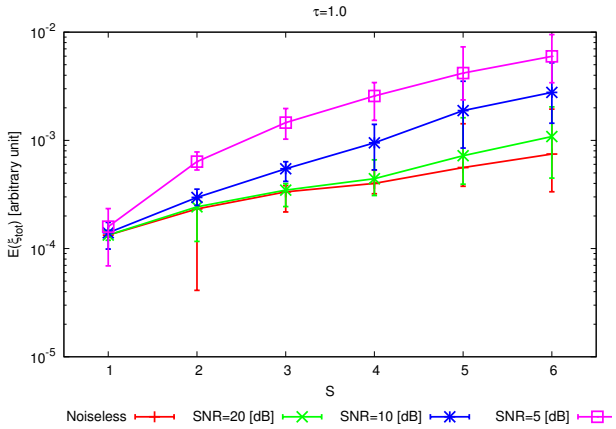

(a)

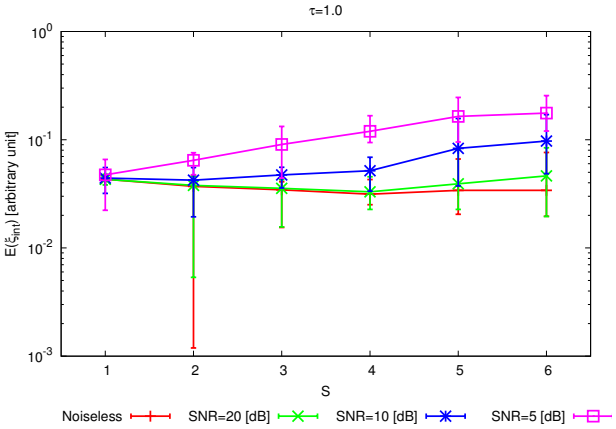

(b)

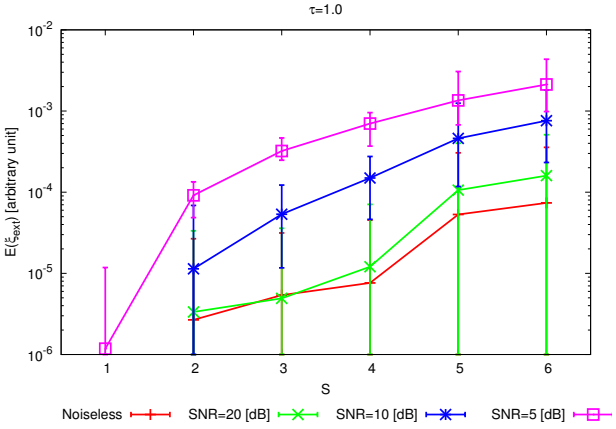

(c)

Figure 157. *Statistical analysis* $[K = 10, \varepsilon_r = 2.0]$ - Behaviour of mean, maximum and minimum of the error figures as a function of S (sparsity factor), for different SNR values: (a) total error ξ_{tot}, (b) internal error ξ_{int}, (c) external error ξ_{ext}.

RESULTS: $\varepsilon_r = 3.0$

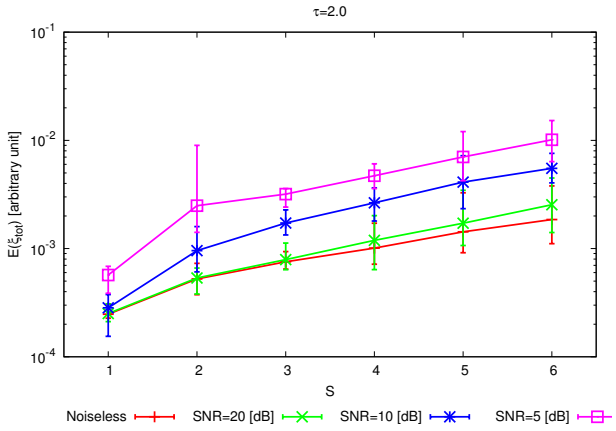

(a)

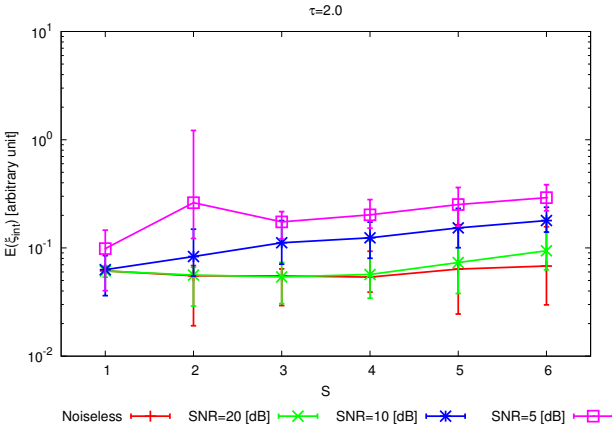

(b)

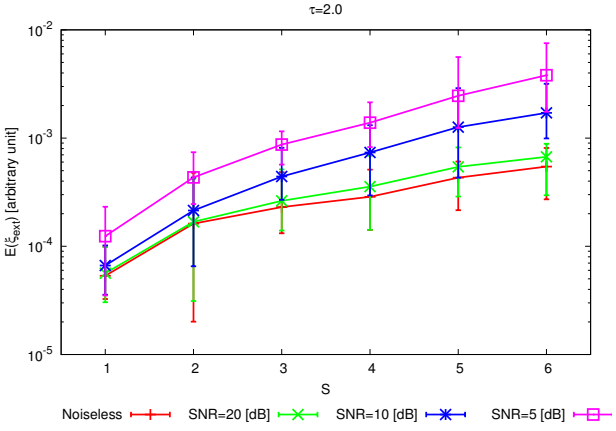

(c)

Figure 158. *Statistical analysis* $[K = 10, \varepsilon_r = 3.0]$ - Behaviour of mean, maximum and minimum of the error figures as a function of S (sparsity factor), for different SNR values: (a) total error ξ_{tot}, (b) internal error ξ_{int}, (c) external error ξ_{ext}.

RESULTS: $\varepsilon_r = 4.0$

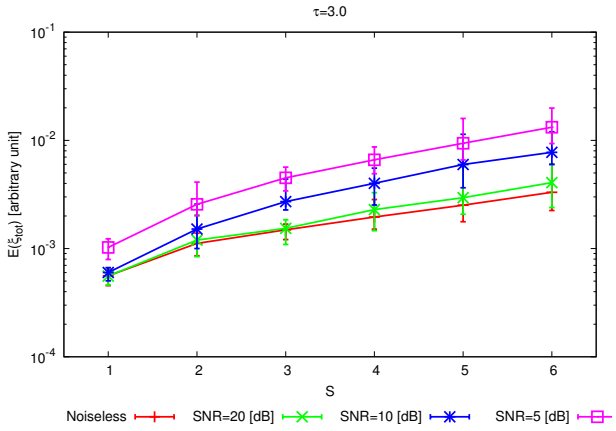

(a)

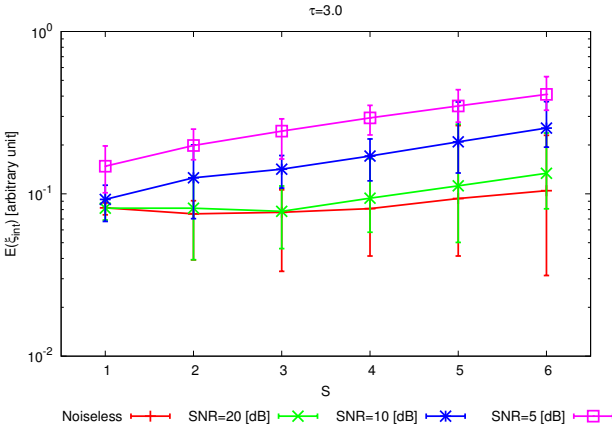

(b)

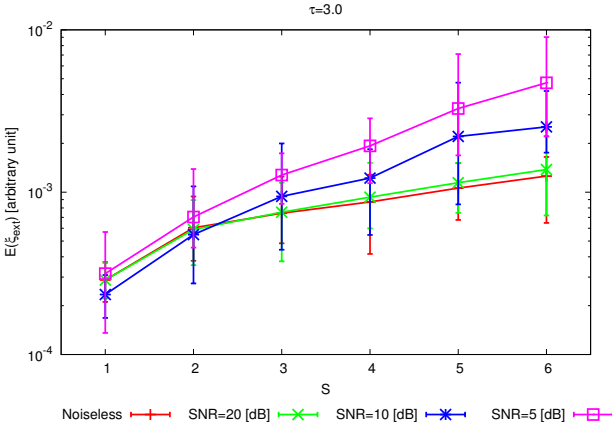

(c)

Figure 159. *Statistical analysis* $[K = 10, \varepsilon_r = 4.0]$ - Behaviour of mean, maximum and minimum of the error figures as a function of S (sparsity factor), for different SNR values: (a) total error ξ_{tot}, (b) internal error ξ_{int}, (c) external error ξ_{ext}.

RESULTS: $\varepsilon_r = 5.0$

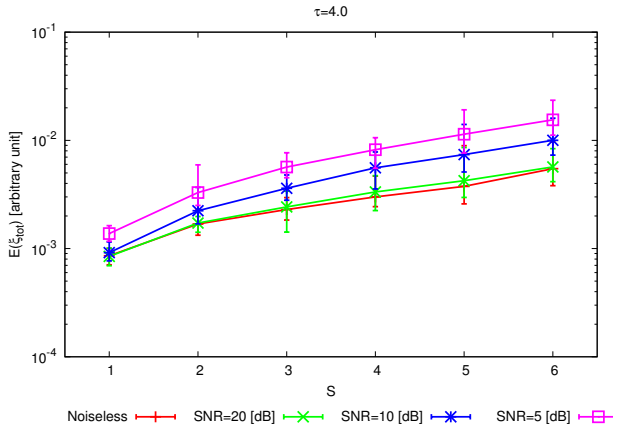

(a)

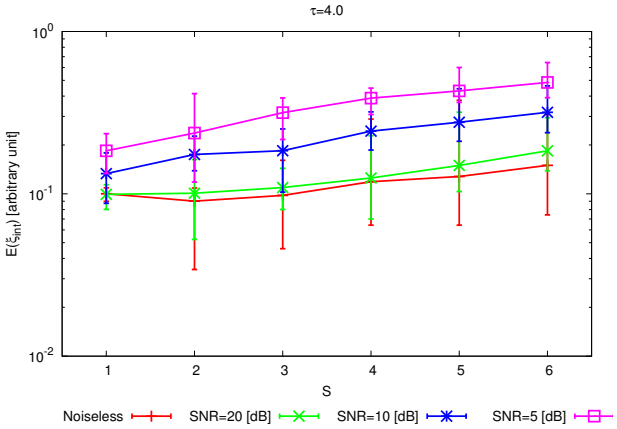

(b)

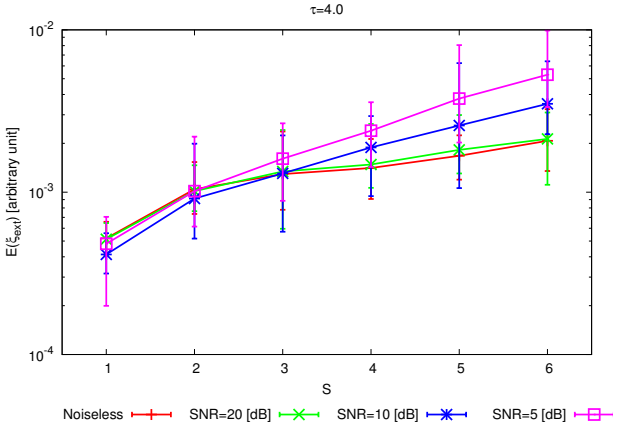

(c)

Figure 160. *Statistical analysis* $[K = 10, \varepsilon_r = 5.0]$ - Behaviour of mean, maximum and minimum of the error figures as a function of S (sparsity factor), for different SNR values: (a) total error ξ_{tot}, (b) internal error ξ_{int}, (c) external error ξ_{ext}.

TEST CASE: Two Square Cylinders on the Diagonal

Goal: evaluate the the performances of BCS

- Number of Views: V
- Number of Measurements: M
- Number of Cells for the Inversion: N
- Number of Cells for the Direct solver: D
- Side of the investigation domain: L

Test Case Description

Direct solver:

- Square domain divided in $\sqrt{D} \times \sqrt{D}$ cells
- Domain side: $L = 3\lambda$
- $D = 1296$ (discretization for the direct solver: $< \lambda/10$)

Investigation domain:

- Square domain divided in $\sqrt{N} \times \sqrt{N}$ cells
- $L = 3\lambda$
- $N = 324$

Measurement domain:

- Measurement points taken on a circle of radius $\rho = 3\lambda$
- Full-aspect measurements
- $M \approx 2ka \rightarrow M = 27$

Sources:

- Plane waves
- $V \approx 2ka \rightarrow V = 27$
- Amplitude $A = 1$
- Frequency: 300 MHz ($\lambda = 1$)

Object:

- Two square cylinders of side $\frac{\lambda}{6} = 0.16667$ at a distance Δx, Δy from each other
- $\varepsilon_r \in \{1.5, 2.0, 3.0, 4.0, 5.0\}$
- $\sigma = 0$ [S/m]

BCS parameters:

- Gamma prior on noise variance parameters: $a = 1 \times 10^{+1}$, $b = 5 \times 10^{-3}$
- Convergenze parameter: $\tau = 1.0 \times 10^{-8}$

Resolution Analysis:

- $\Delta x = \Delta y = \{k\lambda/10,\ k = 0, ..., 14\}$

RESULTS: $\varepsilon_r = 1.5$

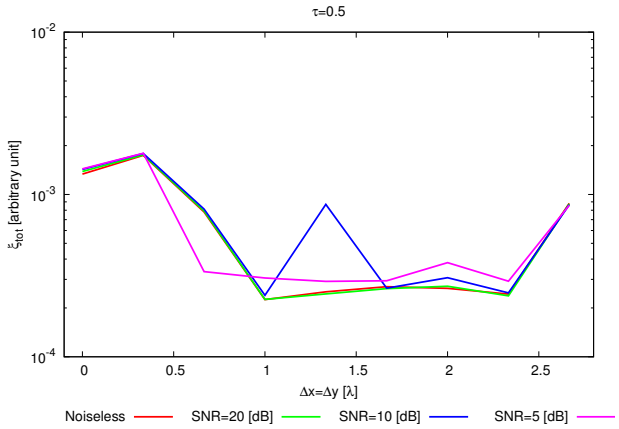

(a)

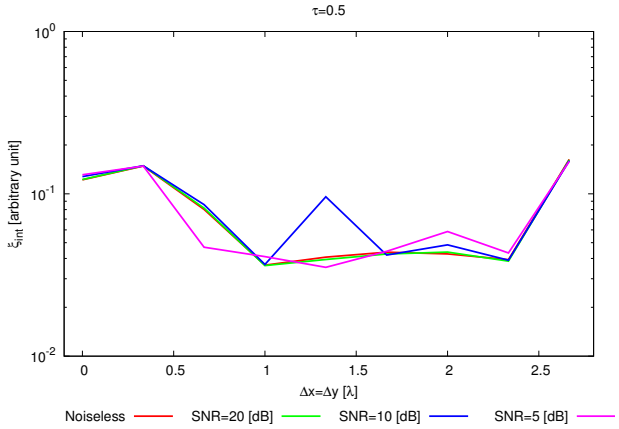

(b)

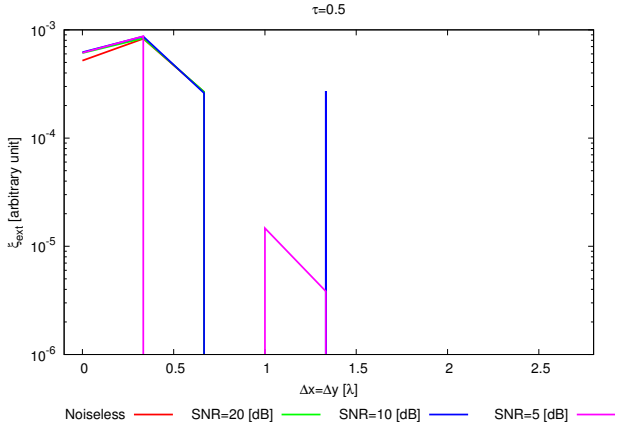

(c)

Figure 161. *Resolution analysis* - Behaviour of error figures as a function of $\Delta x = \Delta y$ for different SNR values: (a) total error ξ_{tot}, (b) internal error ξ_{int}, (c) external error ξ_{ext}.

RESULTS: $\varepsilon_r = 2.0$

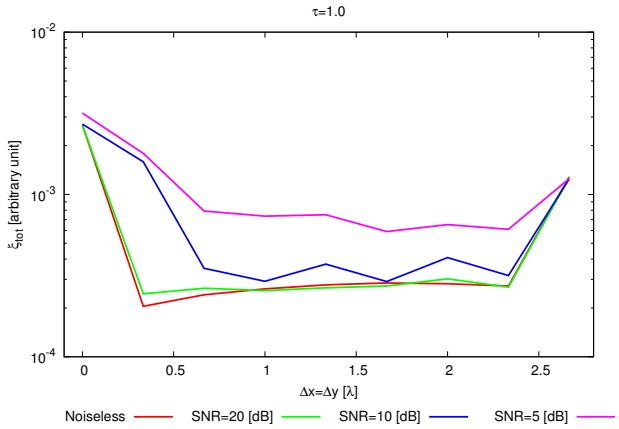

(a)

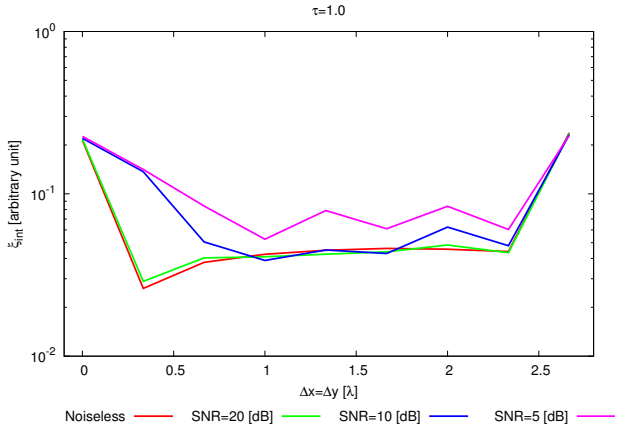

(b)

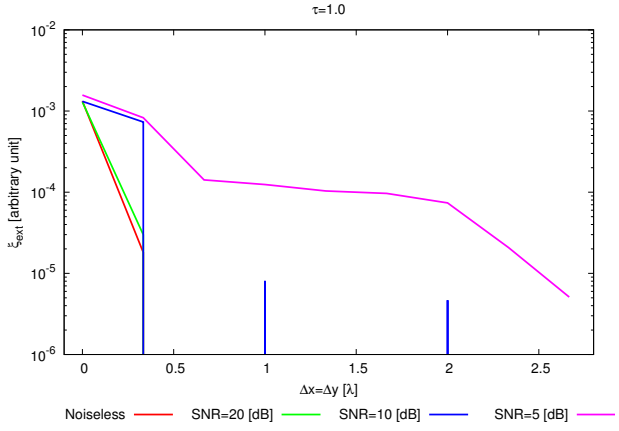

(c)

Figure 162. *Resolution analysis* - Behaviour of error figures as a function of $\Delta x = \Delta y$ for different SNR values: (a) total error ξ_{tot}, (b) internal error ξ_{int}, (c) external error ξ_{ext}.

RESULTS: $\varepsilon_r = 3.0$

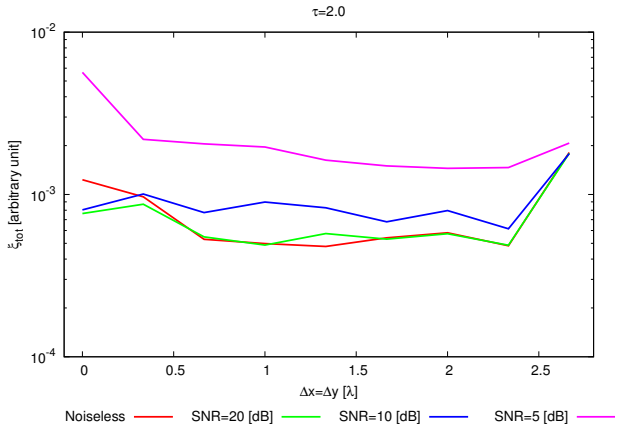

(a)

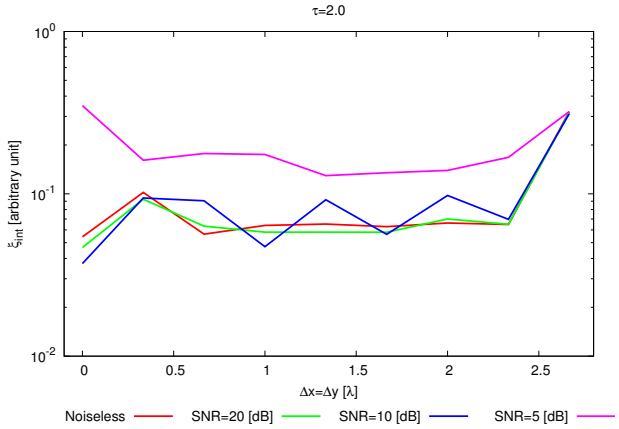

(b)

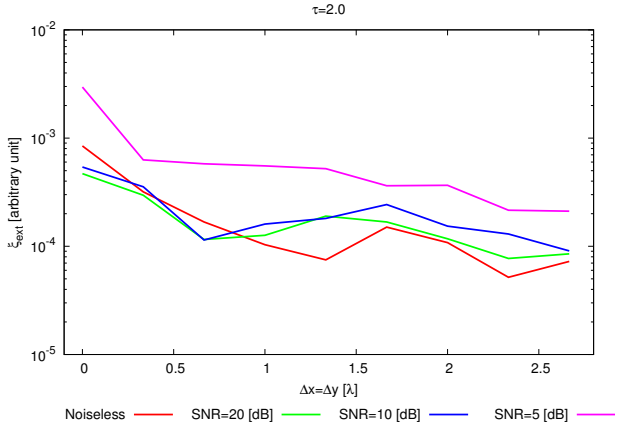

(c)

Figure 163. *Resolution analysis* - Behaviour of error figures as a function of $\Delta x = \Delta y$ for different SNR values: (a) total error ξ_{tot}, (b) internal error ξ_{int}, (c) external error ξ_{ext}.

RESULTS: $\varepsilon_r = 4.0$

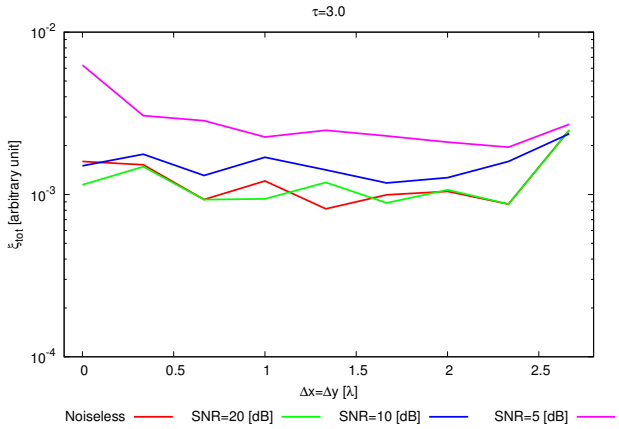

(a)

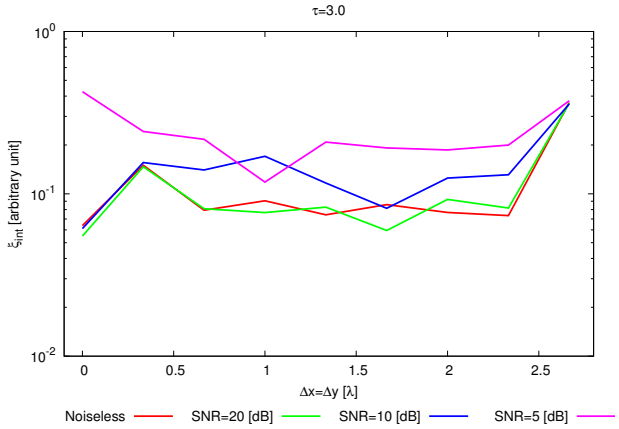

(b)

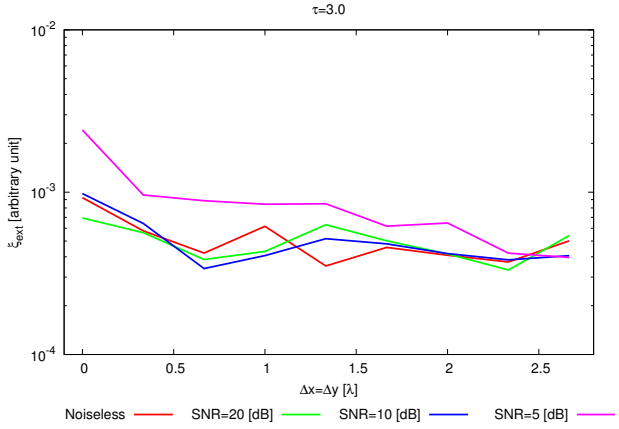

(c)

Figure 164. *Resolution analysis* - Behaviour of error figures as a function of $\Delta x = \Delta y$ for different SNR values: (a) total error ξ_{tot}, (b) internal error ξ_{int}, (c) external error ξ_{ext}.

RESULTS: $\varepsilon_r = 5.0$

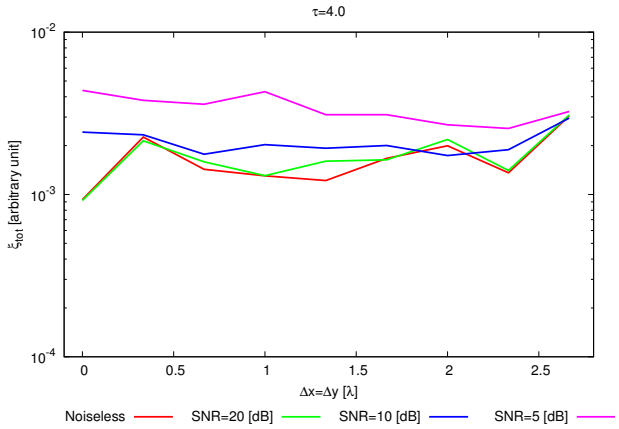

(a)

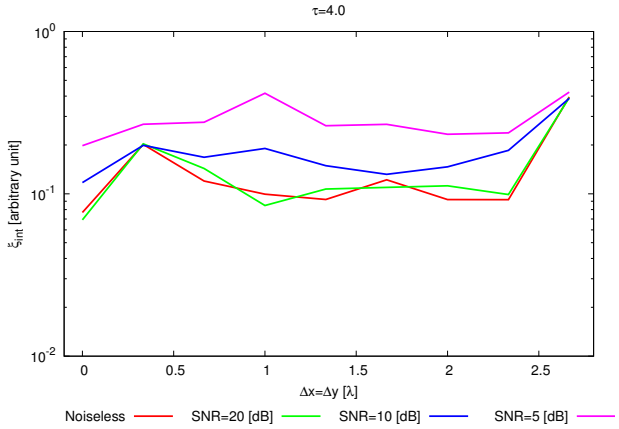

(b)

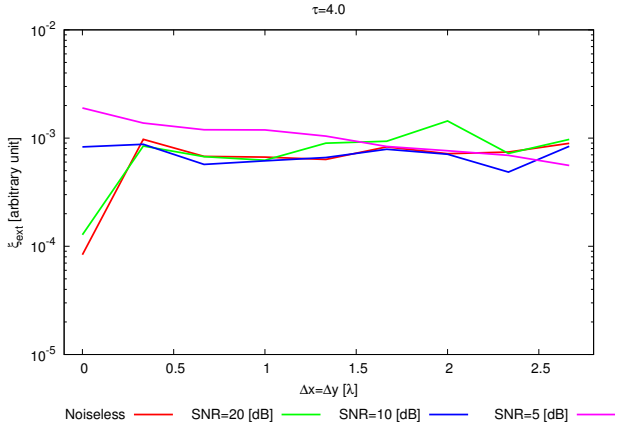

(c)

Figure 165. *Resolution analysis* - Behaviour of error figures as a function of $\Delta x = \Delta y$ for different SNR values: (a) total error ξ_{tot}, (b) internal error ξ_{int}, (c) external error ξ_{ext}.

5 MV-XY-MT-BCS (Exploiting Correlation between Views and Field Components)

5.1 MV-XY-MT-BCS - Calibration

TEST CASE: Square Cylinder

Goal: show the performances of BCS when dealing with a sparse scatterer

- Number of Views: V
- Number of Measurements: M
- Number of Cells for the Inversion: N
- Number of Cells for the Direct solver: D
- Side of the investigation domain: L

Test Case Description

Direct solver:

- Square domain divided in $\sqrt{D} \times \sqrt{D}$ cells
- Domain side: $L = 3\lambda$
- $D = 1296$ (discretization for the direct solver: $< \lambda/10$)

Investigation domain:

- Square domain divided in $\sqrt{N} \times \sqrt{N}$ cells
- $L = 3\lambda$
- $2ka = 2 \times \frac{2\pi}{\lambda} \times \frac{L\sqrt{2}}{2} = 6\pi\sqrt{2} = 26.65$
- $\#DOF = \frac{(2ka)^2}{2} = \frac{(2 \times \frac{2\pi}{\lambda} \times \frac{L\sqrt{2}}{2})^2}{2} = 4\pi^2 \left(\frac{L}{\lambda}\right)^2 = 4\pi^2 \times 9 \approx 355.3$
- N scelto in modo da essere vicino a $\#DOF$: $N = 324$ (18×18)

Measurement domain:

- Measurement points taken on a circle of radius $\rho = 3\lambda$
- Full-aspect measurements
- $M \approx 2ka \rightarrow M = 27$

Sources:

- Plane waves
- $V \approx 2ka \rightarrow V = 27$
- Amplitude: $A = 1$
- Frequency: 300 MHz ($\lambda = 1$)

Object:

- Square cylinder of side $\frac{\lambda}{6} = 0.1667$
- $\varepsilon_r = 2.0$

- $\sigma = 0$ [S/m]

BCS parameters:

- Gamma prior on noise variance parameter: $a \in \{1 \times 10^{-1}, 2 \times 10^{-1}, 5 \times 10^{-1}\ 1 \times 10^{0}, 2 \times 10^{0}, 5 \times 10^{0}, 1 \times 10^{+1}, 2 \times 10^{+1}, 5 \times 10^{+1}, 1 \times 10^{+2}, 2 \times 10^{+2}, 5 \times 10^{+2}, 1 \times 10^{+3}, 2 \times 10^{+3}, 5 \times 10^{+3}, 1 \times 10^{+4}\}$
- Gamma prior on noise variance parameter: $b \in \{1 \times 10^{+0}, 5 \times 10^{-1}, 2 \times 10^{-1}, 1 \times 10^{-1}, 5 \times 10^{-2}, 2 \times 10^{-2}\ 1 \times 10^{-2}, 5 \times 10^{-3}, 2 \times 10^{-3}, 1 \times 10^{-3}, 5 \times 10^{-4}, 2 \times 10^{-4}, 1 \times 10^{-4}\}$
- Convergenze parameter: $\tau = 1.0 \times 10^{-8}$

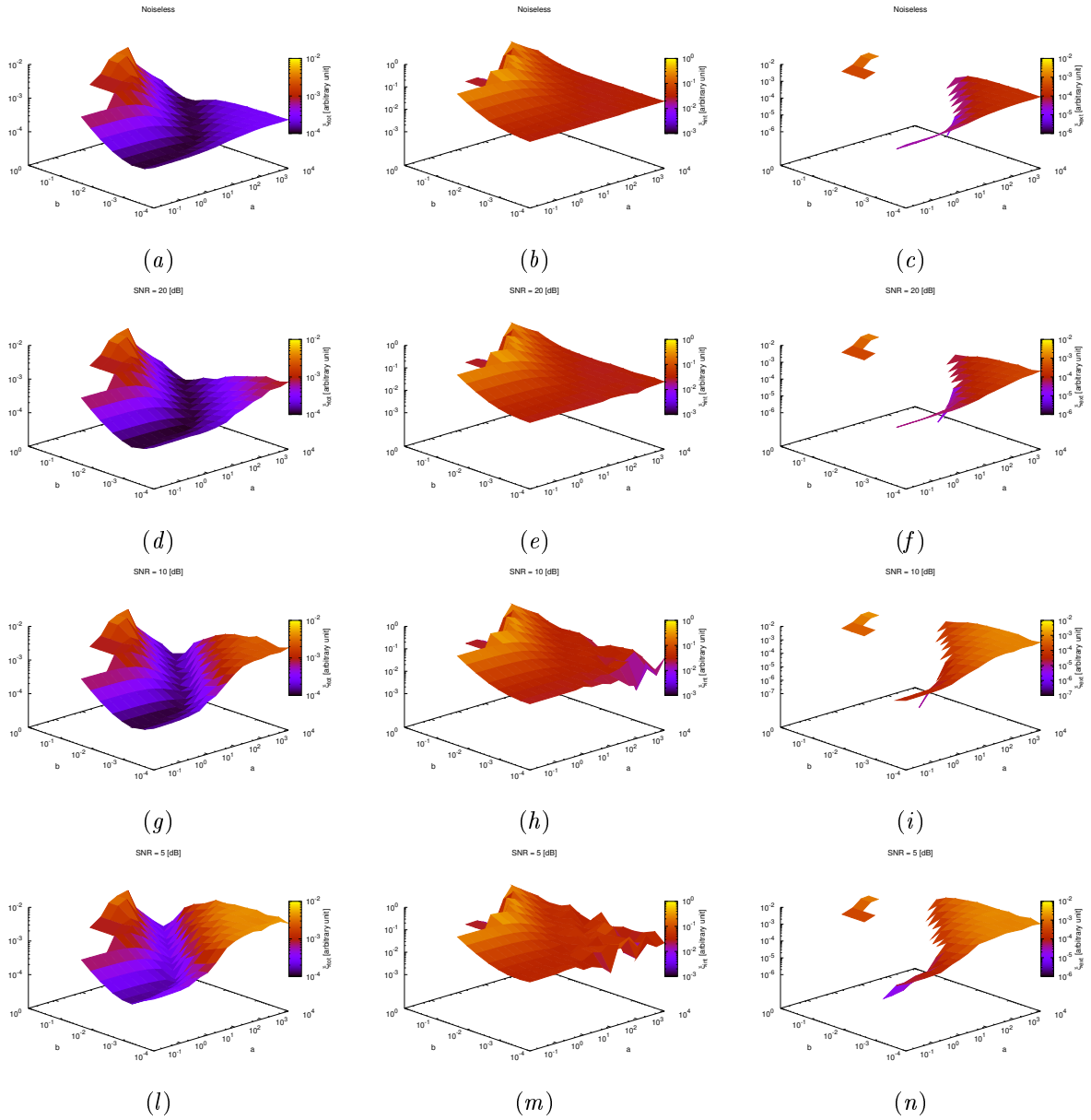

Figure 108. Behaviour of error figures as a function of the initial estimate of the Gamma prior on the noise variance parameters a and b, for different SNR values: (a), (d), (g) and (l) total error ξ_{tot}, (b), (e), (h) and (m) internal error ξ_{int}, (c), (f), (i) and (n) external error ξ_{ext}, for (a), (b) and (c) Noiseless case, (d), (e) and (f) $SNR = 20dB$, (g), (h) and (i) $SNR = 10dB$ and (l), (m) and (n) $SNR = 5dB$.

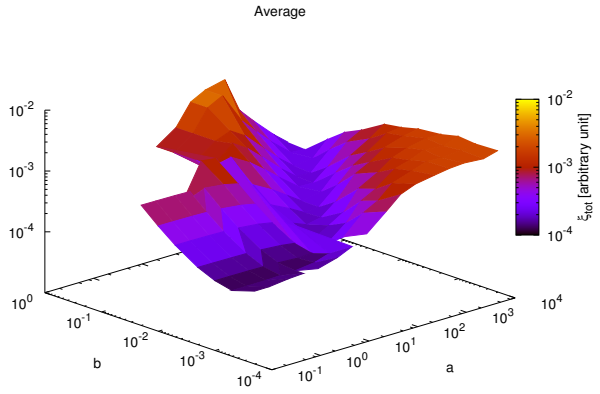

(a)

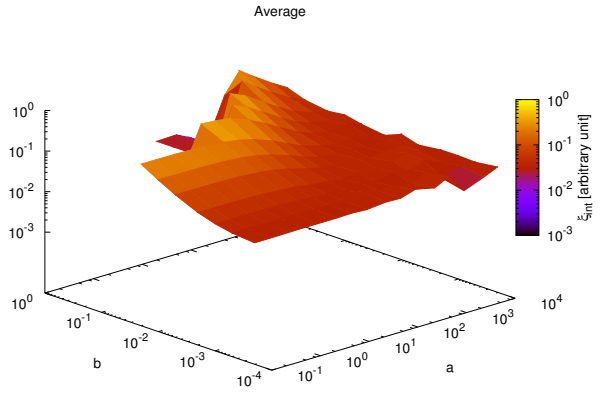

(b)

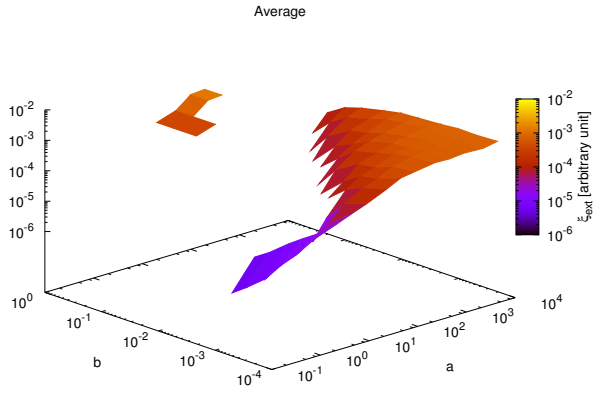

(c)

Figure 109. Averaged behaviour of error figures as a function of the initial estimate of the Gamma prior on the noise variance parameters a and b: (a) total error ξ_{tot}, (b) internal error ξ_{int}, (c) external error ξ_{ext}.

5.2 MV-XY-MT-BCS - Basic Tests

TEST CASE: Square Cylinder $L = 0.16\lambda$

Goal: show the performances of BCS when dealing with a sparse scatterer

- Number of Views: V
- Number of Measurements: M
- Number of Cells for the Inversion: N
- Number of Cells for the Direct solver: D
- Side of the investigation domain: L

Test Case Description

Direct solver:

- Square domain divided in $\sqrt{D} \times \sqrt{D}$ cells
- Domain side: $L = 3\lambda$
- $D = 1296$ (discretization for the direct solver: $< \lambda/10$)

Investigation domain:

- Square domain divided in $\sqrt{N} \times \sqrt{N}$ cells
- $L = 3\lambda$
- $2ka = 2 \times \frac{2\pi}{\lambda} \times \frac{L\sqrt{2}}{2} = 6\pi\sqrt{2} = 26.65$
- $\#DOF = \frac{(2ka)^2}{2} = \frac{(2 \times \frac{2\pi}{\lambda} \times \frac{L\sqrt{2}}{2})^2}{2} = 4\pi^2 \left(\frac{L}{\lambda}\right)^2 = 4\pi^2 \times 9 \approx 355.3$
- N scelto in modo da essere vicino a $\#DOF$: $N = 324$ (18×18)

Measurement domain:

- Measurement points taken on a circle of radius $\rho = 3\lambda$
- Full-aspect measurements
- $M \approx 2ka \rightarrow M = 27$

Sources:

- Plane waves
- $V \approx 2ka \rightarrow V = 27$
- Amplitude: $A = 1$
- Frequency: 300 MHz ($\lambda = 1$)

Object:

- Square cylinder of side $\frac{\lambda}{6} = 0.1667$
- $\varepsilon_r \in \{1.5, 2.0, 2.5, 3.0, 3.5, 4.0, 4.5, 5.0\}$

- $\sigma = 0$ [S/m]

BCS parameters:

- Gamma prior on noise variance parameters: $a = 1 \times 10^{-1}$, $b = 5 \times 10^{-4}$
- Convergenze parameter: $\tau = 1.0 \times 10^{-8}$

RESULTS: $\varepsilon_r = 1.5$

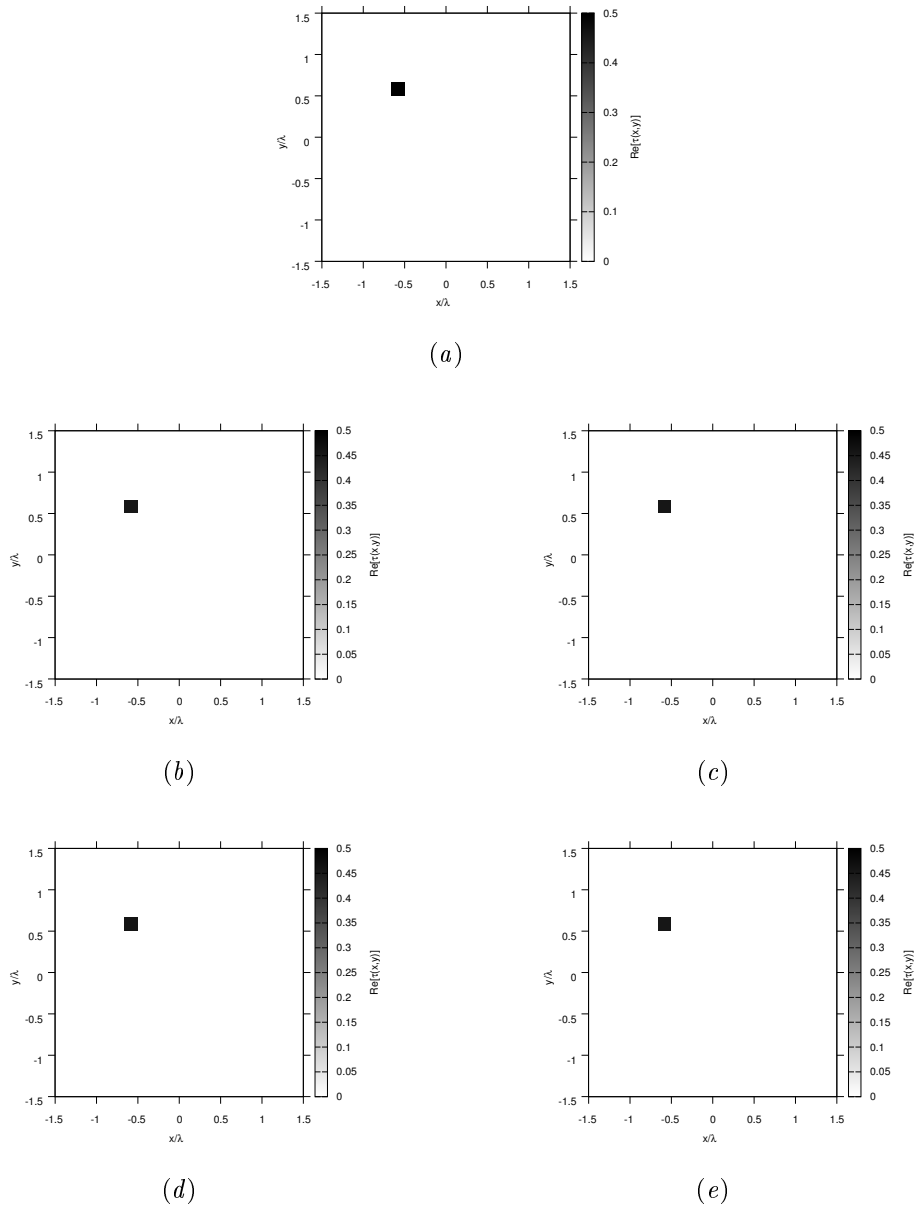

(a) (b) (c) (d) (e)

Figure 110. Actual object (a) and BCS reconstructed object for (b) Noiseless case, (c) $SNR = 20$ [dB] , (d) $SNR = 10$ [dB] , (e) $SNR = 5$ [dB].

RESULTS: $\varepsilon_r = 2.0$

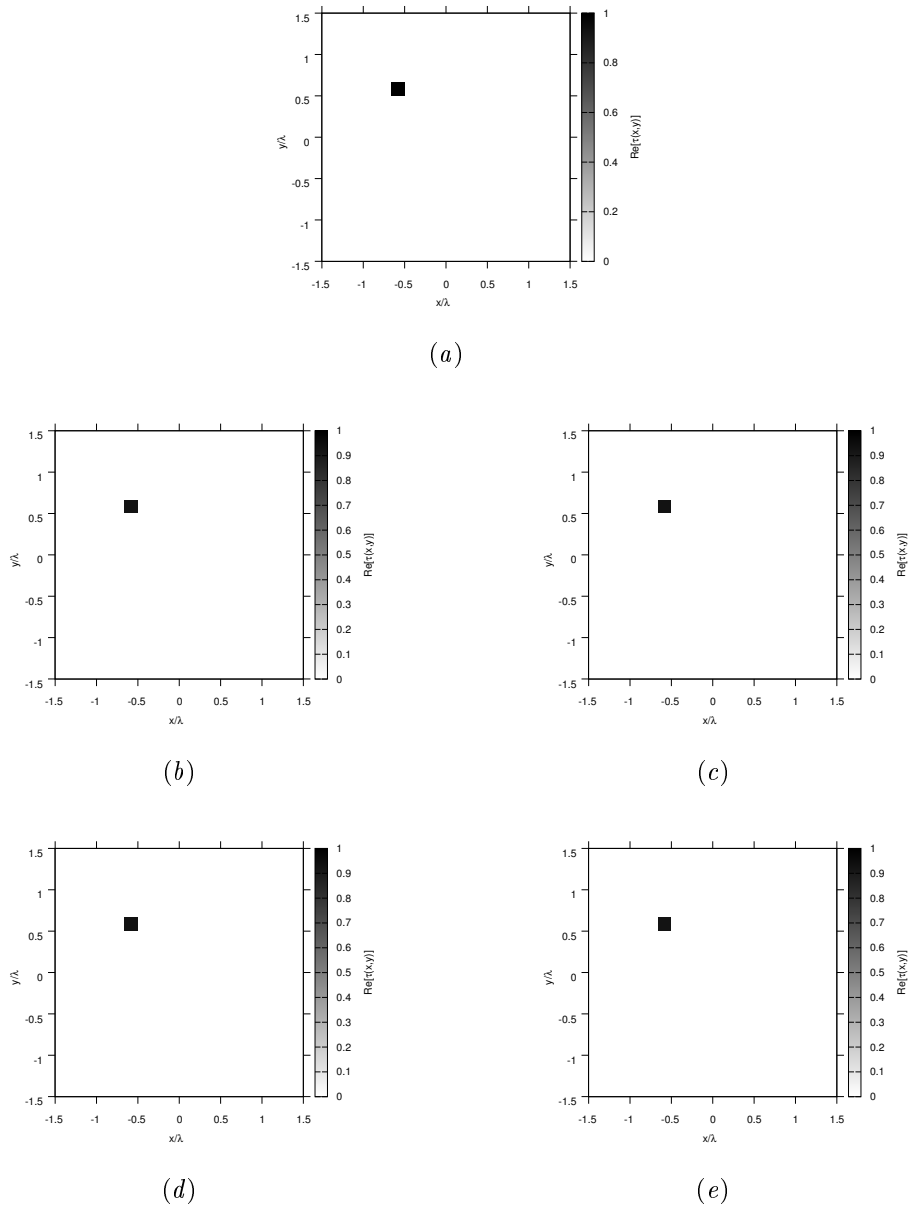

(a) (b) (c) (d) (e)

Figure 111. Actual object (a) and BCS reconstructed object for (b) Noiseless case, (c) $SNR = 20$ [dB] , (d) $SNR = 10$ [dB] , (e) $SNR = 5$ [dB].

RESULTS: $\varepsilon_r = 5.0$

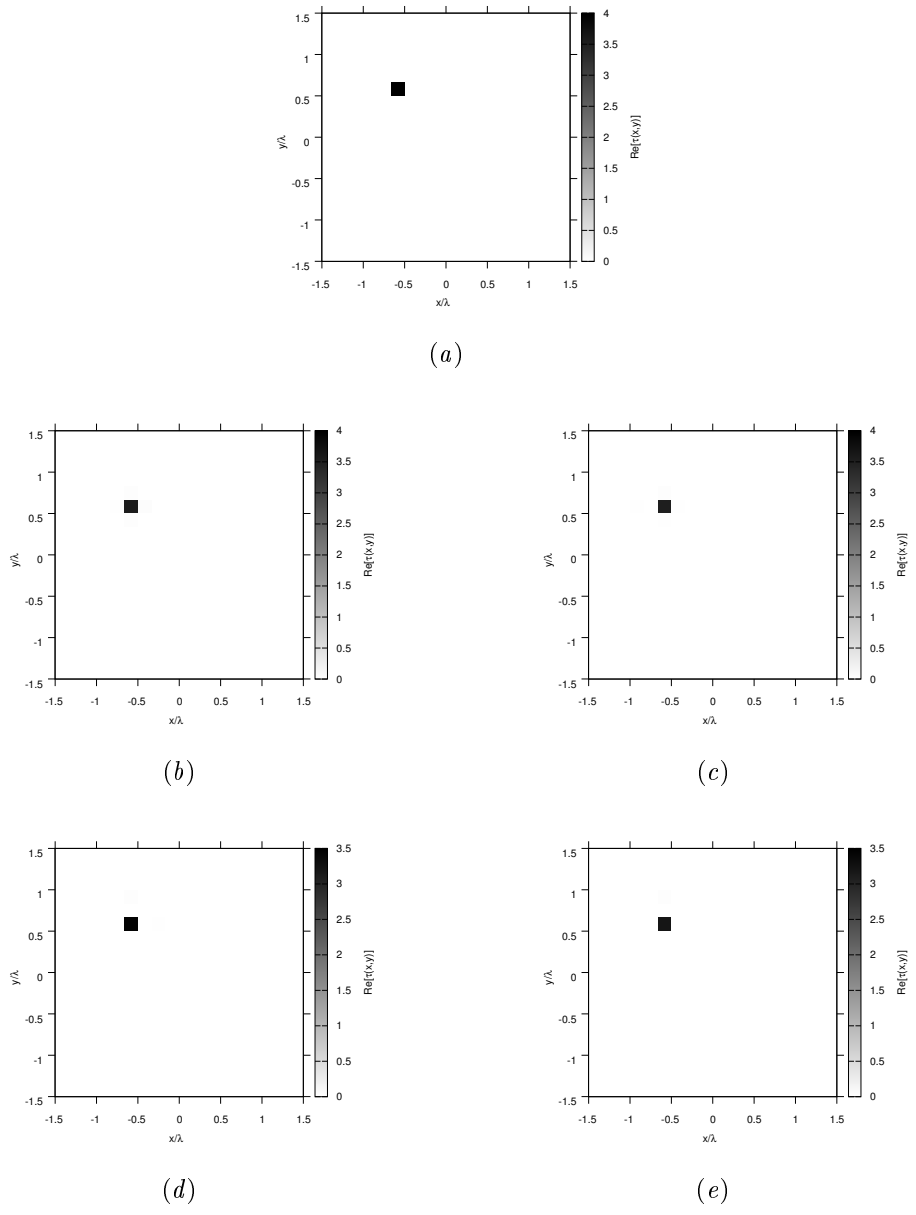

(a)

(b)

(c)

(d)

(e)

Figure 112. Actual object (a) and BCS reconstructed object for (b) Noiseless case, (c) $SNR = 20$ [dB] , (d) $SNR = 10$ [dB] , (e) $SNR = 5$ [dB].

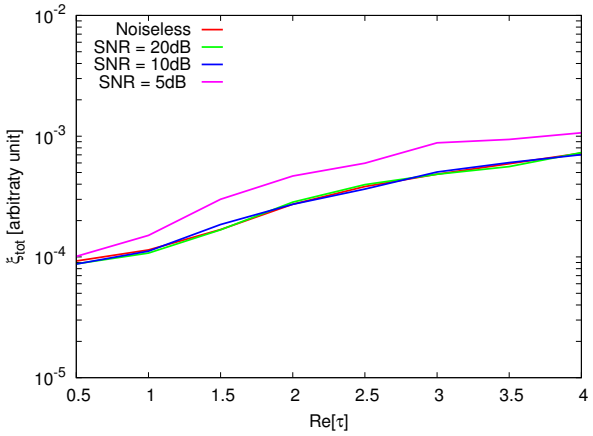

(a)

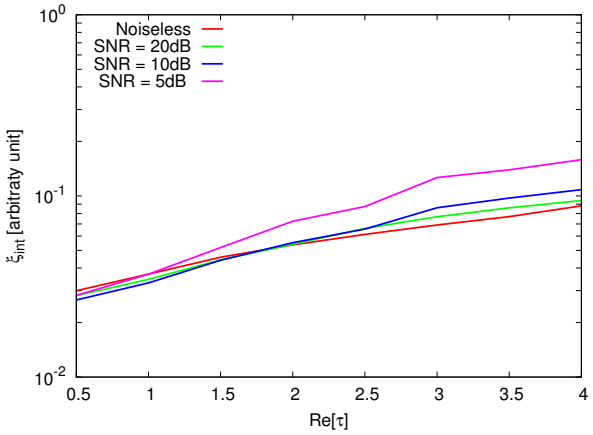

(b)

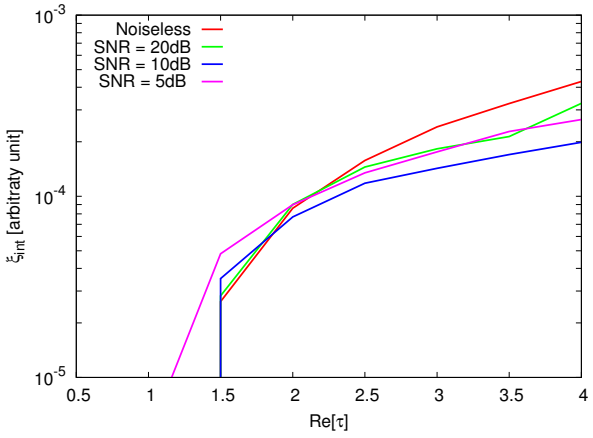

(c)

Figure 113. Behaviour of error figures as a function of ε_r, for different SNR values: (a) total error ξ_{tot}, (b) internal error ξ_{int}, (c) external error ξ_{ext}.

TEST CASE: Two Square Cylinders $L = 0.16\lambda$

Goal: show the performances of BCS when dealing with a sparse scatterer

- Number of Views: V
- Number of Measurements: M
- Number of Cells for the Inversion: N
- Number of Cells for the Direct solver: D
- Side of the investigation domain: L

Test Case Description

Direct solver:

- Square domain divided in $\sqrt{D} \times \sqrt{D}$ cells
- Domain side: $L = 3\lambda$
- $D = 1296$ (discretization for the direct solver: $< \lambda/10$)

Investigation domain:

- Square domain divided in $\sqrt{N} \times \sqrt{N}$ cells
- $L = 3\lambda$
- $2ka = 2 \times \frac{2\pi}{\lambda} \times \frac{L\sqrt{2}}{2} = 6\pi\sqrt{2} = 26.65$
- $\#DOF = \frac{(2ka)^2}{2} = \frac{(2 \times \frac{2\pi}{\lambda} \times \frac{L\sqrt{2}}{2})^2}{2} = 4\pi^2 \left(\frac{L}{\lambda}\right)^2 = 4\pi^2 \times 9 \approx 355.3$
- N scelto in modo da essere vicino a $\#DOF$: $N = 324$ (18×18)

Measurement domain:

- Measurement points taken on a circle of radius $\rho = 3\lambda$
- Full-aspect measurements
- $M \approx 2ka \rightarrow M = 27$

Sources:

- Plane waves
- $V \approx 2ka \rightarrow V = 27$
- Amplitude: $A = 1$
- Frequency: 300 MHz $(\lambda = 1)$

Object:

- Two square cylinders of side $\frac{\lambda}{6} = 0.1667$
- $\varepsilon_r \in \{1.5, 2.0, 2.5, 3.0, 3.5, 4.0, 4.5, 5.0\}$ (one square), $\varepsilon_r = 1.5$ (one square)
- $\sigma = 0$ [S/m]

BCS parameters:

- Gamma prior on noise variance parameters: $a = 1 \times 10^{-1}$, $b = 5 \times 10^{-4}$
- Convergenze parameter: $\tau = 1.0 \times 10^{-8}$

RESULTS: $\varepsilon_r = 1.5$

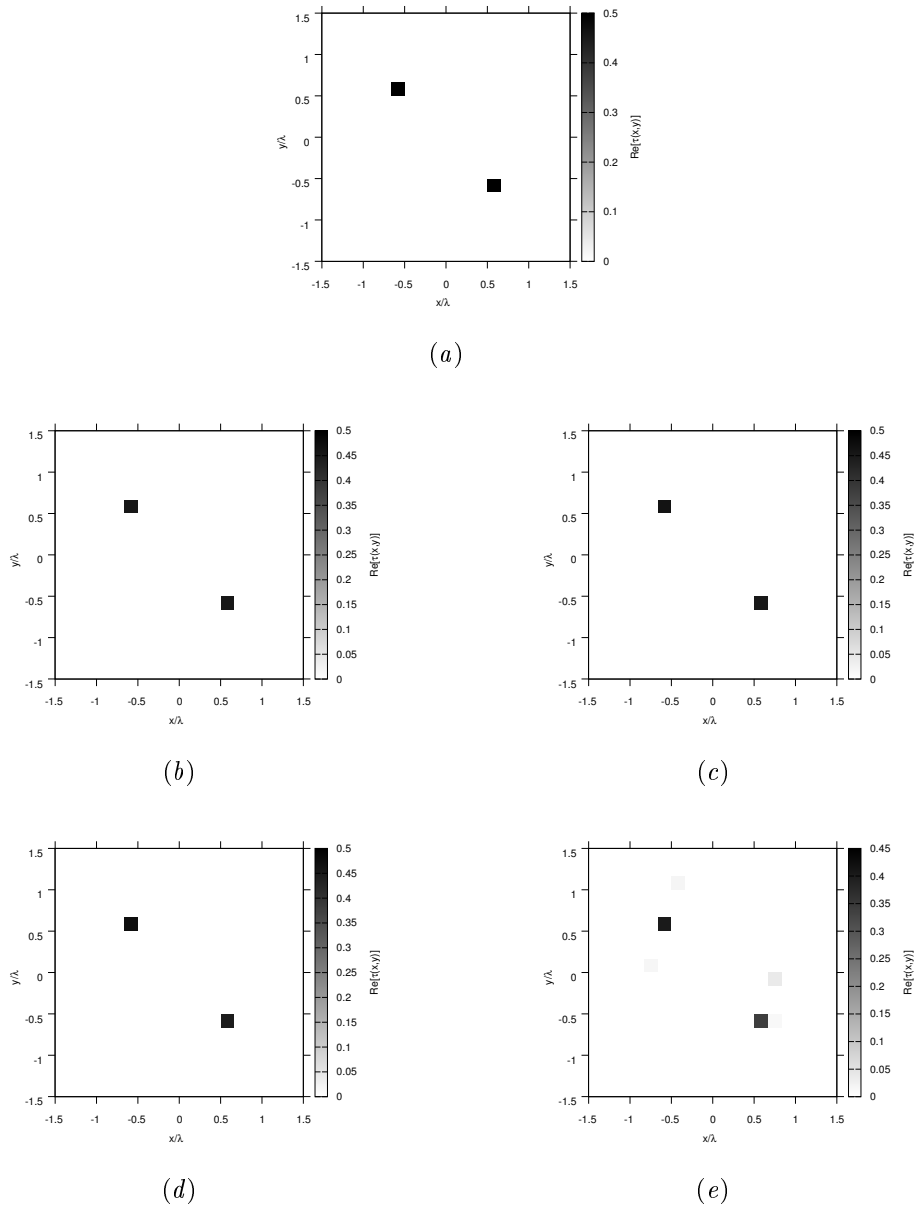

(a) (b) (c) (d) (e)

Figure 114. Actual object (a) and BCS reconstructed object for (b) Noiseless case, (c) $SNR = 20$ [dB] , (d) $SNR = 10$ [dB] , (e) $SNR = 5$ [dB].

RESULTS: $\varepsilon_r = 2.0$

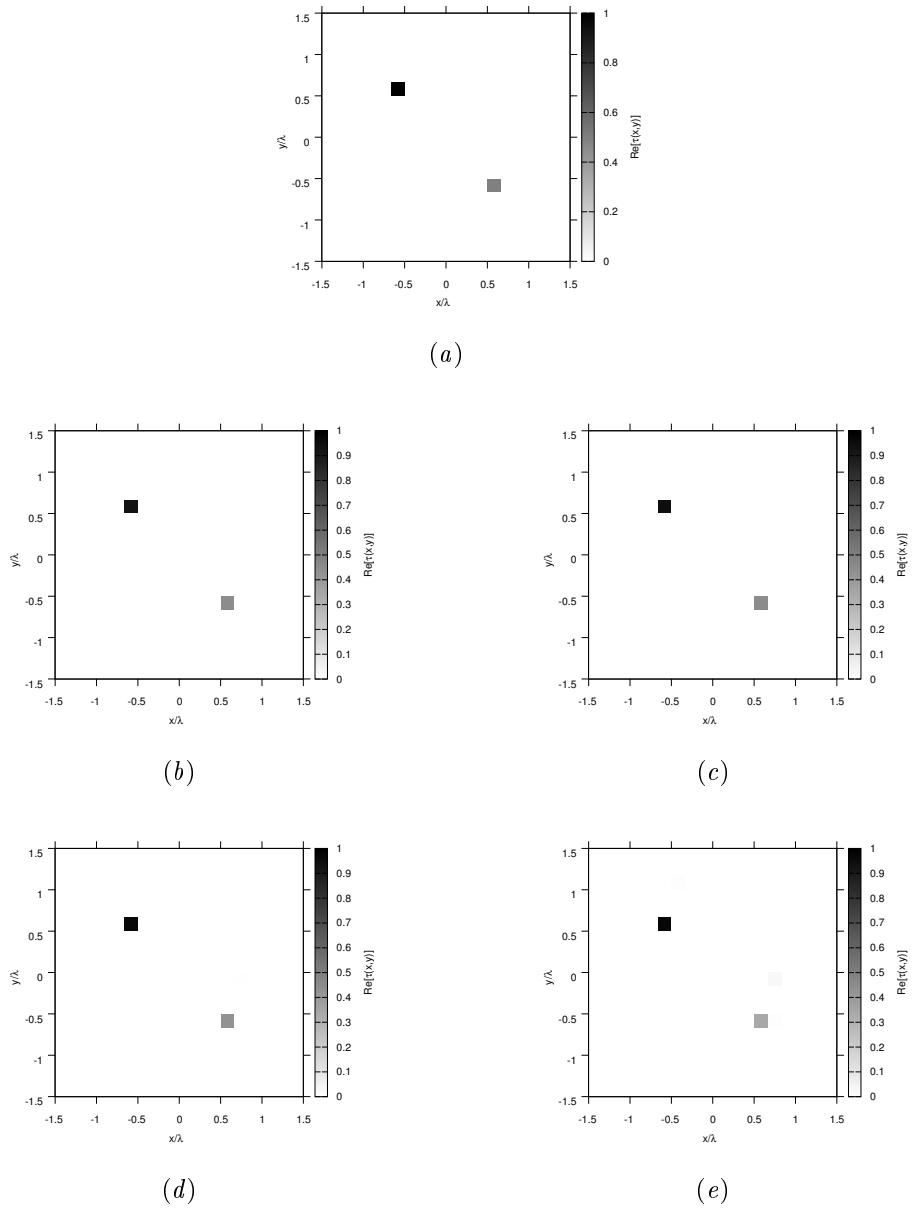

(a) (b) (c) (d) (e)

Figure 115. Actual object (a) and BCS reconstructed object for (b) Noiseless case, (c) $SNR = 20$ [dB] , (d) $SNR = 10$ [dB] , (e) $SNR = 5$ [dB].

RESULTS: $\varepsilon_r = 5.0$

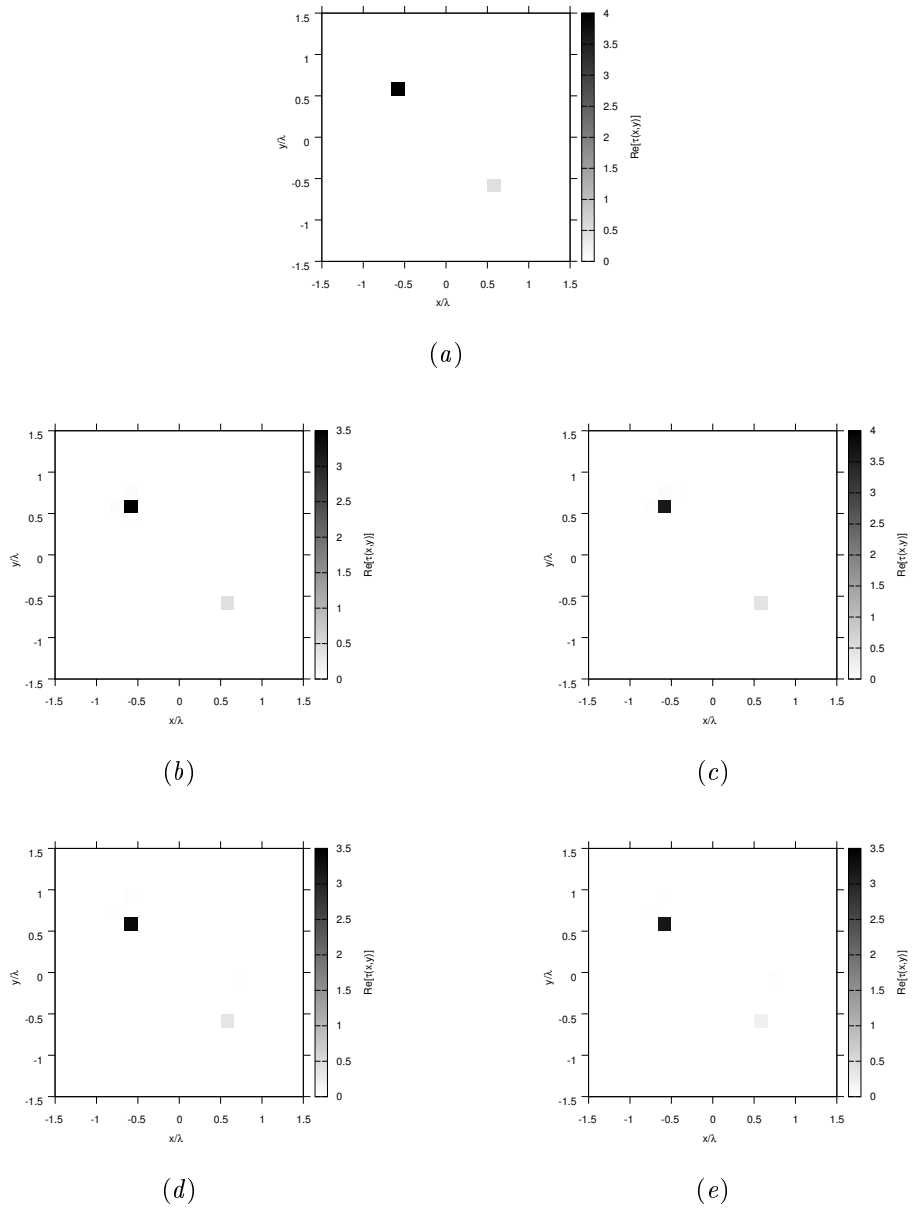

(a)

(b)

(c)

(d)

(e)

Figure 116. Actual object (a) and BCS reconstructed object for (b) Noiseless case, (c) $SNR = 20$ [dB] , (d) $SNR = 10$ [dB] , (e) $SNR = 5$ [dB].

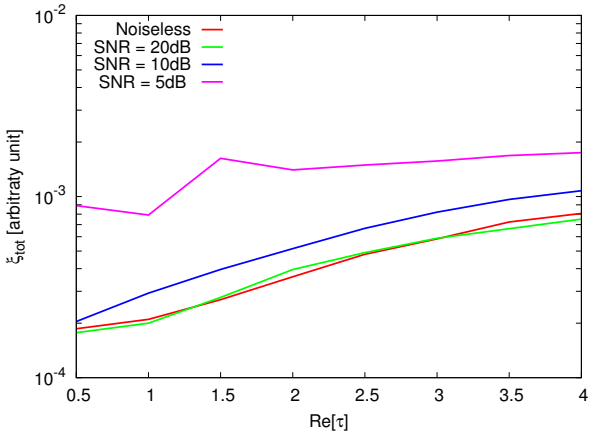

(a)

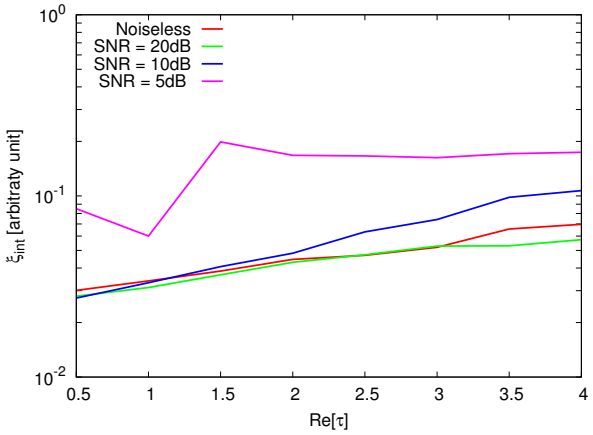

(b)

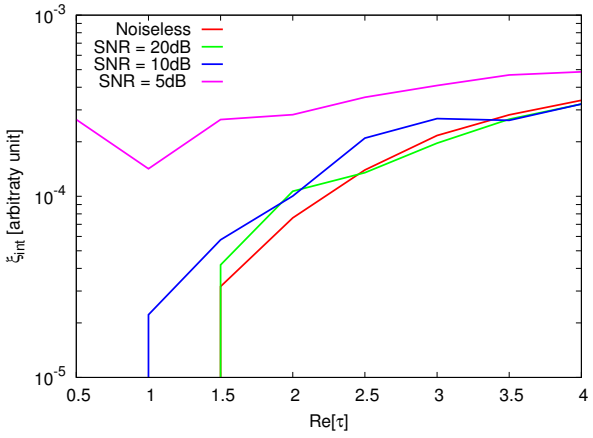

(c)

Figure 117. Behaviour of error figures as a function of ε_r, for different SNR values: (a) total error ξ_{tot}, (b) internal error ξ_{int}, (c) external error ξ_{ext}.

TEST CASE: Square Cylinder $L = 0.33\lambda$

Goal: show the performances of BCS when dealing with a sparse scatterer

- Number of Views: V
- Number of Measurements: M
- Number of Cells for the Inversion: N
- Number of Cells for the Direct solver: D
- Side of the investigation domain: L

Test Case Description

Direct solver:

- Square domain divided in $\sqrt{D} \times \sqrt{D}$ cells
- Domain side: $L = 3\lambda$
- $D = 1296$ (discretization for the direct solver: $< \lambda/10$)

Investigation domain:

- Square domain divided in $\sqrt{N} \times \sqrt{N}$ cells
- $L = 3\lambda$
- $2ka = 2 \times \frac{2\pi}{\lambda} \times \frac{L\sqrt{2}}{2} = 6\pi\sqrt{2} = 26.65$
- $\#DOF = \frac{(2ka)^2}{2} = \frac{(2 \times \frac{2\pi}{\lambda} \times \frac{L\sqrt{2}}{2})^2}{2} = 4\pi^2 \left(\frac{L}{\lambda}\right)^2 = 4\pi^2 \times 9 \approx 355.3$
- N scelto in modo da essere vicino a $\#DOF$: $N = 324$ (18×18)

Measurement domain:

- Measurement points taken on a circle of radius $\rho = 3\lambda$
- Full-aspect measurements
- $M \approx 2ka \rightarrow M = 27$

Sources:

- Plane waves
- $V \approx 2ka \rightarrow V = 27$
- Amplitude: $A = 1$
- Frequency: 300 MHz $(\lambda = 1)$

Object:

- Square cylinder of side $\frac{\lambda}{4} = 0.25$
- $\varepsilon_r \in \{1.5, 2.0, 2.5, 3.0, 3.5, 4.0, 4.5, 5.0\}$
- $\sigma = 0$ [S/m]

BCS parameters:

- Gamma prior on noise variance parameters: $a = 1 \times 10^{-1}$, $b = 5 \times 10^{-4}$
- Convergenze parameter: $\tau = 1.0 \times 10^{-8}$

RESULTS: $\varepsilon_r = 1.5$

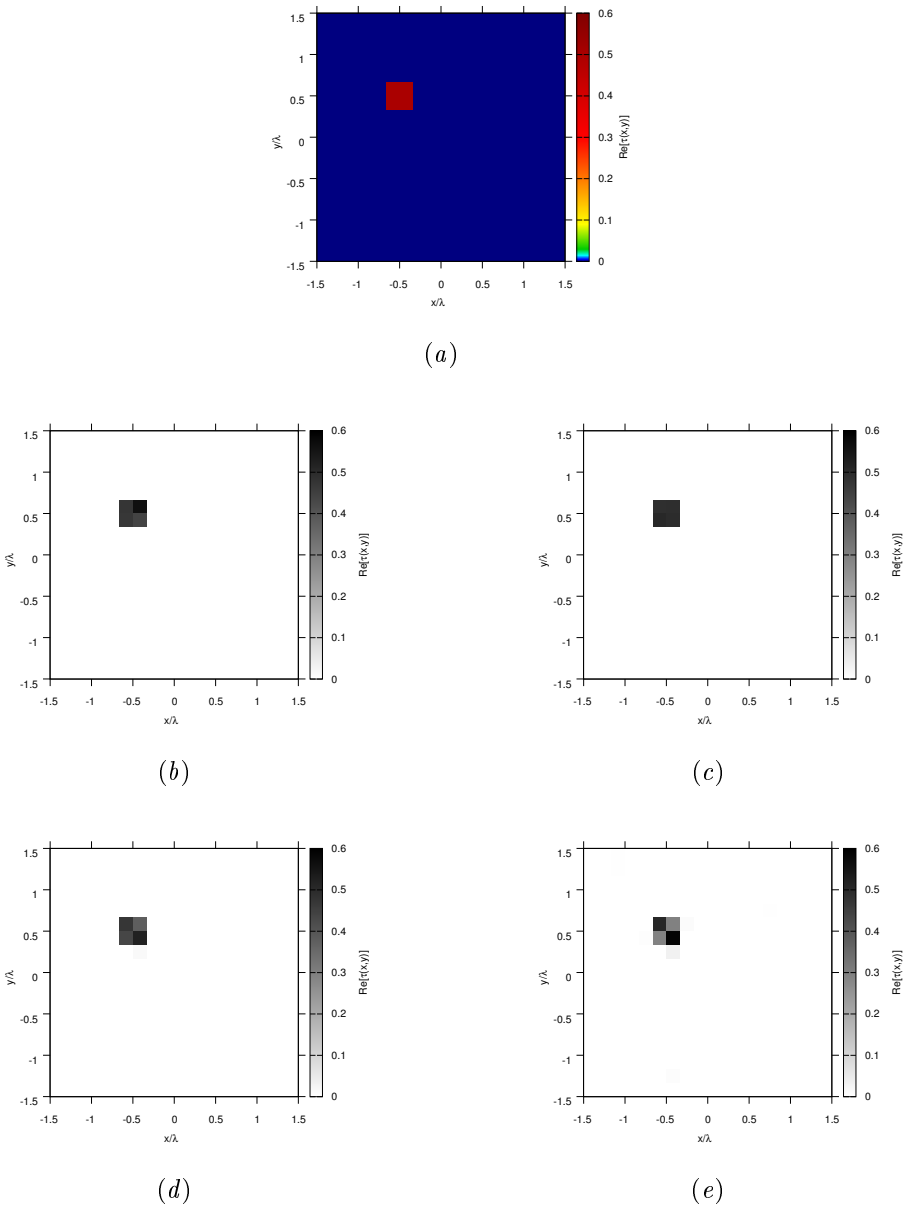

(a)

(b) (c)

(d) (e)

Figure 118. Actual object (a) and BCS reconstructed object for (b) Noiseless case, (c) $SNR = 20$ [dB] , (d) $SNR = 10$ [dB] , (e) $SNR = 5$ [dB].

RESULTS: $\varepsilon_r = 2.0$

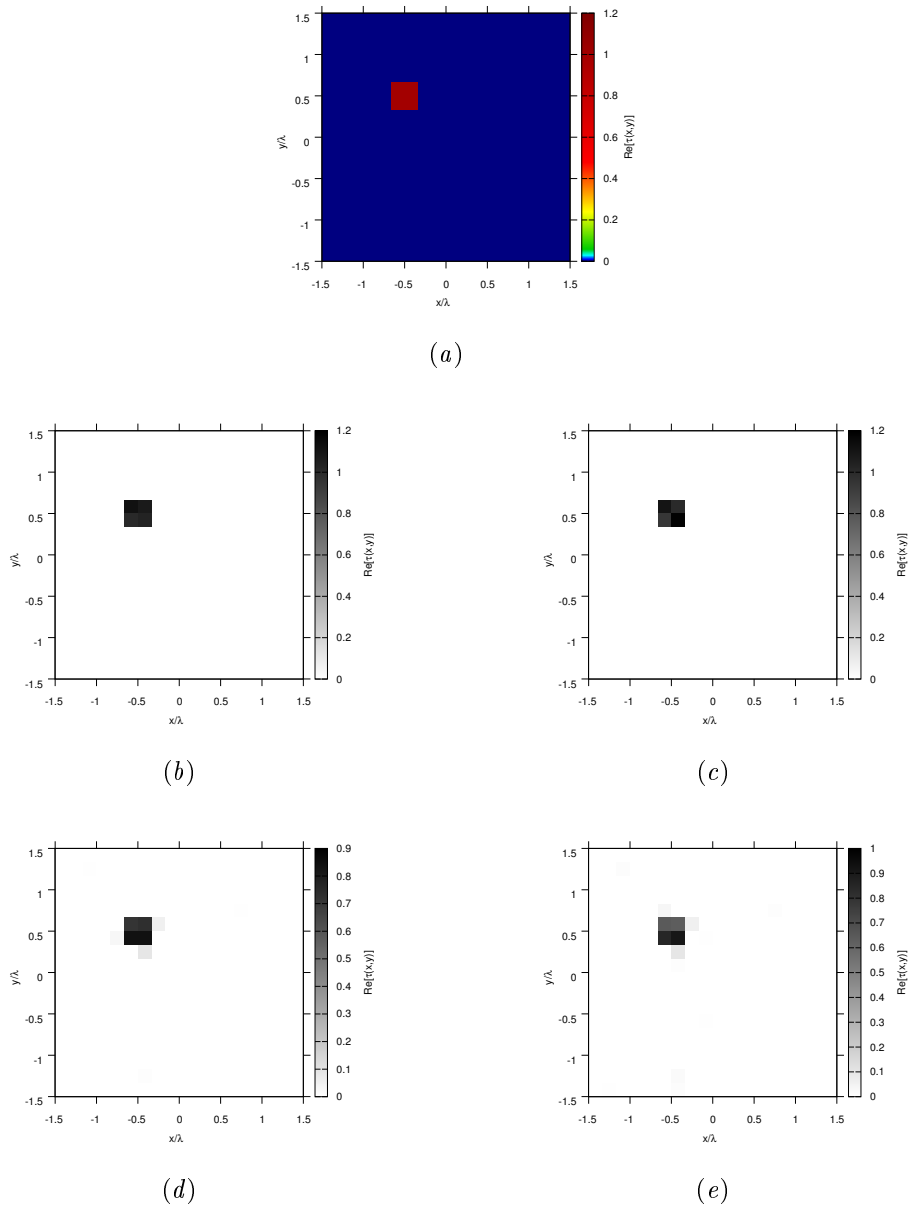

(a) (b) (c) (d) (e)

Figure 119. Actual object (a) and BCS reconstructed object for (b) Noiseless case, (c) $SNR = 20$ [dB] , (d) $SNR = 10$ [dB] , (e) $SNR = 5$ [dB].

RESULTS: $\varepsilon_r = 3.0$

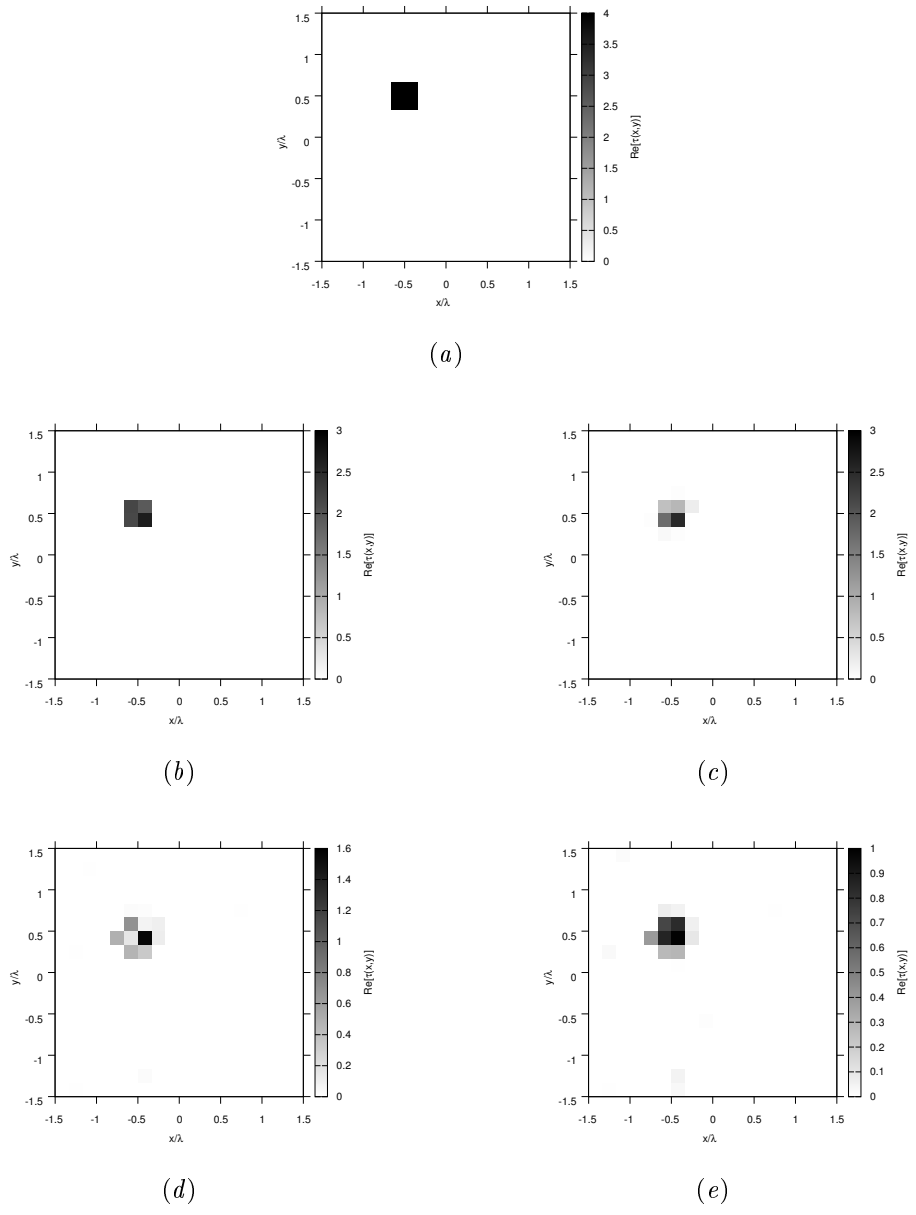

(a)

(b)

(c)

(d)

(e)

Figure 120. Actual object (a) and BCS reconstructed object for (b) Noiseless case, (c) $SNR = 20$ [dB] , (d) $SNR = 10$ [dB] , (e) $SNR = 5$ [dB].

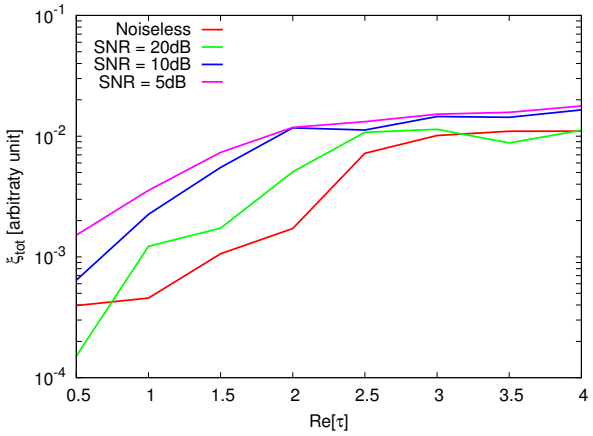

(a)

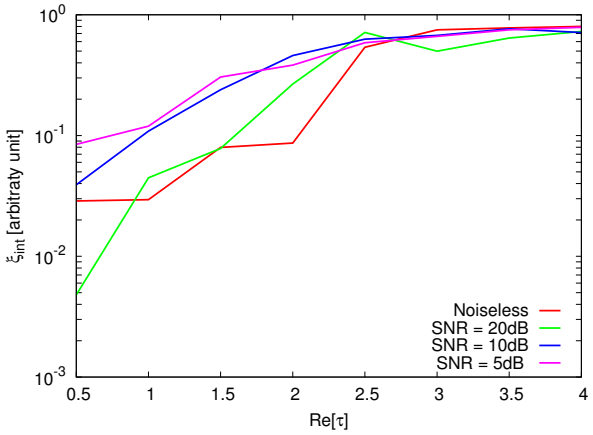

(b)

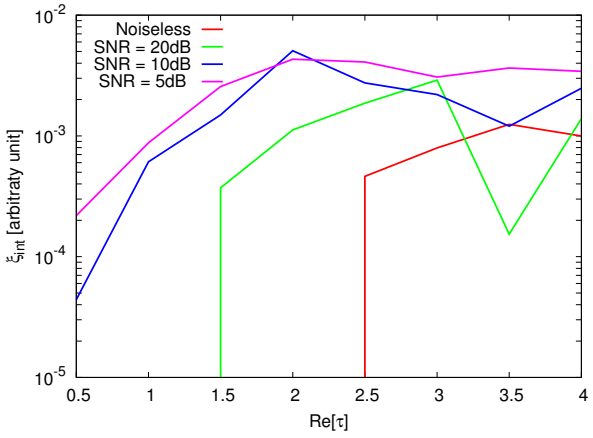

(c)

Figure 121. Behaviour of error figures as a function of ε_r, for different SNR values: (a) total error ξ_{tot}, (b) internal error ξ_{int}, (c) external error ξ_{ext}.

TEST CASE: Cross-Shaped Cylinder

Goal: show the performances of BCS when dealing with a sparse scatterer

- Number of Views: V
- Number of Measurements: M
- Number of Cells for the Inversion: N
- Number of Cells for the Direct solver: D
- Side of the investigation domain: L

Test Case Description

Direct solver:

- Square domain divided in $\sqrt{D} \times \sqrt{D}$ cells
- Domain side: $L = 3\lambda$
- $D = 1296$ (discretization for the direct solver: $< \lambda/10$)

Investigation domain:

- Square domain divided in $\sqrt{N} \times \sqrt{N}$ cells
- $L = 3\lambda$
- $2ka = 2 \times \frac{2\pi}{\lambda} \times \frac{L\sqrt{2}}{2} = 6\pi\sqrt{2} = 26.65$
- $\#DOF = \frac{(2ka)^2}{2} = \frac{(2 \times \frac{2\pi}{\lambda} \times \frac{L\sqrt{2}}{2})^2}{2} = 4\pi^2 \left(\frac{L}{\lambda}\right)^2 = 4\pi^2 \times 9 \approx 355.3$
- N scelto in modo da essere vicino a $\#DOF$: $N = 324$ (18×18)

Measurement domain:

- Measurement points taken on a circle of radius $\rho = 3\lambda$
- Full-aspect measurements
- $M \approx 2ka \rightarrow M = 27$

Sources:

- Plane waves
- $V \approx 2ka \rightarrow V = 27$
- Amplitude: $A = 1$
- Frequency: 300 MHz $(\lambda = 1)$

Object:

- Cross-shaped cylinder
- $\varepsilon_r \in \{1.5, 2.0, 2.5, 3.0, 3.5, 4.0, 4.5, 5.0\}$
- $\sigma = 0$ [S/m]

BCS parameters:

- Gamma prior on noise variance parameters: $a = 1 \times 10^{-1}$, $b = 5 \times 10^{-4}$
- Convergenze parameter: $\tau = 1.0 \times 10^{-8}$

RESULTS: $\varepsilon_r = 1.5$

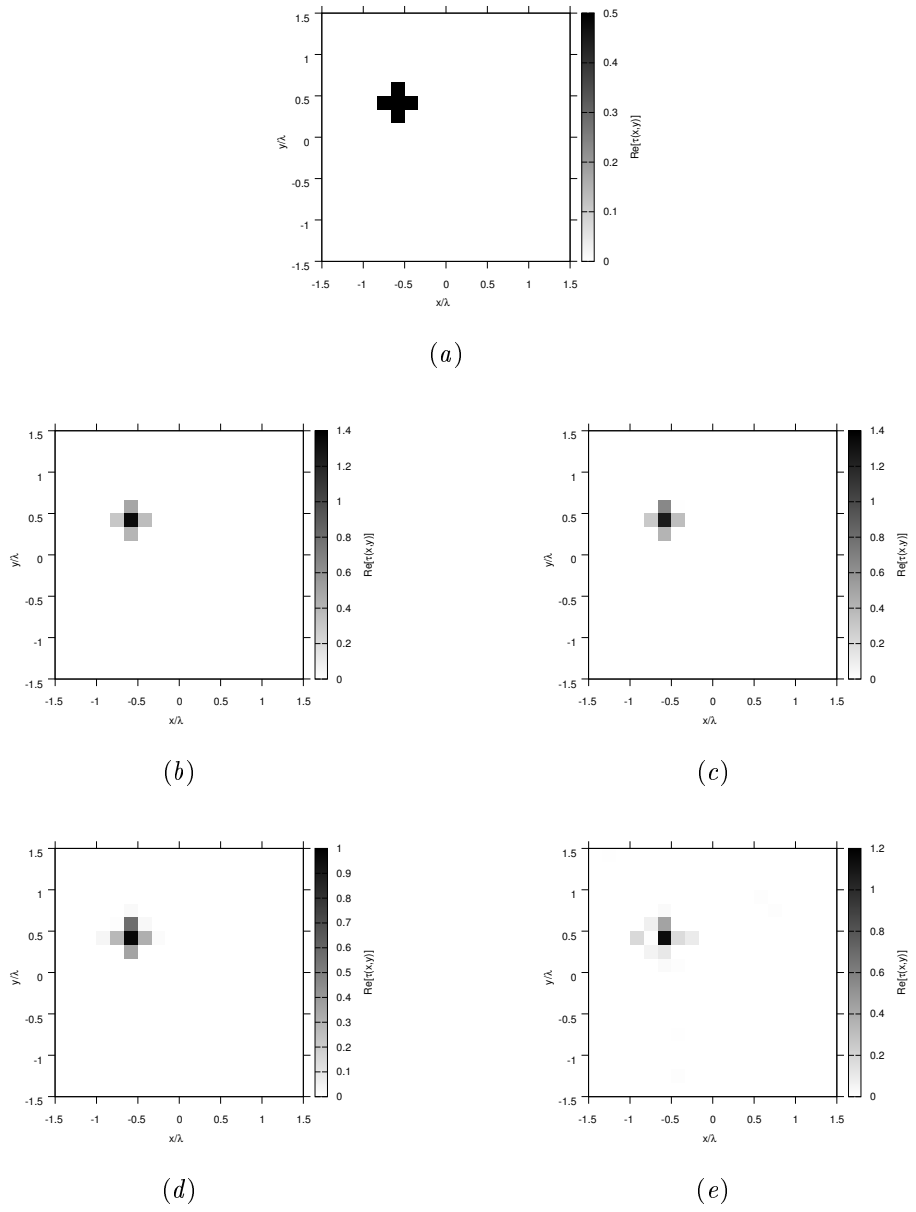

(a)

(b)

(c)

(d)

(e)

Figure 122. Actual object (a) and BCS reconstructed object for (b) Noiseless case, (c) $SNR = 20$ [dB] , (d) $SNR = 10$ [dB] , (e) $SNR = 5$ [dB].

RESULTS: $\varepsilon_r = 2.0$

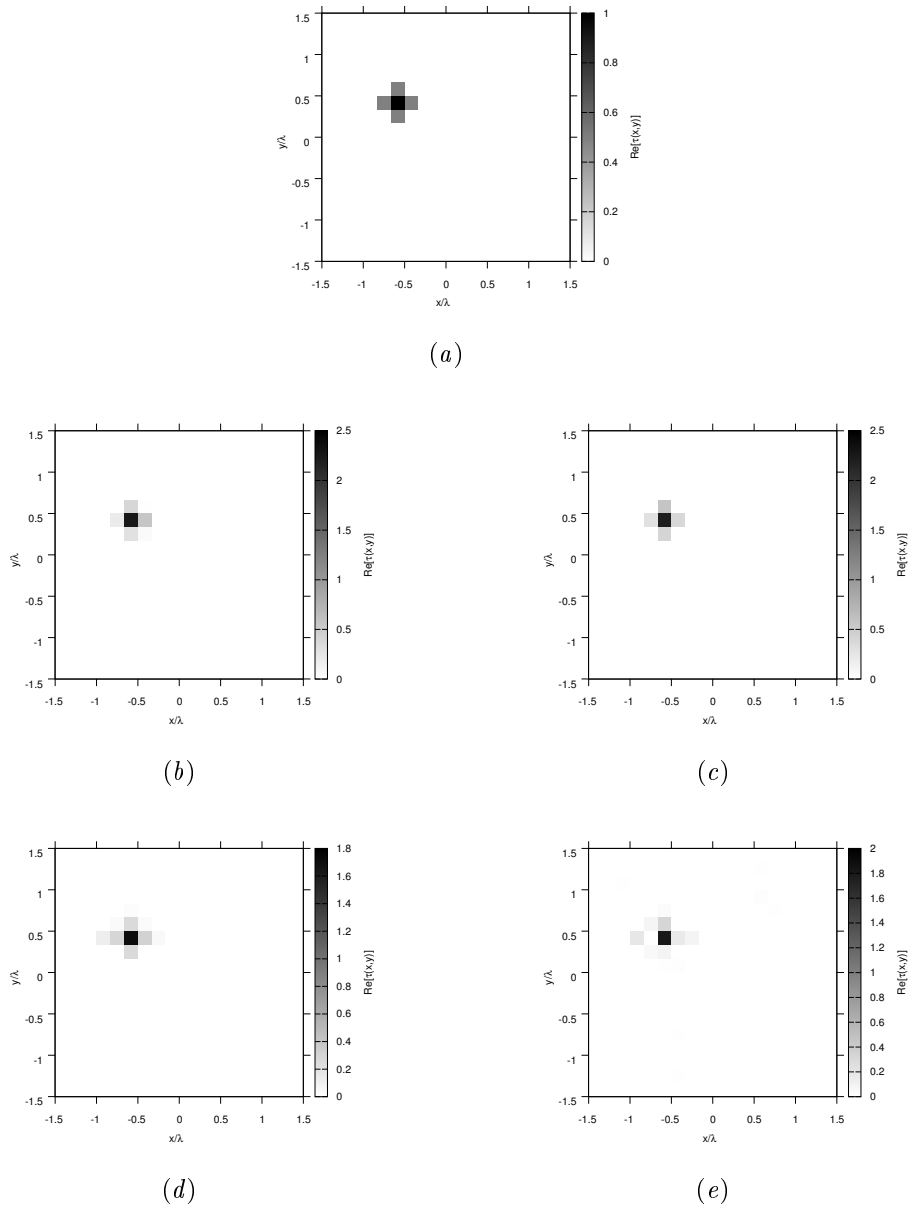

(a) (b) (c) (d) (e)

Figure 123. Actual object (a) and BCS reconstructed object for (b) Noiseless case, (c) $SNR = 20$ [dB] , (d) $SNR = 10$ [dB] , (e) $SNR = 5$ [dB].

RESULTS: $\varepsilon_r = 3.0$

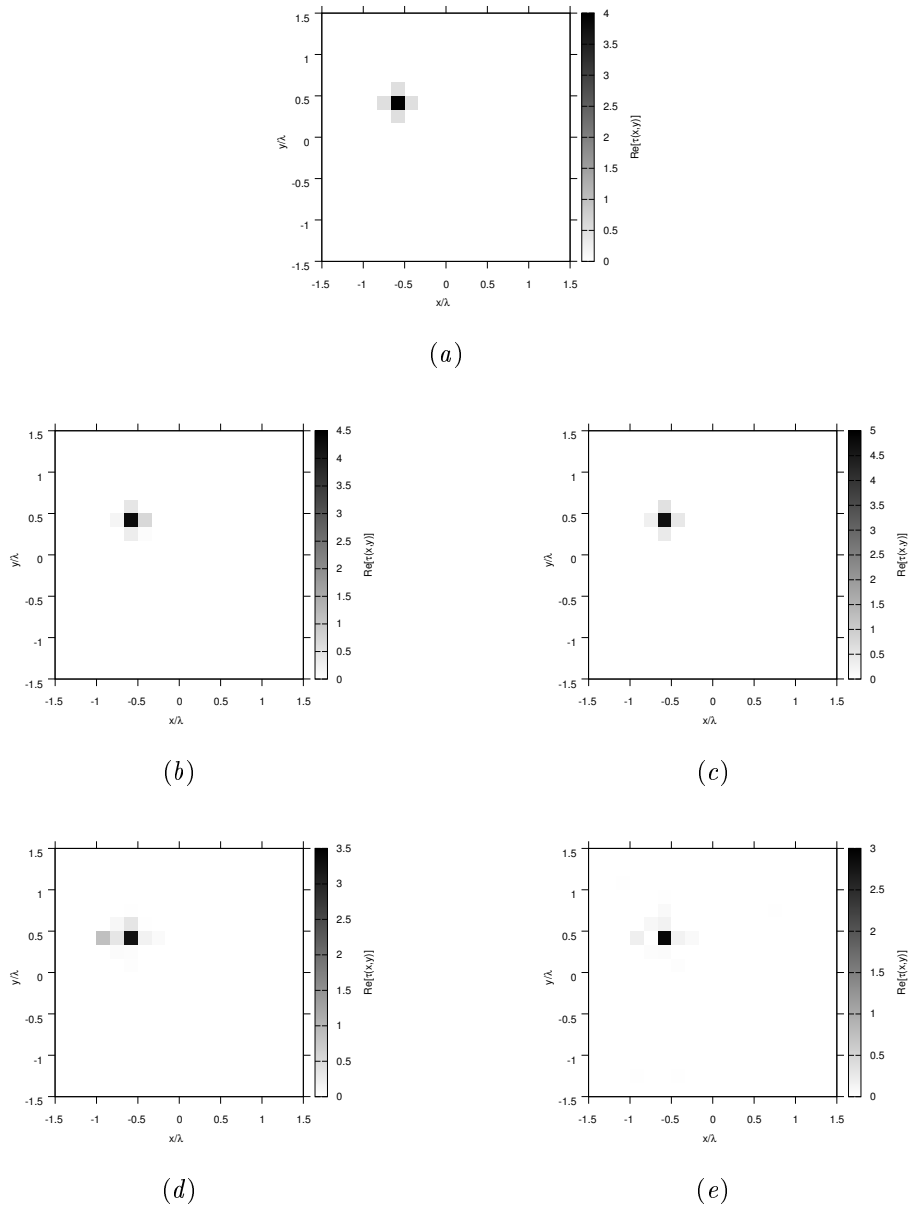

(a)

(b)

(c)

(d)

(e)

Figure 124. Actual object (a) and BCS reconstructed object for (b) Noiseless case, (c) $SNR = 20$ [dB] , (d) $SNR = 10$ [dB] , (e) $SNR = 5$ [dB].

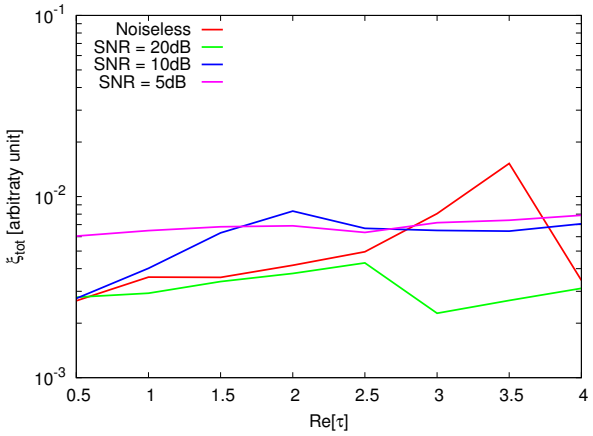

(a)

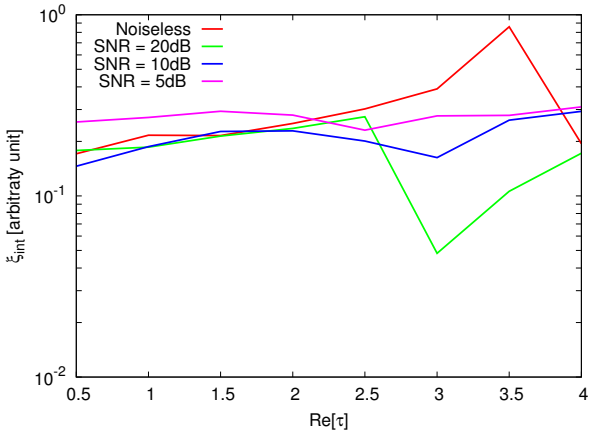

(b)

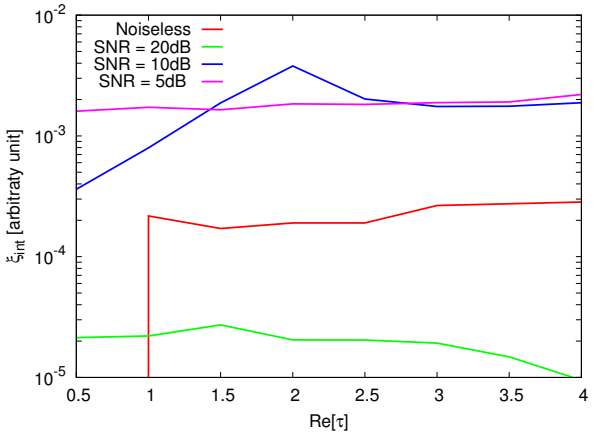

(c)

Figure 125. Behaviour of error figures as a function of ε_r, for different SNR values: (a) total error ξ_{tot}, (b) internal error ξ_{int}, (c) external error ξ_{ext}.

TEST CASE: L-Shaped Cylinder

Goal: show the performances of BCS when dealing with a sparse scatterer

- Number of Views: V
- Number of Measurements: M
- Number of Cells for the Inversion: N
- Number of Cells for the Direct solver: D
- Side of the investigation domain: L

Test Case Description

Direct solver:

- Square domain divided in $\sqrt{D} \times \sqrt{D}$ cells
- Domain side: $L = 3\lambda$
- $D = 1296$ (discretization for the direct solver: $< \lambda/10$)

Investigation domain:

- Square domain divided in $\sqrt{N} \times \sqrt{N}$ cells
- $L = 3\lambda$
- $2ka = 2 \times \frac{2\pi}{\lambda} \times \frac{L\sqrt{2}}{2} = 6\pi\sqrt{2} = 26.65$
- $\#DOF = \frac{(2ka)^2}{2} = \frac{(2 \times \frac{2\pi}{\lambda} \times \frac{L\sqrt{2}}{2})^2}{2} = 4\pi^2 \left(\frac{L}{\lambda}\right)^2 = 4\pi^2 \times 9 \approx 355.3$
- N scelto in modo da essere vicino a $\#DOF$: $N = 324$ (18×18)

Measurement domain:

- Measurement points taken on a circle of radius $\rho = 3\lambda$
- Full-aspect measurements
- $M \approx 2ka \rightarrow M = 27$

Sources:

- Plane waves
- $V \approx 2ka \rightarrow V = 27$
- Amplitude $A = 1$
- Frequency: 300 MHz $(\lambda = 1)$

Object:

- L-shaped cylinder
- $\varepsilon_r \in \{1.5, 2.0, 2.5, 3.0, 3.5, 4.0, 4.5, 5.0\}$
- $\sigma = 0$ [S/m]

BCS parameters:

- Gamma prior on noise variance parameters: $a = 1 \times 10^{-1}$, $b = 5 \times 10^{-4}$
- Convergenze parameter: $\tau = 1.0 \times 10^{-8}$

RESULTS: $\varepsilon_r = 1.5$

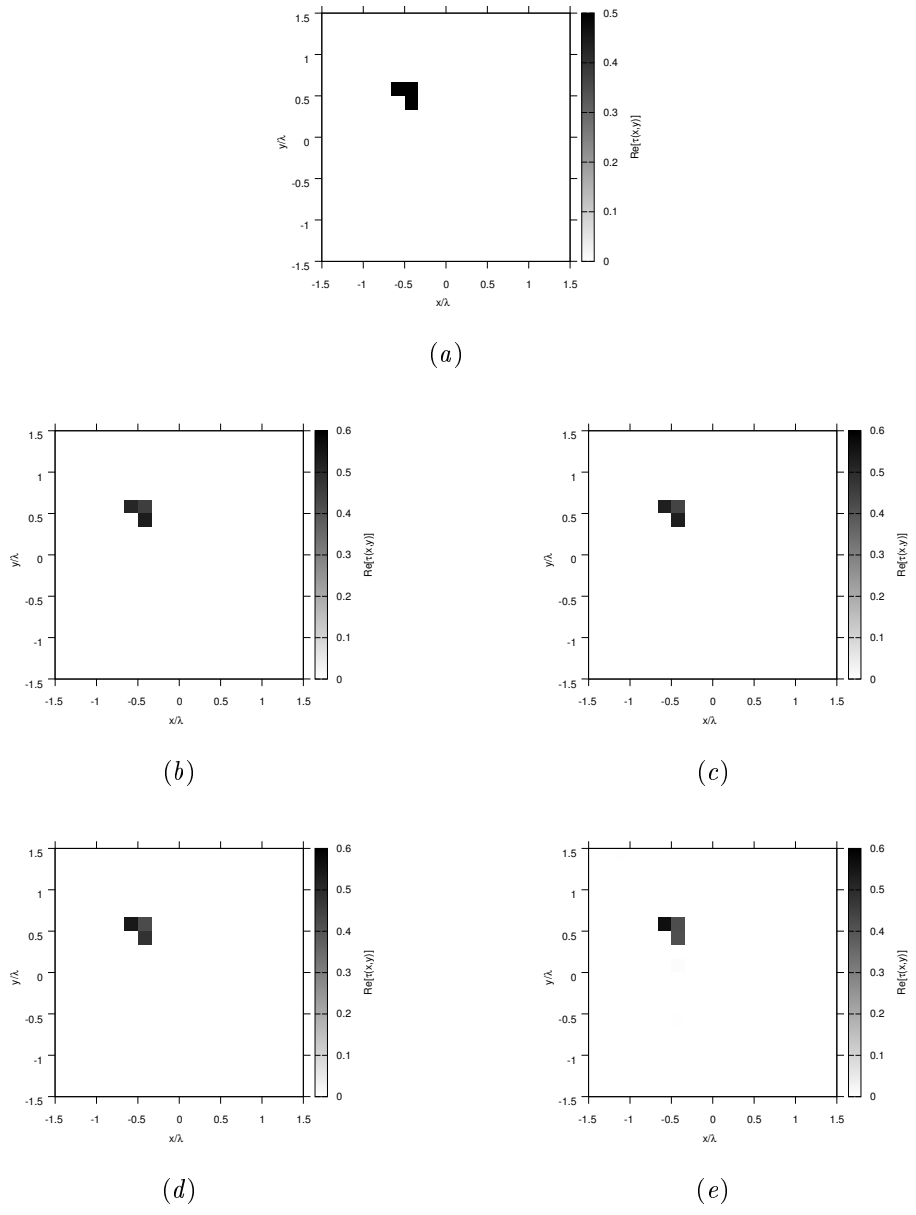

(a) (b) (c) (d) (e)

Figure 126. Actual object (a) and BCS reconstructed object for (b) Noiseless case, (c) $SNR = 20$ [dB] , (d) $SNR = 10$ [dB] , (e) $SNR = 5$ [dB].

RESULTS: $\varepsilon_r = 2.0$

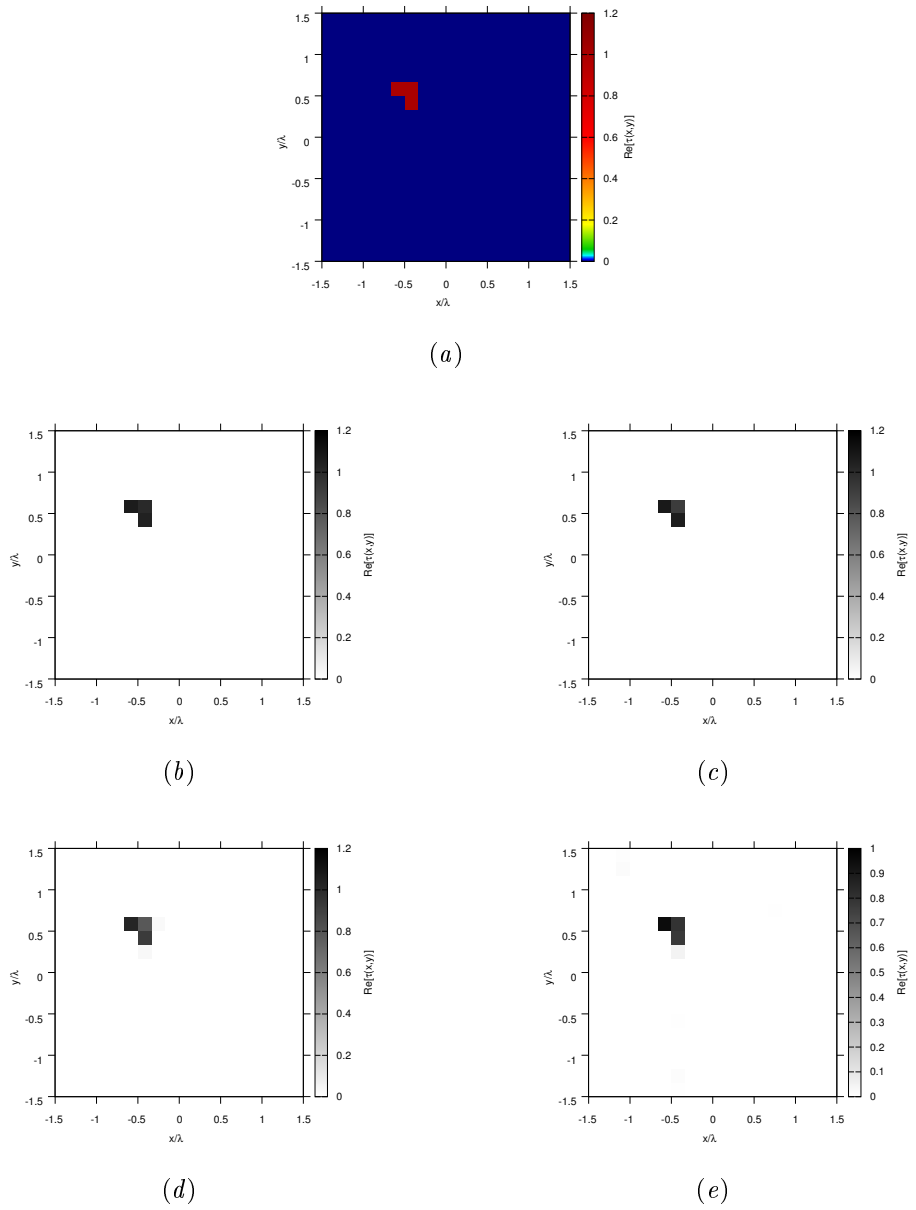

(a)

(b)

(c)

(d)

(e)

Figure 127. Actual object (a) and BCS reconstructed object for (b) Noiseless case, (c) $SNR = 20$ [dB] , (d) $SNR = 10$ [dB] , (e) $SNR = 5$ [dB].

RESULTS: $\varepsilon_r = 3.0$

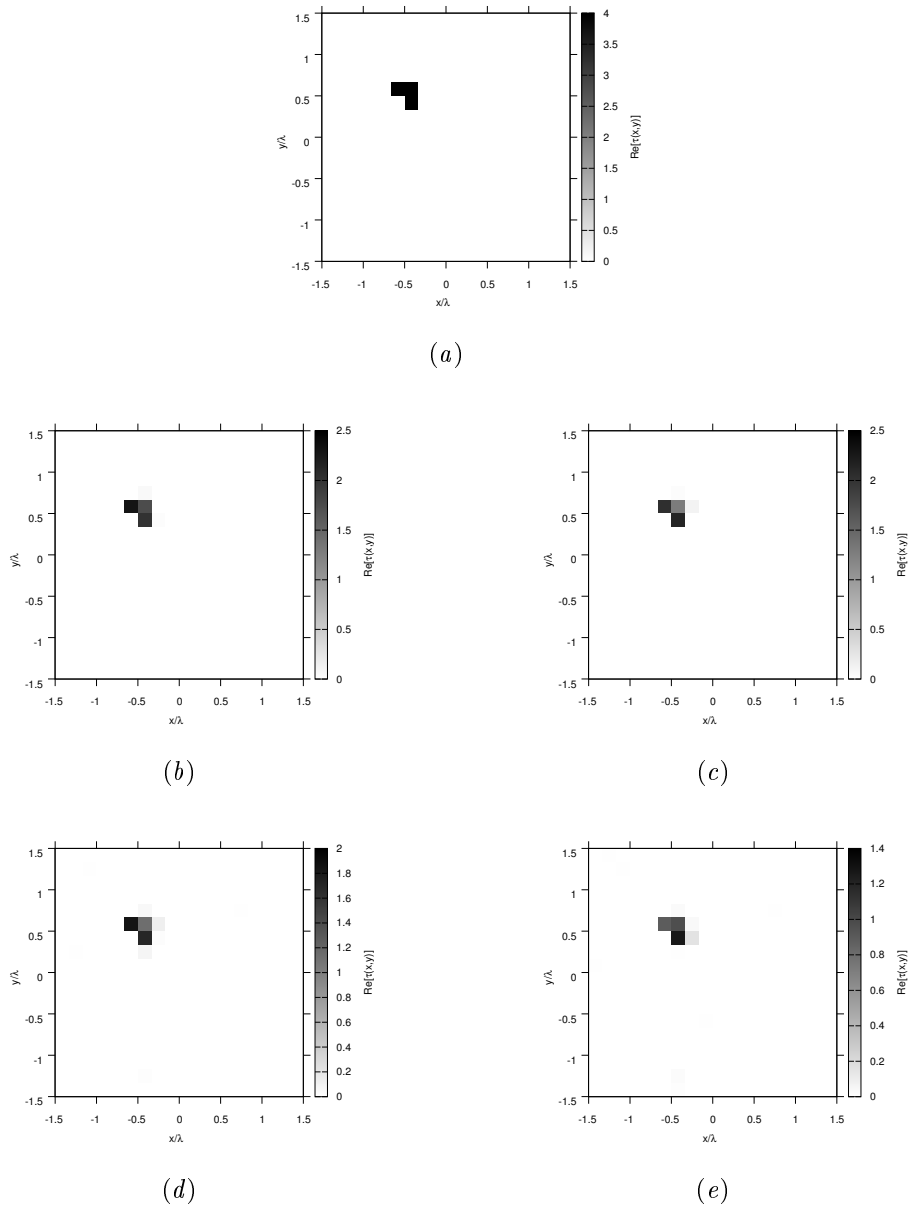

(a)

(b) (c)

(d) (e)

Figure 128. Actual object (a) and BCS reconstructed object for (b) Noiseless case, (c) $SNR = 20$ [dB] , (d) $SNR = 10$ [dB] , (e) $SNR = 5$ [dB].

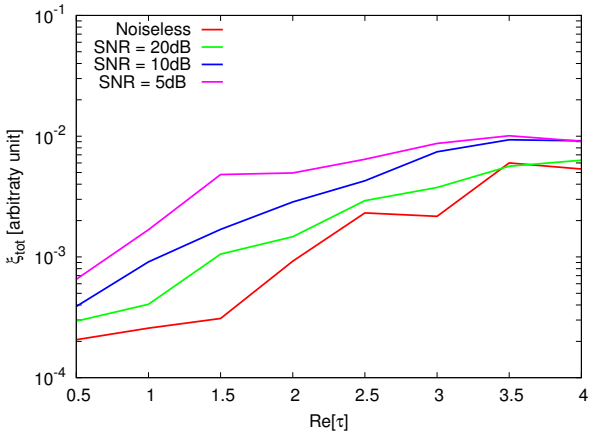

(a)

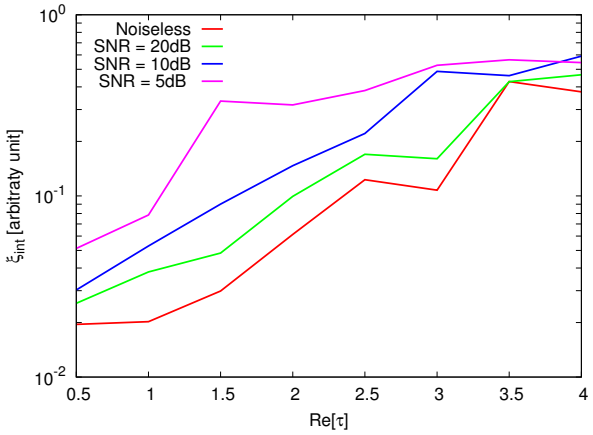

(b)

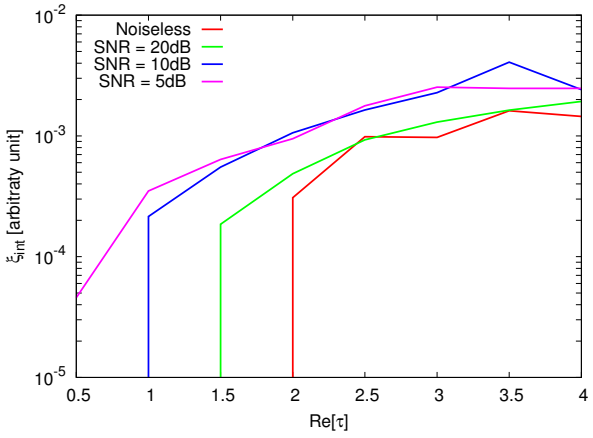

(c)

Figure 129. Behaviour of error figures as a function of ε_r, for different SNR values: (a) total error ξ_{tot}, (b) internal error ξ_{int}, (c) external error ξ_{ext}.

TEST CASE: Inhomogeneous L-Shaped Cylinder

Goal: show the performances of BCS when dealing with a sparse scatterer

- Number of Views: V
- Number of Measurements: M
- Number of Cells for the Inversion: N
- Number of Cells for the Direct solver: D
- Side of the investigation domain: L

Test Case Description

Direct solver:

- Square domain divided in $\sqrt{D} \times \sqrt{D}$ cells
- Domain side: $L = 3\lambda$
- $D = 1296$ (discretization for the direct solver: $< \lambda/10$)

Investigation domain:

- Square domain divided in $\sqrt{N} \times \sqrt{N}$ cells
- $L = 3\lambda$
- $2ka = 2 \times \frac{2\pi}{\lambda} \times \frac{L\sqrt{2}}{2} = 6\pi\sqrt{2} = 26.65$
- $\#DOF = \frac{(2ka)^2}{2} = \frac{(2 \times \frac{2\pi}{\lambda} \times \frac{L\sqrt{2}}{2})^2}{2} = 4\pi^2 \left(\frac{L}{\lambda}\right)^2 = 4\pi^2 \times 9 \approx 355.3$
- N scelto in modo da essere vicino a $\#DOF$: $N = 324$ (18×18)

Measurement domain:

- Measurement points taken on a circle of radius $\rho = 3\lambda$
- Full-aspect measurements
- $M \approx 2ka \rightarrow M = 27$

Sources:

- Plane waves
- $V \approx 2ka \rightarrow V = 27$
- Amplitude $A = 1$
- Frequency: 300 MHz $(\lambda = 1)$

Object:

- Inhomogeneous L-shaped cylinder
- $\varepsilon_r \in \{1.5, 2.0, 2.5, 3.0, 3.5, 4.0, 4.5, 5.0\}$
- **BCS parameters:**
- Gamma prior on noise variance parameters: $a = 1 \times 10^{-1}$, $b = 5 \times 10^{-4}$
- Convergenze parameter: $\tau = 1.0 \times 10^{-8}$

RESULTS: $\varepsilon_r = 1.5$

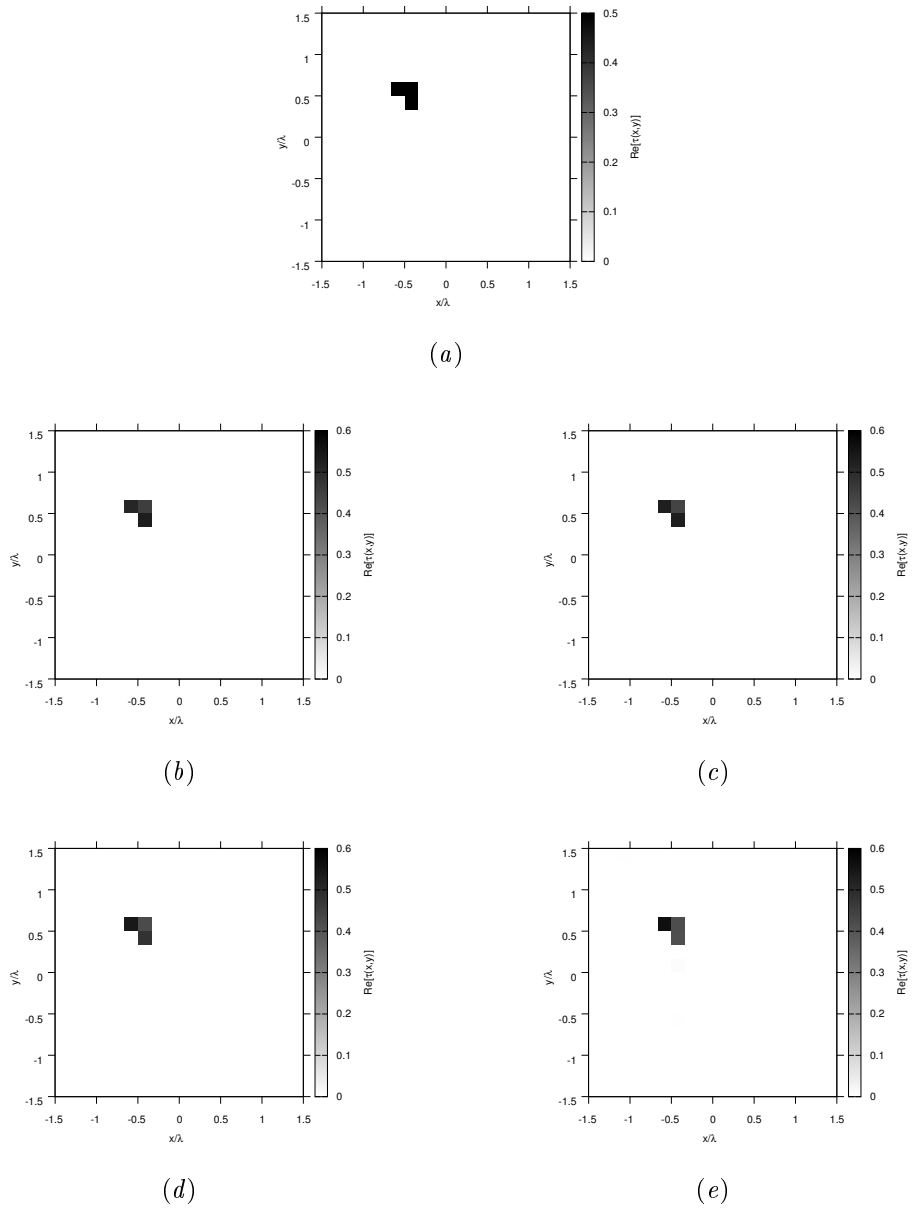

(a)

(b)

(c)

(d)

(e)

Figure 130. Actual object (a) and BCS reconstructed object for (b) Noiseless case, (c) $SNR = 20$ [dB] , (d) $SNR = 10$ [dB] , (e) $SNR = 5$ [dB].

RESULTS: $\varepsilon_r = 2.0$

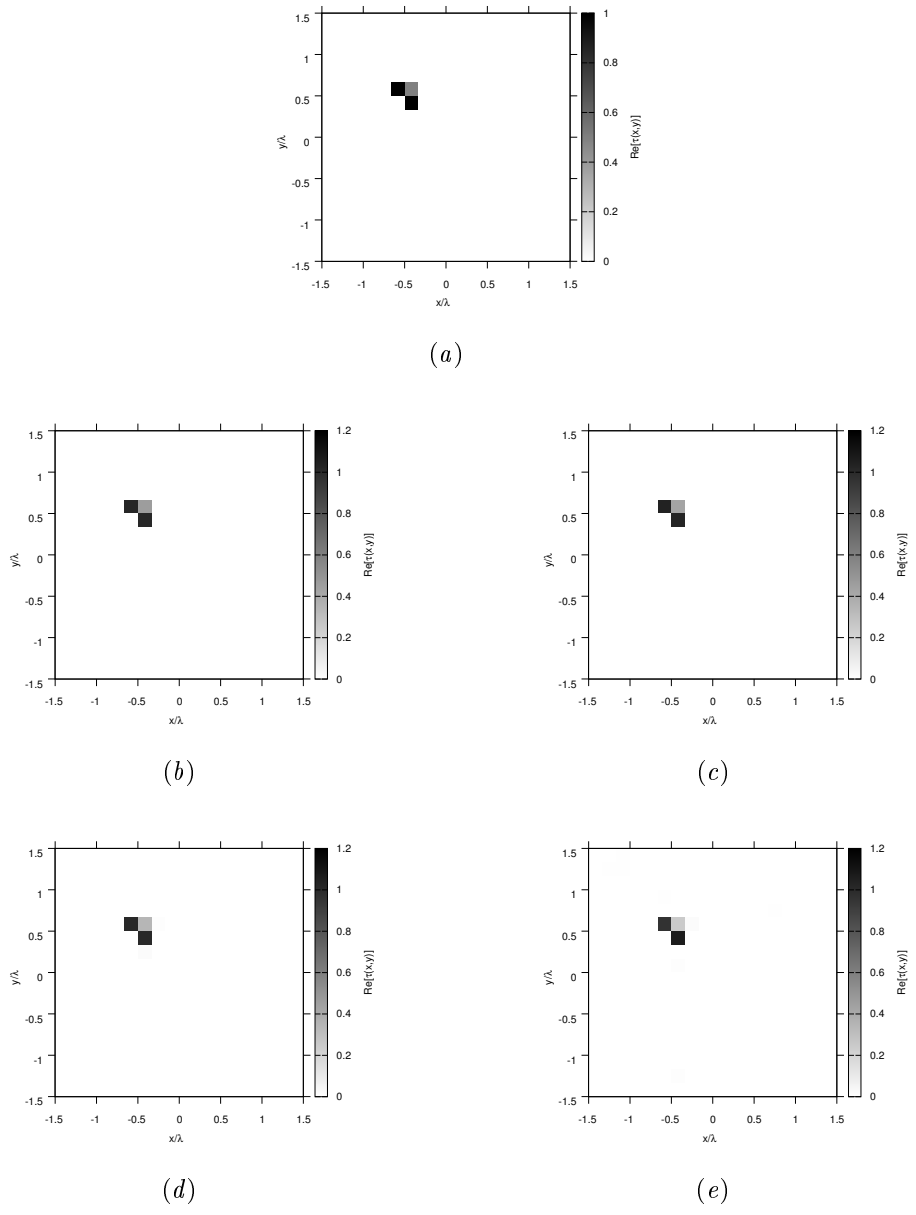

(a)

(b)

(c)

(d)

(e)

Figure 131. Actual object (a) and BCS reconstructed object for (b) Noiseless case, (c) $SNR = 20$ [dB] , (d) $SNR = 10$ [dB] , (e) $SNR = 5$ [dB].

RESULTS: $\varepsilon_r = 5.0$

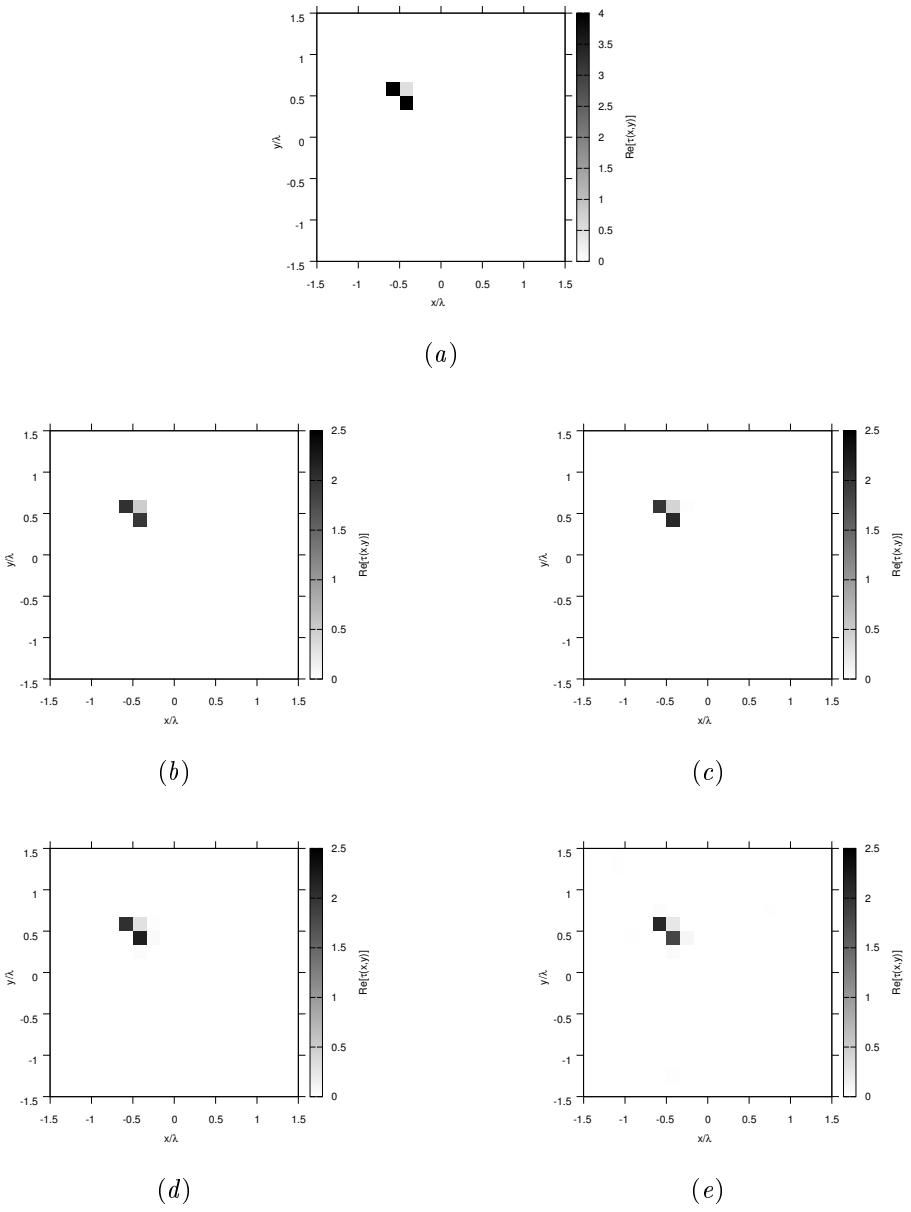

(a) (b) (c) (d) (e)

Figure 132. Actual object (a) and BCS reconstructed object for (b) Noiseless case, (c) $SNR = 20$ [dB] , (d) $SNR = 10$ [dB] , (e) $SNR = 5$ [dB].

RESULTS: $\varepsilon_r = 5.0$

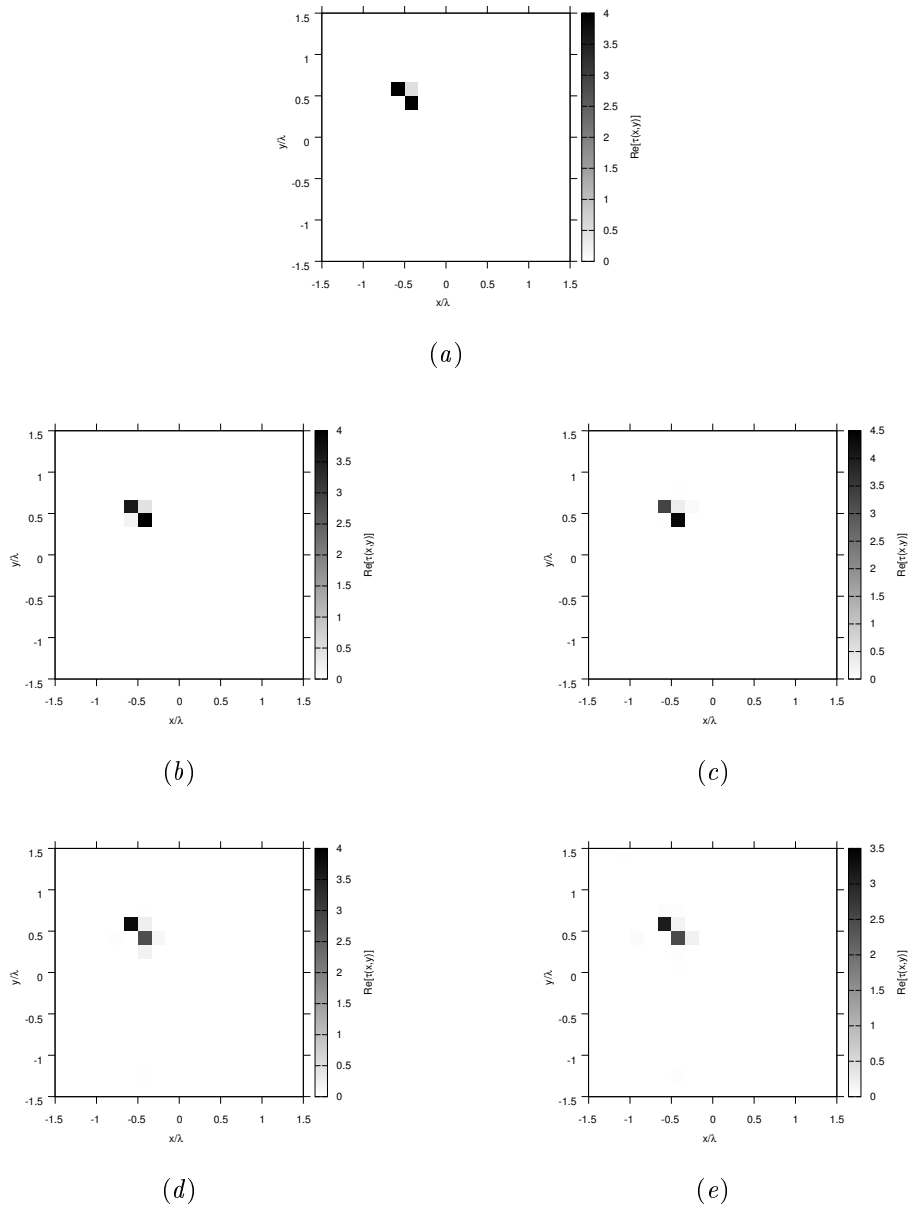

(a)

(b)

(c)

(d)

(e)

Figure 133. Actual object (a) and BCS reconstructed object for (b) Noiseless case, (c) $SNR = 20$ [dB] , (d) $SNR = 10$ [dB] , (e) $SNR = 5$ [dB].

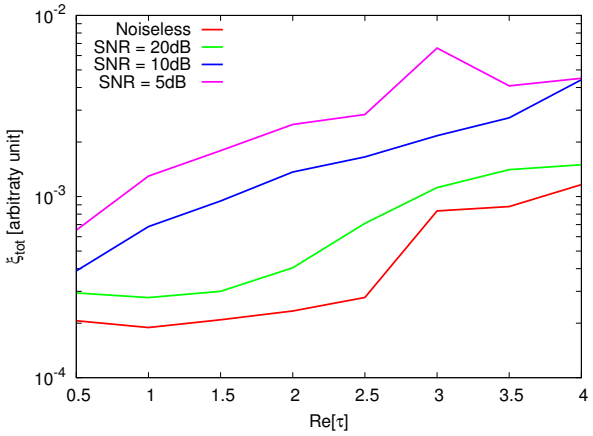

(a)

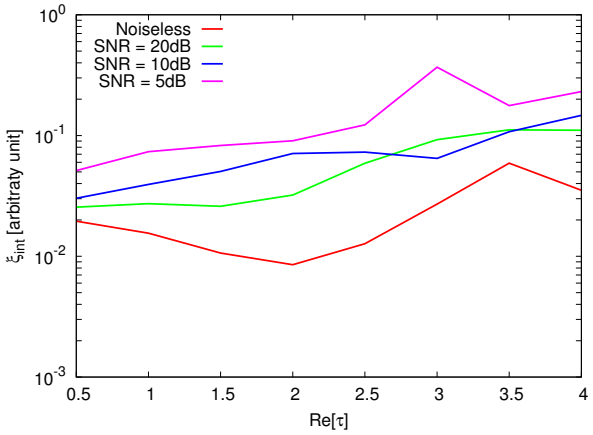

(b)

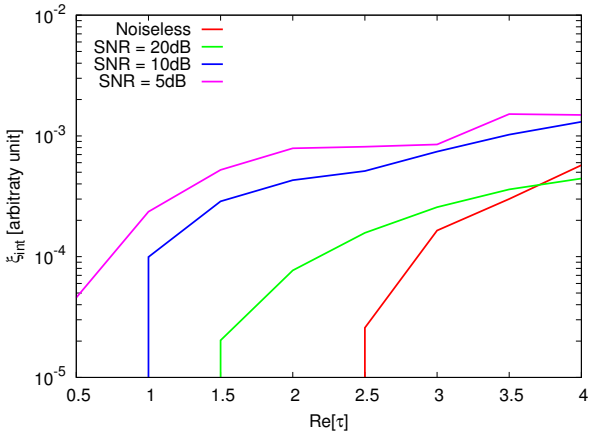

(c)

Figure 134. Behaviour of error figures as a function of ε_r, for different SNR values: (a) total error ξ_{tot}, (b) internal error ξ_{int}, (c) external error ξ_{ext}.

TEST CASE: Line-Shaped Cylinder $L = 0.5\lambda$

Goal: show the performances of BCS when dealing with a sparse scatterer

- Number of Views: V
- Number of Measurements: M
- Number of Cells for the Inversion: N
- Number of Cells for the Direct solver: D
- Side of the investigation domain: L

Test Case Description

Direct solver:

- Square domain divided in $\sqrt{D} \times \sqrt{D}$ cells
- Domain side: $L = 3\lambda$
- $D = 1296$ (discretization for the direct solver: $< \lambda/10$)

Investigation domain:

- Square domain divided in $\sqrt{N} \times \sqrt{N}$ cells
- $L = 3\lambda$
- $2ka = 2 \times \frac{2\pi}{\lambda} \times \frac{L\sqrt{2}}{2} = 6\pi\sqrt{2} = 26.65$
- $\#DOF = \frac{(2ka)^2}{2} = \frac{(2 \times \frac{2\pi}{\lambda} \times \frac{L\sqrt{2}}{2})^2}{2} = 4\pi^2 \left(\frac{L}{\lambda}\right)^2 = 4\pi^2 \times 9 \approx 355.3$
- N scelto in modo da essere vicino a $\#DOF$: $N = 324$ (18×18)

Measurement domain:

- Measurement points taken on a circle of radius $\rho = 3\lambda$
- Full-aspect measurements
- $M \approx 2ka \rightarrow M = 27$

Sources:

- Plane waves
- $V \approx 2ka \rightarrow V = 27$
- Amplitude $A = 1$
- Frequency: 300 MHz $(\lambda = 1)$

Object:

- Inhomogeneous L-shaped cylinder
- $\varepsilon_r \in \{1.5, 2.0, 2.5, 3.0, 3.5, 4.0, 4.5, 5.0\}$
- $\sigma = 0$ [S/m]

BCS parameters:

- Gamma prior on noise variance parameters: $a = 1 \times 10^{-1}$, $b = 5 \times 10^{-4}$
- Convergenze parameter: $\tau = 1.0 \times 10^{-8}$

RESULTS: $\varepsilon_r = 1.5$

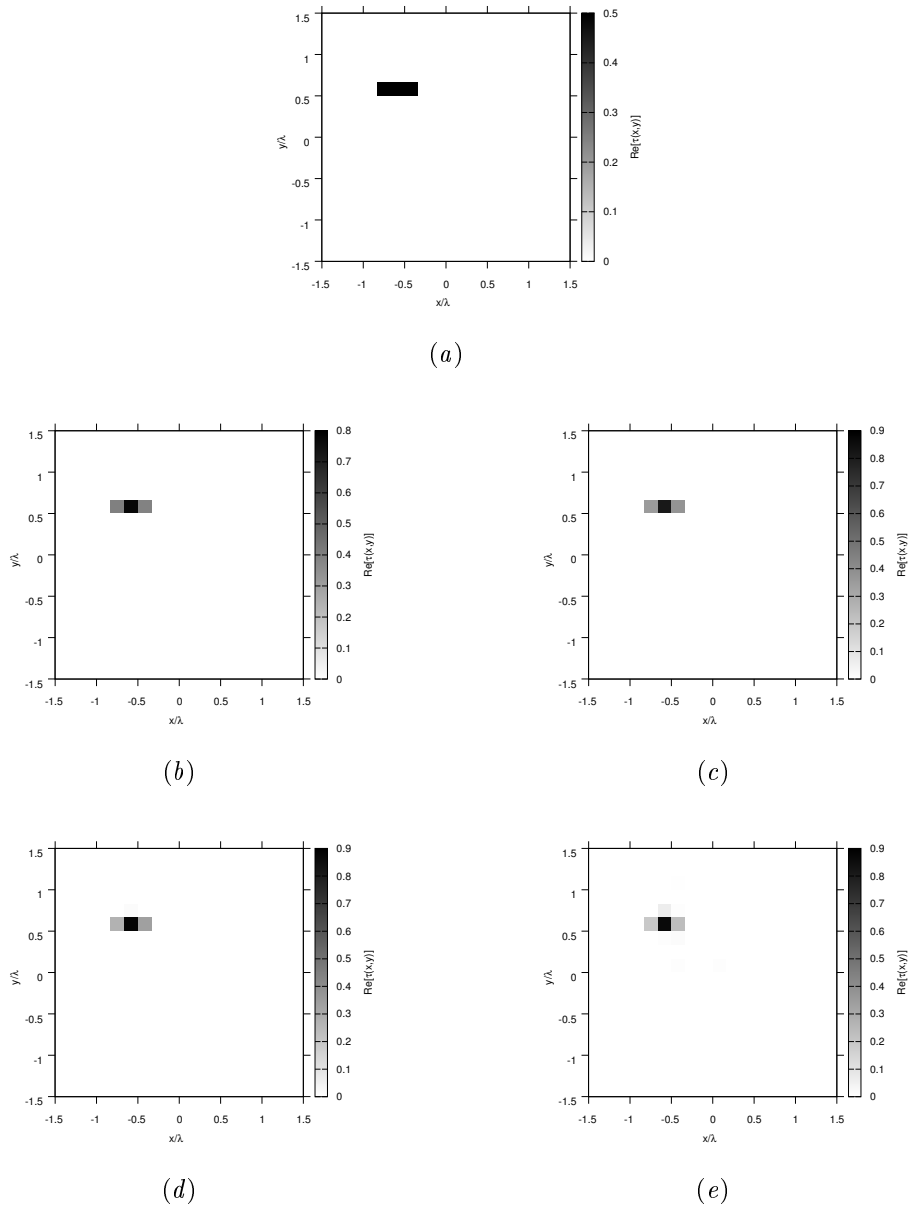

(a) (b) (c) (d) (e)

Figure 135. Actual object (a) and BCS reconstructed object for (b) Noiseless case, (c) $SNR = 20$ [dB] , (d) $SNR = 10$ [dB] , (e) $SNR = 5$ [dB].

RESULTS: $\varepsilon_r = 2.0$

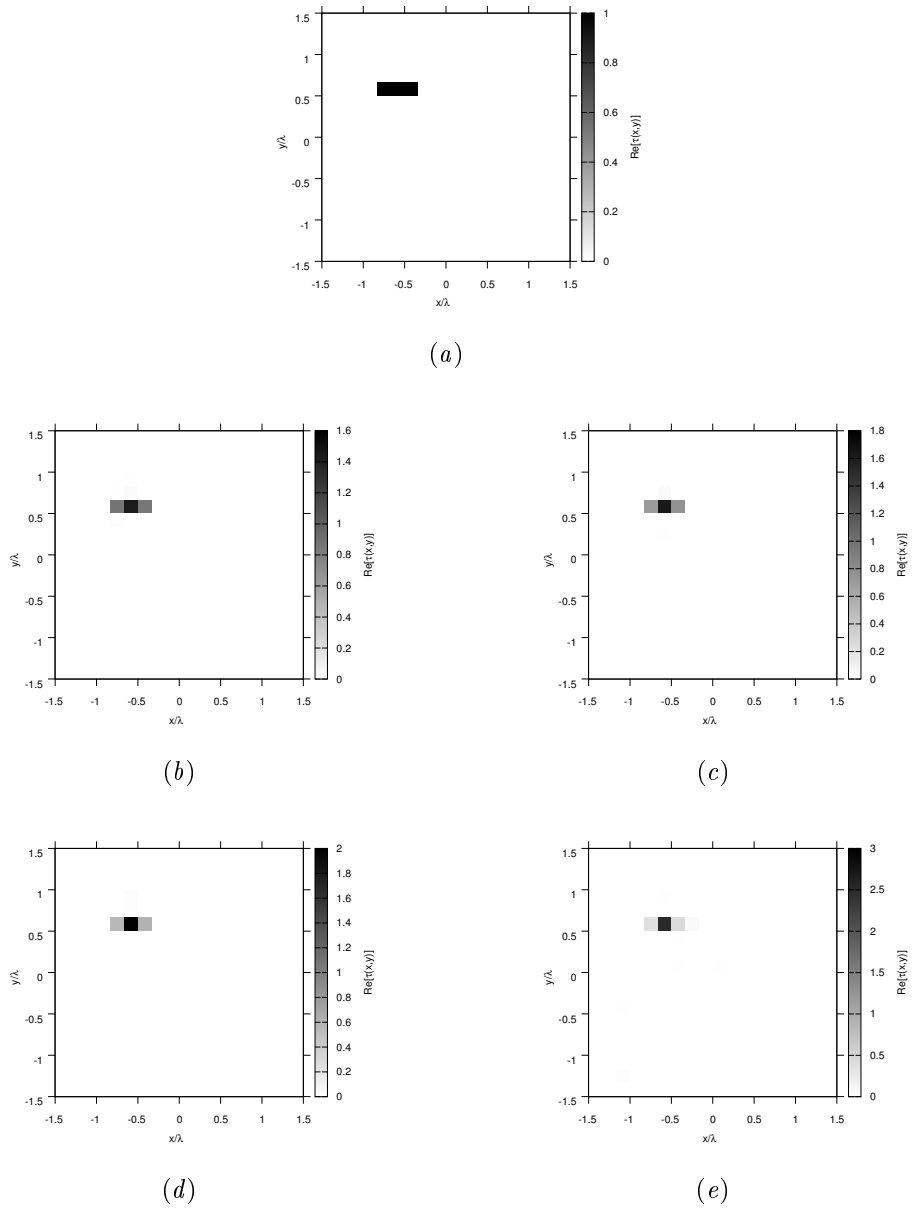

(a) (b) (c) (d) (e)

Figure 136. Actual object (a) and BCS reconstructed object for (b) Noiseless case, (c) $SNR = 20$ [dB] , (d) $SNR = 10$ [dB] , (e) $SNR = 5$ [dB].

RESULTS: $\varepsilon_r = 3.0$

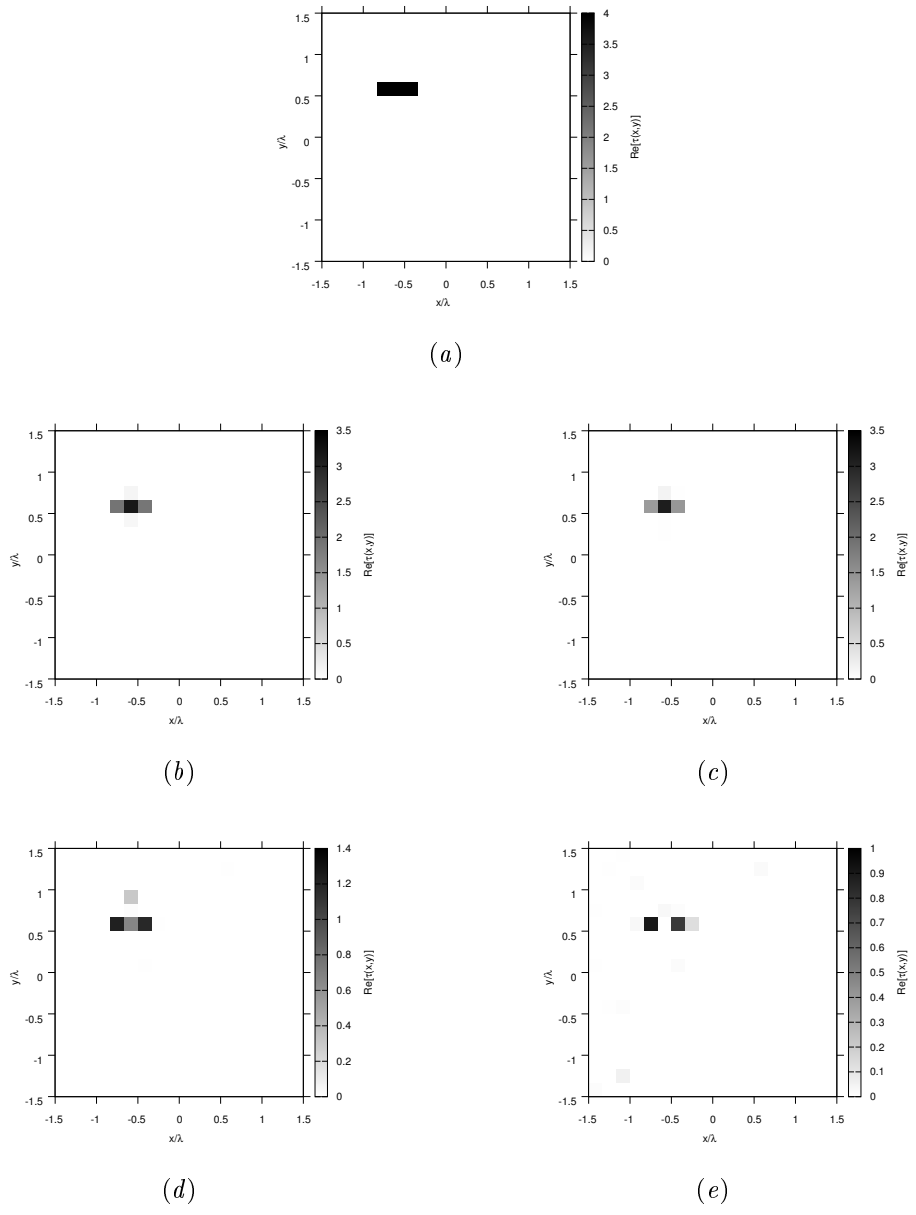

(a) (b) (c) (d) (e)

Figure 137. Actual object (a) and BCS reconstructed object for (b) Noiseless case, (c) $SNR = 20$ [dB] , (d) $SNR = 10$ [dB] , (e) $SNR = 5$ [dB].

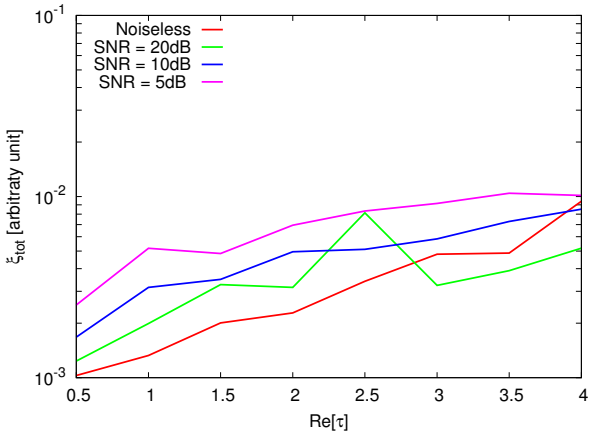

(a)

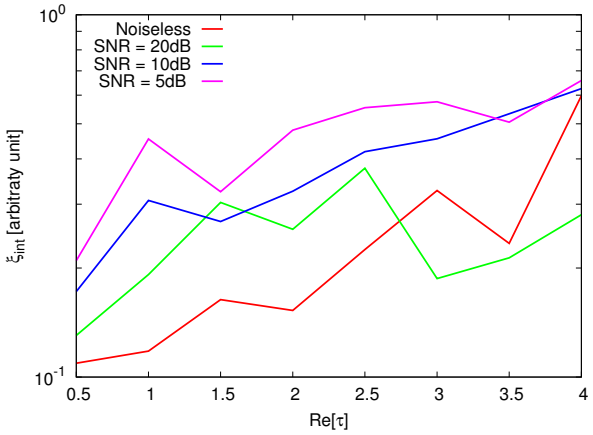

(b)

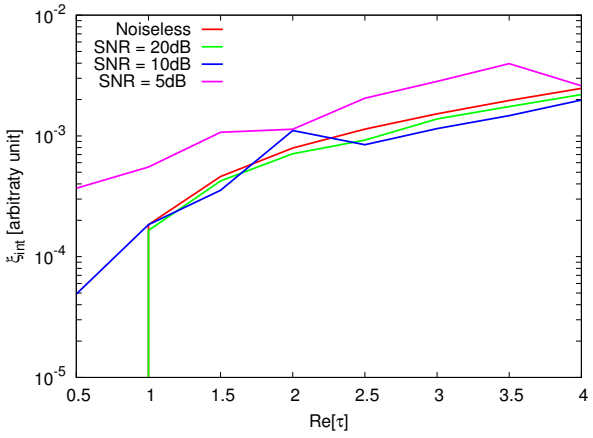

(c)

Figure 138. Behaviour of error figures as a function of ε_r, for different SNR values: (a) total error ξ_{tot}, (b) internal error ξ_{int}, (c) external error ξ_{ext}.

5.3 MV-XY-MT-BCS - Advanced Tests

TEST CASE: Two Square Cylinders $L = 0.33\lambda$

Goal: show the performances of BCS when dealing with a sparse scatterer

- Number of Views: V
- Number of Measurements: M
- Number of Cells for the Inversion: N
- Number of Cells for the Direct solver: D
- Side of the investigation domain: L

Test Case Description

Direct solver:

- Square domain divided in $\sqrt{D} \times \sqrt{D}$ cells
- Domain side: $L = 3\lambda$
- $D = 1296$ (discretization for the direct solver: $< \lambda/10$)

Investigation domain:

- Square domain divided in $\sqrt{N} \times \sqrt{N}$ cells
- $L = 3\lambda$
- $2ka = 2 \times \frac{2\pi}{\lambda} \times \frac{L\sqrt{2}}{2} = 6\pi\sqrt{2} = 26.65$
- $\#DOF = \frac{(2ka)^2}{2} = \frac{(2 \times \frac{2\pi}{\lambda} \times \frac{L\sqrt{2}}{2})^2}{2} = 4\pi^2 \left(\frac{L}{\lambda}\right)^2 = 4\pi^2 \times 9 \approx 355.3$
- N scelto in modo da essere vicino a $\#DOF$: $N = 324$ (18×18)

Measurement domain:

- Measurement points taken on a circle of radius $\rho = 3\lambda$
- Full-aspect measurements
- $M \approx 2ka \rightarrow M = 27$

Sources:

- Plane waves
- $V \approx 2ka \rightarrow V = 27$
- Amplitude: $A = 1$
- Frequency: 300 MHz ($\lambda = 1$)

Object:

- Two square cylinders of side $\frac{\lambda}{3} = 0.33$
- $\varepsilon_r \in \{1.5, 2.0, 2.5, 3.0, 3.5, 4.0, 4.5, 5.0\}$ (two square)

- $\sigma = 0$ [S/m]

BCS parameters:

- Gamma prior on noise variance parameters: $a = 1 \times 10^{-1}$, $b = 5 \times 10^{-4}$
- Convergenze parameter: $\tau = 1.0 \times 10^{-8}$

RESULTS: $\varepsilon_r = 1.5$

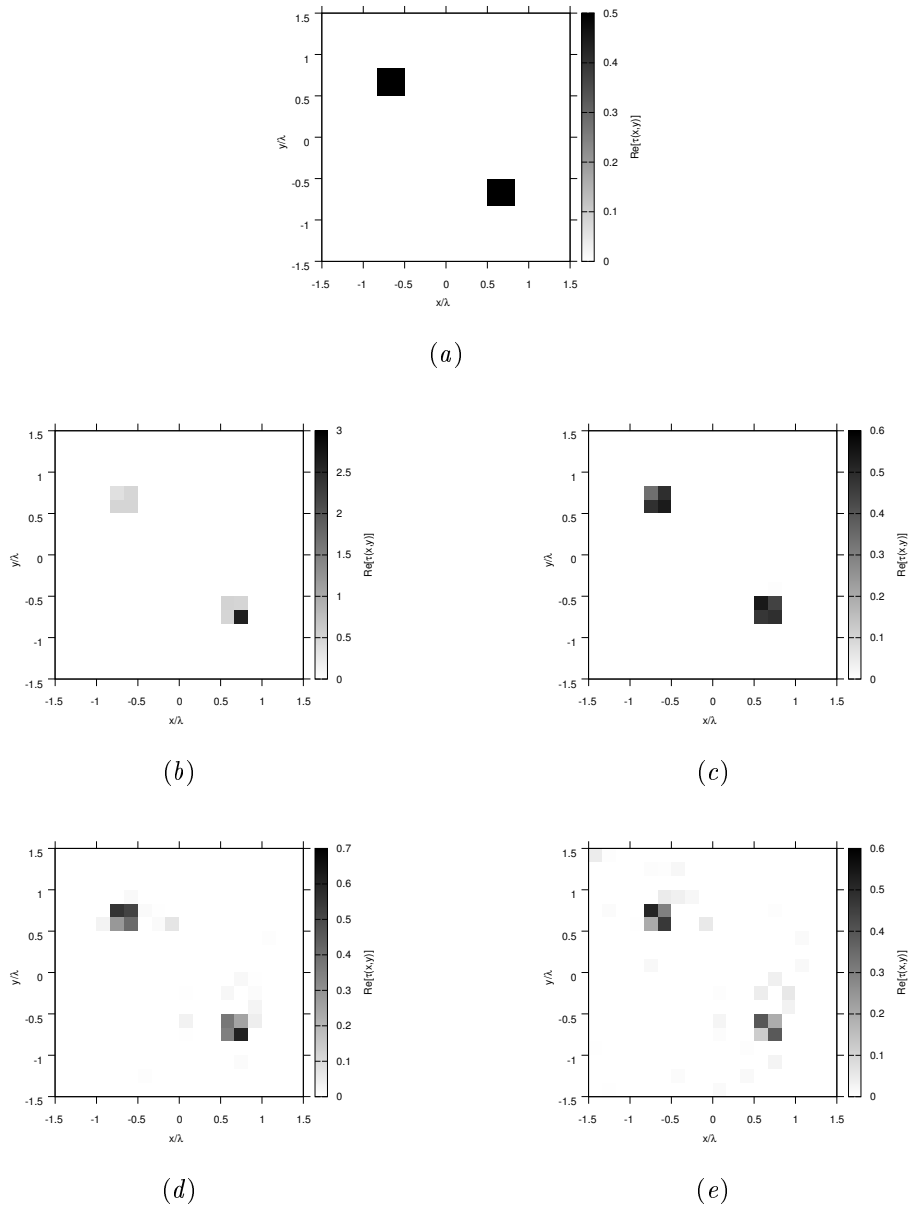

(a) (b) (c) (d) (e)

Figure 139. Actual object (a) and BCS reconstructed object for (b) Noiseless case, (c) $SNR = 20$ [dB] , (d) $SNR = 10$ [dB] , (e) $SNR = 5$ [dB].

RESULTS: $\varepsilon_r = 2.0$

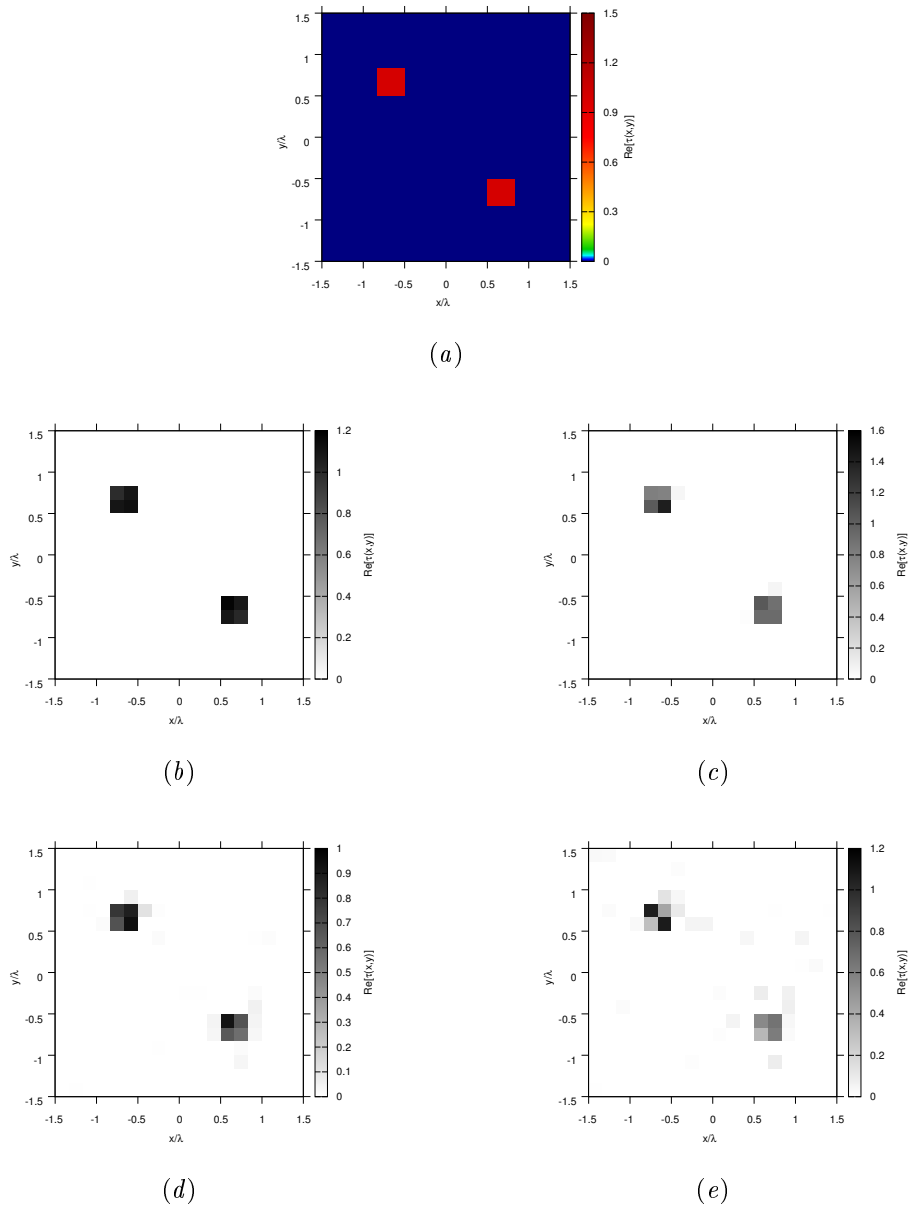

(a)

(b)

(c)

(d)

(e)

Figure 140. Actual object (a) and BCS reconstructed object for (b) Noiseless case, (c) $SNR = 20$ [dB] , (d) $SNR = 10$ [dB] , (e) $SNR = 5$ [dB].

RESULTS: $\varepsilon_r = 3.0$

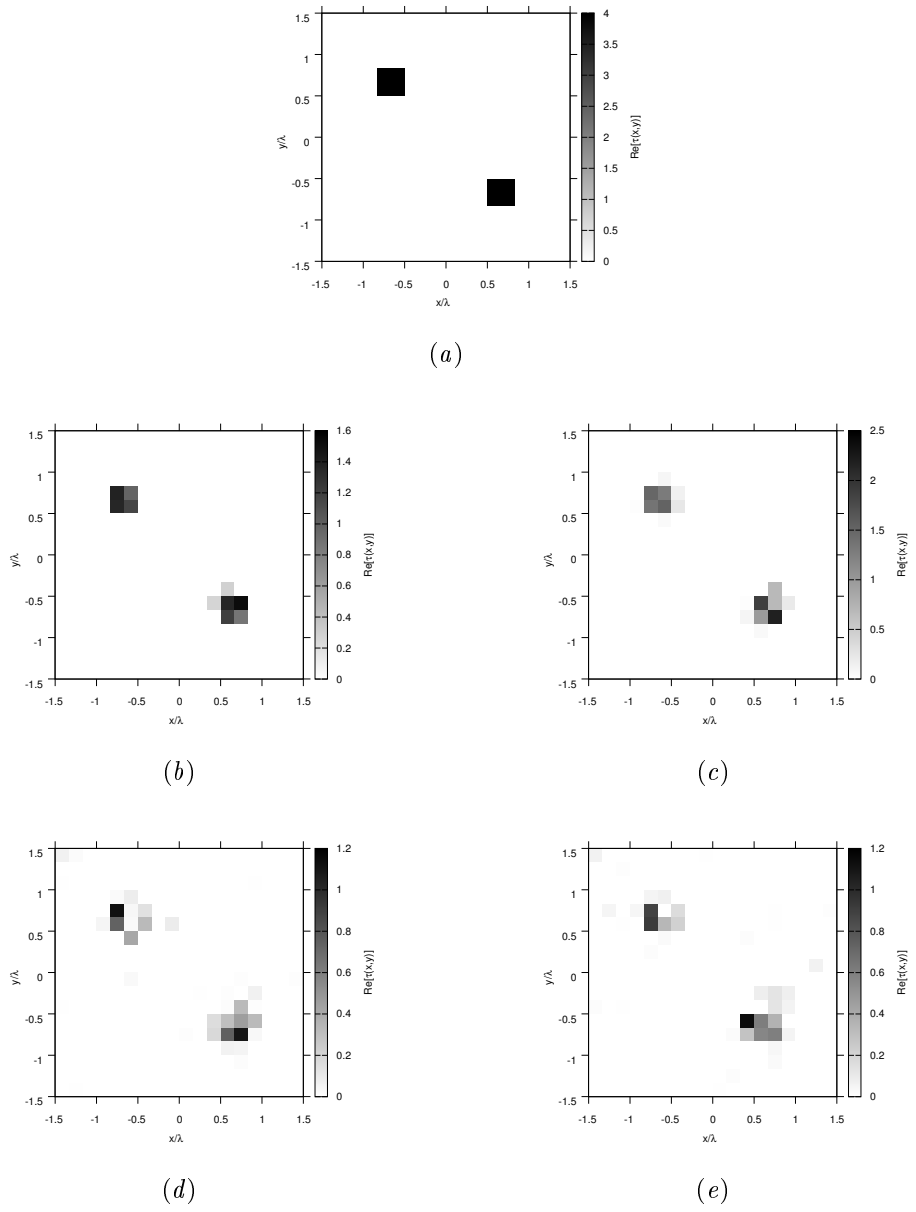

Figure 141. Actual object (a) and BCS reconstructed object for (b) Noiseless case, (c) $SNR = 20$ [dB] , (d) $SNR = 10$ [dB] , (e) $SNR = 5$ [dB].

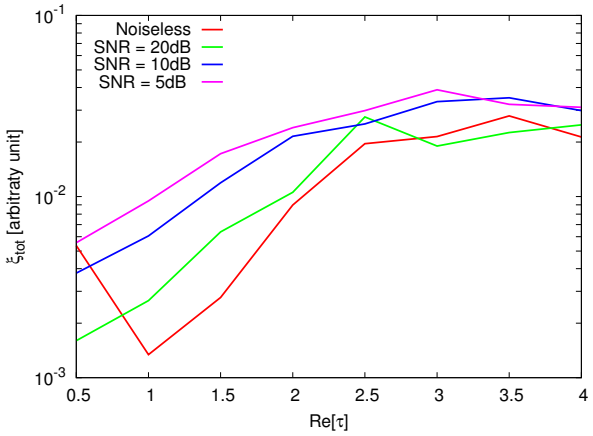

(a)

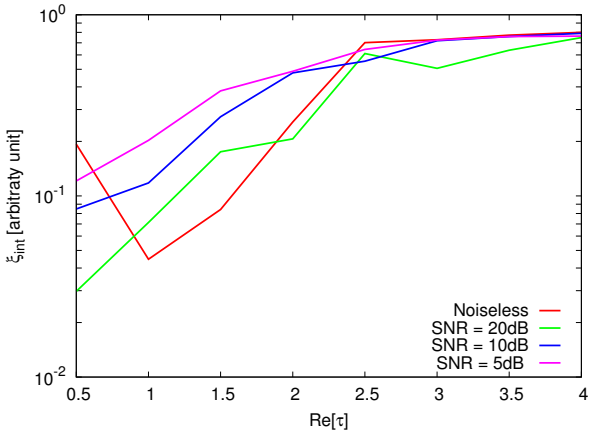

(b)

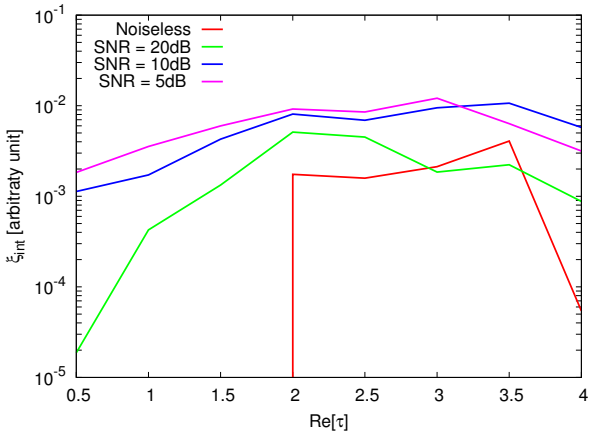

(c)

Figure 142. Behaviour of error figures as a function of ε_r, for different SNR values: (a) total error ξ_{tot}, (b) internal error ξ_{int}, (c) external error ξ_{ext}.

TEST CASE: Square Cylinder $L = 0.50\lambda$

Goal: show the performances of BCS when dealing with a sparse scatterer

- Number of Views: V
- Number of Measurements: M
- Number of Cells for the Inversion: N
- Number of Cells for the Direct solver: D
- Side of the investigation domain: L

Test Case Description

Direct solver:

- Square domain divided in $\sqrt{D} \times \sqrt{D}$ cells
- Domain side: $L = 3\lambda$
- $D = 1296$ (discretization for the direct solver: $< \lambda/10$)

Investigation domain:

- Square domain divided in $\sqrt{N} \times \sqrt{N}$ cells
- $L = 3\lambda$
- $2ka = 2 \times \frac{2\pi}{\lambda} \times \frac{L\sqrt{2}}{2} = 6\pi\sqrt{2} = 26.65$
- $\#DOF = \frac{(2ka)^2}{2} = \frac{(2 \times \frac{2\pi}{\lambda} \times \frac{L\sqrt{2}}{2})^2}{2} = 4\pi^2 \left(\frac{L}{\lambda}\right)^2 = 4\pi^2 \times 9 \approx 355.3$
- N scelto in modo da essere vicino a $\#DOF$: $N = 324$ (18×18)

Measurement domain:

- Measurement points taken on a circle of radius $\rho = 3\lambda$
- Full-aspect measurements
- $M \approx 2ka \rightarrow M = 27$

Sources:

- Plane waves
- $V \approx 2ka \rightarrow V = 27$
- Amplitude: $A = 1$
- Frequency: 300 MHz $(\lambda = 1)$

Object:

- Square cylinder of side $\frac{\lambda}{2} = 0.50$
- $\varepsilon_r \in \{1.5, 2.0, 2.5, 3.0, 3.5, 4.0, 4.5, 5.0\}$
- $\sigma = 0$ [S/m]

BCS parameters:

- Gamma prior on noise variance parameters: $a = 1 \times 10^{-1}$, $b = 5 \times 10^{-4}$
- Convergenze parameter: $\tau = 1.0 \times 10^{-8}$

RESULTS: $\varepsilon_r = 1.5$

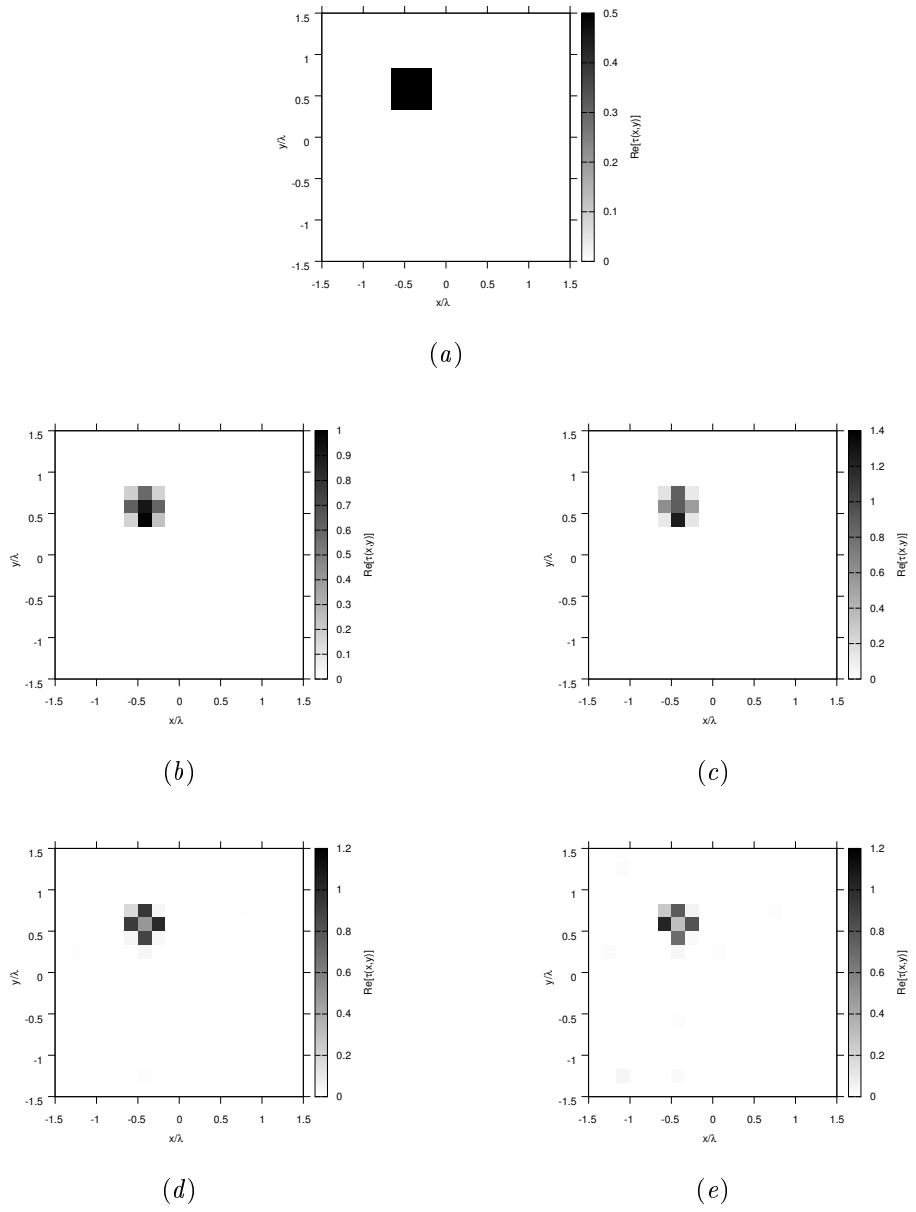

(a) (b) (c) (d) (e)

Figure 143. Actual object (a) and BCS reconstructed object for (b) Noiseless case, (c) $SNR = 20$ [dB] , (d) $SNR = 10$ [dB] , (e) $SNR = 5$ [dB].

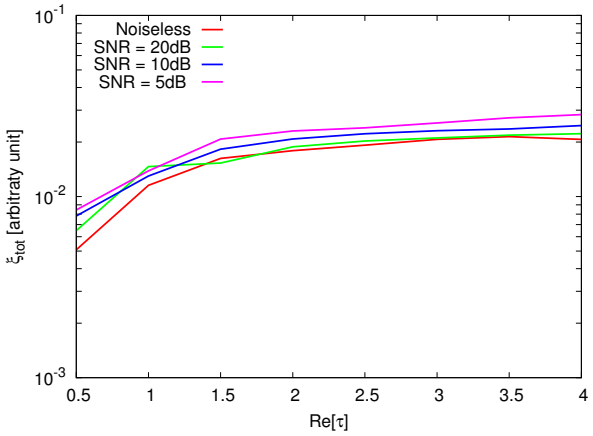

(a)

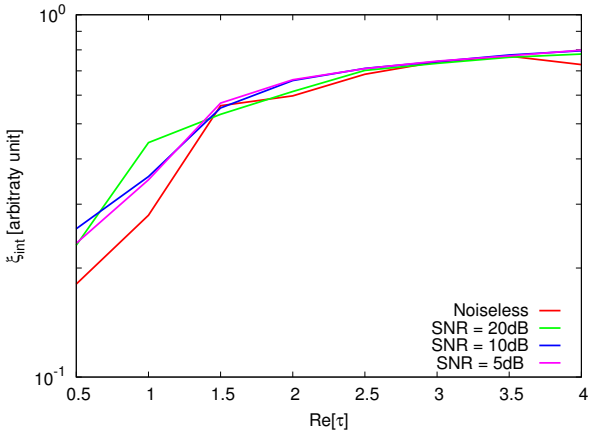

(b)

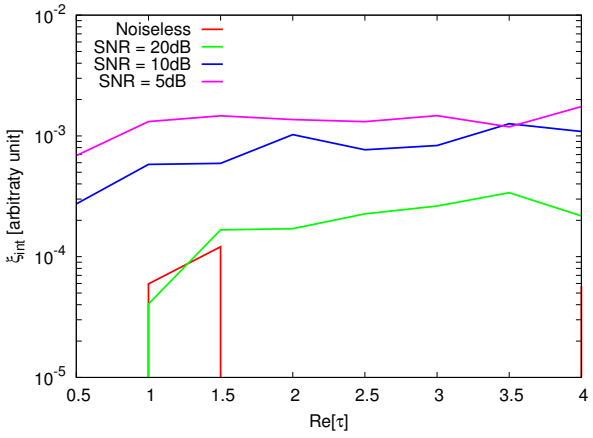

(c)

Figure 144. Behaviour of error figures as a function of ε_r, for different SNR values: (a) total error ξ_{tot}, (b) internal error ξ_{int}, (c) external error ξ_{ext}.

TEST CASE: Hollow Square Cylinder $L = 0.50\lambda$

Goal: show the performances of BCS when dealing with a sparse scatterer

- Number of Views: V
- Number of Measurements: M
- Number of Cells for the Inversion: N
- Number of Cells for the Direct solver: D
- Side of the investigation domain: L

Test Case Description

Direct solver:

- Square domain divided in $\sqrt{D} \times \sqrt{D}$ cells
- Domain side: $L = 3\lambda$
- $D = 1296$ (discretization for the direct solver: $< \lambda/10$)

Investigation domain:

- Square domain divided in $\sqrt{N} \times \sqrt{N}$ cells
- $L = 3\lambda$
- $2ka = 2 \times \frac{2\pi}{\lambda} \times \frac{L\sqrt{2}}{2} = 6\pi\sqrt{2} = 26.65$
- $\#DOF = \frac{(2ka)^2}{2} = \frac{(2 \times \frac{2\pi}{\lambda} \times \frac{L\sqrt{2}}{2})^2}{2} = 4\pi^2 \left(\frac{L}{\lambda}\right)^2 = 4\pi^2 \times 9 \approx 355.3$
- N scelto in modo da essere vicino a $\#DOF$: $N = 324$ (18×18)

Measurement domain:

- Measurement points taken on a circle of radius $\rho = 3\lambda$
- Full-aspect measurements
- $M \approx 2ka \rightarrow M = 27$

Sources:

- Plane waves
- $V \approx 2ka \rightarrow V = 27$
- Amplitude: $A = 1$
- Frequency: 300 MHz $(\lambda = 1)$

Object:

- Hollow square cylinder of side $\frac{\lambda}{2} = 0.5$
- $\varepsilon_r \in \{1.5, 2.0, 2.5, 3.0, 3.5, 4.0, 4.5, 5.0\}$
- $\sigma = 0$ [S/m]

BCS parameters:

- Gamma prior on noise variance parameters: $a = 1 \times 10^{-1}$, $b = 5 \times 10^{-4}$
- Convergenze parameter: $\tau = 1.0 \times 10^{-8}$

RESULTS: $\varepsilon_r = 1.5$

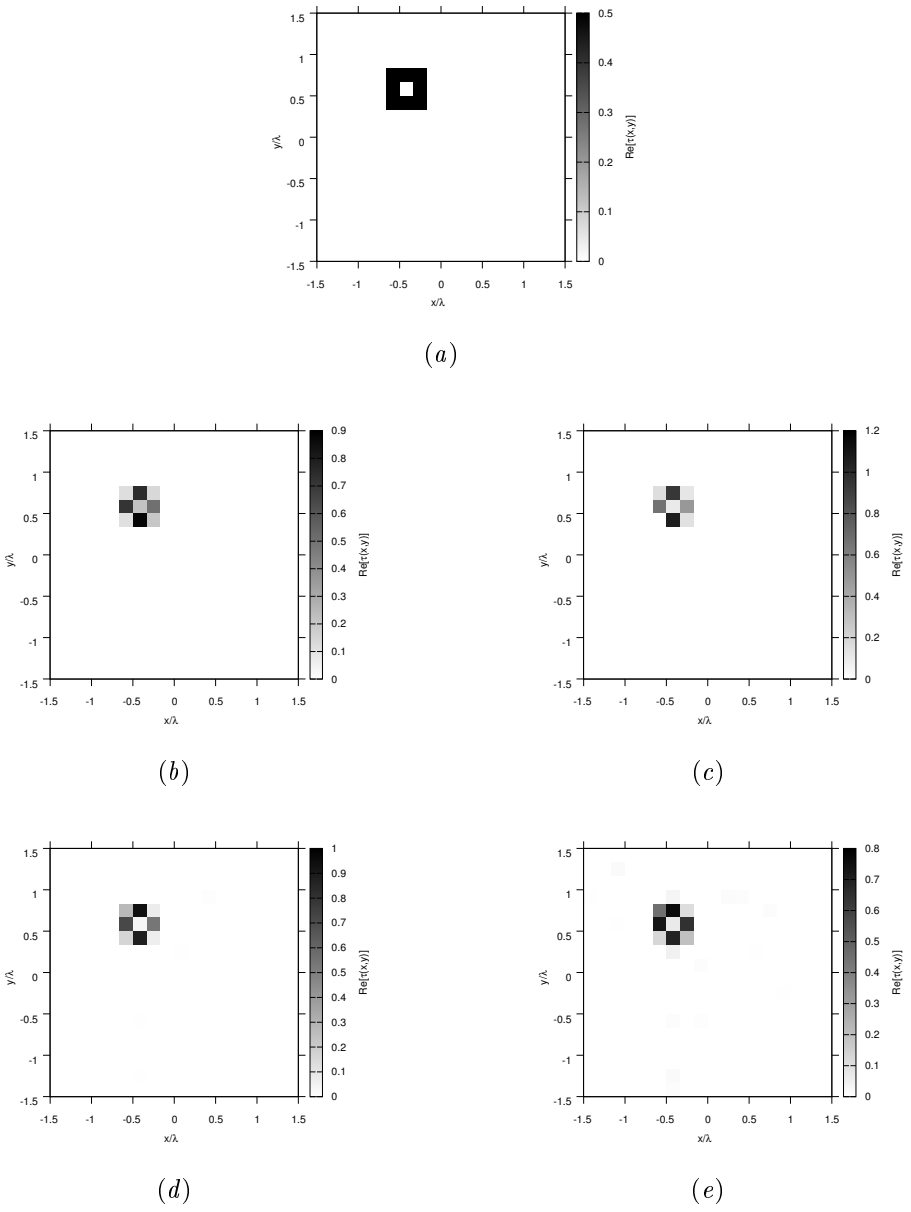

(a) (b) (c) (d) (e)

Figure 145. Actual object (a) and BCS reconstructed object for (b) Noiseless case, (c) $SNR = 20$ [dB] , (d) $SNR = 10$ [dB] , (e) $SNR = 5$ [dB].

RESULTS: $\varepsilon_r = 2.0$

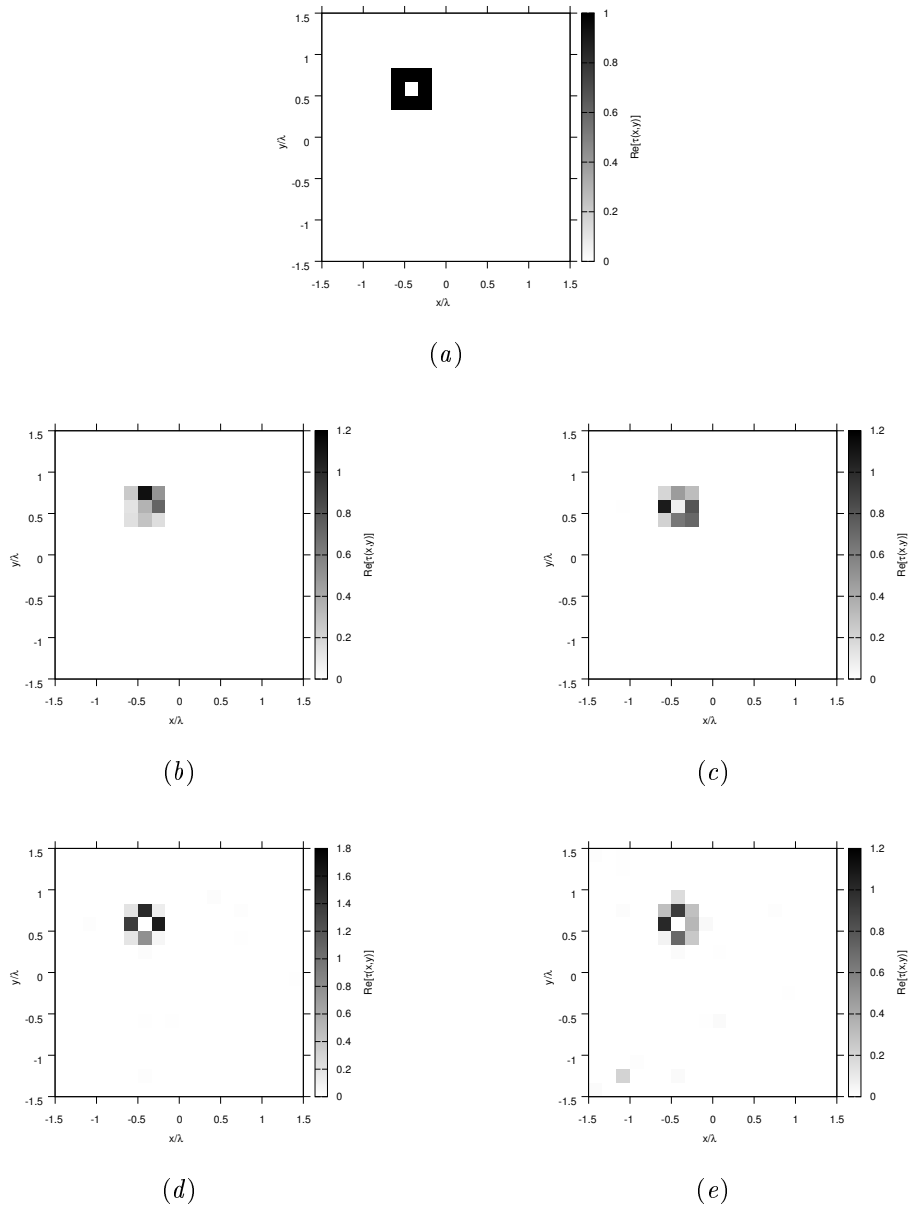

(a)

(b)

(c)

(d)

(e)

Figure 146. Actual object (a) and BCS reconstructed object for (b) Noiseless case, (c) $SNR = 20$ [dB] , (d) $SNR = 10$ [dB] , (e) $SNR = 5$ [dB].

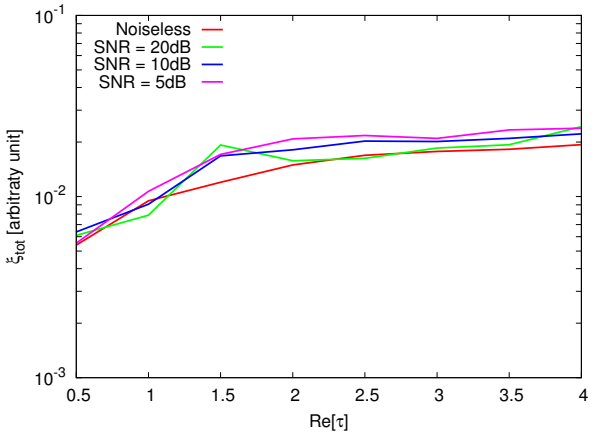

(a)

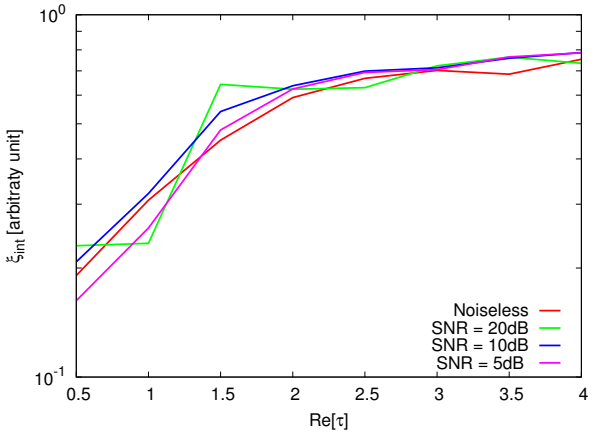

(b)

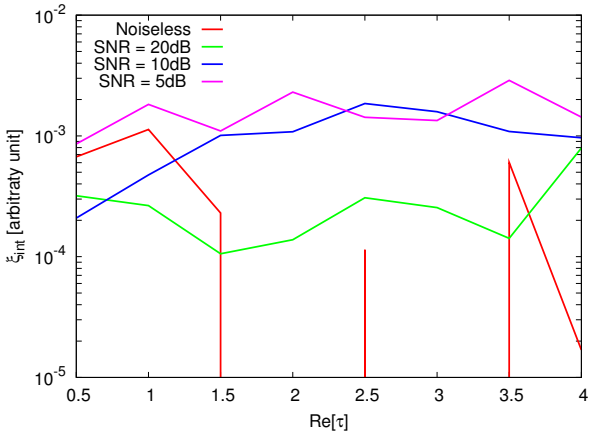

(c)

Figure 147. Behaviour of error figures as a function of ε_r, for different SNR values: (a) total error ξ_{tot}, (b) internal error ξ_{int}, (c) external error ξ_{ext}.

TEST CASE: Big L-Shaped Cylinder

Goal: show the performances of BCS when dealing with a sparse scatterer

- Number of Views: V
- Number of Measurements: M
- Number of Cells for the Inversion: N
- Number of Cells for the Direct solver: D
- Side of the investigation domain: L

Test Case Description

Direct solver:

- Square domain divided in $\sqrt{D} \times \sqrt{D}$ cells
- Domain side: $L = 3\lambda$
- $D = 1296$ (discretization for the direct solver: $< \lambda/10$)

Investigation domain:

- Square domain divided in $\sqrt{N} \times \sqrt{N}$ cells
- $L = 3\lambda$
- $2ka = 2 \times \frac{2\pi}{\lambda} \times \frac{L\sqrt{2}}{2} = 6\pi\sqrt{2} = 26.65$
- $\#DOF = \frac{(2ka)^2}{2} = \frac{(2 \times \frac{2\pi}{\lambda} \times \frac{L\sqrt{2}}{2})^2}{2} = 4\pi^2 \left(\frac{L}{\lambda}\right)^2 = 4\pi^2 \times 9 \approx 355.3$
- N scelto in modo da essere vicino a $\#DOF$: $N = 324$ (18×18)

Measurement domain:

- Measurement points taken on a circle of radius $\rho = 3\lambda$
- Full-aspect measurements
- $M \approx 2ka \rightarrow M = 27$

Sources:

- Plane waves
- $V \approx 2ka \rightarrow V = 27$
- Amplitude: $A = 1$
- Frequency: 300 MHz $(\lambda = 1)$

Object:

- Big L-shaped cylinder
- $\varepsilon_r \in \{1.5, 2.0, 2.5, 3.0, 3.5, 4.0, 4.5, 5.0\}$
- $\sigma = 0$ [S/m]

BCS parameters:

- Gamma prior on noise variance parameters: $a = 1 \times 10^{-1}$, $b = 5 \times 10^{-4}$
- Convergenze parameter: $\tau = 1.0 \times 10^{-8}$

RESULTS: $\varepsilon_r = 1.5$

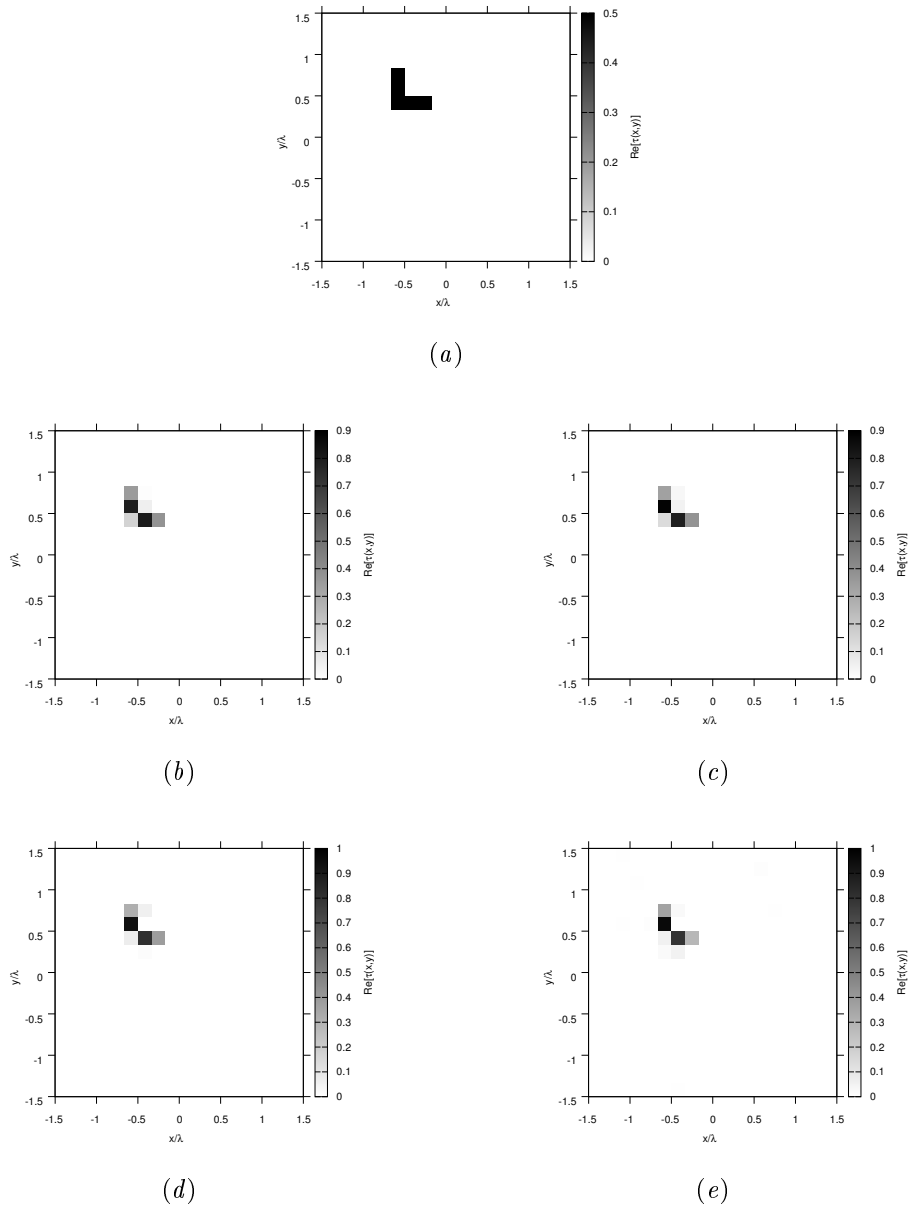

Figure 148. Actual object (a) and BCS reconstructed object for (b) Noiseless case, (c) $SNR = 20$ [dB] , (d) $SNR = 10$ [dB] , (e) $SNR = 5$ [dB].

RESULTS: $\varepsilon_r = 2.0$

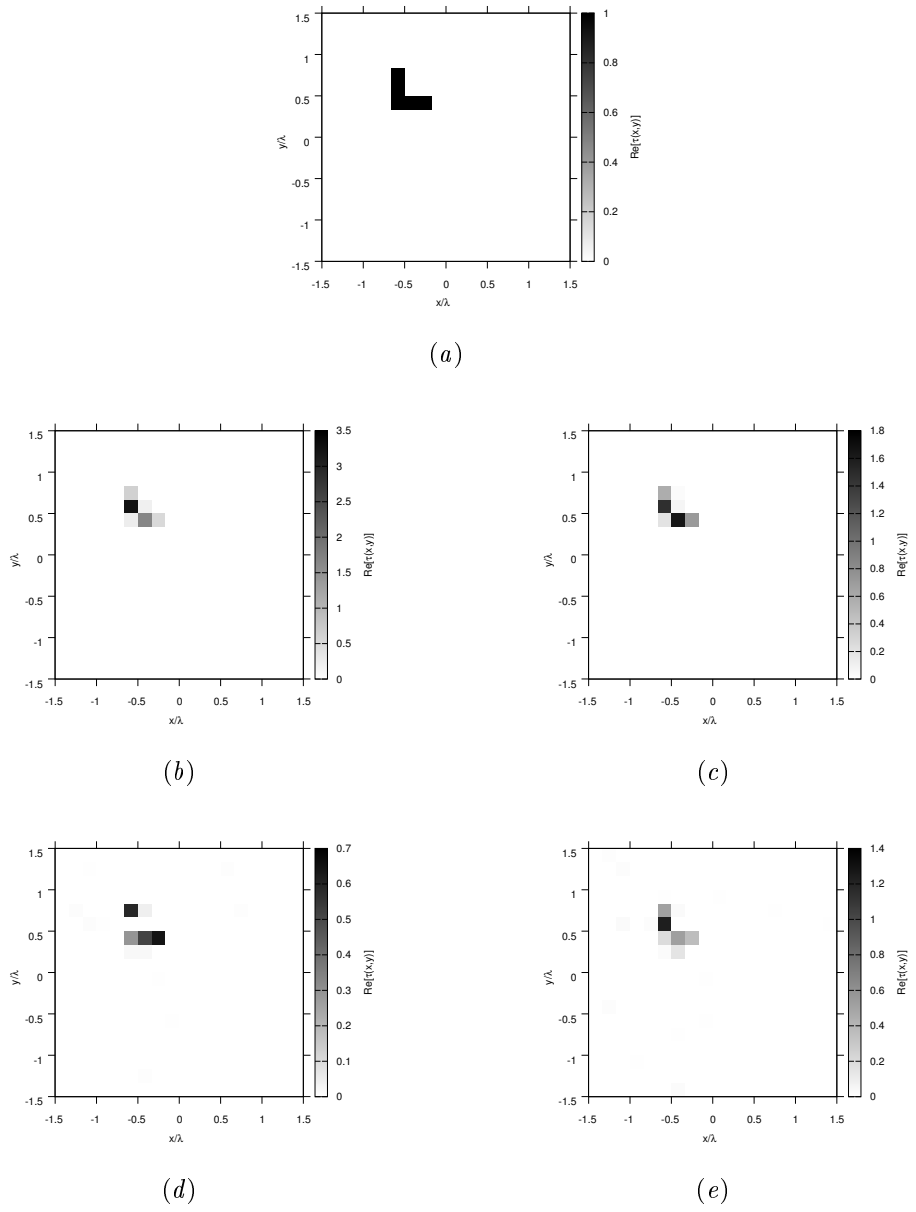

Figure 149. Actual object (a) and BCS reconstructed object for (b) Noiseless case, (c) $SNR = 20$ [dB] , (d) $SNR = 10$ [dB] , (e) $SNR = 5$ [dB].

RESULTS: $\varepsilon_r = 3.0$

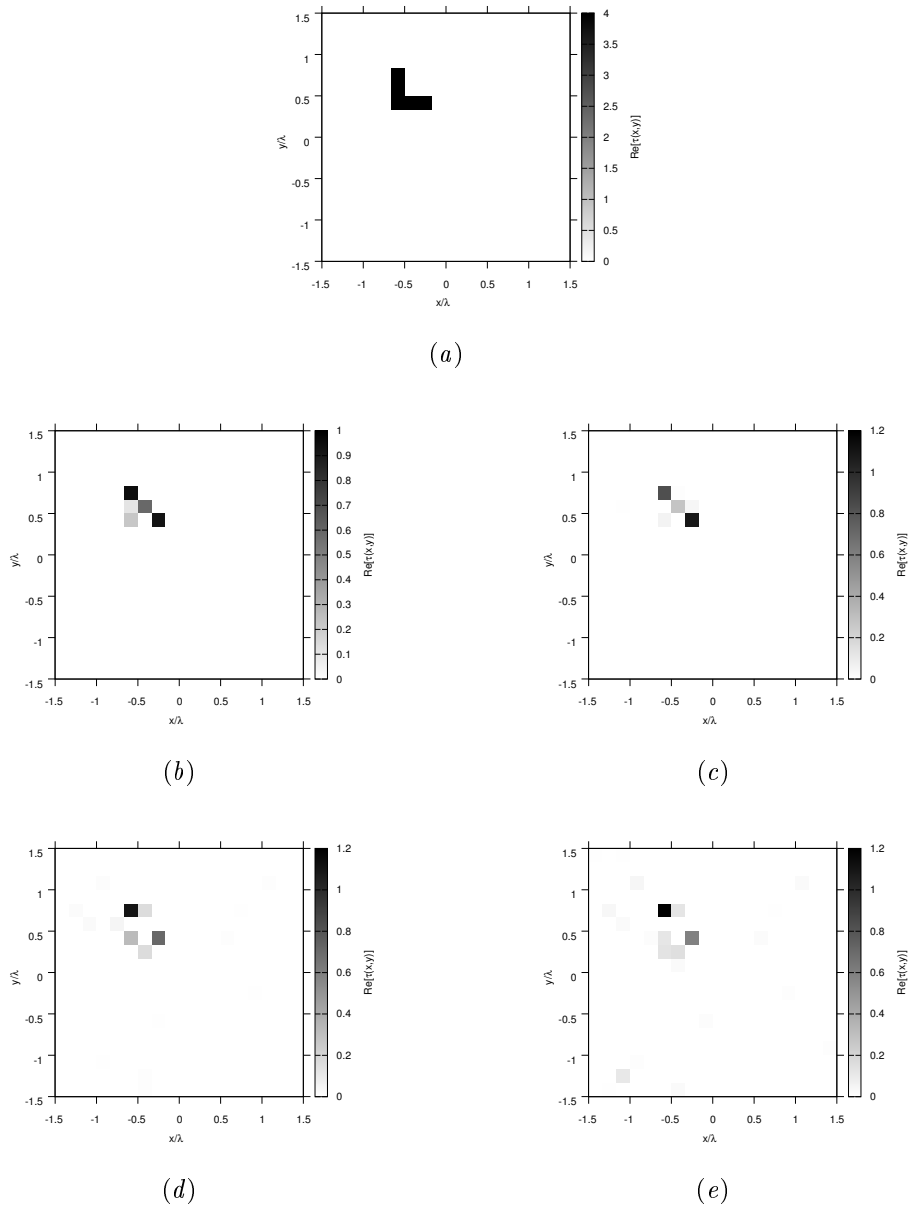

(a) (b) (c) (d) (e)

Figure 150. Actual object (a) and BCS reconstructed object for (b) Noiseless case, (c) $SNR = 20$ [dB] , (d) $SNR = 10$ [dB] , (e) $SNR = 5$ [dB].

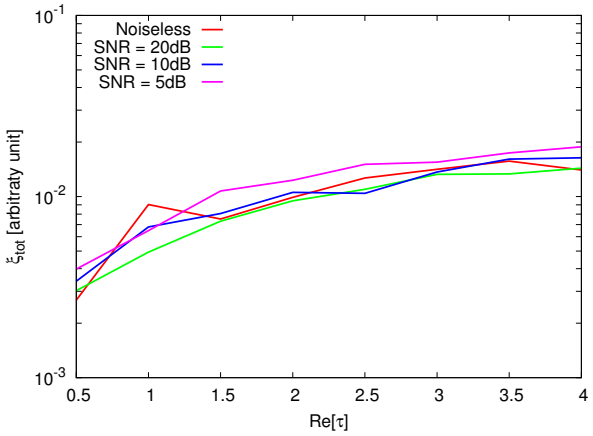

(a)

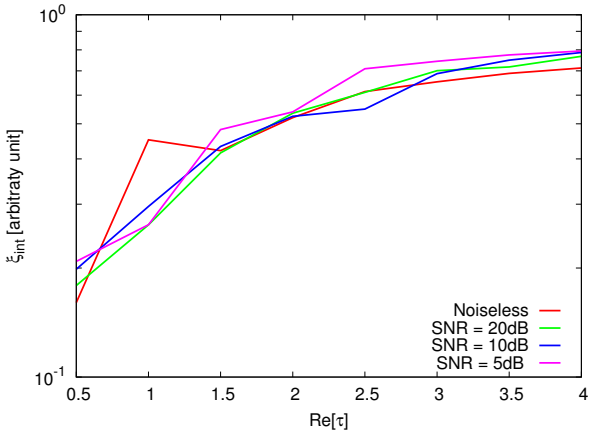

(b)

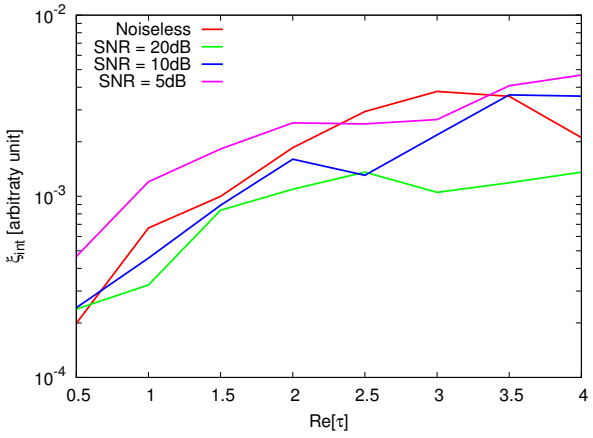

(c)

Figure 151. Behaviour of error figures as a function of ε_r, for different SNR values: (a) total error ξ_{tot}, (b) internal error ξ_{int}, (c) external error ξ_{ext}.

TEST CASE: Big T-Shaped Cylinder

Goal: show the performances of BCS when dealing with a sparse scatterer

- Number of Views: V
- Number of Measurements: M
- Number of Cells for the Inversion: N
- Number of Cells for the Direct solver: D
- Side of the investigation domain: L

Test Case Description

Direct solver:

- Square domain divided in $\sqrt{D} \times \sqrt{D}$ cells
- Domain side: $L = 3\lambda$
- $D = 1296$ (discretization for the direct solver: $< \lambda/10$)

Investigation domain:

- Square domain divided in $\sqrt{N} \times \sqrt{N}$ cells
- $L = 3\lambda$
- $2ka = 2 \times \frac{2\pi}{\lambda} \times \frac{L\sqrt{2}}{2} = 6\pi\sqrt{2} = 26.65$
- $\#DOF = \frac{(2ka)^2}{2} = \frac{(2 \times \frac{2\pi}{\lambda} \times \frac{L\sqrt{2}}{2})^2}{2} = 4\pi^2 \left(\frac{L}{\lambda}\right)^2 = 4\pi^2 \times 9 \approx 355.3$
- N scelto in modo da essere vicino a $\#DOF$: $N = 324$ (18×18)

Measurement domain:

- Measurement points taken on a circle of radius $\rho = 3\lambda$
- Full-aspect measurements
- $M \approx 2ka \rightarrow M = 27$

Sources:

- Plane waves
- $V \approx 2ka \rightarrow V = 27$
- Amplitude: $A = 1$
- Frequency: 300 MHz $(\lambda = 1)$

Object:

- Big T-shaped cylinder
- $\varepsilon_r \in \{1.5, 2.0, 2.5, 3.0, 3.5, 4.0, 4.5, 5.0\}$
- $\sigma = 0$ [S/m]

BCS parameters:

- Gamma prior on noise variance parameters: $a = 1 \times 10^{-1}$, $b = 5 \times 10^{-4}$
- Convergenze parameter: $\tau = 1.0 \times 10^{-8}$

RESULTS: $\varepsilon_r = 1.5$

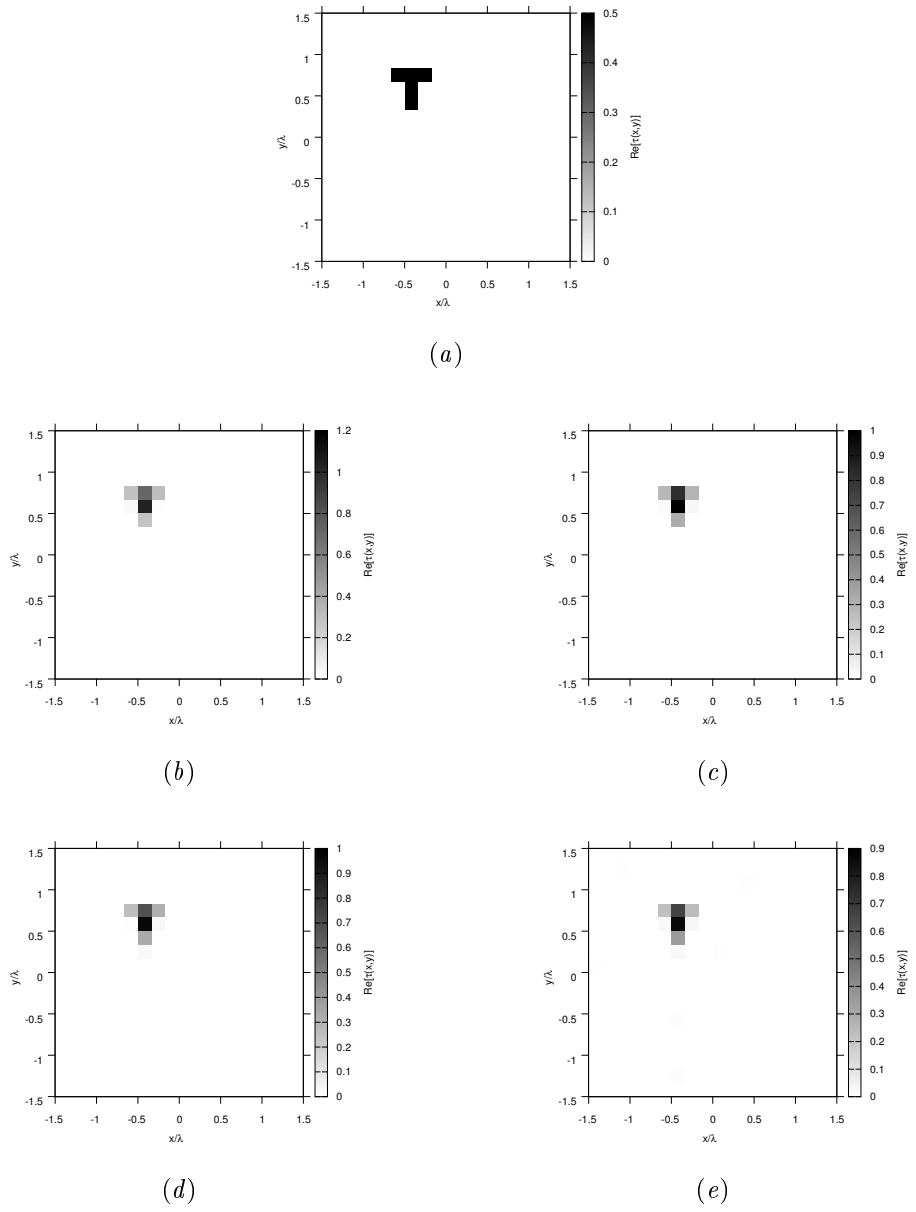

(a) (b) (c) (d) (e)

Figure 152. Actual object (a) and BCS reconstructed object for (b) Noiseless case, (c) $SNR = 20$ [dB] , (d) $SNR = 10$ [dB] , (e) $SNR = 5$ [dB].

RESULTS: $\varepsilon_r = 2.0$

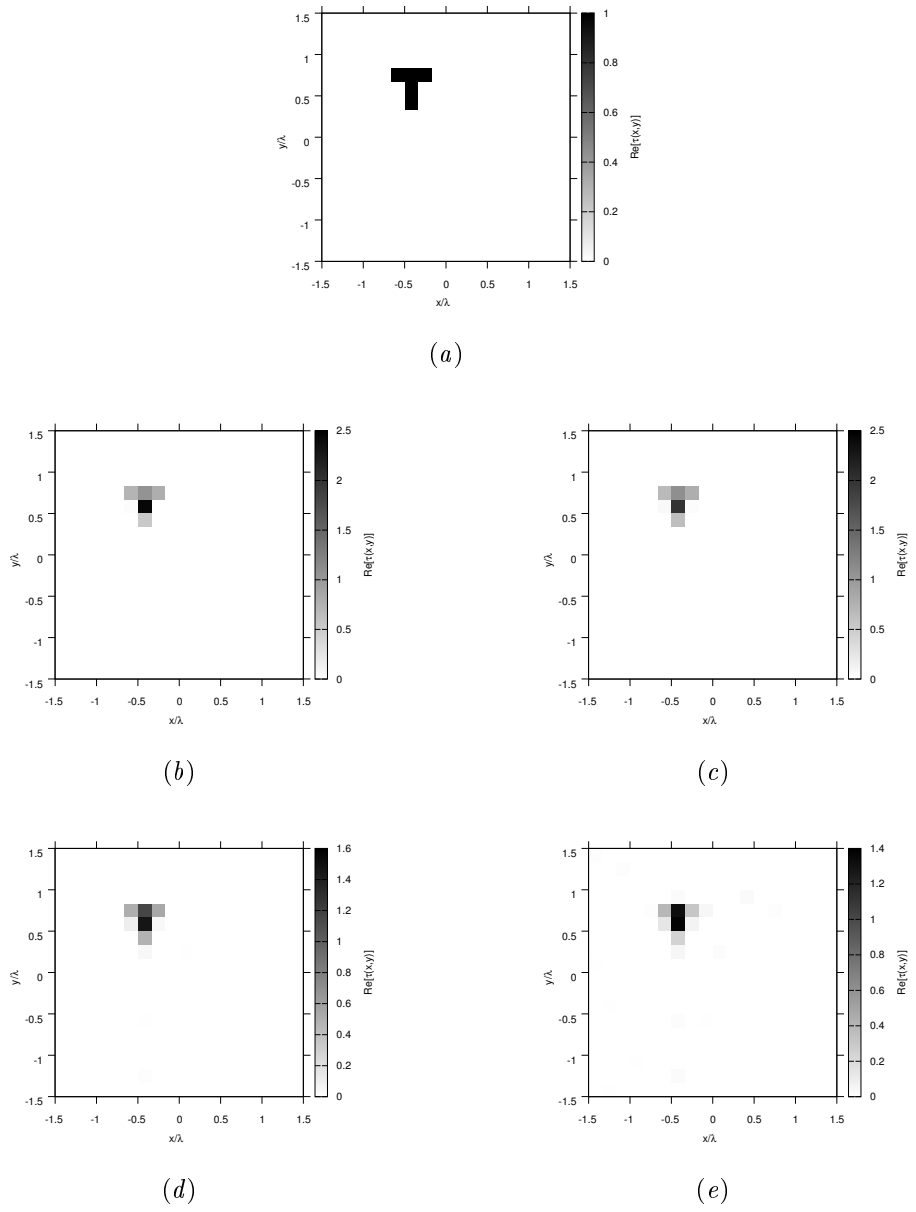

(a)

(b)

(c)

(d)

(e)

Figure 153. Actual object (a) and BCS reconstructed object for (b) Noiseless case, (c) $SNR = 20$ [dB] , (d) $SNR = 10$ [dB] , (e) $SNR = 5$ [dB].

RESULTS: $\varepsilon_r = 3.0$

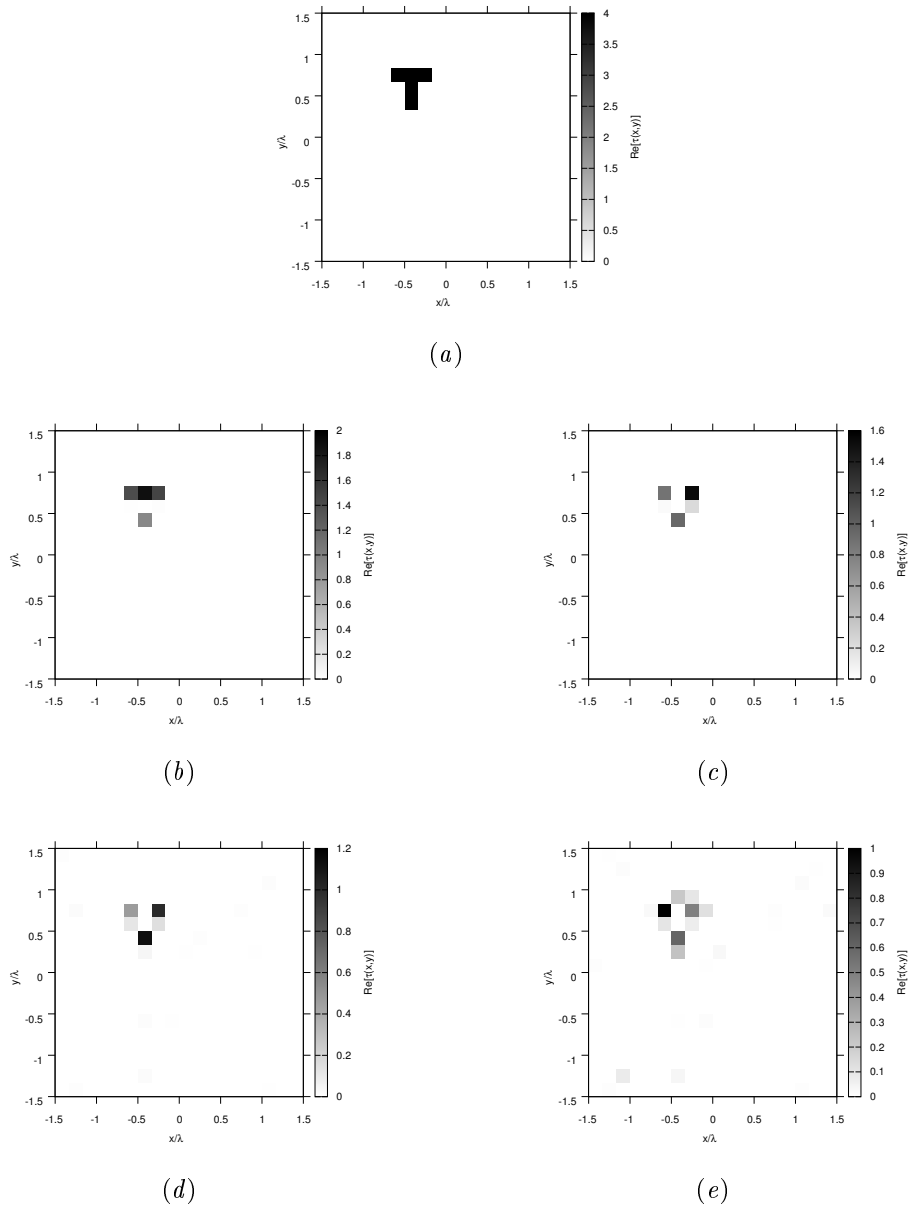

(a) (b) (c) (d) (e)

Figure 154. Actual object (a) and BCS reconstructed object for (b) Noiseless case, (c) $SNR = 20$ [dB] , (d) $SNR = 10$ [dB] , (e) $SNR = 5$ [dB].

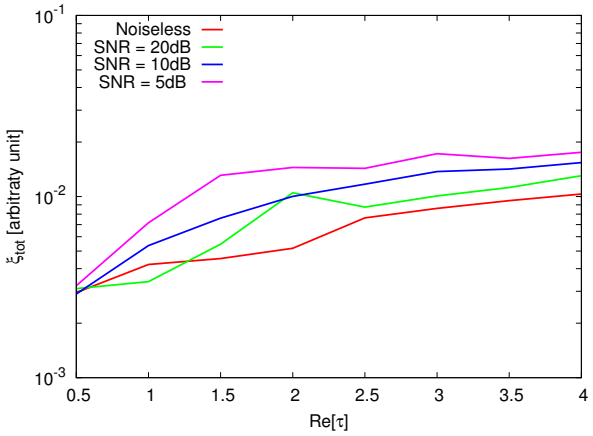

(a)

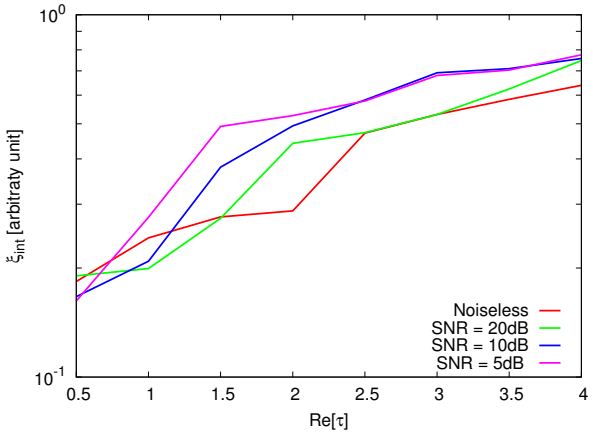

(b)

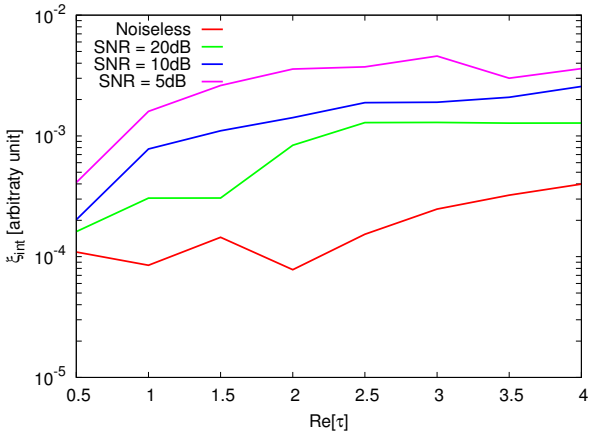

(c)

Figure 155. Behaviour of error figures as a function of ε_r, for different SNR values: (a) total error ξ_{tot}, (b) internal error ξ_{int}, (c) external error ξ_{ext}.

TEST CASE: Test Random Objects (Statistical Test)

Goal: evaluate the performances of BCS

- Number of Views: V
- Number of Measurements: M
- Number of Cells for the Inversion: N
- Number of Cells for the Direct solver: D
- Side of the investigation domain: L

Test Case Description

Direct solver:

- Square domain divided in $\sqrt{D} \times \sqrt{D}$ cells
- Domain side: $L = 3\lambda$
- $D = 1296$ (discretization for the direct solver: $< \lambda/10$)

Investigation domain:

- Square domain divided in $\sqrt{N} \times \sqrt{N}$ cells
- $L = 3\lambda$
- $N = 324$

Measurement domain:

- Measurement points taken on a circle of radius $\rho = 3\lambda$
- Full-aspect measurements
- $M \approx 2ka \rightarrow M = 27$

Sources:

- Plane waves
- $V \approx 2ka \rightarrow V = 27$
- Amplitude $A = 1$
- Frequency: 300 MHz ($\lambda = 1$)

Object:

- S square cylinders of side $\frac{\lambda}{6} = 0.16667$ ($S \in \{1, 2, 3, 4, 5, 6\}$)
- $\varepsilon_r \in \{1.5, 2.0, 3.0, 4.0, 5.0\}$
- $\sigma = 0$ [S/m]

BCS parameters:

- Gamma prior on noise variance parameters: $a = 1 \times 10^{-1}$, $b = 5 \times 10^{-4}$
- Convergenze parameter: $\tau = 1.0 \times 10^{-8}$

Statistical Analysis:

- $K = 10$ random seeds used for each case to determine the position of the objects inside the onvestigation domain

RESULTS: $\varepsilon_r = 1.5$

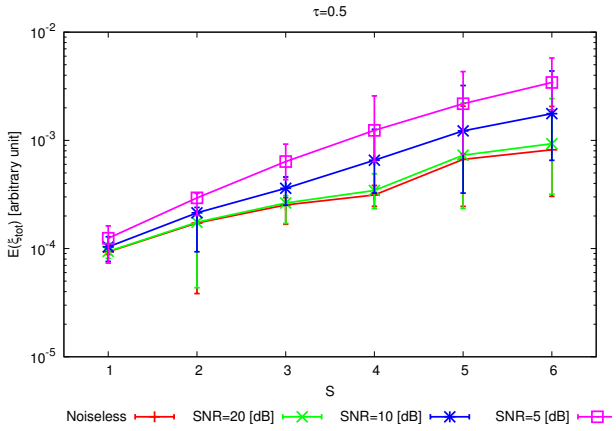

(a)

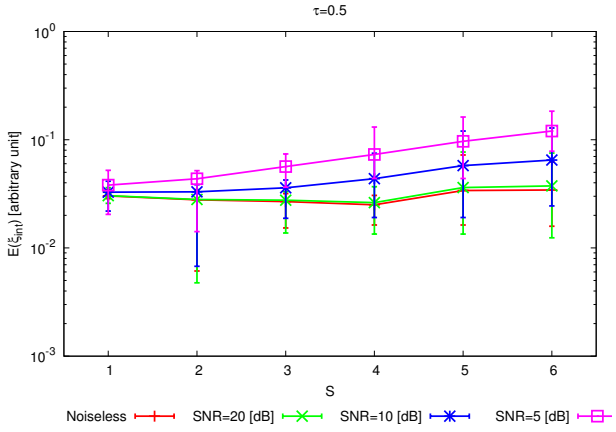

(b)

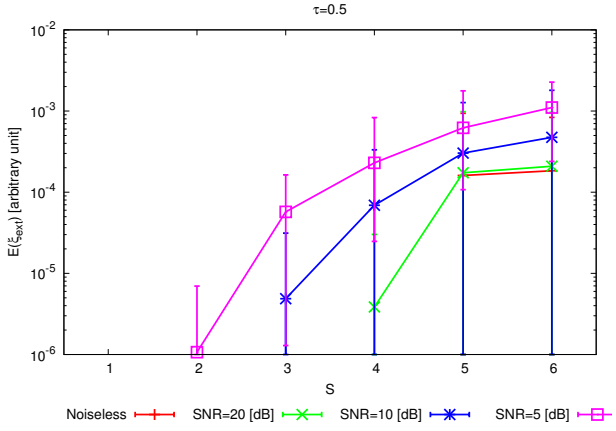

(c)

Figure 156. *Statistical analysis* $[K = 10, \varepsilon_r = 1.5]$ - Behaviour of mean, maximum and minimum of the error figures as a function of S (sparsity factor), for different SNR values: (a) total error ξ_{tot}, (b) internal error ξ_{int}, (c) external error ξ_{ext}.

RESULTS: $\varepsilon_r = 2.0$

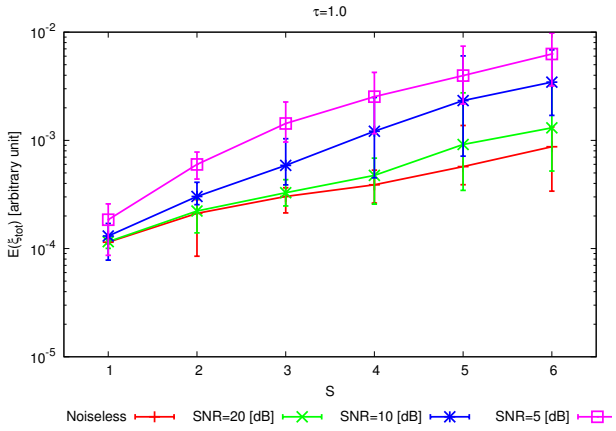

(a)

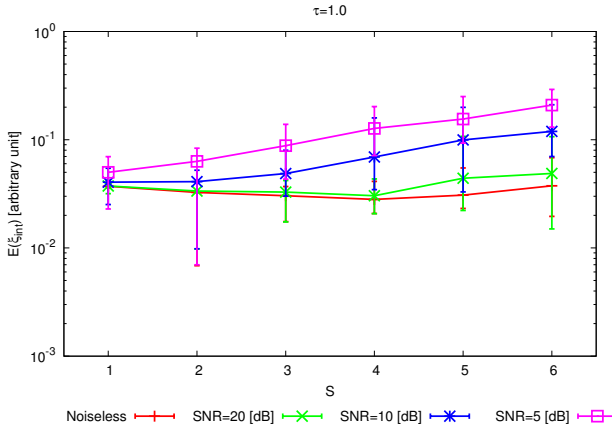

(b)

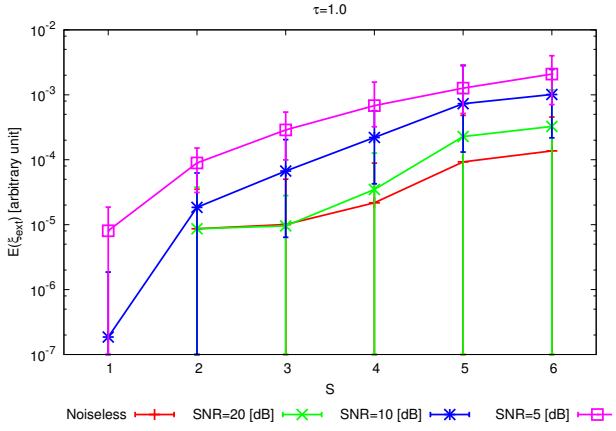

(c)

Figure 157. *Statistical analysis* $[K = 10, \varepsilon_r = 2.0]$ - Behaviour of mean, maximum and minimum of the error figures as a function of S (sparsity factor), for different SNR values: (a) total error ξ_{tot}, (b) internal error ξ_{int}, (c) external error ξ_{ext}.

RESULTS: $\varepsilon_r = 3.0$

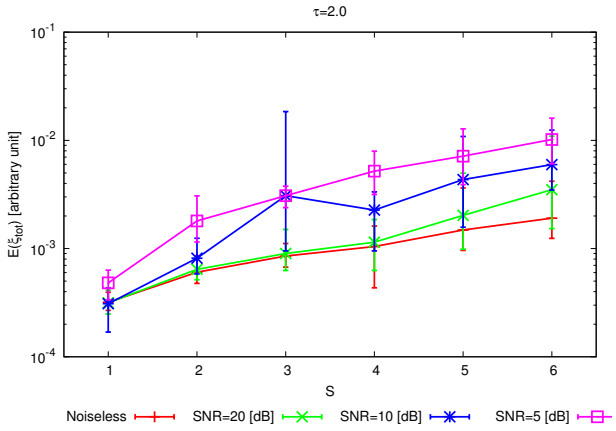

(a)

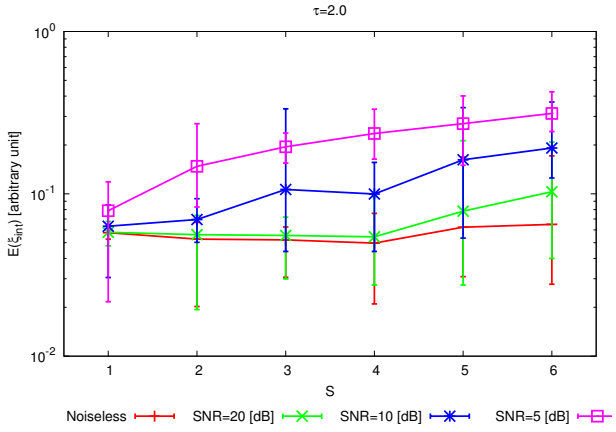

(b)

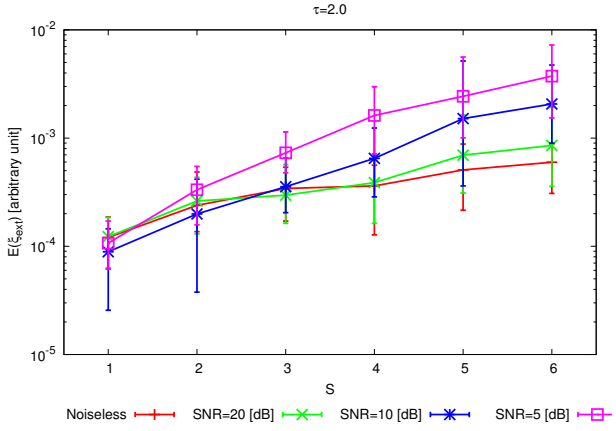

(c)

Figure 158. *Statistical analysis* $[K = 10, \varepsilon_r = 3.0]$ - Behaviour of mean, maximum and minimum of the error figures as a function of S (sparsity factor), for different SNR values: (a) total error ξ_{tot}, (b) internal error ξ_{int}, (c) external error ξ_{ext}.

RESULTS: $\varepsilon_r = 4.0$

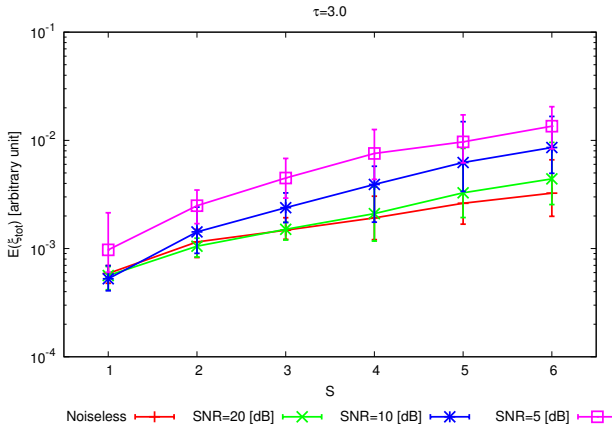

(a)

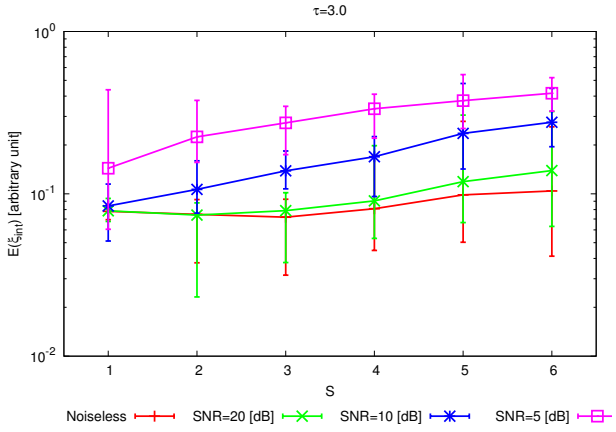

(b)

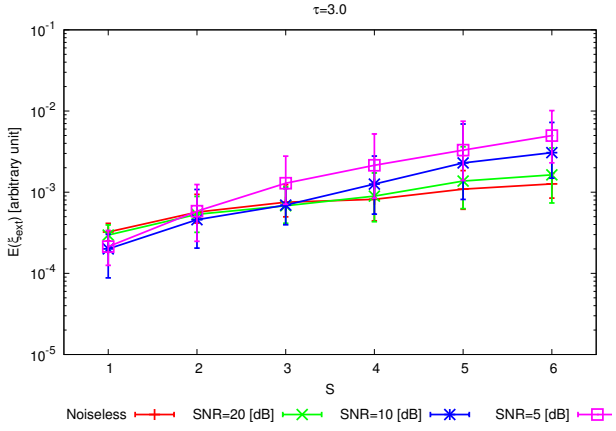

(c)

Figure 159. *Statistical analysis* $[K = 10, \varepsilon_r = 4.0]$ - Behaviour of mean, maximum and minimum of the error figures as a function of S (sparsity factor), for different SNR values: (a) total error ξ_{tot}, (b) internal error ξ_{int}, (c) external error ξ_{ext}.

RESULTS: $\varepsilon_r = 5.0$

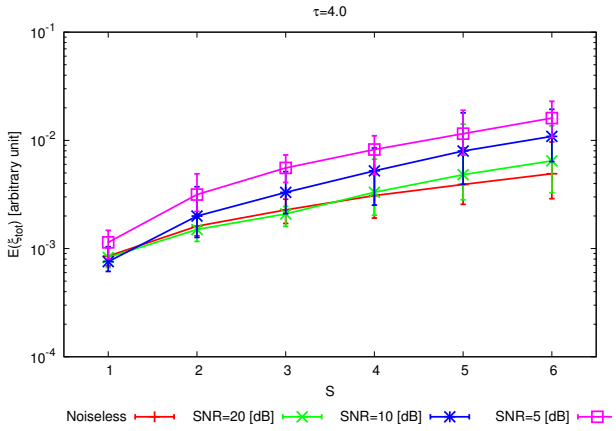

(a)

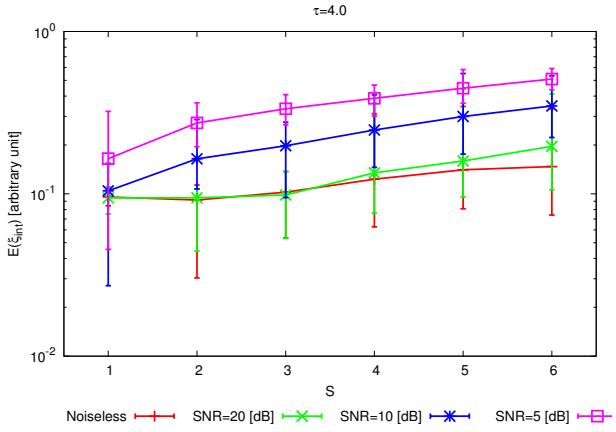

(b)

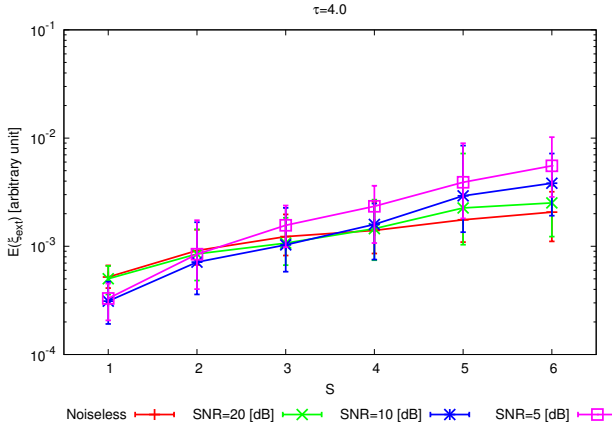

(c)

Figure 160. *Statistical analysis* $[K = 10, \varepsilon_r = 5.0]$ - Behaviour of mean, maximum and minimum of the error figures as a function of S (sparsity factor), for different SNR values: (a) total error ξ_{tot}, (b) internal error ξ_{int}, (c) external error ξ_{ext}.

TEST CASE: Two Square Cylinders on the Diagonal

Goal: evaluate the the performances of BCS

- Number of Views: V
- Number of Measurements: M
- Number of Cells for the Inversion: N
- Number of Cells for the Direct solver: D
- Side of the investigation domain: L

Test Case Description

Direct solver:

- Square domain divided in $\sqrt{D} \times \sqrt{D}$ cells
- Domain side: $L = 3\lambda$
- $D = 1296$ (discretization for the direct solver: $< \lambda/10$)

Investigation domain:

- Square domain divided in $\sqrt{N} \times \sqrt{N}$ cells
- $L = 3\lambda$
- $N = 324$

Measurement domain:

- Measurement points taken on a circle of radius $\rho = 3\lambda$
- Full-aspect measurements
- $M \approx 2ka \rightarrow M = 27$

Sources:

- Plane waves
- $V \approx 2ka \rightarrow V = 27$
- Amplitude $A = 1$
- Frequency: 300 MHz ($\lambda = 1$)

Object:

- Two square cylinders of side $\frac{\lambda}{6} = 0.16667$ at a distance Δx, Δy from each other
- $\varepsilon_r \in \{1.5, 2.0, 3.0, 4.0, 5.0\}$
- $\sigma = 0$ [S/m]

BCS parameters:

- Gamma prior on noise variance parameters: $a = 1 \times 10^{-1}$, $b = 5 \times 10^{-4}$
- Convergenze parameter: $\tau = 1.0 \times 10^{-8}$

Resolution Analysis:

- $\Delta x = \Delta y = \{k\lambda/10,\ k = 0, ..., 14\}$

RESULTS: $\varepsilon_r = 1.5$

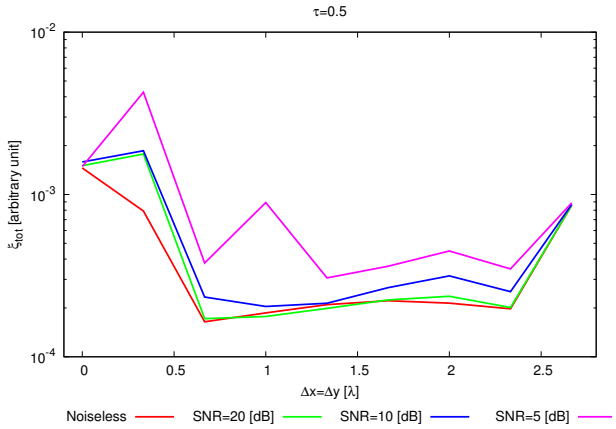

(a)

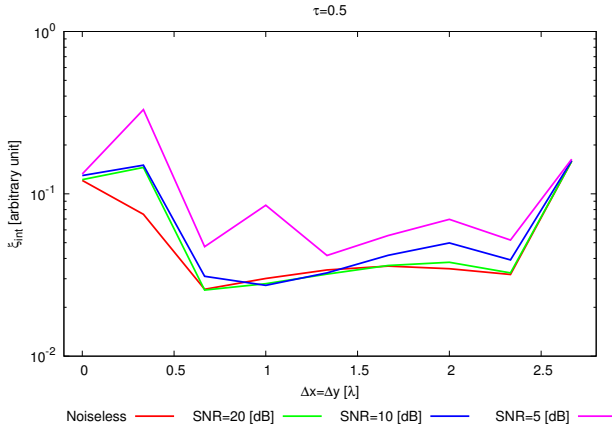

(b)

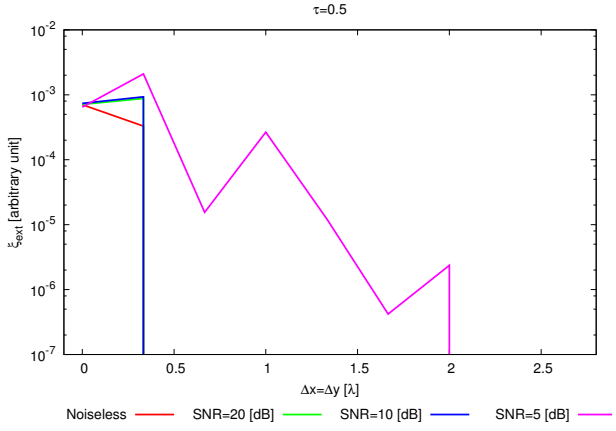

(c)

Figure 161. *Resolution analysis* - Behaviour of error figures as a function of $\Delta x = \Delta y$ for different SNR values: (a) total error ξ_{tot}, (b) internal error ξ_{int}, (c) external error ξ_{ext}.

RESULTS: $\varepsilon_r = 2.0$

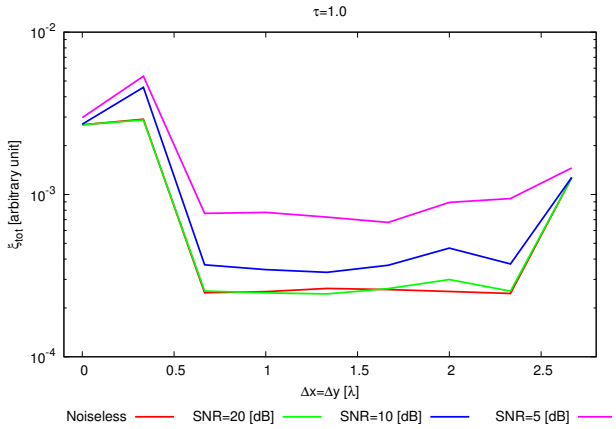

(a)

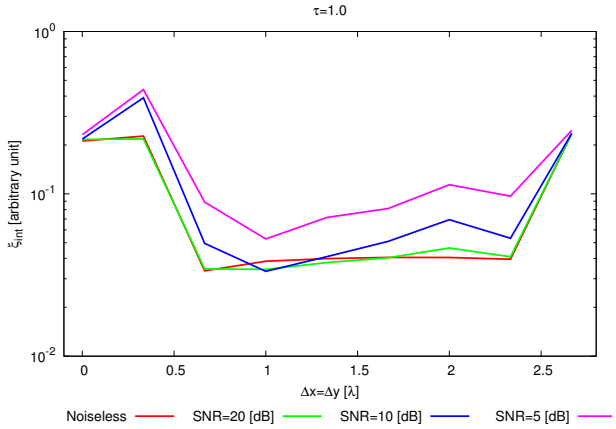

(b)

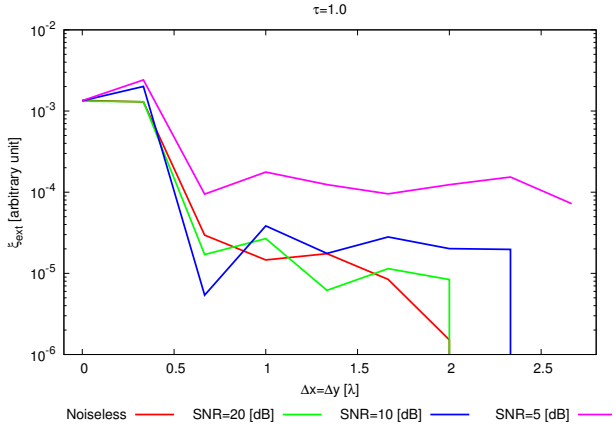

(c)

Figure 162. *Resolution analysis* - Behaviour of error figures as a function of $\Delta x = \Delta y$ for different SNR values: (a) total error ξ_{tot}, (b) internal error ξ_{int}, (c) external error ξ_{ext}.

RESULTS: $\varepsilon_r = 3.0$

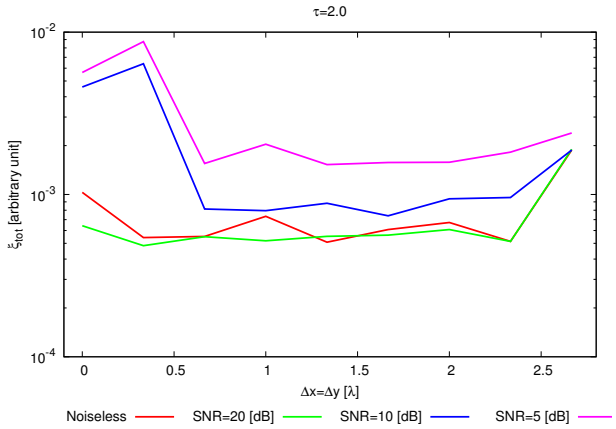

(a)

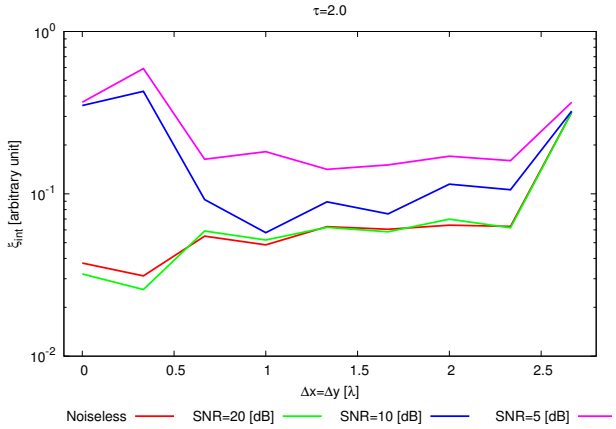

(b)

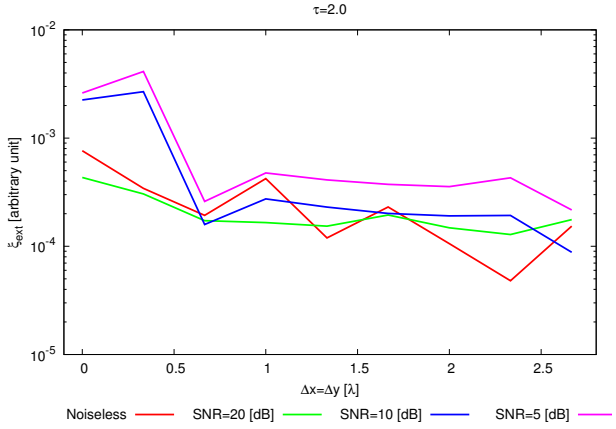

(c)

Figure 163. *Resolution analysis* - Behaviour of error figures as a function of $\Delta x = \Delta y$ for different SNR values: (a) total error ξ_{tot}, (b) internal error ξ_{int}, (c) external error ξ_{ext}.

RESULTS: $\varepsilon_r = 4.0$

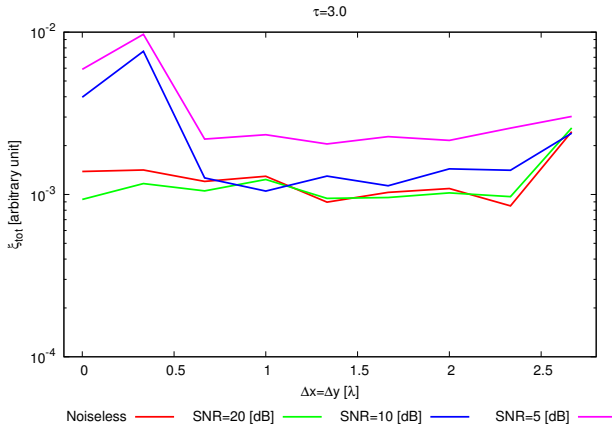

(a)

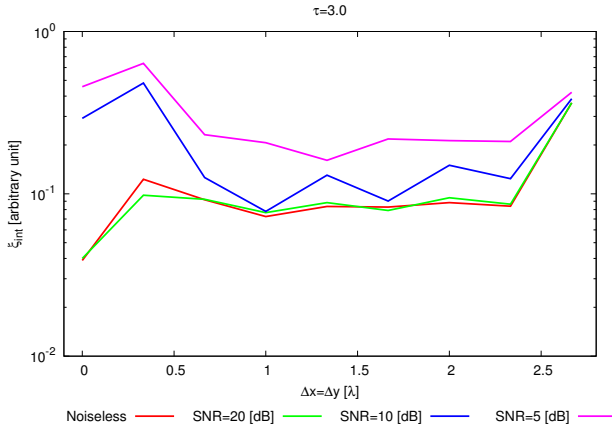

(b)

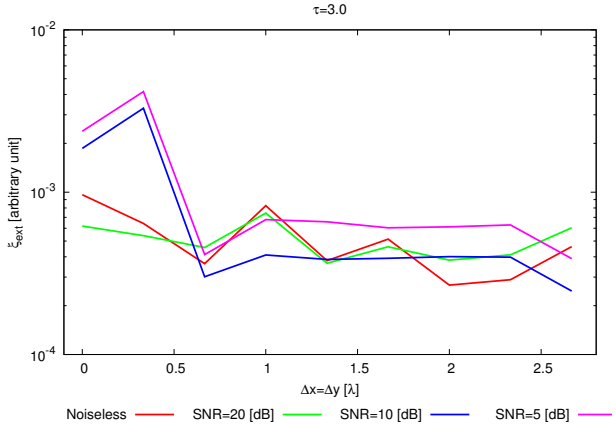

(c)

Figure 164. *Resolution analysis* - Behaviour of error figures as a function of $\Delta x = \Delta y$ for different SNR values: (a) total error ξ_{tot}, (b) internal error ξ_{int}, (c) external error ξ_{ext}.

RESULTS: $\varepsilon_r = 5.0$

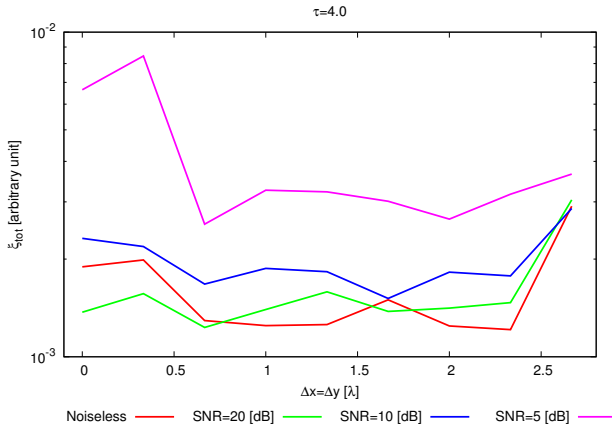

(a)

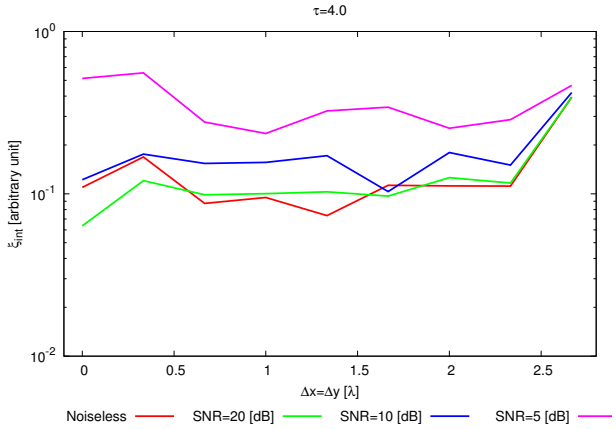

(b)

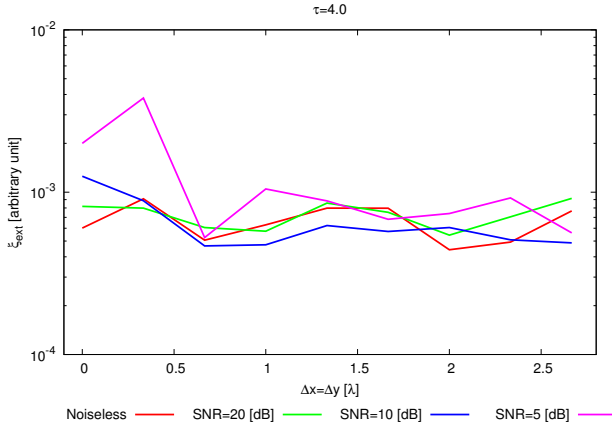

(c)

Figure 165. *Resolution analysis* - Behaviour of error figures as a function of $\Delta x = \Delta y$ for different SNR values: (a) total error ξ_{tot}, (b) internal error ξ_{int}, (c) external error ξ_{ext}.

6 Single/Double Field Components

TEST CASE: L-Shaped Cylinder

Goal: show the performances of BCS when dealing with a sparse scatterer

- Number of Views: V
- Number of Measurements: M
- Number of Cells for the Inversion: N
- Number of Cells for the Direct solver: D
- Side of the investigation domain: L

Test Case Description

Direct solver:

- Square domain divided in $\sqrt{D} \times \sqrt{D}$ cells
- Domain side: $L = 3\lambda$
- $D = 1296$ (discretization for the direct solver: $< \lambda/10$)

Investigation domain:

- Square domain divided in $\sqrt{N} \times \sqrt{N}$ cells
- $L = 3\lambda$
- $2ka = 2 \times \frac{2\pi}{\lambda} \times \frac{L\sqrt{2}}{2} = 6\pi\sqrt{2} = 26.65$
- $\#DOF = \frac{(2ka)^2}{2} = \frac{(2 \times \frac{2\pi}{\lambda} \times \frac{L\sqrt{2}}{2})^2}{2} = 4\pi^2 \left(\frac{L}{\lambda}\right)^2 = 4\pi^2 \times 9 \approx 355.3$
- N scelto in modo da essere vicino a $\#DOF$: $N = 324$ (18×18)

Measurement domain:

- Measurement points taken on a circle of radius $\rho = 3\lambda$
- Full-aspect measurements
- $M \approx 2ka \rightarrow M = 27$

Sources:

- Plane waves
- $V \approx 2ka \rightarrow V = 27$
- Amplitude $A = 1$
- Frequency: 300 MHz $(\lambda = 1)$

Object:

- L-shaped cylinder
- $\varepsilon_r \in \{1.5, 2.0, 2.5, 3.0, 3.5, 4.0, 4.5, 5.0\}$
- $\sigma = 0$ [S/m]

BCS parameters:

- Convergenze parameter: $\tau = 1.0 \times 10^{-8}$

COMPARISON RESULTS: $\varepsilon_r = 2.0$, *Noiseless*

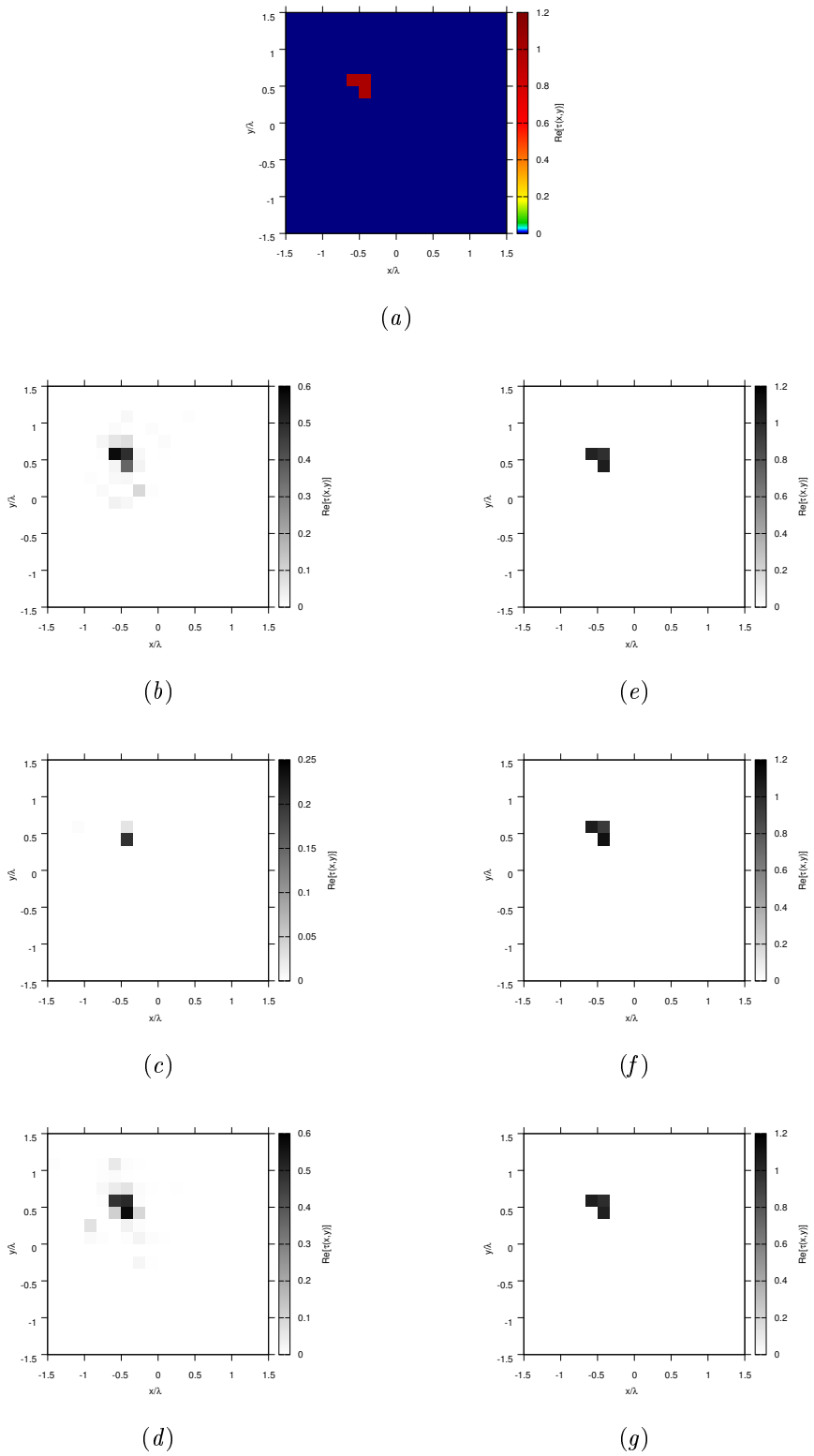

(a) (b) (e) (c) (f) (d) (g)

Figure 166. *Noiseless* case: Actual object (a) and BCS reconstructed object for (b) X-ST-BCS, (c) Y-ST-BCS, (d) ST-BCS, (e) MV-X-MT-BCS, (f) MV-Y-MT-BCS and (g) MV-MT-BCS.

COMPARISON RESULTS: $\varepsilon_r = 2.0, \quad SNR = 20dB$

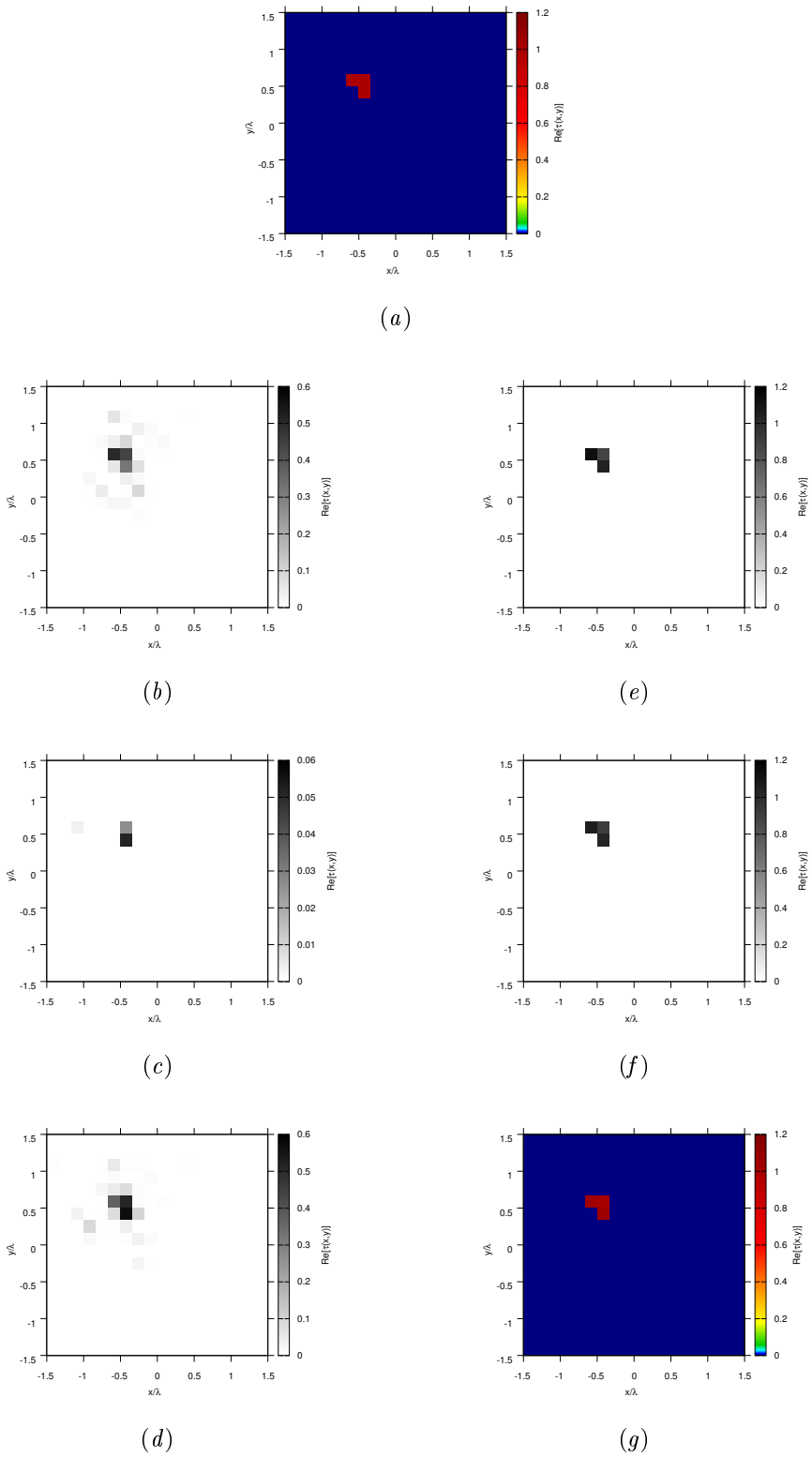

Figure 167. $SNR = 20dB$ case: Actual object (a) and BCS reconstructed object for (b) X-ST-BCS, (c) Y-ST-BCS, (d) ST-BCS, (e) MV-X-MT-BCS, (f) MV-Y-MT-BCS and (g) MV-MT-BCS.

COMPARISON RESULTS: $\varepsilon_r = 2.0, \quad SNR = 10dB$

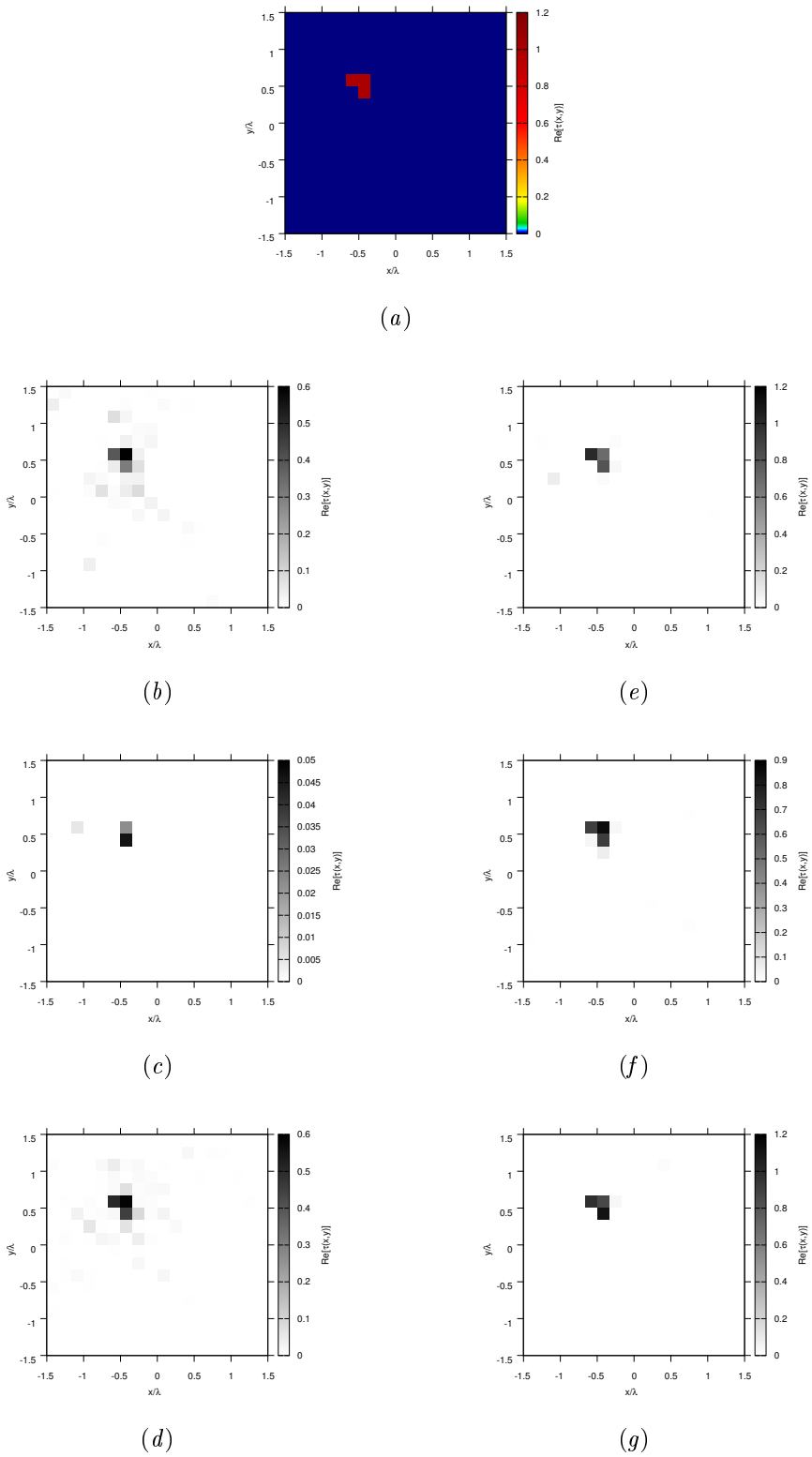

Figure 168. $SNR = 10dB$ case: Actual object (a) and BCS reconstructed object for (b) X-ST-BCS, (c) Y-ST-BCS, (d) ST-BCS, (e) MV-X-MT-BCS, (f) MV-Y-MT-BCS and (g) MV-MT-BCS.

COMPARISON RESULTS: $\varepsilon_r = 2.0, \quad SNR = 5dB$

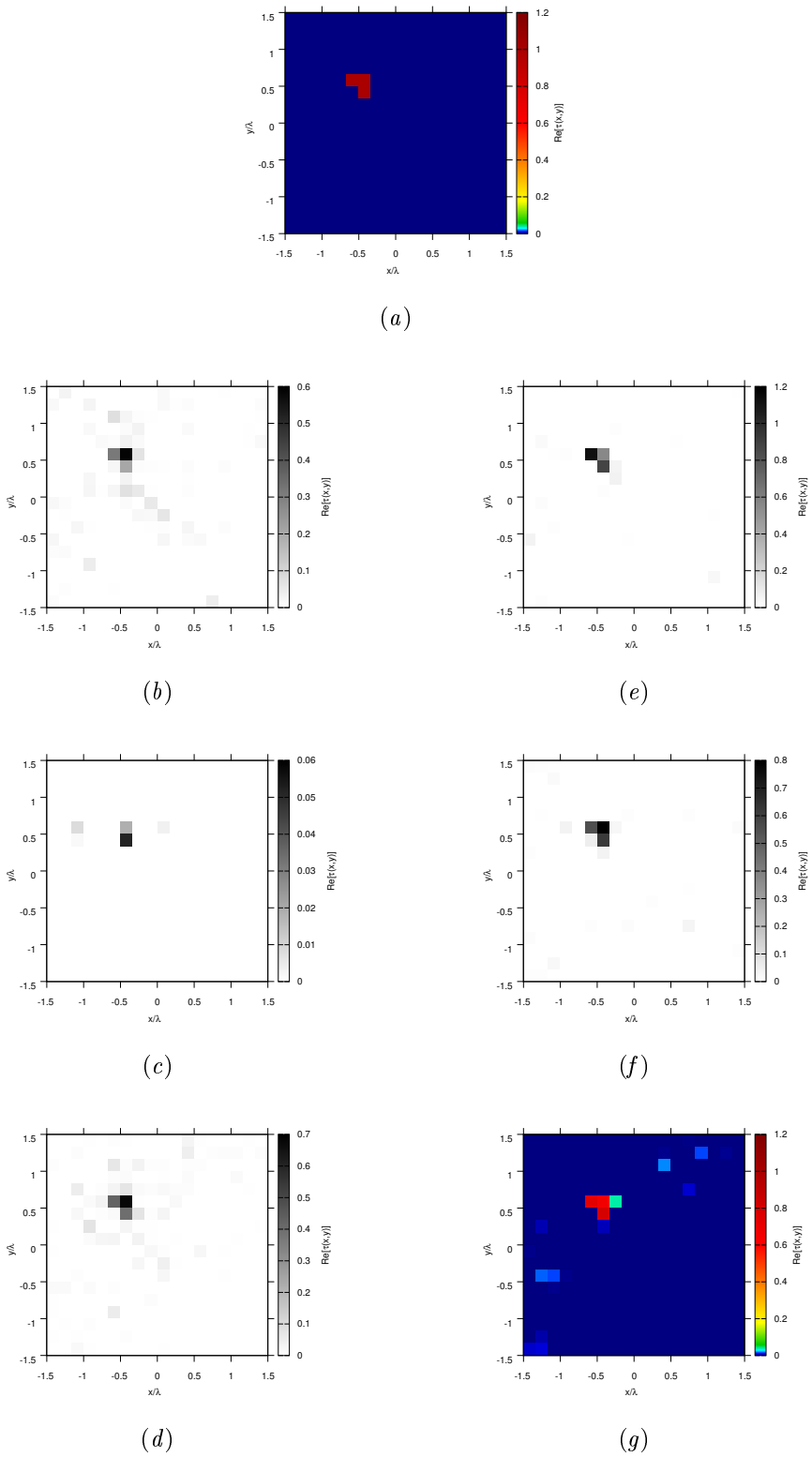

(a) (b) (e) (c) (f) (d) (g)

Figure 169. $SNR = 5dB$ case: Actual object (a) and BCS reconstructed object for (b) X-ST-BCS, (c) Y-ST-BCS, (d) ST-BCS, (e) MV-X-MT-BCS, (f) MV-Y-MT-BCS and (g) MV-MT-BCS.

COMPARISON RESULTS: Total Error ξ_{tot}

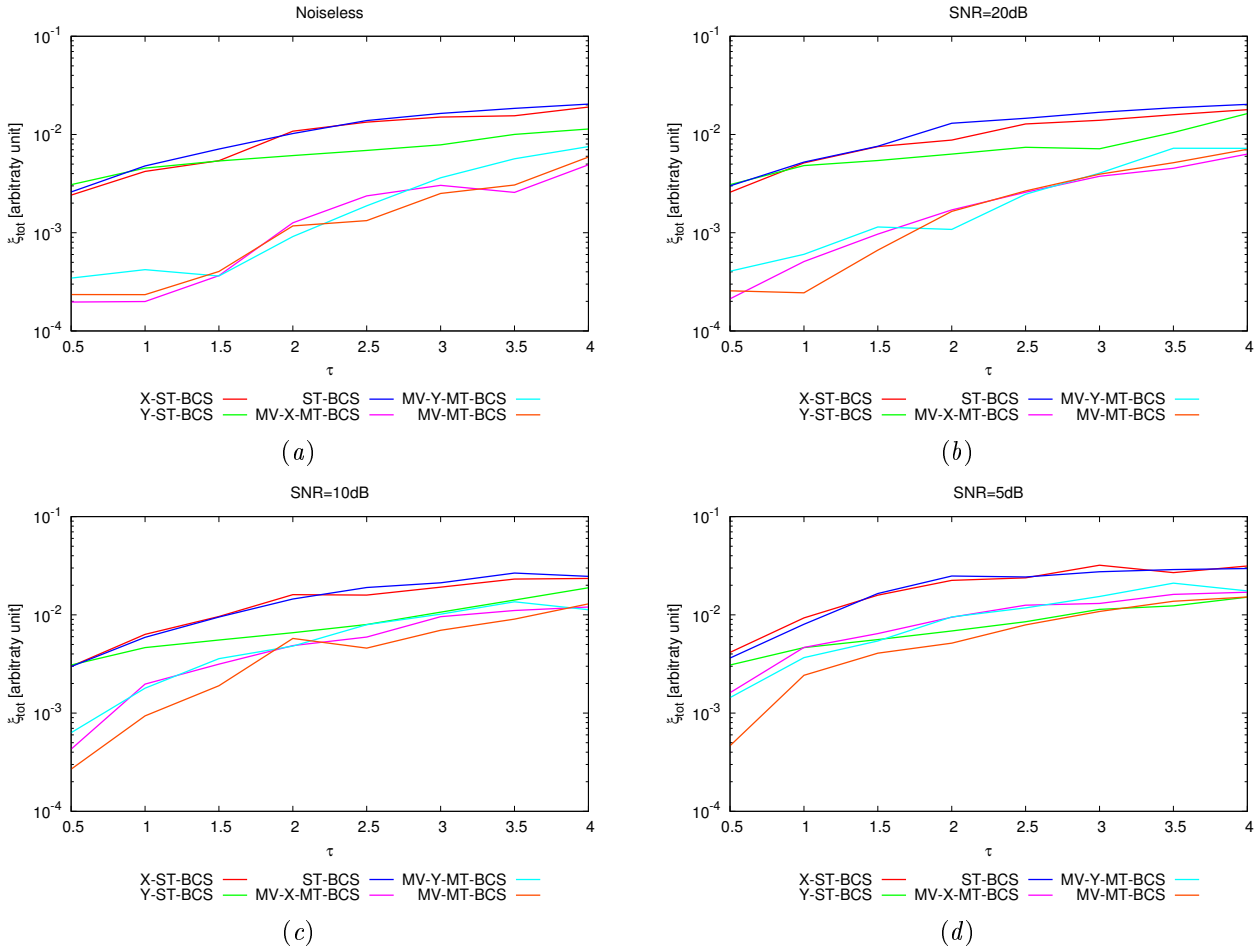

Figure 170. Behaviour of the total error ξ_{tot} as a function of ε_r, for different SNR values: (a) Noiseless case, (b) $SNR = 20$ [dB] , (c) $SNR = 10$ [dB] and (d) $SNR = 5$ [dB].

COMPARISON RESULTS: Internal Error ξ_{int}

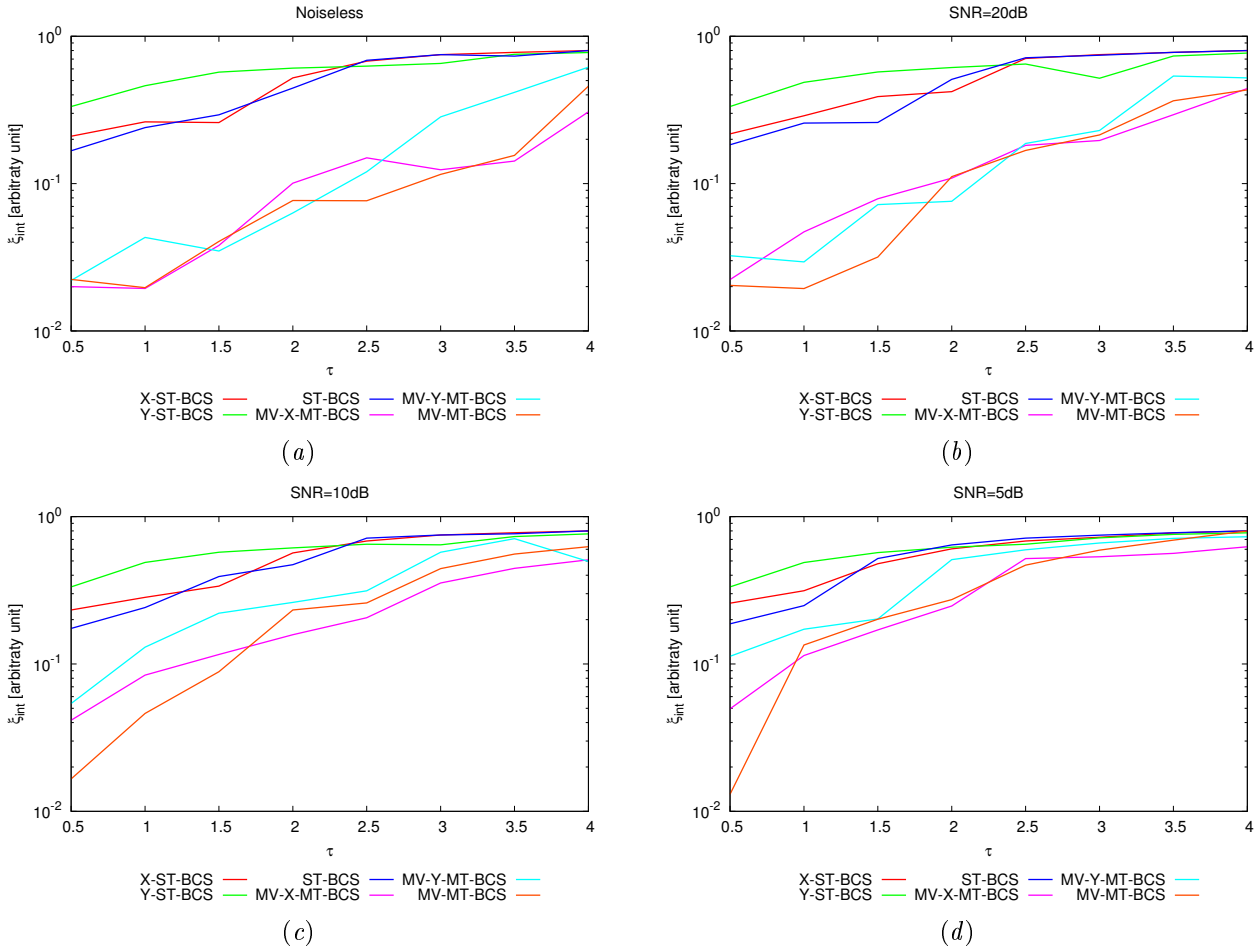

Figure 171. Behaviour of the internal error ξ_{int} as a function of ε_r, for different SNR values: (a) Noiseless case, (b) $SNR = 20$ [dB] , (c) $SNR = 10$ [dB] and (d) $SNR = 5$ [dB].

COMPARISON RESULTS: External Error ξ_{ext}

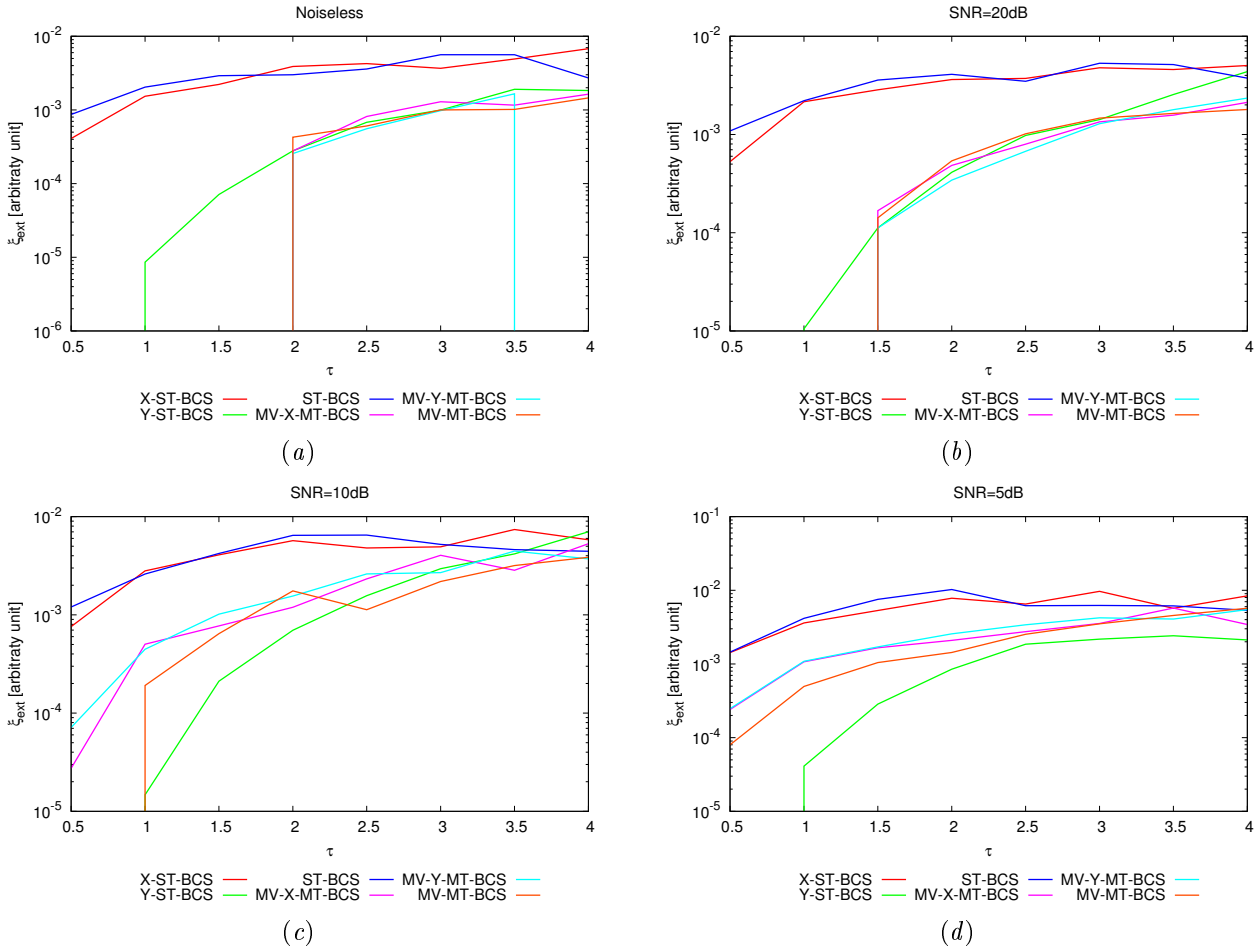

Figure 172. Behaviour of the external error ξ_{ext} as a function of ε_r, for different SNR values: (a) Noiseless case, (b) $SNR = 20$ [dB] , (c) $SNR = 10$ [dB] and (d) $SNR = 5$ [dB].

TEST CASE: Two Square Cylinders $L = 0.33\lambda$

Goal: show the performances of BCS when dealing with a sparse scatterer

- Number of Views: V
- Number of Measurements: M
- Number of Cells for the Inversion: N
- Number of Cells for the Direct solver: D
- Side of the investigation domain: L

Test Case Description

Direct solver:

- Square domain divided in $\sqrt{D} \times \sqrt{D}$ cells
- Domain side: $L = 3\lambda$
- $D = 1296$ (discretization for the direct solver: $< \lambda/10$)

Investigation domain:

- Square domain divided in $\sqrt{N} \times \sqrt{N}$ cells
- $L = 3\lambda$
- $2ka = 2 \times \frac{2\pi}{\lambda} \times \frac{L\sqrt{2}}{2} = 6\pi\sqrt{2} = 26.65$
- $\#DOF = \frac{(2ka)^2}{2} = \frac{(2 \times \frac{2\pi}{\lambda} \times \frac{L\sqrt{2}}{2})^2}{2} = 4\pi^2 \left(\frac{L}{\lambda}\right)^2 = 4\pi^2 \times 9 \approx 355.3$
- N scelto in modo da essere vicino a $\#DOF$: $N = 324$ (18×18)

Measurement domain:

- Measurement points taken on a circle of radius $\rho = 3\lambda$
- Full-aspect measurements
- $M \approx 2ka \rightarrow M = 27$

Sources:

- Plane waves
- $V \approx 2ka \rightarrow V = 27$
- Amplitude: $A = 1$
- Frequency: 300 MHz $(\lambda = 1)$

Object:

- Two square cylinders of side $\frac{\lambda}{3} = 0.3333$
- $\varepsilon_r \in \{1.5, 2.0, 2.5, 3.0, 3.5, 4.0, 4.5, 5.0\}$ (one square)
- $\sigma = 0$ [S/m]

BCS parameters:

- Convergenze parameter: $\tau = 1.0 \times 10^{-8}$

COMPARISON RESULTS: $\varepsilon_r = 2.0$, *Noiseless*

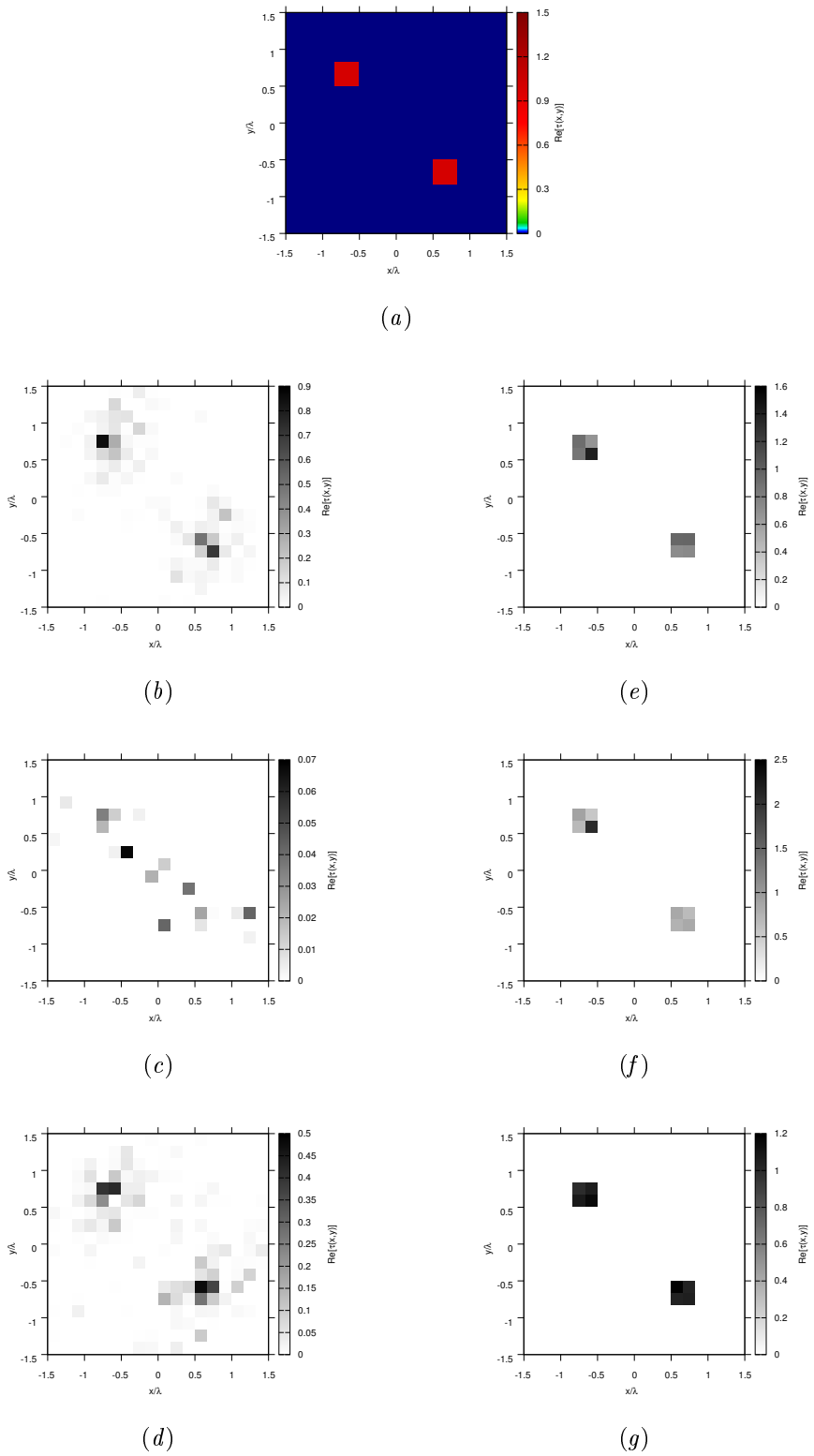

(a) (b) (e) (c) (f) (d) (g)

Figure 173. *Noiseless* case: Actual object (a) and BCS reconstructed object for (b) X-ST-BCS, (c) Y-ST-BCS, (d) ST-BCS, (e) MV-X-MT-BCS, (f) MV-Y-MT-BCS and (g) MV-MT-BCS.

COMPARISON RESULTS: $\varepsilon_r = 2.0, \quad SNR = 20dB$

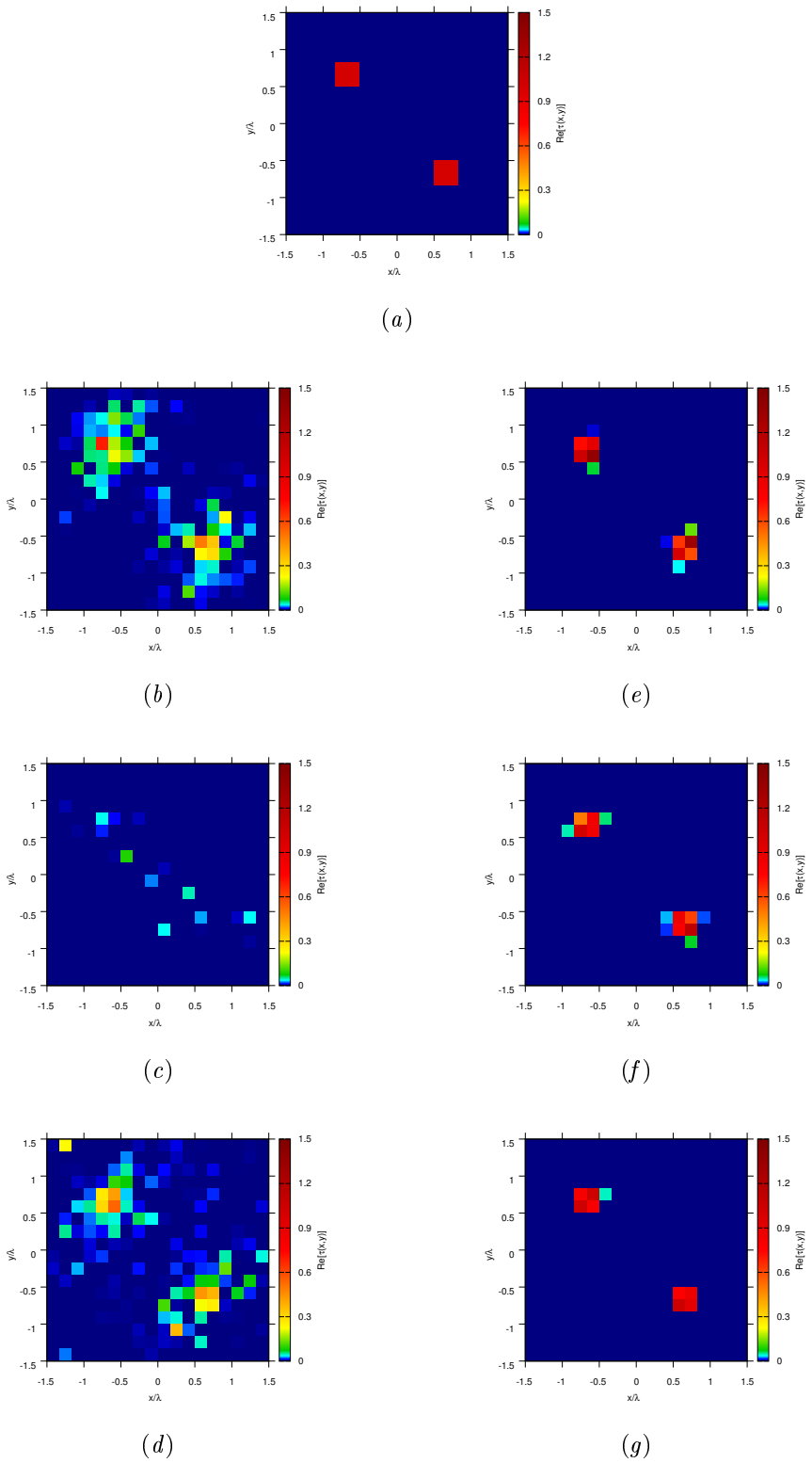

Figure 174. $SNR = 20dB$ case: Actual object (a) and BCS reconstructed object for (b) X-ST-BCS, (c) Y-ST-BCS, (d) ST-BCS, (e) MV-X-MT-BCS, (f) MV-Y-MT-BCS and (g) MV-MT-BCS.

COMPARISON RESULTS: $\varepsilon_r = 2.0, \quad SNR = 10dB$

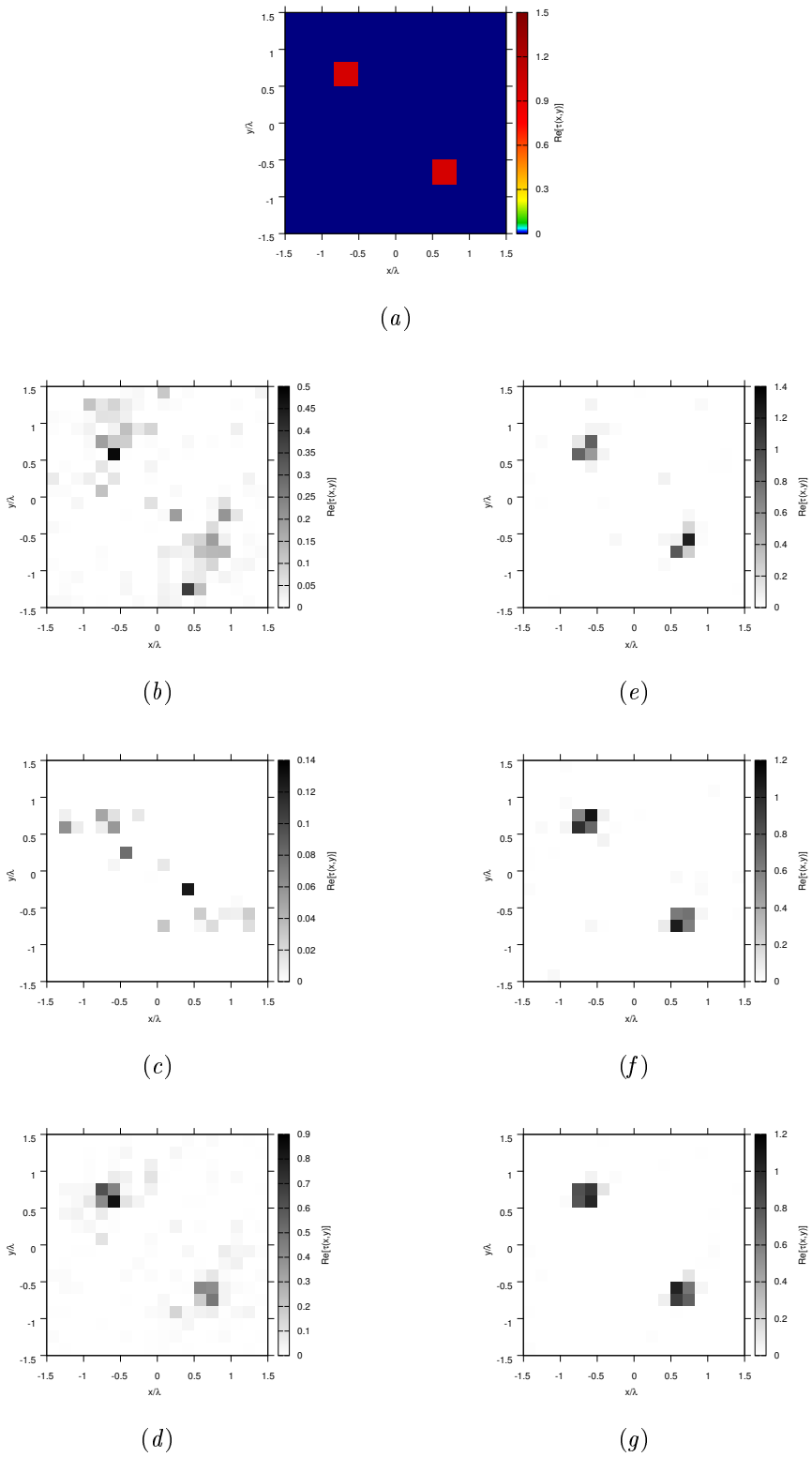

Figure 175. $SNR = 10dB$ case: Actual object (a) and BCS reconstructed object for (b) X-ST-BCS, (c) Y-ST-BCS, (d) ST-BCS, (e) MV-X-MT-BCS, (f) MV-Y-MT-BCS and (g) MV-MT-BCS.

COMPARISON RESULTS: $\varepsilon_r = 2.0, \quad SNR = 5dB$

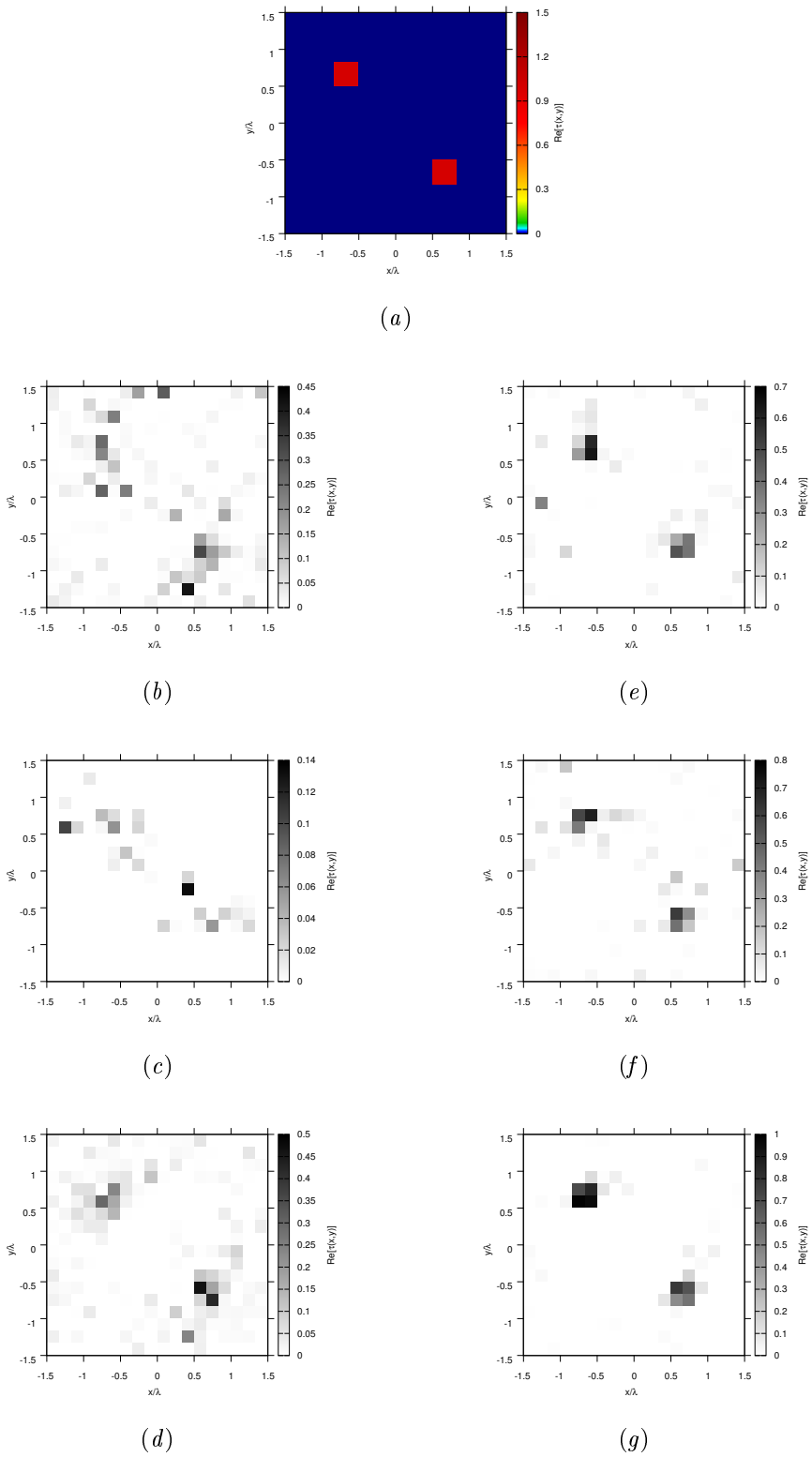

(a) (b) (e) (c) (f) (d) (g)

Figure 176. $SNR = 5dB$ case: Actual object (a) and BCS reconstructed object for (b) X-ST-BCS, (c) Y-ST-BCS, (d) ST-BCS, (e) MV-X-MT-BCS, (f) MV-Y-MT-BCS and (g) MV-MT-BCS.

COMPARISON RESULTS: Total Error ξ_{tot}

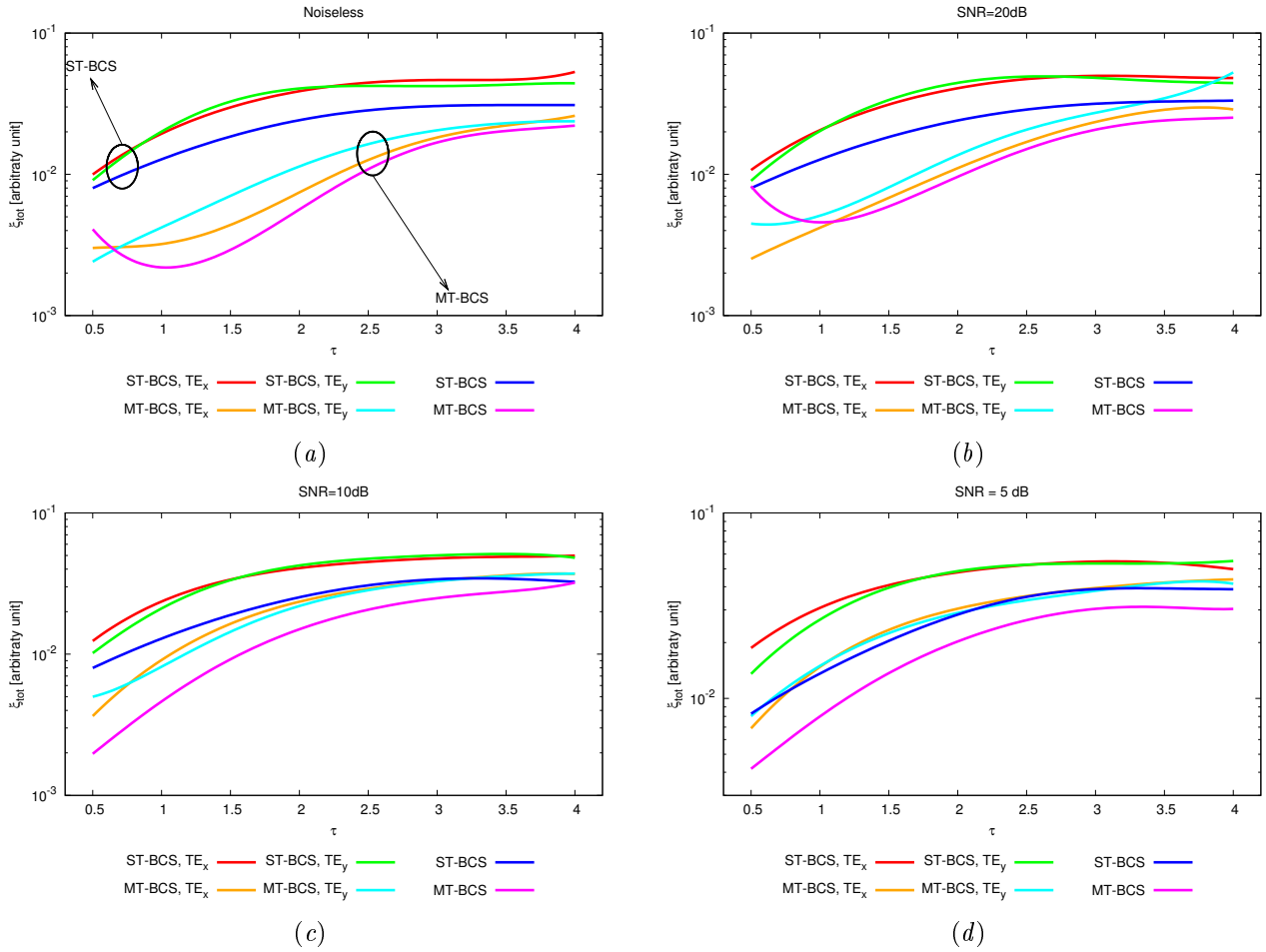

Figure 177. Behaviour of the total error ξ_{tot} as a function of ε_r, for different SNR values: (a) Noiseless case, (b) $SNR = 20$ [dB] , (c) $SNR = 10$ [dB] and (d) $SNR = 5$ [dB].

COMPARISON RESULTS: Internal Error ξ_{int}

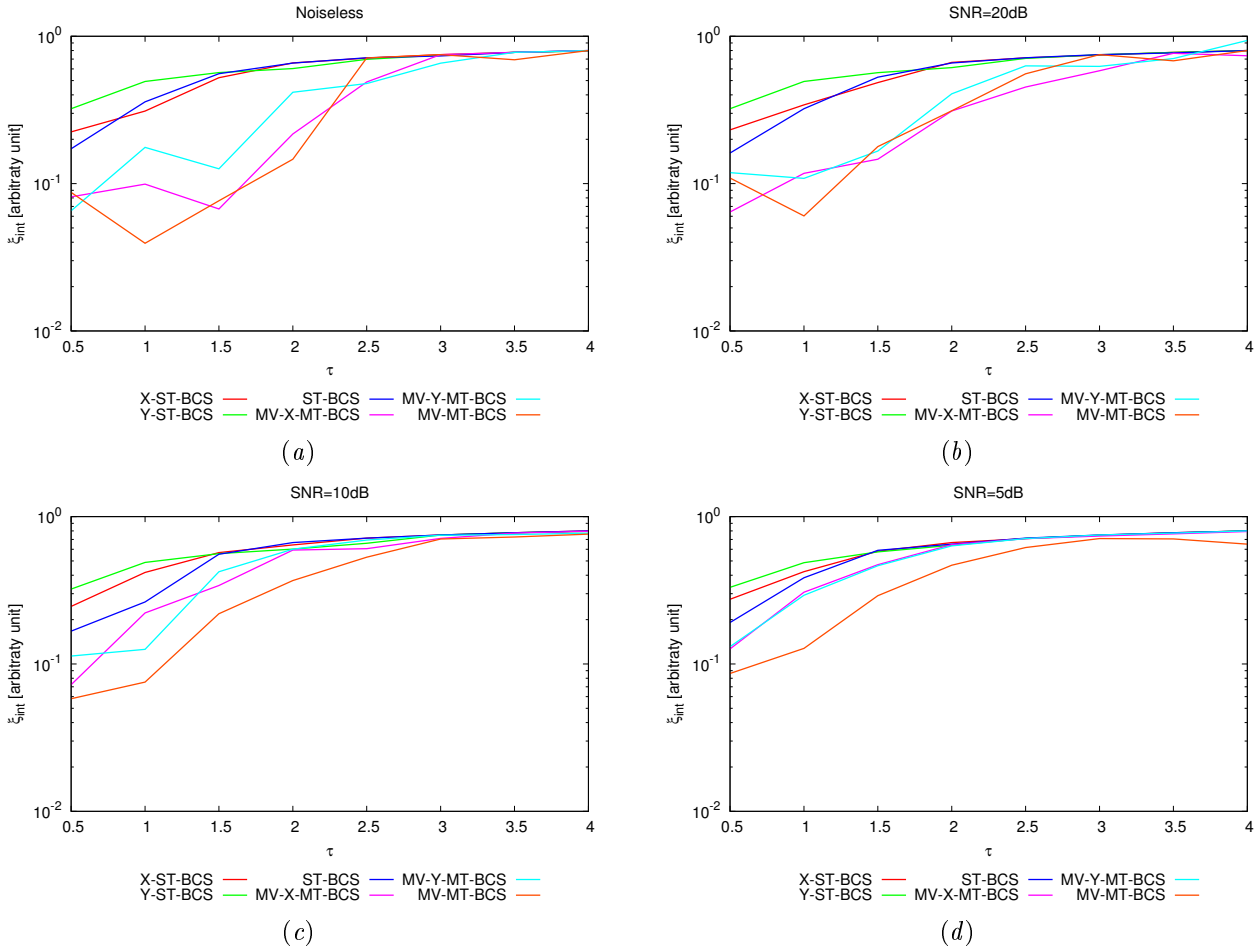

Figure 178. Behaviour of the internal error ξ_{int} as a function of ε_r, for different SNR values: (a) Noiseless case, (b) $SNR = 20$ [dB] , (c) $SNR = 10$ [dB] and (d) $SNR = 5$ [dB].

COMPARISON RESULTS: External Error ξ_{ext}

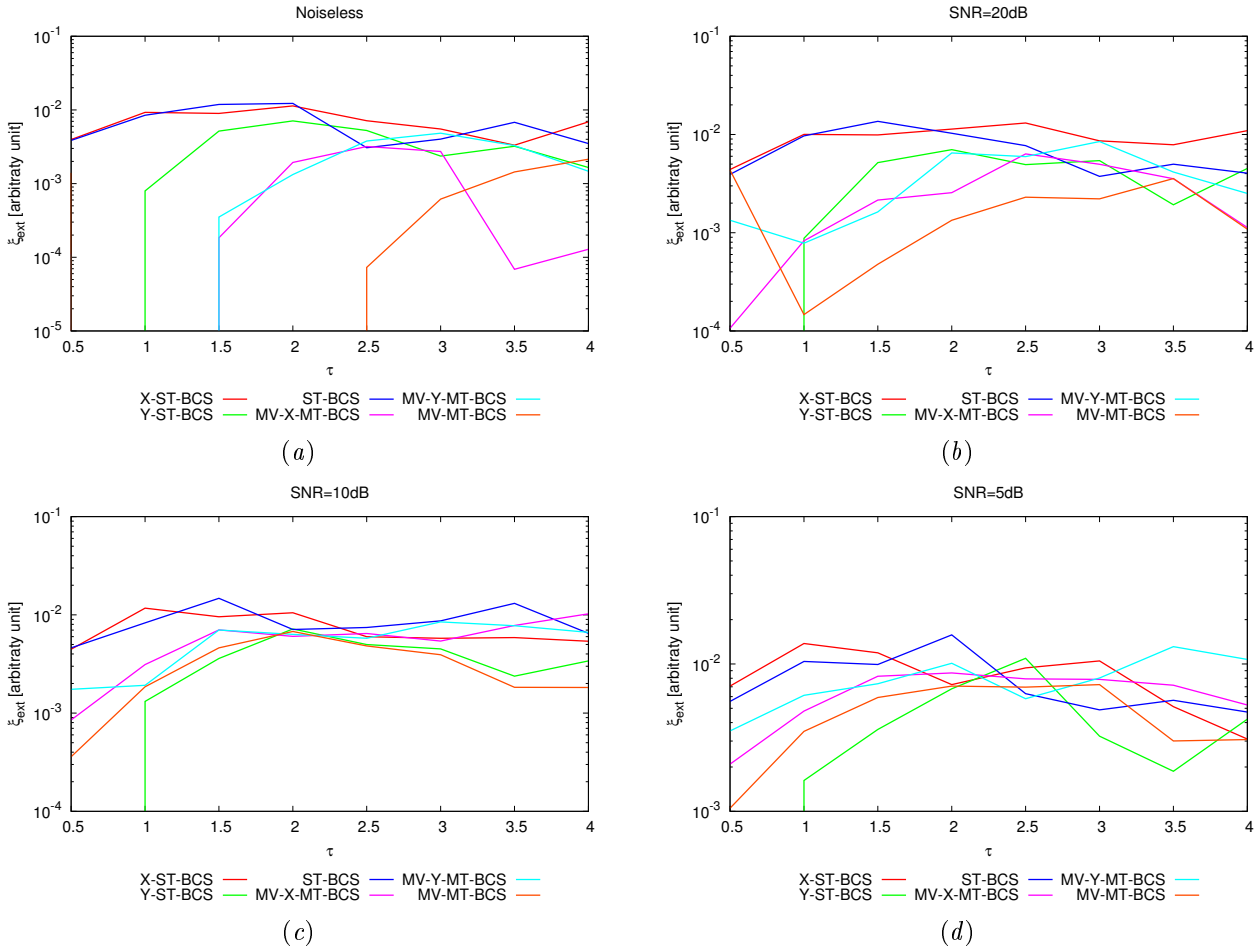

Figure 179. Behaviour of the external error ξ_{ext} as a function of ε_r, for different SNR values: (a) Noiseless case, (b) $SNR = 20$ [dB] , (c) $SNR = 10$ [dB] and (d) $SNR = 5$ [dB].

7 Comparison between BCS techniques

7.1 Basic Tests

TEST CASE: Square Cylinder $L = 0.16\lambda$

COMPARISON: Total Error ξ_{tot}

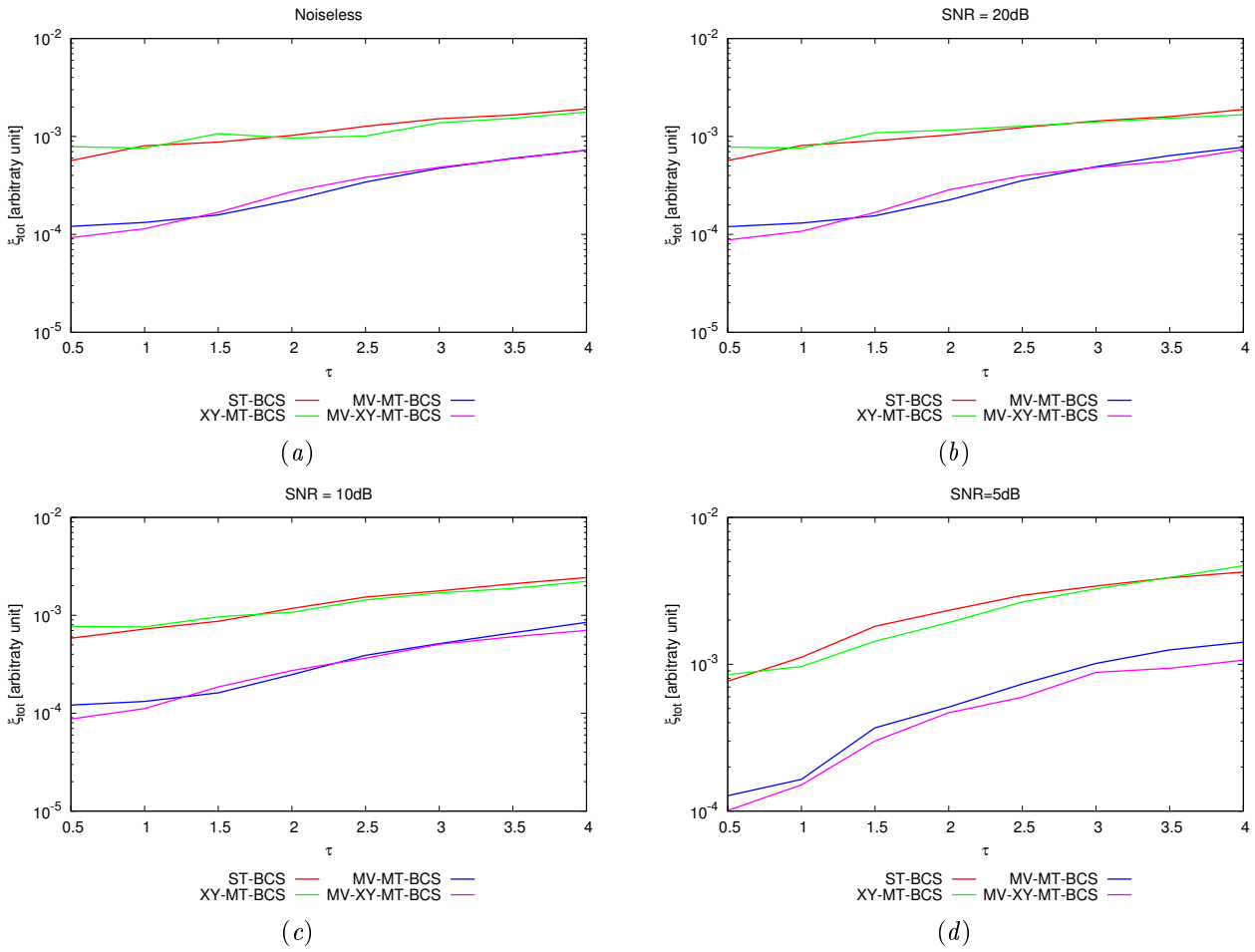

Figure 180. Behaviour of the total error ξ_{tot} as a function of ε_r: comparison between the techniques ST-BCS, XY-MT-BCS, MV-XY-BCS and MV-XY-MT-BCS for different SNR values: (a) Noiseless case, (b) $SNR = 20$ [dB] , (c) $SNR = 10$ [dB] and (d) $SNR = 5$ [dB].

COMPARISON: Internal Error ξ_{int}

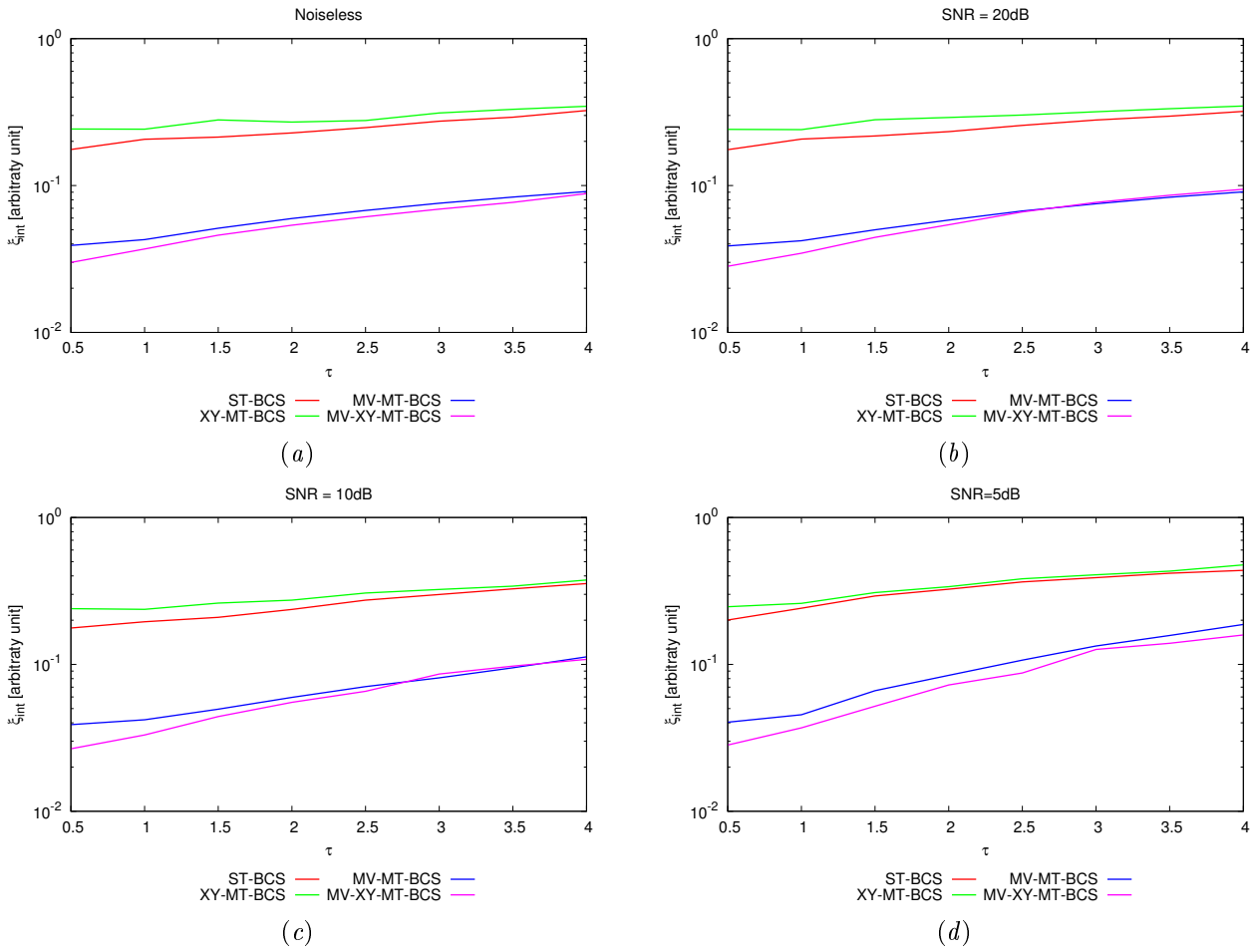

Figure 181. Behaviour of the total error ξ_{int} as a function of ε_r: comparison between the techniques ST-BCS, XY-MT-BCS, MV-XY-BCS and MV-XY-MT-BCS.

COMPARISON: External Error ξ_{ext}

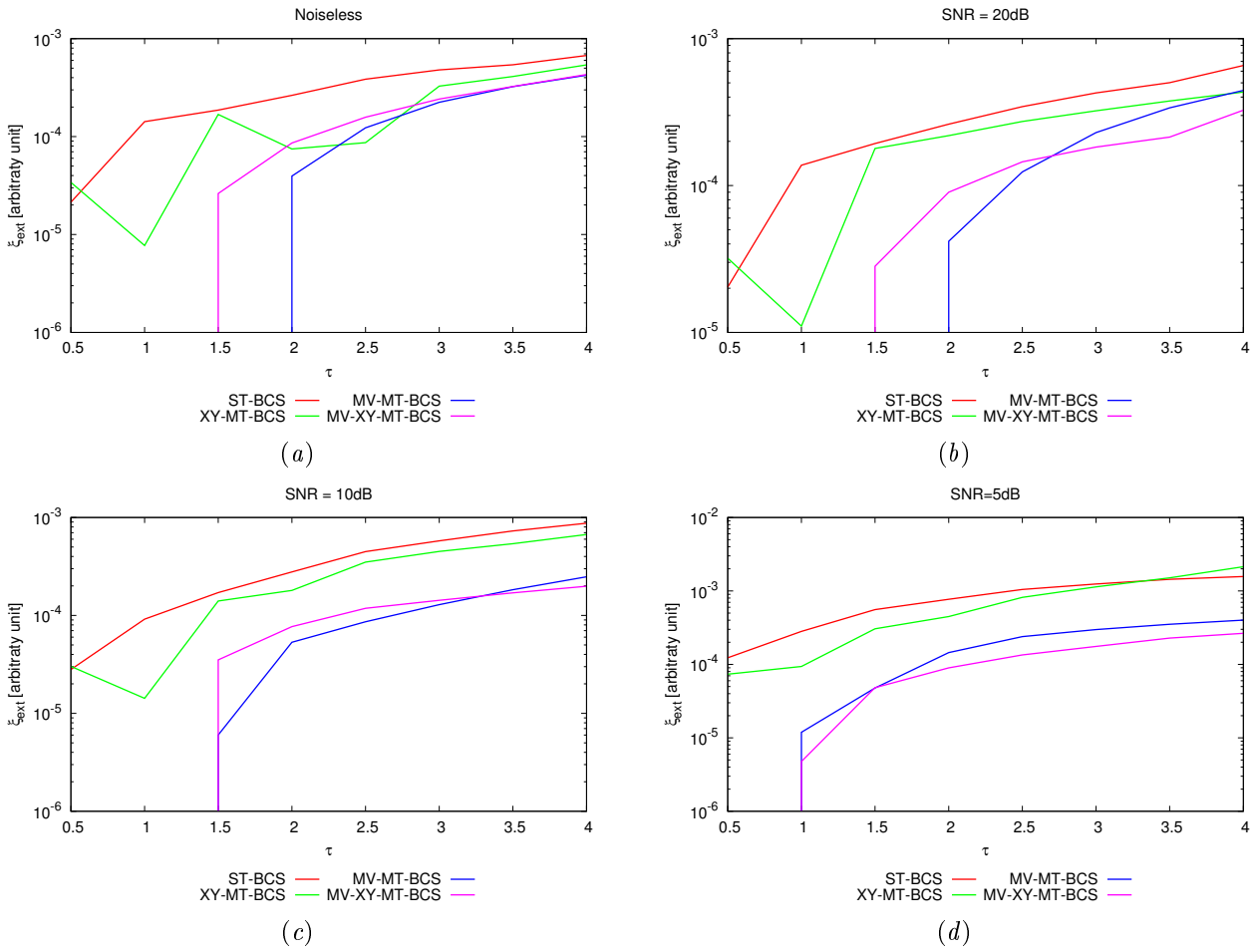

Figure 182. Behaviour of the total error ξ_{ext} as a function of ε_r: comparison between the techniques ST-BCS, XY-MT-BCS, MV-XY-BCS and MV-XY-MT-BCS.

TEST CASE: Two Square Cylinders $L = 0.16\lambda$

COMPARISON: Total Error ξ_{tot}

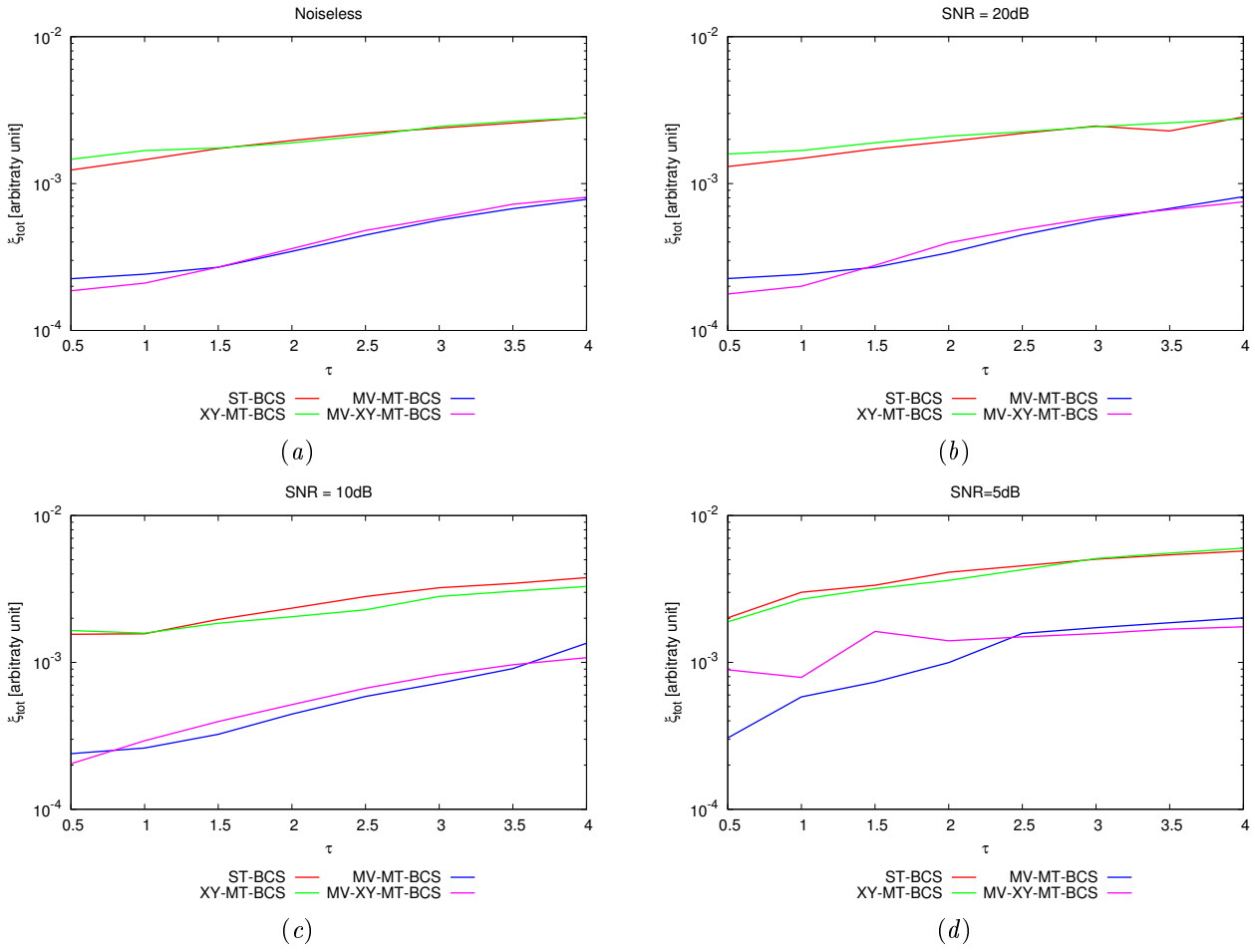

Figure 183. Behaviour of the total error ξ_{tot} as a function of ε_r: comparison between the techniques ST-BCS, XY-MT-BCS, MV-XY-BCS and MV-XY-MT-BCS.

TEST CASE: Square Cylinders $L = 0.33\lambda$

COMPARISON: Total Error ξ_{tot}

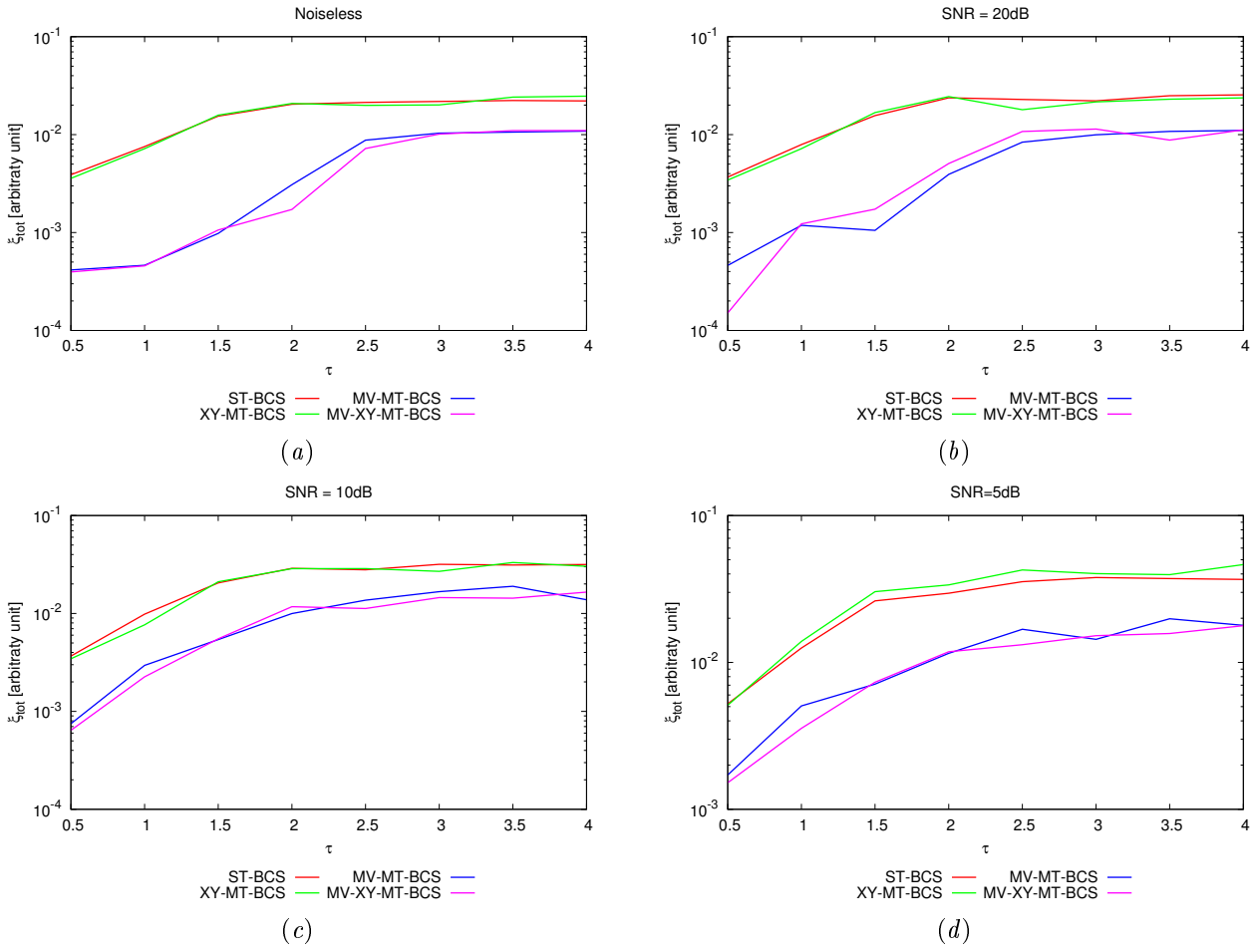

Figure 184. Behaviour of the total error ξ_{tot} as a function of ε_r: comparison between the techniques ST-BCS, XY-MT-BCS, MV-XY-BCS and MV-XY-MT-BCS.

TEST CASE: L-Shaped Cylinder

COMPARISON: Total Error ξ_{tot}

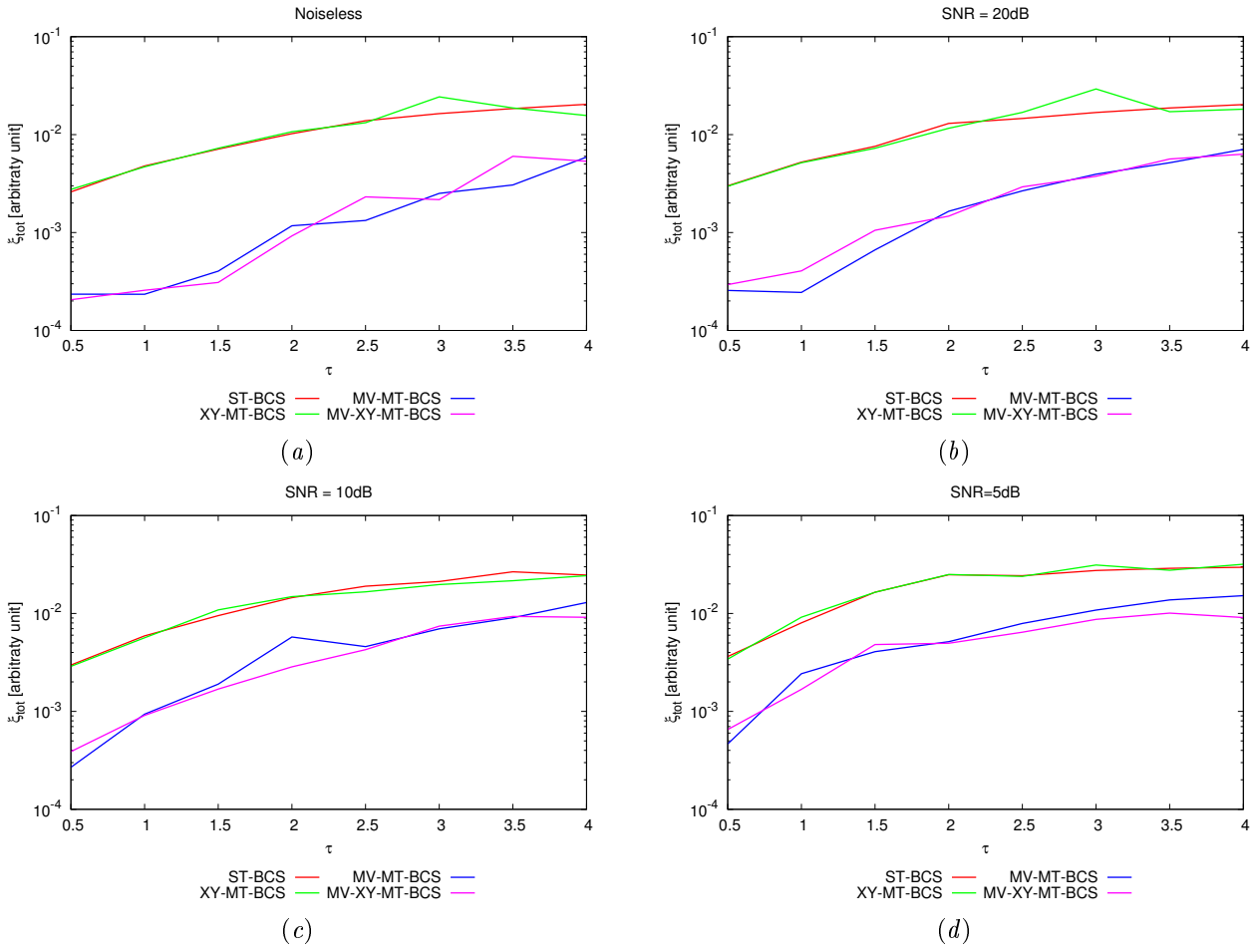

Figure 185. Behaviour of the total error ξ_{tot} as a function of ε_r: comparison between the techniques ST-BCS, XY-MT-BCS, MV-XY-BCS and MV-XY-MT-BCS.

TEST CASE: Inhomogeneous L-Shaped Cylinder

COMPARISON: Total Error ξ_{tot}

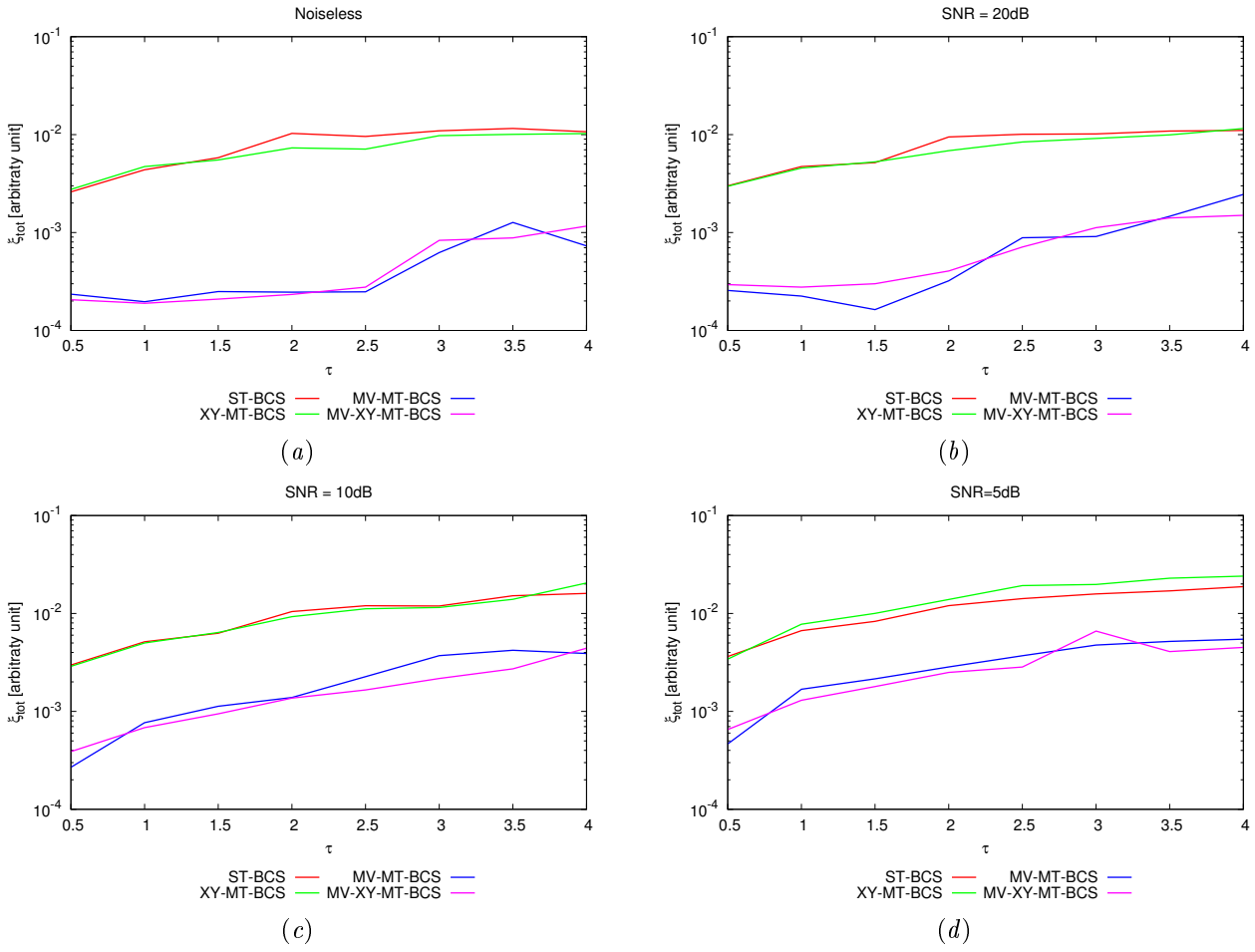

Figure 186. Behaviour of the total error ξ_{tot} as a function of ε_r: comparison between the techniques ST-BCS, XY-MT-BCS, MV-XY-BCS and MV-XY-MT-BCS.

TEST CASE: Cross-Shaped Cylinder

COMPARISON: Total Error ξ_{tot}

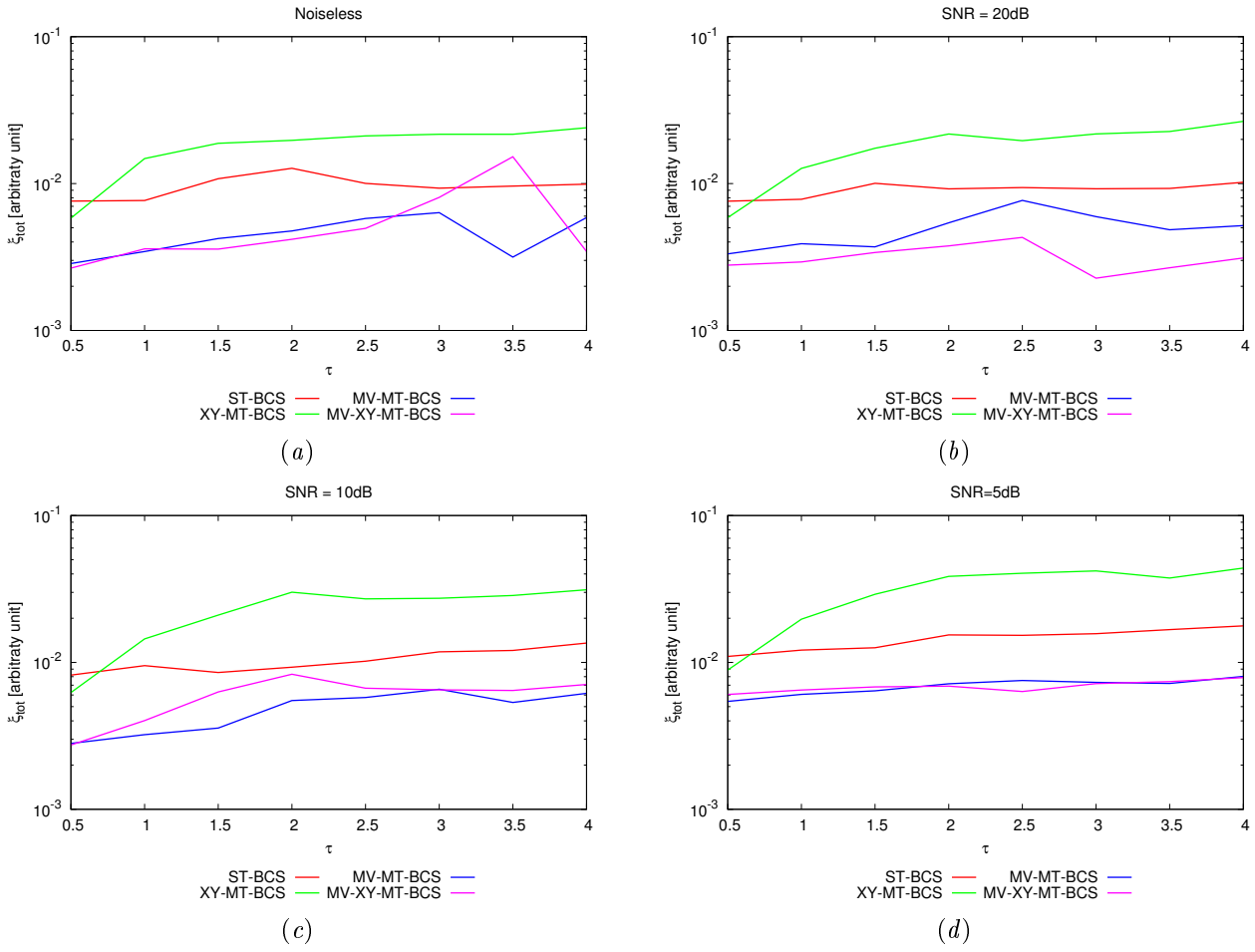

Figure 187. Behaviour of the total error ξ_{tot} as a function of ε_r: comparison between the techniques ST-BCS, XY-MT-BCS, MV-XY-BCS and MV-XY-MT-BCS.

TEST CASE: Line-Shaped Cylinder

COMPARISON: Total Error ξ_{tot}

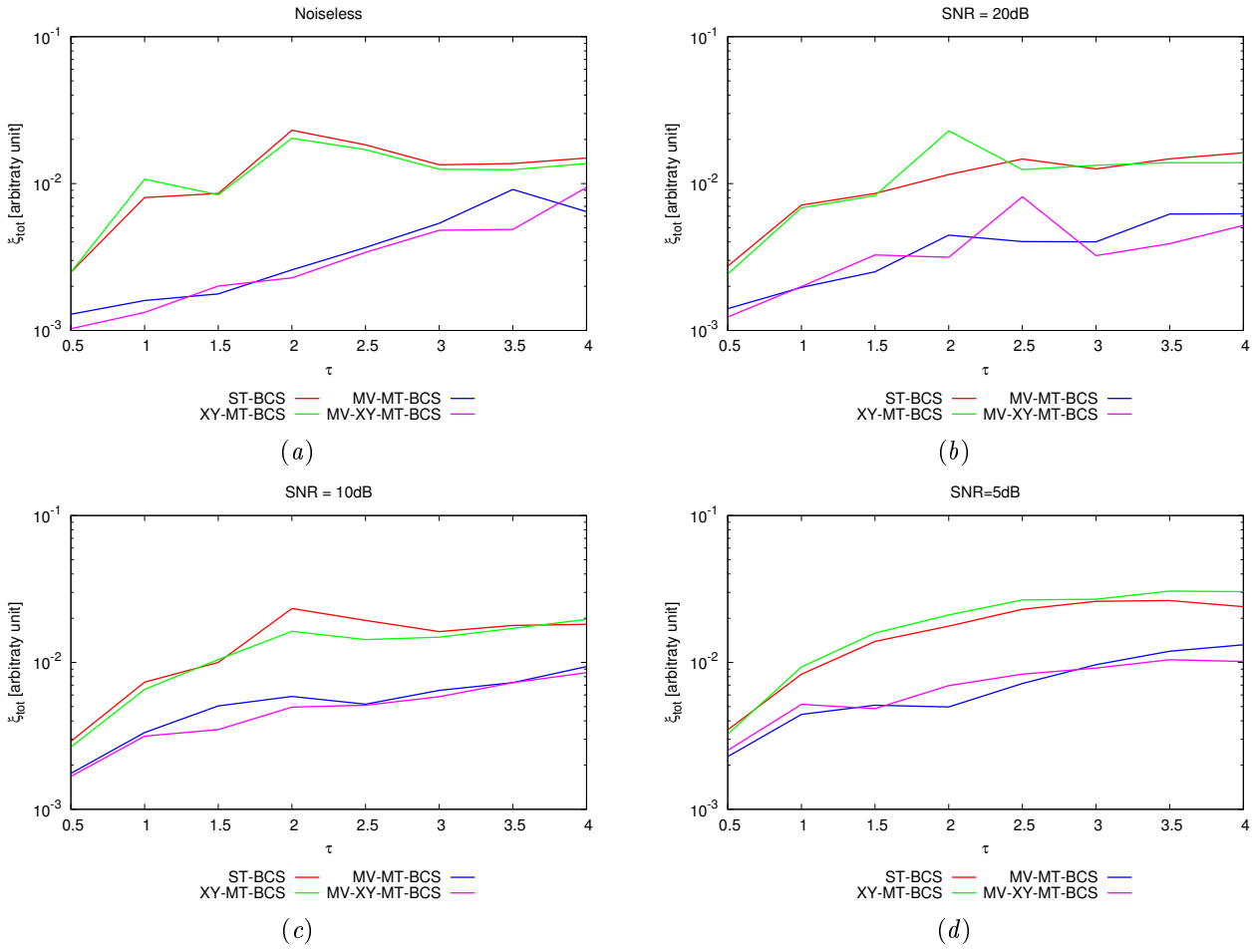

Figure 188. Behaviour of the total error ξ_{tot} as a function of ε_r: comparison between the techniques ST-BCS, XY-MT-BCS, MV-XY-BCS and MV-XY-MT-BCS.

7.2 Advanced Tests

TEST CASE: Big L-Shaped Cylinder

COMPARISON: Total Error ξ_{tot}

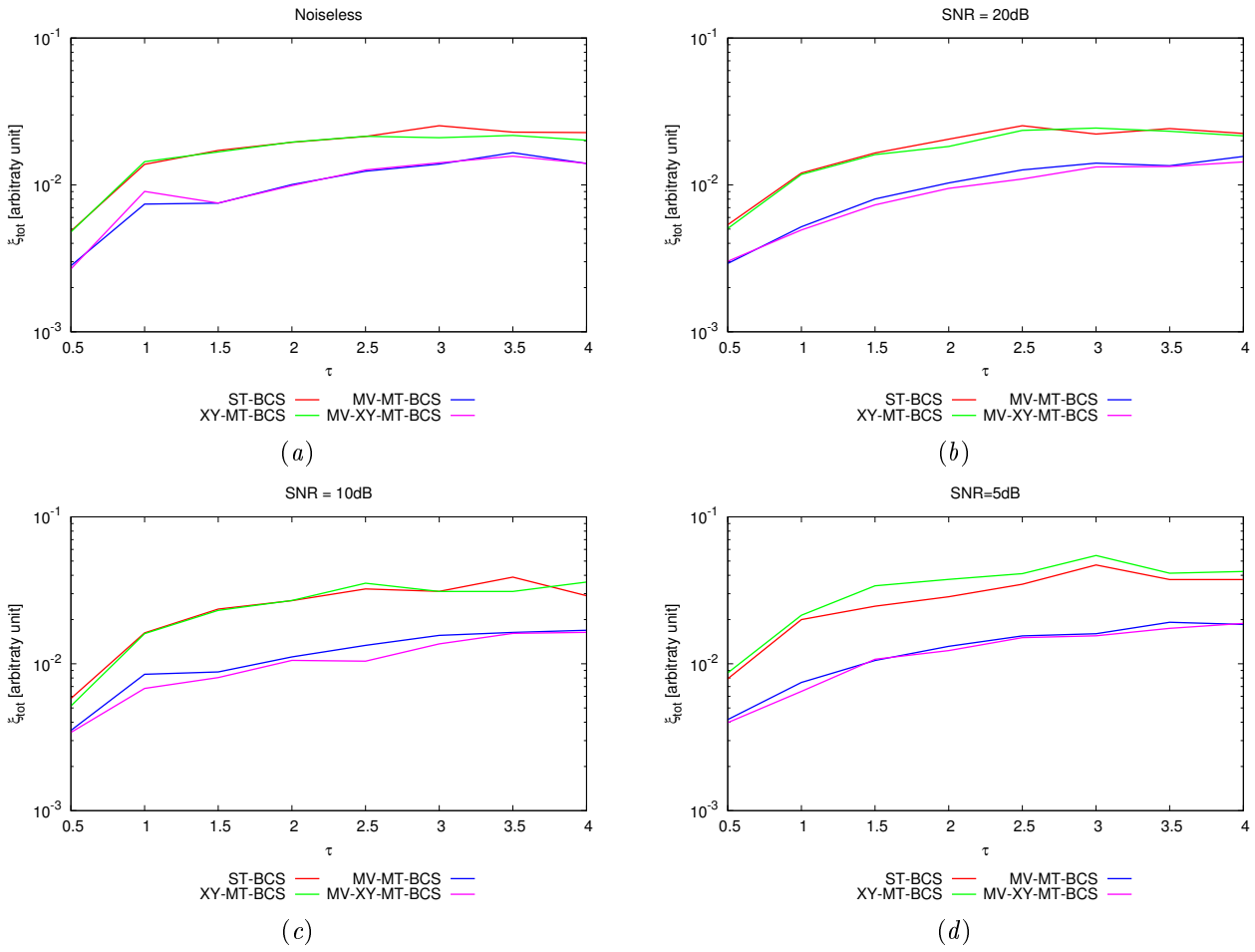

Figure 189. Behaviour of the total error ξ_{tot} as a function of ε_r: comparison between the techniques ST-BCS, XY-MT-BCS, MV-XY-BCS and MV-XY-MT-BCS.

TEST CASE: Big T-Shaped Cylinder

COMPARISON: Total Error ξ_{tot}

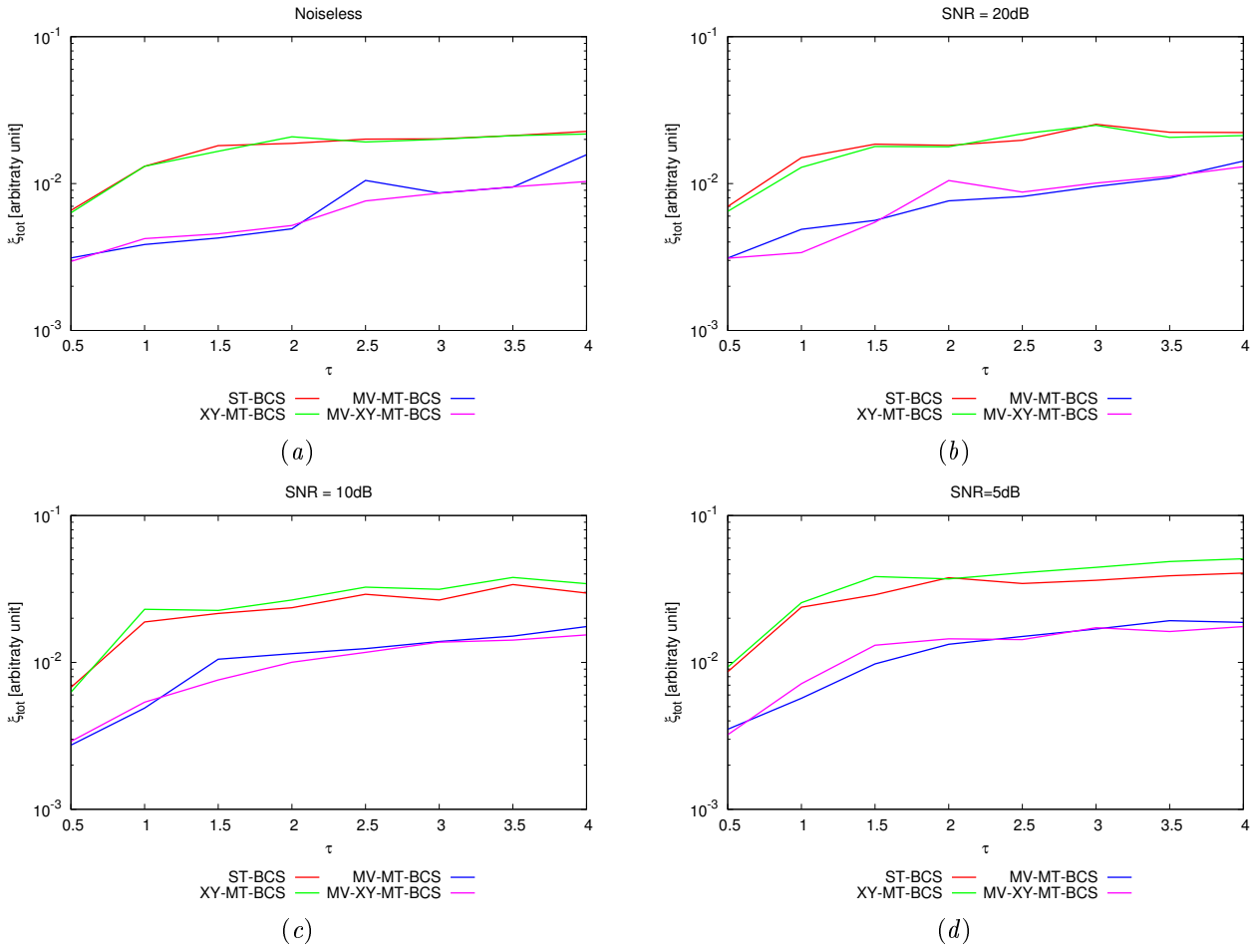

Figure 190. Behaviour of the total error ξ_{tot} as a function of ε_r: comparison between the techniques ST-BCS, XY-MT-BCS, MV-XY-BCS and MV-XY-MT-BCS.

TEST CASE: Hollow Square Cylinder

COMPARISON: Total Error ξ_{tot}

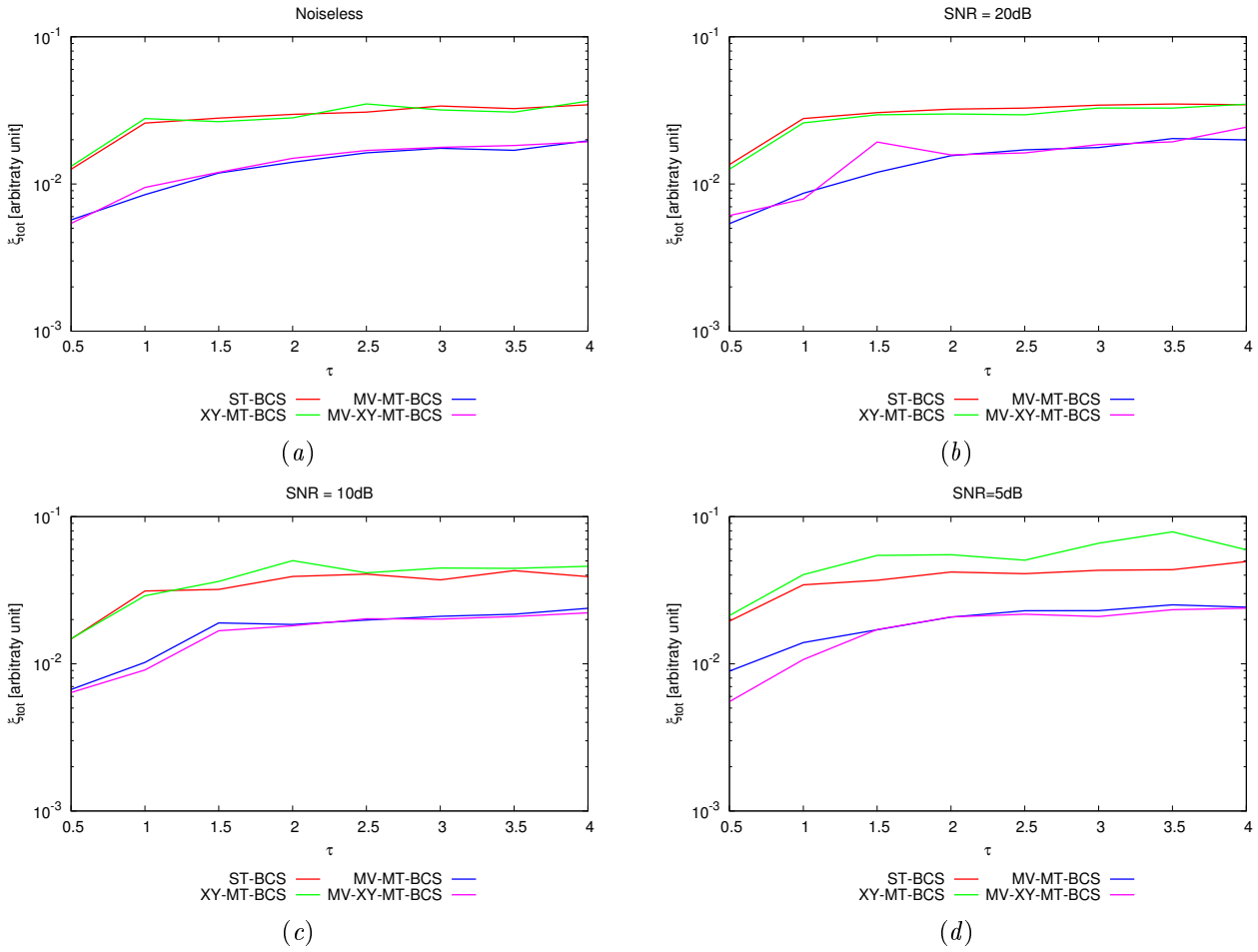

Figure 191. Behaviour of the total error ξ_{tot} as a function of ε_r: comparison between the techniques ST-BCS, XY-MT-BCS, MV-XY-BCS and MV-XY-MT-BCS.

7.3 Test Varying the Number of Views

TEST CASE: L-Shaped Cylinder

Goal: show the performances of BCS when dealing with a sparse scatterer

- Number of Views: V
- Number of Measurements: M
- Number of Cells for the Inversion: N
- Number of Cells for the Direct solver: D
- Side of the investigation domain: L

Test Case Description

Direct solver:

- Square domain divided in $\sqrt{D} \times \sqrt{D}$ cells
- Domain side: $L = 3\lambda$
- $D = 1296$ (discretization for the direct solver: $< \lambda/10$)

Investigation domain:

- Square domain divided in $\sqrt{N} \times \sqrt{N}$ cells
- $L = 3\lambda$
- $2ka = 2 \times \frac{2\pi}{\lambda} \times \frac{L\sqrt{2}}{2} = 6\pi\sqrt{2} = 26.65$
- $\#DOF = \frac{(2ka)^2}{2} = \frac{(2 \times \frac{2\pi}{\lambda} \times \frac{L\sqrt{2}}{2})^2}{2} = 4\pi^2 \left(\frac{L}{\lambda}\right)^2 = 4\pi^2 \times 9 \approx 355.3$
- N scelto in modo da essere vicino a $\#DOF$: $N = 324$ (18×18)

Measurement domain:

- Measurement points taken on a circle of radius $\rho = 3\lambda$
- Full-aspect measurements
- $M \approx 2ka \rightarrow M = 27$

Sources:

- Plane waves
- $V \in \{2, 3, 4, 5, 6, 7, 8, 9, 10, 11, 12, 13, 14, 15, 16, 17, 18, 19, 20, 21, 22, 23, 24, 25, 26, 27\}$
- Amplitude: $A = 1$
- Frequency: 300 MHz $(\lambda = 1)$

Object:

- L-shaped cylinder
- $\varepsilon_r = 2.0$
- $\sigma = 0$ [S/m]

RESULTS: Error Figures - *Noiseless*

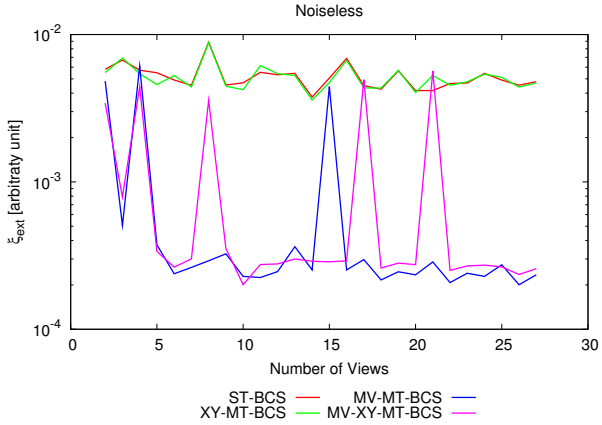

(a)

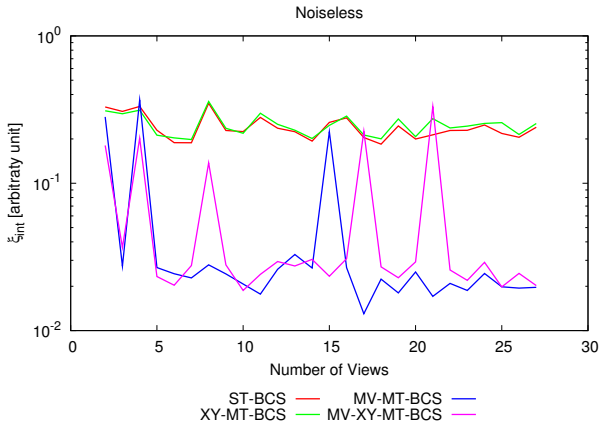

(b)

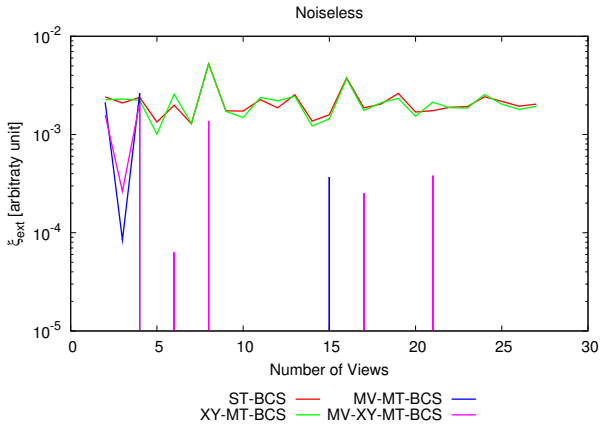

(c)

Figure 192. Behaviour of error figures as a function of the number of views V: (a) total error ξ_{tot}, (b) internal error ξ_{int}, (c) external error ξ_{ext}.

RESULTS: Error Figures - $SNR = 20$ [dB]

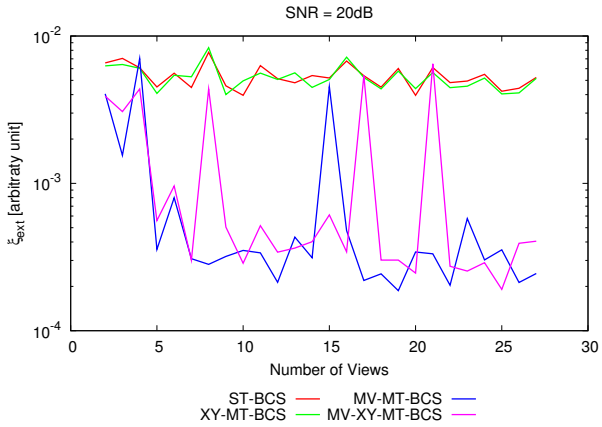

(a)

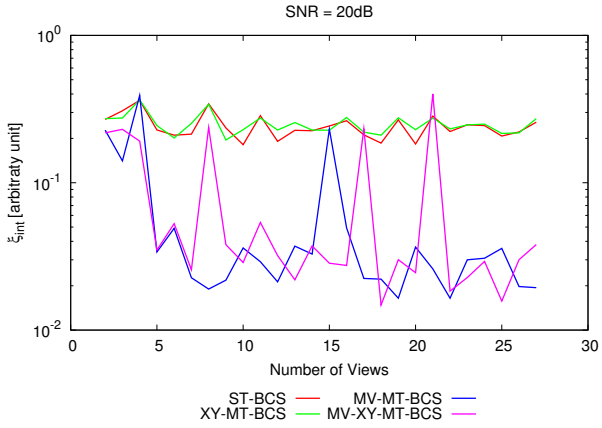

(b)

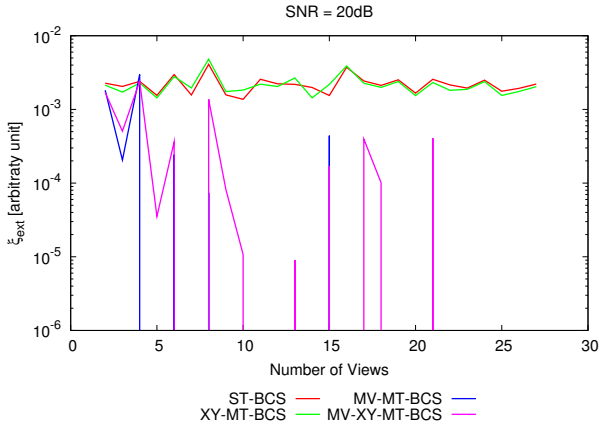

(c)

Figure 193. Behaviour of error figures as a function of the number of views V: (a) total error ξ_{tot}, (b) internal error ξ_{int}, (c) external error ξ_{ext}.

RESULTS: Error Figures - $SNR = 10$ [dB]

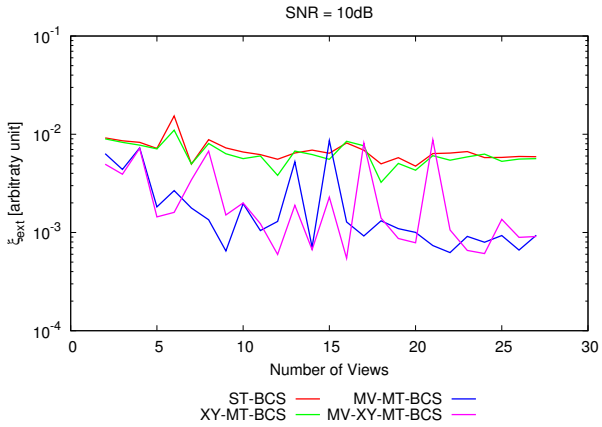

(a)

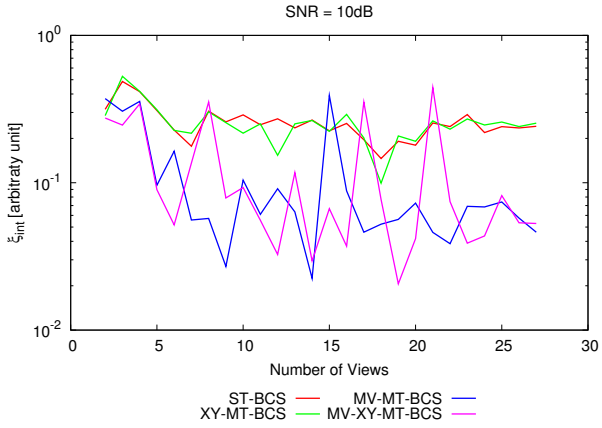

(b)

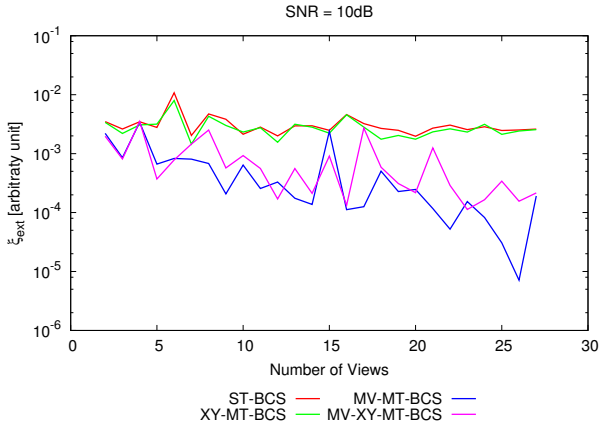

(c)

Figure 194. Behaviour of error figures as a function of the number of views V: (a) total error ξ_{tot}, (b) internal error ξ_{int}, (c) external error ξ_{ext}.

RESULTS: Error Figures - $SNR = 5$ [dB]

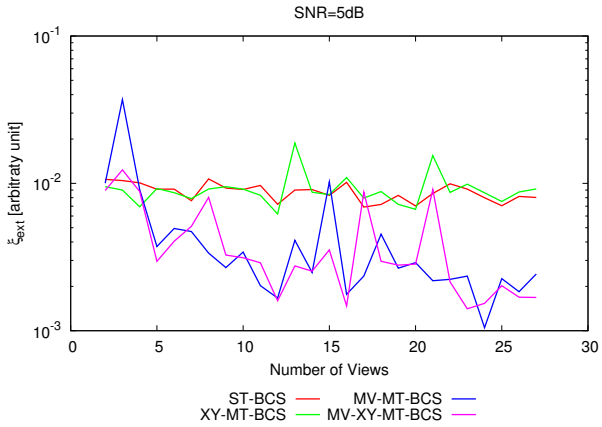

(a)

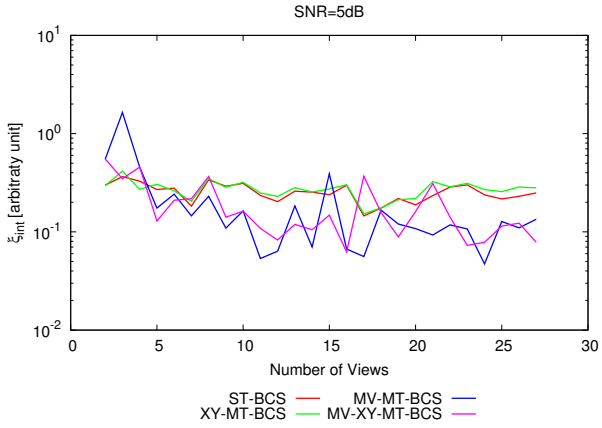

(b)

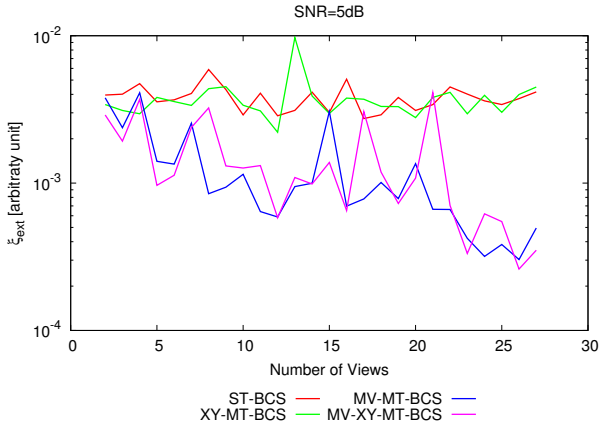

(c)

Figure 195. Behaviour of error figures as a function of the number of views V: (a) total error ξ_{tot}, (b) internal error ξ_{int}, (c) external error ξ_{ext}.

7.4 Test Varying the Number of Measurement Points

TEST CASE: L-Shaped Cylinder

Goal: show the performances of BCS when dealing with a sparse scatterer

- Number of Views: V
- Number of Measurements: M
- Number of Cells for the Inversion: N
- Number of Cells for the Direct solver: D
- Side of the investigation domain: L

Test Case Description

Direct solver:

- Square domain divided in $\sqrt{D} \times \sqrt{D}$ cells
- Domain side: $L = 3\lambda$
- $D = 1296$ (discretization for the direct solver: $< \lambda/10$)

Investigation domain:

- Square domain divided in $\sqrt{N} \times \sqrt{N}$ cells
- $L = 3\lambda$
- $2ka = 2 \times \frac{2\pi}{\lambda} \times \frac{L\sqrt{2}}{2} = 6\pi\sqrt{2} = 26.65$
- $\#DOF = \frac{(2ka)^2}{2} = \frac{(2 \times \frac{2\pi}{\lambda} \times \frac{L\sqrt{2}}{2})^2}{2} = 4\pi^2 \left(\frac{L}{\lambda}\right)^2 = 4\pi^2 \times 9 \approx 355.3$
- N scelto in modo da essere vicino a $\#DOF$: $N = 324$ (18×18)

Measurement domain:

- Measurement points taken on a circle of radius $\rho = 3\lambda$
- Full-aspect measurements
- $M \in \{2, 3, 4, 5, 6, 7, 8, 9, 10, 11, 12, 13, 14, 15, 16, 17, 18, 19, 20, 21, 22, 23, 24, 25, 26, 27\}$

Sources:

- Plane waves
- $V \approx 2ka \rightarrow V = 27$
- Amplitude: $A = 1$
- Frequency: 300 MHz $(\lambda = 1)$

Object:

- L-shaped cylinder
- $\varepsilon_r = 2.0$
- $\sigma = 0$ [S/m]

RESULTS: Error Figures - *Noiseless*

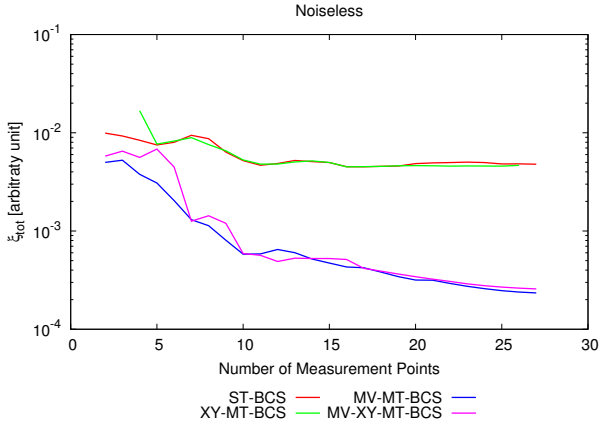

(a)

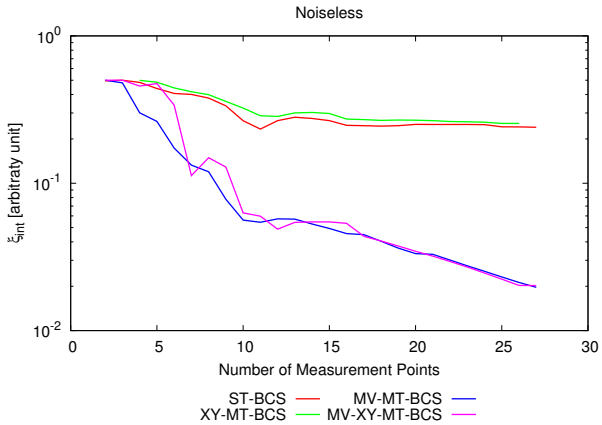

(b)

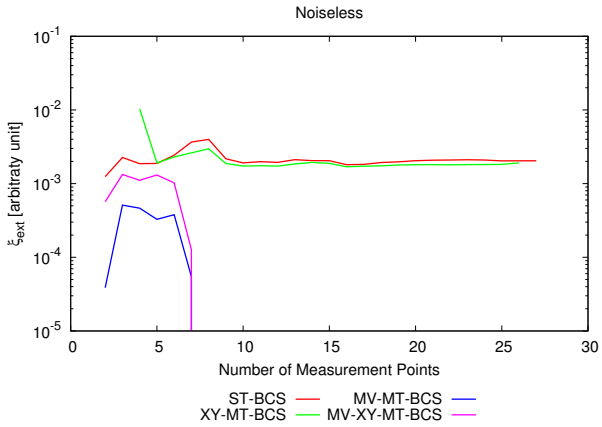

(c)

Figure 196. Behaviour of error figures as a function of the number of measurement points M: (a) total error ξ_{tot}, (b) internal error ξ_{int}, (c) external error ξ_{ext}.

RESULTS: Error Figures - $SNR = 20$ [dB]

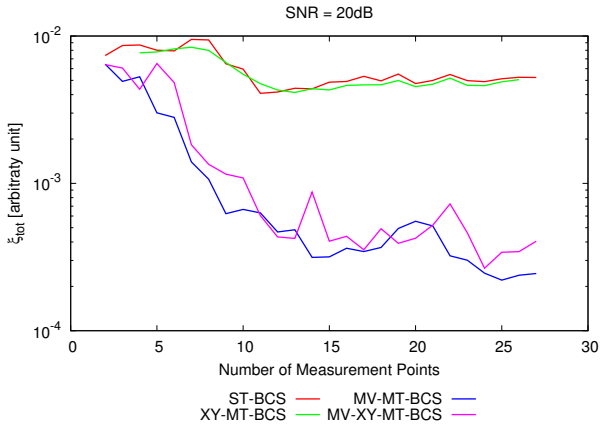

(a)

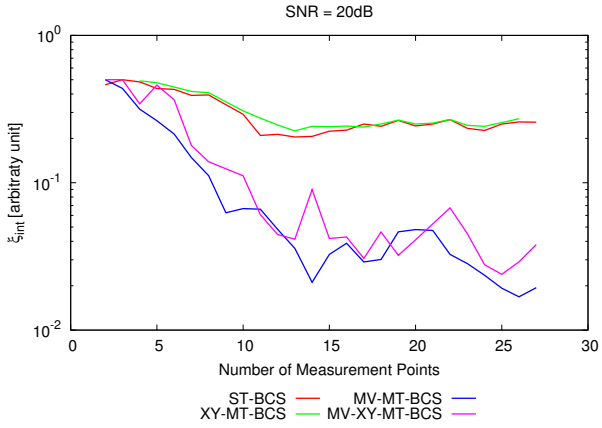

(b)

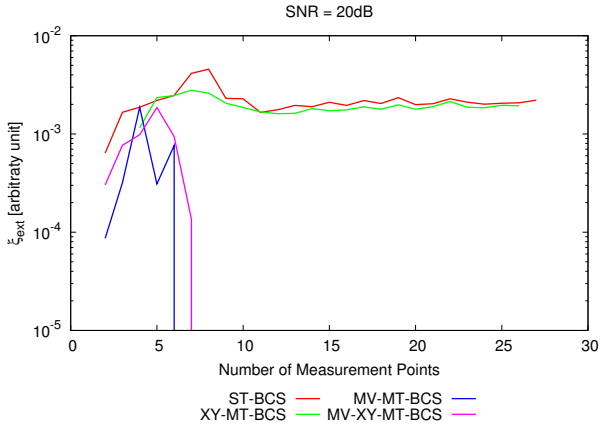

(c)

Figure 197. Behaviour of error figures as a function of the number of measurement points M: (a) total error ξ_{tot}, (b) internal error ξ_{int}, (c) external error ξ_{ext}.

RESULTS: Error Figures - $SNR = 10$ [dB]

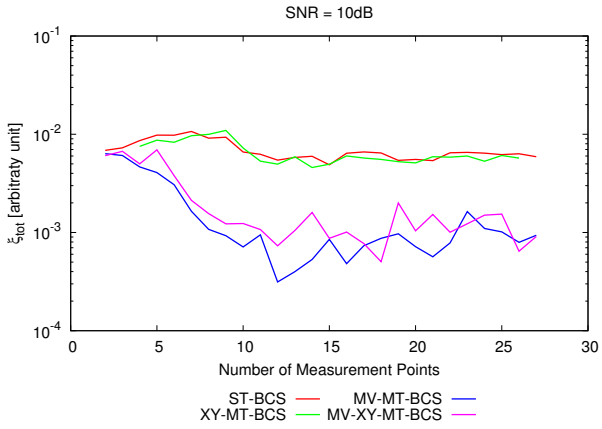

(a)

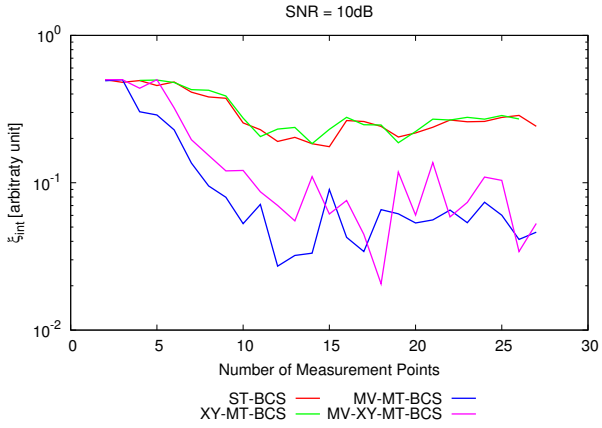

(b)

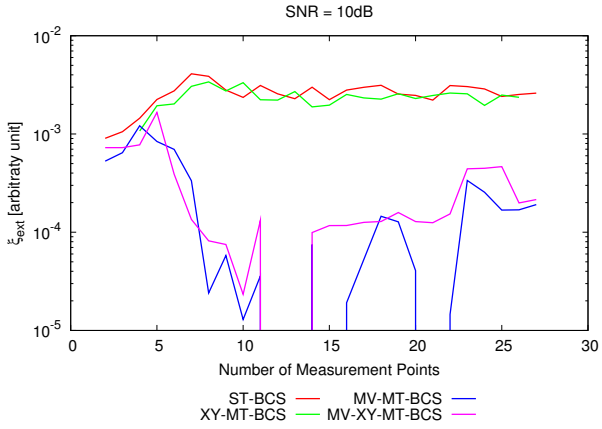

(c)

Figure 198. Behaviour of error figures as a function of the number of measurement points M: (a) total error ξ_{tot}, (b) internal error ξ_{int}, (c) external error ξ_{ext}.

RESULTS: Error Figures - $SNR = 5$ [dB]

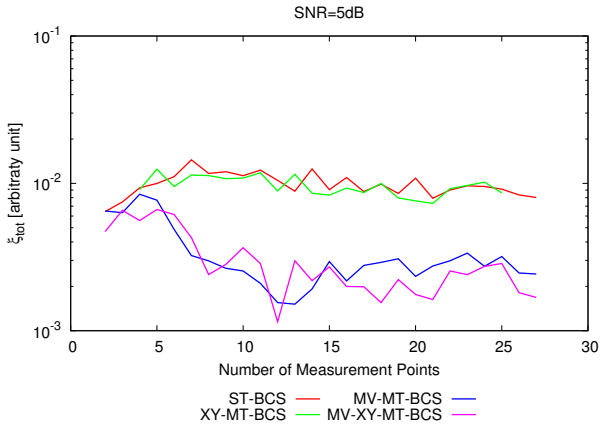

(a)

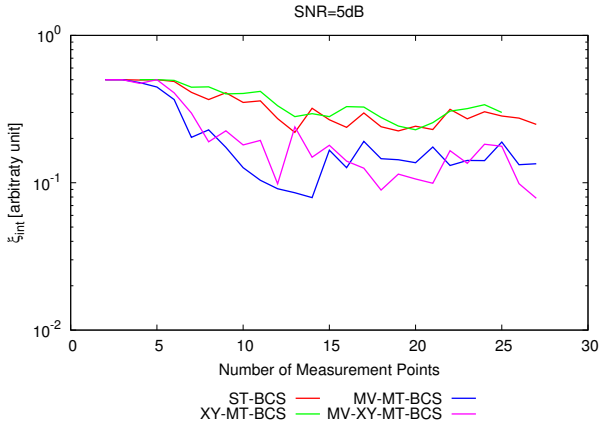

(b)

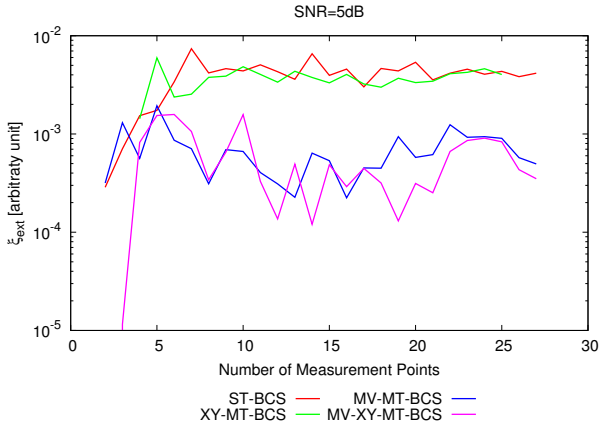

(c)

Figure 199. Behaviour of error figures as a function of the number of measurement points M: (a) total error ξ_{tot}, (b) internal error ξ_{int}, (c) external error ξ_{ext}.

7.5 Test Varying the Number of Views/Measurement Points

TEST CASE: L-Shaped Cylinder

Goal: show the performances of BCS when dealing with a sparse scatterer

- Number of Views: V
- Number of Measurements: M
- Number of Cells for the Inversion: N
- Number of Cells for the Direct solver: D
- Side of the investigation domain: L

Test Case Description

Direct solver:

- Square domain divided in $\sqrt{D} \times \sqrt{D}$ cells
- Domain side: $L = 3\lambda$
- $D = 1296$ (discretization for the direct solver: $< \lambda/10$)

Investigation domain:

- Square domain divided in $\sqrt{N} \times \sqrt{N}$ cells
- $L = 3\lambda$
- $2ka = 2 \times \frac{2\pi}{\lambda} \times \frac{L\sqrt{2}}{2} = 6\pi\sqrt{2} = 26.65$
- $\#DOF = \frac{(2ka)^2}{2} = \frac{(2 \times \frac{2\pi}{\lambda} \times \frac{L\sqrt{2}}{2})^2}{2} = 4\pi^2 \left(\frac{L}{\lambda}\right)^2 = 4\pi^2 \times 9 \approx 355.3$
- N scelto in modo da essere vicino a $\#DOF$: $N = 324$ (18×18)

Measurement domain:

- Measurement points taken on a circle of radius $\rho = 3\lambda$
- Full-aspect measurements
- $M \in \{2, 3, 4, 5, 6, 7, 8, 9, 10, 11, 12, 13, 14, 15, 16, 17, 18, 19, 20, 21, 22, 23, 24, 25, 26, 27\}$

Sources:

- Plane waves
- $V = M$
- Amplitude: $A = 1$
- Frequency: 300 MHz $(\lambda = 1)$

Object:

- L-shaped cylinder
- $\varepsilon_r = 2.0$
- $\sigma = 0$ [S/m]

RESULTS: Error Figures - *Noiseless*

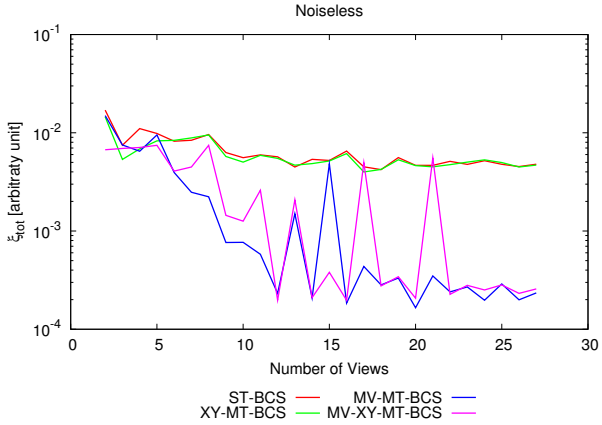

(a)

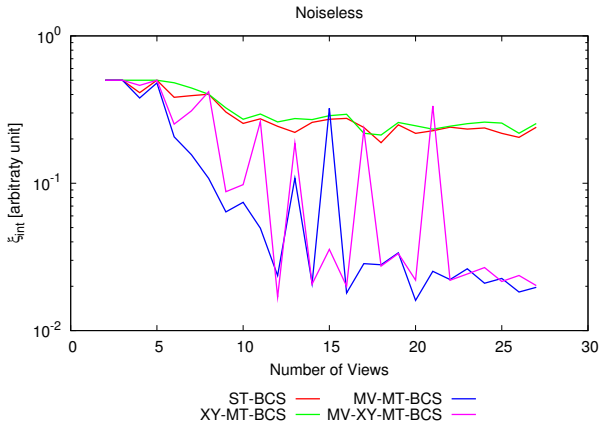

(b)

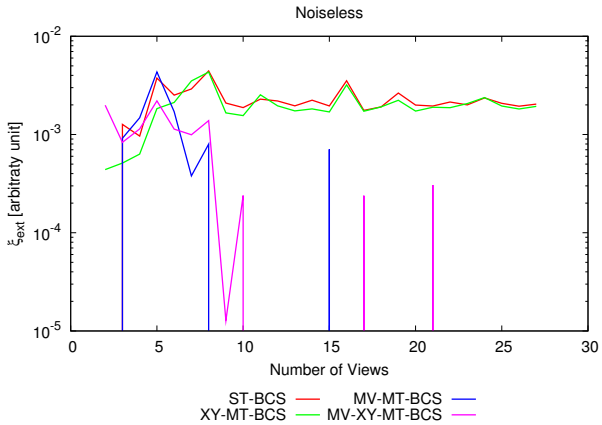

(c)

Figure 200. Behaviour of error figures as a function of the number of views/measurement points V/M: (a) total error ξ_{tot}, (b) internal error ξ_{int}, (c) external error ξ_{ext}.

RESULTS: Error Figures - $SNR = 20$ [dB]

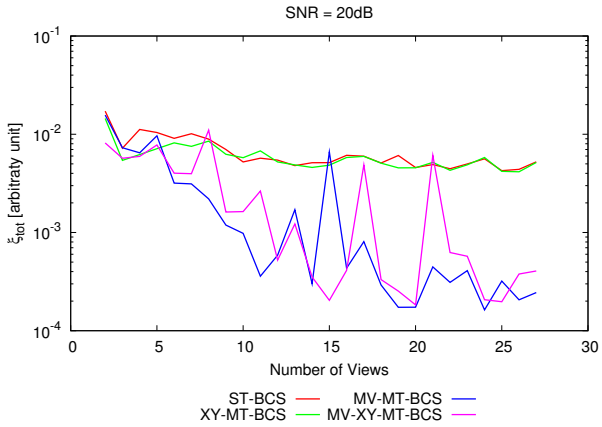

(a)

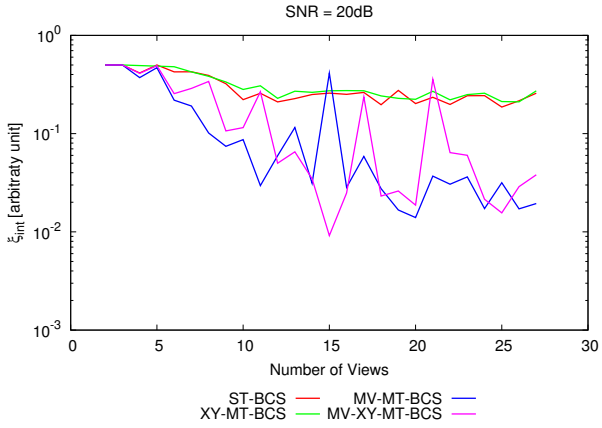

(b)

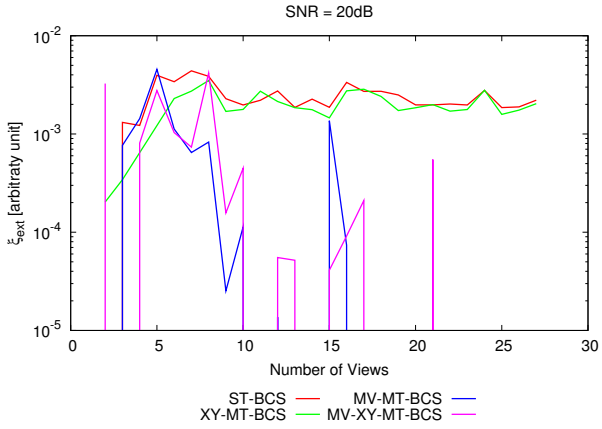

(c)

Figure 201. Behaviour of error figures as a function of the number of views/measurement pointsV/M: (a) total error ξ_{tot}, (b) internal error ξ_{int}, (c) external error ξ_{ext}.

RESULTS: Error Figures - $SNR = 10$ [dB]

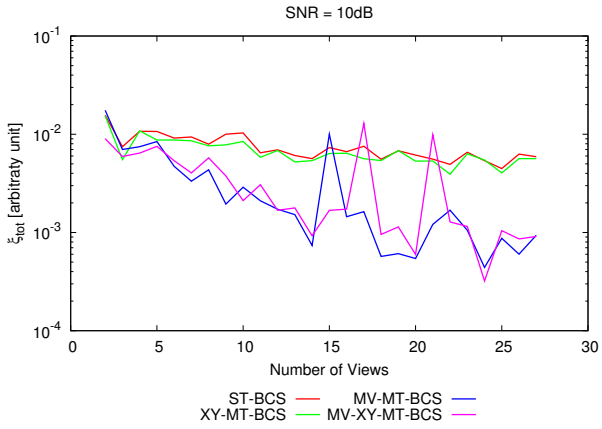

(a)

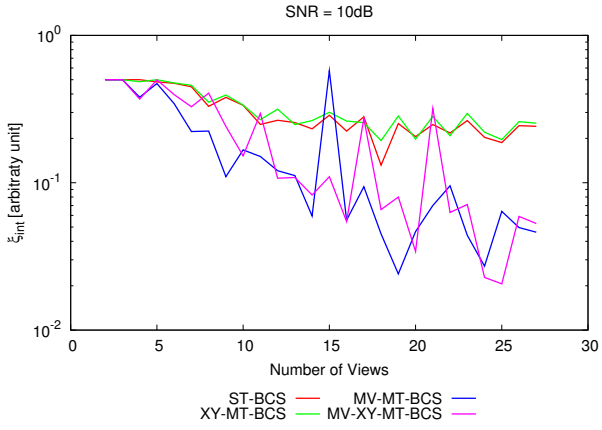

(b)

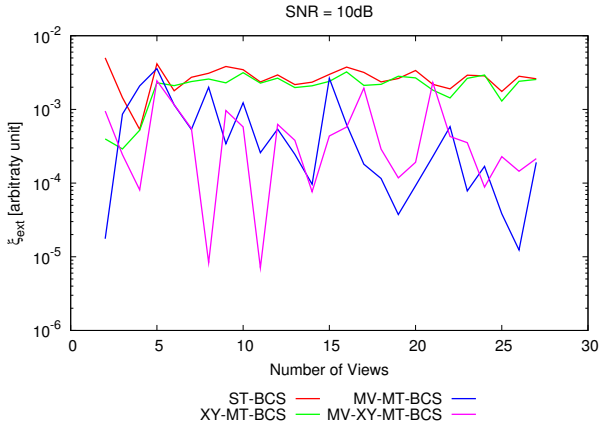

(c)

Figure 202. Behaviour of error figures as a function of the number of views/measurement points V/M: (a) total error ξ_{tot}, (b) internal error ξ_{int}, (c) external error ξ_{ext}.

RESULTS: Error Figures - $SNR = 5$ [dB]

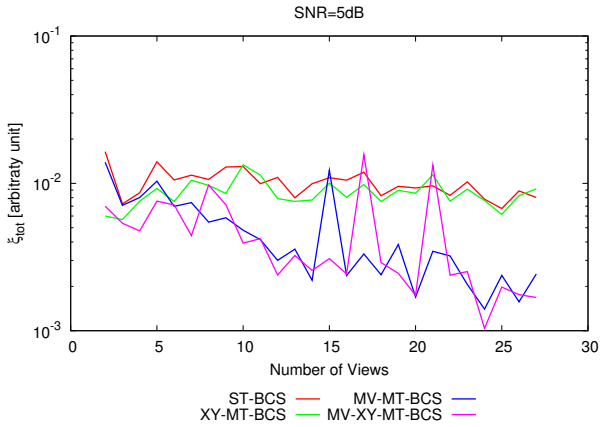

(a)

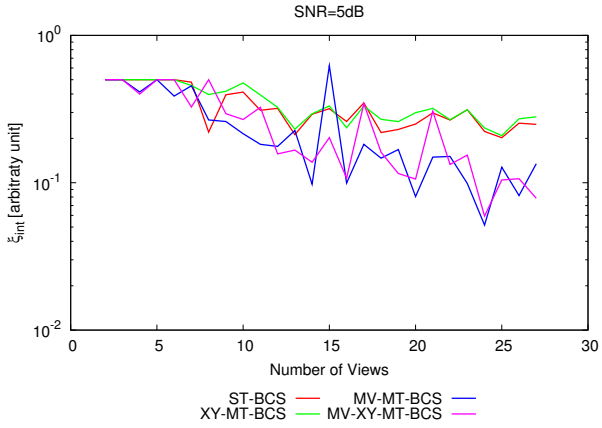

(b)

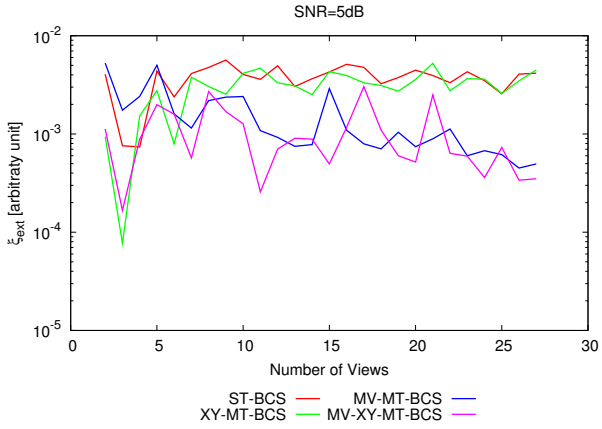

(c)

Figure 203. Behaviour of error figures as a function of the number of views/measurement points V/M: (a) total error ξ_{tot}, (b) internal error ξ_{int}, (c) external error ξ_{ext}.

8 Comparison with CG

TEST CASE: L-Shaped Cylinder

Goal: show the performances of BCS when dealing with a sparse scatterer

- Number of Views: V
- Number of Measurements: M
- Number of Cells for the Inversion: N
- Number of Cells for the Direct solver: D
- Side of the investigation domain: L

Test Case Description

Direct solver:

- Square domain divided in $\sqrt{D} \times \sqrt{D}$ cells
- Domain side: $L = 3\lambda$
- $D = 1296$ (discretization for the direct solver: $< \lambda/10$)

Investigation domain:

- Square domain divided in $\sqrt{N} \times \sqrt{N}$ cells
- $L = 3\lambda$
- $2ka = 2 \times \frac{2\pi}{\lambda} \times \frac{L\sqrt{2}}{2} = 6\pi\sqrt{2} = 26.65$
- $\#DOF = \frac{(2ka)^2}{2} = \frac{(2 \times \frac{2\pi}{\lambda} \times \frac{L\sqrt{2}}{2})^2}{2} = 4\pi^2 \left(\frac{L}{\lambda}\right)^2 = 4\pi^2 \times 9 \approx 355.3$
- N scelto in modo da essere vicino a $\#DOF$: $N = 324$ (18×18)

Measurement domain:

- Measurement points taken on a circle of radius $\rho = 3\lambda$
- Full-aspect measurements
- $M \approx 2ka \rightarrow M = 27$

Sources:

- Plane waves
- $V \approx 2ka \rightarrow V = 27$
- Amplitude $A = 1$
- Frequency: 300 MHz ($\lambda = 1$)

Object:

- L-shaped cylinder
- $\varepsilon_r \in \{1.5, 2.0, 3.0, 4.0, 5.0\}$
- $\sigma = 0$ [S/m]

CG parameters:

- Number of Iterations: $I = 10000$

COMPARISON RESULTS: $\varepsilon_r = 1.5$

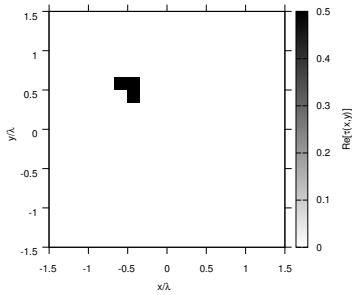

(a)

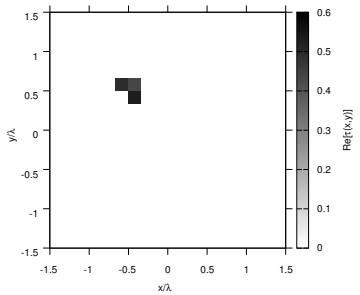

(b)

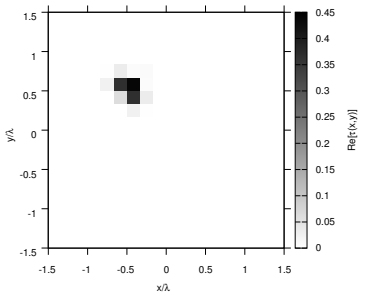

(f)

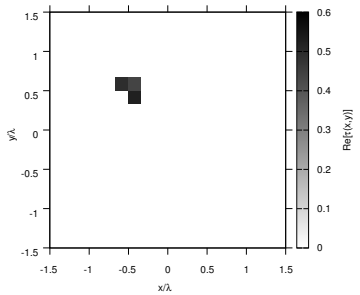

(c)

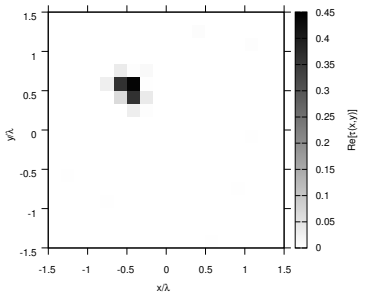

(g)

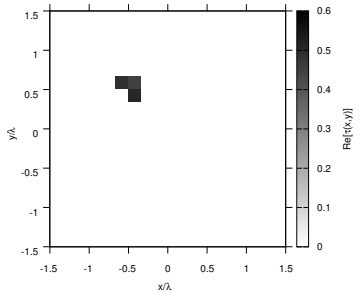

(d)

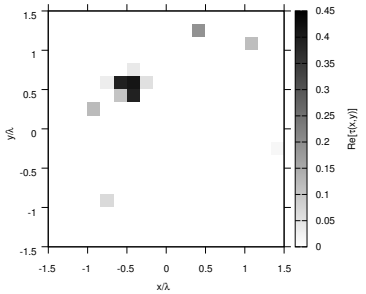

(h)

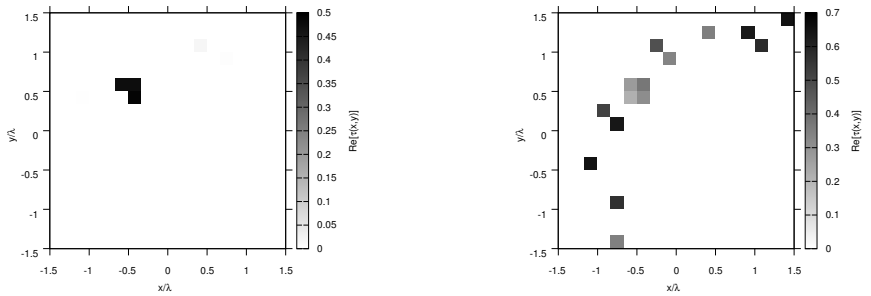

(e) (i)

Figure 204. Actual object (a), MV-MT-BCS reconstructed object $(b)(c)(d)(e)$ and CG reconstructed object $(f)(g)(h)(i)$ for Noisless case $(b)(f)$, $SNR = 20$ [dB] $(c)(g)$, $SNR = 10$ [dB] $(d)(h)$ and $SNR = 5$ [dB] $(e)(i)$.

COMPARISON RESULTS: $\varepsilon_r = 2.0$

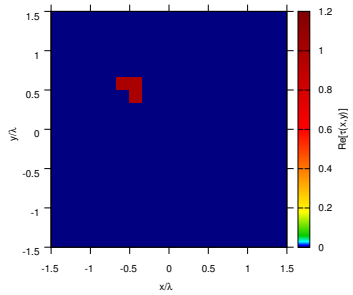

(a)

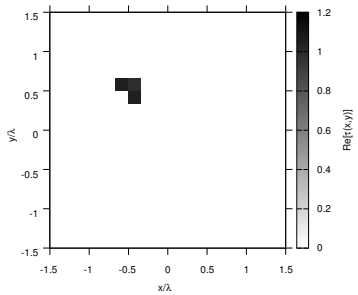

(b)

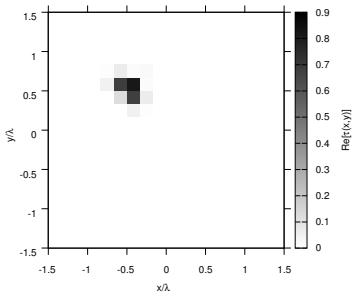

(f)

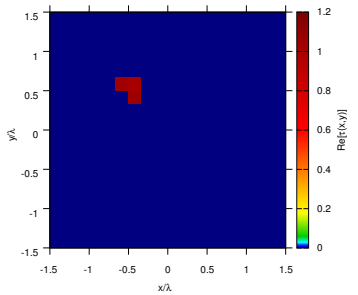

(c)

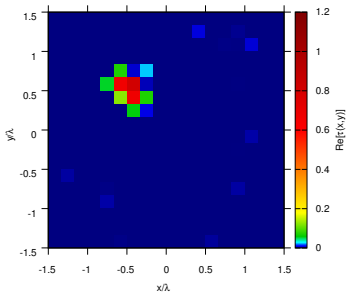

(g)

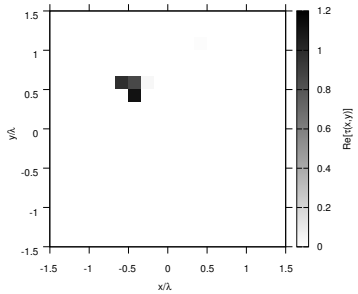

(d)

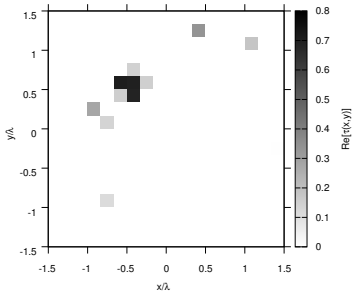

(h)

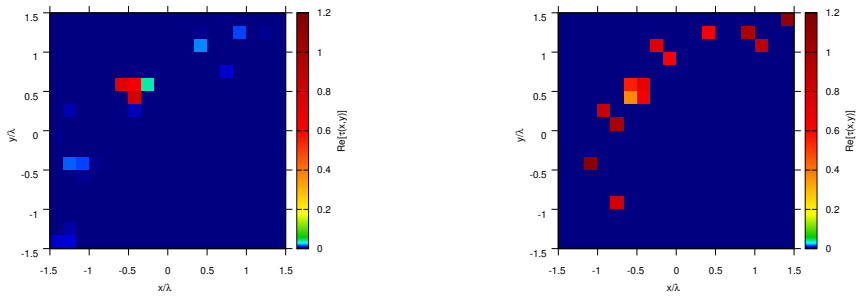

(e) (i)

Figure 205. Actual object (a), MV-MT-BCS reconstructed object $(b)(c)(d)(e)$ and CG reconstructed object $(f)(g)(h)(i)$ for Noisless case $(b)(f)$, $SNR = 20$ [dB] $(c)(g)$, $SNR = 10$ [dB] $(d)(h)$ and $SNR = 5$ [dB] $(e)(i)$.

COMPARISON RESULTS: $\varepsilon_r = 3.0$

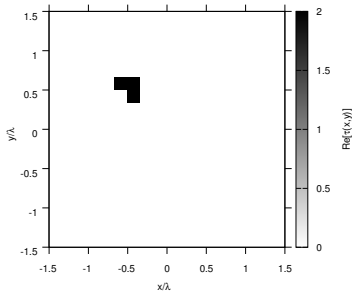

(a)

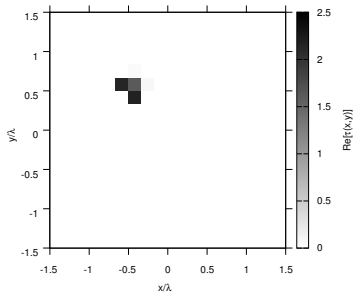

(b)

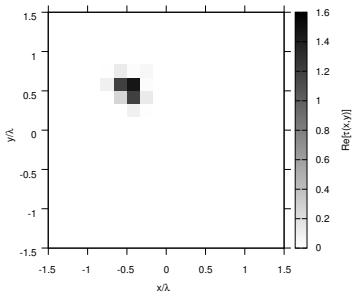

(f)

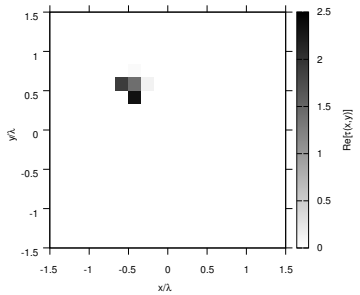

(c)

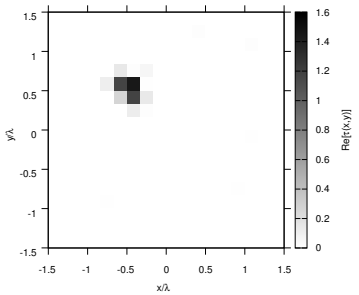

(g)

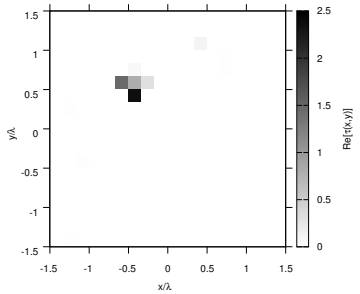

(d)

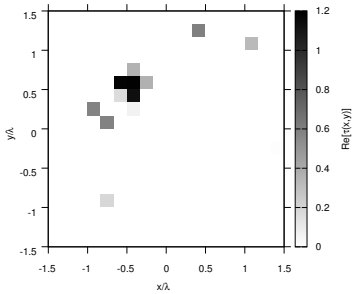

(h)

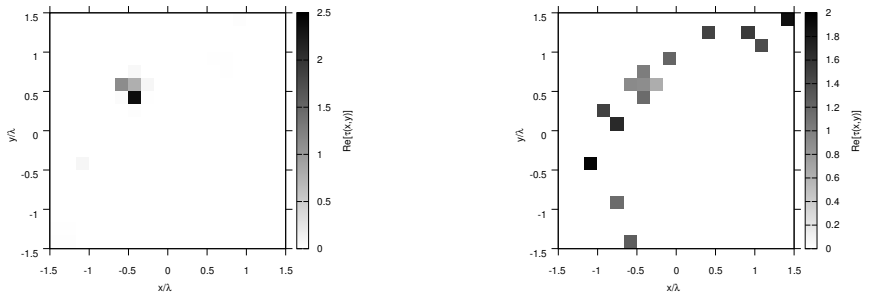

(e) (i)

Figure 206. Actual object (a), MV-MT-BCS reconstructed object $(b)(c)(d)(e)$ and CG reconstructed object $(f)(g)(h)(i)$ for Noisless case $(b)(f)$, $SNR = 20$ [dB] $(c)(g)$, $SNR = 10$ [dB] $(d)(h)$ and $SNR = 5$ [dB] $(e)(i)$.

COMPARISON RESULTS: $\varepsilon_r = 4.0$

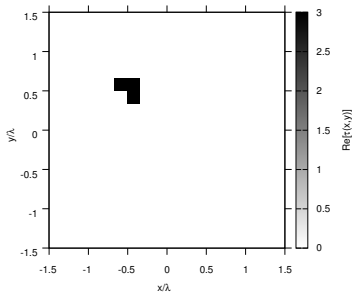

(a)

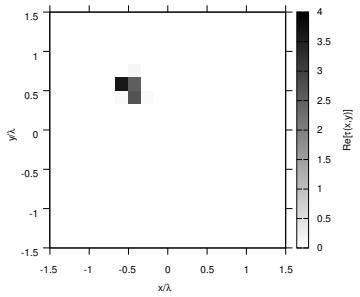

(b)

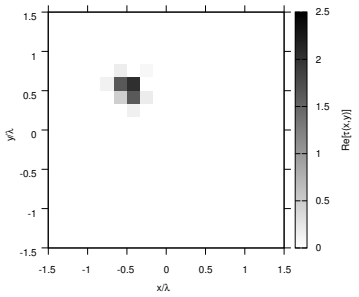

(f)

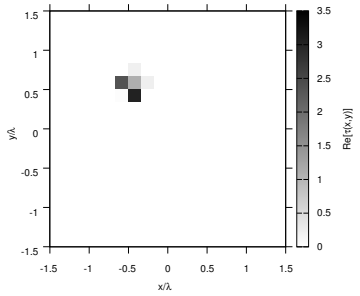

(c)

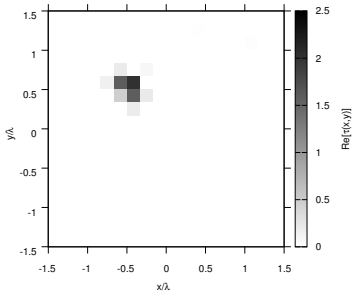

(g)

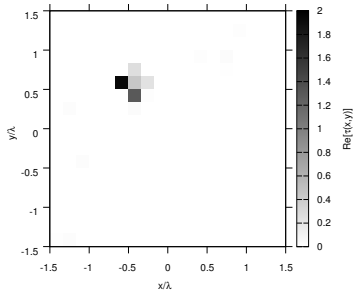

(d)

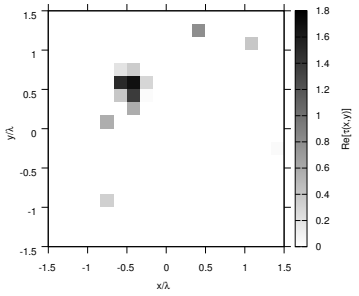

(h)

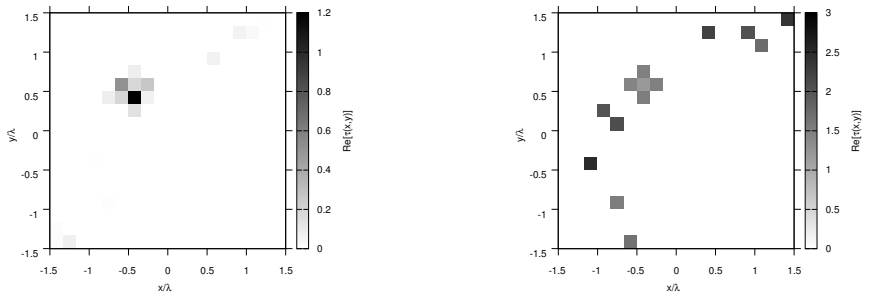

(e) (i)

Figure 207. Actual object (a), MV-MT-BCS reconstructed object $(b)(c)(d)(e)$ and CG reconstructed object $(f)(g)(h)(i)$ for Noisless case $(b)(f)$, $SNR = 20$ [dB] $(c)(g)$, $SNR = 10$ [dB] $(d)(h)$ and $SNR = 5$ [dB] $(e)(i)$.

COMPARISON RESULTS: $\varepsilon_r = 5.0$

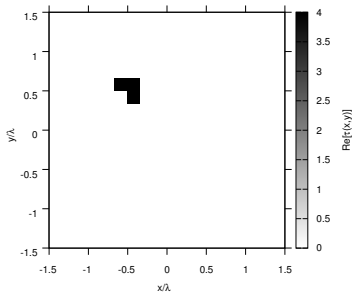

(a)

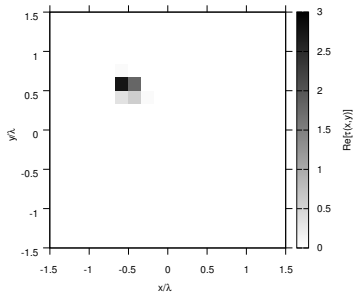

(b)

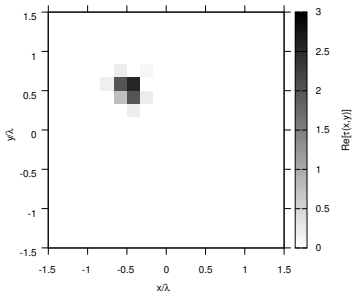

(f)

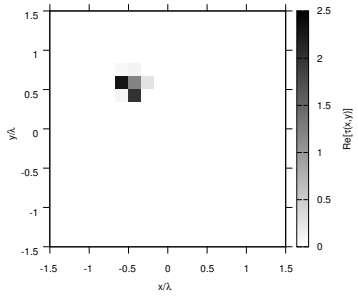

(c)

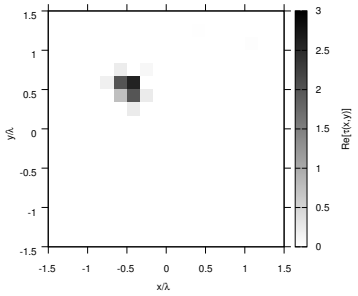

(g)

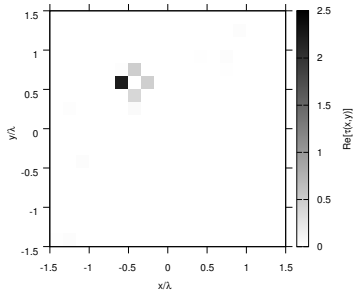

(d)

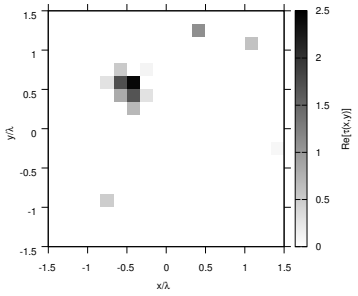

(h)

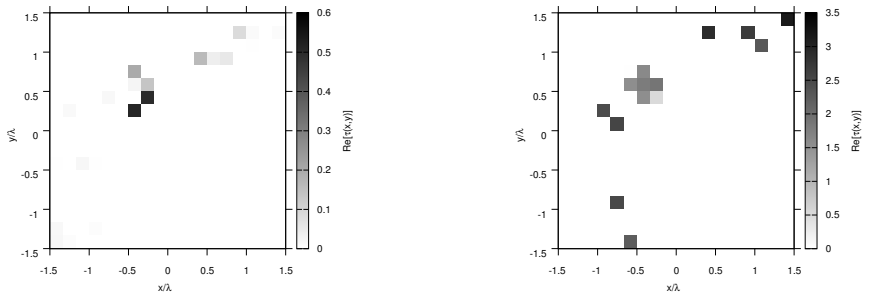

(e) (i)

Figure 208. Actual object (a), MV-MT-BCS reconstructed object $(b)(c)(d)(e)$ and CG reconstructed object $(f)(g)(h)(i)$ for Noisless case $(b)(f)$, $SNR = 20$ [dB] $(c)(g)$, $SNR = 10$ [dB] $(d)(h)$ and $SNR = 5$ [dB] $(e)(i)$.

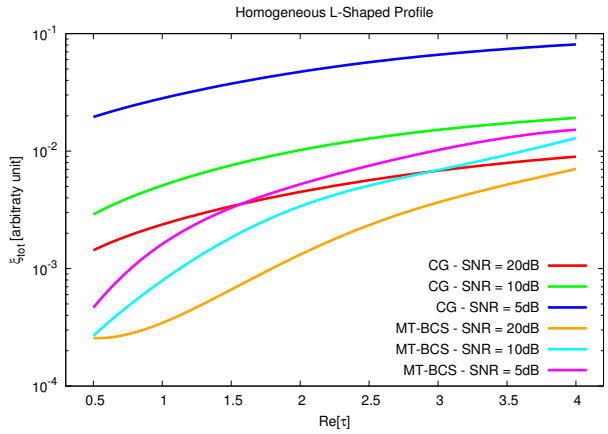

(a)

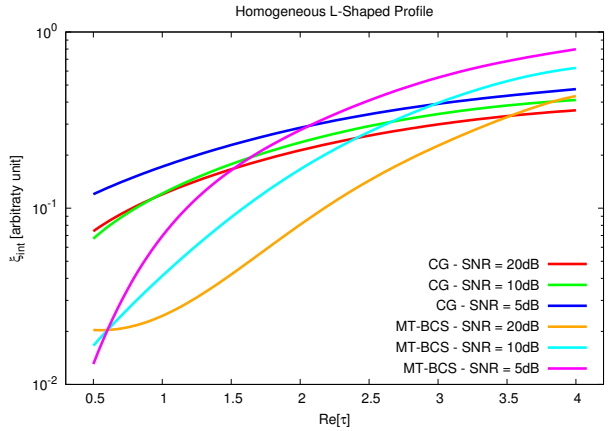

(b)

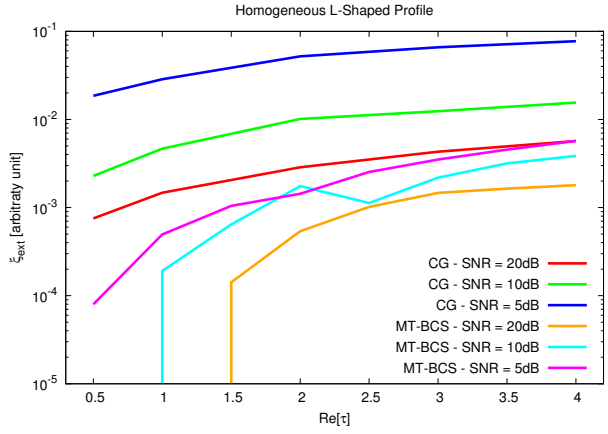

(c)

Figure 209. Behaviour of error figures as a function of ε_r, for different SNR values: (a) total error ξ_{tot}, (b) internal error ξ_{int}, (c) external error ξ_{ext}; comparison between CG and MV-MT-BCS.

COMPARISON: Error Figures

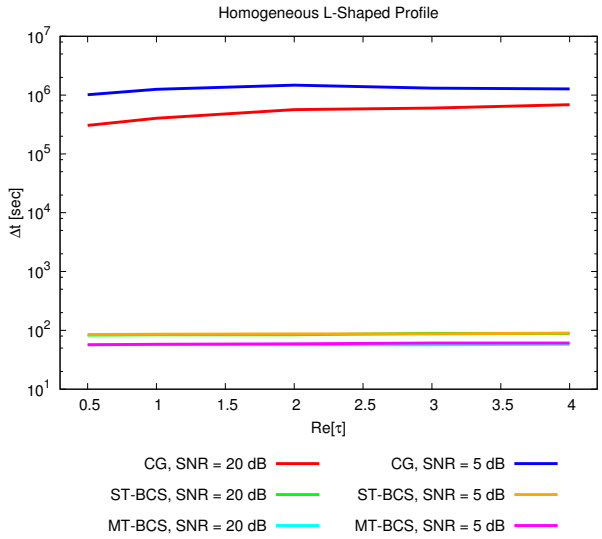

(a)

Figure 210. Inversion time comparison between CG and MV-MT-BCS.

References

[1] E. J. Candes and M. B. Wakin, "An introduction to compressive sampling", *IEEE Signal Processing Magazine*, vol. 25, no. 2, pp. 21-30, March 2008.

[2] S. Ji, Y. Xue, and L. Carin, "Bayesian compressive sampling", *IEEE Trans. on Signal Processing*, vol. 56, no. 6, pp. 2346-2356, June 2008.

[3] R. F. Harrington, *Field computation by moment methods*, New York: IEEE Press, 1993.

[4] J. H. Richmond, "TE-wave scattering by a dielectric of arbitrary cross-section shape," *IEEE Trans. Antennas Propagat.,* vol.14, pp. 460-464, July 1966.

[5] C.-C. Chiu and P.-T. Liu, "Image reconstruction of a complex cylinder illuminated by TE waves," *IEEE Trans. Microwave Theory Tech.,* vol.44, pp. 1921-1927, Oct 1996.

[6] A. Qing, "Electromagnetic imaging of two-dimensional perfectly conducting cylinders with transverse electric scattered field," *IEEE Trans. Microwave Theory Tech.,* vol. 50, pp. 1786-1794, Dec 2002.

[7] J. Ma, W. C. Chew, C.-C. Lu and J. Song, "Image reconstruction from TE scattering data using equation of strong permittivity fluctuation," *IEEE Trans. Microwave Theory Tech.,* vol. 48, pp. 860-867, Jun 2000.

[8] N. Joachimowicz and C. Pichot, "Comparison of three integral formulations for the 2-D TE scattering problem," *IEEE Trans. Microwave Theory Tech.,* vol. 38, pp. 178-185, Feb. 1990.

[9] C.-P. Chou and Y.W. Kiang, "Inverse scattering of dielectric cylinders by a cascaded TE-TM method," *IEEE Trans. Microwave Theory Tech.,* vol. 47, pp. 1923-1930, Oct 1999.

[10] L. Poli, G. Oliveri, and A. Massa, "Imaging sparse metallic cylinders through a Local Shape Function Bayesian Compressive Sensing approach," in press.

[11] F. Viani, L. Poli, G. Oliveri, F. Robol, and A. Massa, "Sparse scatterers imaging through approximated multitask compressive sensing strategies," Microwave and Optical Technology Letters, vol. 55, no. 7, pp. 1553-1558, Jul. 2013.

[12] L. Poli, G. Oliveri, P. Rocca, and A. Massa, "Bayesian compressive sensing approaches for the reconstruction of two-dimensional sparse scatterers under TE illumination," IEEE Transactions on Geoscience and Remote Sensing, vol. 51, no. 5, pp. 2920-2936, May. 2013.

[13] L. Poli, G. Oliveri, and A. Massa, "Microwave imaging within the first-order Born approximation by means of the contrast-field Bayesian compressive sensing," IEEE Transactions on Antennas and Propagation, vol. 60, no. 6, pp. 2865-2879, Jun. 2012.

[14] G. Oliveri, P. Rocca, and A. Massa, "A bayesian compressive sampling-based inversion for imaging sparse scatterers," IEEE Transactions on Geoscience and Remote Sensing, vol. 49, no. 10, pp. 3993-4006, Oct. 2011.

[15] G. Oliveri, L. Poli, P. Rocca, and A. Massa, "Bayesian compressive optical imaging within the Rytov approximation," Optics Letters, vol. 37, no. 10, pp. 1760-1762, 2012.

[16] G. Oliveri, M. Carlin, and A. Massa, "Complex-weight sparse linear array synthesis by bayesian compressive sampling," IEEE Transactions on Antennas and Propagation, vol. 60, no. 5, pp. 2309-2326, May 2012.

[17] G. Oliveri and A. Massa, "Bayesian compressive sampling for pattern synthesis with maximally sparse non-uniform linear arrays," IEEE Transactions on Antennas and Propagation, vol. 59, no. 2, pp. 467-481, Feb. 2011.

[18] G. Oliveri, P. Rocca, and A. Massa, "Reliable Diagnosis of Large Linear Arrays - A Bayesian Compressive Sensing Approach," IEEE Transactions on Antennas and Propagation, vol. 60, no. 10, pp. 4627-4636, Oct. 2012.

[19] M. Carlin, P. Rocca, G. Oliveri, F. Viani, and A. Massa, "Directions-of-Arrival Estimation through Bayesian Compressive Sensing strategies," IEEE Transactions on Antennas and Propagation, in press.

[20] G. Oliveri, Y. Zhong, X. Chen, and A. Massa, "Multi-resolution subspace-based optimization method for inverse scattering," Journal of Optical Society of America A, vol. 28, no. 10, pp. 2057-2069, Oct. 2011.

[21] A. Randazzo, G. Oliveri, A. Massa, and M. Pastorino, "Electromagnetic inversion with the multiscaling inexact-Newton method - Experimental validation," Microwave and Optical Technology Letters, vol. 53, no. 12, pp. 2834-2838, Dec. 2011.

[22] G. Oliveri, L. Lizzi, M. Pastorino, and A. Massa, "A nested multi-scaling inexact-Newton iterative approach for microwave imaging," IEEE Transactions on Antennas and Propagation, vol. 60, no. 2, pp. 971-983, Feb. 2012.

[23] G. Oliveri, A. Randazzo, M. Pastorino, and A. Massa, "Electromagnetic imaging within the contrast-source formulation by means of the multiscaling inexact Newton method," Journal of Optical Society of America A, vol. 29, no. 6, pp. 945-958, 2012.